



***Ministry of Higher Education and Scientific Research***

***Dijlah University College***

***Refrigeration and Air Conditioning***

***Technologies Engineering Department***

## **Study the Forced Harmonic Vibration in Two Degree of Freedom System Using CAD/FEM**

***A project***

***Submitted to the Refrigeration and Air Condition Technology Engineering Department at Dijlah University College in partial fulfillment of the requirements for Degree of Bachelor in Refrigeration and Air Conditioning Technologies Engineering Department***

***By:***

**Anmar Samir Jabir Matar**

**Bashir Sabry Asaad Yassen**

**Haider Abbas Hussain**

**Mohammed Yassen Khalil Ahmed**

**Moataz Abd Abbas**

***Supervisor by:***

**Asst. lecture. Saif Medhat**

***1442 A.H.***

***2021 A.D.***

# بسم الله الرحمن الرحيم

﴿ يَأْتِيهَا الَّذِينَ ءَامَنُوا إِذَا قِيلَ لَكُمْ تَفَسَّحُوا  
فِي الْمَجَالِسِ فَأَفْسَحُوا يَفْسَحِ اللَّهُ لَكُمْ وَإِذَا  
قِيلَ ائْشُرُوا فَأَشُرُوا ﴾

## صدق الله العظيم

ويقول النبي محمد - صل الله عليه وسلم - عن العلم : " (مَنْ سَلَكَ طَرِيقًا يَلْتَمِسُ فِيهِ عِلْمًا سَهَّلَ اللَّهُ لَهُ بِهِ  
طَرِيقًا إِلَى الْجَنَّةِ).

## ***Supervisor Certificate***

***We certify that this project entitled ((Study the Forced Harmonic Vibration in Two Degree of Freedom System Using CAD/FEM))***

***Prepared by:***

***Anmar Samir Jabir Matar***

***Bashir Sabry Asaad Yassen***

***Haider Abbas Hussain***

***Mohammed Yassen Khalil Ahmed***

***Moataz Abd Abbas***

***Has been carried out completely under our supervision at the Dijlah university college in partial fulfillment of the requirements for Degree of Bachelor in Refrigeration and Air Conditioning Technologies Engineering.***

***Signature:***

***Asst.lecture. Saif Medhat***

***Date: / /2021***

***Approved by the head of Air condition and refrigeration engineering department:***

***Signature***

***Dr.***

***Head of Refrigerating and Air  
Conditioning Engineering Department***

***Date: / /2021***

# ***Examining committee certificate***

**We certify that this project entitled ( Study the Forced Harmonic Vibration in Two Degree of Freedom System Using CAD/FEM )**

**Submitted by:**

*Anmar Samir Jabir Matar*

*Bashir Sabry Asaad Yassen*

*Haider Abbas Hussain*

*Mohammed Yassen Khalil Ahmed*

*Moataz Abd Abbas*

and as an examining committee examined the students in its content and that in our opinion it meets the standards of a project for the for Degree of Bachelor in Refrigeration and Air Conditioning Technologies Engineering.

Signature

**Asst.lecture. Saif Medhat**

***Date: / /2021***

***(supervisor)***

***Signature***

***Name:***

***Date: / /2021***

***(Member)***

***Signature***

***Name:***

***Date: / /2021***

***(Member)***



## الاهداء

الحمد لله وكفى والصلاة على الحبيب المصطفى واهله ومن وافاه واما بعد:  
الحمد لله الذي وفقنا لتثمين هذه الخطوة في مسيرتنا الدراسية بذكرتنا هذه ثمرة الجهد  
والنجاح بفضلته تعالى مهداة الى

سيدي وحببي وأطيب من وطئت قدماه على سطح المعمورة...

معلمنا وشفيعنا يوم التناد...

إلى مُحَمَّدٍ صَلَّى الله عليه وسلّم...

الى شهداء بلد العظام عراق السلام...

المُكرَّمان والمُحمولان على الأعناق، اللذان قدَّما لي يد العون في مسيرتي دون مُقابل...

إلى أبويَّيَّ الجليلين...

لن تستقيم الحياة دون أخلاء أوفياء؛ نلتمس مساعدتهم في وقت الشدَّة...

ونجدهم دوماً في الميعاد...

إلى أصدقائي المُحترمين...

أساتذتي الكرام أصحاب الفكر المُستتير...

## ***Abstract***

In this project, the forced harmonic vibration will be studied in a system with two degrees of freedom, and how the response changes by changing the frequency of the external forces affecting it. With the presentation of the response results that represent the amplitude, speed and vibration acceleration using the finite element method (FEM).

Theoretical analysis in the project covered the equations by derivation of the two-degree oscillation system using Newton's second law.

The results of the numerical analysis were done using Matlab and Ansys Workbench, version (2019) with the application of external forces affecting.

## ***Content***

## **Chapter one**

### **INTRODUCTION**

**P/**

**9-.....1.1 Elementary Parts of Vibrating Systems..**

**10-.....1.2 Number of Degrees of Freedom.**

**13-..... 1.3 Discrete and Continuous Systems.**

**14-..... 1.4. Classification of Vibration.**

**14-..... Free Vibration.**

**14-..... Forced Vibration.**

**15-.....1.5. Undamped and Damped Vibration.**

## **Chapter two**

### **Theory**

**17-.....2-1 Introduction**

**17-18-19.....2.2 Using newton's second law**

## **Chapter three**

### **Finite Element Method**

**21-.....3-1What is the finite element method**

**21-22-.....3-2 How the FEM works**

## **Chapter Four**

### **Result and discussion**

**25-.....4-1 Introduction**

**25-.....4-2 Results of displacement, velocity and acceleration**

# Chapter one

## INTRODUCTION

Chapter one

# **INTRODUCTION**

Any motion that repeats itself after an interval of time is called vibration or oscillation. The swinging of a pendulum and the motion of a plucked string are typical examples of vibration. The theory of vibration deals with the study of oscillatory motions of bodies and the forces associated with them.

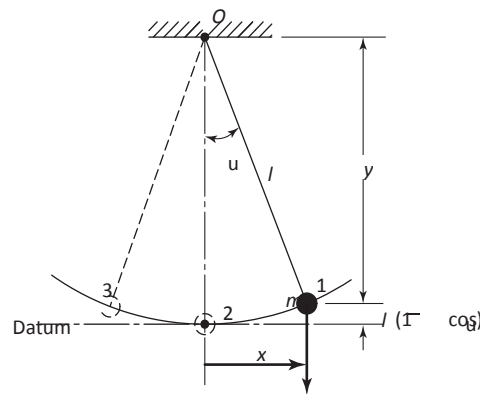
## **1.1 Elementary Parts of Vibrating Systems**

A vibratory system, in general, includes a means for storing potential energy (spring or elasticity), a means for storing kinetic energy (mass or inertia), and a means by which energy is gradually lost (damper). [1]

The vibration of a system involves the transfer of its potential energy to kinetic energy and of kinetic energy to potential energy, alternately. If the system is damped, some energy is dissipated in each cycle of vibration and must be replaced by an external source if a state of steady vibration is to be maintained.

As an example, consider the vibration of the simple pendulum shown in Let the bob of mass  $m$  be released after being given an angular displacement  $u$ . At position 1 the velocity of the bob and hence its kinetic energy is zero. But it has a potential energy of magnitude  $mgl(1 - \cos u)$  with respect to the datum position 2. Since the gravitational force  $mg$  induces a torque  $mgl \sin u$  about the point  $O$ , the bob starts swinging to the left from position 1. This gives the bob certain angular acceleration in the clockwise direction, and by the time it reaches position 2, all of its potential energy will be converted into kinetic energy. Hence the bob will not stop in position 2 but will continue to swing to position 3. However, as it passes the mean position 2, a counterclockwise torque due to gravity starts acting on the bob and causes the bob to decelerate.

The velocity of the bob reduces to zero at the left extreme position. By this time, all the kinetic energy of the bob will be converted to potential energy. Again due to the gravity torque, the bob continues to attain a counterclockwise velocity. Hence the bob starts swinging back with progressively increasing velocity and passes the mean position again. This process keeps repeating, and the pendulum will have oscillatory motion. However, in practice, the magnitude of oscillation ( $u$ ) gradually decreases and the pendulum ultimately stops due to the resistance (damping) offered by the surrounding medium (air). This means that some energy is dissipated in each cycle of vibration due to damping by the air. [1]

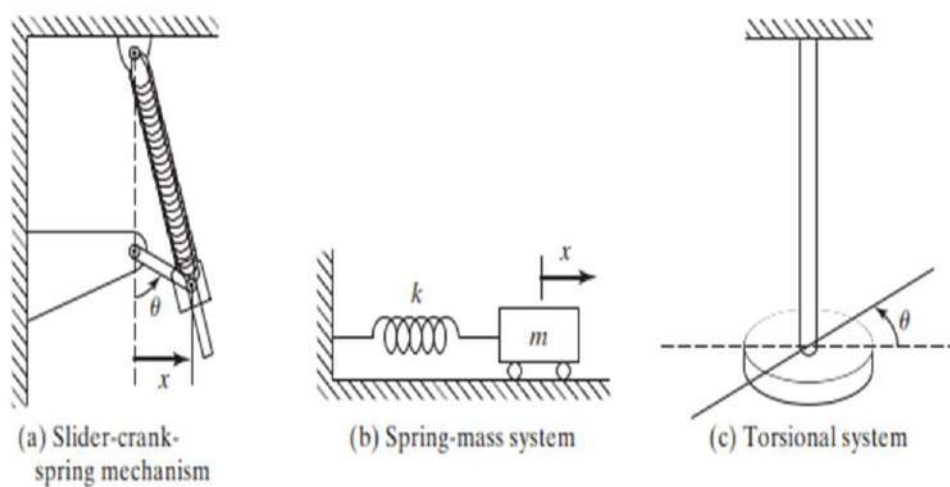


**FIGURE (1-1)** simple pendulum. [1]

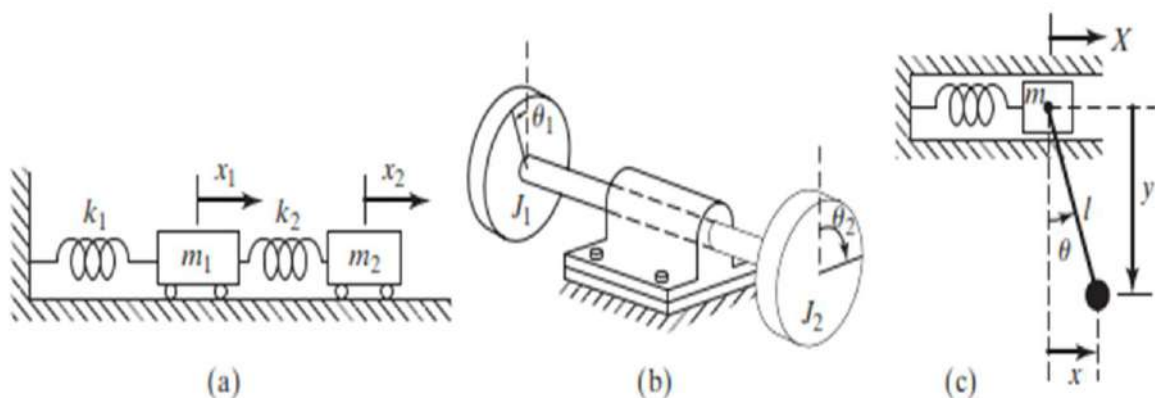
## 1.2 Number of Degrees of Freedom

The minimum number of independent coordinates required to determine completely the positions of all parts of a system at any instant of time defines the number of degrees of freedom of the system. The simple pendulum, as well as each of the systems, represents a single-degree-of-freedom system. For example, the motion of the simple pendulum can be stated either in terms of the angle  $u$  or in terms of the Cartesian coordinates  $x$  and  $y$ . If the coordinates  $x$  and  $y$  are used to describe the motion, it must be recognized that these coordinates are not independent.

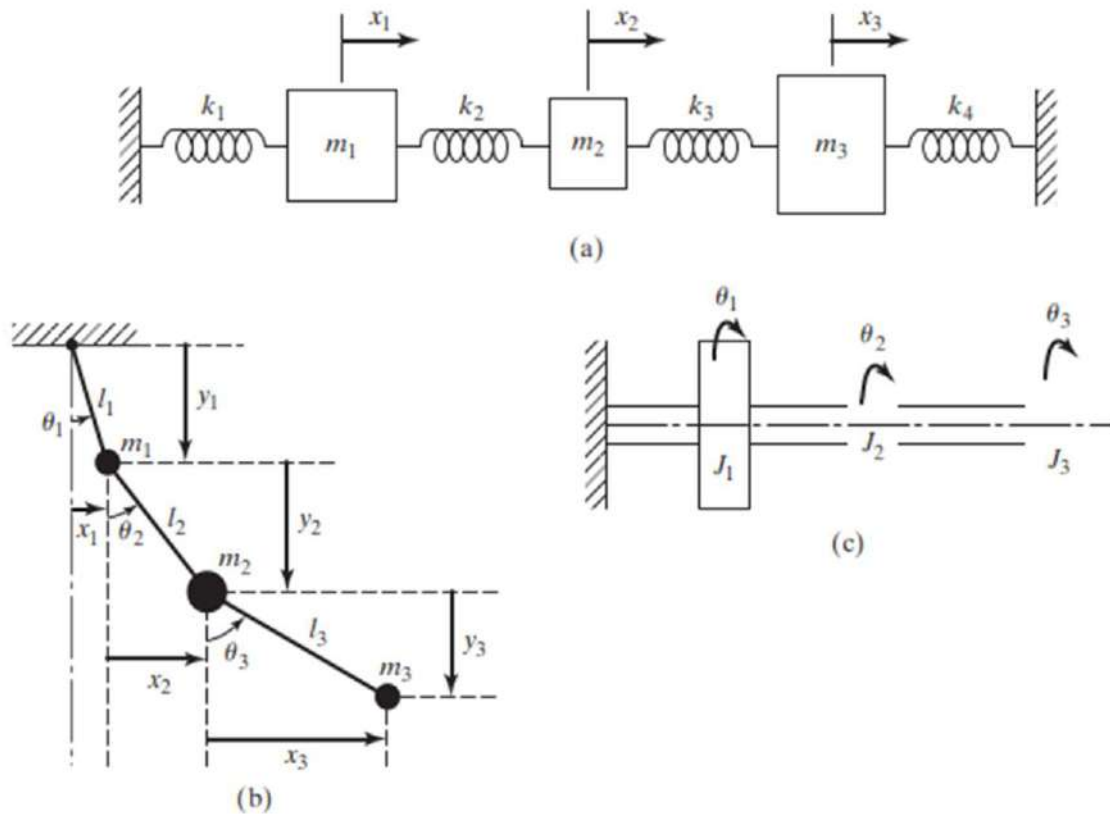
They are related to each other through the relation  $x^2 + y^2 = l^2$ , where  $l$  is the constant length of the pendulum. Thus any one coordinate can describe the motion of the pendulum. In this example, we find that the choice of  $\theta$  as the independent coordinate will be more convenient than the choice of  $x$  or  $y$ . For the slider shown in Fig. (1-1)(a), either the angular coordinate  $\theta$  or the coordinate  $x$  can be used to describe the motion. In Fig (1-1) (b), the linear coordinate  $x$  can



**Fig (1-1)** single – degree of freedom system[1]



**Fig(1-2)** Two-degree-of-freedom systems. [1]



**Fig (1-3)** Three degree-of-freedom systems[1]

be used to specify the motion. For the torsional system (long bar with a heavy disk at the end) shown in Fig (1-1) (c), the angular coordinate  $\theta$  can be used to describe the motion. Fig (1-2) and fig(1.3), respectively. Some examples of two- and three-degree-of-freedom systems are Figure (a) shows a two-mass, two-spring system that is described by the two linear coordinates  $x_1$  and  $x_2$ . Figure (b) denotes a two-rotor system whose motion can be specified in terms of  $\theta_1$  and  $\theta_2$ . The motion of the system shown in Fig. (c) can be described completely either by  $(X, \theta)$  or by  $\theta, x, y$ , and  $X$ . In the latter case,  $x$  and  $y$  are constrained as  $x^2 + y^2 = l^2$  where  $l$  is a constant.

For the systems shown in Fig(1-3). (a) and (c), the coordinates  $x_i$  ( $i = 1, 2, 3$ ) and  $\theta_i$  ( $i = 1, 2, 3$ ) can be used, respectively, to describe the



motion. In the case of the system shown in Fig.(1-3) (b),  $\theta_i$  ( $i = 1, 2, 3$ ) specifies the positions of the masses  $m_i$  ( $i = 1, 2, 3$ ).

An alternate method of describing this system is in terms of  $x_i$  and  $y_i$  ( $i = 1, 2, 3$ ); but in this case the constraints  $x_i^2 + y_i^2 = l_i^2$  ( $i = 1, 2, 3$ ) have to be considered. [1]

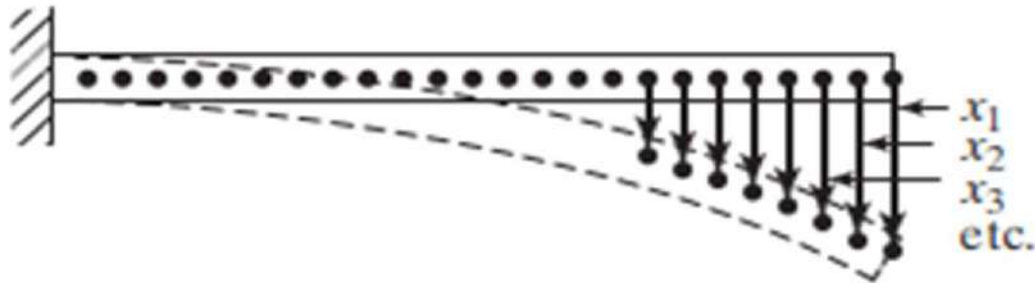
### **1.3 Discrete and Continuous Systems**

A large number of practical systems can be described using a finite number of degrees of freedom, such as the simple systems shown in figs.(1-1) to(1-3) Some systems, especially those involving continuous elastic members, have an infinite number of degrees of freedom. As a simple example, consider the cantilever beam shown in fig. (1-4) since the beam has an infinite number of mass points, we need an infinite number of coordinates to specify its deflected configuration. The infinite number of coordinates defines its elastic deflection curve. Thus the cantilever beam has an infinite number of degrees of freedom. Most structural and machine systems have deformable (elastic) members and therefore have an infinite number of degrees of freedom.

Systems with a finite number of degrees of freedom are called discrete or lumped parameter systems, and those with an infinite number of degrees of freedom are called continuous or distributed systems.

Most of the time, continuous systems are approximated as and solutions are obtained in a simpler manner. Although treatment of a system as continuous gives exact results, the analytical methods available for dealing with continuous systems are limited to a narrow selection of problems, such as uniform beams, slender rods, and thin plates. Hence most of the practical systems are studied by treating them as finite lumped masses, springs, and dampers. In general, more accurate results are obtained by increasing the

number of masses, springs, and dampers that is, by increasing the Number of degrees of freedom. [1]



**Fig. (1-4)** A cantilever beam  
(an infinite-number-of-degrees-of-freedom System). [1]

## 1.4 Classification of Vibration

Vibration can be classified in several ways. Some of the important classifications are as follows.

**Free Vibration.** If a system, after an initial disturbance, is left to vibrate on its own, the ensuing vibration is known as *free vibration*. No external force acts on the system. The oscillation of A simple pendulum is an example of free vibration. [1]

**Forced Vibration.** If a system is subjected to an external force (often, a repeating type of force), the resulting vibration is known as *forced vibration*. The oscillation that arises in machines such as diesel engines is an example of forced vibration.

If the frequency of the external force coincides with one of the natural frequencies of the system,

a condition known as resonance occurs, and the system undergoes dangerously large oscillations. Failures of such structures as buildings, bridges, turbines, and airplane wings have been associated with the occurrence of resonance.

## **1.5 Undamped and Damped Vibration**

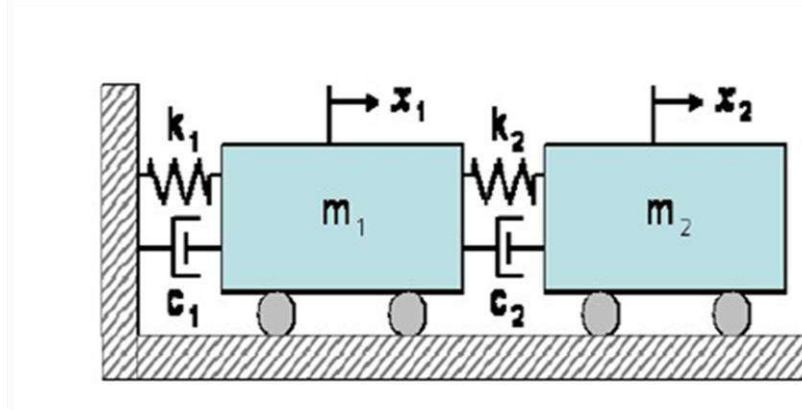
If no energy is lost or dissipated in friction or other resistance during oscillation, the vibration is known as *undamped vibration*. If any energy is lost in this way, however, it is called damped vibration. In many physical systems, the amount of damping is so small that it can be disregarded for most engineering purposes. However, consideration of damping becomes extremely important in analyzing vibratory systems near resonance. [1]

# **Chapter Two**

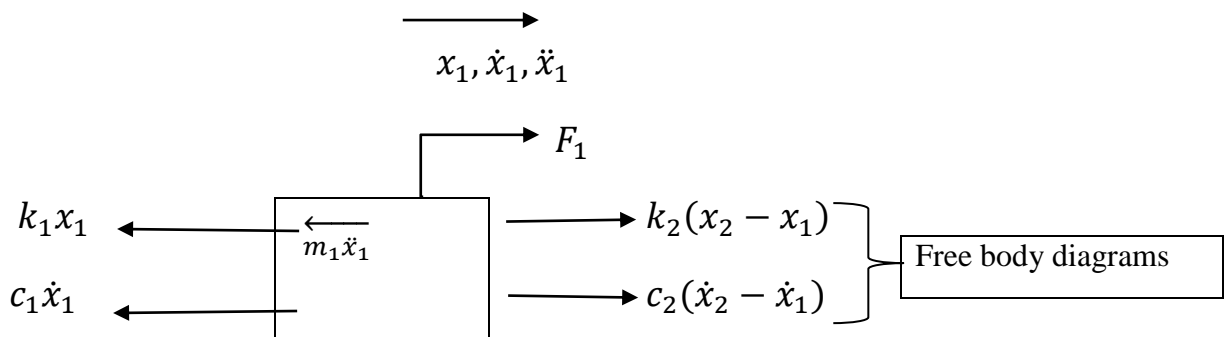
## **Theory**

## Introduction

This chapter covers theoretical work of with solving mathematical equations in the model using Newton's second law to solve mathematical equations.



**Fig.(3-1)** Two degree of freedom



Using newton's second law:--

For first mass

$$\sum \overset{+}{\leftarrow} F = ma \Rightarrow \sum F = m_1 \ddot{x}_1$$

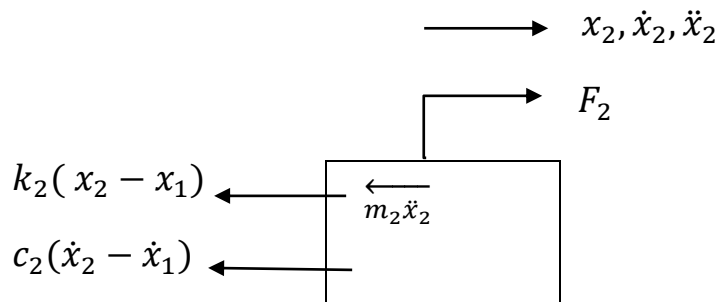
$$m_1 \ddot{x}_1 + k_1 x_1 + c_1 \dot{x}_1 - k_2 (x_2 - x_1) - c_2 (\dot{x}_2 - \dot{x}_1) - F_1 = 0$$

$$\therefore m_1 \ddot{x}_1 + k_1 x_1 + c_1 \dot{x}_1 + k_2 x_1 - k_2 x_2 - c_2 \dot{x}_1 - c_2 \dot{x}_2 - F_1 = 0$$

$$m_1 \ddot{x}_1 + (k_1 + k_2)x_1 + (c_1 + c_2)\dot{x}_1 - k_2x_2 - c_2\dot{x}_2 = F_1$$

$$\therefore m_1 \ddot{x}_1 + (k_1 + k_2)x_1 + (c_1 + c_2)\dot{x}_1 - k_2x_2 - c_2\dot{x}_2 = F_1 \quad \dots\dots\dots 1$$

$\therefore$  Free body diagram for second mass is :



Using Newton's Second law:-

$$\sum^+ F = m_2 \ddot{x}_2$$

$$m_2 \ddot{x}_2 + K_2(x_2 - x_1) + C_2(\dot{x}_2 - \dot{x}_1) - F_2 = 0$$

$$\therefore m_2 \ddot{x}_2 + c_2 \dot{x}_2 - c_2 \dot{x}_1 + k_2 x_2 - k_2 x_1 = F_2$$

$$\therefore m_2 \ddot{x}_2 - c_2 \dot{x}_1 + c_2 \dot{x}_2 - k_2 x_1 + k_2 x_2 = F_2 \quad \dots\dots\dots 2$$

Using matrix equation of motion

$$[M] \{ \ddot{x}_{(t)} \} + [C] \{ \dot{x}_{(t)} \} + [K] \{ x_{(t)} \} = \{ F_{(t)} \}$$

For equation (1) & (2)

$$\therefore [M] = \begin{bmatrix} m_1 & 0 \\ 0 & m_2 \end{bmatrix} \quad (\text{mass matrix})$$

$$[C] = \begin{bmatrix} (c_1 + c_2) & -c_2 \\ -c_2 & c_2 \end{bmatrix} \quad (\text{damping matrix})$$

$$[K] = \begin{bmatrix} (k_1 + k_2) & -k_2 \\ -k_2 & k_2 \end{bmatrix} \quad (\text{stiffness matrix})$$

$$\{x\} = \begin{Bmatrix} x_1 \\ x_2 \end{Bmatrix}$$

$$\{\dot{x}\} = \begin{Bmatrix} \dot{x}_1 \\ \dot{x}_2 \end{Bmatrix}$$

$$\{\ddot{x}\} = \begin{Bmatrix} \ddot{x}_1 \\ \ddot{x}_2 \end{Bmatrix}$$

$$\{F\} = \begin{Bmatrix} F_1 \\ F_2 \end{Bmatrix}$$

$\therefore$  general equation

$$\begin{bmatrix} m_1 & 0 \\ 0 & m_2 \end{bmatrix} \begin{Bmatrix} \ddot{x}_1 \\ \ddot{x}_2 \end{Bmatrix} + \begin{bmatrix} (c_1 + c_2) & -c_2 \\ -c_2 & c_2 \end{bmatrix} \begin{Bmatrix} \dot{x}_1 \\ \dot{x}_2 \end{Bmatrix} + \begin{bmatrix} (k_1 + k_2) & -k_2 \\ -k_2 & k_2 \end{bmatrix} \begin{Bmatrix} x_1 \\ x_2 \end{Bmatrix} = \begin{Bmatrix} F_1 \\ F_2 \end{Bmatrix}$$

# **Chapter three**

# **Finite Element**

# **Method**



### **3-1-What is the finite element method**

The finite element method (**FEM**) is a numerical technique for solving problems which are described by partial differential equations or can be formulated as functional minimization. A domain of interest is represented as an assembly of finite elements. Approximating functions in finite elements are determined in terms of nodal values of a physical field which is sought. A continuous physical problem is transformed into a discretized finite element problem with unknown nodal values. For a linear problem a system of linear algebraic equations should be solved. Values inside finite elements can be recovered using nodal values. Two features of the FEM are worth to be mentioned: 1) Piece-wise approximation of physical fields on finite elements provides good precision even with simple approximating functions (increasing the number of elements we can achieve any precision). 2) Locality of approximation leads to sparse equation systems for a discretized problem. This helps to solve problems with very large number of nodal unknowns. [2]

### **3-2 -How the FEM works**

To summarize in general terms how the finite element method works we list main steps of the finite element solution procedure below.

1. Discretize the continuum. The first step is to divide a solution region into finite elements. The finite element mesh is typically generated by a preprocessor program. The description of mesh consists of several arrays main of which are nodal coordinates and element connectivities.
2. Select interpolation functions. Interpolation functions are used to interpolate the field variables over the element. Often, polynomials are selected as interpolation functions. The degree of the polynomial depends on the number of nodes assigned to the element.
3. Find the element properties. The matrix equation for the finite element should be established which relates the nodal values of the unknown function

to other parameters. For this task different approaches can be used; the most convenient are: the variational approach and the Galerkin method.

4. Assemble the element equations. To find the global equation system for the whole solution region we must assemble all the element equations. In other words we must combine local element equations for all elements used for discretization. Element connectivities are used for the assembly process. Before solution, boundary conditions (which are not accounted in element equations) should be imposed. [2]

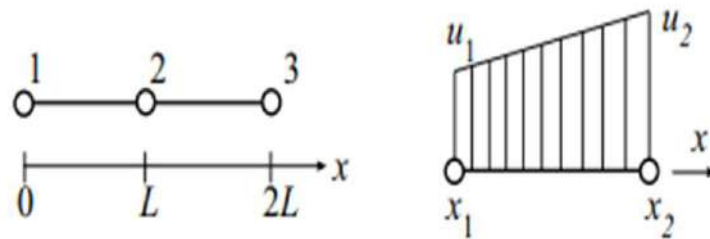
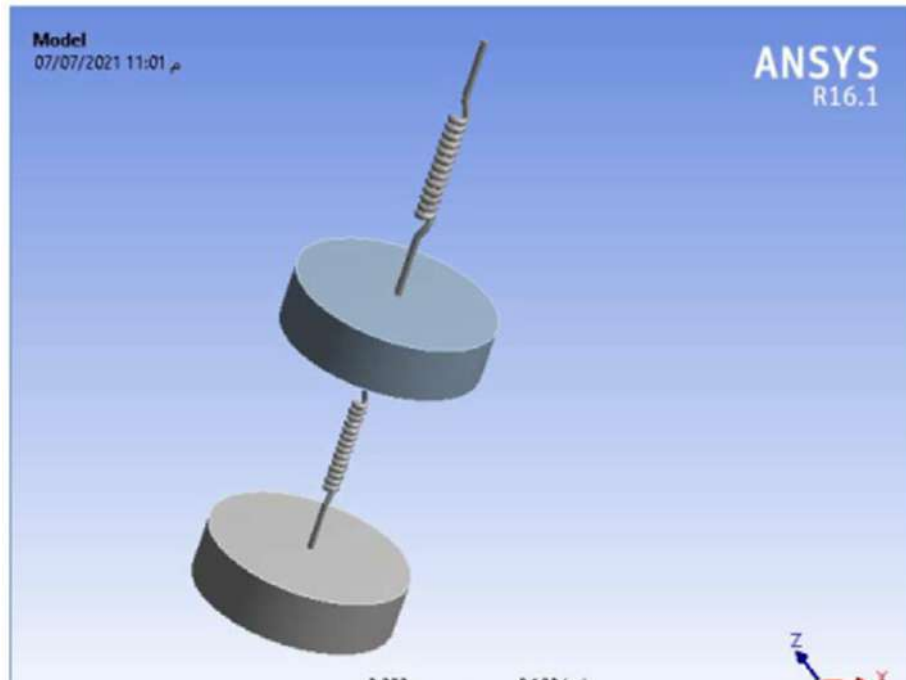


Figure 3.1: Two one-dimensional linear elements and function interpolation inside element.

5. Solve the global equation system. The finite element global equation system is typically sparse, symmetric and positive definite. Direct and iterative methods can be used for solution. The nodal values of the sought function are produced as a result of the solution.

6. Compute additional results. In many cases we need to calculate additional parameters. For example, in mechanical problems strains and stresses are of interest in addition to displacements, which are obtained after solution of the global equation system.



**Fig (3-2)**

# **Chapter Four**

## **Result and discussion**

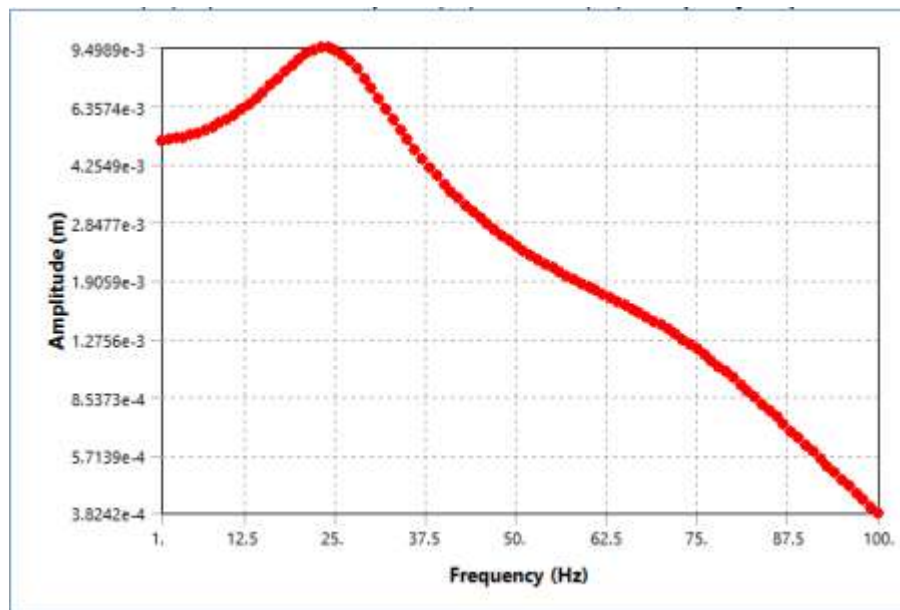
## 4-1 Introduction

In this chapter, the finite element method is used to solve equations for a body with two degree of freedom motions. The results were extracted for displacement, velocity and acceleration for different values of frequency using the (ANSYS) program, and also the ( Matlab) program to extract the values of displacement, velocity and acceleration.

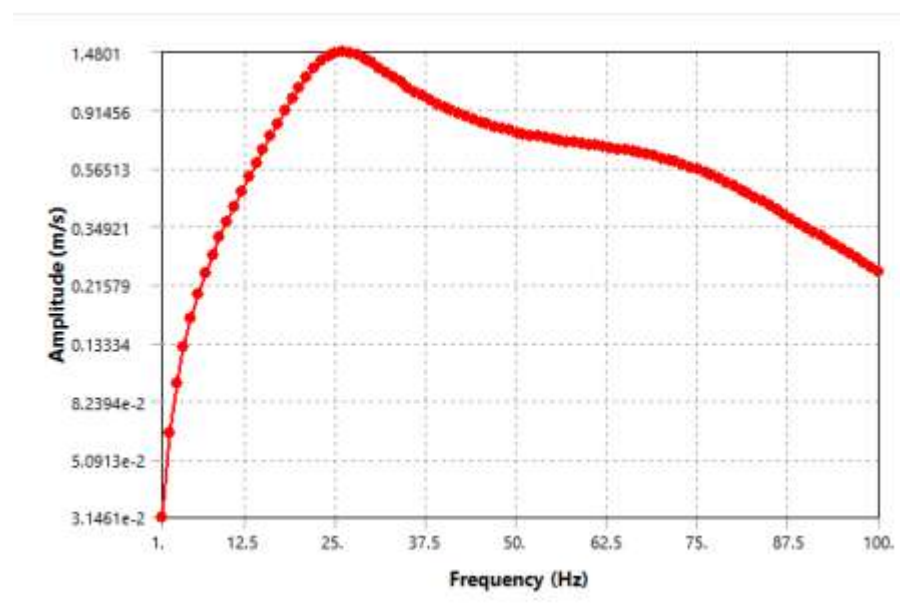
## 4-2 Results of displacement, velocity and acceleration

Figures (4-1) to (4-3) show the results of displacement, velocity and acceleration for the first mass whose value is (5 kg), take the damping ratio (0.25) and the spring stiffness of ( 300,000 N/ sec), where the results showed that the highest value of displacement is (  $9.4989 * 10^{-3}m$ ) and the highest speed (1.480 m/s) and the highest acceleration ( $270.29m/s^2$ ).

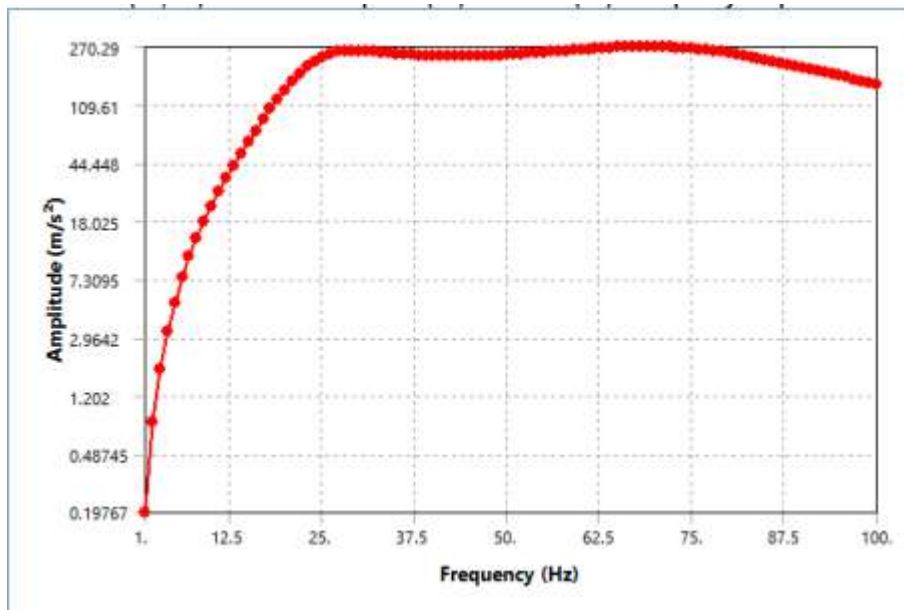
Figures (4-4) to (4-6) show the results of displacement, velocity and acceleration of the second mass whose value is (5 kg) and the forced harmonic acting on it ( $150 \sin \omega t$ ), the frequency range from (0 to 100 )HZ and the damping ratio (0.25). And the spring stiffness of is (500000) N/sec. The results showed that the highest value of displacement is ( $1.34 * 10^{-2}$ ), the highest speed is (2.03 m/sec) and the highest acceleration is ( $355.82m/s^2$ ).



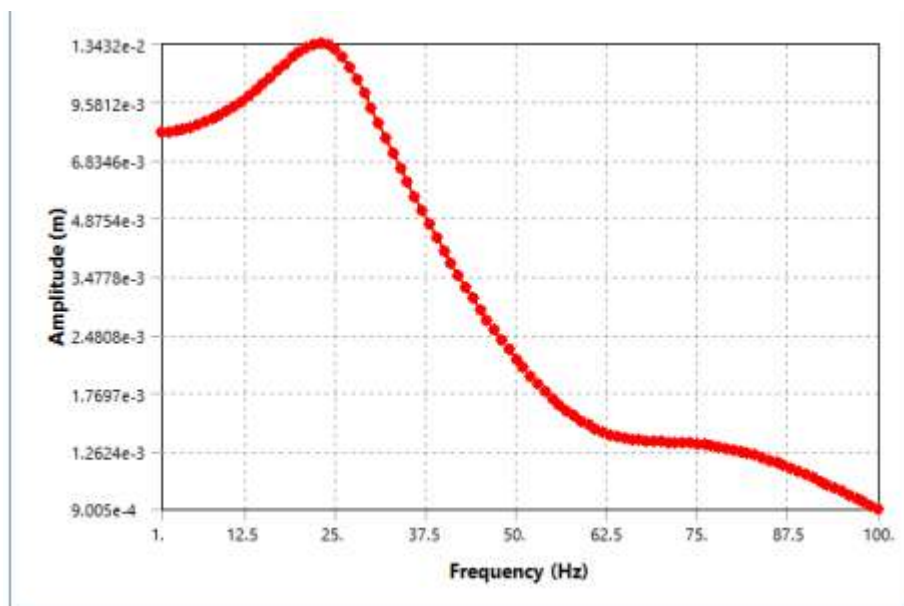
**Fig. 4-1**



**Fig. 4-2**



**Fig.4-3**



**Fig. 4-4**

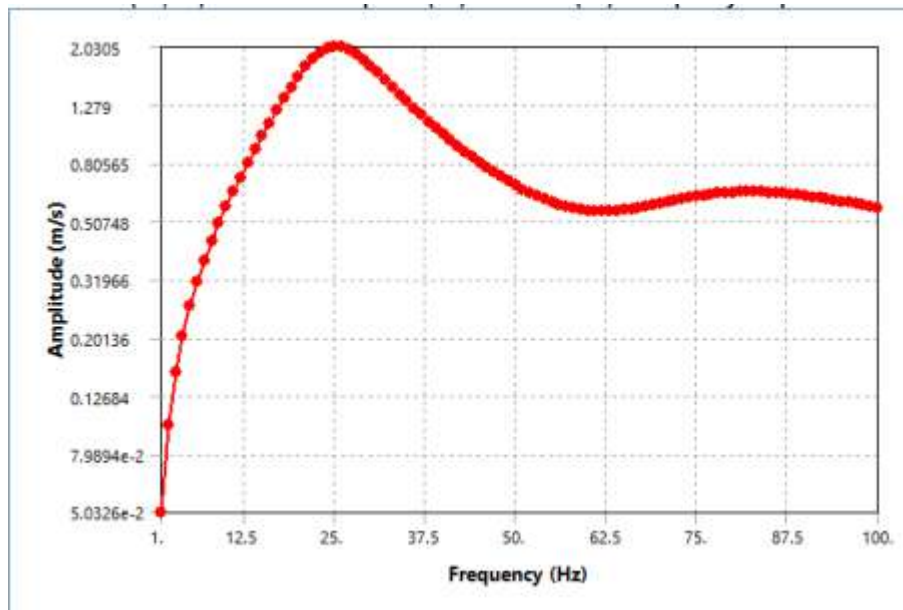


Fig. 4-5

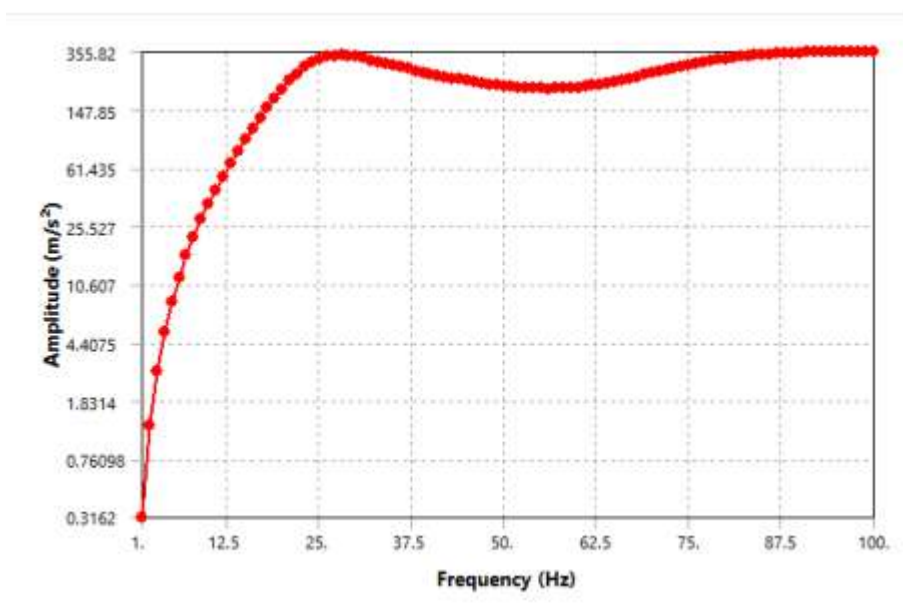


Fig. 4-6

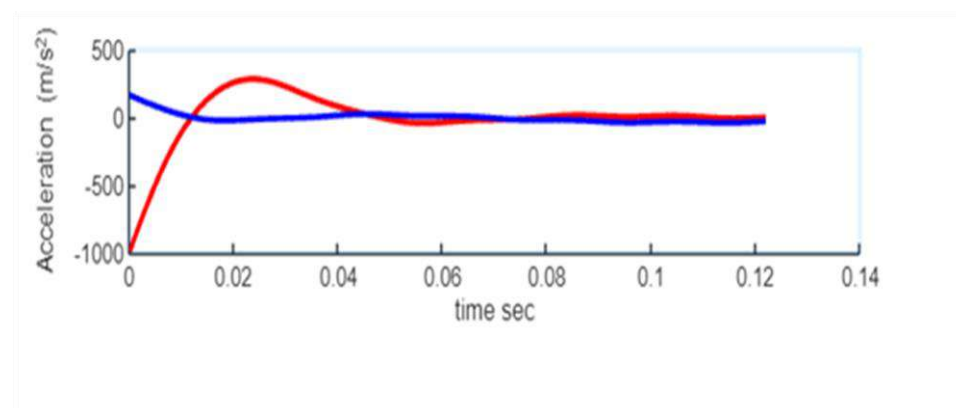
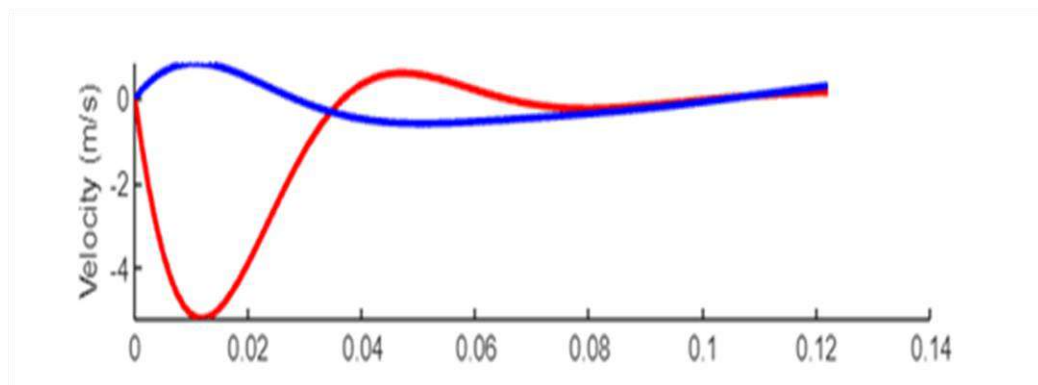
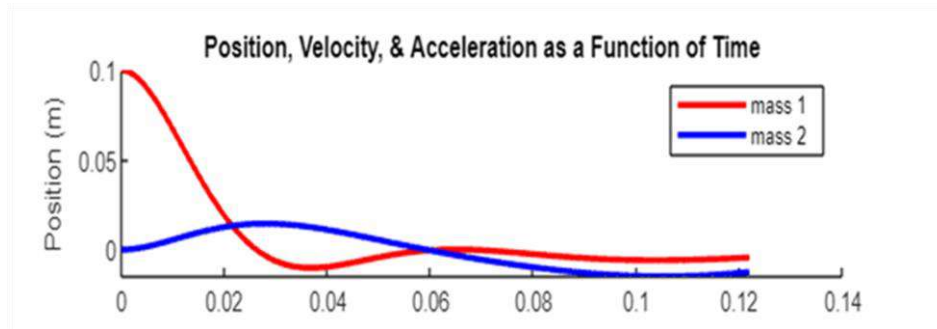


#### **4-4 Result of matlab**

When the two masses are subjected to a forced vibration force, we will notice the change in the location of the blocks at a certain time. At the beginning of the vibration, the displacement between the blocks is as large as possible. Through this graph, we notice that there is a relationship between mass and vibration, as the mass increases, the less vibration.

Through the graph between speed and time, we notice that there is a relationship between speed and mass, where the less mass, the higher the speed, and there is a direct relationship between speed and frequency, where the higher the speed, the higher the frequency.

The smaller the change in time, the greater the acceleration, meaning that the relationship is direct between acceleration and change in speed, and the inverse relationship between acceleration and change in time



# REFERENCES

## REFERENCES

- 1:- Singiresu S. Rao,( mechanical vibration) 5th edition.
- 2- (Fundamental FEA Concepts and Applications), A Guidebook for the use and Applicability of Workbench Simulation Tools from ANSYS, Inc.

## الخلاصة

في هذا المشروع سيتم دراسة الاهتزاز التناغمي القسري في نظام يحتوي على درجتين من الحرية ، وكيف تتغير الاستجابة بتغيير تردد القوى الخارجية المؤثرة عليه .مع عرض نتائج الاستجابة التي تمثل سعة الاهتزاز و سرعة الاهتزاز وتعجيل الاهتزاز باستخدام طريقة العناصر المحددة (FEM). التحليل النظري في المشروع غطى المعادلات من خلال الاشتقاق الخاص بالنظام الاهتزاز ذو الدرجتين من الحرية باستخدام قانون نيوتن الثاني.

نتائج التحليل العددي انجزت باستخدام برنامج ماتلاب وبرنامج انسر ورك بينج النسخة (٢٠١٩) مع تطبيق القوى الخارجية المؤثرة عليه



وزارة التعليم العالي والبحث العلمي

كلية دجلة الجامعة الأهلية

قسم هندسة تقنيات التبريد والتكييف

دراسة الامتزاز التناغمي القسري لنظام ذو درجتين من الحرية باستخدام

العناصر المحددة المعالجة بالحاسوب

بحث مقدم إلى كلية دجلة الجامعة الأهلية/ قسم هندسة تقنيات التبريد والتكييف وهو جزء من

متطلبات نيل شهادة البكالوريوس في هندسة تقنيات التبريد والتكييف

من قبل

-انمار سمير جبير

- بشير صبري اسعد

-حيدر عباس إحسان

-محمد ياسين خليل

-معتز عبد عباس

بإشراف

م.م. سيف مدحت

٥ ١٤٤٢

م ٢٠٢١

***Ministry of Higher Education and Scientific  
Research***

***Dijlah University College***

***Refrigeration and Air Conditioning***

***Technologies Engineering Department***



***project name***

***A numerical study to improve performance at shell and tube  
temperatures by inserting moving balls inside***

***A project***

***Submitted to the Refrigeration and Air Condition Technology  
Engineering Department at Dijlah University College in  
partial fulfillment of the requirements for Degree of Bachelor  
in Refrigeration and Air Conditioning Technologies  
Engineering Department***

***By:***

***1\_Haider Kazem***

***2\_Ali Firas***

***3\_Ali Kamal***

***4\_Saif ali***

***5\_Muhammad Jabbar***

***Supervisor by: Dr. Haider Laft***

***1442 A.H.***

***2021 A.D.***

قال تعالى

﴿ قَالَ الَّذِي عِنْدَهُ عِلْمٌ مِنَ الْكِتَابِ أَنَا آتِيكَ بِهِ قَبْلَ أَنْ يَرْتَدَّ إِلَيْكَ طَرْفُكَ فَلَمَّا رآه مُسْتَقِرًّا  
عِنْدَهُ قَالَ هَذَا مِنْ فَضْلِ رَبِّي لِيَبْلُوَنِي أَأَشْكُرُ أَمْ أَكْفُرُ وَمَنْ شَكَرَ فَإِنَّمَا يَشْكُرُ لِنَفْسِهِ  
وَمَنْ كَفَرَ فَإِنَّ رَبِّي غَنِيٌّ كَرِيمٌ ﴾

[النمل: 40]

صدق الله العظيم



***Supervisor Certificate***

***We certify that this project entitled  
A numerical study to improve performance at shell and tube  
temperatures by inserting moving balls inside))***

***Prepared by:***

***(Haider Kazem \_ Ali Firas \_ Ali Kamal \_ Saif ali \_  
Muhammad Jabbar)***

***Has been carried out completely under our supervision at the  
Dijlah university college in partial fulfillment of the  
requirements for Degree of Bachelor in Refrigeration and Air  
Conditioning Technologies Engineering.***

***Signature:***

***Date: / /2021***

***Approved by the head of Air condition and refrigeration  
engineering department:***

***Signature***

***Dr.***

***Head of Refrigerating and Air***

***Conditioning Engineering Department***

***Date: / /2021***

***Examining committee certificate***

***We certify that this project entitled ( A numerical study to improve performance at shell and tube temperatures by inserting moving balls inside)) )***

***Submitted by:***

***Haider Kazem***

***Ali Firas***

***Ali Kamal***

***Saif ali***

***Muhammad Jabbar***

***and as an examining committee examined the students in its content and that in our opinion it meets the standards of a project for the for Degree of Bachelor in Refrigeration and Air Conditioning Technologies Engineering.***

***Signature***

***Name of lecturer***

***Date: / /2021***

***(supervisor)***

***Signature***

***Name:***

***Date: / /2021***

***(Member)***

***Signature***

***Name:***

***Date: / /2021***

***(Member)***

## الاهداء

### إهداءنا

إلى البلسم الذي يداوي جروحنا...

إلى من ربيانا صغيرا...

إلى من أحببنا ولن ننسى...إلى أبائنا وأمهاتنا...

إلى أشقائنا و شقيقاتنا الذين وقفوا بجانبنا طيلة السنين الماضية

إلى أصدقائنا الذين دعمونا وساندونا خلال دراستنا

إلى قادة المستقبل وبناءة الغد...طلبة العراق..

إلى من له حق علينا...نهدي هذا العمل المتواضع

### *Nomenclature*

*CRTs*    *circular-ring turbulators*

*DR*      *diameter ratio=d/D*

*PR*      *pitch ratio=p/D*

*n*        *the number of bidirectional conical strip*

*x*        *central angle of single bidirectional conicalstrip*

*PEC*    *comprehensive heat transfer performance coefficient*

*P*        *pitch ratio*

*Re*      *Reynolds number*

*Nu*      *nusselt number*

*R3*      *comprehensive heat transfer performance coefficient*

<b>WQABSTRACT</b>	8
<b>CHAPTER ONE</b>	9
<b>INTRODUCTION</b>	9
(1-1)General	10
(3-1)methodology	<b>Error! Bookmark not defined.</b>
<b>CHAPTER THREE</b>	25
<b>THEORETICAL INVESTIGATION</b>	25
3-1 INTRODUCTION	26
3-3 SIMULATION PROCEDURE	28
3-3-1 FLUENT AND CFD-POSTPROCESSING	28
3-3-2 CREATING THE GEOMETRY	31
3-3-3 MESHING THE GEOMETRY	33
3-3-4 SETTING UP THE CFD SIMULATION	37
<b>CHAPTER FOUR</b>	44
<b>RESULTS AND DISCUSSION</b>	44
4-1 introduction	45
4-2 Results and Discussion	45
الخلاصة	56

## ***Abstract***

***Work on this project transferred and optimized models are represented by ANSYS 19 R1 software. Two parameters in the Reynolds number range (2500-15000) have been changed. The first parameter is the diameter of the ball and the maximum performance is achieved. And that the data and results obtained from the simulation process, collected and compared with the literature studies. Initial setup of prototype units correctly Production uni Where the Reynolds number, Nusselt number, Prantel number and the thermal performance factor were calculated by isothermal pumping method before and after adding the moving balls and compared with a variable setting of Reynolds number. The second parameter is the speed of the moving ball. The percentage increase in the thermal performance factor is calculated by diameter (0.422), the performance factor (14.4%), by the diameter (0.563), and the reinforcement percentage (27.8%). Finally, the maximum value of the boost is (40.8%) and the diameter ratio is (0.704 .).t***

# CHAPTER ONE

## INTRODUCTION

## General (1\_1)

*There are many ways to intensify heat transfer in heat exchangers e.g. by using different inserts inside or outside tubes of the heat exchanger, twisted bands, wire coils or internal ribs of different shapes. All the methods mentioned above are considered to be passive, which means they do not require extra energy from outside to improve the heat transfer. Nevertheless, they cause an increase in the flow resistance, and consequently there is a greater power demand to pump the fluid. A comparison of the two opposite values shows the actual benefit of using the method, as compared to a smooth tube. Reaching a highly intensified heat transfer with a simultaneous low increase in the pressure drop is a challenge for designers of heat exchangers. Thermal performance factor  $g$  (TPF) [1] is one of the most common parameters used to evaluate heat channels. It helps compare the studied channel to a smooth circular tube at the same heat conditions and the same pumping power. If the TPF is greater than one, the channels is considered to be more heat efficient than a smooth tube (the goal is to reach the highest values possible). If the value is one, its heat performance is the same as heat performance of a smooth tube, while the value lower than one indicates heat performance of a channel smaller than in a smooth tube. Many scientists apply this evaluation method to study heat channels with turbulators. Unfortunately, limited literature resources devoted to moving ball inserts makes it impossible to refer directly to such geometry. The best way to find the value of the thermal performance factor is a method of equal pumping power in which the increase in the amount of heat transferred as a result of adding an object inside the tube is compared with the amount of increase in pressure drop as a result of that body being trapped in the tube*

### *(1-2) Types of heat exchangers*



*-1Liquid or gas heating*

*2 Liquid or gas cooling*

*-3Steam condensation*

*-4 Evaporating liquid*

*Heat exchangers are called according to their function as follows :*

*-1Heaters: They are heat exchangers that use a liquid to heat a fluid .*

*2 They are heat exchangers that cool the fluids with another liquid. Water is usually used for this purpose and it is called Cooling Water*

*-3 Condensers: They are heat exchangers that are used to condense steam or a mixture of fumes or in the presence of condensable gases (such as the presence of air with water vapor) and their action. The main is to remove or absorb the latent heat of vaporization, and water is usually used for this.*

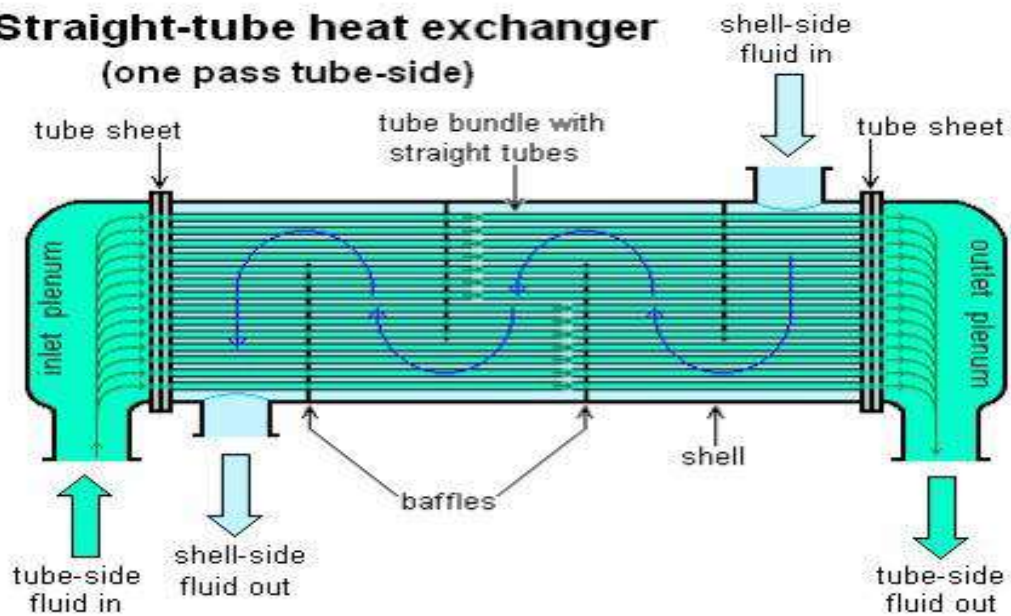
*-4 Evaporators: Evaporators are used to evaporate a solvent liquid from a specific solution and are usually used to concentrate solutions by evaporating water (from these aqueous solutions (*

*-5Reboilers: They are heat exchangers that are usually used to heat the bottom of distillation towers to separate derivatives from each other or for retail towers (to separate some gases from Liquids) water vapor is widely used in the oil industry .Heat exchangers can also be classified according to the number of phases. As follows:*

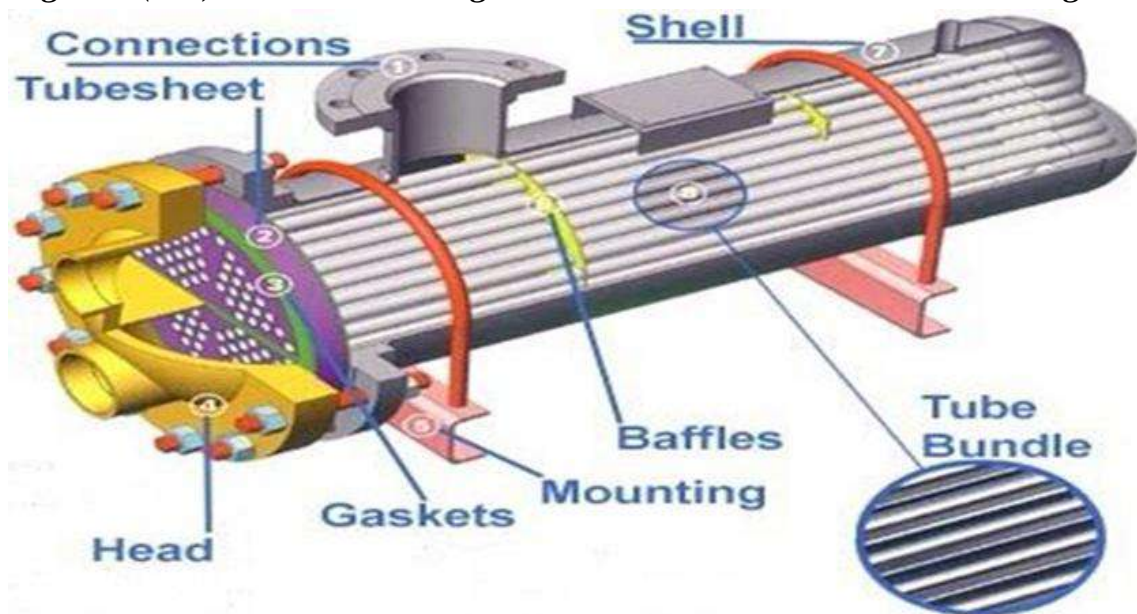
*-1 Single-phase exchangers: They are heat exchangers in which heat exchange takes place between two fluids (with the same phase) and there is no change in the state (phase) of one of these fluids.*

*2-Multiphase exchangers: They are heat exchangers in which heat exchange takes place with a change in the state (phase) of one of these fluids, for example, one of them evaporates or condenses during heat exchange, as shown in the figure (1-1), (1-2) , (1-3) [2].*

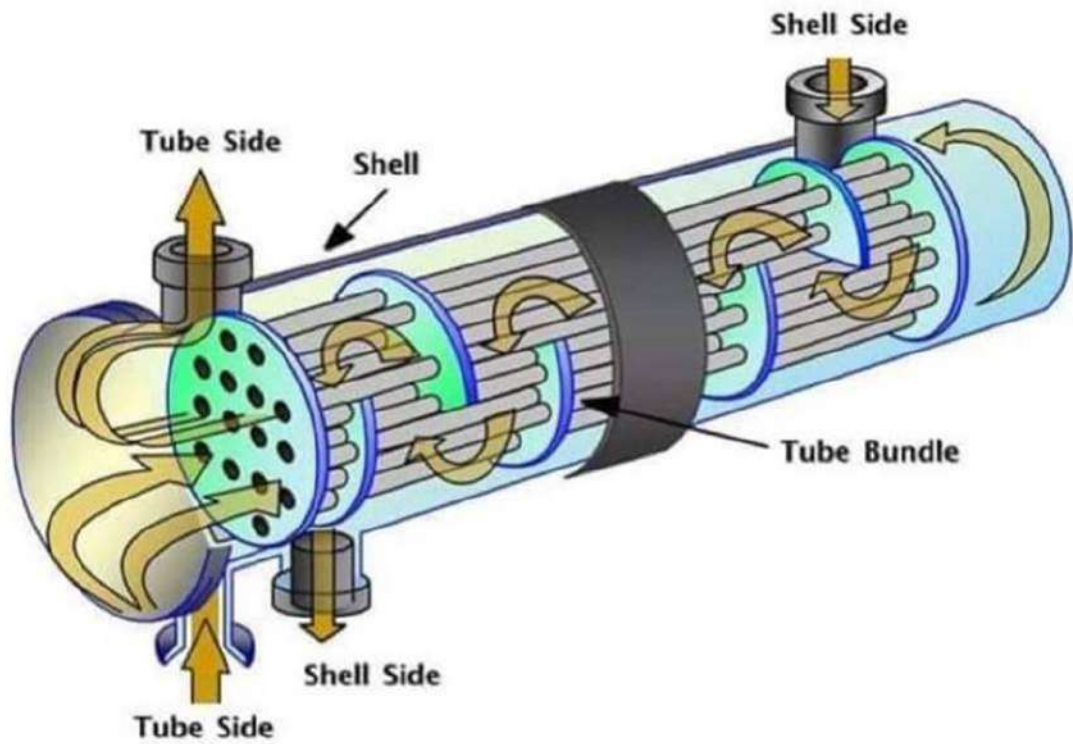
### **Straight-tube heat exchanger (one pass tube-side)**



*Figure (1-1) schematic diagram shell and tube heat exchanger*



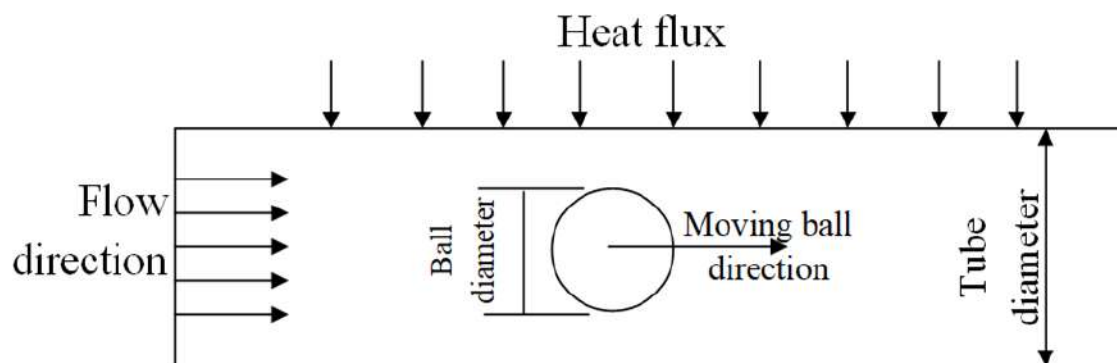
*Figure (1-2) iso-view shell and tube heat exchanger*



*Figure (1-3) two passes water-cooled heat exchangers*

### (1-3) methodology

*In this project, moving balls were used inside the tube, as shown in the figure (1-4), the case is simulated numerically and optimum dimensions are found by the ANSYS 19 R1 program. Two parameters were changed at range of Reynolds number (2500- 15000). First parameter is the diameter of the ball insert and the maximum amount of increase in improving thermal performance was calculated*



*Figure (1-4) schematic diagram of the case study*

*The non-dimensional setting was calculated to correctly compare the prototype with the production unit, as the Reynolds number, the Nusselt number, the Prandtl number and the thermal performance factor was calculated by the method of equal pumping before and after adding the moving balls and comparing them with a variable setting For Reynolds number. The second parameter is the velocity of the moving ball. After that, the data and results obtained from the simulation process are collected and compared with the literature studies .*

#### *(Aim of the current study*

- 1 Investigation numerically the moving ball inside tube by ANSYS FLUENT*
- 2- Enhancement the heat performance of the heat exchanger*

# CHAPTER TWO

## LITERATURE SURVE

## 2.1-Introduction

*The amount of heat transferred from the tube to space. We are working on in this project is the amount of heat transfer from the smooth cylindrical tubes by placing moving balls inside the tubes that increase the turbulence intensity of the fluid entering the tube, and thus an increase in heat exchange*

## **-2.2Previous research**

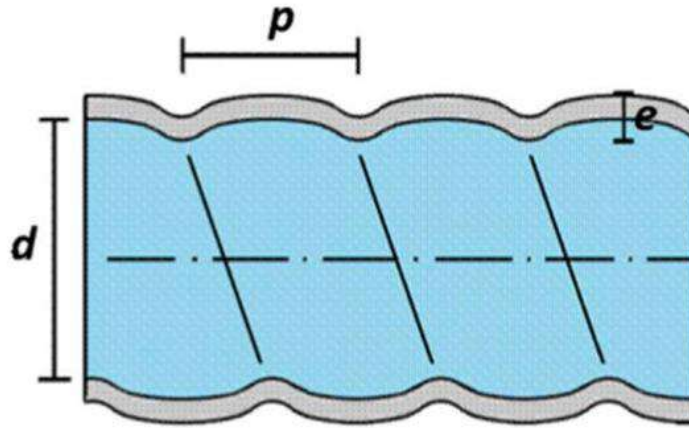
*There are some important studies that increase the transfer of heat from the liquid inside the tube to the outer space.*

*F. Andradaet. al.. 2019 [3] investigated the operating conditions of the pre-heater zone of an automotive vehicle waste heat recover heat exchanger occurs in, or close to, the transitional flow regime. For such an application the use of corrugated tubes in a cross flow tube heat exchanger is of particular interest. However, not much work has been done in the transitional flow regime in corrugated tubes where the internal flow changes from laminar to turbulent with heat transfer at high heat fluxes.*

*Therefore, more data is needed. Hence, the main purpose of this work is the characterization of the heat transfer and pressure drop of internal flow in corrugated tubes. To this end an experimental setup was developed and validated for the study of a smooth tube and two corrugated tubes that have an internal diameter of 5.75 mm and a heating length of 0.38 m. The experiments were conducted in laminar, transitional and turbulent regime, with Reynolds numbers in the range from 429 to 6212, under both adiabatic and adiabatic flow conditions. The heat flux imposed on the tube wall ranged from 5.5 kW/m<sup>2</sup> to 21.1 kW/m<sup>2</sup>. The flow was hydro-dynamically fully developed at test section inlet. The results revealed that the friction factor of the corrugated tubes presented a smoother transition than in the case of the smooth tube, being the adiabatic and adiabatic friction factor for the corrugated tubes quite similar from laminar to turbulent regime .*



*The corrugated tubes are more effective under transitional flow regime. The highest heat transfer augmentation occurs at  $Re = 2000$ , specifically, the Nusselt number augmentation ( $Nu/Nu_s$ ) increases up to 4.7 for the corrugated tube with helical pitch  $p = 6$  mm and up to 3.8 for the corrugated tube with  $p = 12$  mm.*

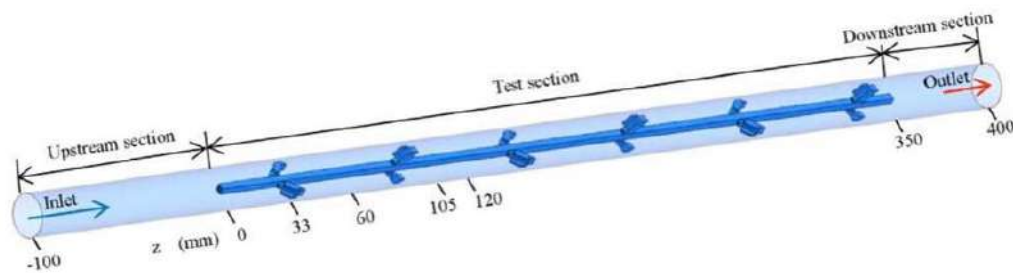


*Fig.(2-1). longitudinal section of a corrugated tube*

*weiliu et. al. 2016 [4] studied the heat transfer and flow performance in turbulent flow of the tube fitted with the drainage inserts are investigated. The results show that the new-type insert can lead the fluid at the core to*

*the tube wall, strengthening the mixing of cold and hot fluid. And the insert also generates the vortex to make perturbation in the fluid domain. The experiment investigates the influence of pitch ratio on the Nusselt number and friction factor. The Nusselt number and friction factor both increase with the decrease of pitch ratio. And the pitch ratio of 3.3 is recommended for the insert. Some numerical results validated by the experimental results are also shown in the study to analyze the influence of slant angle on heat transfer and flow performance. The results indicate that  $45^\circ$  is suggested as the best slant angle for the insert. The numerical results of  $Nu/Nu_{p.f/fg}$  and PEC range from 1.82 to 1.94, 6.70 to 7.15 and 0.95 to 1.04, respectively, for the insert with the slant angle of  $45^\circ$  and the pitch ratio of 3.3. The results show that the*

*insert is of good performance and the correlations of  $Nu$  and  $f$  are developed in the study.*



**Fig.(2-2).schematic diagram of the computation domin**

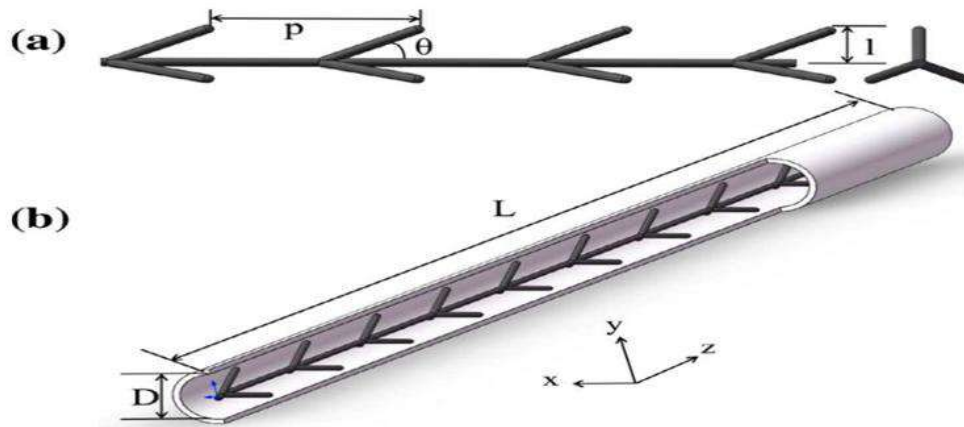
*Peng Liu et. al. 2015 [5] conducted a numerical study on the characteristics of heat transfer and friction factor of laminar water flow in a circular tube fitted with a new tube insert (central slant rod inserts) is presented. Results reveal that the new inserts can fully disturb the core flow in the tube and create multiple longitudinal vortex structures, which are confirmed to be excellent flow structures for heat transfer enhancement. In addition, we carried out stereoscopic particle image velocimetry (SPIV) measurements in exactly the same facility as that of the numerical study to validate the accuracy of our numerical study.*

*The results show good agreement between the experiment and numerical simulation. Following this, the effects of three parameters of central slant rods, including the slant angle. pitch and length in the radial direction are discussed numerically. The computational results indicate that a moderate slant angle ranging from 20 to 30 can obtain the largest Nusselt number; however, the effect of slant angle on the friction factor is quite limited. The Nusselt number and friction factor both increase with a decrease in rod pitch and an increase in rod length in the radial direction. The simulation results show that the Nusselt number and friction factor are enhanced by 1.81-5.05 times and 2.49-6.92 times, respectively, to that of a plain tube .*



*The performance ratio  $R3$  values are in the range of 1.74-460. Empirical formulas for  $Nu$  and  $f$  are obtained based on calculation results .*

*All results indicate that the central slant rod is a promising high-performance tube insert for heat transfer enhancement in practical.*

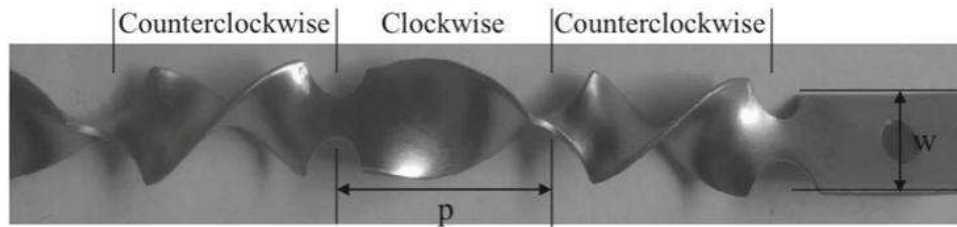


*Figure (2-3) A-geometry of the central slant rod insert, and*

*B-circular tube fitted with central slant rod inserts.*

*Changzhong Man, et. al..2016 [6] In this paper , experimental investigation on heat transfer and friction characteristics of dual - pipe heat exchanger for single - phase forced convective flow with alternation of clockwise and counterclockwise twisted tape ( ACCT tape ) and typical twisted tape ( TT tape ) inserted in the inner tube has been carried out . And effects of different lengths of twisted tapes on heat transfer enhancement were studied through a circular tube using water as testing fluid in turbulent conditions with a range of Reynolds number between 3000 and 9000. In the dual - pipe heat exchanger , hot water was cooled in the inner tube and cold water was as cooling fluid between the inner tube and the outer tube . The results showed that the ACCT tapes performed better on heat transfer enhancement than the typical twisted tapes and the best effect appeared with the full - length (  $I$  - 2400 mm ) ACCT tape insert in comparison with the twisted tapes of other lengths . The maximum values of PEC ( performance evaluation criteria ) with the full - length ACCT tape insert reached 1.42 in*

*experimental flowing conditions . Empirical correlations for Nusselt number and friction factors were established and found to fit the experimental data with a deviation within 8 % © 2016 Elsevier Ltd. All rights reserved*



**Figure (2-4). the ACCT tape**

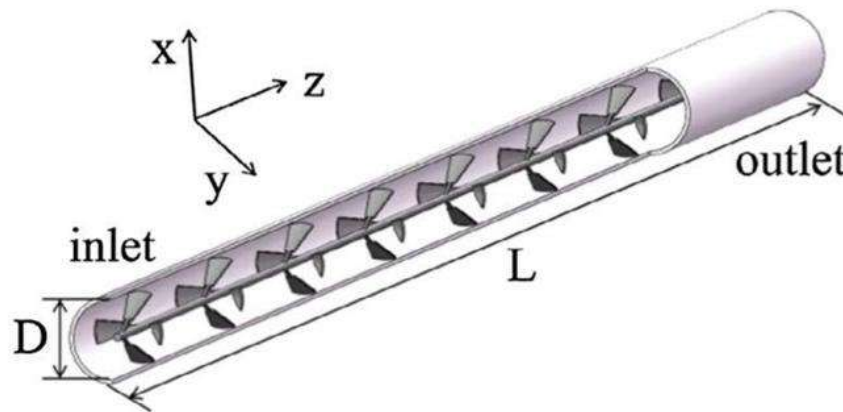
*Peng Liuet. at.. 2017 [7] investigated a novel tube insert (bidirectional conical strip inserts) is proposed, and the heat transfer performance and flow characteristics of this insert are studied numerically. Effects of three geometric parameters (numbers of bidirectional conical strip, central angle ( $\alpha$ ) and pitch ratio ( $P - p/D$ ) are also investigated .*

*The results indicate that cold fluid in the core region and the hot fluid near the tube wall are rapidly exchanged as the fluid flows through the bidirectional conical strip, and multiple longitudinal swirling flows are formed downstream of the bidirectional conical strip. Therefore, the heat transfer (the Nusselt number) is significantly enhanced by 2.35-9.85 times compared to the smooth tube. Moreover, because of the cooperation between the forward and the reverse conical strips, the formation of the dead zone and eddy on the back of the conical strips is inhibited.*

*Thus, the increase in flow resistance is smaller than many other published works, as the friction factor is enhanced to 2.37-21.18 times of the smooth tube. The overall heat transfer performance (PEC value) is located in range of 1.75-3.93. Both the Nusselt number and friction*

*factor increase with the increasing numbers of bidirectional conical strip, central angle and the decreasing pitch ratio .*

*However, the friction factor is more sensitive to geo- metric parameters, so the maximum overall heat transfer performance (PEC value) is obtained at moderate geometric parameters ( $n = 3$ ,  $\alpha = 40^\circ$  and  $P = 3$ ). In addition, Correlation formulas for Nusselt number and friction factor are derived.*



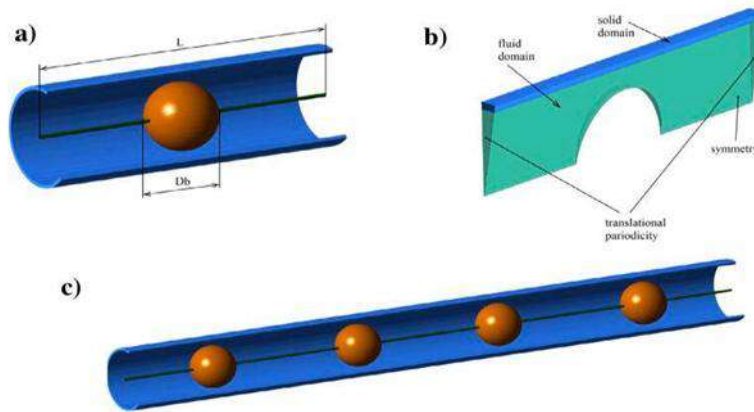
*Figure (2-5).geometry model of bidirectional conical strip inserts, and the*

*schematic diagram of a tube with bidirectional conical strip inserts .*

*poitrboguslaw et. al..2016 [8] studied numerically a thermo-hydraulic characteristics in a circular tube with ball turbulators. The paper contains an analysis of heat transfer performance of the tested turbulators, taking into account the criterion of the same pumping power. The studies were carried out for the Re number range of 10,000-300,000, for balls with different diameters ( $D_b = 7, 10, 13, 16$  and  $19$  mm) and a variable longitudinal distance between the balls ( $L = 20, 24, 28, 32, 36, 40, 48, 60$  and  $85$  mm ).(*

*The results revealed that the highest gain in the Nu number and flow resistance was observed for inserts made of balls with the largest diameters but the maximum values of the thermal performance factor reaching 1.22, were observed for turbulators made of the smallest balls with a diameter of 7 mm.*

*It was demonstrated that for balls of the same diameter the highest value of the factor occurred for the greatest longitudinal distance. Moreover, the paper presents characteristics (Re) for all abovementioned parameters and geometric configurations of the insert.*

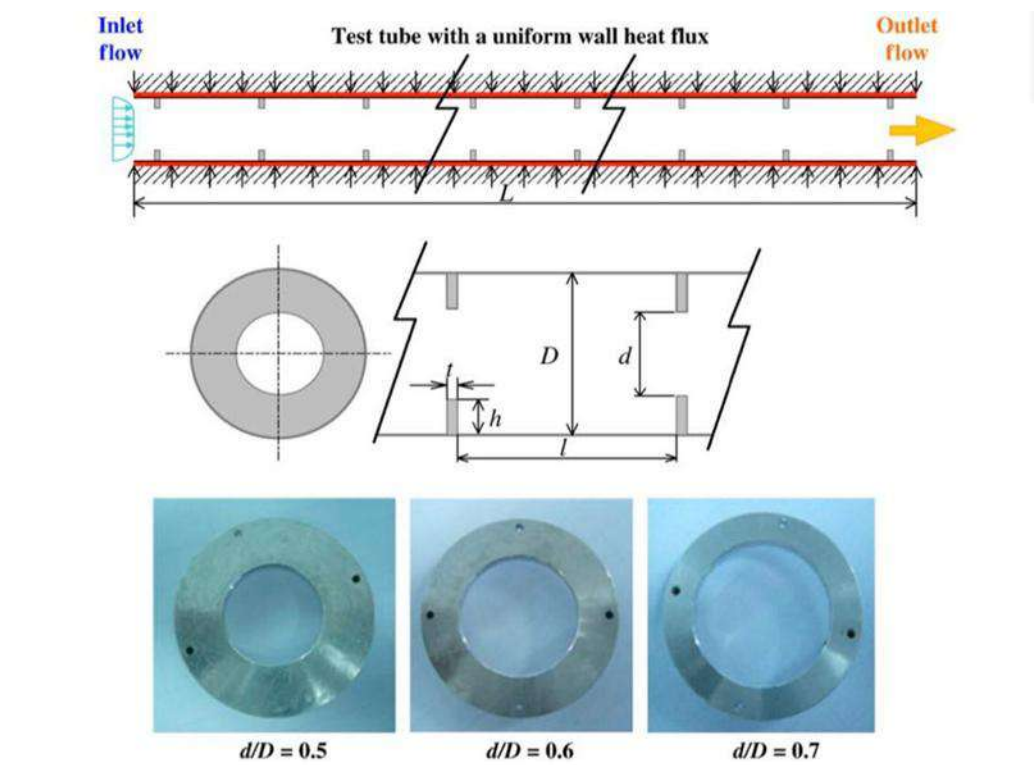


**Figure (2-6). repeatable segment of the insert:**

*a) 3D view, b) computational domain, c) several elements of insert*

*V. Kongkai paiboonet. al..2010 [9] conducted the effect of the circular-ring turbulator (CRT) on the heat transfer and fluid friction characteristics in a heat exchanger tube. The experiments were conducted by insertion of CRTs with various geometries, including three different diameter ratios ( $DR=d/D=0.5, 0.6$  and  $0.7$ ) and three different pitch ratios ( $PR= p/D=6, 8$  and  $12$ ). During the test air at  $27^{\circ}\text{C}$  was passed through the test tube which was controlled under uniform wall heat flux condition. The Reynolds number was varied from 4000 to 20,000 .*

*According to the experimental results, heat transfer rates in 57% to 195% compared to that in the plain tube, depending upon operating conditions. In addition, the results also reveal the CRT with the smallest pitch and diameter ratios offers the highest heat transfer rate in accompany with the largest pressure loss. tube fitted with CRTs are augmented around*

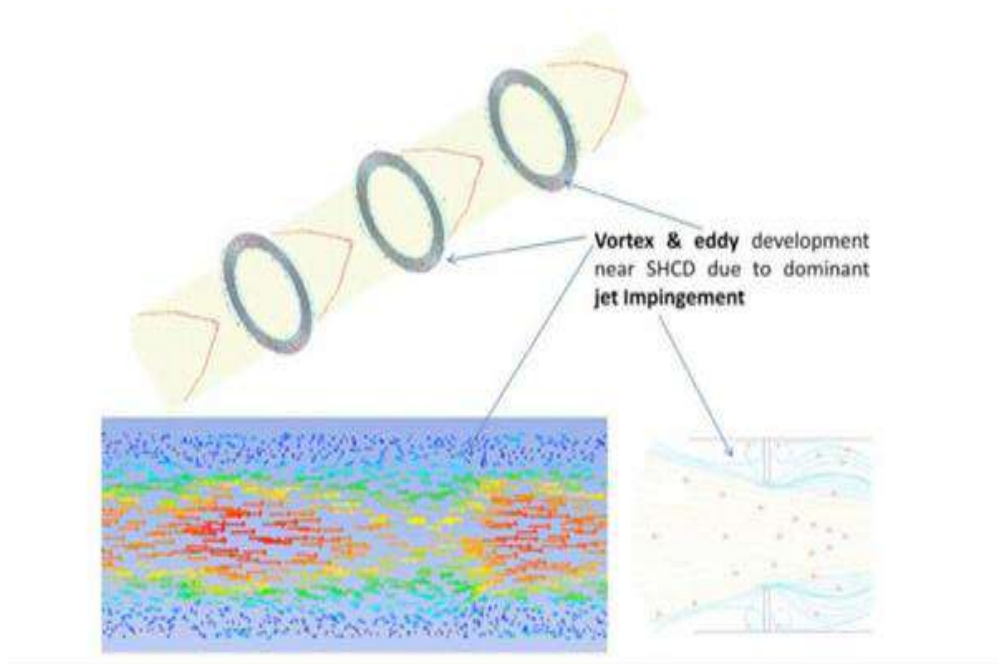


**Figure (2-7). test section with circular-ring turbulators (crt.)**

*Alok Kumar et al. 2015 [10] studied Enhancement in heat transfer by generating turbulence in the fluid stream inside the heat exchanger tube has become an innovative area of the research for the researchers. Hence, many techniques have been investigated and adopted on enhancement of heat transfer rate to reduce the size and cost of the heat exchangers. In the present study the effect of solid hollow circular disk (SHCD) turbulators on heat transfer, friction factor and thermal performance factor the heat exchanger is evaluated through experimentation. The different parameters used for the experimentation include fixed thickness ratio ( $t / D$ ) of SHCD, i.e. 0.0075, diameter ratios ( $d / D = 0.6, 0.7$  and  $0.8$ ) and pitch ratios ( $1 / D = 1, 2, 3$  and  $4$ ). The experiments are conducted in the range of Reynolds number from 6500 to 23,000. The test setup comprises of the test section (1.4 m long) with a hydraulic diameter ( $D$ ) of 68 mm. Constant heat flux is provided in the test section with the help of a variable voltage transformer and coiled wire heater. On the basis of experimental investigation, there is around 4.45 times enhancement in*



*heat transfer in case of  $PR = 1$  and  $DR = 0.6$ , and around 1.4 times enhancement in thermal performance factor for  $PR = 1$  and  $DR = 0.8$  when compared to smooth tube heat exchangers.*



*Figure (2-8).velocity vector contour and flow behavior*

### ***-2.3scope of the present work***

*It is also clear in previous experiments of some scientists that any change in the shape of the tube makes a significant difference in the amount of heat transferred to and from the tube. As it is when we mix the liquid (water) inside the tube by placing obstacles that cause disturbance of the fluid flow or mixing the fluid through a cylinder containing feathers, this all produces fluid disturbance and*

*an increase in the amount of heat transferred to and from the tube*

# CHAPTER THREE

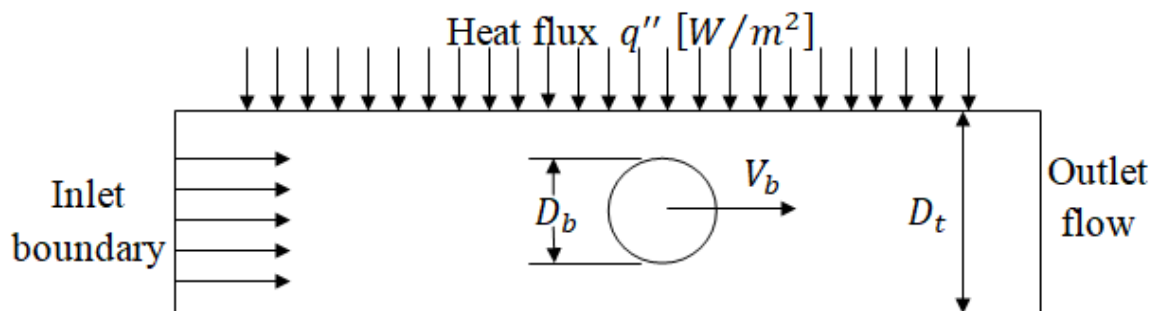
## THEORETICAL INVESTIGATION

### 3-1 Introduction

*Set up and solve a turbulent fluid-flow and heat-transfer problem in a tube numerically. It is designed to introduce you to the ANSYS Workbench tool set using a simple geometry. Guided by the steps that follow, creation the elbow geometry and the corresponding computational mesh using the geometry and meshing tools within ANSYS Workbench. ANSYS Fluent is used to set up and solve the CFD problem, then visualize the results in both ANSYS Fluent and in the CFD-Post processing tool.*

### 3-2 Problem Specification

*Simulation is done by software (Fluent 19R1) of the CFD process in which the solution is dependent on finite volume method. Where the simulation of this research is by applying a constant heat flux on the wall of the tube as shown in the figure (3-1). And one of the followed hypotheses is that the velocity of the flow is equal to zero at the walls and also fully developed flow with a temperature of the inlet water is constant. The range used for Reynolds number is from 50,000 to 350,000. The criteria of convergence is Prepared on ( $10^{-6}$ ) for all variables. It is also hypotheses that the thickness of the tube has been neglected, and this means that equation (3-1) can be used to extract the local Nusselt number for each point of the tube for a given and fixed length, after which the average is calculated for the Nusselt number of the entire tube.*



*Figure (3-1) schematic diagram of the boundary of the case study*



*The following equations were used to calculate the number of Nusselt, the equation (3-1) through the numerical calculation of a certain number of points on the tube, and after that the mean value was extracted for the number of Nusselt in the case of balls inside the tube. Equation (3-2) is an empirical equation of Nusselt number applied on a smooth tube without an insert of balls from Dittus-Boelter equation [11],[12]:*

$$Nu = \frac{h.D_t}{\lambda} \dots\dots\dots (3-1)$$

$$Nu)_s = 0.023 (Re)^{0.8} . (Pr)^{0.4} \dots\dots\dots (3-2)$$

*Where Reynolds number (Re) is proportional to the average velocity (u) and the diameter of the tube  $D_t$ :*

$$Re = \frac{\rho.u.D_t}{\mu} \dots\dots\dots (3-3)$$

*Numerical calculation of the friction factor was calculated when the balls inside tube from Darcy-Weisbach equation:*

$$f = \frac{2.\Delta p.D_t}{L.\rho.u^2} \dots\dots\dots (3-4)$$

$$f_s = 0.3164 (Re)^{-0.25} \dots\dots\dots (3-5)$$

*The equation (5) is empirical formula for smooth tube found by Blasius solution.*

$$\eta = \frac{Nu/Nu)_s}{(f/f_s)^{1/3}} \dots\dots\dots (3-6)$$

*The equation (3-6) is thermal performance factor which represented a comparison between tube with insertion of balls and smooth tube; it is based on equal surface area of the heat transfer at equal pumping power. The k–w SST (Shear Stress Transport) turbulence model was used. It is one of the most commonly used models in CFD applications due to much better mapping of fluid-thermal phenomena for calculation of cases with a stream separation as such is the nature of the flow of the inserts under investigation than the standard k–e model*

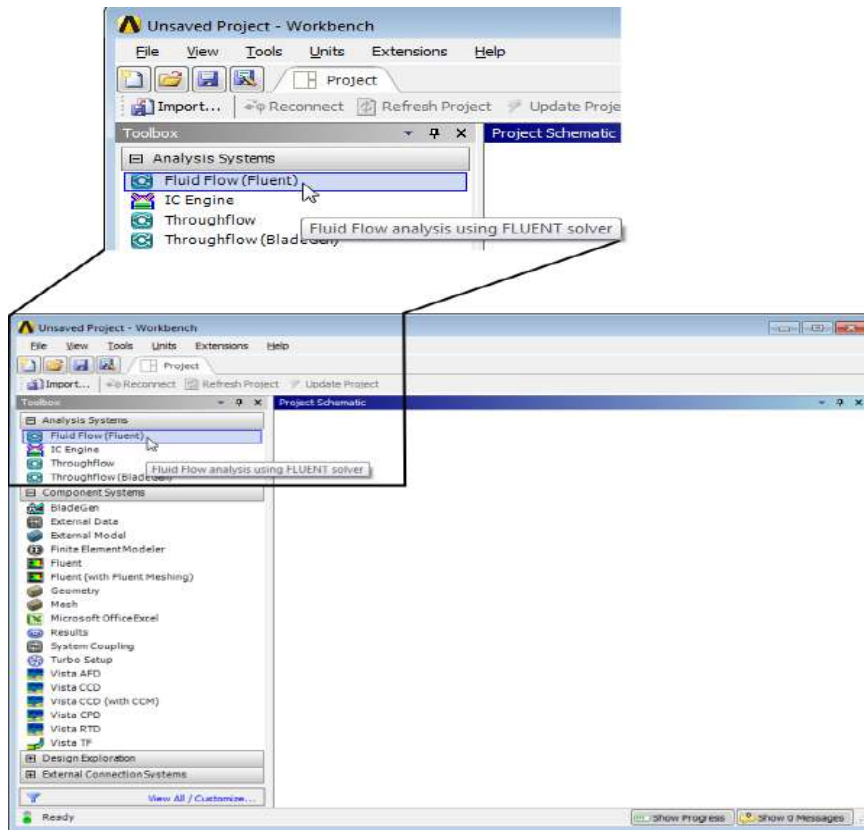
*because this kind of flow structure is caused by the tested insert. The main feature of the SST model is its ability to take into account a viscous sublayer by applying the  $k$ - $\omega$  model near the wall and to use the standard  $k$ - $\epsilon$  model in the turbulent core. For the choice of a suitable model for calculation, a special function (called a blending function) implemented in the SST model [13] is responsible.*

### **3-3 Simulation procedure**

- 1. Launch ANSYS Workbench.*
- 2. Create a Fluent fluid flow analysis system in ANSYS Workbench.*
- 3. Create the tube geometry using ANSYS DesignModeler.*
- 4. Create the computational mesh for the geometry using ANSYS Meshing.*
- 5. Set up the CFD simulation in ANSYS Fluent, which includes:*
  - a. Setting material properties and boundary conditions for a turbulent forced-convection problem.*
  - b. Initiating the calculation with residual plotting.*
  - c. Calculating a solution using the pressure-based solver.*
  - d. Examining the flow and temperature fields using ANSYS*

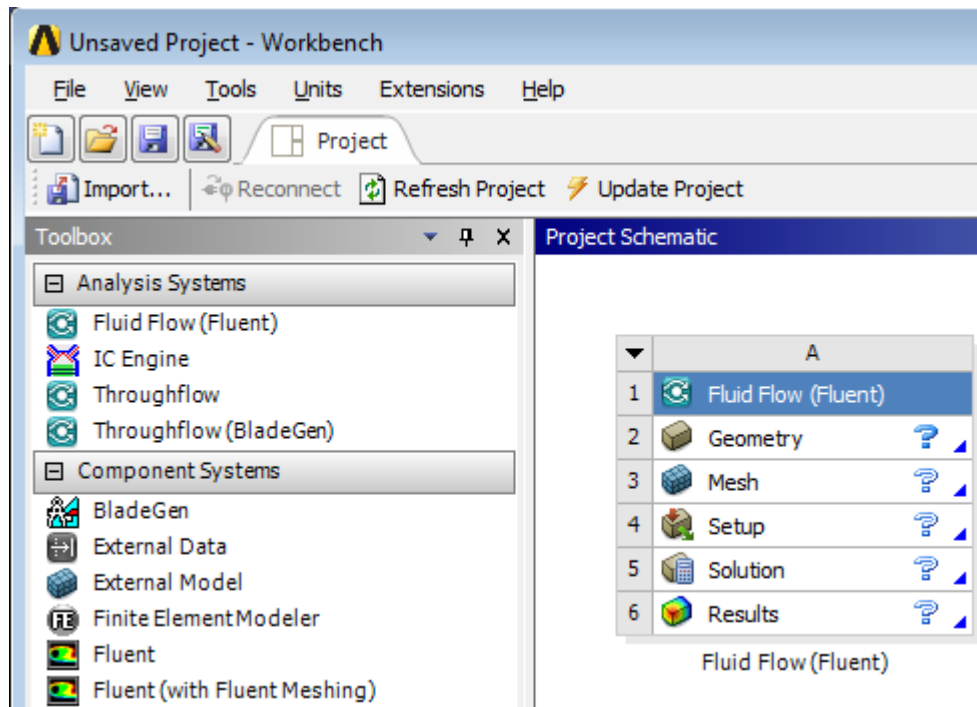
#### **3-3-1 Fluent and CFD-Postprocessing**

*In this step, start ANSYS Workbench, create a new fluent fluid flow analysis system, and then review the list of files generated by ANSYS Workbench.*



**Figure (3-2) Start ansys19Program session**

- 1- From the Windows Start menu, select Start > All Programs > ANSYS 19> Workbench 16.0 to start anew ANSYS Workbench session. This displays the ANSYS Workbench application window, which has the Toolbox on the left and the Project Schematic to its right. Various supported applications are listed in the Toolbox and the components of the analysis system will be displayed in the Project Schematic.
- 2- Create a new fluent fluid flow analysis system by double-clicking the Fluid Flow (Fluent) option under Analysis Systems in the Toolbox.



**Figure (3-3) Creation a new fluid flow analysis system**

### **3- Name the analysis.**

**a- Double-click the Fluid Flow (Fluent) label underneath the analysis system**

**b. Enter tube for the name of the analysis system.**

### **4. Save the project.**

**a. Select the Save option under the File menu in ANSYS Workbench.**

**File → Save**

**This displays the Save As dialog box, where you can browse to your working folder and enter a specific name for the ANSYS Workbench project.**

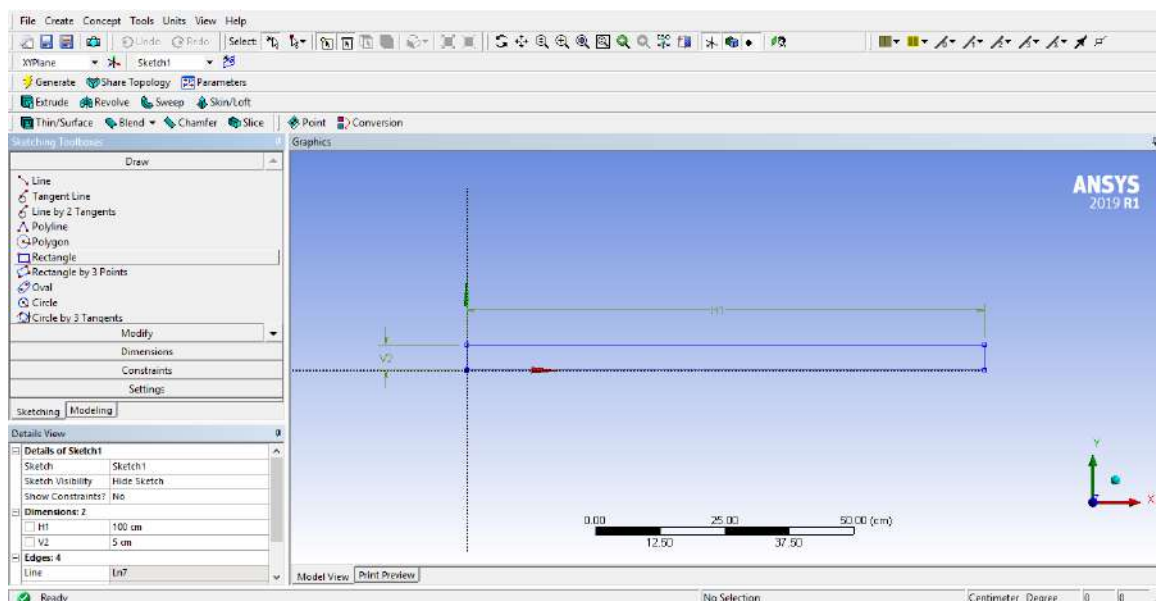
**b. In your working directory, enter tube-workbench as the project File name and click the Save button to save the project. ANSYS Workbench**

*saves the project with a “.wbpj” extension and also saves supporting files for the project.*

### 3-3-2 Creating the Geometry

*For the geometry of your fluid flow analysis, you can create geometry in ANSYS DesignModeler, or import the appropriate geometry file. In this step, you will create the geometry in ANSYS DesignModeler, and then review the list of files generated by ANSYS Workbench.*

#### 1. Start ANSYS Design Modeler



**Figure (3-4) Start ANSYS Design Modeler**

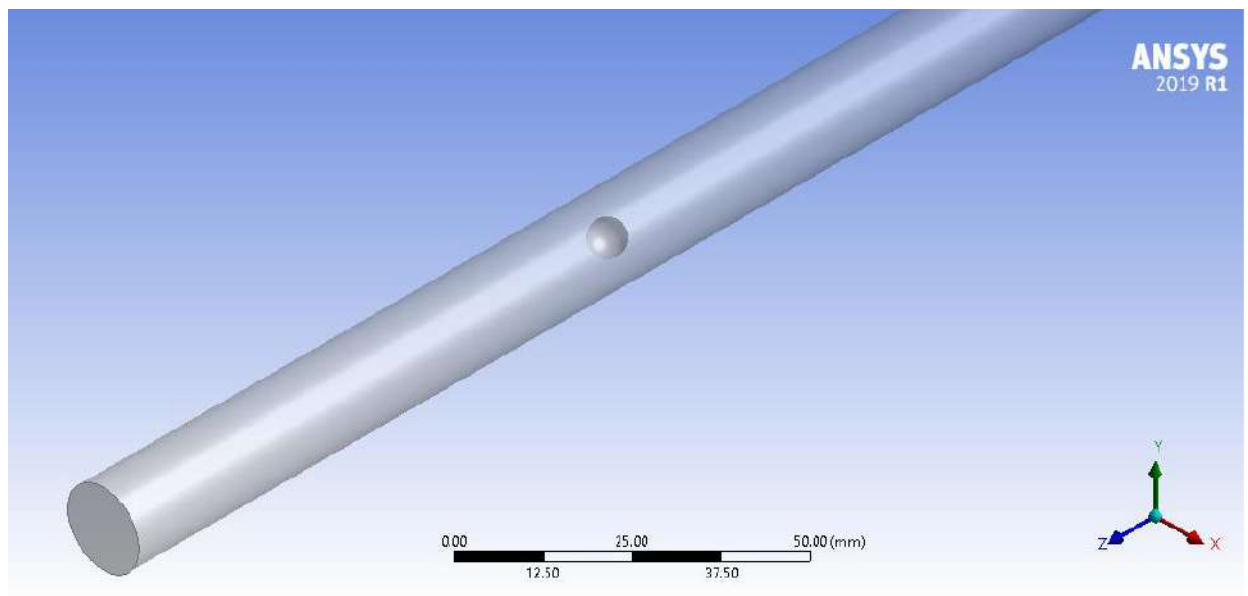
#### 2. Set the units in ANSYS Design Modeler.

*When ANSYS Design Modeler first appears, you should select desired system of length units to work from. For the purposes of this tutorial*

*(where you will create the geometry in millimeters and perform the CFD analysis using SI units) set the units to Millimeter. Units→ Millimeter*

### **3. Create the geometry.**

*ANSYS Design Modeler provides various geometry primitives that can be combined to rapidly create geometries such as this one.*



**Figure (3-5) creation the geometry by ANSYS Design Modeler**

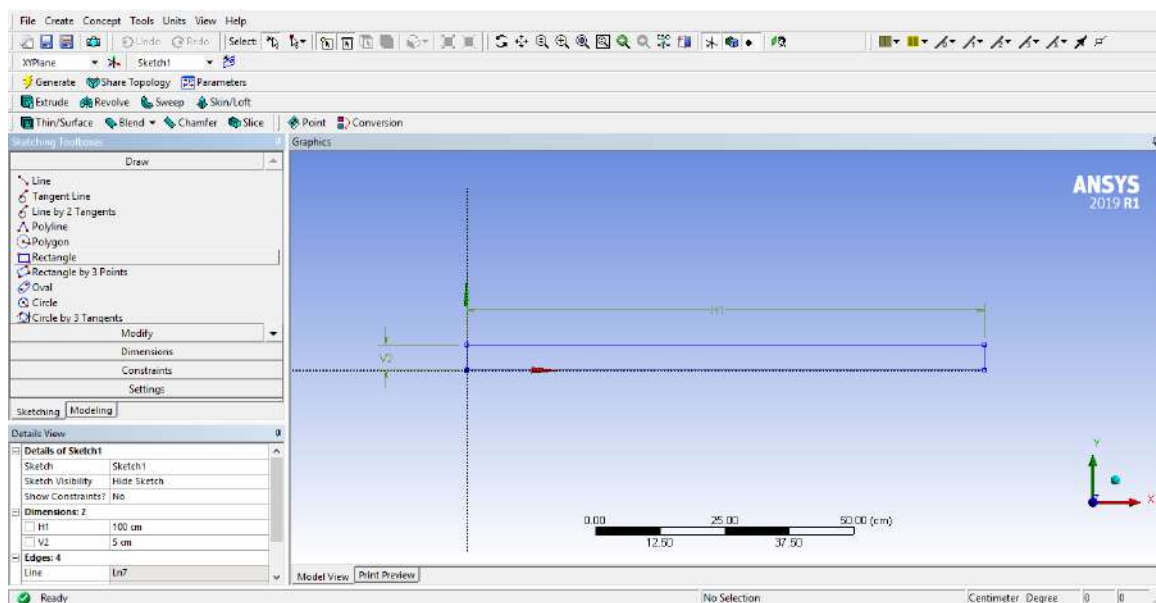
- 4- Close ANSYS Design Modeler by selecting File →Close Design Modeler or by clicking the 'X' icon in the upper right-hand corner. ANSYS Workbench automatically saves the geometry and updates the Project Schematic accordingly. The question mark in the Geometry cell is replaced by a check mark, indicating that there is a geometry now associated with the fluid flow analysis system.**

### 3-3-3 Meshing the Geometry

*Use the ANSYS Meshing application to create a mesh for the CFD analysis, and then review the list of files generated by ANSYS Workbench.*

*Workbench.*

#### 1. Start ANSYS Design Modeler



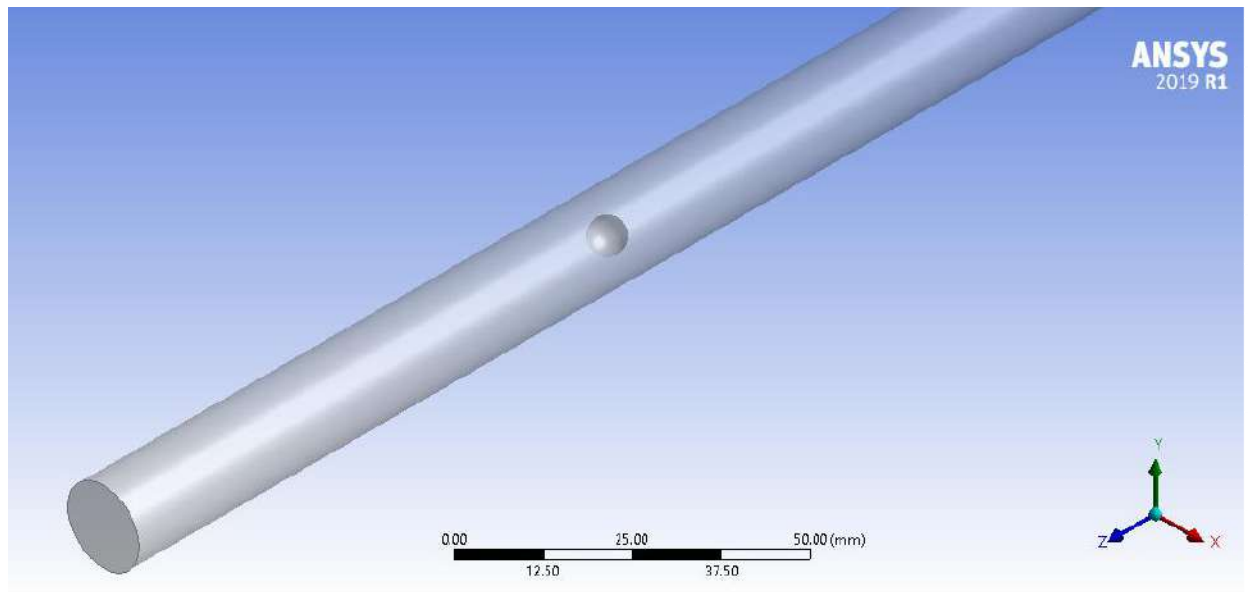
*Figure (3-4) Start ANSYS Design Modeler*

#### 2. Set the units in ANSYS Design Modeler.

*When ANSYS Design Modeler first appears, you should select desired system of length units to work from. For the purposes of this tutorial (where you will create the geometry in millimeters and perform the CFD analysis using SI units) set the units to Millimeter. Units→ Millimeter*

### ***3. Create the geometry.***

***ANSYS Design Modeler provides various geometry primitives that can be combined to rapidly create geometries such as this one.***



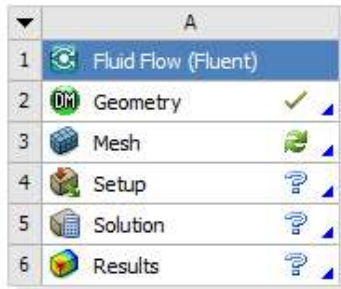
***Figure (3-5) creation the geometry by ANSYS Design Modeler***

- 5- Close ANSYS Design Modeler by selecting File →Close Design Modeler or by clicking the ‘X’ icon in the upper right-hand corner. ANSYS Workbench automatically saves the geometry and updates the Project Schematic accordingly. The question mark in the Geometry cell is replaced by a check mark, indicating that there is a geometry now associated with the fluid flow analysis system.***



### 3-3-3 Meshing the Geometry

*Use the ANSYS Meshing application to create a mesh for the CFD analysis, and then review the list of files generated by ANSYS Workbench.*



*Figure (3-6) creation the mesh for the CFD analysis*

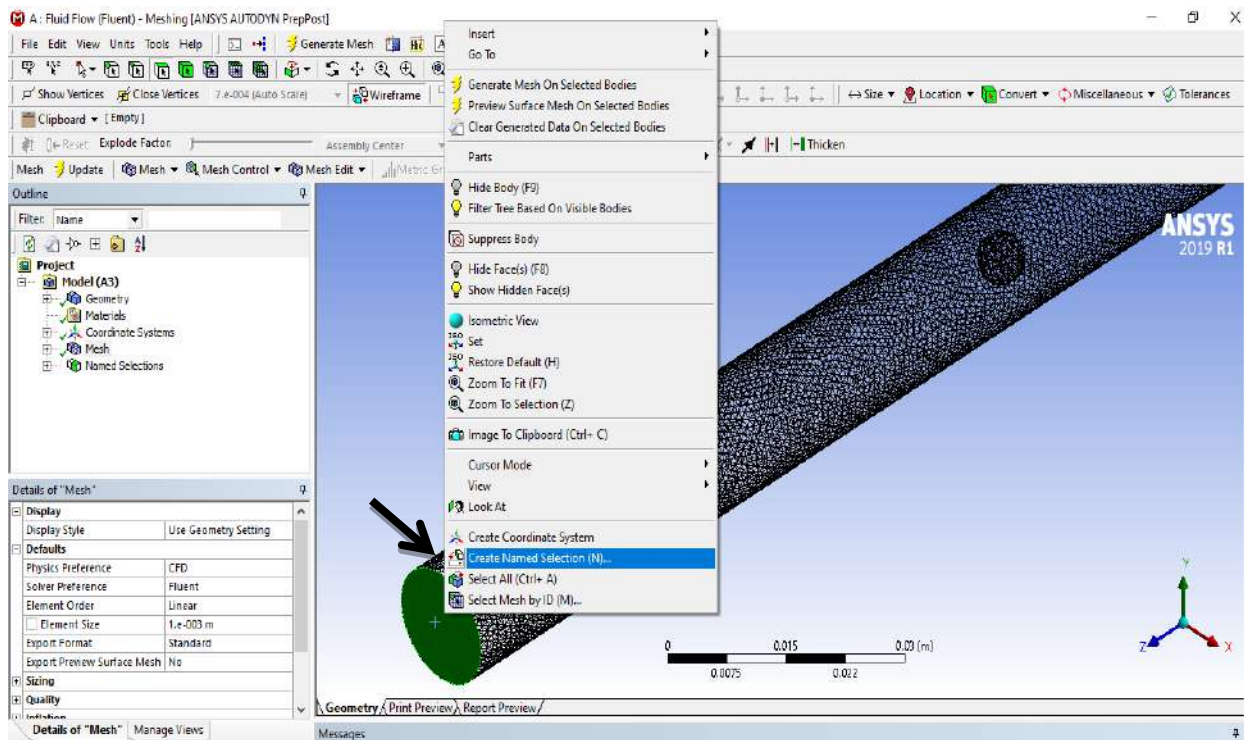
#### *1. Open the ANSYS Meshing application.*

*In the ANSYS Workbench Project Schematic, double-click the Mesh cell in the tube fluid flow analysis system. This displays the ANSYS Meshing application with the tube geometry already loaded. also right-click the Mesh cell to display the context menu where you can select the Edit option.*

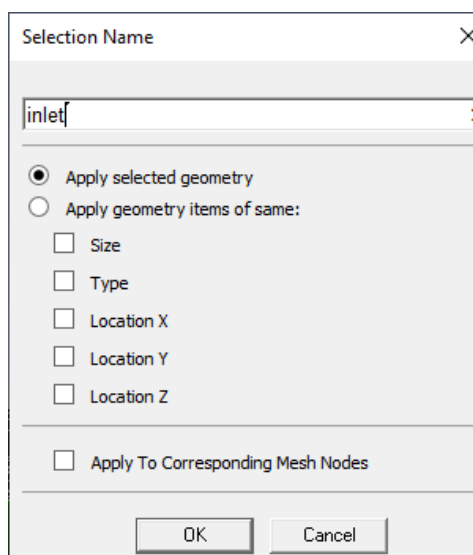
#### *2. Create named selections for the geometry boundaries.*

*In order to simplify the work later on in ANSYS Fluent, should be label each boundary in the geometry by creating named selections for the tube inlets, the outlet. Select the inlet in the geometry that is displayed in the ANSYS Meshing application.*

- a) Right-click and select the Create Named Selection option.*
- b) In the Selection Name dialog box, enter velocity-inlet-large for the name and click OK.*



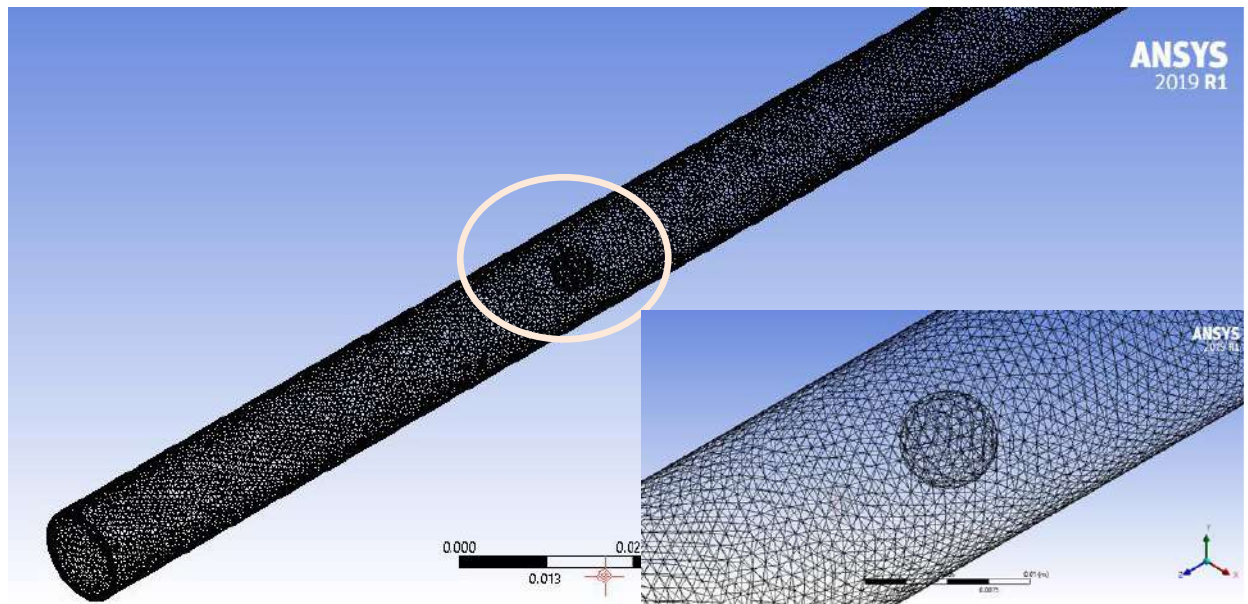
**Figure (3-7) Right-click and select the Create Named Selection option.**



**Figure (3-8) Name the boundary Selected option**

### **3. Generate the mesh.**

**Right-click Mesh in the project Outline tree, and select Update in the context menu.**



**Figure (3-9) mesh generation**

#### **4. Close the ANSYS Meshing application.**

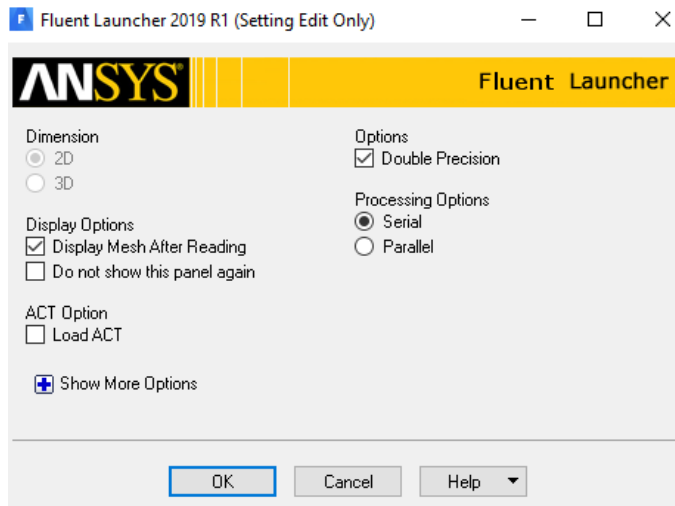
*When closed the ANSYS Meshing application without saving, the ANSYS Workbench automatically saves the mesh and updates the Project Schematic accordingly. The Refresh required icon in the Mesh cell has been replaced by a check mark, indicating that there is a mesh now associated with the fluid flow analysis system.*

### **3-3-4 Setting Up the CFD Simulation**

*In this step, make a setup of CFD analysis using ANSYS Fluent, then review the list of files generated by ANSYS Workbench.*

#### **1. Start ANSYS Fluent.**

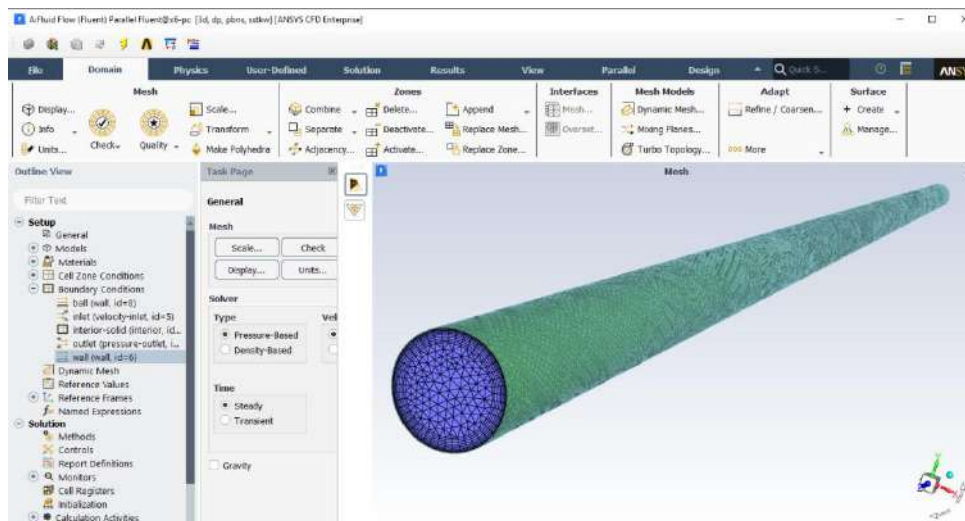
*In the ANSYS Workbench Project Schematic, double-click the Setup cell in the elbow fluid flow analysis system. You can also right-click the Setup cell to display the context menu where you can select the Edit option.*



**Figure (3-10) fluent setup launcher**

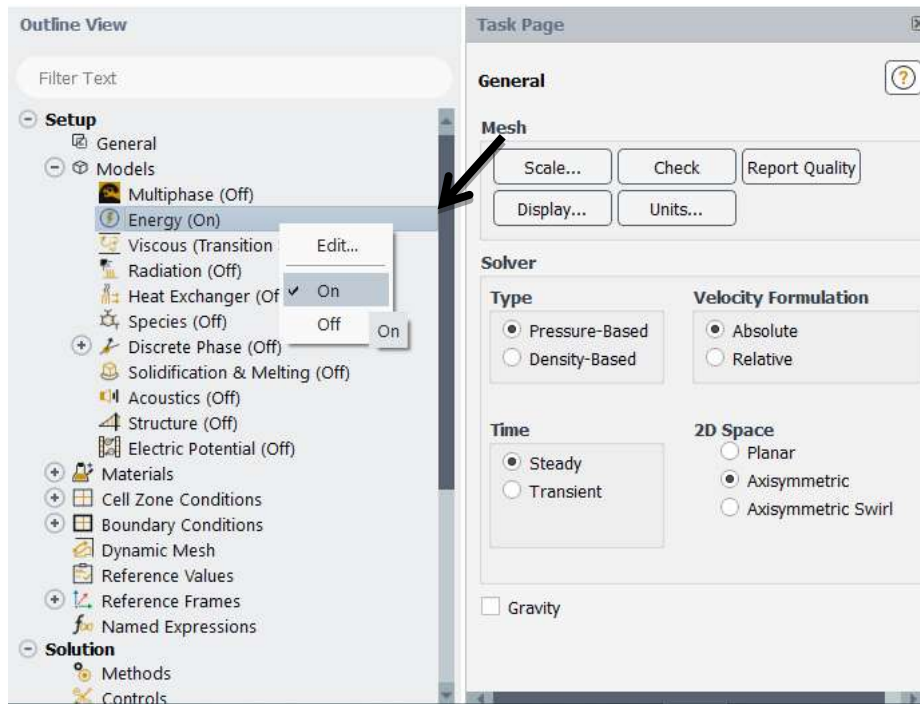
## **2. Set general settings for the CFD analysis.**

**Click General in the tree to open the General task page where you can perform the mesh-related activities and to choose a solver.**

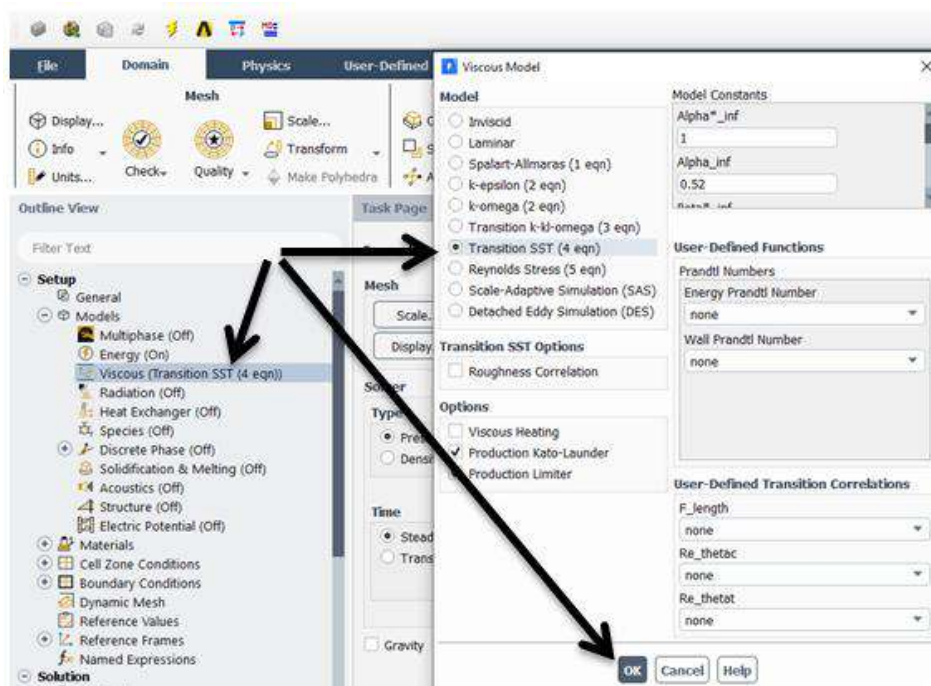


**Figure (3-11) general settings**

## **3. Set up your models for the CFD simulation.**

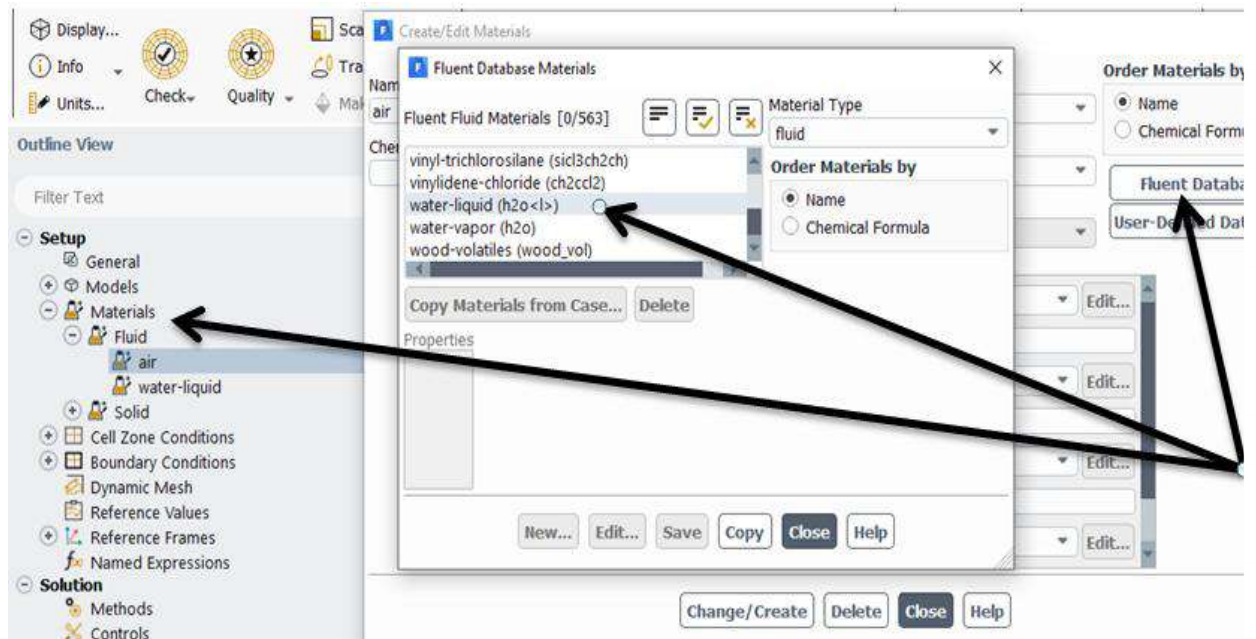


**Figure (3-12) activate the energy equation**

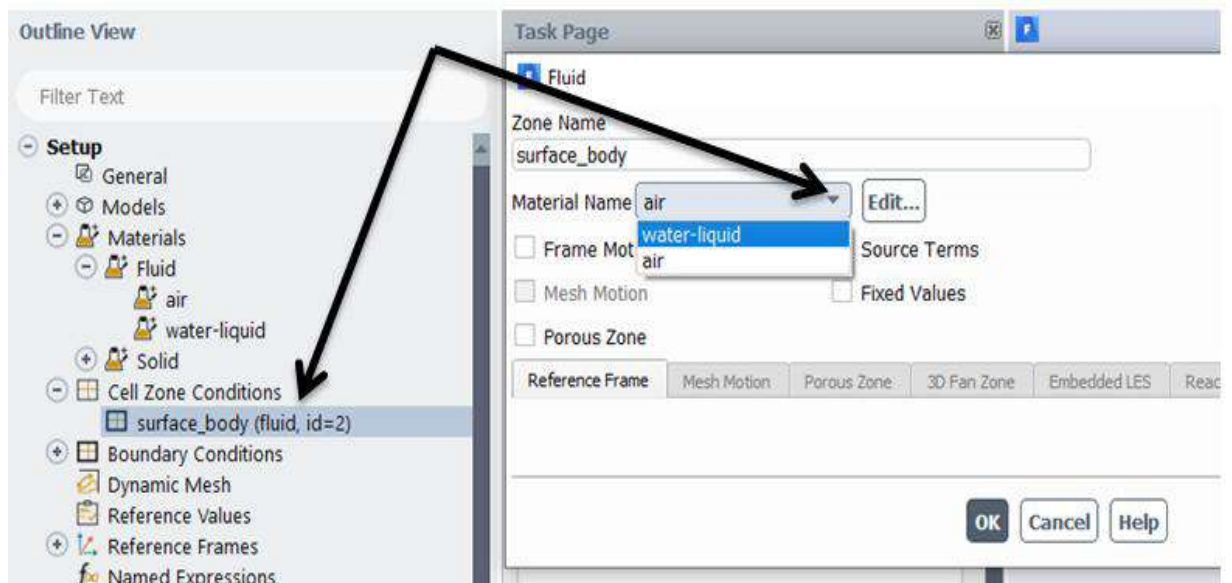


**Figure (3-13) select the turbulence model**

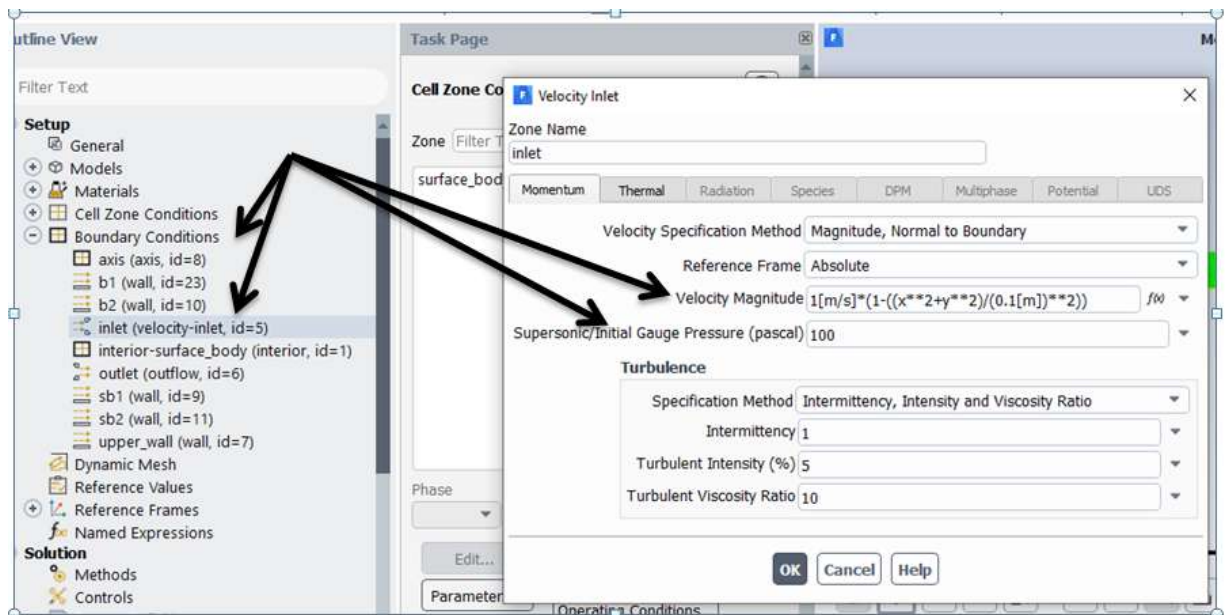




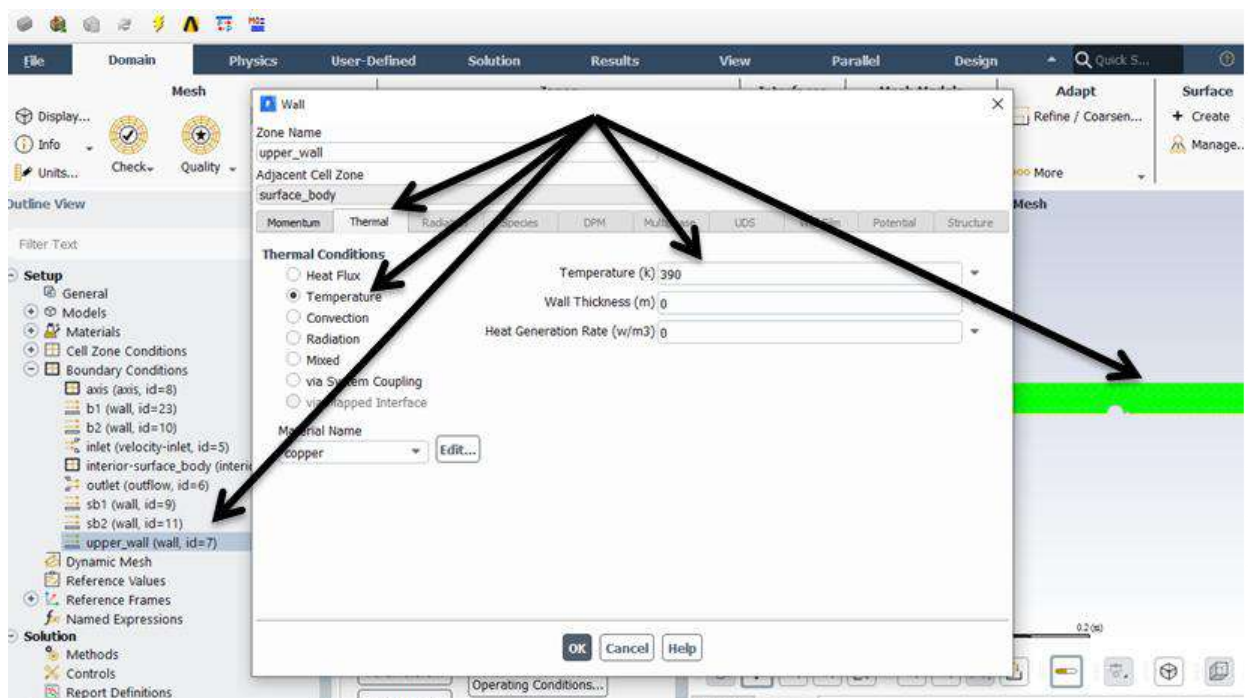
**Figure (3-14) Setup the materials for the case study.**



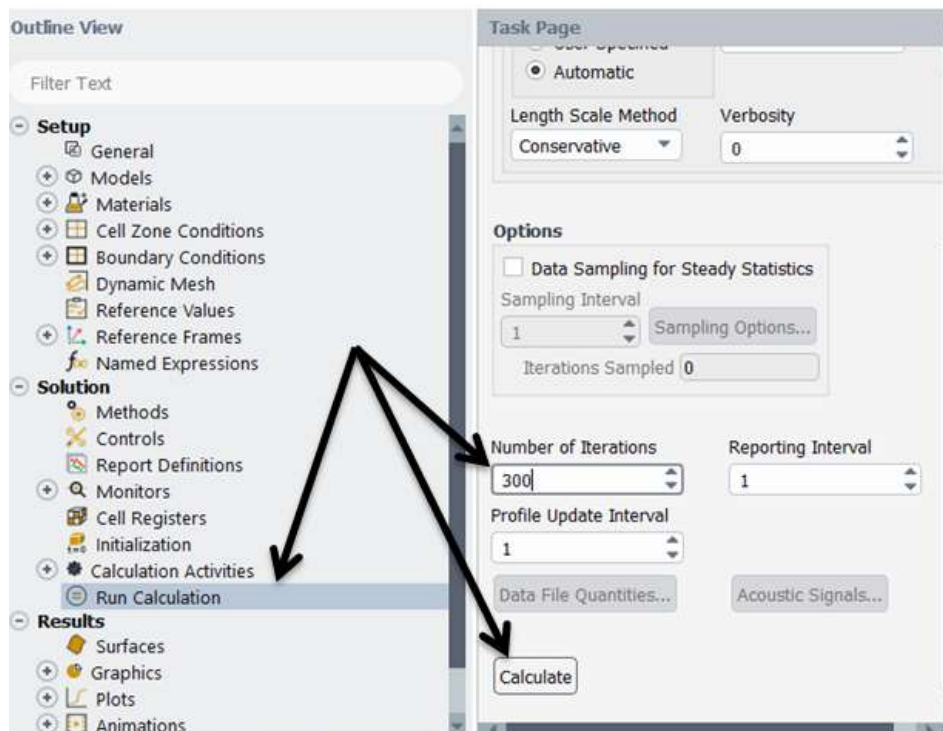
**Figure (3-15) Set up the cell zone conditions for the CFD simulation.**



**Figure (3-15) Set up the boundary conditions for the CFD analysis.**

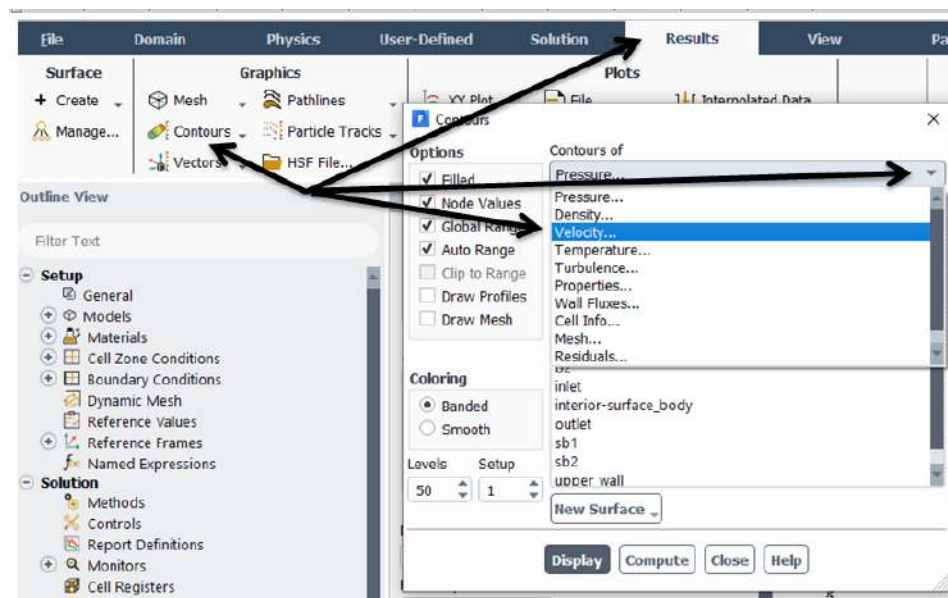


**Figure (3-16) Set up the boundary conditions for the CFD analysis.**



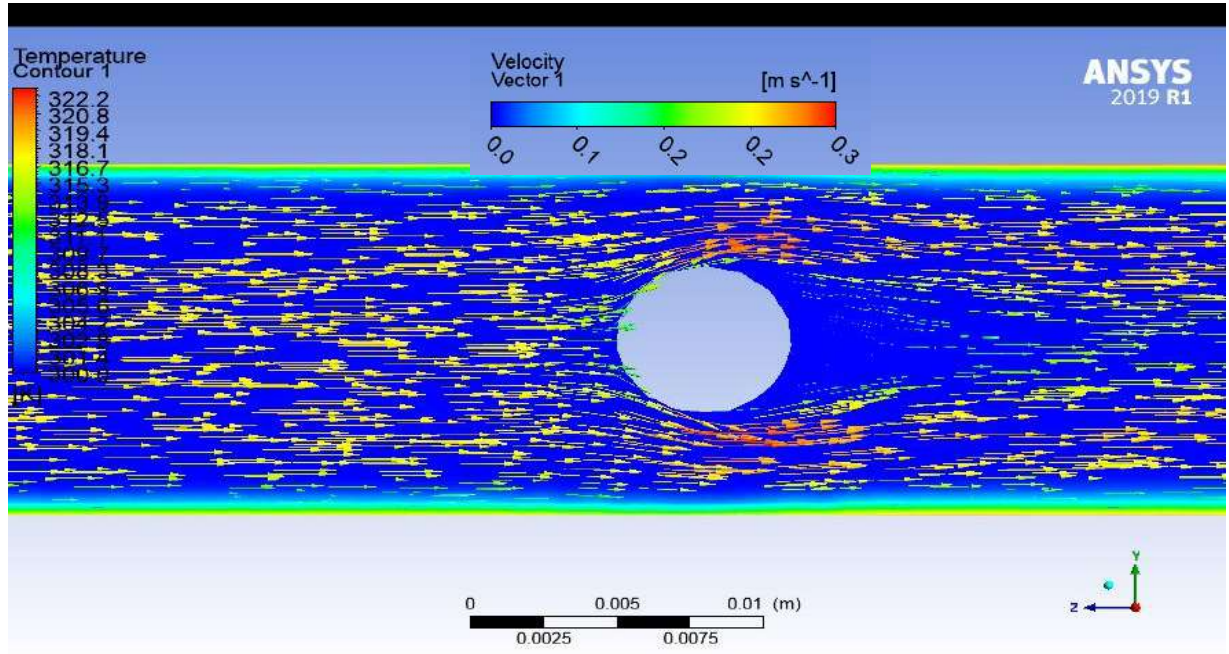
**Figure (3-17) calculate a solution.**

#### **4. Display Results**



**Figure (3-18) Displaying Results**





*Figure (3-19) show the temperature contour and velocity vector of the flow inside the tube over the moving ball*

# CHAPTER FOUR

## RESULTS AND DISCUSSION

## 4-1 introduction

*In the fourth chapter reviewed the results from Simulation code (ANSYS FLUENT R19) and comparing the condition of the smooth tube with the state in which the moving ball at different position with different dimensions to optimize the best thermal performance factor. And also discuss the diameters of the moving ball.*

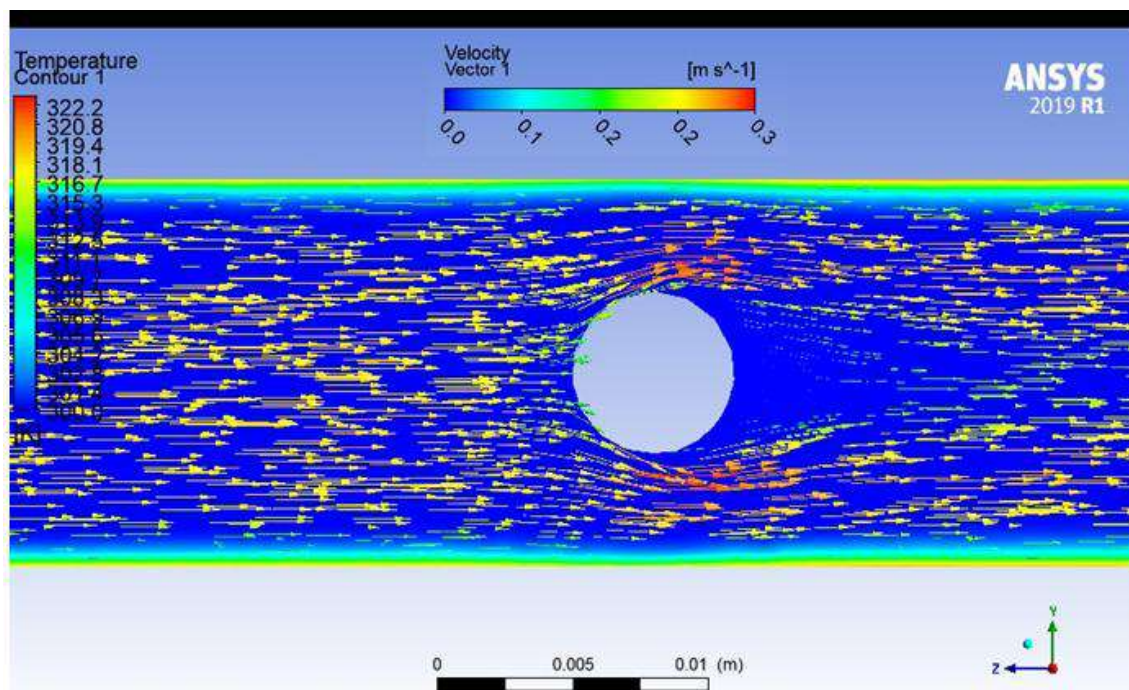
## 4-2 Results and Discussion

*The purpose of these simulations is to study the effects of inserting the moving ball inside tube to enhance the heat transfer performance of the heat exchangers. Figure (1-4) show the temperature contour and velocity vector of the flow inside the tube over the moving ball. By observing the figure (4-1), it was found that there is an increase in the amount of heat transferred around the ball due to the increase in velocity on both sides of the ball near the wall of the tube. velocity is a key factor in the process of heat transfer, as it leads to an increase in the mixing process between the layers of the flow, and the higher the velocity on the two sides of the ball, the greater the intensity of the flow turbulence .*

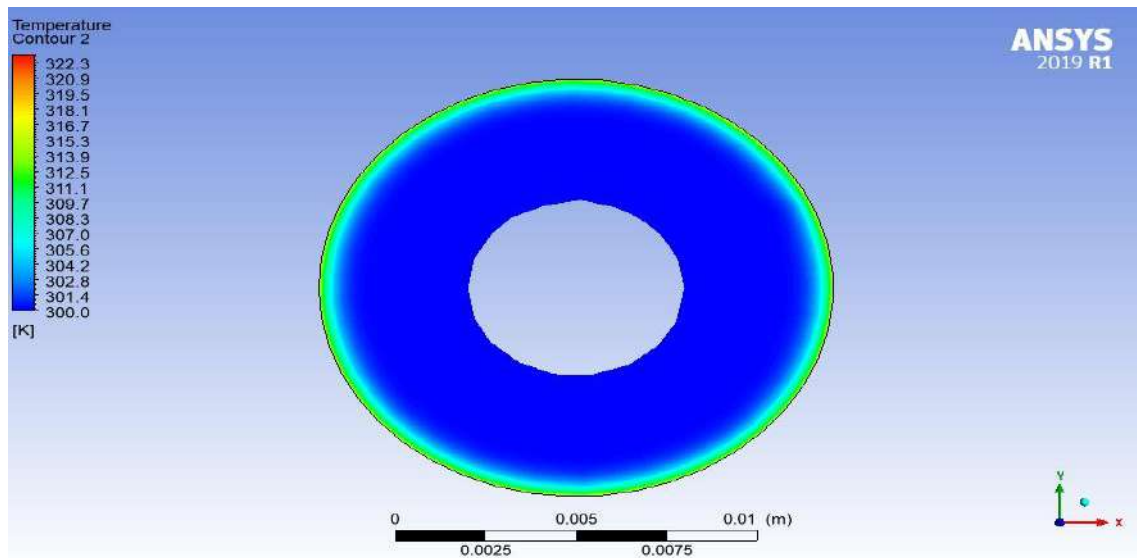
*In the figure (4-2) showed the cross sectional view of temperature contour, the temperature distribution around the ball explain the temperature drop because the high amount of heat is transferred. And the figures (4-3) & (4-4) show the comparison between the different positions of cross sectional view, the region near the ball is better than all positions of the tube because the flow is mixed, therefore; the heat transfer performance enhanced.*

*Figure (4-5) shows that the thermal performance factor at different value of Reynolds number, there are three cases chosen of the optimum diameter ratios of ball inserted inside the tube to tube diameter, the figure (4-6) represent the results of pressure drop and Nusselt number , as the ball diameter ratio increase, the pressure drop and Nusselt number increase too. Therefore; there are limit of increasing the diameter ratio to reduce the pressure drop of the entire*

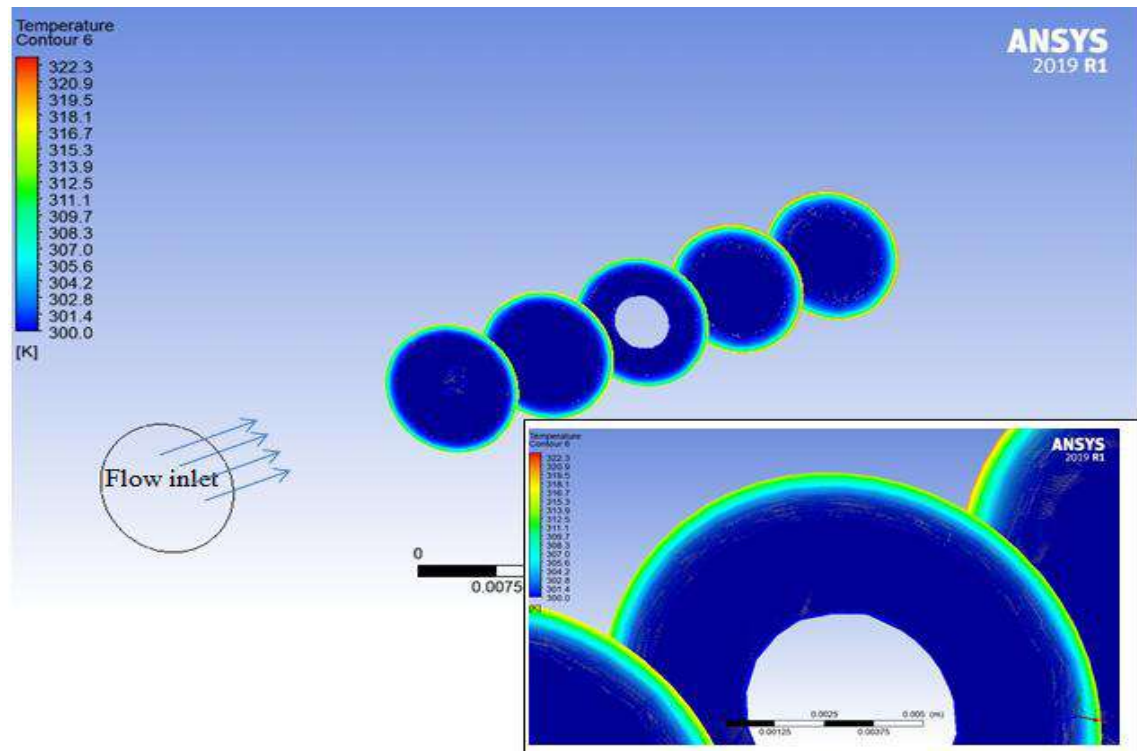
*tube. The percentage of increase in thermal performance factor calculated from figure (4-5), at the diameter ratio of (0.422) the performance factor increase percentage is (14.4%) and at (0.563) diameter ratio, the enhancement percentage is (27.8%). Finally, the maximum value of enhancement increase is (40.8%) at diameter ratio of (0.704). the reason of this enhancement in the thermal performance factor is the mixing of the layers near the wall by the effect of the ball moving inside the tube.*



*Figure (4-1) temperature contour and velocity vector of the flow inside the tube over the moving ball*

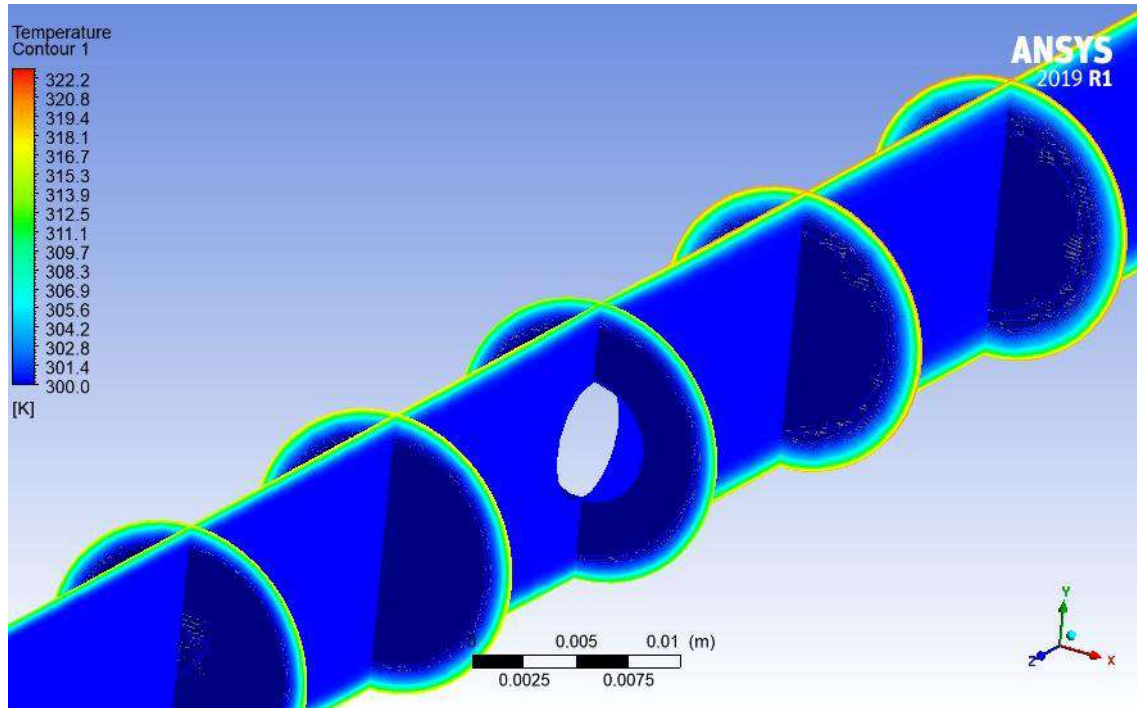


*Figure (4-2) front view of ball inside tube*

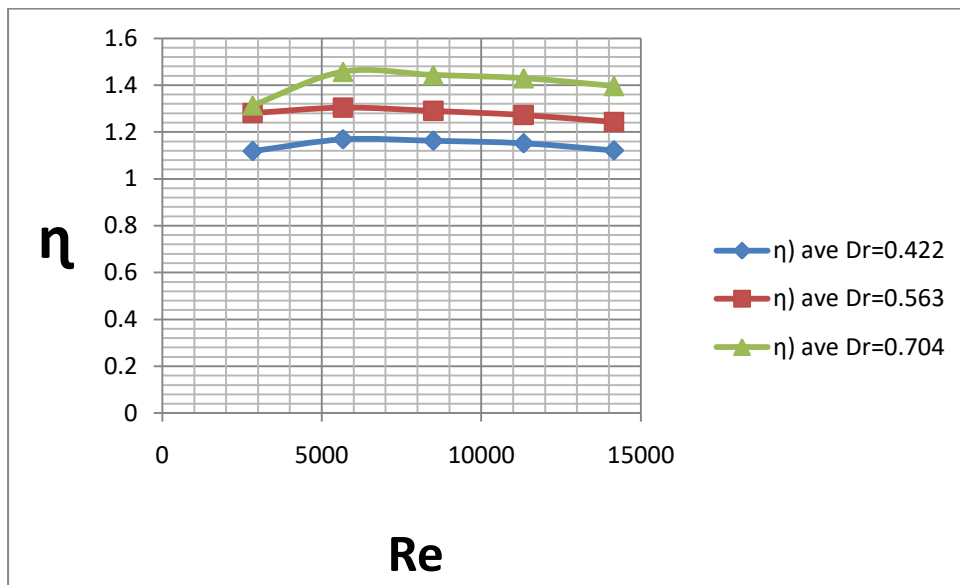


*Figure (4-3) multi-position plane of the tube*

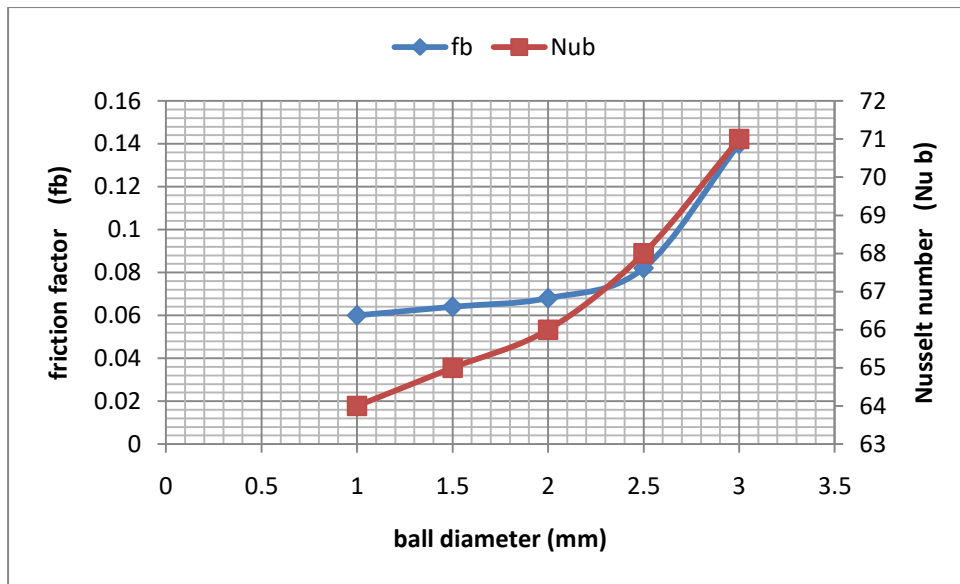




**Figure (4-4) multi-position plane and YZ plane of the tube**



**Figure (4-5) thermal performance factor at different Reynolds number**



*Figure (4-6) friction factor and Nusselt number at different ball diameter*

# CHAPTER FIVE

## CONCLUSIONS AND RECOMMENDATIONS



## **5-1 Conclusions**

*The present numerical simulation shows an acceptable agreement with the literature studies results for the same flow conditions. The CFD methods require very fine computational grids to realistically capture the flow and temperature near the wall of tube and the ball. At present, this leads to high computation times to get the results.*

**1-**

*The CFD results with k-w (sst) turbulence model much better mapping of fluid-thermal phenomena for calculation of cases with a stream separation as such is the nature of the flow of the inserts under investigation*

**2-**

*The percentage of increase in thermal performance factor calculated at the diameter ratio of (0.422) the performance factor is (14.4%) and at (0.563) diameter ratio, the enhancement percentage is (27.8%). Finally, the maximum value of enhancement increase is (40.8%) at diameter ratio of (0.704).*

## 5-2 Recommendations

*Through the general overview of previous studies, several recommendations were reached related to the current research -:*

**1-**

*Changing the surface roughness of the moving ball, allowing the flow to change its properties*

**2-**

*Study whether there is an improvement when adding more than one ball in the same tube*

**3-**

*Study of the effect of ball movement on the cleaning process of heat exchangers*

**4-**

*Changing the density of the ball used, which affects its speed and thus will affect turbulence and heat transfer*

## references

Rui, Z. Guangbei, T. Jihong, L. *Study on biological contaminant control strategies under different ventilation models in hospital operating room. Building and Environment* 43 (2008) 793–803

[2]Randall, David J .; Warren W. Burggren; Kathleen French; Roger Eckert (2002). *Eckert animal physiology: mechanisms and adaptations. Macmillan. ISBN 0-7167-3863-5. Archived from the original on December 17, 2019*

[3]F. Andrade, A.S. Moita, A. Nikulin , A.L.N. Moreira'', H. Santosb far“ *Experimental investigation on heat transfer and pressure drop of internal flow in corrugated tubes” International Journal of Heat and Mass Transfer*21 June 2019

[4]Pengxiao Li, Peng Liu, Zhichun Liu'', Wei Liu “*Experimental and numerical study on the heat transfer and flow performance for the circular tube fitted with drainage inserts” International Journal of Heat and Mass Transfer*27 November 2016

[5]Peng Liu, Nianben Zheng, Feng Shan, Zhichun Liu, Wei Liu“ *Numerical study on characteristics of heat transfer and friction factor in a circular tube with central slant rods” International Journal of Heat and Mass Transfer*15 March 2016

[6]Changzhong Man, Xiaogang Lv''. Jingwei Hu, Peiyan Sun, Yunbang Tang *Experimental study on effect of heat transfer enhancement for single- phase forced convective flow with twisted tape inserts International Journal of Heat and Mass Transfer*8 October 2016

[7]Peng Liu, Nianben Zheng, Feng Shan, Zhichun Liu, Wei Liu “ *Heat transfer enhancement for laminar flow in a tube using bidirectional conical strip inserts” International Journal of Heat and Mass Transfer*25 July 2018Piotr

***[8]Bogusław Jasiński “Numerical study of thermo- hydraulic characteristics in a circular tube with ball turbulators. Part 3: Thermal performance analysis” International Journal of Heat and Mass Transfer 15 November 2016***

***[9]V. Kongkai Paiboon, K. Nanan, S. Eiamsa-ard “ Experimental investigation of convective heat transfer and pressure loss in a round tube fitted with circular-ring turbulators” International Communications in Heat and Mass transfer 14 February 2010***

***[10]Alok Kumar, Sunil Chamoli , Manoj Kumar “Experimental investigation on thermal performance and fluid flow characteristics in heat exchanger tube with solid hollow circular disk inserts” Applied Thermal Engineering 12 February 2016***

***[11]Piotr Bogusław Jasiński (2017) “Numerical study of thermo- hydraulic characteristics in a circular tube with ball turbulators. Part 3: Thermal performance analysis” International Journal of Heat and Mass Transfer 107, 1138–1147***

***[12]Jasiński. Piotr (2012) “Numerical study of friction factor and heat transfer characteristics for single-phase turbulent flow in tubes with helical microfins” Arch. Mech. Eng. LIX (4) 469–485.***

***[13] Ansys-Cfx manual v.***



وزارة التعليم العالي والبحث العلمي

كلية دجلة الجامعة الأهلية

قسم هندسة تقنيات التبريد والتكييف

دراسة عددية لتحسين الأداء الحراري لانتقال الحرارة في المبادلات الحرارية ذات  
القشرة والأنابيب بواسطة حشر كرات متحركة داخل الأنابيب ((

بحث مقدم إلى كلية دجلة الجامعة الأهلية/ قسم هندسة تقنيات التبريد والتكييف وهو  
جزء من متطلبات نيل شهادة البكالوريوس في هندسة تقنيات التبريد والتكييف

من قبل

1. حيدر كاظم\_
2. علي فراس\_
3. علي كمال
4. سيف علي
5. محمد جبار

مشرف المشروع

م.م حيدر لفته

1437 هـ

2016 م

## الخلاصة

نعمل في هذا المشروع على كمية الحرارة المنقولة من الأنابيب الأسطوانية الملساء عن طريق وضع كرات داخل الأنابيب تزيد من شدة اضطراب دخول السائل إلى الأنبوب ، وبالتالي زيادة التبادل الحراري ، وهناك أحجام مختلفة و الأبعاد التي سننظر إليها لاحقاً. وفي هذا المشروع تم استخدام الكرات المتحركة داخل الأنبوب وتم محاكاة العلبة عددياً وتم إيجاد الأبعاد المثلى تم تغيير معلمتين في نطاق رقم رينولدز (  $2500 - 15000$  ) ANSYS 19 R1 بواسطة برنامج المعلمة الأولى هي قطر إدراج الكرة وتم حساب أقصى قدر من الزيادة في تحسين الأداء الحراري. وأن البيانات والنتائج التي تم الحصول عليها من عملية المحاكاة يتم جمعها ومقارنتها مع الدراسات الأدبية. وايضاً تم حساب الإعداد غير الأبعاد لمقارنة النموذج الأولي بشكل صحيح مع وحدة الإنتاج ، حيث تم حساب رقم رينولدز ورقم نسلت ورقم برانتل وعامل الأداء الحراري بطريقة الضخ المتساوي قبل وبعد إضافة الكرات المتحركة و مقارنتها بإعداد متغير لرقم رينولدز. المعلمة الثانية هي سرعة الكرة المتحركة. نسبة الزيادة في معامل الأداء الحراري محسوبة بنسبة قطر (  $0.422$  ) عامل الأداء (  $14.4\%$  ) ونسبة قطر (  $0.563$  ) ونسبة التعزيز (  $27.8\%$  ). وأخيراً بلغت القيمة القصوى لزيادة التعزيز (  $40.8\%$  ) ونسبة

قطرها (  $0.704$  )



Ministry of Higher Education and Scientific  
Research  
Dijlah University College  
Refrigeration and Air Conditioning  
Technologies Engineering Department



## **"ANALYSIS OF STEAM POWER PLANT USING (EES) PROGRAM"**

### **PROJECT**

Submitted to the Refrigeration and air Conditioning Technology  
Engineering Department, Dijlah University College in partial fulfillment  
requirement for the degree of B.Sc in Refrigeration and Air Conditioning  
Technology Engineering

By

Omar Ali  
Murtada Thamer  
Hassan Muhammed  
Mustafa Adel  
Yasser Adel

**Supervisor**

**Dr. Abbas Fadhil Mahmood  
2021.**

We certify that we have read this project entitled **“Analysis of steam power plant using (EES) program”**

Which is prepared by Dijlah university's college students /air conditioning and refrigeration department

Omar Ali  
Murtada Thamer  
Hassan Muhammed  
Mustafa Adel  
Yasser Adel

Has been carried out completely under our supervision at the dijlah university college in partial fulfillment of requirements for degree of:

**B. Sc in Air Conditioning and Refrigeration Engineering.**

Signature:

**Dr. Abbas Fadhil Mahmood**

Date: // 2021

Approved for the chairman of air condition and refrigeration engineering department

Signature:

Chairman of air conditioning and refrigeration

Engineering department

Dijlah University College

Date: // 2021



### **Examining committee certificate**

We certify that we have read this project entitled — “**Analysis of steam power plant using (EES) program**” which is prepared by Dijlah university's college students /air conditioning and refrigeration department.

Omar Ali  
Murtada Thamer  
Hassan Muhammed  
Mustafa Adel  
Yasser Adel

Has been carried out completely under our supervision at the Dijlah University College in partial fulfillment of the requirement for degree of B.Sc in  
**Refrigeration and Air conditioning Techniques Engineering Department.**

**Dr. Abbas Fadhil Mahmood**  
**Supervisor**  
**Date: / /2021 Supervisor**

Signature:  
Name:  
Date: / /2021  
(Member)

Signature:  
Name:  
Date: / /2021  
(Member)

## DEDICATION

To ....

Our Doctor, Teachers, who taught us, for their loyalty, patience and appreciable advice. We hope we shall give them back what they deserve of gratitude and respect, furthermore our extended thanks to the staff of teaching and administrators, in the college and special thanks to the director of Air-conditioning & cooling engineering division. Not forgetting and well remembering thanks and gratefulness to those who raised us up and brought us up to what we are now , and finally special thanks to our fellow -membership in the class rooms of the years 2017-2021



## ACKNOWLEDGMENT

We would like to express our sincere feelings and thankfulness to our supervisor **Dr. Abbas Fadhil Mahmood** for what he has done to us fulfilling our project in this final script and manner.

We also appreciate efforts of our teaching staff of Air-conditioning & cooling department who did not lose a single moment for helping, easing, transforming data, lectures and science. Our sincere greetings to all the staff and administrators of the department.

May God bless our parents for helping, raising us Special thanks to those who were pioneers of plotting theory and applied science of this department and branch of this science.

Omar Ali  
Murtada Thamer  
Hassan Muhammed  
Mustafa Adel  
Yasser Adel

﴿ هُوَ الَّذِي جَعَلَ الشَّمْسَ ضِيَاءً وَالْقَمَرَ نُورًا  
وَقَدَّرَهُ مَنَازِلَ لِتَعْلَمُوا عَدَدَ السِّنِينَ وَالْحِسَابَ مَا  
خَلَقَ اللَّهُ ذَلِكَ إِلَّا بِالْحَقِّ يُفَصِّلُ الْآيَاتِ لِقَوْمٍ  
يَعْلَمُونَ ﴾ { يونس } 5 :

## CONTEENTS

<b>Title</b>	<b>Page No.</b>
<b>Abstract, <i>Keywords</i></b>	<b>1</b>
<b>Chapter One</b>	<b>2</b>
<b>Introduction</b>	<b>3</b>
<b>1.1 EES</b>	<b>3</b>
<b>1.2 Rankine cycle</b>	<b>3</b>
<b>1.3 Methods of Increasing the Efficiency of the Rankine Cycle</b>	<b>4</b>
<b>1-4 Aim of project</b>	<b>5</b>
<b>Chapter Two</b>	<b>6</b>
<b>Literature survey</b>	<b>7-8</b>
<b>Chapter three</b>	<b>9</b>
<b>3-1 Rankine cycle &amp; its features</b>	<b>10-12</b>
<b>Chapter four</b>	<b>13</b>
<b>4-1 Results</b>	<b>14-19</b>
<b>4-2 Discussions</b>	<b>20</b>
<b>Chapter five</b>	<b>21</b>
<b>5-1Conclusions</b>	<b>22</b>
<b>5-1 Recommendations</b>	<b>22</b>
<b>References</b>	<b>23</b>

## **Abstract.**

**Engineering Equation Solver** (EES) is a commercial software package used for solution of systems of simultaneous non-linear equations. It provides many useful specialized functions and equations for the solution of thermodynamics and heat transfer problems, making it a useful and widely used program for mechanical engineers working in these fields. EES stores thermodynamic properties, which eliminates iterative problem solving by hand through the use of code that calls properties at the specified thermodynamic properties. EES performs the iterative solving, eliminating the tedious and time-consuming task of acquiring thermodynamic properties with its built-in functions.

In this graduation project, we study the change in some parameters of the Rankine cycle and their effect on the efficiency of the cycle. We will focus on the boiler temperature pressure of the Rankine cycle.

**Keywords:** Rankine cycle, steam-turbine, efficiency, Feed Water Heater (FWH), irreversibility, reheat cycle, regeneration, condensers

# **Chapter One**

## **Introduction**

## **Introduction**

### **1.1 EES**

EES [11] (Engineering Equation Solver) is a non-free general equation-solving program that can numerically solve systems of non-linear algebraic and differential equations. It can handle a wide range of technical problems and it is particularly well suited for modelling thermal systems. The programming environment is a causal which permits to reuse the same code even after modifying the models inputs and outputs. For example, a same code can firstly size an ORC system and then be used for assessing the system performance under off-design conditions. Additionally, EES provides many useful functionalities permitting to perform optimizations, uncertainty analysis, units checking or parametric studies. It also contains its own thermodynamic and transport database covering a wide range of substances, including organic fluids and refrigerants. EES is particularly interesting for simple studies and basic thermal systems. It is robust (as long as a proper initialization is ensured by the user) and the model development is really fast. However, simulations with EES demonstrate convergence issues when investigating more complex systems. For example, the part-load simulation of an ORC when only considering the boundary conditions to define the equilibrium state of the system is a real challenge, especially if the ORC features an advanced architecture like several heat exchangers in series (e.g. with a recuperator). Although EES proposes some useful functionalities, it does not provide a user-friendly environment to conduct cascaded tasks.

### **1.2 Rankine cycle**

The Rankine cycle or Rankine Vapor Cycle is the process widely used by power plants such as coal-fired power plants or nuclear reactors. In this mechanism,



a fuel is used to produce heat within a boiler, converting water into steam which then expands through a turbine producing useful work. This process was developed in 1859 by Scottish engineer William J.M. Rankine.[1] This is a thermodynamic cycle which converts heat into mechanical energy—which usually gets transformed into electricity by electrical generation. Heat energy is supplied to the system via a boiler where the working fluid (typically water) is converted to a high pressure gaseous state (steam) in order to turn a turbine. After passing over the turbine the fluid is allowed to condense back into a liquid state as waste heat energy is rejected before being returned to boiler, completing the cycle. Friction losses throughout the system are often neglected for the purpose of simplifying calculations as such losses are usually much less significant than thermodynamic losses, especially in larger systems.

### **1.3 Methods of Increasing the Efficiency of the Rankine Cycle**

There are three ways to increase the efficiency of the simple ideal Rankine cycle.

- a) Decreasing the condenser pressure.
- b) Superheating the steam to a high temperature.
- c) Increasing the boiler pressure.

To take advantage of the increased efficiencies at higher boiler pressure without facing the excessive moisture at the final stages of the turbine, reheating is used. In the ideal *reheating cycle*, the expansion process takes place in two stages, i.e., the high- pressure and low-pressure turbines.

The *regeneration process* in steam power plants is accomplished by extracting (or bleeding) steam from turbine at various stages and feed that steam in heat exchanger where the feedwater is heated. These heat exchangers are called regenerator or feedwater heater (FWH).

The objective of the work presented here is to perform a Rankine cycle analysis and demonstrate the potential of the EES program.

**1-4 Aim of project:**

The purpose of this project is the use of the full potential of the (ESS) to study the effect of the changes in some Rankin cycle's data such as pressure and temperature and their effect on its efficiency

# **Chapter Two**

## **Literature Survey**

## **Literature survey**

- 2.1** In order to remain general and accessible to as many people as possible, three widely used programming languages are covered within organic Rankine cycles, i.e. Matlab, Python and EES (Engineering Equation Solver). Besides source codes, organic Rankine cycles also includes calibration tools for empirical and semi- empirical models as well as a complete documentation for ease of use [3].
- 2.2** A thermodynamic model was developed using then gingering Equation Solver (EES) software to determine its performance using different working fluids (toluene, R245fa and R123) under the same operating conditions, taking into account the effect of certain operating parameters and the selection of organic fluids on cycle performance. The results obtained show that the toluene organic fluid has the best thermal efficiency of the cycle compared to the other fluids; 14.38% for toluene, 13.68% for R123 and 13.19 for R245fa [4].
- 2.3** Recently, the TLC (trilateral power cycle) has attracted significant interest as it provides better matching between the temperature profiles in the evaporator compared to conventional power cycles. This article investigates the performance of this cycle and compares it with those for the ORC (organic Rankine cycle) and the Kalina cycle, from the viewpoints of thermodynamics and thermoeconomics. A low-grade heat source with a temperature of 120 °C is considered for all the

three systems. Parametric studies are performed for the systems for several working fluids in the ORC and TLC. The systems are then optimized for either maximum net output power or minimum product cost, using the EES (engineering equation solver) software. The results for the TLC indicate that an increase in the expander inlet temperature leads to an increase in net output power and a decrease in product cost for this power plant, whereas this is not the case for the ORC system [5].

# **Chapter Three**

## **An analysis of Rankine Cycle**

### **3-1 Rankine cycle & its features**

Rankine cycle has less practical difficulties and it is found to be more economical. For the steam boiler, this would be a reversible constant pressure heating process of water to form steam, for the turbine the ideal process would be a reversible adiabatic expansion of steam, for the condenser it would be a reversible constant pressure heat rejection as the steam condenses till it becomes saturated liquid, and for the pump, the ideal process would be the reversible adiabatic compression of this liquid ending at the initial pressure. When all these four processes are ideal, the cycle is an ideal cycle, called a Rankine cycle.

### **3-2 Components associated with Rankine cycle**

The four basic components of a vapor power plant are shown in Fig 1. Each component in the cycle is regarded as a control volume, operating at steady state.

**Turbine:** The vapor leaving the boiler enters the turbine, where it expands isentropically to the condenser pressure at the state 2 (shown in Fig 1 & 2).

The work produced by the turbine is rotary (shaft) work and is used to drive an electric generator.

**Condenser:** The condenser is attached at the exit of the turbine. The vapor leaving the turbine is wet vapor and it is condensed completely in the condenser to the state 3 (shown in Fig 1 & 2), by giving its latent heat to some other cooling fluid like water.

**Pump:** The liquid condensate leaving the condenser at the state 3 (shown in Fig1&2) is pumped to the operating pressure of the boiler. The pump operation is considered isentropic.

**Boiler:** The heat is supplied to the working fluid (feed water) in the boiler and thus vapor is generated. The vapor leaving the boiler is either saturated at the state 1 or superheated at the state 1' (shown in Fig1&2), depending upon the amount of heat supplied in the boiler.

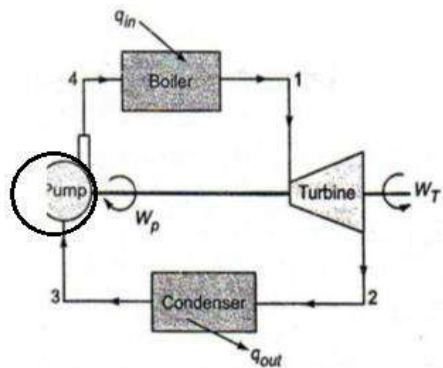


Fig 3-1: Basic components of Rankine cycle.

The Figure 2 shows Rankine cycle on T-s coordinates. The liquid, vapour and wet vapour regions are also indicated with the help of saturation curve.

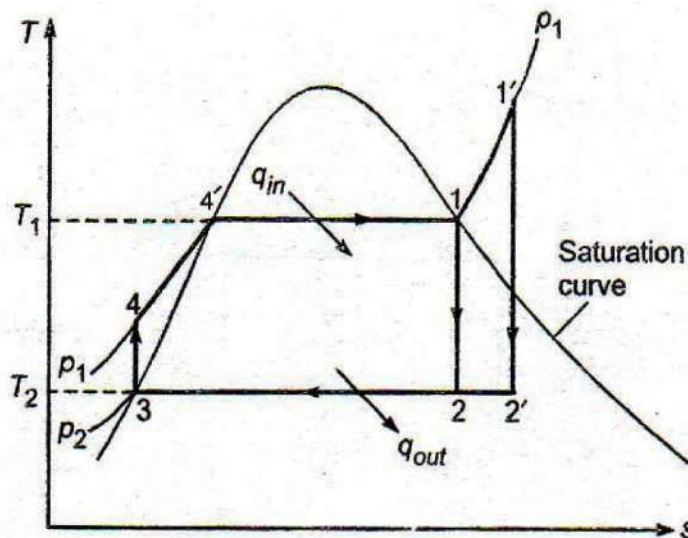




Fig 3-2: T-S diagram of Rankine cycle.

**For 1kg fluid**

The S.F.E.E. for the boiler control volume) gives:

$$h_4 + Q_1 = h_1 \quad \dots\dots\dots (1)$$

So,  $Q_1 = h_1 - h_4 \quad \dots\dots\dots (2)$

The S.F.E.E. for the turbine as the control volume gives:

$$h_1 = W_T + h_2 \quad \dots\dots\dots (3)$$

So,  $W_T = h_1 - h_2 \quad \dots\dots\dots (4)$

The S.F.E.E. for the pumps gives:

$$h_3 + W_P = h_4 \quad \dots\dots\dots (5)$$

So,  $W_P = h_4 - h_3 \quad \dots\dots\dots (6)$

A measure of the effectiveness of an energy conversion device is its thermal efficiency. By using the above equation the Rankin cycle thermal efficiency in terms of cycle enthalpies is given as:

$$\frac{W_T - W_P}{Q_1} = \frac{(h_1 - h_2) - (h_4 - h_3)}{h_1 - h_4}$$

The pump handles liquid water which is incompressible, i.e. its density or specific volume undergoes little change with an increase in pressure. For reversible adiabatic compression, by the use of the general property relation,

$$Tds = dh - vdp ; ds=0$$

And  $dh = vdp$

Since change in specific volume is negligible

$$dh = vdp$$

Or  $h_4 - h_3 = v(p_1 - p_2) \quad \dots\dots\dots (7)$

Usually, the pump work is quite small compared to the turbine work and is sometimes neglected.

Then  $h_4 = h_3$ , and the cycle efficiency approximately becomes

$$\eta_{\text{rankine}} \cong \frac{h_1 - h_2}{h_1 - h_4} \dots\dots\dots (8)$$

# Chapter Four

## Results and Discussions

## 4-1 Results

In our scientific research, we will analyze the performance of the reheat Rankine cycle with the following specifications (Steam enters the high-pressure turbine at 15 MPa and 500°C and is condensed in the condenser at a pressure of 75 kPa. If the moisture content of the steam at the exit of the low-pressure turbine is not to exceed 10.4 percent)

In addition, we will analyze the same cycle with reheat. All calculations will be done by (EES).

Now, let's solve using EES to see how the program can help speed up the process and also help solve for multiple variables. Enter the problem information as shown in Fig. 4-1.

Equations window	Format Equations
P1=75 [kpa]	P1 = 75
h1=Enthalpy(Steam_IAPWS,x=0,P=P1)	h1 = h SteamIAPWS , x =0, P =P1
s1=Entropy(Steam_IAPWS,x=0,P=P1)	s1 = s SteamIAPWS , x =0, P =P1
P2=P3	P2 = P3
T3=500 [c]	T3 = 500
h2=wp+h1	h2 = wp + h1
s2=Entropy(Steam_IAPWS,h=h2,P=P3)	s2 = s SteamIAPWS , h =h2, P =P3

---

<p> <math>P3=15000 \text{ [kPa]}</math>  <math>w_p=v1*(P2-P1)</math>  <math>v1=\text{Volume}(\text{Steam\_IAPWS},x=0,P=P1)</math>  <math>P1=P4</math>  <math>h3=\text{Enthalpy}(\text{Steam\_IAPWS},T=T3,P=P3)</math>  <math>s3=\text{Entropy}(\text{Steam\_IAPWS},T=T3,P=P3)</math>  <math>s4=s3</math>  <math>h4=\text{Enthalpy}(\text{Steam\_IAPWS},s=s4,P=P4)</math>  <math>w_t=h3-h4</math>  <math>w_{net}=w_t-w_p</math>  <math>q_{in}=h3-h2</math>  <math>q_{out}=h4-h1</math>  <math>\eta=1-q_{out}/q_{in}</math> </p>	<p> <math>P3 = 15000</math>  <math>w_p = v1 \cdot P2 - P1</math>  <math>v1 = v \text{ SteamIAPWS}, x = 0, P = P1</math>  <math>P1 = P4</math>  <math>h3 = h \text{ SteamIAPWS}, T = T3, P = P3</math>  <math>s3 = s \text{ SteamIAPWS}, T = T3, P = P3</math>  <math>s4 = s3</math>  <math>h4 = h \text{ SteamIAPWS}, s = s4, P = P4</math>  <math>w_t = h3 - h4</math>  <math>w_{net} = w_t - w_p</math>  <math>q_{in} = h3 - h2</math>  <math>q_{out} = h4 - h1</math>  <math>\eta = 1 - q_{out}/q_{in}</math> </p>
--	---

---

Fig. 4-1. Problem information

An additional property given to us in the problem statement, the saturated vapor or the vapor quality of the fluid at state one, which can be represented as  $x1$ . EES has built in property tables that follow the thermodynamics rule that for saturated vapor the value of  $x$  is 1 and for saturated liquid the value is 0.

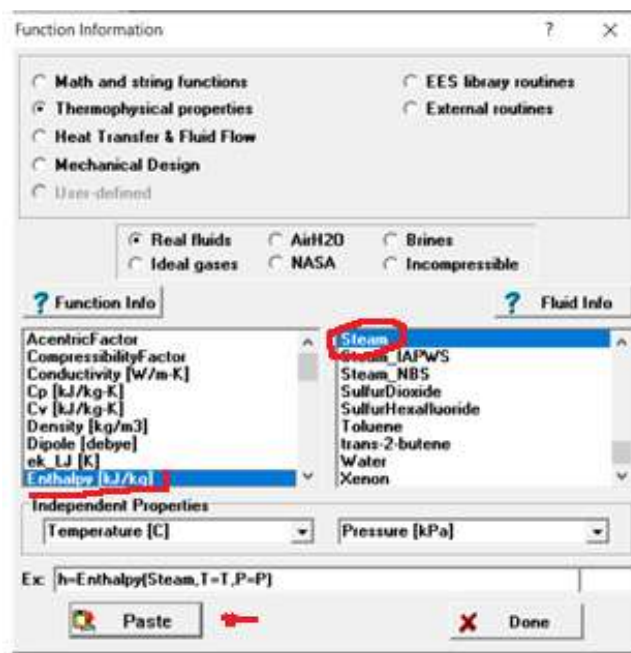


Fig. 4-2. Function information

The second problem could be that EES does not know the units of the variables we assigned for it. Even though we defined them in text, we did not define them in EES. EES allows us to assign properties by using the Unit System Manager, accessed through Diagram Window Toolbar, shown in Fig. 6.

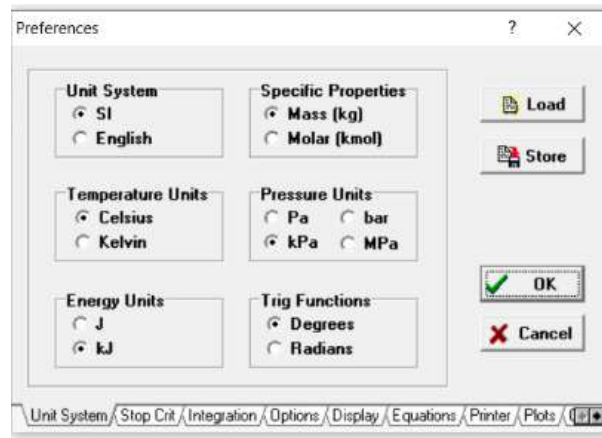


Fig. 4-3. Unit System Manager

The next step is to find the value of the cycle efficiency and the value

**Unit Settings: SI C kPa kJ mass deg**

$\eta = 0.3563$	$h_1 = 384.4 \text{ [kJ/kg]}$	$h_2 = 399.9 \text{ [kJ/kg]}$	$h_3 = 3311 \text{ [kJ/kg]}$
$h_4 = 2258 \text{ [kJ/kg]}$	$P_1 = 75 \text{ [kPa]}$	$P_2 = 15000 \text{ [kPa]}$	$P_3 = 15000 \text{ [kPa]}$
$P_4 = 75 \text{ [kPa]}$	$q_{in} = 2911 \text{ [kJ/kg]}$	$q_{out} = 1874 \text{ [kJ/kg]}$	$s_1 = 1.213 \text{ [kJ/kg-K]}$
$s_2 = 1.213 \text{ [kJ/kg-K]}$	$s_3 = 6.348 \text{ [kJ/kg-K]}$	$s_4 = 6.348 \text{ [kJ/kg-K]}$	$T_3 = 500 \text{ [C]}$
$v_1 = 0.001037 \text{ [m}^3\text{/kg]}$	$w_{net} = 1037 \text{ [kJ/kg]}$	$w_p = 15.48 \text{ [kJ/kg]}$	$w_t = 1053 \text{ [kJ/kg]}$

Fig. 4-4. Solution parameters

In Figure (8) we tested the boiler temperature to study the effect of the changes on the station efficiency and the turbine work.

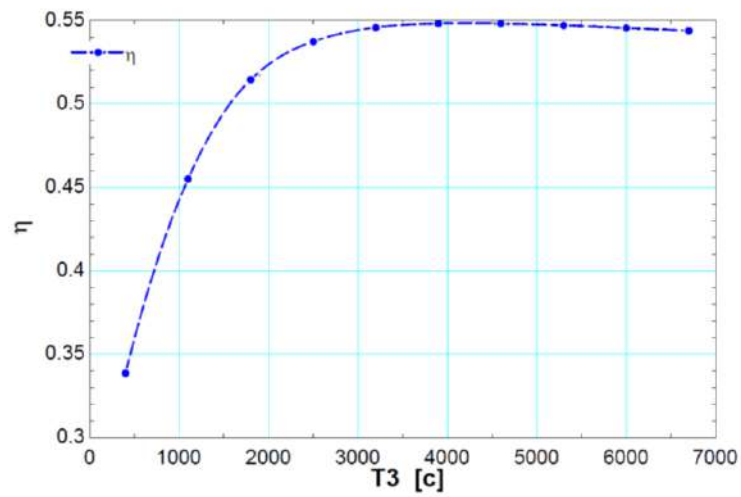


Fig. 8. The effect of temperature on efficiency

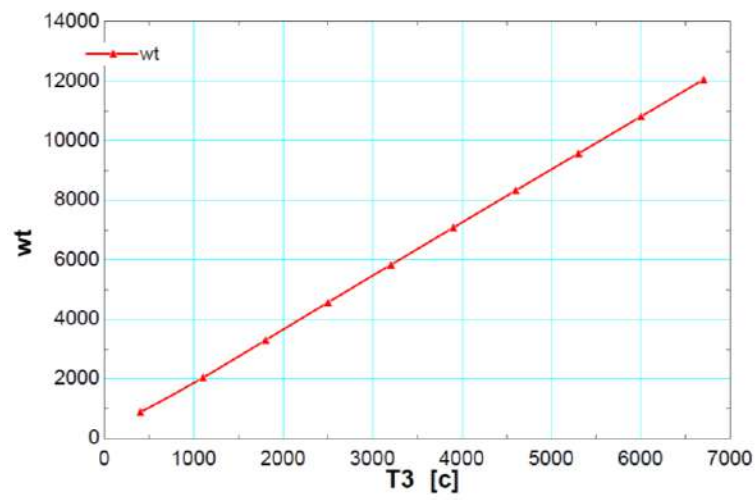


Fig. 4-5. The effect of temperature on turbine work

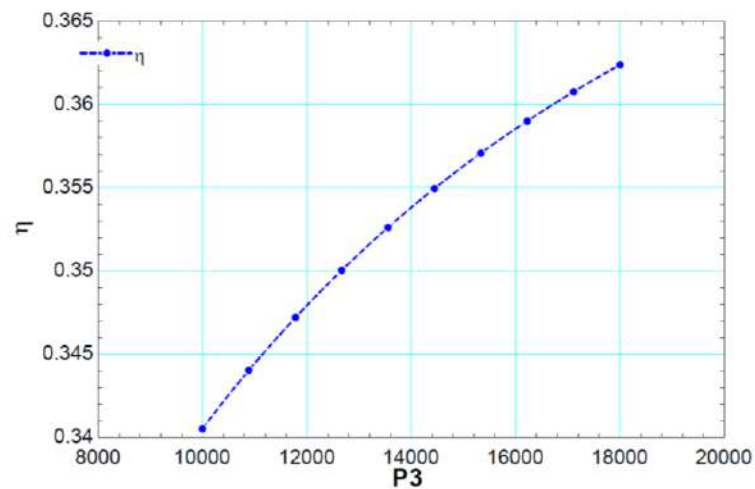


Fig. 4-6. The effect of boiler pressure on efficiency

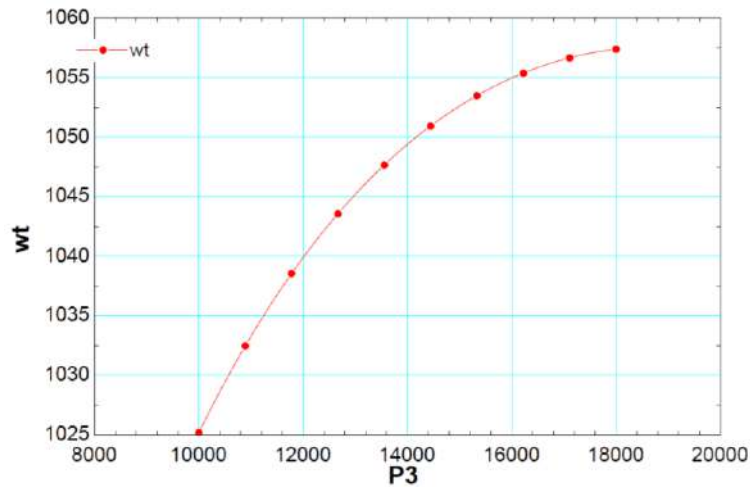


Fig. 4-7. The effect of boiler pressure on turbine work

**Build a Parametric Table for a range of temperatures at state three.**

To find solutions for multiple input of temperature, pressure, etc. For this problem we will find solutions for the temperatures mentioned previously (300 to 525 °C)

**4-2** With the same specifications as the simple cycle (temperature and pressure) by adding reheat we performed the same calculations to find the relationship between  $(\eta - P_3)$ ,  $(\eta - T_3)$  and  $(W_T - P_3)$ ,  $(W_T - T_3)$  using EES the results shown in the following figures:

**Unit Settings: SI C kPa kJ mass deg**

$\eta = 0.369$	$h_1 = 384.4$ [kJ/kg]	$h_2 = 399.9$ [kJ/kg]	$h_3 = 3311$ [kJ/kg]
$h_4 = 3088$ [kJ/kg]	$h_5 = 3412$ [kJ/kg]	$h_6 = 2426$ [kJ/kg]	$P_1 = 75$ [kPa]
$P_2 = 15000$ [kPa]	$P_3 = 15000$ [kPa]	$P_4 = 6916$ [kPa]	$q_{in} = 3235$ [kJ/kg]
$q_{out} = 2041$ [kJ/kg]	$s_1 = 1.213$ [kJ/kg-K]	$s_2 = 1.213$ [kJ/kg-K]	$s_3 = 6.348$ [kJ/kg-K]
$s_4 = 6.348$ [kJ/kg-K]	$s_6 = 6.807$ [kJ/kg-K]	$T_3 = 500$ [C]	$T_5 = 500$ [C]
$v_1 = 0.001037$ [m <sup>3</sup> /kg]	$W_{net} = 1194$ [kJ/kg]	$W_p = 15.48$ [kJ/kg]	$W_t = 1209$ [kJ/kg]

Fig. 4-8. Solution parameters reheat cycle

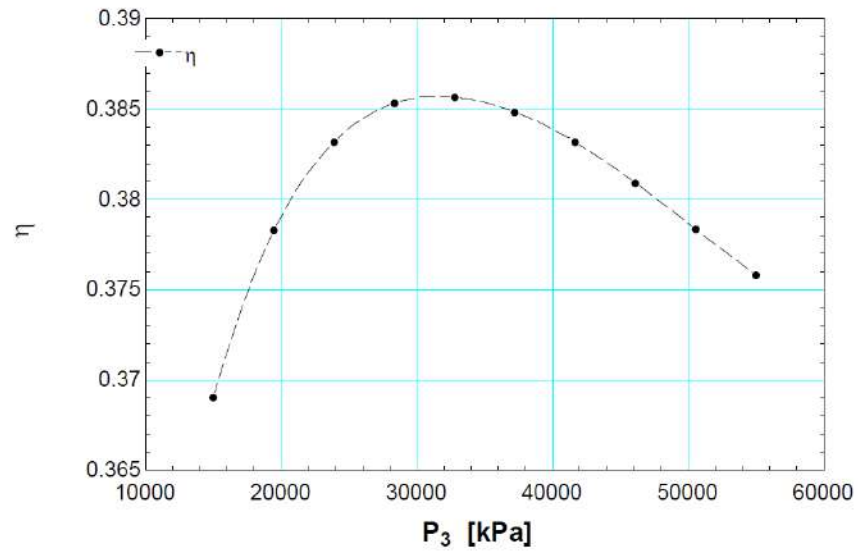


Fig. 9. The effect of pressure on efficiency (reheat cycle)

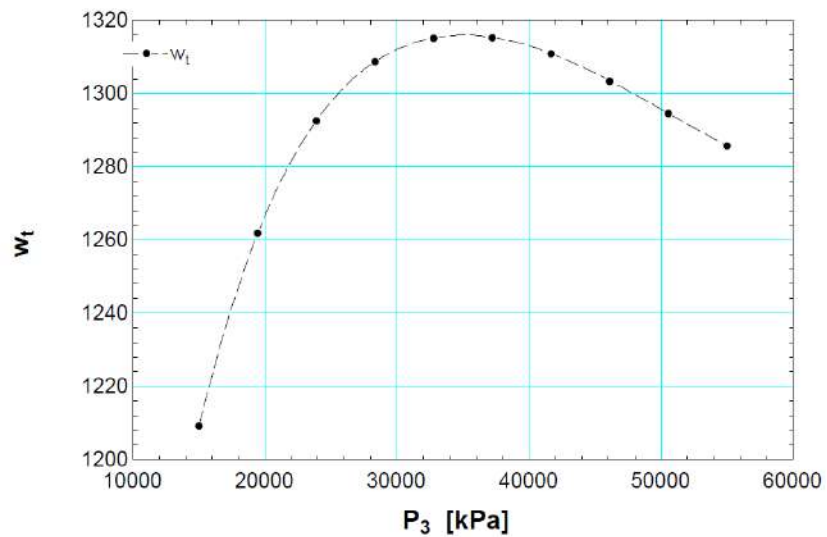


Fig. 4-10. The effect of boiler pressure on turbine work (reheat cycle)



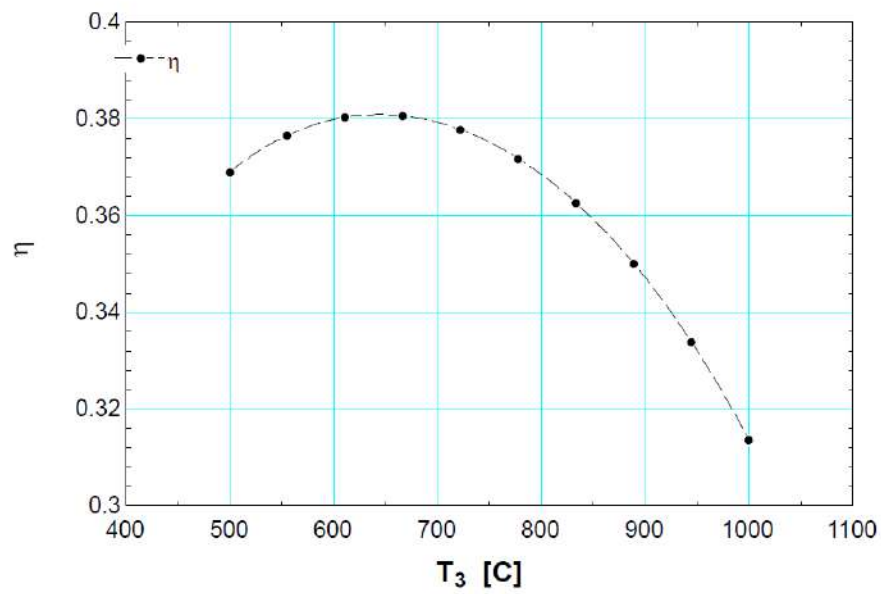


Fig. 4-11. The effect of boiler pressure on efficiency (reheat cycle)

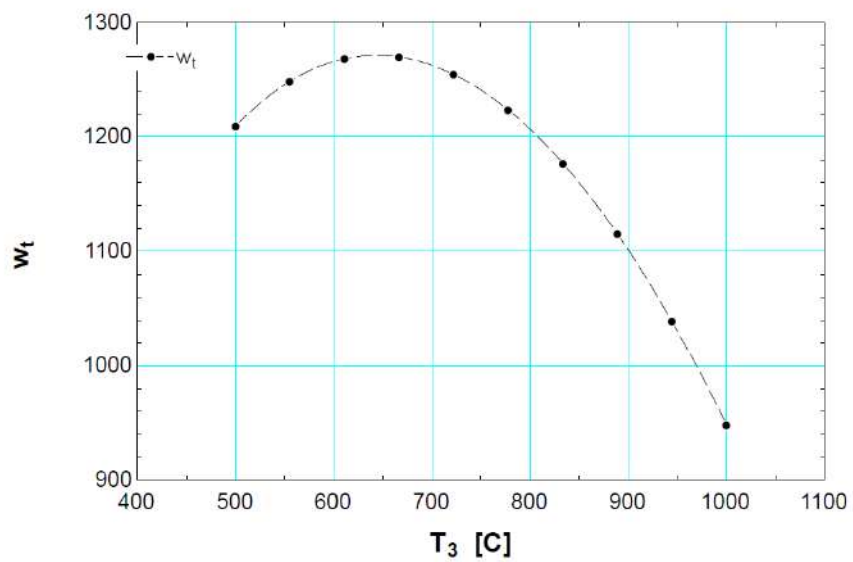


Fig. 4-12. The effect of temperature on turbine work (reheat cycle)

## **4-2 Discussions**

By reviewing the results, it becomes clear how important the use of EES program is, using this program we can get the change in some parameters and its effect on the efficiency of the (steam) cycle, for example, or any cycle that is subjected to the laws of thermodynamics. This program helps scientific researchers to solve a lot of problems, it keeps them do real experiences.

# **Chapter five**

## **Conclusions and Recommendations**

## **5-1Conclusions**

The search results showed how important it is to use (ESS) in solving special thermodynamic equations and specifically steam power stations. Through this program, we can study the effect change in some station barometers on its efficiency and those results are close to reality.

Through the results, we noticed that the increase in temperature to  $680^{\circ}\text{C}$  we get the highest efficiency when the boiler pressure  $p_3 = 15000 \text{ kpa}$  and when stabilizing the boiler temperature  $T_3=500^{\circ}\text{C}$ , Efficiency reaches maximum when pressure reaches  $3300 \text{ kpa}$  .

## **5-1 Recommendations**

In the future, we could compare the results using the (ESS) Software with the results of genuine experiments to determine the differences between them

## REFERENCES

1. ASHRAE Handbook of Fundamentals, (1989, 1993, 1997), American Society of Heating, Refrigerating and Air Conditioning Engineers, Atlanta, GA
2. L. Albright, L. Angenent, F. Vanek. (May 6, 2015). "Stationary Combustion Systems" in *Energy Systems Engineering*, 2nd Edition. McGraw Hill. 2012. ch.6, pp.161-167
3. Dickes, R., Ziviani, D., De Paepe, M., van den Broek, M., Quoilin, S., & Lemort, V. (2016). ORCmKit: an open-source library for organic Rankine cycle modelling and analysis. In *The 29th International Conference on Efficiency, Cost, Optimization, Simulation and Environmental impact of energy systems* (pp. 1-14).
4. Spayde, E., Mago, P. J., & Luck, R. (2018). Economic, energetic, and environmental performance of a solar powered organic Rankine cycle with electric energy storage in different commercial buildings. *Energies*, 11(2), 276.
5. Shams Ghoreishi, S. M., Akbari Vakilabadi, M., Bidi, M., Khoeini Poorfar, A., Sadeghzadeh, M., Ahmadi, M. H., & Ming, T. (2019). Analysis, economical and technical enhancement of an organic Rankine cycle recovering waste heat from an exhaust gas stream. *Energy Science & Engineering*, 7(1), 230-254.
6. ASHRAE, Thermophysical Properties of Refrigerants, American Society of Heating,
7. Refrigerating, and Air-Conditioning Engineers, Atlanta, GA, (1976)
8. Bertagnolio, S., Masy, G., Lebrun, J., & André, P. (2008). Building and HVAC System simulation with the help of an engineering equation solver. *Proceedings of SimBuild*, 3(1), 53-60.

## الخلاصة

(EES) عبارة عن حزمة برامج تجارية تستخدم لحل أنظمة المعادلات غير الخطية المتزامنة. يوفر العديد من الوظائف المتخصصة المفيدة والمعادلات لحل مسائل الديناميكا الحرارية وانتقال الحرارة ، مما يجعله برنامجاً مفيداً ومستخدماً على نطاق واسع للمهندسي الميكانيكيين العاملين في هذه المجالات. تخزن EES الخصائص الديناميكية الحرارية ، والتي تقضي على حل المشكلات التي تصاحب التكرار يدوياً من خلال استخدام الكود الذي يستدعي الخصائص الديناميكية الحرارية المحددة. تقوم EES بالحل التكراري ، مما يلغي المهمة الشاقة والمستهلكة للوقت لكتساب الخصائص الديناميكية الحرارية من خلال وظائفها المضمنة . في مشروع التخرج هذا ، ندرس التغيير في بعض متغيرات دورة رانكين وتأثيرها على كفاءة الدورة . سنركز على ضغط و درجة حرارة الغلاية في دورة رانكين.



وزارة التعليم العالي والبحث العلمي  
كلية دجلة الجامعة  
قسم هندسة تقنيات التبريد والتكييف



## تحليل محطة طاقة بخارية باستخدام برنامج (EES)

بحث مقدم الى قسم هندسة تقنيات التبريد والتكييف في كلية دجلة الجامعة  
كمطلب جزئي لأستحقاق درجة بكالوريوس  
في  
هندسة تقنيات التكييف والتبريد

اعداد

عمر علي  
ياسر عادل  
مصطفى عادل  
حسن محمد  
مرتضى ثامر

المشرف  
د. عباس فاضل محمود  
تموز ٢٠٢١

*Ministry of Higher Education and Scientific Research*

*Dijlah University College*

*Refrigeration & Air Conditioning Department*



***Data Acquisition System for temperature  
Measurements***

*A project*

*Submitted to the Refrigeration and Air Condition Technology Engineering  
Department, Dijlah University College in partial  
Fulfillment requirement for the degree of B.Eng in Refrigeration and Air-  
Conditioning Technical Engineering*

*By:*

- *Majed Taha Yaseen*
- *Abd -Alrahman Muthana Hadi*
- *Mohamad Shihab Nasif*
- *Saif Salah-Alden Sabar*
- *Hussain Ali jasim*
- *Rafid Hasan Mahdi*

*Supervisor by:*

*Dr. Firas Maan Abdulsattar*

*2021-2020*



قال تعالى :

قَالُوا سُبْحَانَكَ لَا عِلْمَ لَنَا إِلَّا مَا عَلَّمْتَنَا إِنَّكَ أَنْتَ الْعَلِيمُ  
الْحَكِيمُ

صدق الله  
العظيم

سورة البقرة الآية " 32 "

## Dedication

أهدأنا

الى البلسم الذي يداوي جروحنا ...  
الى من رببونا صغيرا...

الى من احببنا ولن ننسى ... الى ابائنا وامهاتنا ...  
الى اشقائنا وشقيقاتنا الذين وقفوا بجانبنا طيلة  
السنين الماضية

الى اصدقائنا الذين دعمونا وساندونا خلال  
دراستنا

الى قادة المستقبل وبناءة الغد ...

طلبة العراق

## Acknowledgment

الحمد لله الذي علم بالقلم , علم الانسان ما لم يعلم , الحمد لله المنان , الملك القدوس السلام , مدبر الليالي والايام , مصرف الشهور والاعوام , قدر الأمور فأجراها على أحسن نظام , ما شاء الله كان وما لم يشأ لم يكن , الحمد لله على ما أنعم به على من فضله الخير الكثير والعلم الوفير وأعاننا على إنجاز هذا العمل .

وبعد حمد الله تعالى وشكره على انهائنا لهذه الرسالة نقدم بخالص الشكر وعظيم الامتنان للدكتور فراس معن عبدالستار على ما قدمه لنا من علم نافع وعطاء متميز وارشاد مستمر , وعلى ما بذله من جهد متواصل ونصح وتوجيه من بداية المرحلة البحث حتى اتمام هذه الرسالة , ومهما كتبنا من عبارات وجمل فأن كلمات الشكر تظل عاجزة عن ايفاء حقه , فجزاه الله عنا خير الجزاء وجعل ذلك في موازين حسناته .

وكما نقدم بأسمى عبارات الشكر والتقدير الى كل من غرس فينا حب العلم من الصغر , والى عوائلنا التي قدمت لنا كل ما هوه غالي ونفيس , وكان لهم الفضل بعد الله فيما وصلنا اليه الآن .

ونقدم الشكر لكل من مد لنا يد العون , واسدى معروفاً لنا , او قدمة لنا نصحية , او كانت له اسهامه صغيرة او كبيرة في انجاز هذه العمل فله خالص الشكر والتقدير .

والحمد لله رب العالمين اولاً و آخرأ .

*Examining committee certificate*

*Project Title*

*Data Acquisition System for temperature Measurements*

*Submitted by:*

- *Majed Taha Yaseen*
- *Abd -Alrahman Muthana Hadi*
- *Mohamad Shihab Nasif*
- *Saif Salah-Alden Sabar*
- *Hussain Ali jasim*
- *Rafid Hasan Mahdi*

*Has been carried out completely under our supervision at the Dijlah university college in partial fulfillment of the requirements for degree of B.Eng.*

*In Refrigeration and Air Conditioning Techniques Engineering Department*

*Signature*

*Dr. Firas Maan Abdulsattar*

*Date: / /2021*

*(Supervisor)*

*Signature*

*Name:*

*Date: / /2021*

*(Member)*

*Signature*

*Name:*

*Date: / /2021*

*(Member)*

## *Supervisor Certificate*

*We certify that this project entitled ((Data Acquisition System for temperature Measurements))*

*Prepared by:*

- *Majed Taha Yaseen*
- *Abd -Alrahman Muthana Hadi*
- *Mohamad Shihab Nasif*
- *Saif Salah-Alden Sabar*
- *Hussain Ali jasim*
- *Rafid Hasan Mahdi*

*Has been carried out completely under our supervision at the Djlal university college in partial fulfillment of the requirements for degree of B.Eng in Air Conditioning and Refrigeration Engineering.*

*Signature:*

*Dr. Firas Maan Abdulsattar*

*Date: / /2021*

*Approved by the charm in of Air condition and refrigeration engineering department:*

*Signature*

*Dr. Firas Maan Abdulsattar*

*Charmin of Refrigerating and Air Conditioning Engineering  
Department*

*Date: / /2021*

### *List of symbols*

DAQ	Data acquisition system
RTD <sub>s</sub>	resistance temperature detectors
LED	Light sensors detect light
PWM	Pulse-width modulation
USB	Universal Serial Bus
DC	Direct current
mA	Milli Ampere

## *List of Figures*

### Chapter 1

Figure (1.1) (functional diagram of a PC-based data acquisition system).....3

Figure (1.2) (Data acquisition system block diagram and the elements of the modern digital data acquisition system).....3

Figure (1.3) (Light Detection).....5

### Chapter 2

Figure (2.1) (Device components connecting digram).....9

Figure (2.2) (The form of connecting the components of the device).10

Figure (2.3) (The final shape of device).....11

Figure (2.4) (Arduino Mega 2560).....12

Figure (2.5) (Arduino Mega 2560).....13

Figure (2.6) (Arduino UNO R3).....15

Figure (2.7) (Arduino Lenardo) .....15

Figure (2.8) (Arduino YUN).....16

Figure (2.9) (Arduino Due) .....17

Figure (2.10) (Arduino micro) .....18

Figure (2.11) (Arduino Nano).....18

Figure (2.12) (Arduino Mini).....18

Figure (2.13) (GLCD 12864).....19

Figure (2.14) (thermocouple K-Type).....20

Figure (2.15) (Temperature to voltage conversion chart).....21

Figure (2.16) (J- Type thermocouple).....22

Figure (2.17) (N-Type thermocouple).....23

Figure (2.18) (S-Type thermocouple).....23

Figure (2.19) (Power Supply).....24

Figure (2.20) (USB 2.0 CABLE TYPE).....24

Figure (2.21) (Sensor max6675 type k).....	25
Figure (2.22) (Types of Sensors).....	26
Figure (2.23) ( Jumping wires).....	27
Figure (2.24) (Breadbord).....	27
Figure (2.25) (PVC BOX).....	28
Chapter 3	
Figure (3.1) (water cooler).....	41
Figure (3.2) (thermocouples location).....	43
Chapter 4	
Figure (4.1) Developments.....	47
Figure (4.2) (The power source).....	48
Figure (4.3) (Internal storage unit) ((SD card)).....	49
Figure (4.4) (sensors) .....	50
Figure (4.5) (Wi-Fi device).....	51

### *List of tables*

Chapter 2	
Table (2.1).....	14
Chapter 3	
Table (3.1).....	42
Table (3.2).....	44

### *List of charts*

Chapter 3	
Chart (3.1).....	45



## *Content*

### **Abstract**

<b>Chapter One</b> .....	1
<b>Introduction</b> .....	1
<b>Chapter Two</b> .....	8
<b>2-1 Hardware</b> .....	8
2-1-1 <b>ARDUINO MEGA 2560</b> .....	12
2-1-2 <b>Types of Arduino</b> .....	15
2-1-3 <b>Arduino UNO R3</b> .....	15
2-1-4 <b>Arduino Leonardo</b> .....	15
2-1-5 <b>Arduino YUN</b> .....	16
2-1-6 <b>Arduino Due</b> .....	17
2-1-7 <b>Arduino Micro</b> .....	18
2-1-8 <b>Arduino Nano</b> .....	18
2-1-9 <b>Arduino Mini</b> .....	18
<b>2-2 GLCD 12864</b> .....	19
<b>2-3 Thermocouple K-Type</b> .....	20
2-3-1 <b>Types of Thermocouple</b> .....	22
2-3-2 <b>J-Type Thermal Double (Iron/Constantin)</b> .....	22
2-3-3 <b>T-type thermocouple (copper / constantanne)</b> .....	22
2-3-4 <b>E-type thermocouple (nickel-chrome / constantanne)</b> .....	22
2-3-5 <b>N-type has similar properties to type K but is more stable</b> .....	23
2-3-6 <b>Type R, S and B thermocouples (precious metal thermocouples)</b> .....	23
2-3-7 <b>S-type thermocouple (platinum rhodium - 10% / platinum)</b> .....	23

2-4 Power Supply.....	24
2-5 USB 2.0 CABLE TYPE.....	24
2-6 Sensor max6675 type. K.....	25
2-7 Jumping wires.....	27
2-8 Breadboard.....	27
2-9 PVC BOX.....	28
2-10 Software.....	29
<b>Chapter three.....</b>	<b>41</b>
3-1 Practical experiment.....	41
3-2 Temperature readings table.....	44
<b>Chapter four.....</b>	<b>46</b>
4-1 Conclusion.....	46
4-2 Future work.....	47
<b>Reference .....</b>	<b>52</b>

### *Abstract*

In this project, a device was manufactured to measure the temperature with high accuracy and transport it on the computer and record readings and store them when measuring the temperature of the surrounding air or water.

Temperature is one of the determining factors in every aspect of life it is necessary to be able to measure with high accuracy.

Was used k-type thermocouple and a max 6675 thermocouple chip, which is characterized by communication and self-calibration, and an electronic circuit board (Arduino Mega 6025) powered by a 5 volt power supply and (Arduino) is an open source circuit with a microcontroller programmed by computer The programming code is entered using 6 thermal sensors of type k and max6675 side by side and sensing the ambient air for a period of 00:00:01:643 second to raise the accuracy of the thermal sensors of type k and max 6675. With a simple technique, calibration and data analysis is done through the electronic circuit (Arduino). The readings were recorded on the computer screen for each sensor, and the average of the readings was taken for each sensor.

This study aimed to record temperature and reading time history used by thermal sensors of type k and sensors of type max6675 to read different temperature values and using (Arduino) microprocessor.

# CHAPTER ONE

## INTRODUCTION

### 1.1 Introduction

Data acquisition (commonly abbreviated as DAQ or DAS) is the process of sampling signals that measure real-world physical phenomena and converting them into a digital form that can be manipulated by a computer and software.

DAQ is the process of measuring an electrical or physical phenomenon, such as voltage, current, temperature, pressure, or sound. A DAQ system consists of sensors, DAQ measurement hardware, and a computer with programmable software.

A typical Data Acquisition System consists of individual sensors with the necessary signal conditioning, data conversion, data processing, multiplexing, data handling and associated transmission, storage and display systems. In order to optimize the characteristics of the system in terms of performance, handling capacity and cost, the relevant sub systems can be combined together. Analog Data Acquisition System is generally acquired and converted into digital form for the purpose of processing, transmission, display and storage.

We can create our own DAQ using Arduino. As a converter to read from one or more sensors and convert the reading to an initial measurement value, many DAQs can be programmed to read over different time intervals, at certain data rates.

Using a Type K thermocouple and a Max 6675 sensor, the thermocouple consists of two different types of metals connected together at one end. When the junction of the two metals is heated or cooled, a voltage is created that can be linked back to the temperature. Thermocouples are commonly used in a wide variety of applications.

Data may be transmitted over long distances (from one point to another) or short distances (from test Centre to a nearby PC). [1]

## 1.2 Fundamentals of Data Acquisition Systems

Data acquisition (DAQ) systems are the main instruments used in laboratory research from scientists and engineers; in particular, for test and measurement, Automation, and so on. Typically, DAQ systems are general-purpose DAQ instruments that are well suited for measuring voltage or current signals. However, Many sensors and transducers output signals must be conditioned before that a board Can acquire and transform in digital the signal. The basic elements of DAQ are Shown in Fig. 1.1 and are:

- Sensors and transducers
- Field wiring
- Signal conditioning
- DAQ hardware
- DAQ software
- PC (with operating system)

### 1.2.1 Components of Data Acquisition System

Modern digital data acquisition systems consist of four essential components that form the entire measurement chain of physics phenomena:

- Sensors
- Signal Conditioning
- Analog-to-Digital Converter
- Computer with DAQ software for signal logging and analysis

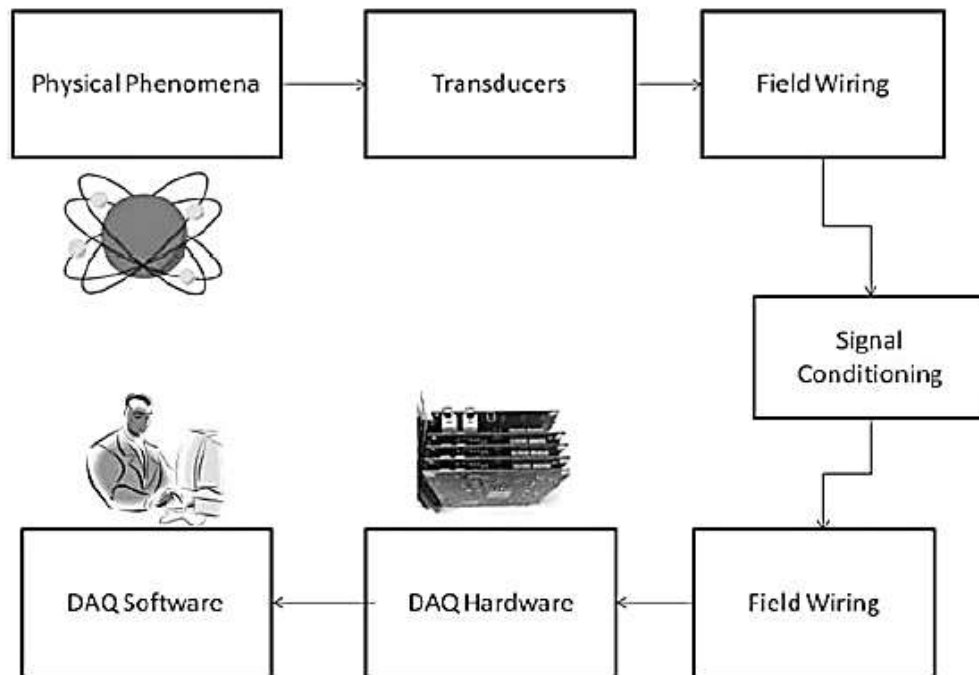


Fig. 1.1 Functional diagram of a PC-based data acquisition system

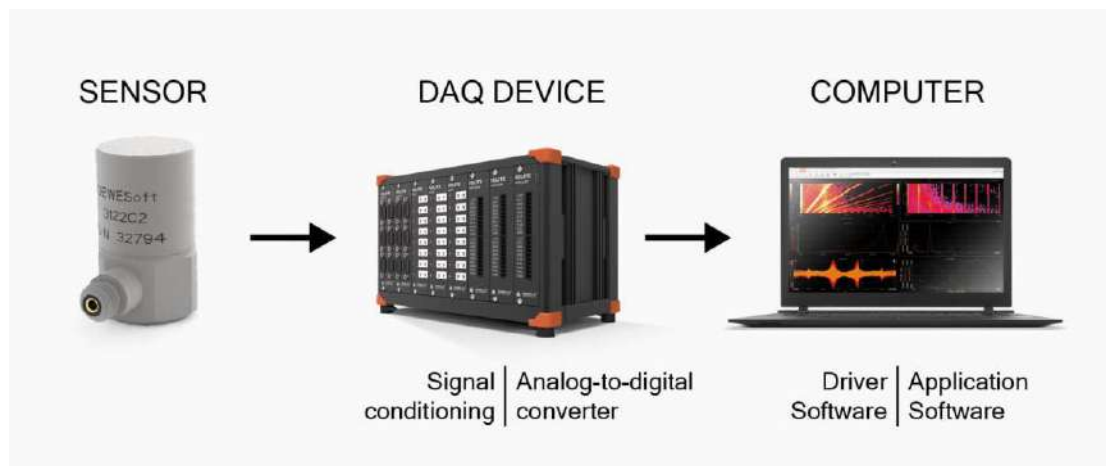


Figure 1.2. Data acquisition system block diagram and the elements of the modern digital data acquisition system.

Transducers can be used to detect a wide range of different physical phenomena

Such as movement, electrical signals, radiant energy, and thermal, magnetic, or mechanical energy. They are used to convert one kind of energy into another kind.

The type of input or output of the transducer used depends on the type of signal detected or process controlled; in other ways, we can define a transducer as a device that converts one physical phenomena into another one. Devices with input function are called sensors because they detected a physical event that changes according to. [2]

### 1.3 Sensors and Transducers

Transducers and sensors are used to convert a physical phenomenon into an electrical signal (voltage or current) that will be then converted into a digital signal used [2] for the next stage such as a computer, digital system, or memory board.

#### 1.3.1 Temperature Sensors

Several techniques for detection of temperature are currently used. The most common of these are resistance temperature detectors (RTDs), thermocouples, thermistors, and sensor ICs. The choice of one for your application can depend on some factors such as: required temperature range, linearity, accuracy, cost, and features.

#### 1.3.2 *Magnetic Field Sensors*

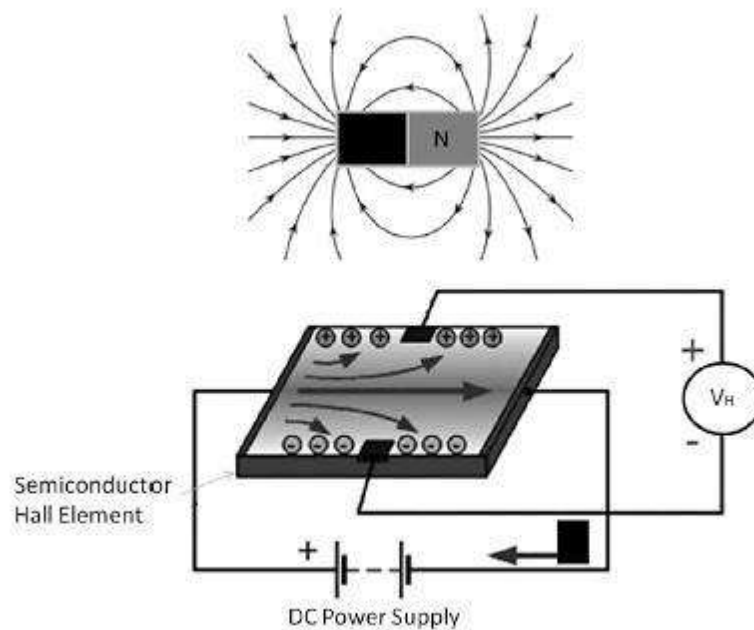
Magnetic sensors convert magnetic energy into electrical signals for processing by electronic system. Magnetic sensors are designed to respond to a wide range of magnetic field; they are mainly used in different applications, in particular in automotive systems for the sensing of position, distance, and speed.

#### 1.3.3 Potentiometers

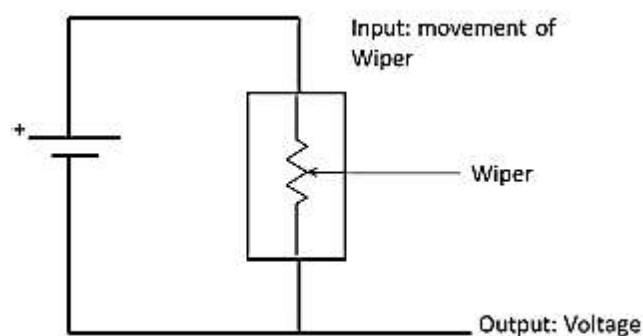
A potentiometer is an electromechanical device that contains a movable wiper arm with the goal of maintaining electrical contact with a resistive surface; the wiper is coupled mechanically to a movable linkage. It gives a voltage signal by divider circuit when voltage is applied across the entire resistance within the potentiometer.

### 1.3.4 Light Detection

Light sensors detect light emitted or given off from an object, such as LED, reflected from surfaces, transmitted from electronics device, and so on. LED or light emitting diode is a solid-state semiconductor that emits light when current passes through it in the forward direction as in the figure below.



**Fig. 1.2** Hall effect sensor



**Fig. 1.3** Potentiometers

Figure 1.3 (Light Detection)



#### 1.4 The Purposes of Data Acquisition

The primary purpose of a data acquisition system is to acquire and store the data. But they are also intended to provide real-time and post-recording visualization and analysis of the data. Furthermore, most data acquisition systems have some analytical and report generation capability built-in.

A recent innovation is the combination of data acquisition and control, where a high-quality DAQ system is connected tightly and synchronized with a real-time control system. You can read more about this topic in the related article: “Merging Data Acquisition with a Real-Time Control System”.

Engineers in different applications have various requirements, of course, but these key capabilities are present in varying proportion:

- Data recording
- Data storing
- Real-time data visualization
- Post-recording data review
- Data analysis using various mathematical and statistical calculations
- Report generation

#### 1.5 Objectives of Data Acquisition

- It must acquire the necessary data, at correct speed and at the correct
- Use of all data efficiently to inform the operator about the state of the
- It must monitor the complete plant operation to maintain on-line optimum and safe operations.

- It must provide an effective human communication system and be able to identify problem areas, thereby minimizing unit availability and maximizing unit through point at minimum cost.
- It must be able to collect, summarise and store data for diagnosis of operation and record purpose.
- It must be able to compute unit performance indices using on-line, real-time data.
- It must be flexible and capable of being expanded for future require
- It must be reliable, and not have a down time greater than 0.1%.

## 1.6 General Configuration of Data Acquisition System

### 1. Single channel possibilities

Direct conversion

Pre-amplification and direct conversion

Sample and hold, and conversion

Pre-amplification, signal conditioning and any of the above.

### 2. Multi-channel possibilities

Multiplexing the outputs of single channel converters.

Multiplexing the output of sample-hold circuits.

Multiplexing the inputs of sample-hold circuits.

Multiplexing low level data. [3]

## CHAPTER TWO

### Experimental Setup

This chapter consists of the experimental preparation of the project and the experimental apparatus as it consists of:

**Hardware**

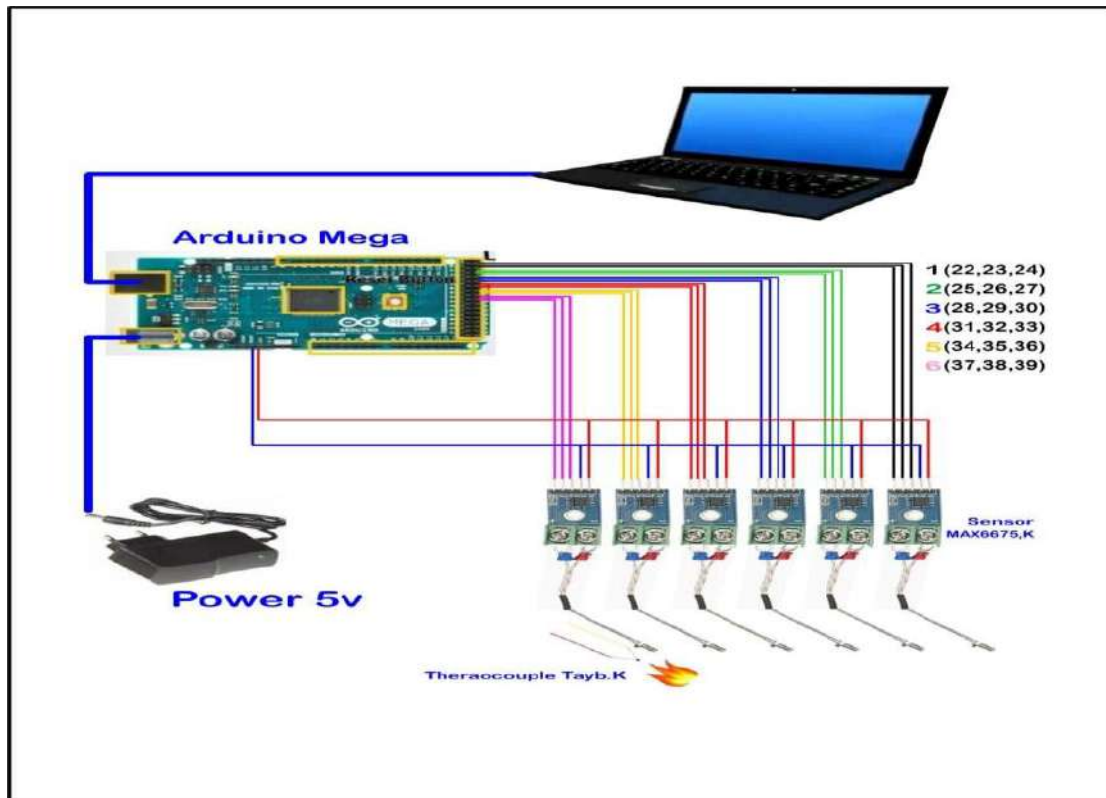
**Software**

#### 2-1 Hardware (components)

Hardware of the experimental setup consist of as shownen in figures.

1. ARDUINO MEGA 2560
2. Max 6675 type K
3. 6-Thermocouple K-Type
4. GLCD 12864
5. Power Supply
6. USB 2.0 CABLE TYPE
7. Jumping wires
8. Breadboard
9. PVC BOX

**Figure( 2-1) Device components connection diagram**



The Arduino is fed to a 5V supply as shown in the figure.

The red wire (+) is connected to Pin 5V and the blue wire to pin GND (-).

And the red and blue wires are connected to sensor No. 1 and fed to the rest of the sensors by connecting in parallel with all sensors via PIN No. 1 GND and 2 VIN.

Wires are connected from the first sensor via PIN 3 SCK, PIN 4 CS, and PIN 5 SO and connected to the Arduino and connected in PIN No. 22,23,24 indicated in black as in the figure 2-1.

The rest of the sensors are connected according to the diagram in the above diagram.

The programming is done and the information is transferred via the Arduino to the computer by using USB cable and the readings are taken with high accuracy for each sensor.

The components are assembled inside the BOX as shown in the figure 2-2.

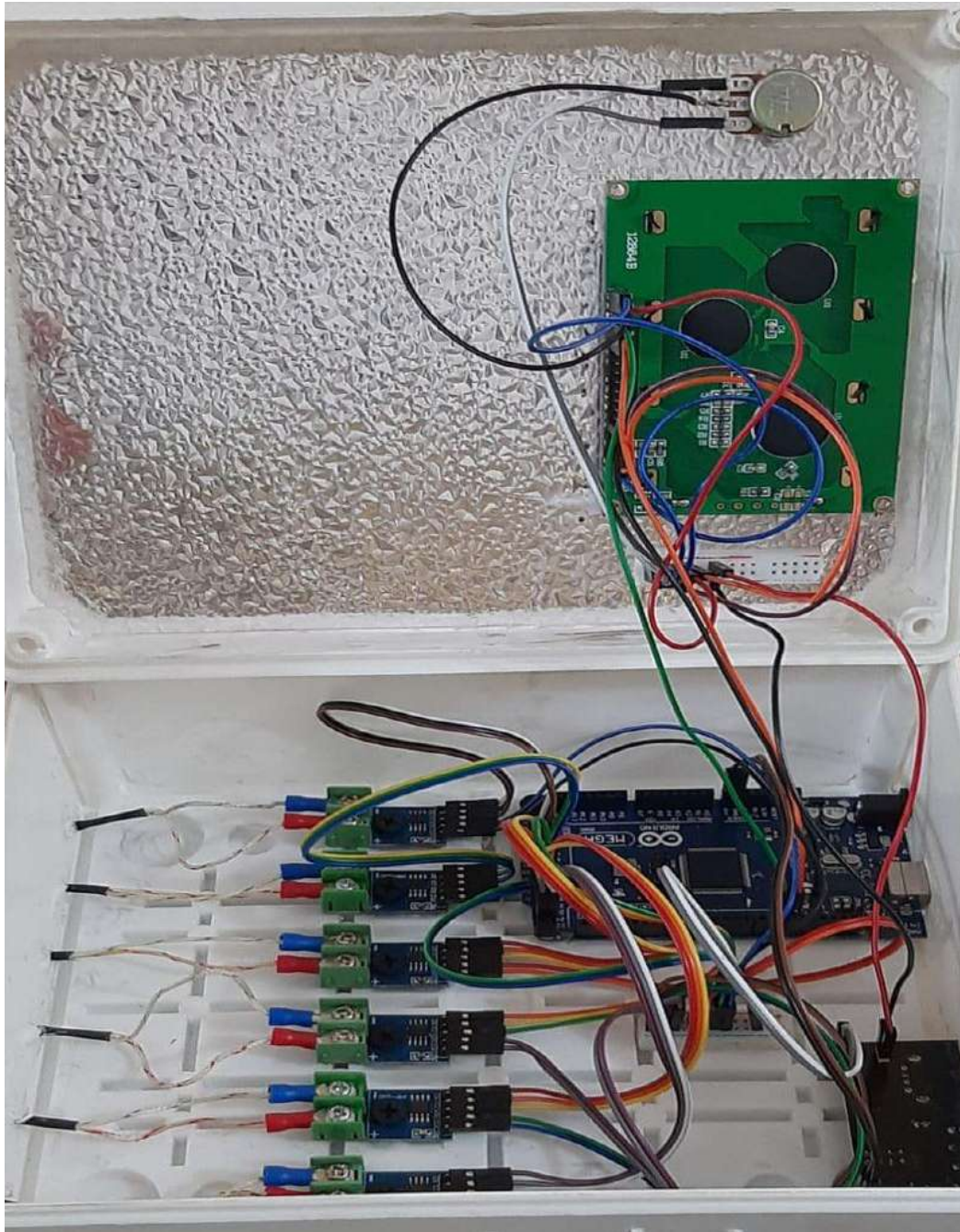


Figure 2.2

(The form of connecting the components of the device)

A GLCD 12864 screen was added to the device and it became possible to read the temperatures on the screen after it was programmed by its code in sequence 24 in the programming codes. The wires were connected between the Arduino and the screen and a lighting controller was added. The device was assembled and the final form as in the figure 2-3.



Figure 2.3 ( The final shape of device)



2-1-1

### ARDUINO MEGA 2560

They are small computers that can interact and control the surrounding environment better than a desktop computer, and the strength of Arduino is reflected in its ability to communicate with other electronic devices such as switches and sensors to take advantage and obtain data such as temperature, humidity, intensity of light and its characteristics Great effectiveness in controlling motors and photodiodes. And the Arduino connects it to the computer and makes it deal with one of the existing programs and can run independently, as shown in Figure 2.4 and figure 2.5. [4]



Figure 2.4 (ARDUINO MEGA 2560)

The Arduino Mega is a microcontroller board containing 54 digital I/O pins (15 of which can be used as PWM outputs), 16 analog inputs, 4 (hardware serial ports), a 16MHz crystal oscillator, a link (USB), and a power socket, and a reset button. It contains everything needed to support the microcontroller; simply connect it to a computer with a USB cable or run it on a DC adapter or battery to start programming. [4]

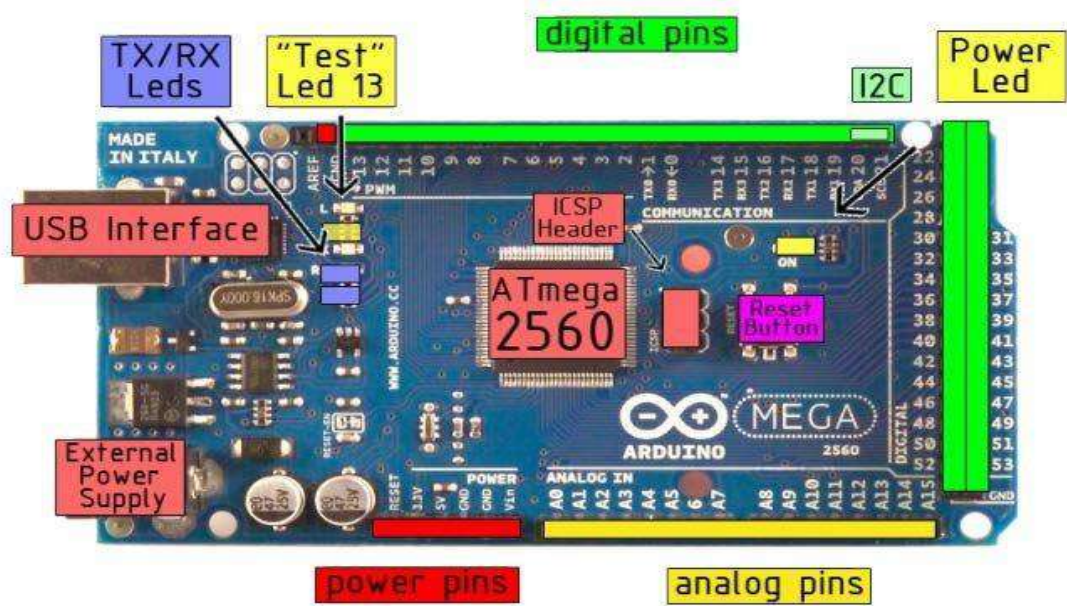


Figure 2.5 (ARDUINO MEGA 2560)

And this specification are presented in table 2.1.



Table 2.1 Specifications

Microcontroller	A Tmega2560
Operating voltage	5V
Input voltage (recommended)	7-12V
Input voltage (limits)	6-20V
Digital I/O Pins	54(of which 14 provide PW output)
Analog Input Pins	16
DC Current per/O Pin	40 mA
DC current for 3.3V Pin	50 mA
Flash Memory	256 KB of which 8 KB used by boot loader
SRAM	8 KB
EEPROM	4 KB
Clock Speed	16 MHz

## 2-1-2 Types of Arduino

### 2-1-3 Arduino UNO R3

The most famous type of Arduino board, we have explained it and presented its pictures in detail previously. Most of this book will focus on it. The most important feature of this board is the possibility of replacing the microcontroller chip. This allows you to repair your own circuit after programming the chip as shown in figure 2.6. [5]

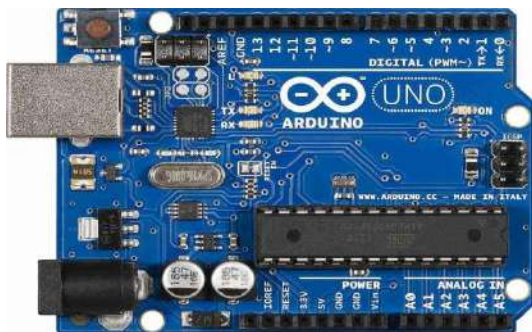


Figure 2.6 (Arduino UNO R3)

### 2-1-4 Arduino Leonardo

It does not differ in anything from the Arduino UNO except that the microcontroller chip is installed and cannot be replaced as shown in figure 2.7. And the USB port used is micro USB, not USB type B like before. Its price is cheaper than UNO too. [5]



Figure 2.7 (Arduino Leonardo)

### 2-1-5 [Arduino YUN](#)

The YUN is characterized by being integrated with WiFi. The "Yun" also provides advanced programming options in the Linux system, but programming to "Yun" is usually like any Arduino using the Arduino IDE programming program. It can also be programmed wirelessly if WiFi is defined on the same network as the computer. When you start the Boon, it will create a wireless network called arduino Yun Connect to it, enter the browser and then enter the address 192.168.240.1 and enter the password: arduino You will be faced with a page with the Yun settings. as shown in figure 2.8. [5]



Figure 2.8 ([Arduino YUN](#))

### 2-1-6 [Arduino Due](#)

Arduino Due is similar to Mega in size and number of ports. But it has a different processor that works at a higher speed (84MHz) and it works on a voltage of 3.3V and not 5V like the rest of the Arduino. This makes some additional circuits not working on the Arduino Due.

Small versions of the Arduino Micro, Nano, Mini

In some applications, you will need to make the circuit as small as possible. There are many smaller models of Arduino, and their drawback is the difficulty of using the usual shields with them. Note here you will place the products of the parent company Arduino. We will not include the types produced by other companies. as shown in figure 2.9. [5]



Figure 2.9 ([Arduino Due](#))

### 2-1-7 [Arduino Micro](#)

Dimensions: 48 \* 18 mm

Digital Ports: 20 of which are 7 pwm

Analogue Inputs: 12 [5]

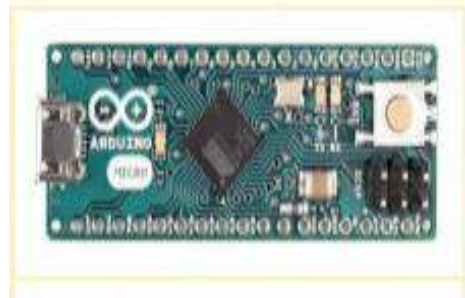


Figure 2.10 ([Arduino Micro](#))

as shown in figure 2.10

### 2-1-8 [Arduino Nano](#)

Dimensions: 45 \* 18 mm

Digital Ports: 22 of which 6 pwm

Analogue Inputs: 6 [5]

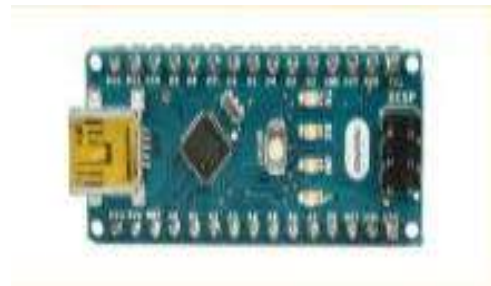


Figure 2.11 ([Arduino Nano](#))

as shown in figure 2.11

### 2-1-9 [Arduino Mini](#)

Dimensions: 30 \* 18 mm

Digital ports 14 of which 6 pwm

Analogue Inputs: 8 [5]



Figure 2.12 ([Arduino Mini](#))

as shown in figure 2.12

Note: The mini cannot be connected to the computer directly, an intermediate circuit must be used.

Note: For each type, you must know the distribution of the terminals, the location of the analog outlets, the location of the power supply terminals, and so on.

The GLCD12864 is a 2.7- inch 128×64 Graphical LCD display module which is the graphical upgrade to those popular 16×2 LCDs, but allows full graphical control. It communicates via 8080 8-bit parallel interface and negative voltage built in on module. This 128 x 64 LCD module can be operating at temperatures from -20°C to +70°C; its storage temperatures range from -30°C to +80°C. as shown in figure 2.13.



Figure 2.13 (**GLCD 12864**)



2-3

### Thermocouple K-Type

K type thermocouple (nickel-chromium/nickel-alumel)

This is the most common type of thermocouple with a wide range of measurement ranging from -200 to 1350°C

K-type thermocouple temperature range: -200 to 1350 °C

K-type wiring temperature range: 0°C to 200°C. as shown in figure 2.14.



Figure 2.14 (Thermocouple K-Type)

#### The method of work

The doublet consists of two different metals joined together at the end of the doublet.

When a thermal difference occurs at the end of the doublet, which in turn contains the two ends of the two different metals, an electrical tension is formed proportional to the heat passing through each of the metals. The hotter the metal, the more electric current is generated. In this way, each end of the metal passes a different temperature than that of the other metal, and two different electric currents are reached at the other end. At this end, which connects the two metals together, an electric potential is generated due to the difference in current.

An electronic component measures this generated voltage, and converts its value as needed into a heat value that appears on a display screen, or passes the value to another component for use in another standard machine or the like. [6]

## Advantages of thermocouple

Ease of manufacture. •

- Standard wide temperature range.

It does not need an external power source to operate. •

It does not depend on a specific type of wire. •

- The resistance of the used wires does not affect the quality of the measurement.

## Disadvantages of thermocouple

- Small values of electro-thermal current generated.

- Difficulty in correcting the value of the error in the measurement.

- Difficulty in welding wires consisting of the aforementioned metals.

- The danger that dirt or rust takes place between the object to be measured and the pair, so the measured value is affected.

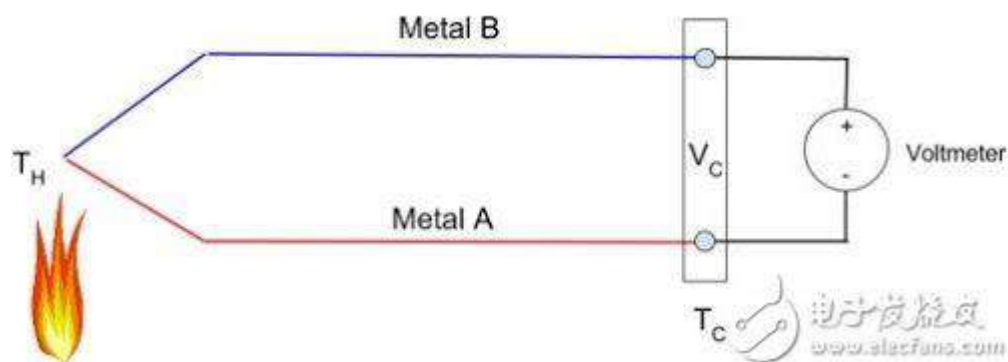


Figure 2.15 (Temperature to voltage conversion chart.)



### 2-3-1 Types of Thermocouple

#### 2-3-2 J-Type Thermocouple (Iron/Constantine)

These also can be used in a wide range of temperatures, but have a shorter life at higher temperatures.

J-type thermocouple temperature range: -210 to 760°C

J-type wiring temperature range: 0°C to 200°C. as shown in figure 2.16.



Figure 2.16 (J-Type Thermal Double)

#### 2-3-3 T-type thermocouple (copper / Constantine)

This type is especially for sub-zero applications as it gives the best results

The temperature range of a T-type thermocouple is: -270 to 370 degrees Celsius

T-type wiring temperature range: 0°C to 200°C

#### 2-3-4 E-type thermocouple (nickel-chrome / Constantine)

Type E is more accurate at medium temperatures

-The temperature range of an E-type thermocouple is: -270 to 870°C

E-Type Wiring Temperature Range: 0°C to 200°C

Double Thermal Type (Nicursil / Nesyl) [7]

2-3-5 N-type has similar properties to type K but is more stable.

The most effective temperature range for N-type thermocouple: 270 to 392°C

The temperature range of N-type wiring is 0 to 200°C.

as shown in figure 2.17.



Figure 2.17 (N-type thermocouple)

2-3-6 Type R, S and B thermocouples (precious metal thermocouples)

These are known as precious metal thermocouples and are very expensive. This is especially suitable for applications at very high temperatures

The most effective temperature range for precious metal thermocouples: 600 to 1300°C

2-3-7 S-type thermocouple (platinum rhodium - 10% / platinum)

This type is used when stable results are desired over a very wide temperature range with evenly accurate results. The temperature range of an S-type thermocouple is: -50 to 1480°C, S-type wiring temperature range: 0°C to 200°C. as shown in figure 2.18. [7]



Figure 2.18 (S-type thermocouple)

## 2-4

### Power Supply

Electronic component kit for beginners has a complete set of accessories that can be used for Arduino R3, which can meet your needs.

Comes with breadboard and power supply module, various LEDs, resistors, buttons, capacitors, some transistors and diodes. as shown in figure 2.19.

All parts and components are clearly listed in a box, easy to carry and store.

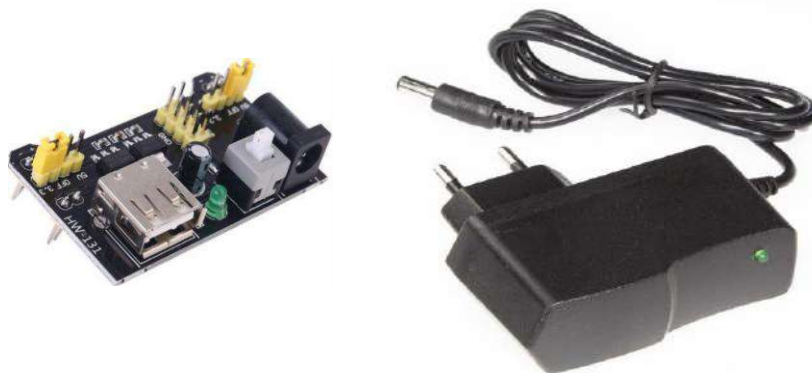


Figure 2.19 (Power Supply)

## 2-5

### USB 2.0 CABLE TYPE A/B

Use it to connect Arduino Uno, Arduino Mega 2560, Arduino 101 or any board with the USB female a port of your computer. as shown in figure 2.20.



Figure 2.20 (USB 2.0 CABLE TYPE)

## 2-6 Sensor max6675 type.k

MAX6675 K-Type Thermocouple Temperature Sensor performs cold-junction compensation and digitizes the signal from a type-K thermocouple. The data is output in a 12-bit resolution, SPI™-compatible, read-only format.

MAX6675 converter resolves temperatures to 0.25°C, allows readings as high as +1024°C, and exhibits thermocouple accuracy of 8 LSBs for temperatures ranging from 0°C to +700°C. as shown in figure 2.21.

### Specification of MAX6675 K-Type Thermocouple Temperature Sensor:

- Working Voltage: DC 5V
- Operating Current: 50 mA
- Test Temperature Range: 0°C – 1024°C, the converter temperature resolution is 0.25°C
- The Temperature Measurement Accuracy: +/-1.5C
- The Temperature Resolution : 0.25C
- The Output mode: SPI digital signal
- With a Fixing hole for easy to fix and install. [8]

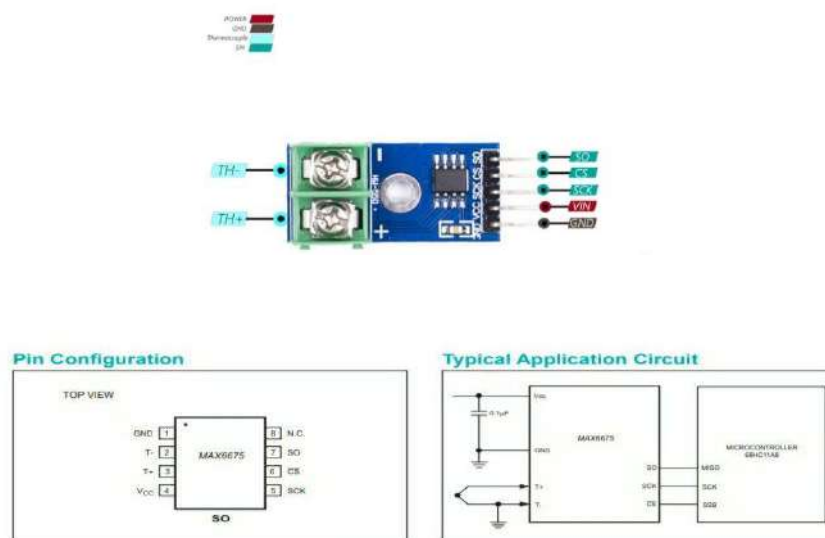


Figure 2.21 (Sensor max6675 type. k)

### 2-6-1 Types of Sensors

There are many different types of sensors, each of which is used for a specific purpose or application and to measure a specific physical quantity. as shown in figure 2.22. [8]



(Ultrasonic-sensor –HC-SR04)

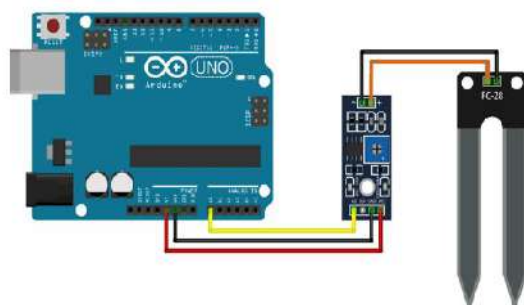


(Gas sensors-MQ2)

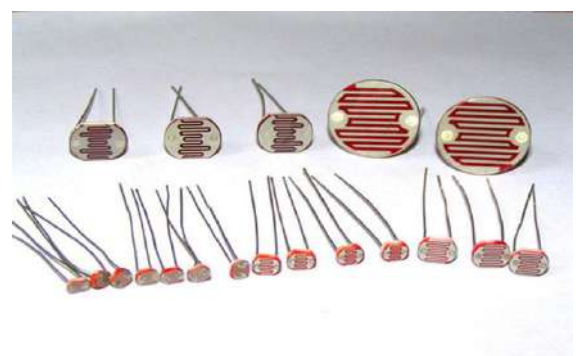


(IR-sensor)

(Tilt-sensor)



Soil Moisture sensor



(Light- dependent sensor)

Figure 2.22 (Types of Sensors)

## 2-7 **Jumping wires**

A **jump wire** (also known as jumper, jumper wire, jumper cable, DuPont wire or cable) is an electrical wire, or group of them in a cable, with a connector or pin at each end (or sometimes without them – simply "tinned"), which is normally used to interconnect the components of a breadboard or other prototype or test circuit, internally or with other equipment or components, without soldering.

Individual jump wires are fitted by inserting their "end connectors" into the slots provided in a breadboard, the header connector of a circuit board, or a piece of test equipment. as shown in figure 2.23.



Figure 2.23 (**Jumping wires**)

## 2-8 **Breadboard**

It is a flat plate used as a base for connecting electronic components to build electronic circuits. and prototyping of electronic devices. It is solderless and reusable, which makes it easy to use to create temporary prototypes and circuit design experiments. as shown in figure 2.24.

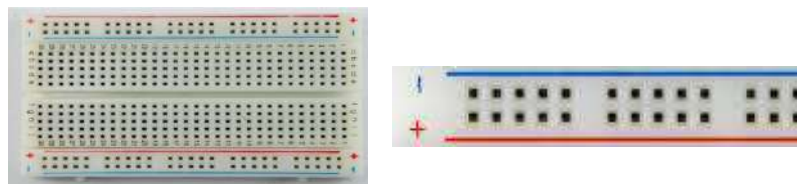


Figure 2.24 (**Breadboard**)

## 2-9 **PVC BOX**

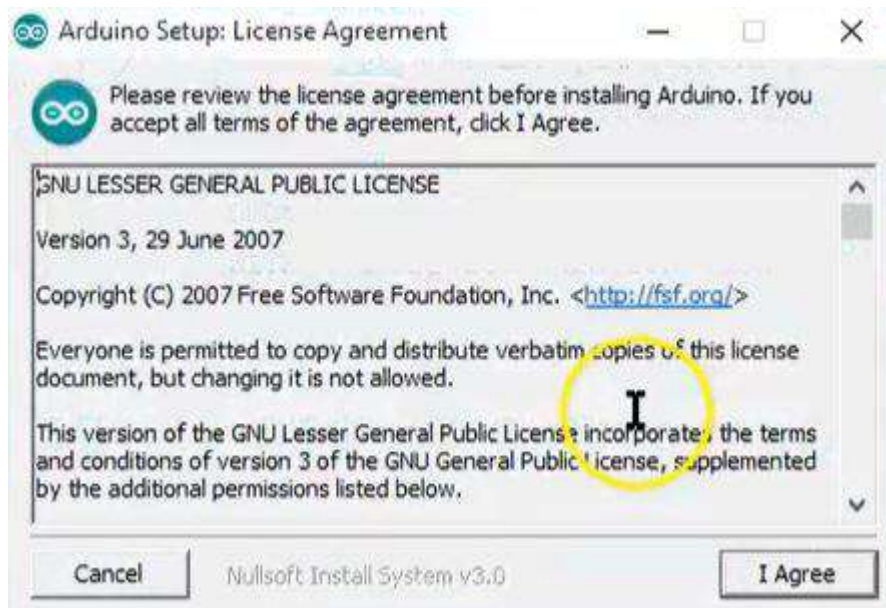
Electrical junction boxes are simply standard electrical boxes that house and protect the connections of two or more circuit cables or wires. Junction boxes are the communal meeting spot for electrical wires--- where they connect before moving in different directions through conduit and other electrical fittings. as shown in figure 2.25.



Figure 2.25 (PVC BOX)

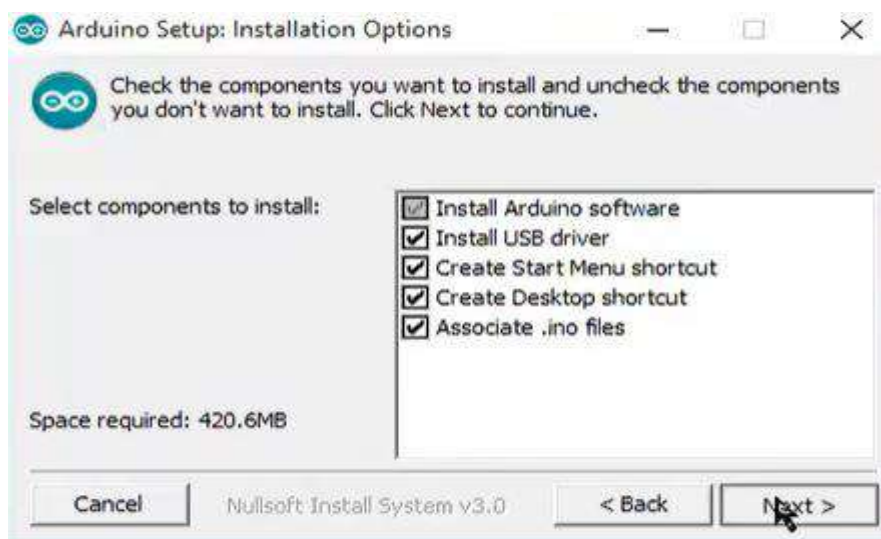


- 1) Visit the website and download the Arduino software.
- 2) Save the .exe file. on the hard disk.
- 3) Open the .exe file. which was downloaded.
- 4) Click I Agree.



- 5) Installation components:

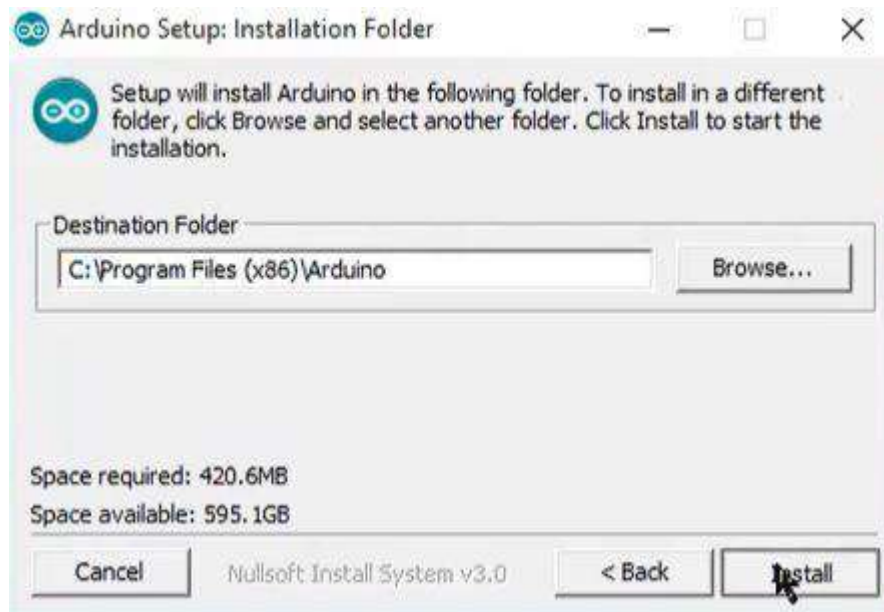
Select the components to be installed, then click Next.



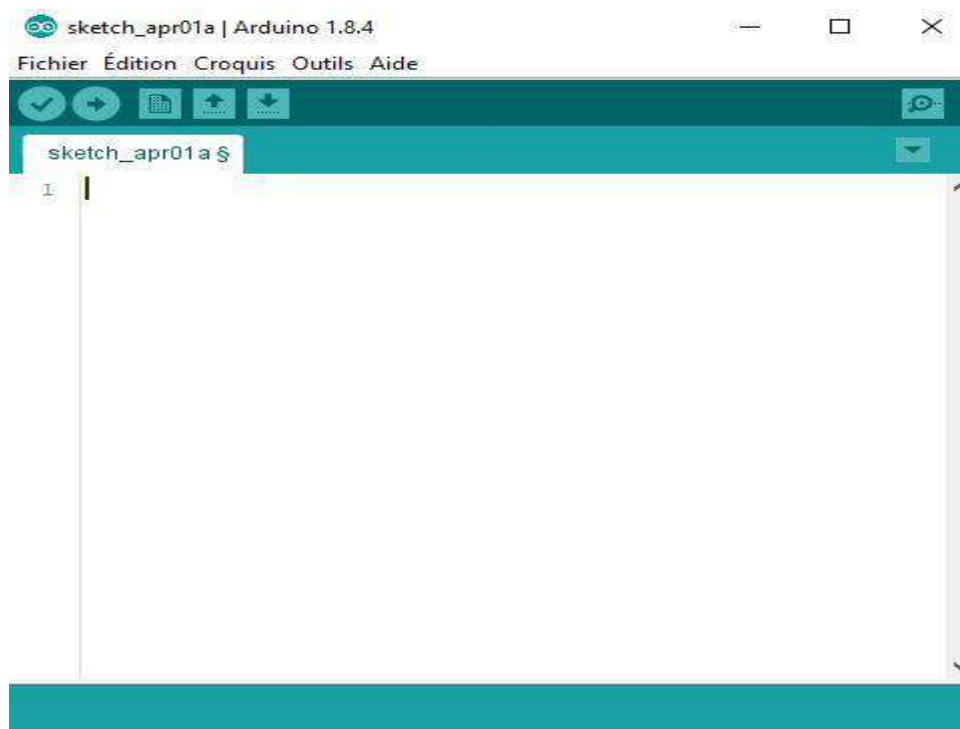
- 6) Choose the installation location



Select the folder where you want to install the program, then click “Install”.



7)Open the program:



We will put the basic commands in the Arduino programming regarding the project in order to write the code.

The goal is to measure the ambient temperature using the thermocouple and a sensor (Max 6675,k), where the sensor gives ready numbers to the Arduino through the chip in the sensor after receiving it from the thermocouple, which consists of two different types of metals connected together in One end when the junction of the two metals is heated or cooled.

The Data Acquisition (DAQ) information is collected from temperature sensors.

This is done by programming the Arduino Mega by entering the programming code.

Relying on libraries written from the community to avoid having to write driver code to communicate with the sensors which saves us time.

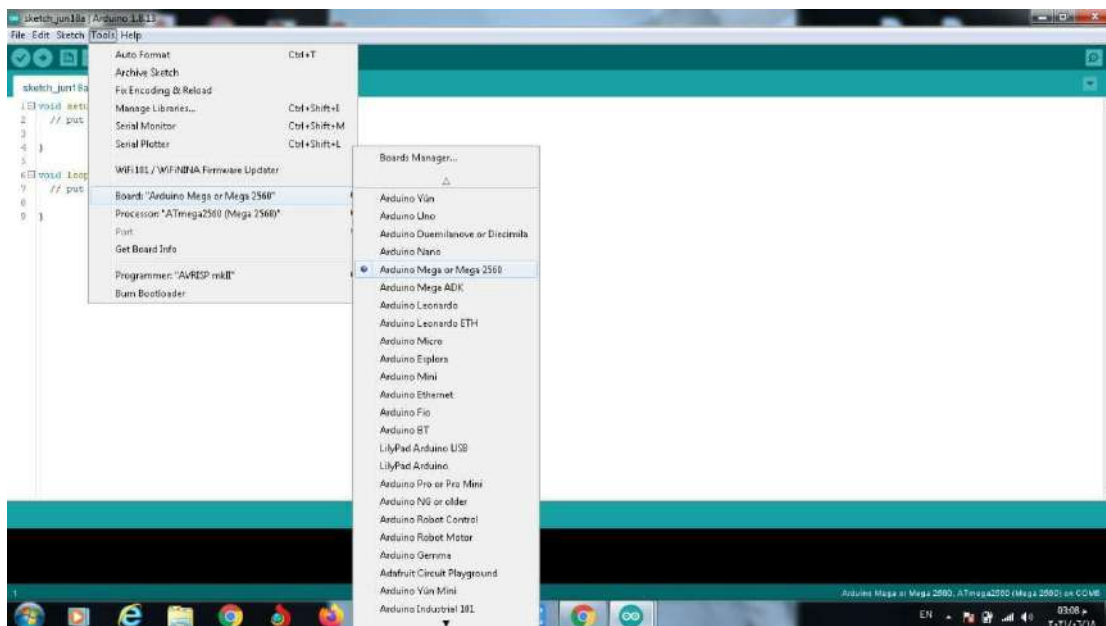
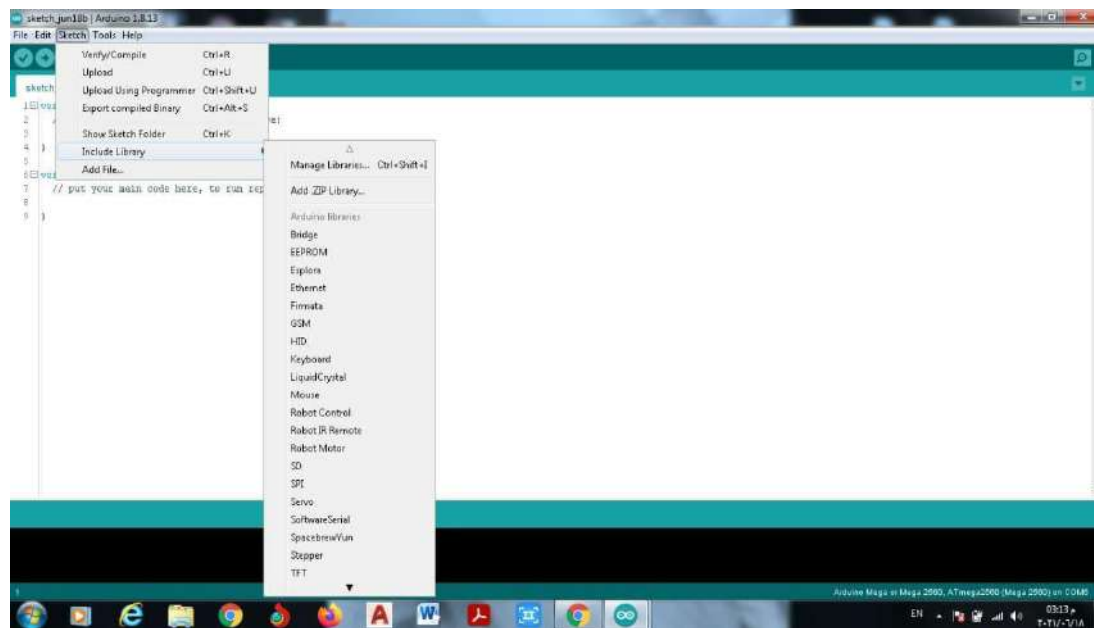
After entering the Arduino programming code, the data is collected from the 6 temperature sensors (Max 6675).

The data is read in the form of numbers to measure temperatures on the computer directly, and the readings are taken for each sensor within 15 seconds, and the average value is given to each sensor.

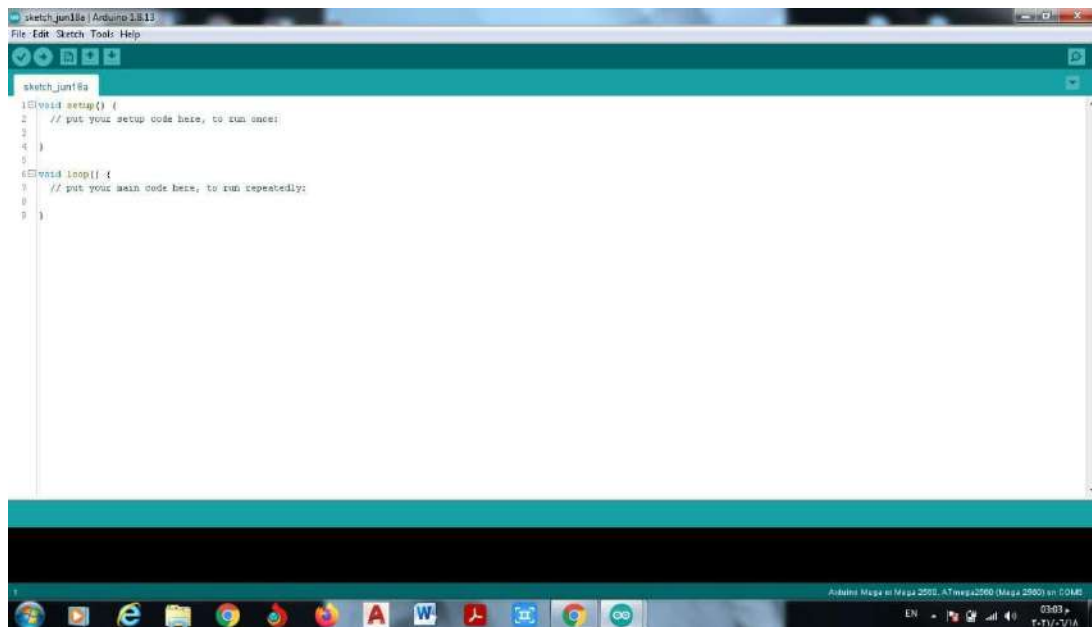
After installing the program on the computer, the manufacturer has put free programming through the library by giving the ready-made code and the basic commands in programming the Arduino in a short and easy way for free. As shown in the figure below.

And you can choose the Arduino for your project according to the list in the figure below.

We used (Arduino Mega2560) in our project



Enter the programming code



After this window appears

We use void loop. The commands between parentheses will be executed repeatedly as long as the Arduino is running.

```
serialthermocouple
1 #include "max6675.h"
2
3 #include <Arduino.h>
4 #include <U8g2lib.h>
5 #ifdef U8X8_HAVE_HW_SPI
6 #include <SPI.h>
7 #endif
8 #ifdef U8X8_HAVE_HW_I2C
9 #include <Wire.h>
10 #endif
11
12 MAX6675 thermocouple_1(22, 23, 24);
13
14 MAX6675 thermocouple_2(25, 26, 27);
15
16 MAX6675 thermocouple_3(28, 29, 30);
17
18 MAX6675 thermocouple_4(31, 32, 33);
19
20 MAX6675 thermocouple_5(34, 35, 36);
21
22 MAX6675 thermocouple_6(37, 38, 39);
23
24 U8G2_ST7920_128X64_1_SW_SPI u8g2(U8G2_R0, /* clock=*/ 13, /* data=*/ 11, /* CS=*/ 10, /* reset=*/ 8);
25
26 const char s[] PROGMEM = "Avg for 6 sensor...";
27
28 void setup() {
```

From sequence 1 to sequence 10 are library commands for the manufacturer and are ready to enter the code for programming the Arduino Mega and can be added to it.

From sequence 11 to sequence 22, the code is entered to communicate information from the sensor to the Arduino.

And sequence 24 is for programming the GLCD 12864 screen.

```
serialthermocouple
28 void setup() {
29     u8g2.begin();
30     Serial.begin(9600);
31     delay(500);
32 }
33
34
35 float sensor_1[30];
36 float sensor_2[30];
37 float sensor_3[30];
38 float sensor_4[30];
39 float sensor_5[30];
40 float sensor_6[30];
41
42 float avg_c = 0;
43 float avg_f = 0;
44
45 int counter = 0;
46
47 void loop() {
48     if(counter < 30){
49         sensor_1[counter] = thermocouple_1.readCelsius();
50         sensor_1[counter+1] = thermocouple_1.readFahrenheit();
51
52         sensor_2[counter] = thermocouple_2.readCelsius();
53         sensor_2[counter+1] = thermocouple_2.readFahrenheit();
54
55         sensor_3[counter] = thermocouple_3.readCelsius();
```

From sequence 35 to 40 is intended to store 30 containers at a rate of 15 Celsius and 15 Fahrenheit.

From sequence 42 and 43 it is for the average temperature gauge of each sensor per second.

Fahrenheit.

Celsius.

From the sequence 48 is a counter for the temperature in Celsius and Fahrenheit and the code was written to the sequence 66.

Sequence 68 is the delay of 1000 per/s .

```

serialthermocouple
55     sensor_3[counter] = thermocouple_3.readCelsius();
56     sensor_3[counter+1] = thermocouple_3.readFahrenheit();
57
58     sensor_4[counter] = thermocouple_4.readCelsius();
59     sensor_4[counter+1] = thermocouple_4.readFahrenheit();
60
61     sensor_5[counter] = thermocouple_5.readCelsius();
62     sensor_5[counter+1] = thermocouple_5.readFahrenheit();
63
64     sensor_6[counter] = thermocouple_6.readCelsius();
65     sensor_6[counter+1] = thermocouple_6.readFahrenheit();
66     counter+=2;
67
68     delay(1000);
69
70
71
72 }
73
74 else{
75 //screen code here:
76     u8g2.firstPage();
77     do{
78         printlcdSensor("1");
79         printlcdSensor("2");
80         printlcdSensor("3");
81         printlcdSensor("4");
82         printlcdSensor("5");

```

```

serialthermocouple
82     printlcdSensor("5");
83     printlcdSensor("6");
84     } while ( u8g2.nextPage() );
85
86     //Serial print here:
87     newScreen();
88     printSensor("1");
89     printSensor("2");
90     printSensor("3");
91     printSensor("4");
92     printSensor("5");
93     printSensor("6");
94
95 }
96 }
97
98
99 void prepareTable(){
100 // Serial.println(" Sensor          Second -01-          Second -02-          Second
101 // Serial.println("#####");
102 }
103
104
105 void printSensor(String sensorNumber){
106
107     counter = 0;
108     float avg_c = 0;
109     float avg_f = 0;

```



```

serialthermocouple
109 float avg_f = 0;
110
111 Serial.print("Sensor_"+sensorNumber);
112 for(counter; counter < 30; counter+=2){
113
114     if(sensorNumber == "1"){
115         avg_c+=sensor_1[counter];
116         avg_f+=sensor_1[counter+1];
117
118     }else if(sensorNumber == "2"){
119         avg_c+=sensor_2[counter];
120         avg_f+=sensor_2[counter+1];
121
122     }else if(sensorNumber == "3"){
123         avg_c+=sensor_3[counter];
124         avg_f+=sensor_3[counter+1];
125
126     }else if(sensorNumber == "4"){
127         avg_c+=sensor_4[counter];
128         avg_f+=sensor_4[counter+1];
129
130     }else if(sensorNumber == "5"){
131         avg_c+=sensor_5[counter];
132         avg_f+=sensor_5[counter+1];
133
134     }else if(sensorNumber == "6"){
135         avg_c+=sensor_6[counter];
136         avg_f+=sensor_6[counter+1];

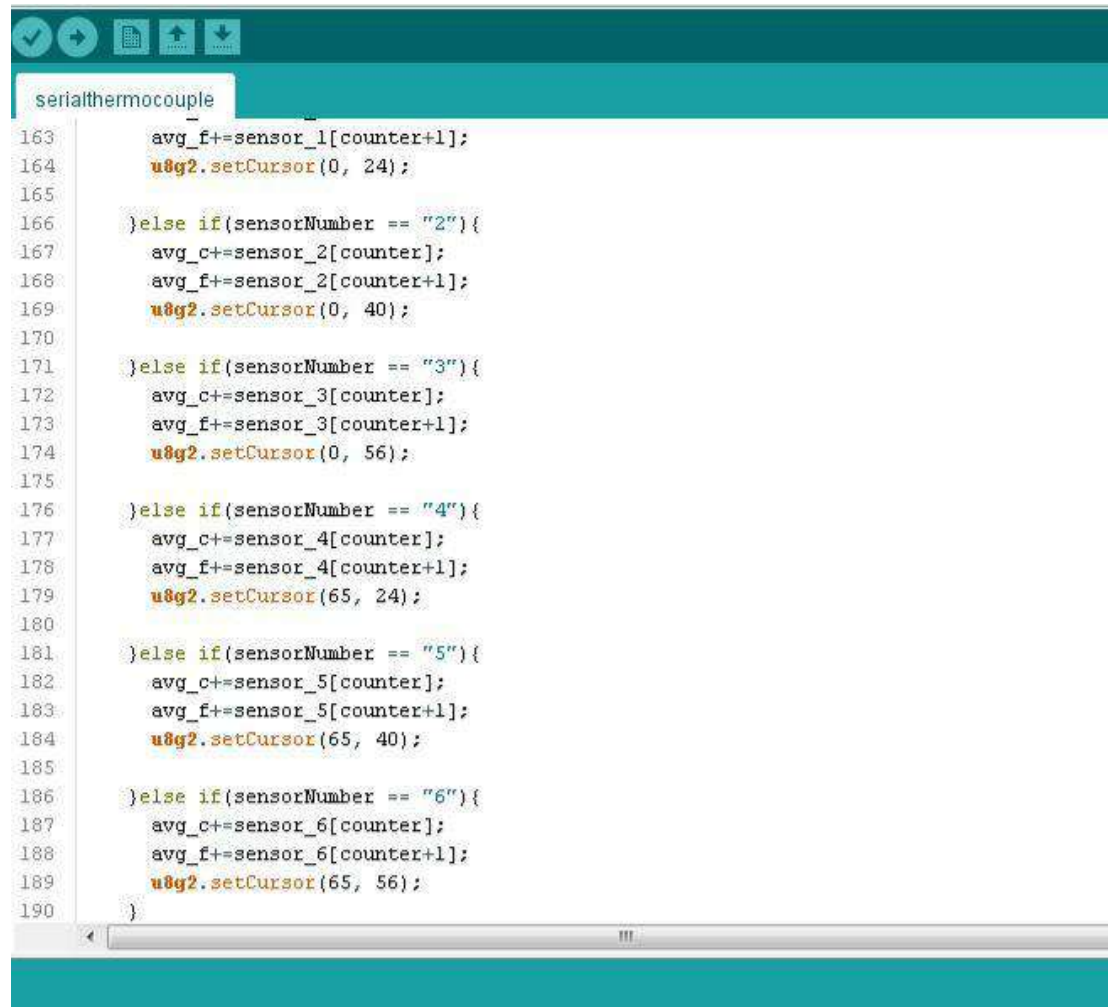
```

```

serialthermocouple
136     avg_f+=sensor_6[counter+1];
137 }
138 }
139 Serial.print(" ");
140 Serial.print(avg_c/15);
141 Serial.print(" C / ");
142 Serial.print(avg_f/15);
143 Serial.print(" F");
144 Serial.println("");
145
146 counter = 0;
147
148 }
149
150 void printlcdSensor(String sensorNumber){
151
152     counter = 0;
153     float avg_c = 0;
154     float avg_f = 0;
155     u8g2.setFont(u8g2_font_profont11_mr);
156     u8g2.setCursor(0, 7);
157     u8g2.print((class __FlashStringHelper *)s); // print a sting, located in PROGMEM
158     u8g2.setFont(u8g2_font_haxrcorp4089_tr);
159     for(counter; counter < 30; counter+=2){
160
161         if(sensorNumber == "1"){
162             avg_c+=sensor_1[counter];
163             avg_f+=sensor_1[counter+1];

```





```
163     avg_f+=sensor_1[counter+1];
164     u8g2.setCursor(0, 24);
165
166 }else if(sensorNumber == "2"){
167     avg_c+=sensor_2[counter];
168     avg_f+=sensor_2[counter+1];
169     u8g2.setCursor(0, 40);
170
171 }else if(sensorNumber == "3"){
172     avg_c+=sensor_3[counter];
173     avg_f+=sensor_3[counter+1];
174     u8g2.setCursor(0, 56);
175
176 }else if(sensorNumber == "4"){
177     avg_c+=sensor_4[counter];
178     avg_f+=sensor_4[counter+1];
179     u8g2.setCursor(65, 24);
180
181 }else if(sensorNumber == "5"){
182     avg_c+=sensor_5[counter];
183     avg_f+=sensor_5[counter+1];
184     u8g2.setCursor(65, 40);
185
186 }else if(sensorNumber == "6"){
187     avg_c+=sensor_6[counter];
188     avg_f+=sensor_6[counter+1];
189     u8g2.setCursor(65, 56);
190 }
```

```
serialthermocouple
189     u8g2.setCursor(65, 56);
190 }
191 }
192 u8g2.print(data(sensorNumber, avg_c/15)); // print a sting (PROGMEM) via RAM array.
193 counter = 0;
194
195 }
196
197 void newScreen(){
198     Serial.println("");
199     Serial.println("////////new value\\\\\\\\\\\\\\\\\\\\\\\\\\\\\\\\\\\\\\\\");
200     Serial.println("");
201 }
202
203
204 String data (String Sensor_number, float Sensor_value ){
205     String str = "S " + String(Sensor_number) + " = " + String(Sensor_value);
206
207     // Length (with one extra character for the null terminator)
208     int str_len = str.length() + 1;
209
210     // Prepare the character array (the buffer)
211     char char_array[str_len];
212
213     // Copy it over
214     str.toCharArray(char_array, str_len);
215     return char_array;
216 }
```

From sequence 78 to sequence 215 is for underlining and printing orders and the results of temperatures.

```

01:00:28.891 ->
01:00:28.891 -> //new value
01:00:28.891 ->
01:00:28.891 -> Sensor_1      32.17 C / 89.90 F
01:00:28.938 -> Sensor_2      32.07 C / 89.72 F
01:00:28.938 -> Sensor_3      32.18 C / 89.93 F
01:00:28.985 -> Sensor_4      32.63 C / 90.74 F
01:00:29.032 -> Sensor_5      32.75 C / 90.95 F
01:00:29.079 -> Sensor_6      32.50 C / 90.50 F
01:00:44.523 ->
01:00:44.523 -> //new value
01:00:44.569 ->
01:00:44.569 -> Sensor_1      32.25 C / 90.05 F
01:00:44.616 -> Sensor_2      32.32 C / 90.17 F
01:00:44.616 -> Sensor_3      32.15 C / 89.87 F
01:00:44.663 -> Sensor_4      32.68 C / 90.83 F
01:00:44.710 -> Sensor_5      32.82 C / 91.07 F
01:00:44.710 -> Sensor_6      32.47 C / 90.44 F
01:01:00.201 ->
01:01:00.201 -> //new value
01:01:00.247 ->
01:01:00.247 -> Sensor_1      32.42 C / 90.35 F
01:01:00.247 -> Sensor_2      32.50 C / 90.50 F
01:01:00.294 -> Sensor_3      32.22 C / 89.99 F
01:01:00.341 -> Sensor_4      32.75 C / 90.95 F
01:01:00.388 -> Sensor_5      33.05 C / 91.49 F
01:01:00.388 -> Sensor_6      32.60 C / 90.68 F
01:01:15.863 ->
01:01:15.863 -> //new value
01:01:15.910 ->
01:01:15.910 -> Sensor_1      32.57 C / 90.62 F
01:01:15.957 -> Sensor_2      32.58 C / 90.65 F
01:01:15.957 -> Sensor_3      32.43 C / 90.38 F
01:01:16.004 -> Sensor_4      32.88 C / 91.19 F
01:01:16.050 -> Sensor_5      33.20 C / 91.76 F
01:01:16.050 -> Sensor_6      32.82 C / 91.07 F

```

☒ Autoscroll ☒ Show timestamp

## The Results

## Chapter Three: Experimental result

3-1

### Practical experiment

For the purpose of examining the device designed and manufactured in an actual cooling system and studying the temperature readings taken and the stability of temperatures over time as shown (figure 3.1)



Figure 3.1

(Water cooler)

When the appliance is connected to a medium-sized water cooler

Where each sensor is connected individual Table (3.1)

Sensor .NO	Location
1	<i>compresor</i>
2	<i>condenser</i>
3	<i>evaporator</i>
4	<i>coold water</i>
5	<i>ambient temp</i>
6	<i>normal water</i>

Table (3.1)





Figure (3.2) thermocouples location

3-2

### Temperature readings table

After that, all readings were taken at fixed intervals of ( 15 second) , and a timeline was taken for a group of readings to show the effectiveness of the device Table(3.2) Chart (3.1)

TEMP ERAT URE	TI M E											
n	0	15	30	45	60	75	90	10 5	12 0	13 5	15 0	16 5
1	32.55	31. 95	31. 93	31. 77	31. 97	31. 97	32. 02	31. 87	31. 92	32	32. 02	31. 82
2	32.07	24. 23	24. 13	24. 12	24. 38	24. 55	25. 25	25. 15	25. 22	24. 97	25. 57	25. 42
3	32.13	12. 62	12. 92	12. 95	13. 18	13. 27	13. 37	13. 52	13. 52	13. 6	13. 75	13. 85
4	32.32	23. 63	23. 22	22. 97	22. 58	22. 17	21. 92	21. 48	21. 25	20. 97	20. 55	20. 32
5	32.15	43. 82	43. 72	43. 52	43. 3	43. 1	43. 03	42. 93	42. 83	42. 68	42. 53	42. 32
6	32.32	50. 5	50. 95	51. 23	51. 47	51. 67	51. 95	52. 3	52. 67	52. 73	52. 95	53

Table (3.2)

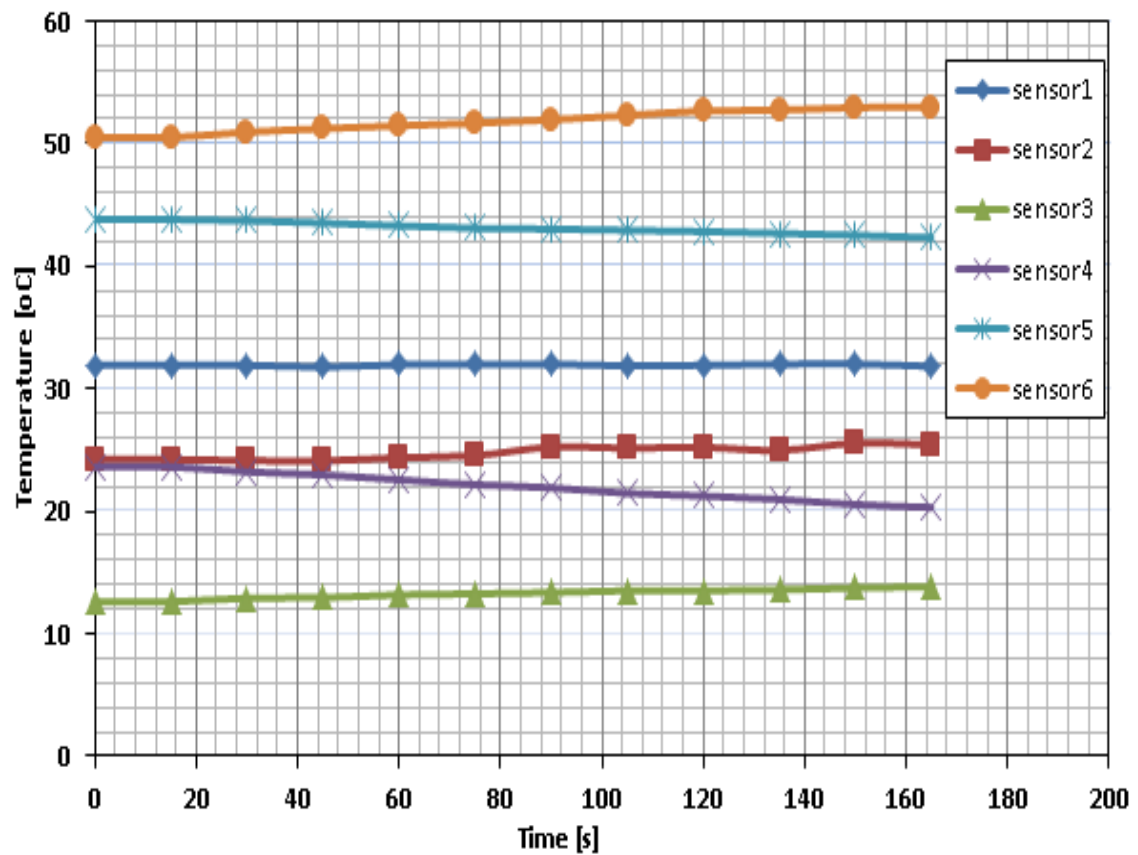


Chart (3.1)

After drawing a diagram of the readings and obtaining results, it was confirmed that the device was working correctly and that there was no problem with the temperature sensors.



# Chapter Four

## Conclusion and Future work

### 4-1 Conclusion

After measuring the temperature and making sure that the device works well, it can be said that it is easy to use and can be used in all disciplines that need to measure temperatures, whether the temperatures are gas, liquid, or solid matter. It can be used by connecting it to a computer or directly by connecting it to an electrical source and displaying the results are through the device screen. One of the advantages of the device is that it is light in weight, easy to maintain, and at a low cost. It also gives results in a short time according to the desire of the user of the device. One or more sources of heat sensors can also be used, and it does not require electrical energy to operate the device and obtain accurate results with less than 0.3. Table(4.1)

no	S1	m	S1-m	(s1-m) <sup>2</sup>	n-1	$\sqrt{\Sigma(s1-m)^2/n-1}$
1	32.55	32	0.55	0.30	0	0
2	31.95	32	-0.05	1/400	1	0.70
3	31.93	32	-0.07	49/10000	2	0.49
4	31.77	32	-0.23	0.0529	3	0.40
5	31.97	32	-0.03	9/10000	4	0.35
6	31.97	32	-0.03	9/10000	5	0.31
7	32.2	32	0.2	0.04	6	0.28
8	31.87	32	-0.13	0.0169	7	0.26
9	31.92	32	-0.08	4/625	8	0.24
10	32	32	0	0	9	0.23
11	32.2	32	0.2	0.04	10	0.22
12	31.82	32	-0.18	0.032	11	0.21
				$\Sigma=0.497$		Av=0.3

Table(4.1)

## Future work

4-2

- 1\_Increase the number of sensors by using all the ports on the Arduino board.
- 2\_Wired temperature sensors can be replaced with wireless ones. Figure (4.1).



Figure (4.1)

3\_The power source can be dispensed with when using the device by placing a small (9v) battery that is charged from time to time. Figure (4.2)

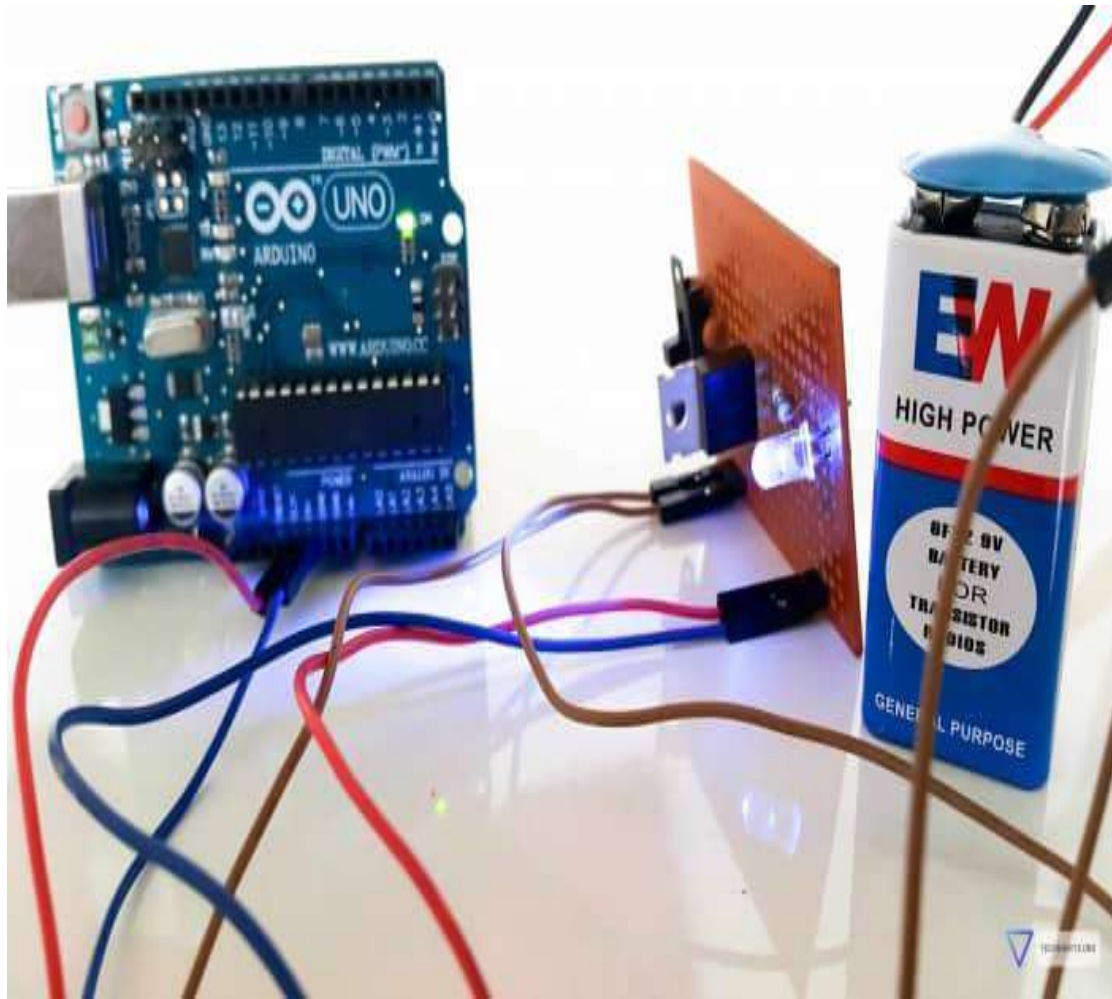


Figure (4.2)

4\_ An internal storage unit (SD card) can be added that saves temperature data. Figure (4.3)

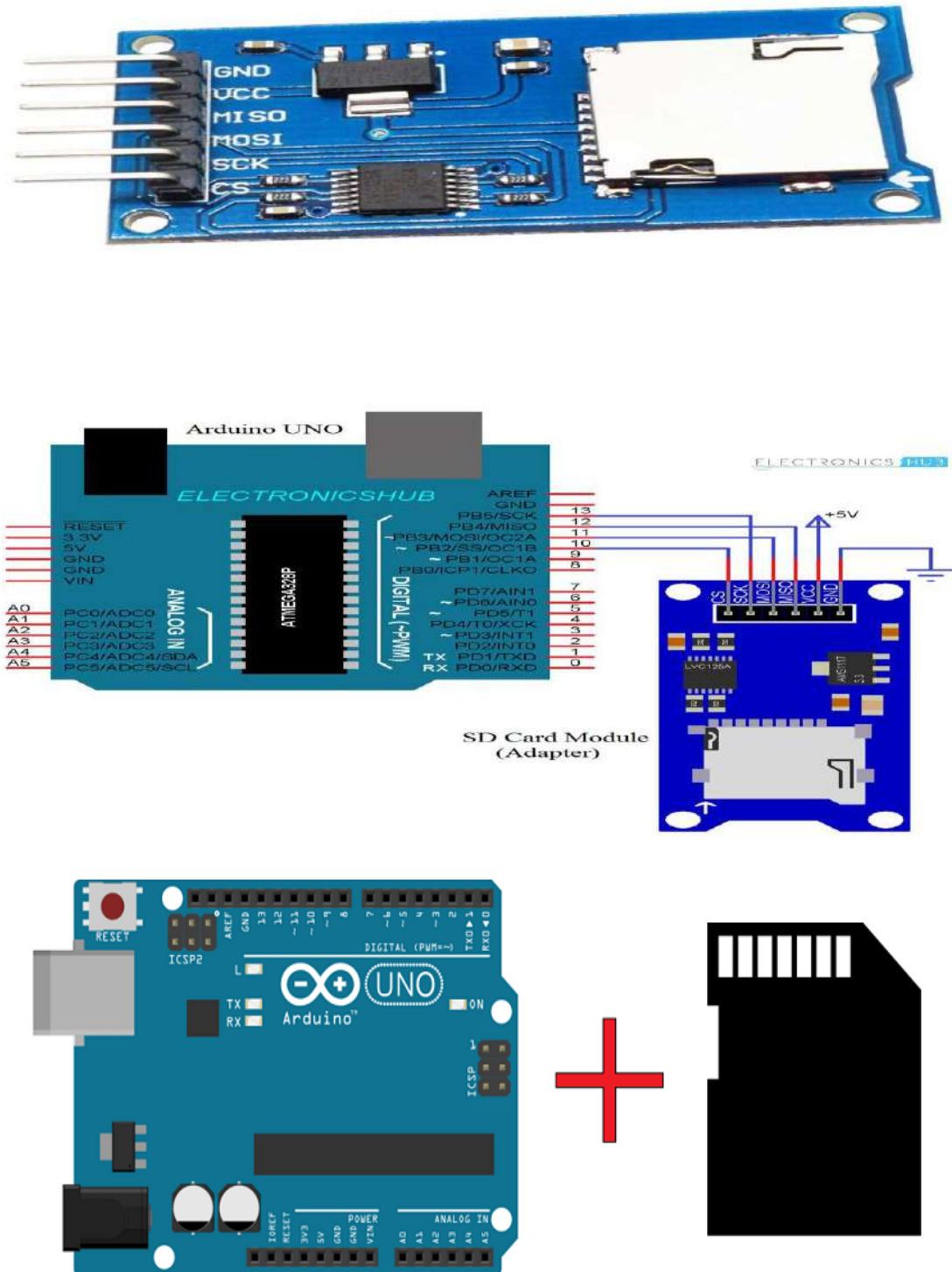


Figure (4.3)

5\_ Other sensors can be used in the same device such as pressure sensor, humidity sensor, sound sensor, etc. figure (4.4)



(Pressure sensor)



(Humidity sensor)



(sound sensor)

Fig(4.4)



6\_It is possible to receive data from the device without the need for a wired connection by adding a (Wi-Fi) unit to the device fig (4.5)



Figure (4.5) Wi-Fi device

## References:

1. Park J, Mackqy S (2003) Practical data acquisition for instrumentation and system control. Elsevier, Oxford.
2. Lacanette K (1997) Temperature Sensor Handbook – Application Note National Semiconductor Corporation
3. National Instruments (2002) Data Acquisition Fundamentals, Application Note 007, National Instruments Corporation.
4. <http://www.mantech.co.za/datasheets/products/A000047.pdf>
5. Arduino program.pdf - <https://www.moys.gov.iq>
6. [https://ar.wikipedia.org/wiki/%D9%85%D8%B2%D8%AF%D9%88%D8%AC%D8%A9\\_%D8%AD%D8%B1%D8%A7%D8%B1%D9%8A%D8%A9](https://ar.wikipedia.org/wiki/%D9%85%D8%B2%D8%AF%D9%88%D8%AC%D8%A9_%D8%AD%D8%B1%D8%A7%D8%B1%D9%8A%D8%A9)
7. [https://www.danomsk.ru/upload/iblock/e47/194131\\_0a2c3de5f3b04f1ab5f0344b0e7b458a.pdf](https://www.danomsk.ru/upload/iblock/e47/194131_0a2c3de5f3b04f1ab5f0344b0e7b458a.pdf)
8. <https://www.electricaltechnology.org/2018/11/types-sensors-applications.html>
9. <https://www.noor-book.com/%D9%83%D8%AA%D8%A7%D8%A8-%D8%A7%D8%B1%D8%AF%D9%88%D9%8A%D9%86%D9%88-%D8%A8%D8%A8%D8%B3%D8%A7%D8%B7%D8%A9-%D8%A7%D9%84%D8%A7%D8%B5%D8%AF%D8%A7%D8%B1%D8%A7%D9%84%D9%83%D8%A7%D9%85%D9%84-pdf>

## الخلاصة

في هذا المشروع تم تصنيع جهاز لقياس درجة الحرارة بدقة عالية ونقلها على الكمبيوتر وتسجيل القراءات وتخزينها عند قياس درجة حرارة الهواء المحيط أو الماء.

تعتبر درجة الحرارة أحد العوامل المحددة في كل جانب من جوانب الحياة ، فمن الضروري أن تكون قادرًا على قياسها بدقة عالية.

تم استخدام مزدوج حراري من النوع k ورقاقة حرارية 6675 كحد أقصى ، والتي تتميز بالاتصال والمعايرة الذاتية ، ولوحة دوائر إلكترونية (Arduino Mega 6025) مدعومة بمصدر طاقة 5 فولت و (Arduino) عبارة عن دائرة مفتوحة المصدر مع متحكم مبرمج بالحاسوب يتم إدخال كود البرمجة باستخدام 6 مجسات حرارية من النوع k و max6675 جنبًا إلى جنب واستشعار الهواء المحيط لمدة 15 ثانية لرفع دقة أجهزة الاستشعار الحرارية من النوع k و max 6675. تقنية بسيطة يتم إجراء المعايرة وتحليل البيانات من خلال الدائرة الإلكترونية (Arduino). تم تسجيل القراءات على شاشة الكمبيوتر لكل مستشعر ، وتم أخذ متوسط القراءات لكل مستشعر.

تهدف هذه الدراسة إلى تسجيل درجة الحرارة وقراءة التاريخ الزمني الذي تستخدمه المستشعرات الحرارية من النوع k وأجهزة الاستشعار من النوع max6675 لقراءة قيم درجات الحرارة المختلفة واستخدام المعالجات الدقيقة (Arduino).





وزارة التعليم العالي والبحث العلمي

كلية دجلة الجامعة الأهلية

قسم هندسة تقنيات التبريد والتكييف

### نظام نقل البيانات لقياسات درجة الحرارة

بحث مقدم إلى كلية دجلة الجامعة الأهلية/ قسم هندسة تقنيات التبريد والتكييف وهو جزء من متطلبات نيل درجة بكالوريوس في هندسة تقنيات التبريد والتكييف

من قبل

ماجد طه ياسين

عبدالرحمن مثنى هادي

محمد شهاب نصيف

سيف صلاح الدين صبار

حسن علي جاسم

رافد حسن مهدي

بإشراف

د. فراس معن عبد الستار

2021-2020

Ministry of Higher Education  
and Scientific Research  
Dijlah University College  
Refrigeration and Air Conditioning  
Technologies Engineering Department



# ***Different Types of Solar Dryers***

## ***“Theoretical Study”***

A Project

Submitted to the Dijlah University College in partial fulfillment of the requirements for the Degree of Bachelor in Refrigeration and Air Conditioning Technologies Engineering.

By:

***Aymin T. saken***

***Dhafer A. Hamid***

***Mohammed A.R. Neamah***

***Munther A. Dahad***

***Naseef J. Mohammad***

Supervised by

***Asst. Lec. Amir F. Hussein***

**1441 A.H.**

**2021 A.D.**



## ***Supervisor Certificate***

We certify that this project entitled “***Different Types of Solar Dryers - Theoretical Study***” prepared by: -

- ***Aymin T. Saken***
- ***Dhafer A. Hamid***
- ***Mohammed A.R. Neamah***
- ***Munther A. Dahad***
- ***Naseef J. Mohammad***

has been carried out completely under our supervision at the Dijlah University College in partial fulfillment of the requirements for Degree of ***Bachelor in Refrigeration and Air Conditioning Technologies Engineering.***

Signature:

***Asst. Lec.: Amir F. Husain***

Refrigeration and Air Conditioning  
Technologies Engineering.

Dijlah University college

Date:     /     / 2021

Approved by the Charmin of Air condition and refrigeration engineering department:

Signature:

***Dr. Firas Mean***

Charmin of ***Refrigeration and Air  
Conditioning Technologies Engineering.***

Dijlah University college

Date:     /     / 2021

## ***Examining Committee Certificate***

We certify that we have read this project entitled “*Different Types of Solar Dryers - Theoretical Study*” prepared by: -

- ***Aymin T. Saken***
- ***Dhafer A. Hamid***
- ***Mohammed A.R. Neamah***
- ***Munther A. Dahad***
- ***Naseef J. Mohammad***

and as an examining committee examined the students in its content and that in our opinion it meets the standards of a project for the Degree of ***Bachelor in Refrigeration and Air Conditioning Technologies Engineering.***

***Signature:***

***Name: Asst. Lec. Amir F. Husain***

***Date / / 2021***

***(Supervisor)***

***Signature:***

***Name:***

***Date / / 2021***

***(Member)***

***Signature:***

***Name:***

***Date / / 2021***

***(Chairman)***

Approved for the Dijlah University College:

***Signature:***

***Name:***

***Dean of the Dijlah University College***

***Date: / / 2021***

# ***Acknowledgements***

With deep sense of gratefulness, we would like to express my deepest thanks and sincere gratitude to our supervisor *Asst. prof. Amir F. Husain* for his invaluable help, advice and encouragement during the project.

We indebted to all *Refrigeration & Air Conditioning Techniques Department staff* at *Dijlah University College* who enriched this work with their academic experience.

We offer our sincere thanks, special gratitude and appreciation from our heart to our families who provided us with unfailing support and encouragement throughout the period of our study and for their support, encouragement and understanding during our study in college.

At last, we deeply thank all who helped us in carrying out this project and research.

***Project Students***

**2021**

**List of figures:**

<b>No. of Figure</b>	<b>Details</b>	<b>Page No.</b>
Figure 2-1	Simultaneous Heat and Mass Transfer Process on a Food Surface.....	5
Figure 2-2	Classifications of Dryers and Drying Modes.....	11
Figure 2-3	Typical Solar Energy Dryer Designs.....	12
Figure 2-4	Solar Photovoltaic Panel -powered the Fan of Dryer.....	13
Figure 2-5	Schematic diagram of a forced-convection, transparent-roof solar barn.....	14
Figure 2-6	Schematic diagram of an active collector–roof solar energy storage dryer.....	14
Figure 2-7	Schematic diagram of a distributed-type active solar dryer.....	15
Figure 2-8	Schematic diagram of a mixed-mode-type active solar dryer.....	15
Figure 2-9	Schematic diagram of an integral-type passive solar dryer.....	17
Figure 2-10	A typical natural-circulation solar-energy cabinet dryer.....	17
Figure 2-11	A greenhouse type natural-circulation solar–energy dryer.....	18
Figure 2-12	Schematic diagram of a distributed-type passive solar dryer.....	19
Figure 2-13	Schematic diagram of a natural circulation, mixed-mode solar energy dryer.....	20
Figure 2-14	Working principle of open sun drying.....	21
Figure 2-15	Working principle of direct solar drying.....	21
Figure 2-16	Working principle of indirect solar drying system.....	22
Figure 2-17	Different Types of Fans used in Solar Dryers.....	28
Figure 2-18	Photovoltaics Cells for Energy Supply for Fans of Solar Dryers.	30
Figure 2-19	Different Designs of Different Types of Solar Dryers.....	33
Figure 4-1	Table-like Solar Dryer.....	45
Figure 4-2	Scheme of the Solar Dryer for Bananas.....	46
Figure 4-3	Fruit Dryer.....	47

Figure 4-4	Fruit and Vegetable Dryers.....	47
Figure 4-5	Solar coffee drying system using a wood furnace as back-up system.....	49
Figure 4-6	Schematic layout of the Solar Biomass Heating System.....	50
Figure 4-7	Side view of the Solar Dryer with Biomass Burner.....	51
Figure 4-8	Greenhouse solar dryer type a) load supporting wall design and b) shell design.....	52
Figures 4-9	Cross section of the solar-assisted drying kiln.....	54
Figures 4-10	Longitudinal section of the solar-assisted drying kiln.....	54
Figure 4-11	Solar Rice Dryer.....	55
Figure 4-12	The schematic layout of the solar assisted heat pump granary.....	56
Figure 4-13	Solar Tunnel Dryer.....	57

### ***List of Tables:***

<b><i>No. of Table</i></b>	<b><i>Details</i></b>	<b><i>Page No.</i></b>
Table 2-1	Solar driers compared with open-air and fuel drying.....	7
Table 2-2	The drying process (air enters at 20 °C and leaves at 80% RH) ...	8
Table 2-3	Materials used for the Construction of the Solar Dryer.....	24
Table 2-4	Tilt angle for different latitudes and seasons.....	26
Table 3-1	Typical checklist for preliminary evaluation and selection of solar dryers.....	36
Table 4-1	Agricultural Commodities Traded in Market.....	43
Table 4-2	Range of Moisture Contents of some Agricultural Commodities.....	44
Tables 4-3	Technical data of Fruit and Vegetable Dryer.....	48
Tables 4-4	Details of the components installed.....	56
Table 4-5	Options for adapting a solar tunnel dryer.....	58
Table 4-6	Technical data of the tunnel dryer.....	58



# ***Content***

Supervisor Certificate.....	ii
Examining Committee Certificate.....	iii
Acknowledgements.....	iv
List of Figures and Tables .....	v
Abstract.....	vii
Content.....	viii
<b>1: Introduction.....</b>	<b>1-3</b>
1-1: Introduction.....	2
1-2: Objective of the project .....	3
<b>2: Theoretical Analysis.....</b>	<b>4-33</b>
2-1: Introduction.....	5
2-2: Comparison between Solar Dryer and Conventional Dryers.....	6
2-2-1: Comparison between Solar dryer with Conventional form of dryer.....	6
2-2-2: Comparison between Solar dryer with open air drying .....	7
2-3: Processes during Solar Drying.....	8
2-4: Advantages and Disadvantages of Solar Dryers .....	9
2-4-1: Advantages of Solar Dryers .....	9
2-4-2: Disadvantages of Solar Dryers .....	10
2-5: Classification of Solar Dryers.....	10
2-5-1: Active Solar Energy Dryers.....	13
2-5-1-1: Integral Type.....	14
2-5-1-2: Distributed Type.....	15
2-5-1-3: Mixed-mode Type.....	15
2-5-2: Passive Solar Energy Dryers.....	16
2-5-2-1: Integral Type.....	16
2-5-2-2-1: Solar Cabinet Dryers.....	17
2-5-2-1-2: Natural-Circulation Greenhouse Dryers.....	18

2-5-2-2: Distributed Type.....	19
2-5-2-3: Mixed-mode Type.....	19
2-6: Working Principle of Solar Energy Dryers.....	20
2-6-1: Open Sun Drying.....	20
2-6-2: Direct Solar Drying.....	21
2-6-3: Indirect Solar Drying.....	22
2-6-4: Hybrid Solar Drying.....	23
2-7: Construction of Solar Dryers.....	23
2-7-1: Materials and Tools of Solar Dryer.....	23
2-7-2: Solar Dryer Components.....	24
2-8: The Orientation of Solar Dryers.....	25
2-9: Explain the Components of Solar Dryers.....	26
2-9-1: Air Collectors.....	26
2-9-2: Ventilation.....	27
2-9-2-1: Natural ventilation.....	27
2-9-2-2: Electrical Fans.....	27
2-9-3: Fan Control.....	29
2-9-4: Power Supply from Solar Cells.....	29
2-10: Design of Solar Dryers.....	31
<b>3- Selection of Solar Dryers.....</b>	<b>34-41</b>
3-1: Selection of Solar Dryers.....	36
3-1-1: Initial selection of solar dryers.....	38
3-1-2: Initial comparison of solar dryers.....	38
3-1-3: Solar Drying Tests.....	38
3-1-4: Final Selection of Solar Dryer.....	38
3-2: Non-technical Aspects for Selection Solar Dryers.....	39
3-2-1: Weather conditions.....	39
3-2-2: Storage.....	39
3-2-3: Capacity.....	40
3-2-4: Selection, Cleaning and Pre-treatment.....	40
3-3: Economics of Solar Dryers.....	41

<b>4- Applications and Experiences of Solar Dryers.....</b>	<b>42-59</b>
4-1: Solar Drying of some Selected Commodities.....	44
4-1-1: Fruit and Vegetable Drying.....	44
4-1-1-1: Table-like Solar Dryer.....	44
4-1-1-2: Banana Dryer.....	45
4-1-1-3: The Fruit Dryer.....	46
4-1-1-4: Fruit and Vegetable Dryers.....	47
4-1-2: Coffee Drying.....	48
4-1-3: Chili Drying.....	49
4-1-4: Nuts Drying.....	51
4-1-5: Tobacco Drying.....	52
4-1-5: Timber and Wood Drying.....	53
4-1-6: Rice Drying.....	55
4-1-7: Corn Drying.....	55
4-1-8: Fish Drying.....	57
4-2: Product Quality Consideration.....	59
<b>5- Conclusion and Suggestions.....</b>	<b>60-62</b>
5-1: Conclusions.....	61
5-2: Suggestions for Future Work.....	62
<b>6: References.....</b>	<b>63-65</b>
<b>7: Appendix .....</b>	<b>A1-A2</b>

***Abstract:***

Solar drying is one of the effective applications of solar energy. Drying means moisture removal from the product. Drying is helpful in preserving agricultural and food product for long time; it prevents product from contamination.

Drying involves the application of heat to vaporize moisture and some means of removing water vapor after its separation from the food products. It is thus a combined and simultaneous heat and mass transfer operation for which energy must be supplied. The removal of moisture prevents the growth and reproduction of microorganisms like bacteria, yeasts and molds causing decay and minimizes many of the moisture-mediated deteriorative reactions. It observed that reduction in weight and volume, minimizing packing, storage, and transportation costs and enables storability of the product under ambient temperatures.

There are various products which are dried by solar dryer like various fruits, grains, timber, fish. Open to the sun drying means products are exposed directly to sun, allowed to absorbed solar radiation. It was reported that this method has many disadvantages like poor quality, contamination of product. These disadvantages can be eliminated by indirect type of dryer which is used for drying products as application of solar energy. In this project, we studied the different technique of drying and various modes of solar drying.

Direct solar drying, indirect solar drying, and mixed mode solar drying these are different solar drying methods.

The purpose of a dryer is to supply more heat to the product than that available naturally under ambient conditions, thus increasing sufficiently the vapor pressure of the crop moisture. Therefore, moisture migration from the crop is improved. The dryer also significantly decreases the relative humidity of the drying air, and by doing so, its moisture-carrying capability increases, thus ensuring sufficiently low equilibrium moisture content.

The use of solar drying systems for agricultural products to preserve fruits, vegetables and other crops has been proven to be cheap, reliable, and environmentally friendly. It also provides a viable alternative to traditional techniques of drying.

The traditional method of Sun drying presents issues of dust, rodents and insects as well as loss of color. Solar dryers offer advantages of better-quality produce, shorter periods of drying, reduced loss of raw materials.

A classification of drying equipment classifies dryers as direct or indirect, with subclasses. Solar energy drying systems are classified primarily according to their heating modes and the manner in which the solar heat is utilized. They are classified into two main methods (Active dryers and Passive dryers).

This project presents the state of various kinds of solar dryers that are widely used today and about drying process that has been perform during drying of various food products and percentage containing moisture in different food products. The indirect, direct and mixed mode dryers that have shown potential in drying agricultural products are discussed.

We also highlight the Influencing factors and environmental influence that plays a vital role in the solar drying sector and says that the indirect solar dryer is more suitable than other dryers and recirculation of air in an indirect dryer can reduce the drying time of product in comparison to normal indirect solar dryers. The dryer having recirculation of air have more efficiency than other dryers.

The locally available material for construction of solar dryers can use. Drying systems could be designed utilizing solar photovoltaic panels. As solar energy is necessarily intermittent, advances in thermal and electrical energy storage is needed to make use of renewable energy viable in drying. To minimize use of oil or gas, biomass can be used for heating in the absence of insolation.

It have been explained and discusses numerous types of solar drying systems designed and developed to improving of the drying operation to save energy and improve product quality and to utilize free, renewable, and non-polluting energy source provided by the sun.

In this project discuss the development, technical and performance of solar drying system with aspect to the agriculture product being dried were presented. The use of solar drying systems to conserve vegetables, fruits and crops has shown to be practical, economical and the responsible approach environmentally.

***Chapter -1-***  
***Introduction***

## **Chapter -1**

### **Introduction**

#### **1-1: Introduction:**

Several technologies have been employed by the scientist to preserve food products. Some major techniques are (canning, freezing and dehydration). The drying not only provides storage life but also improves quality, easy handling.

Solar drying is important application of solar energy. Solar dryers use air collectors to collect solar energy. Solar dryers are used primarily by the agricultural industry. The purpose of drying an agricultural product is to reduce its moisture content to a level that prevents its deterioration.

In drying, two processes take place:

1-Heat transfer to the product using energy from the heating source.

2- Mass transfer of moisture from the interior of the product to its surface and from the surface to the surrounding air.

Due to higher cost of fossil fuels and uncertainty regarding future cost and availability, use of solar energy in food processing will probably increase and become more economical in future.

Solar dryers give the better result than sun drying when it properly designed. They provide faster drying rate when heating the air above atmospheric temperature which causes air to circulate faster through the dryer.

Solar dryers also protect foods from dust, insects, birds and animals. However, care must be taken when drying fruits to prevent too fast drying, which will prevent complete drying and would result in case hardening and subsequent mold growth.

“Relative humidity” and “absolute humidity” are two important technical factors for designing solar dryers.

Agricultural and other products have been dried by the sun and wind in the open air for thousands of years. The purpose is either to preserve them for later use, as is the case with fruit; or as an integral part of the production process, as with timber and tobacco.

Solar dryer are simple devices to heat agricultural products by utilizing solar energy and employed in many applications requiring low to moderate temperature below 80 [°C]. Drying processes play an important role in the preservation of agricultural products.

Thus, the solar dryer is one of the many ways of making use of solar energy efficiently in meeting man's demand for energy and food and agricultural products supply.

Total system cost is a most important Consideration in designing a solar dryer for agricultural uses.

***1-2: Objective of the Project:***

Study and explain the different types of solar dryers, which include:

- Working principle of solar dryers.
- The classification of solar dryers.
- Features and characteristics of solar dryers.
- Designs, main components and manufacturing of solar dryers.
- Applications and experiences of solar dryers



*Chapter -2-*

***Theoretical Analysis***

## Chapter - 2

### Theoretical Analysis

#### 2-1: Introduction:

Drying is a complicated process involving simultaneous heat and mass transfer. The required amount of energy to dry a particular product depends on many factors, such as initial moisture content, final moisture content, drying air temperature, relative humidity and velocity. In order to improve the quality, the traditional natural sun drying must be replaced by modern drying methods. Drying characteristics of specific products should be determined to improve the quality. The simultaneous heat and mass transfer process on a food Surface is shown in figure below.

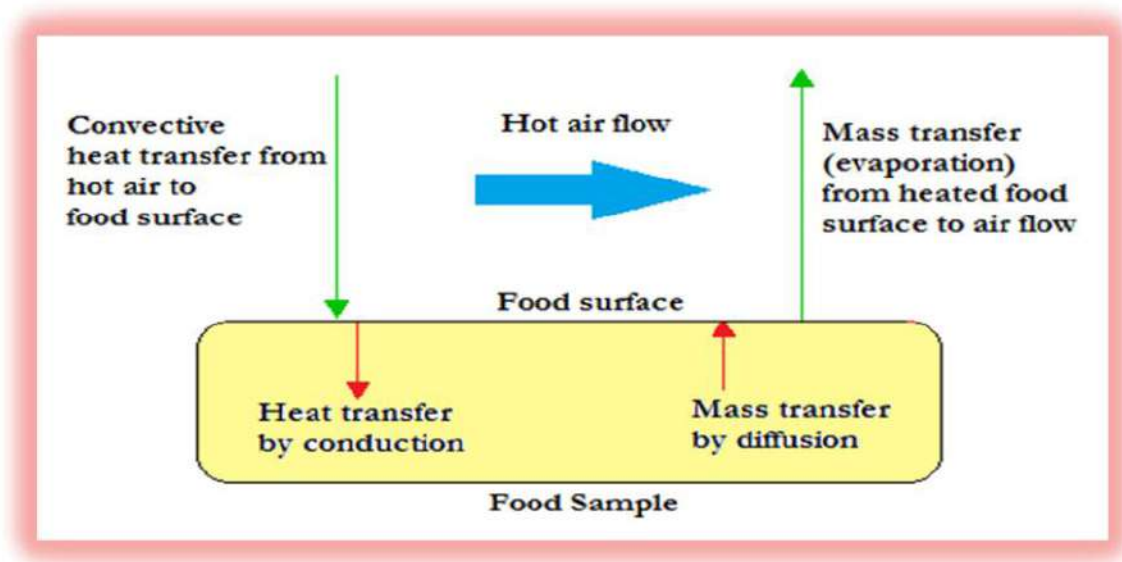


Figure (2-1): Simultaneous Heat and Mass Transfer Process on a Food Surface.

Among the numerous methods used for food conservation, drying is unquestionably the most ancient but still very much used nowadays. It is a process by which water is removed from the food, by vaporization or sublimation, thus reducing the water available for degradation reactions of chemical, enzymatic or microbial nature. The drying rate is influenced by transfer mechanisms, such as the vapor pressures of the food and of the drying air, temperature and air velocity, moisture diffusion in the product, thickness and surface exposed for drying [1].

### ***2-2: Comparison between Solar Dryer and Conventional Dryers:***

All drying systems can be classified primarily according to their operating temperature ranges into two main groups of high temperature dryers and low temperature dryers. However, dryers are more commonly classified broadly according to their heating sources into fossil fuel dryers (more commonly known as conventional dryers) and solar-energy dryers.

Strictly, all practically-realized designs of high temperature dryers are fossil fuel powered, while the low temperature dryers are either fossil fuel or solar-energy based systems.

Drying is most cost-effective application of solar energy. There are various products which are dried by solar dryer like various fruits, grains, meat, timber, fish, cloths. Food products are preserved by drying. In developing nations, open to the sun drying technique is used for drying agricultural products. Open to the sun drying means products are exposed directly to sun, allowed to absorb solar radiation. It was reported that this method has many disadvantages like poor quality, contamination of product [2,3].

The dryer is container which is powered by electricity or fuel as source of heat, design for house product like cloths or agricultural product and used air for drying the products is called as mechanized form of dryer. This is faster dryer but it needs large initial cost for various equipment's as well as for fuel. Following gives advantages and disadvantages between solar dryer with other means of drying [4,5].

#### ***2-2-1: Comparison between Solar dryer with Conventional form of dryer:***

Advantages:

- a. It reduces environmental impact.
- b. Easily managed.
- c. Prevent fuel dependence.
- d. Often less expensive.

Disadvantages:

- a. Requires adequate solar radiation.
- b. Hot and dry climate preferred (relative humidity below 60% needed).
- c. Requires more time.

### 2-2-2: Comparison between Solar dryer with open air drying:

Advantages:

- a. It gives better quality of drying product.
- b. It reduces losses and bacterial contamination.
- c. Requires less area for drying.
- d. May reduce labor required.
- e. Drying time reduces.

Disadvantages:

- a. More expensive.
- b. It may requires some parts material to be import.

Table (2-1) lists the primary benefits and disadvantages of solar drying when compared with traditional open-air drying, and then with the use of fueled driers.

Table 2-1: Solar driers compared with open-air and fuel drying. [6,7 and 8].

Type of Drying	Benefits(+) & Disadvantages(-) of Solar Driers
Solar vs. Open-air	<ul style="list-style-type: none"> <li>+ Can lead to better quality dried products, and better market prices</li> <li>+ Reduces losses and contamination from insects, dust, and animals</li> <li>+ Reduces land required (by roughly 1/3)</li> <li>+ Some driers protect food from sunlight, better preserving nutrition &amp; color</li> <li>+ May reduce labor required</li> <li>+ Faster drying time reduces chances of spoilage</li> <li>+ More complete drying allows longer storage</li> <li>+ Allows more control (sheltered from rain, for example)</li> <li>- More expensive, may require importing some materials</li> <li>- In some cases, food quality is not significantly improved</li> <li>- In some cases, market value of food will not be increased</li> </ul>
Solar vs. Fueled	<ul style="list-style-type: none"> <li>+ Prevents fuel dependence</li> <li>+ Often less expensive</li> <li>+ Reduced environmental impact (consumption of non-renewables)</li> <li>- Requires adequate solar radiation</li> <li>- Hot &amp; dry climates preferred (usually RH below 60% needed)</li> <li>- Requires more time</li> <li>- Greater difficulty controlling process, may result in lower quality product</li> </ul>

### 2-3: Processes during Solar Drying:

The objective of a dryer is to supply the product with more heat than is available under ambient conditions, thereby increasing sufficiently the vapor pressure of the moisture held within the crop and decreasing significantly the relative humidity of the drying air and thereby increasing its moisture carrying capacity and ensuring sufficiently low equilibrium moisture content [9].

Warm air can hold more moisture than cold air, so the amount required depends on the temperature to which it is heated in the collector as well as the amount held (absolute humidity) when it entered the collector. The way in which the moisture absorption capability of air is affected by its initial humidity and by the temperature to which it is subsequently heated is shown in Table (2-2).

Table (2-2): The drying process (air enters at 20 °C and leaves at 80% Relative Humidity) [10]

Initial relative humidity	Moisture absorption capability (grams of water per m <sup>3</sup> of air [g/m <sup>3</sup> ])		
	Not heated	Heated to 40 °C	Heated to 60 °C
40 %	4,3	9,2	16,3
60 %	1,4	8,2	15,6
80 %	0	7,1	14,9

The objective of most drying processes is to reduce the moisture content of the product to a specified value. Moisture content (wet basis) is expressed as the weight of water as a proportion of total weight (see Appendix-1 for initial moisture content of different crops). For example, the moisture content of rice has typically to be reduced from 24 % to 14 %. So, to dry one ton of rice, 100 kg of water must be removed. If the heated air has an absorption capacity of 8 g/m<sup>3</sup> then  $100/0.0008 = 12,500$  m<sup>3</sup> of air are required to dry one ton of rice. The heat required to evaporate water is 2.26 kJ/kg. Hence, approximately 250 MJ (70 kWh) of energy are required to vaporize the 100 kg water.

Solar energy can be used to temperatures needed for most of the drying applications. Solar dryers use is heated through solar energy collectors, which can be installed in modules

according to the requirements of hot air. Drying is basically a heat and mass transfer process: moisture from the surface and inside of the product is vaporized, and the vapor is removed by flowing hot air. Important factors affecting the drying process are listed below:

- 1- Relative humidity and temperature of air.
- 2- Airflow rate.
- 3- Initial moisture content of the product.
- 4- Final desired moisture content of the product.

#### ***2-4: Advantages and Disadvantages of Solar Dryers:***

Solar dryers can be utilized for various domestic purposes. They also find numerous applications in industries such as textiles, wood, fruit and food processing, paper, pharmaceutical, and agriculture industries.

The advantages and disadvantages of solar dryers can be summarized as follows:

##### ***2-4-1: Advantages of Solar Dryers:***

- 1- Solar dryers are more economical compared to dryers that run on conventional fuel/electricity.
- 2- The drying process is completed in the most hygienic and eco-friendly way.
- 3- Solar drying systems have low operation and maintenance costs.
- 4- Solar dryers last longer. A typical dryer can last 15-20 years with minimum maintenance.
- 5- The higher temperature, movement of the air and lower humidity, increases the rate of drying.
- 6- Food is enclosed in the dryer and therefore protected from dust, insects, birds and animals and ultra violet protection of solar dryers maintains colors and nutrients of fruits and vegetables and this led to better product quality (color, skin, taste).
- 7- The higher temperature deters insects and the faster drying rate reduces the risk of spoilage by microorganisms.

8- The higher drying rate also gives a higher throughput of food and hence a smaller drying area (roughly 1/3).

9- The dryers are water proof and the food does not therefore need to be moved when it rains.

10- Dryers can be constructed from locally available materials and are relatively low cost.

#### ***2-4-2: Disadvantages of Solar Dryers:***

1- Drying can be performed only during sunny days, unless the system is integrated with a conventional energy-based system.

2- Due to limitations in solar energy collection, the solar drying process is slow in comparison with dryers that use conventional fuels.

3- Normally, solar dryers can be utilized only for drying at 40-80°C.

4- Solar dryers must provide the equivalent performance to that of the conventional processes in terms of capacity, labor input, the quality of the final product, the total drying costs and reliability.

5- A backup heating system should be installed to ensure drying during the critical periods when the weather is bad.

#### ***2-5: Classification of Solar Dryers:***

Numerous types of solar dryers were developed to reduce post-harvest losses and to improve the product quality. In the following they are classified and some of them are described.

To classify the various types of solar dryers, it is necessary to simplify the complex constructions and various modes of operation to the basic principles. Solar dryers can be classified based on the following criteria:

1- Mode of air movement.

2- Exposure to insulation.

- 3- Direction of air flow.
- 4- Arrangement of the dryer.
- 5- Status of solar contribution.

Drying equipment may be classified in several ways. The two most useful classifications are based on:

- 1- The method of transferring heat to the wet solids.
- 2- The handling characteristics and physical properties of the wet material.

The first method of classification reveals differences in dryer design and operation, while the second method is most useful in the selection of a group of dryers for preliminary consideration in a given drying problem.

A classification chart of drying equipment on the basis of heat transfer is shown in Figure 2-2 [5,10].

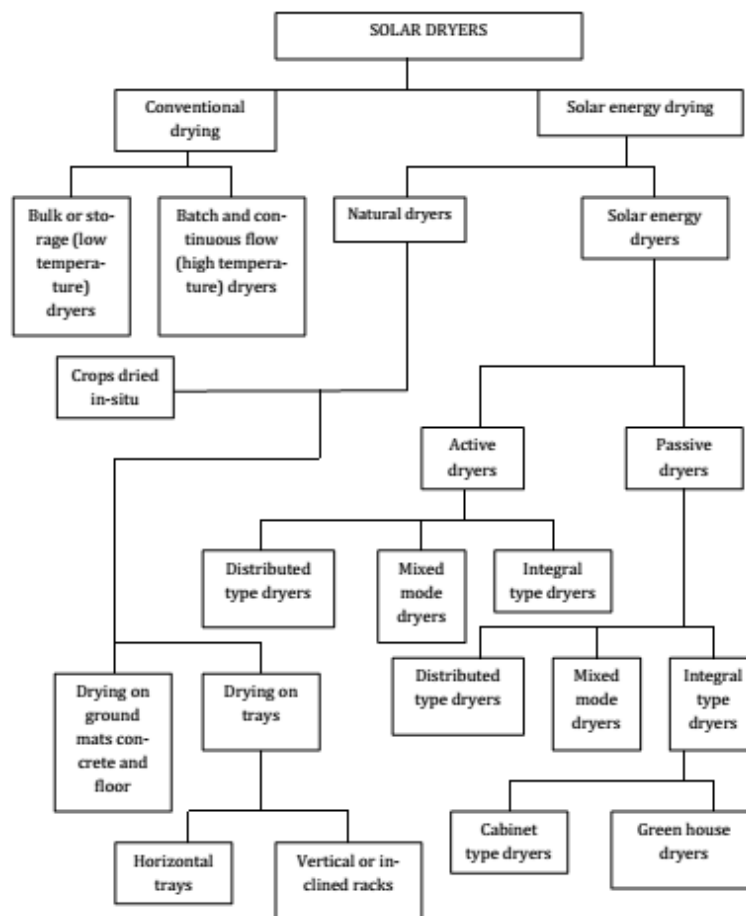


Figure 2-2: Classifications of Dryers and Drying Modes.



solar dryers can be classified primarily according to their heating modes and the manner in which the solar heat is utilized. In broad terms, they can be classified into two major groups, namely:

1- active solar-energy drying systems (most types of which are often termed hybrid solar dryers).

2- passive solar-energy drying systems (conventionally termed natural-circulation solar drying systems).

Three distinct sub-classes of either the active or passive solar drying systems can be identified (which vary mainly in the design arrangement of system components and the mode of utilization of the solar heat, namely [9]:

- Integral-type solar dryers.
- Distributed-type solar dryers.
- Mixed-mode solar dryers.

The main features of typical designs of the various classes of solar-energy dryers are illustrated in Figure 2-3, showing three main groups for solar dryers on the basis of the energy sources used [11].

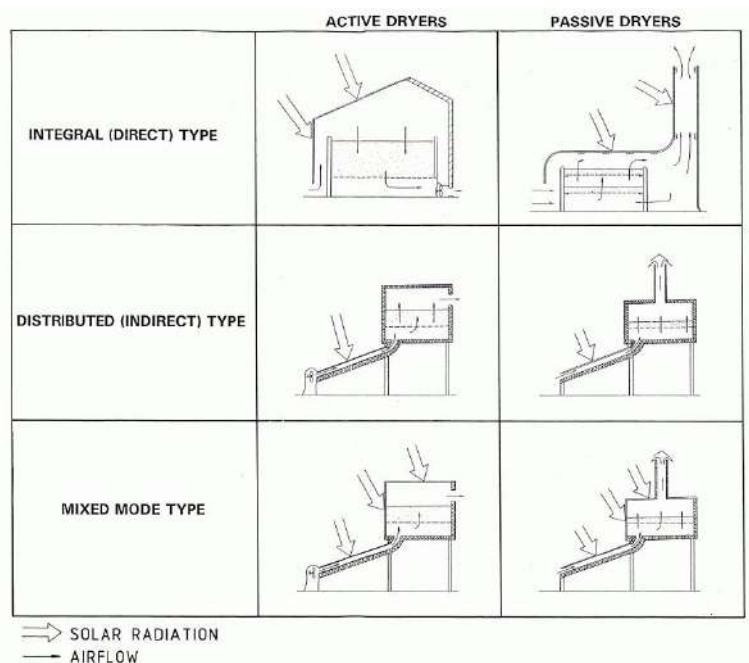


Figure 2-3: Typical Solar Energy Dryer Designs.

The design of solar dryers is adjusted to the quantity, character, and designation of the material to be dried as well as to the energy sources used and accordingly, various types of solar dryers have been developed and are in use to date.

### 2-5-1: Active Solar Energy Dryers:

Active solar dryers are also called forced convection or hybrid solar dryers. Optimum air flow can be provided in the dryer throughout the drying process to control temperature and moisture in wide ranges independent of the weather conditions. Furthermore, the bulk depth is less restricted and the air flow rate can be controlled. Hence, the capacity and the reliability of the dryers are increased considerably compared to natural convection dryers. It is generally agreed that well-designed forced-convection distributed solar dryers are more effective and more controllable than the natural-circulation types.

The use of forced convection can reduce drying time by three times and decrease the required collector area by 50 %. Consequently, dryer using fans may achieve the same throughput as a natural convection dryer with a collector six times as large [10]. Fans may be powered with utility electricity if it is available, or with a solar photovoltaic panel.

In a solar photovoltaic panel -powered system (Figure 2-4), the fan is directly coupled to the solar module, working without an accumulator and load controller. Increasing solar radiation increases the module's output, thus speeding up the fan. This has the advantage of permitting a simple temperature control merely by appropriately designing the components of the solar photovoltaic panel system, thus obviating any additional control devices as long as the system is suitably dimensioned.

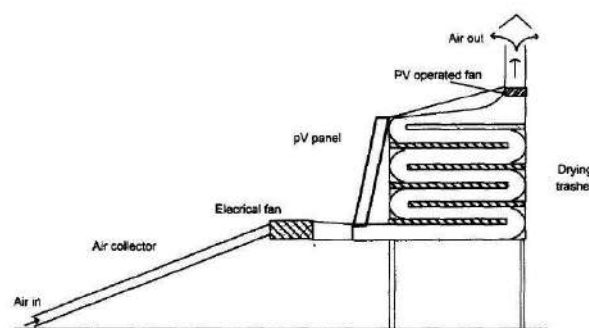


Figure 2-4: Solar Photovoltaic Panel -powered the Fan of Dryer

### 2-5-1-1: Integral Type:

Large-scale, commercial, forced-convection, greenhouse-type dryers are like transparent roof solar barns and are used for solar timber drying kilns (see Figure 2-5). Small-scale forced dryers are often equipped with auxiliary heating.

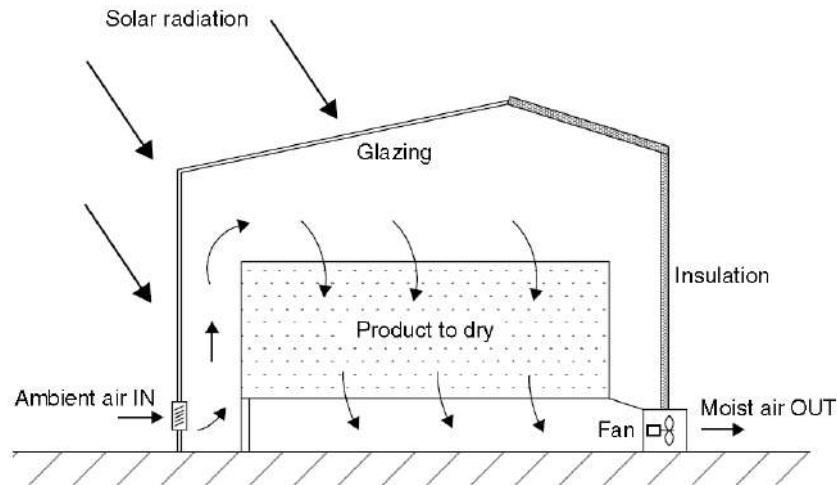


Figure 2-5: Schematic diagram of a forced-convection, transparent-roof solar barn

Another variation of this type of dryer is the solar collector–roof/wall, in which the solar heat collector forms an integral part of the roof and/or wall of the drying chamber. A solar-roof dryer is shown in Figure (2-6). A collector-wall system is a black painted concrete block wall with outside glazing forms the solar collector and serves as a thermal storage.

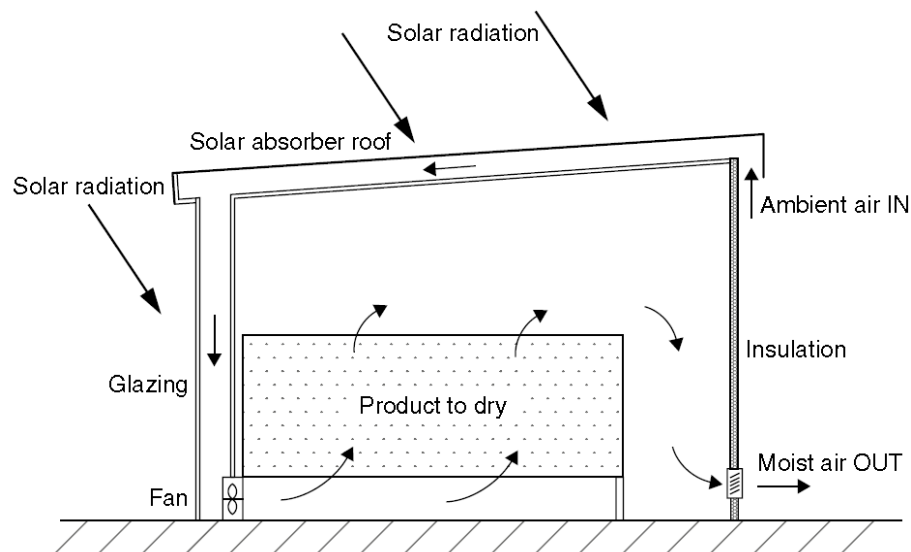


Figure 2-6: Schematic diagram of an active collector–roof solar energy storage dryer

### 2-5-1-2: Distributed Type:

A typical distributed-type active solar dryer is shown in Figure (2-6). It comprises four components: a drying chamber, a solar energy air heater, a fan, and ducting to transfer the hot air from the collector to the dryer.

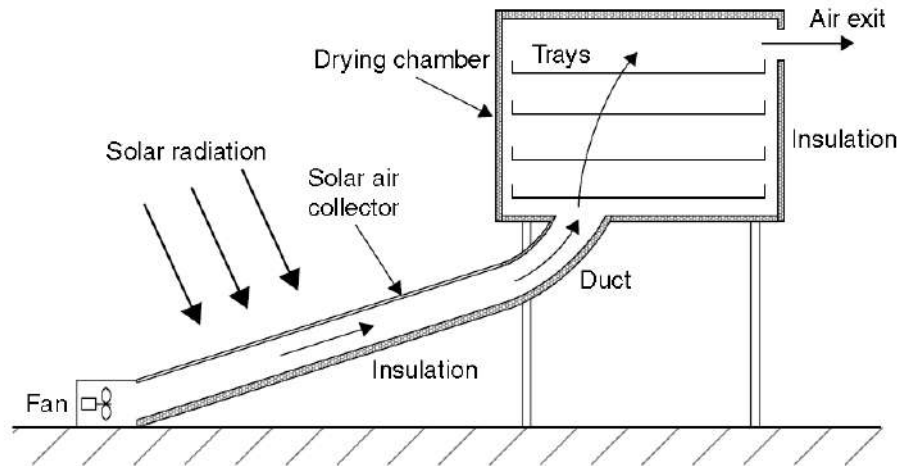


Figure 2-7: Schematic diagram of a distributed-type active solar dryer.

### 2-5-1-3: Mixed-mode Type:

The mixed-mode dryer is similar to the distributed type with the difference that the walls and roof of the dryer are made from glass, to allow solar energy to warm the products directly, as shown in Figure (2-8).

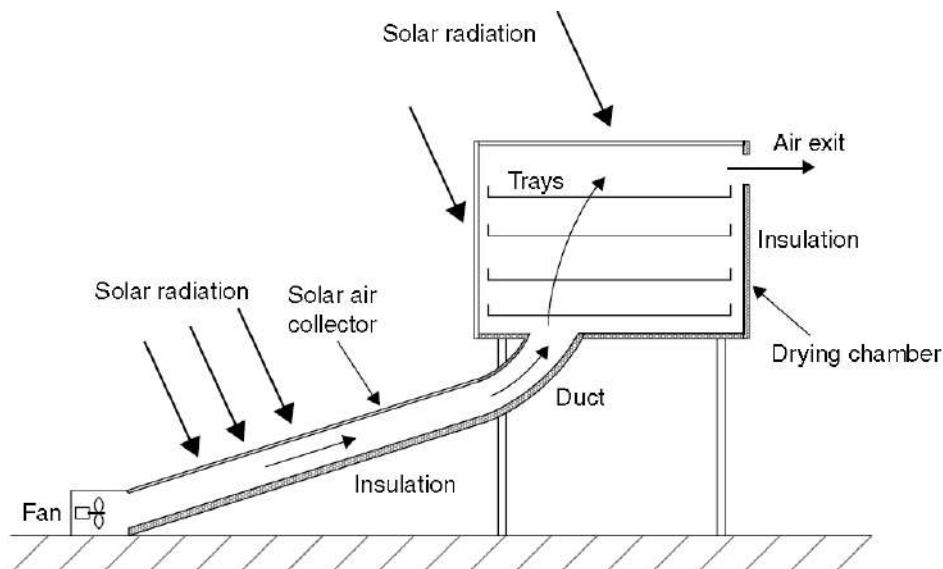


Figure 2-8: Schematic diagram of a mixed-mode-type active solar dryer

Most air heaters use metal or wood absorbers, whereas black polythene absorbers have been used in a few designs in an attempt to minimize cost.

### ***2-5-2: Passive Solar Energy Dryers:***

Passive solar dryers are also called natural circulation or natural convection systems. They are generally of a size appropriate for on-farm use. They can be either direct or indirect.

Natural-circulation solar dryers depend for their operation entirely on solar-energy. In such systems, solar-heated air is circulated through the crop by buoyancy forces or as a result of wind pressure, acting either singly or in combination.

Passive or natural circulation solar energy dryers operate by using entirely renewable sources of energy, such as solar and wind.

#### ***2-5-2-1: Integral Type:***

Integral-type, natural circulation, solar energy dryers are also called direct passive solar energy dryers.

In this system, the crop is placed in a drying chamber, which is made with transparent walls; therefore, the necessary heat is obtained by the direct absorption of solar radiation at the product, from the internal surfaces of the chamber, and by convection from the heated air mass within the chamber.

The heat removes the moisture from the product and, at the same time, lowers the relative humidity of the resident air mass, thus increasing its moisture-carrying capacity. The air in the chamber is also expanded because the density of the hot air is lower than the cold, thus generating natural circulation, which also helps in the removal of moisture, along with the warm air. Because heat is transferred to the crop by both convection and radiation, the rate of drying for direct dryers is greater than that for indirect dryers.

Integral-type, natural circulation solar energy dryers can be of a very simple construction, as shown in Figure (2-9).

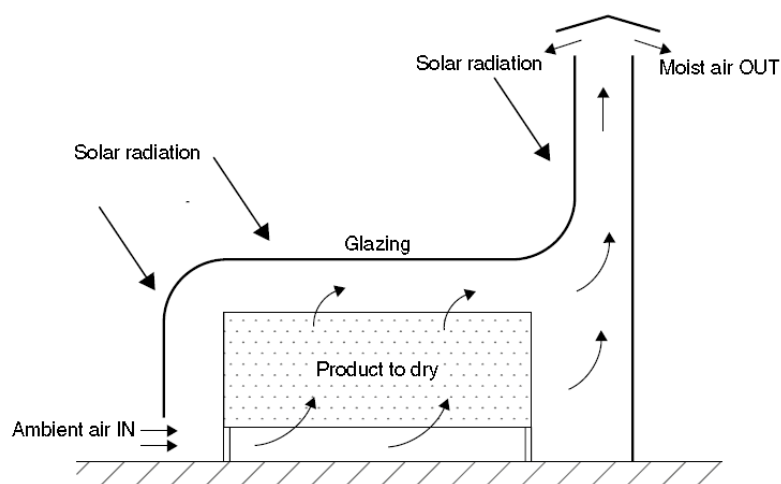


Figure 2-9: Schematic diagram of an integral-type passive solar dryer.

#### 2-5-2-2-1: Solar Cabinet Dryers:

The passive solar cabinet dryers are generally simple and inexpensive units having high applications for domestic purposes. They are suitable for drying of agricultural products, spices and herbs etc., constructed normally with a drying area of 1-2 m<sup>2</sup> and capacities of 10-20 kg. Figure 2-10 shows a typical passive solar cabinet dryer.

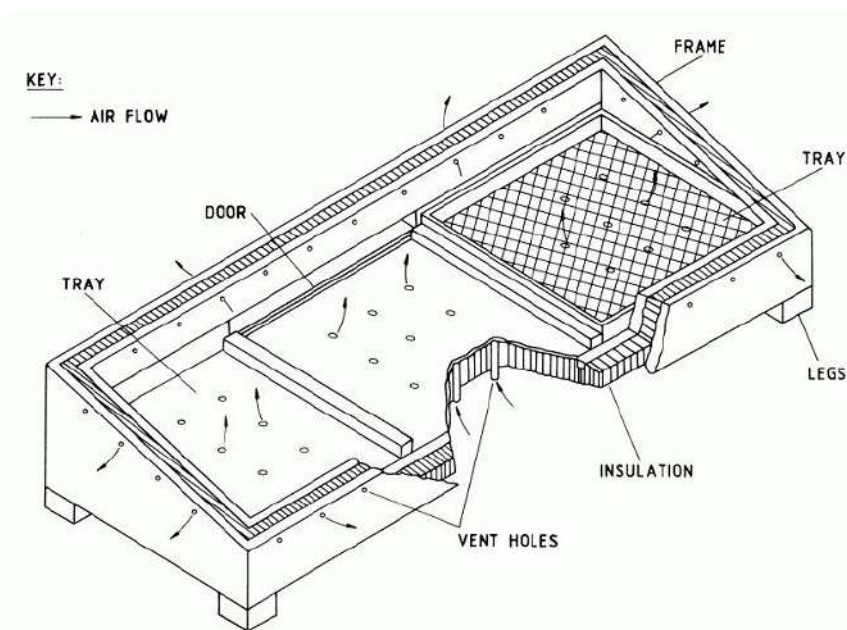


Figure 2-10: A typical natural-circulation solar-energy cabinet dryer

The heat for drying is transmitted through the glass cover and is absorbed on the blackened interior and crops as well. The required air circulation is maintained by the warm

moist air leaving via the upper vent under the action of buoyancy forces and generating suction of fresh air from the base inlet.

The passive solar cabinet dryer has an advantage of being cheap and easy in construction from locally available material, however their major drawback is poor moist removal rates and very high temperature (70-100°C) causing overheating of the product.

#### ***2-5-2-1-2: Natural-Circulation Greenhouse Dryers:***

These are also called as tent dryers and are basically modified greenhouses. They are designed with vents of appropriate size and position to have a controlled air flow. They are characterized by extensive glazing by the transparent cover of polyethylene sheet.

A typical greenhouse type solar dryer with a transparent semi-cylindrical chamber with a cylindrical solar chimney posted vertically at one end and a door for air inlet and access to the chamber at another end as shown in Figure 2-11.

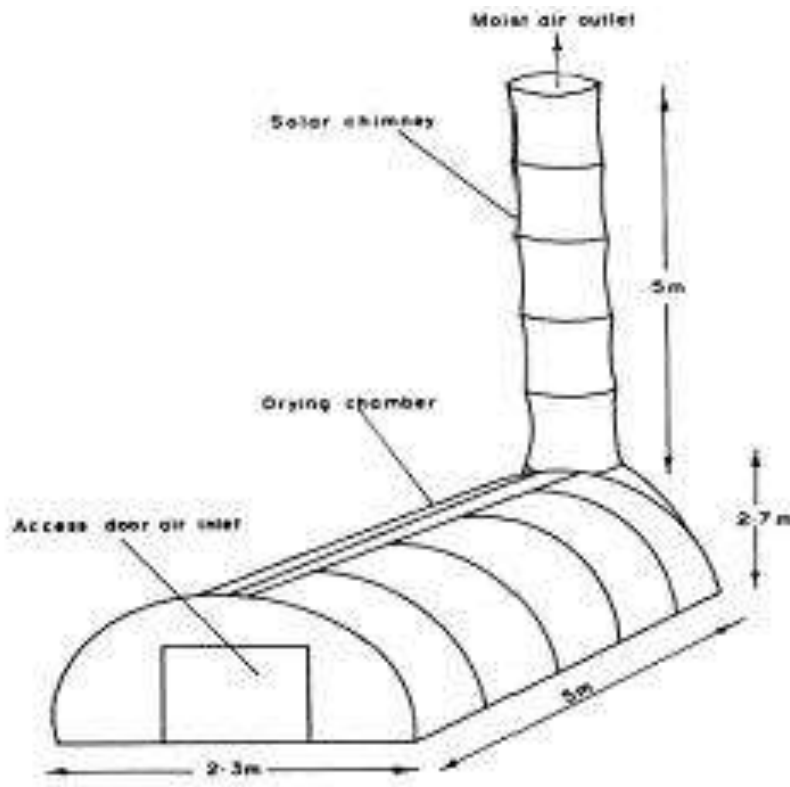


Figure 2-11: A greenhouse type natural-circulation solar-energy dryer

### 2-5-2-2: Distributed Type:

Distributed, natural circulation, solar energy dryers are also called indirect passive dryers. A typical distributed natural circulation solar energy dryer comprises an air heating solar energy collector, appropriate insulated ducting, a drying chamber, and a chimney, as shown in Figure (2-12).

In this design, the crop is located on trays or shelves inside an opaque drying chamber, which does not allow the solar radiation to reach the product directly. Air, which is heated during its passage through an air solar collector, is ducted to the drying chamber to dry the product.

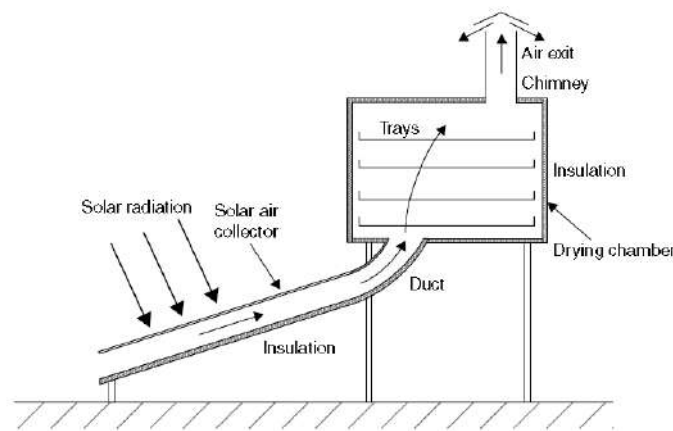


Figure 2-12: Schematic diagram of a distributed-type passive solar dryer.

### 2-5-2-3: Mixed-mode Type:

Mixed-mode, natural circulation, solar energy dryers combine the features of the integral-type and the distributed-type natural circulation solar energy dryers.

In this case, the combined action of solar radiation incident directly on the product to be dried and the air heated in a solar air collector provide the necessary heat required for the drying process.

A mixed-mode, natural circulation solar energy dryer has the same structural characteristics as the distributed type, i.e., a solar air heater, a separate drying chamber, and a chimney; in addition, the drying chamber walls are glazed so that the solar radiation can reach the product directly as in the integral-type dryers, as shown in Figure (2-13).



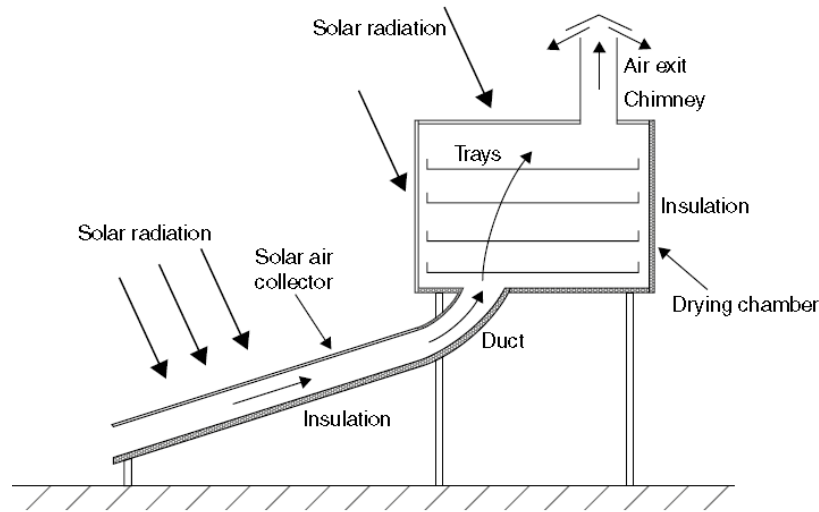


Figure 2-13: Schematic diagram of a natural circulation, mixed-mode solar energy dryer.

### 2-6: Working Principle of Solar Energy Dryers:

Solar energy dryers can broadly be classified into direct, indirect and hybrid solar dryers. The working principle of these dryers mainly depends upon the method of solar energy collection and its conversion to useful thermal energy for drying [12].

#### 2-6-1: Open Sun Drying:

Figure 2-14 shows the working principle of open sun drying by using only the solar energy. The crops are generally spread on the ground, mat, cement floor where they receive short wavelength solar energy during a major part of the day and also natural air circulation. A part of the energy is reflected back and the remaining is absorbed by the surface depending upon the color of the crops.

The absorbed radiation is converted into thermal energy and the temperature of the material starts to increase. However, there are losses like the long wavelength radiation loss from the surface of crop to ambient air through moist air and also convective heat loss due to the blowing wind through moist air over the crop surface. The process is independent of any other source of energy except sunlight and hence the cheapest method however but has a number of limitations.

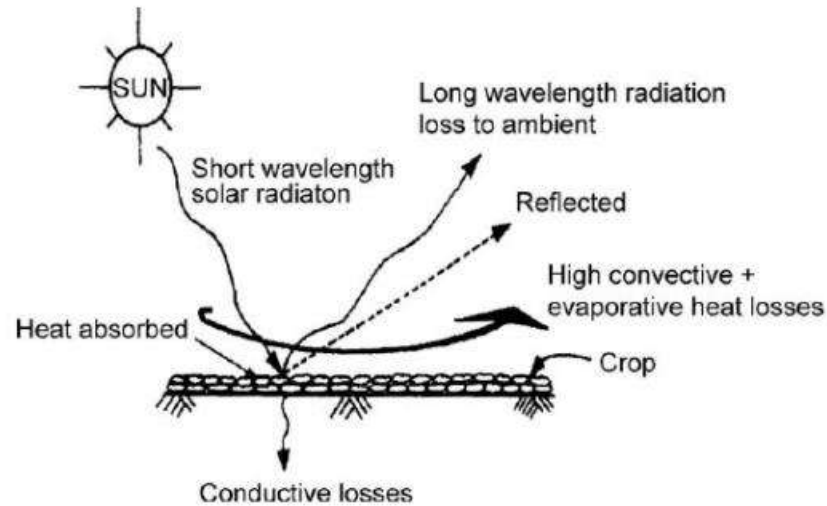


Figure 2-14: Working principle of open sun drying

In general, the open sun drying method does not fulfill the required quality standards and sometimes the products cannot be sold in the international market. With the awareness of inadequacies involved in open sun drying, a more scientific method of solar-energy utilization for crop drying has emerged termed as solar drying.

### 2-6-2: Direct Solar Drying:

The working principle of direct solar crop drying is shown in Figure 2-15, also known as a solar cabinet dryer. Here the moisture is taken away by the air entering into the cabinet from below and escaping through at the top exit as shown in Figure.

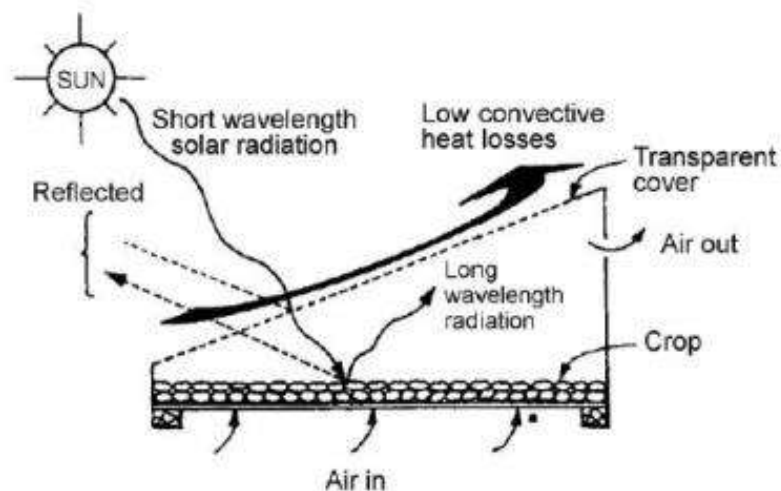


Figure 2-15: Working principle of direct solar drying

In the cabinet dryer, of the total solar radiation impinging on the glass cover, a part is reflected back to atmosphere and the remaining is transmitted inside the cabinet. A part of the transmitted radiation is then reflected back from the crop surface and the rest is absorbed by the surface of the crop which causes its temperature to increase and thereby emit long wavelength radiations which are not allowed to escape to atmosphere due to the glass cover.

The overall phenomena cause the temperature above the crop inside the cabinet to be higher. The glass cover in the cabinet dryer thus serves in reducing direct convective losses to the ambient which plays an important role in increasing the crop and cabinet temperature.

### 2-6-3: Indirect Solar Drying:

Figure 2-16 describes the working principle of indirect solar drying. These differ from direct dryers with respect to heat transfer and vapor removal.

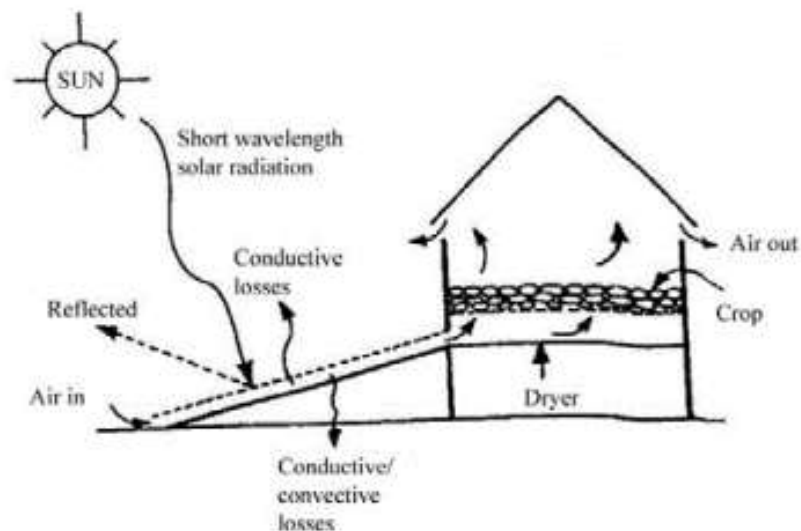


Figure 2-16: Working principle of indirect solar drying system (Sharma et al. 2009)

The crops in these indirect solar dryers are located in trays or shelves inside an opaque drying cabinet and a separate unit termed as solar collector is used for heating of the entering air into the cabinet.

The heated air is allowed to flow through/over the wet crop that provides the heat for moisture evaporation by convective heat transfer between the hot air and the wet crop. Drying takes place due to the difference in moisture concentration between the drying air and the air in the vicinity of crop surface.

#### **2-6-4: Hybrid Solar Drying:**

The hybrid solar dryers combine the features of the direct and indirect type solar energy dryers. Here the combined action of incident direct solar radiation on the product to be dried and air pre-heated in a solar collector heater produces the necessary heat required for the drying process.

#### **2-7: Construction of Solar Dryers:**

The materials used for the construction of the solar dryer are cheap and easily obtainable in the local market. The solar dryer consists of the solar collector (air heater), the fans (for active solar dryer) the drying cabinet and drying trays.

##### **2-7-1: Materials and Tools of Solar Dryer:**

The following materials were used for the construction of the solar dryer:

- 1- Wood - as the casing (housing) of the entire system; wood was selected being a good insulator and relatively cheaper than metals.
- 2- Glass - as the solar collector cover and the cover for the drying chamber. It permits the solar radiation into the system but resists the flow of heat energy out of the systems.
- 3- Aluminum sheet of suitable gauge thickness and aluminum painted black – for absorption of solar radiation.
- 4- Wooden or metals frames for constructing the trays.

5- Nails and glue as fasteners and adhesives.

6- Hinges and handle for the dryer's door.

7- Paint (black).

The materials used for the construction of the solar dryer are listed in Table 2-3:

Table 2-3: Materials used for the Construction of the Solar Dryer

No.	Component	Material
1	Solar Collector	Glass
2	Absorber Plate	Aluminum
3	Heating Chamber	Wood
4	Drying Chamber	Wood
5	Insulation	Glass wool
6	Tray	Aluminum
7	Roof	Wood

The following tools are used in the construction of solar dryer:

(Hand saw or skill saw, if available, Hammer, Tape measure, framing square or tri-square, Wood rasp, Screw driver, Tin snips, Staple gun, Keyhole saw, Paint brush, Chalking gun, Scissors, Pencils, Soaking pan).

### 2-7-2: Solar Dryer Components:

**a- Drying chamber:** the drying chamber was made up highly polished wood wish consist of three d trays also made of wood, the material has been chosen since wood is a poor conductor of heat and its smooth surface finish and also heat loss by radiation is minimized.

#### **b- Heating chamber:**

It consists of following components: Cover plate, absorber plate, insulation.

**Cover plate:** This is a transparent sheet used to cover the absorber, thereby preventing

dust and rain from coming in contact with the absorber, it also retards the heat from escaping, common Materials used for cover plates are glass or flexi glass.

**Absorber plate:** This is a metal painted black and placed below the cover to absorb, the incident solar radiation transmitted by cover thereby heating the air between it and the cover, the aluminum is chosen because its quick response in absorption of solar radiation and also copper because of its good ability to keep the absorbed solar radiation.

**Insulation:** This is used to minimize heat loss from the system, it is under the absorber plate, the insulator can withstand stagnation temperature, it is fire resistant and not subject to out-going gassing and it is damageable by moisture or insect, insulating materials are usually fiber glass, mineral wool.

### ***2-8: The Orientation of Solar Dryers:***

Apart from the effect of the characteristics of the collector itself, the output of the solar system is strongly dependent on the inclination angle of the collector to the sun.

The flat-plate solar collector was always tilted and oriented in such a way that it receives maximum solar radiation during the desired season of used.

The best stationary orientation is due south in the northern hemisphere and due north in southern hemisphere. Therefore, solar collector in this work is oriented facing south and tilted at approximately  $15^\circ$  more than the local geographical latitude, is the best recommended orientation for stationary absorber. This inclination is also to allow easy run and enhance air circulation.

The largest yield is obtained when the collector is always orientated perpendicular to the sun. However, the optimal tilt angle for the collectors varies according to the season, as the sun is higher in the sky in summer than in winter.

As a general rule, the optimum angle of tilt is equal to the degree of latitude of the site. But the minimum angle of the collector should be  $15^\circ$  to assist the thermosiphon effect. The Table (2-4) shows optimum tilt angles of different latitudes and seasons [11].

Table 2-4: Tilt angle for different latitudes and seasons

Latitude [degree]	Best collector tilt in:					
	June	Orientation	Sept./March	Orientation	December	Orientation
50 N	26.5	S	50	S	73.5	S
40 N	16.5	S	40	S	63.5	S
30 N	6.5	S	30	S	53.5	S
20 N	3.5	N	20	S	43.5	S
15 N	8.5	N	15	S	38.5	S
10 N	13.5	N	10	S	33.5	S
<b>Equator = 0</b>	<b>23.5</b>	<b>N</b>	<b>0</b>	<b>-</b>	<b>23.5</b>	<b>S</b>
10 S	33.5	N	10	N	13.5	S
15 S	38.5	N	15	N	8.5	S
20 S	43.5	N	20	N	3.5	S
30 S	53.5	N	30	N	6.5	N
40 S	63.5	N	40	N	16.5	N
50 S	73.5	N	50	N	26.5	N

## 2-9: Explain the Components of Solar Dryers:

### 2-9-1: Air Collectors:

The solar air collector is designed to heat air when irradiated by the sun. The basic components are: cover, absorber, air passage and insulation. Solar radiation transmitted through the cover heats the absorber, which in turn heats the air in the air passage [12].

The Advantages and disadvantages of air collectors in comparison to liquids collectors are:

#### **Advantages:**

- Air will not boil, cannot freeze and no damage results when there is a leakage.
- Nearly no corrosion problems.
- The system will not malfunction if there are small leaks.
- Air is non-toxic (at least, no more toxic than the air we breathe) and is freely available anywhere and at any time.
- Well-designed solar air heating systems require less technical equipment than liquid-based systems.

#### **Disadvantages:**

- Low heat capacity of air.
- High volume flow-rates, big duct-dimensioning.
- Low heat transfer between absorber and air.

### 2-9-2: Ventilation:

The air flow rate is crucial to the overall system performance. Too high an air flow consumes excessive fan power and too low rates cause poor thermal performance of the system.

In summary:

- The higher the mass-flow rates, the higher the efficiency of the collector.
- The electrical energy for the fan increases with the mass flow rate.
- The effect of leakages increases with the air flow rate.
- For drying purposes, a certain temperature level is often needed.

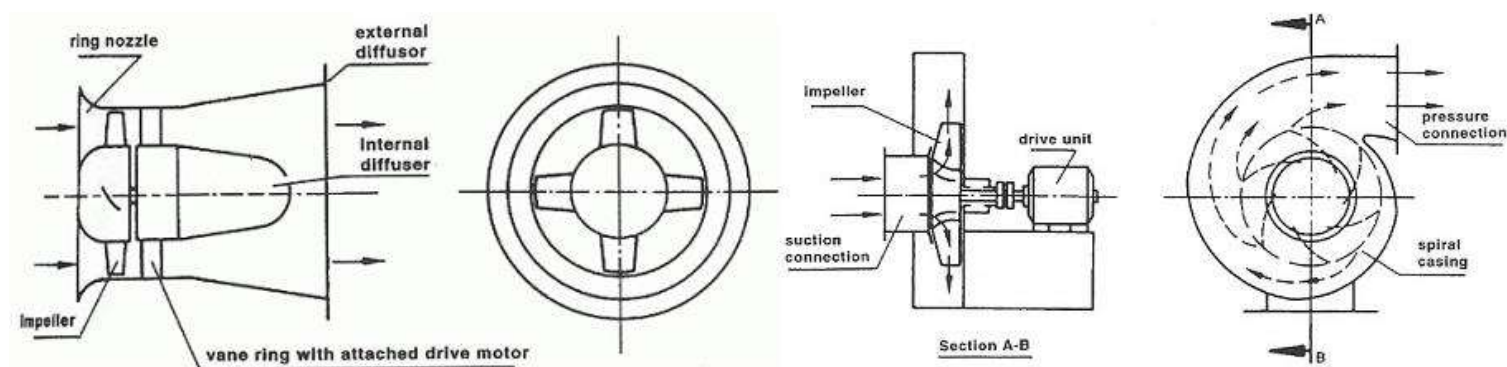
#### 9-2-2-1: Natural ventilation:

The natural ventilation due to the chimney effect is depends on the wind velocity available in the site, dimensions and structure of inlet entrance of air and dimensions and structure of chimney.

#### 9-2-2-2: Electrical Fans:

Fans are flow machines designed to convey a certain air volume and to increase the pressure in order to overcome the resistance of the system. They should work with the best possible efficiency and at lowest possible noise level.

Fans can be divided and classified according to the air flow direction through the fan. The major types are axial flow, radial flow and mixed flow. Figure (12-17) shows different types of fans used in solar dryers.



Axial fan (left) and radial fan (right)



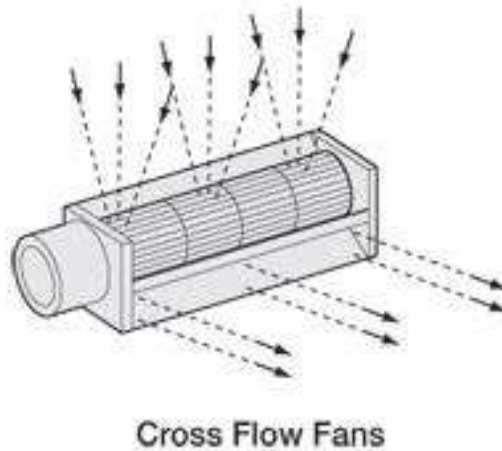


Figure 2-17: Different Types of Fans used in Solar Dryers.

***a-Axial fan:***

The air enters and leaves the fan axially. The main modules of an axial ventilator are the hub with the blades, the casing and the drive. There are several components designed to increase the efficiency of an axial blower, such as an inlet nozzle, stator, diffuser and moveable blades. The air flow of an axial fan can be controlled by:

- dampers on the extraction or pressure side of the fan;
- variation of the blade angle;
- variation of the rotational speed.

If energy savings are considered, the best way to change the air flow rate of a fan is to vary the speed of rotation. A common position for the drive is the hub of the fan.

The motor is cooled by the air flow and all the heat from the motor can be used, while the open cross section is reduced. Typical operating conditions of standard axial fans are high volume rates and low delivery pressure, e.g., ventilation of a sunspace or exhaust-air extraction from rooms.

***b- Radial fan:***

The air enters axially and leaves radially. These fans have usually a spiral casing with single or double inlet. Some special casings allow the use of a radial fan in a round duct. There

are different shapes of blades, which can be forward-curved, radial or back-ward-curved. It is possible to have the motor external to withstand high flow temperatures and to avoid heat gains due to the motor. A radial fan typically achieves a lower volume rate and a higher pressure increase than an axial fan. Radial fans are typically used in ducts with a higher flow resistance, e.g., ducts with air heating, cooling and filter devices.

### ***c-Cross-flow fan:***

The air flow runs through the impeller transversally. The volume increases proportionally to the impeller width. Cross-flow fans are suitable for blowing into narrow ducts or grooves with a broad width but with typically low volume rate and efficiency. An advantage of cross-flow fans is their low noise emission, on account of which they are used in applications where the fan is placed near the user, e.g., an underfloor convector.

### ***2-9-3: Fan Control:***

The air flow or the required pressure increase is adjusted to the respective requirements by way of different control mechanisms, such as:

- On/off control.
- Change of rotational speed with electronic controllers or with coupled to insulation on photovoltaic system.
- Throttling with a damper or throttling flap.
- Bypass control.

### ***2-9-4: Power Supply from Solar Cells:***

Photovoltaics cells offer an ideal energy supply for fans. The electricity produced by the solar cells is not only supplied at the same time but also increases automatically with an increasing demand. As solar cells produce DC, the choice of DC motors is obvious. Figure (12-18) shows the use of photovoltaics cells for energy supply for fans of solar dryers.

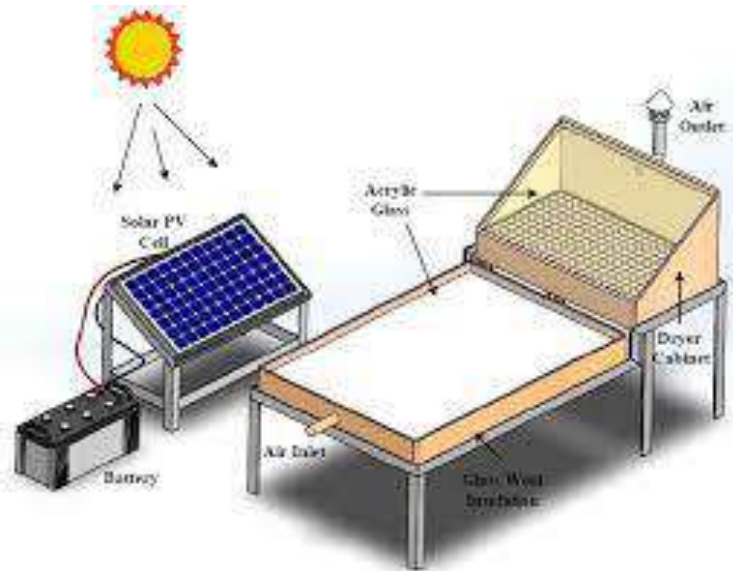


Figure 2-18: Photovoltaics Cells for Energy Supply for Fans of Solar Dryers.

In particular, it is essential to ensure that the fan starts to operate even at low levels of radiation. This is necessary to remove the moisture from the drying compartment so as to prevent spoilage and or growth of mold and yeast.

Cooling fans of cars, which have been used instead of the original ones in several attempts due to their ease of availability and low cost, do not meet this requirement and should therefore not be used.

By the use of DC motors in combination with a photovoltaic panel, it is necessary to take into account that the start-up power can be up to five times higher than the maximum power during operation.

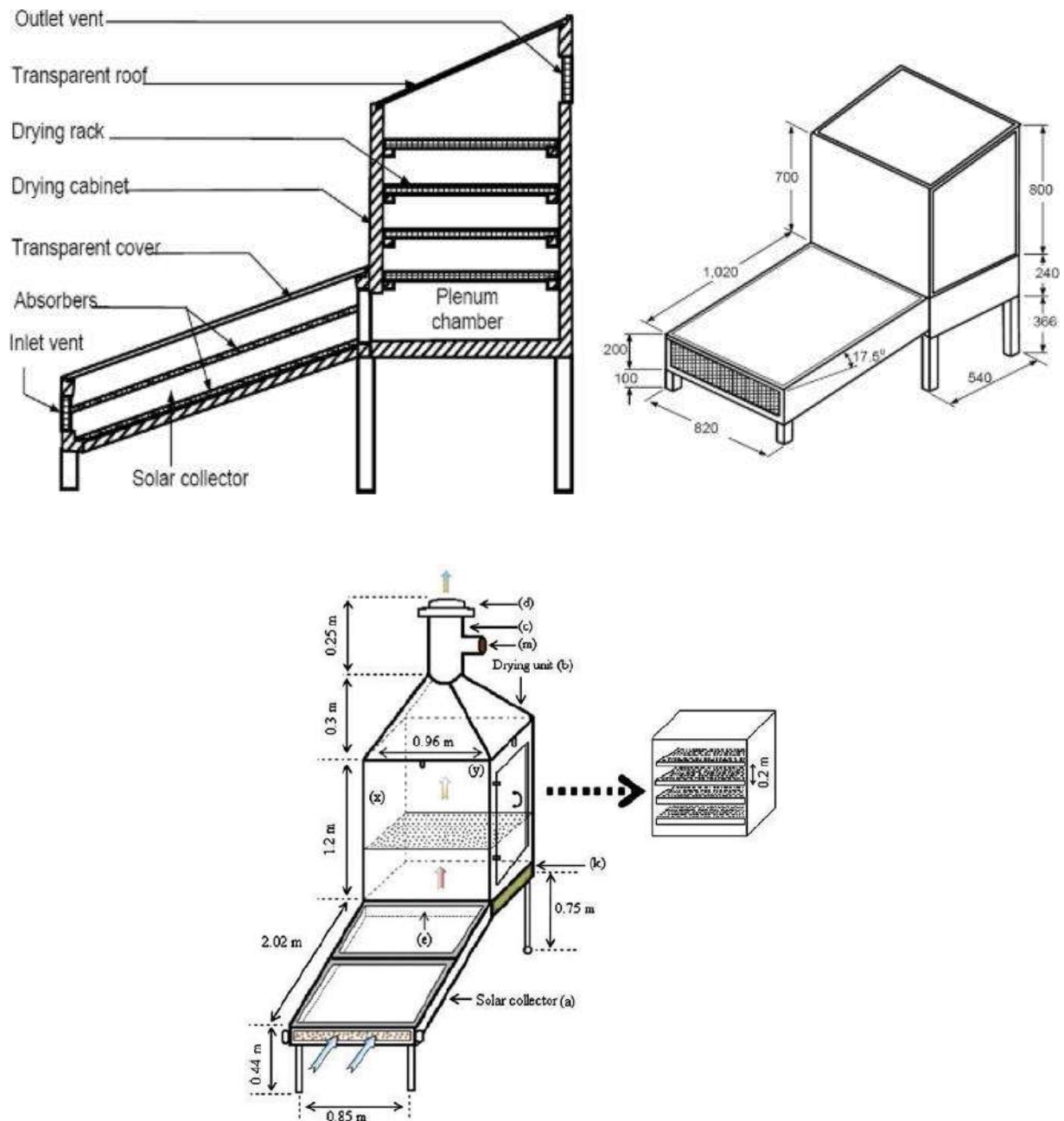
Table (2-5) show exemplary technical data of the drive systems.

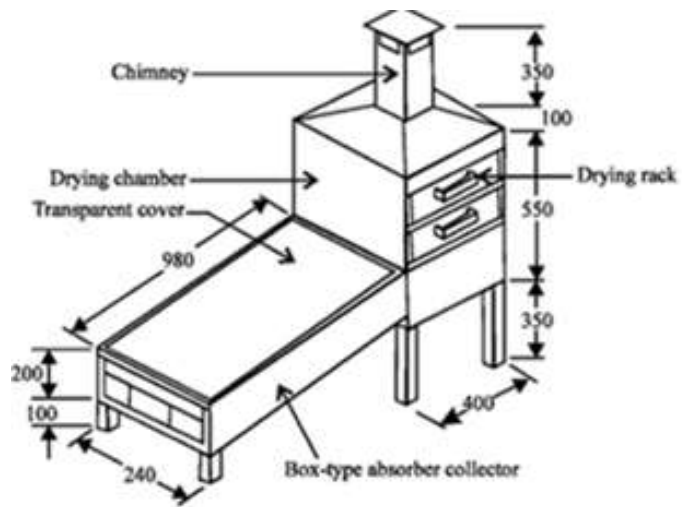
Table 2-5: Exemplary technical data of the drive systems (freely blowing) [6]

Drive system	Mains-powered	Photovoltaic (PV)	
Components	Radial fan	Axial fan	Solar module
Maker	ebm	Fiat	Solarex
Type	R4E 280-AD0805	Uno, gasoline-fueled model	MSX 83
Rated voltage [V]	220	12	16.9
Rated current [A]	0.33	7.0	4.92
Nominal consumption [W]	70	84.0	83.2
Air flow rate [m <sup>3</sup> /h]	1360	1520	
Rated speed [RPM]	1400	2800	

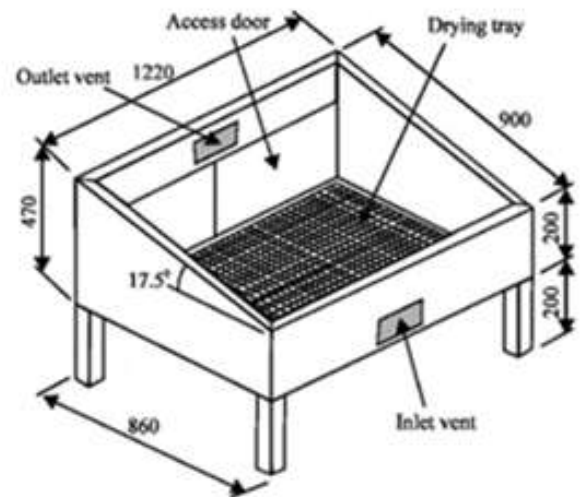
### 2-10: Design of Solar Dryers:

The designed and constructed solar dryer consists of two major compartments or chambers being integrated together, the solar collector compartment, which can also be referred to as the air heater, and the drying chamber, designed to accommodate layers of drying trays on which the produces are placed for drying. Figures (2-19) shows different designs of different types of solar dryers [10, 11 and 12].

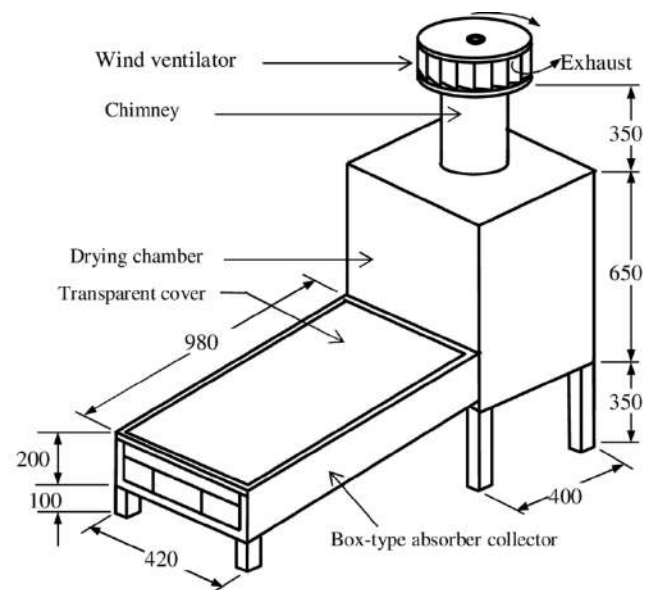
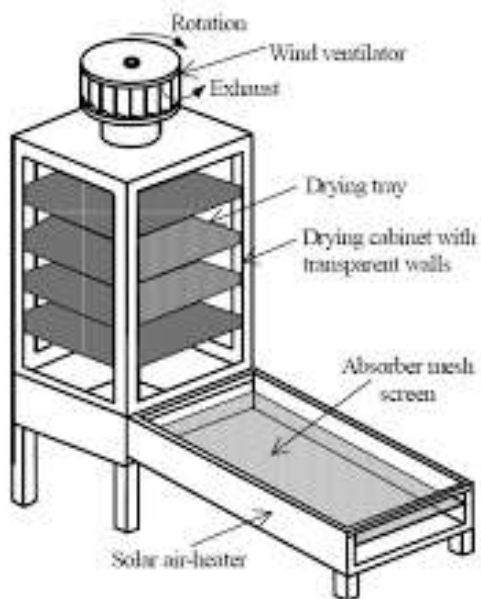


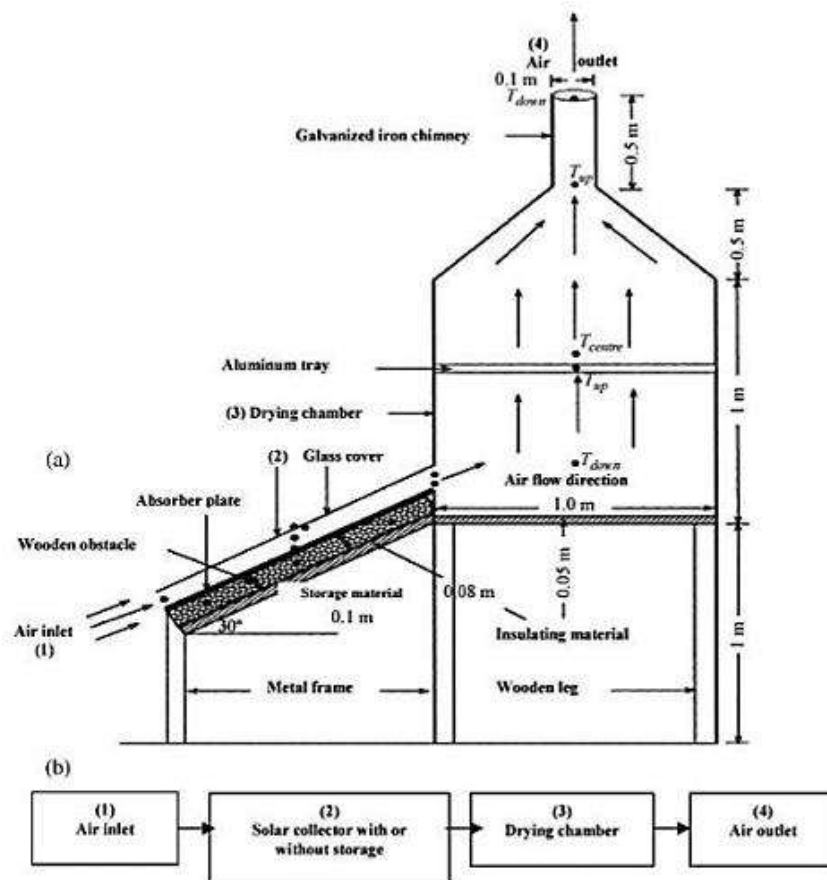
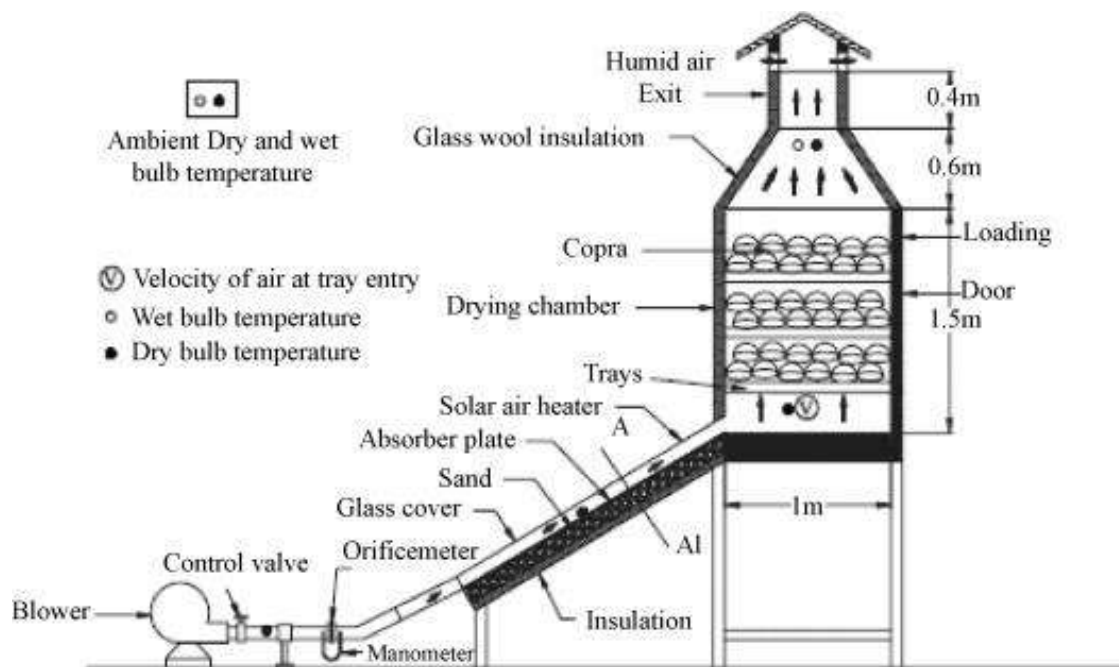


All dimensions in mm



All dimensions in mm





Figures 2-19: Different Designs of Different Types of Solar Dryers.

***Chapter -3-***  
***Selection of Solar***  
***Dryers***

### *Chapter - 3*

#### *Selection of Solar Dryers*

A huge advantage of solar dryers is the fact that different types of fruits and vegetables can be dried. The quality of products dried in this way is excellent, due to the fact that the food is not in direct sunlight (cabinet or in-house dryer), and due to a shorter drying process – up to a 1/3 of the time in comparison to traditional sun drying.

The drying operation must not be considered as merely the removal of moisture since there are many quality factors that can be adversely affected by incorrect selection of drying conditions and equipment.

The desirable properties of high-quality, e.g., for grains (for example), include:

- Low and uniform moisture content.
- Minimal proportion of broken and damaged grains.
- Low susceptibility to subsequent breakage.
- High viability.
- Low mould counts.
- High nutritive value.
- Consumer acceptability of appearance and organoleptic properties.

Apart from weather conditions the drying behavior of agricultural crops during drying depends on the [1]:

- Product.
- Size and shape.
- Initial moisture content.
- Final moisture content.
- Bulk density.
- Thickness of the layer.
- Mechanical or chemical pre-treatment.
- Turning intervals.



- Temperature of grain.
- Temperature, humidity of air in contact with the grain.
- Velocity of air in contact with the grain.

Look for details about the physics of drying in the appendix A-1.

### 3-1: Selection of Solar Dryers:

The diversity of food products has introduced many types and combinations of solar dryers to the food industry. The methods of supplying heat and transporting the moisture and the drying product are the basic variations among different types of solar dryers [12].

Table 3-1 enumerates the typical checklist for evaluation and selection for solar dryers.

Table 3-1: Typical checklist for preliminary evaluation and selection of solar dryers

No.	Parameters	Features
1	<b>Physical features of dryer</b>	<ul style="list-style-type: none"> <li>• Type, size and shape.</li> <li>• Collector area.</li> <li>• Drying capacity/loading density (kg/unit tray area).</li> <li>• Tray area and number of trays.</li> <li>• Loading/unloading convenience.</li> </ul>
2	<b>Thermal performance</b>	<ul style="list-style-type: none"> <li>• Solar insolation.</li> <li>• Drying time/drying rate.</li> <li>• Dryer/drying efficiency.</li> <li>• Drying air temperature and relative humidity.</li> <li>• Airflow rate</li> </ul>
3	<b>Properties of the material being handled</b>	<ul style="list-style-type: none"> <li>• Physical characteristics (wet/dry).</li> <li>• Acidity.</li> <li>• Corrosiveness.</li> <li>• Toxicity.</li> <li>• Flammability.</li> <li>• Particle size.</li> </ul>

		<ul style="list-style-type: none"> <li>• Abrasiveness</li> </ul>
4	<b>Drying characteristics of the material</b>	<ul style="list-style-type: none"> <li>• Type of moisture (bound, unbound, or both).</li> <li>• Initial moisture content.</li> <li>• Final moisture content (maximum).</li> <li>• Permissible drying temperature.</li> <li>• Probable drying time for different dryers</li> </ul>
5	<b>Flow of material to and from the dryer</b>	<ul style="list-style-type: none"> <li>• Quantity to be handled per hour.</li> <li>• Continuous or batch operation.</li> <li>• Process prior to drying.</li> <li>• Process subsequent to drying</li> </ul>
6	<b>Product qualities</b>	<ul style="list-style-type: none"> <li>• Shrinkage.</li> <li>• Contamination.</li> <li>• Uniformity of final moisture content.</li> <li>• Decomposition of product.</li> <li>• Over-drying.</li> <li>• State of subdivision.</li> <li>• Appearance.</li> <li>• Flavor.</li> <li>• Bulk density</li> </ul>
7	<b>Recovery problems</b>	<ul style="list-style-type: none"> <li>• Dust recovery.</li> <li>• Solvent recovery.</li> </ul>
8	<b>Facilities available at site of proposed installation</b>	<ul style="list-style-type: none"> <li>• Space.</li> <li>• Temperature, humidity, and cleanliness of air.</li> <li>• Available fuels.</li> <li>• Available electric power.</li> <li>• Permissible noise, vibration, dust, or heat losses.</li> <li>• Source of wet feed.</li> <li>• Exhaust-gas outlets</li> </ul>
9	<b>Economics</b>	<ul style="list-style-type: none"> <li>• Cost of dryer.</li> <li>• Cost of drying.</li> <li>• Payback.</li> </ul>

10	<b>Other parameters</b>	<ul style="list-style-type: none"> <li>• Skilled technician and operator requirements.</li> <li>• Safety and reliability.</li> <li>• Maintenance</li> </ul>
----	-------------------------	---

### ***3-1-1: Initial selection of solar dryers:***

The initial selection can be of the type of solar dryer that appears best suited for handling the wet material and dry product, that fits well into the continuity of the process as a whole, and that produces the product of desired properties.

### ***3-1-2: Initial comparison of solar dryers:***

The solar dryers selected in step one should then be evaluated from the available cost and performance data selecting a few. The rests should then be eliminated from further considerations.

### ***3-1-3: Solar Drying Tests:***

Drying tests should then be conducted in small-scale units based on the solar dryers selected in step two. These tests are expected to establish the optimum operating conditions, the ability of the dryer to handle the material physically, product quality and characteristics, and dryer size. Occasionally, simple laboratory experiments can serve to reduce further the number of dryers under consideration, as there is rare scope for changes to be made once the dryer is installed. Based on the results of these drying tests that establish size and operating characteristics formal quotations and guarantees should be obtained from dryer manufacturers. Initial costs, installation costs, operating costs, product quality, dryer operability, and dryer flexibility can then be given proper weight in final evaluation and selection.

### ***3-1-4: Final Selection of Solar Dryer:***

From the results of the drying tests and quotations, the final selection of the most suitable solar dryer can be made. The physical nature of the material to be handled is one of the primary features for consideration as these are different for coarse solid, slurry and sheet material. After

the preliminary selection of the suitable type of solar dryer, a further analysis for revaluation of its size and cost should be done to select the most economical one.

After analyzing adequate data on the cost and performance obtained from the equipment manufacturers the factors governing their performance should be due considered. This may involve at times compromising certain steps that precede or follow drying process, like sorting, conveying or packaging and hence must be considered carefully.

### ***3-2: Non-technical Aspects for Selection Solar Dryers:***

#### ***3-2-1: Weather conditions:***

The performance of solar dryers is significantly dependent on the weather conditions. Both the heat required for removing the moisture as well as the electricity necessary for driving the fans are generated in the most cases by solar energy only. In addition to the pre-treatment of the product, the weather conditions have the biggest influence on the capacity of product that can be dried within a certain time period.

The drying time is short under sunny conditions and accordingly extended during adverse weather conditions. The difference in drying capacity between dry and rainy season has to be taken into consideration for the calculation of the yearly capacity of the dryer.

The utilization of solar energy as the only energy source is recommended for small-scale dryers where the risk of spoilage of big quantities of crops due to bad weather is low. If large-scale solar dryers are used for commercial purposes, it is strongly recommended to equip the dryer with a back-up heater to bridge periods with bad weather.

#### ***3-2-2: Storage:***

For small farmers the main purpose in storing grains is to ensure household food supplies. Farm storage also provides a form of saving, to cover future cash need through sale, or for barter exchange or gift-giving. Grain is also stored for seed and as inputs into household enterprises such as beer brewing, or the preparation of cooked food.

There is an ongoing debate about whether farmers are forced to sell because of debt and economic dependence on others, or whether they sell because they regard storage as

- too costly (in terms of time), or
- too risky (given the risk of losses and unpredictability of future prices), or
- unprofitable in relation to other investments such as cattle.

There is no single answer to the debate, since there is much variation in the circumstances under which individual farmers operate, both within and between nations [14].

### **3-2-3: Capacity:**

The capacity of a solar dryer mainly depends on the crop itself and the shape. On the one hand, it should not be too big to ensure that the preparation (washing, slicing and pre-drying processing) of the product to be dried can be completed within a certain time period. On the other hand it should be big enough to enable the user to generate income and thus to create new jobs.

### **3-2-4: Selection, Cleaning and Pre-treatment:**

A process similar to the following seven steps is usually used when drying fruits and vegetables (and fish, with some modifications) [27]:

- 1- Selection (fresh, undamaged produce).
- 2- Cleaning (washing & disinfection).
- 3- Preparation (peeling, slicing, etc.).
- 4- Pre-treatment (sulfurizing, blanching, salting).
- 5- Drying.
- 6- Packaging.
- 7- Storage or sale.

Only fresh, undamaged food should be selected for drying to reduce the chances of spoilage and to help to ensure a quality product. After selection, it is important to clean the produce. This is because drying does not always destroy microorganisms, but only inhibits their growth.

Fruits, vegetables, and meats generally require a pre-treatment before drying. The quality of dried fruits and vegetables is generally improved with one or more of the following pre-treatments: anti-discoloration by coating with vitamin C, de-waxing by briefly boiling and

quenching, and sulfurization by soaking or fumigating. Fish is often salted. A small amount of chemical will treat a large amount of produce, and thus the cost for these supplies is usually small. However, potential problems with availability and the complexity of the process should be considered.

For strict quality control, the drying rate may be monitored and correlated to the food moisture content to help determine the proper drying parameters (see the Appendix A for more information).

### ***3-3: Economics of Solar Dryers:***

Solar dryers are generally capital intensive and therefore the financial viability is the key to successfully compete with any of the other dryers. The financial analysis generally includes the cost of dryer (fixed cost), cost of drying (operating expenses) and payback. They can be viable only if the annual cost of extra investment (on the solar dryer) could be balanced against fuel savings, or if the equipment cost could be reduced.

The user or dryer designer looks for a favorable combination of cost, energy efficiency, quality, and price of the final product. Payback is the measure of time (number of days/months/years) it takes to recoup the total investment made on a dryer, in the form of operational cash inflow. Payback analysis does not measure the profitability of dryer as it does not take the service life of dryer into consideration.

Continued use of the dryer rather than seasonal use will decrease the drying cost and payback. Economic analysis on a solar dryer should also incorporate the cost benefits due to improved quality, higher yields, less floor area and quicker drying [15].

*Chapter -4-*

**Applications and  
Experiences of Solar  
Dryers**

## **Chapter - 4**

### **Applications and Experiences of Solar Dryers**

The following chapter show examples of applied drying systems and different experiences from all over the world. Discussion will be based on some selected commodities where drying is the major step involved in processing.

World commodities can be classified into food and non-food types Table (4-1). Most agricultural commodities are traded in dried form for transportation, storage and handling purposes.

Table 4-1: Agricultural Commodities Traded in Market

Type	Examples of commodities
Food	Sugarcane, maize, wheat, rice, paddy, cow milk, vegetables, potatoes, cassava, sugar beet, soybeans, tomatoes, barley, meat, watermelons, bananas, onions, cocoa, coffee, palm oil, fruits etc
Non food	Timber, wool, rubber, cotton etc

The moisture contents of the dried products are often specified in standards issued by specific governing bodies. Failure to comply with these requirements would result in penalty imposed to the sellers/exporters.

The additional weight due to the higher moisture content not only has an implication on cost, but also on health-related issue for some commodities i.e., molds growth or mycotoxin.

The preservation of these commodities is limited by its moisture content as indicated in Table (4-2). Considerable losses can occur due to failure to reach the safe moisture level susceptible to quality degradation [16].



Table 4-2: Range of Moisture Contents of some Agricultural Commodities

	Moisture content	
Commodity	Initial	Final
Wheat, barley, rye	20 – 25%wb	14 – 16 %wb
Oats, paddy, corn	25 – 45 %wb	12 – 14 %wb
Coffee	50 %db	11 %db
Cocoa	50 %db	7 %db
Pepper	-	5 %db
Onions, garlic	80 %db	4 %db
Wood	Green	10-12 %db
Cotton seed	-	8 %db

**4-1: Solar Drying of some Selected Commodities:****4-1-1: Fruit and Vegetable Drying:****4-1-1-1: Table-like Solar Dryer:**

This dryers' design and construction is relatively simple, artisans and carpenters are not required to build the dryers (Figure 4-1).

These types performed equally well for drying vegetables. The dryer could produce approximately 1.5 kg of dried vegetables, if the vegetables were thinly spread to facilitate faster drying. On average, the dryers were used three times a week, with drying times ranging from four to six hours per use, depending on the type of vegetable and intensity of the sun.

For example, it would take about four hours to dry amaranth (mchicha) leaves on a sunny day, but six hours for sweet potato. Drying one kilogram of fresh vegetables would yield approximately 250 grams of the dried food product.

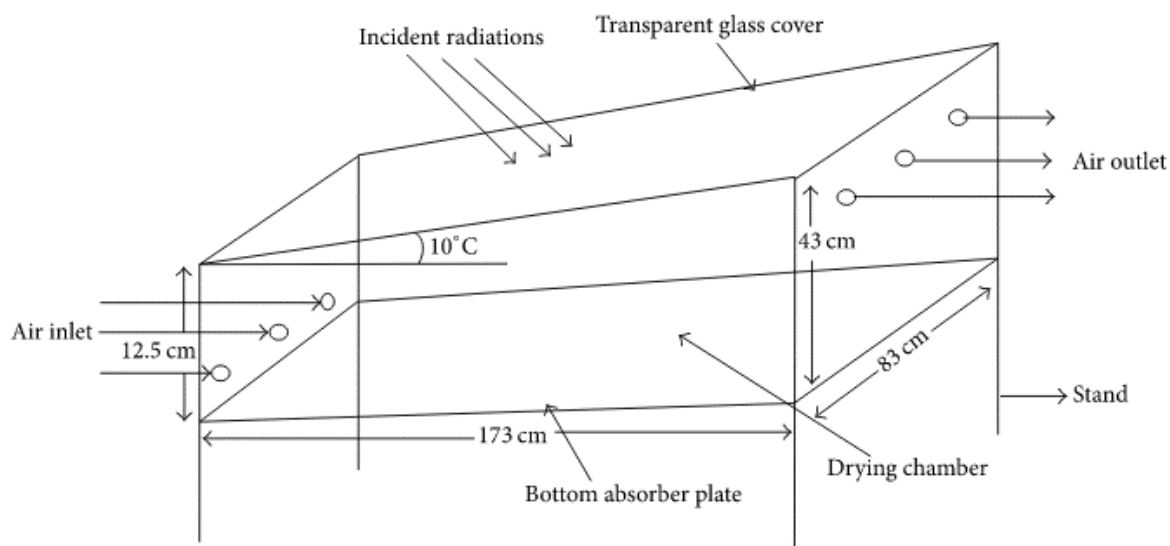


Figure 4-1: Table-like Solar Dryer.

#### 4-1-1-2: Banana Dryer:

The solar dryer system is operating in a mixed mode, which uses indirect heating through forced convection, which gives high yield and good quality for the dried product.

The system is composed of:

- An electrical ventilator allowing an independent air flow rate.
- A solar collector in which its characteristics and dimensions were determined.
- according to hot air flow rate and operating temperature.
- A special designed dryer for tropical fruits.

A scheme of the solar dryer is shown in Figure (4-2). The innovation of this work is not only in the dryer design and dimension, but also in its configuration, material and in the solar collector dimension. The collector was constructed in such a way that its use can be versatile. It is made of flexible PVC, in a cylinder shape with two cones at the both ends. At the bottom, 50% of the collector is made of dark plastic in order to absorb heat and at the top with transparent plastic, in which the solar rays penetrate.

The trays, which contain the fruits to be dried, can be arranged one on top of the other. An exhauster provides air circulation, through an exit in the superior part.

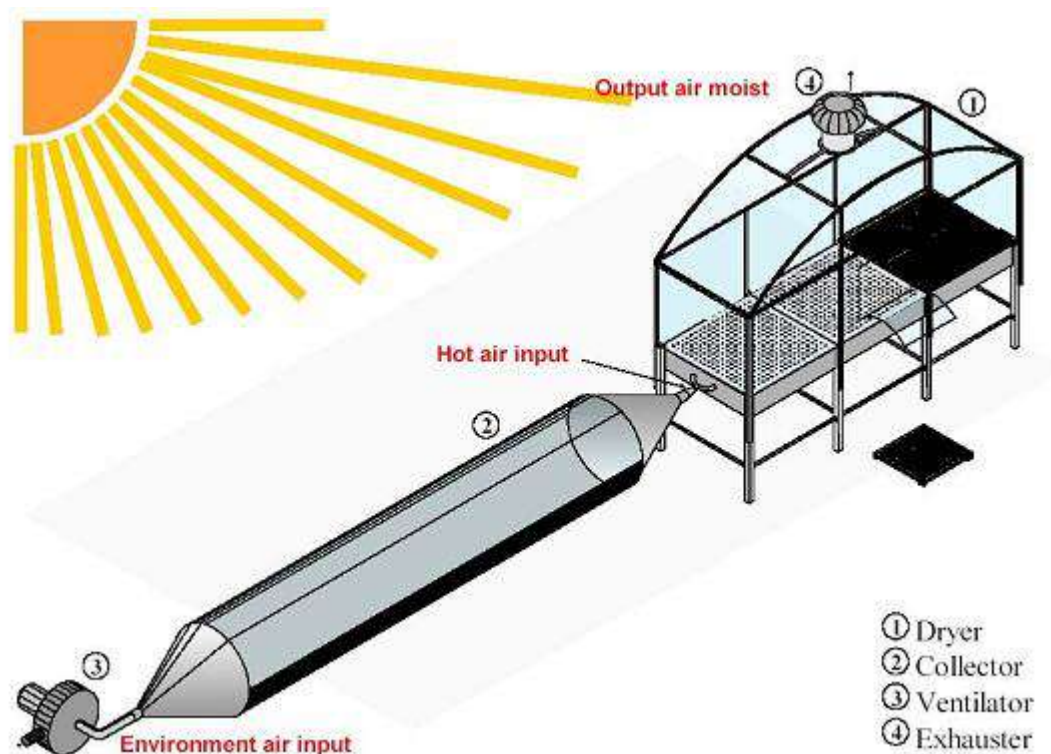


Figure 4-2: Scheme of the Solar Dryer for Bananas

#### 4-1-1-3: The Fruit Dryer:

The fruit dryer shown in Figure (4-3) was designed from basic materials locally available and was constructed by local crafts-men. The solar dryer consists of:

- A wooden frame, constructed as box with shelf for the fruit trays.
- A number of trays made of wooden frame with nylon chicken nets, which allow the air circulation.
- A transparent plastic (acrylic glazing), used as glazing keeping and increasing the heat capacity.
- Used oil around the dryer's legs to protect the wood from being eaten by termites and prevent access of ants and termites to the fruits.

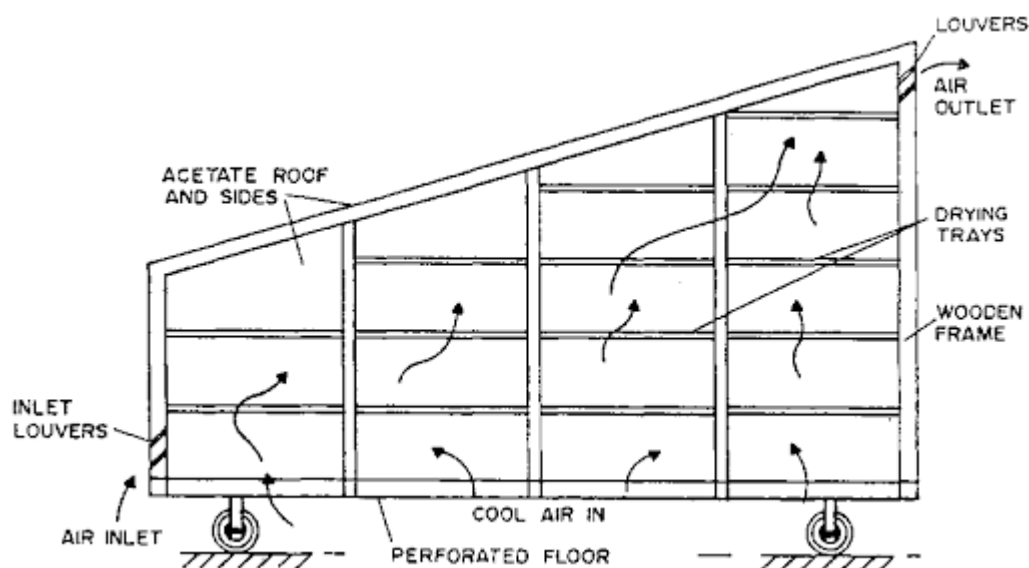


Figure 4-3: Fruit Dryer.

#### 4-1-1-4: Fruit and Vegetable Dryers:

It is house type solar dryer for fruits and vegetables Figure (4-4). A huge advantage of these systems, which are increasingly approved by users, is the fact that different types of fruit and vegetables can be dried, e.g., tomatoes, onions, cabbage, okra, carrots, hibiscus blossoms, mangoes, bananas and pineapples.

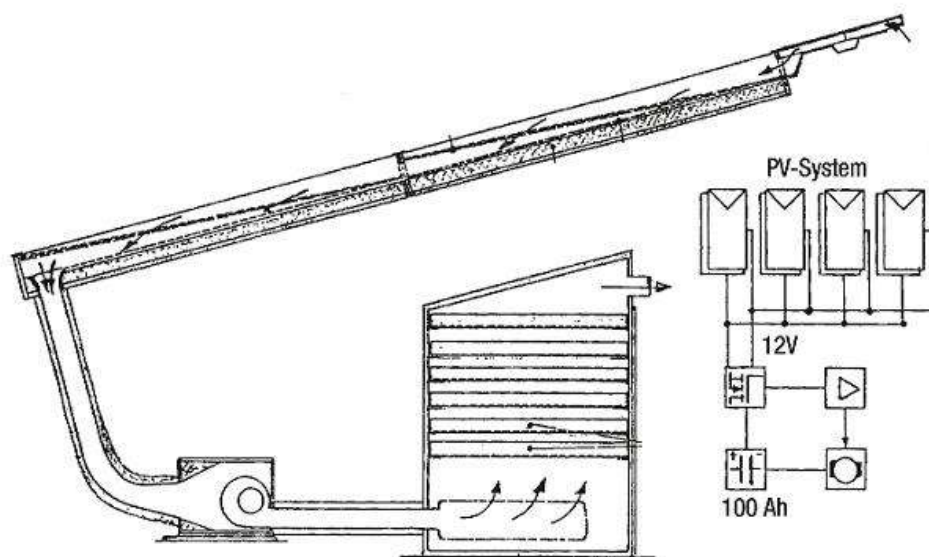


Figure 4-4: Fruit and Vegetable Dryers

The quality of products dried in this way is excellent, due to the fact that the food is not in direct sunlight, and due to a shorter drying process – 1.5 days in comparison to 4 – 5 days for traditional drying.

The dryer where build inside a 3 x 4 [m<sup>2</sup>] house with a 15° inclined roof. The house consists of three rooms, one for preparing, one for storage and the drying room. The house has the advantage of being more hygienic and resistant to rainfall and wind.

The Technical data of this dryer is shown in table below:

Table 4-3: Technical data of Fruit and Vegetable Dryer.

<b>Collector</b>		
	Total area:	9 m <sup>2</sup>
	Outer dimensions:	2,02 m x 0,79 m x 0,23 m
	Material	Wood, aluminium, glass
	Number of collectors:	6
	Insulation:	8 cm
<b>PV</b>		
	Numbers:	2 parallel
	Voltage:	24 V
	Power:	each 110 W <sub>p</sub>
	Accumulator:	2 x 60 Ah, 12 V, serial
<b>Dryer</b>		
	Total drying area:	12 m <sup>2</sup>
	Frame:	wood
	Trays:	aluminium
	Max. temperature:	65 °C (80 °C @ 176 kg/h air flow rate)
<b>Fan</b>		
	Air flow rate	445 / 750 m <sup>3</sup> /h
	Power	65 / 145 W

#### 4-1-2: Coffee Drying:

One opportunity for large scale coffee drying is a hybrid system, containing two independents' sources of thermal energy –solar and biomass.

Under normal conditions (day and sunshine) solar air collectors are used to heat up the air for coffee drying. To enable a continuous drying, during night time the hot air for the drying process is provided by a wood furnace. The design of the dryer is shown in Figure (4-5).

The floor size was 6 m x 2.2 m with height 2.8 m. The roof forms a simple bare plate solar collector black painted corrugated iron with a transparent board ceiling of 30 cm above it. Air is drawn through the cavity between the roof and ceiling by means of a fan.

The drying floor loaded with 1.1 ton of wet coffee berries at 0.3 m depth. Drying temperatures of 40 – 60 °C can be achieved by adjusting the air flowrate from 400– 900 m<sup>3</sup>/hr. Fermented coffee beans of 500 – 600 kg were loaded into the dryer and it took 50 hours to reach the final moisture content below 125 while sun drying required 75 hours.

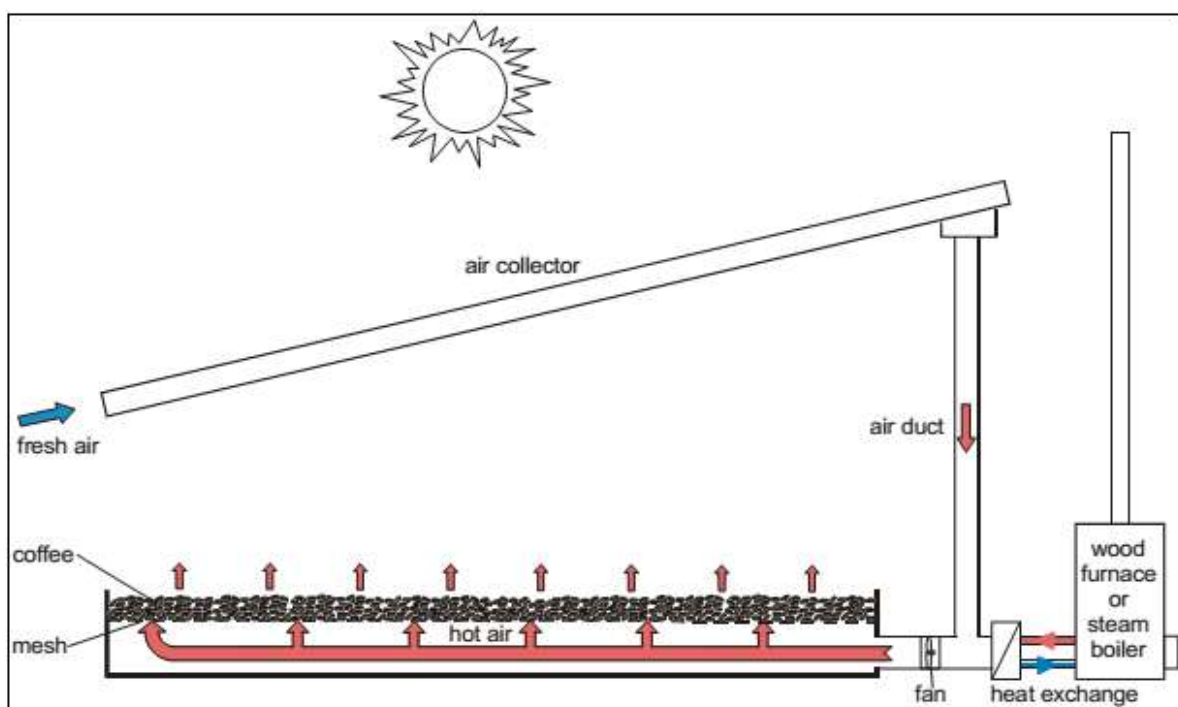


Figure 4-5: Solar coffee drying system using a wood furnace as back-up system

#### 4-1-3: Chili Drying:

A solar assisted biomass drying system with thermal storage is used in drying chili. This drying system was adopted as solar energy-based air heaters/dryers often suffered from fluctuation in temperature, relative humidity and air flow rate. The system aimed to deliver air at 55–60 °C at 70 – 100 m<sup>3</sup>/hr continuously day and night. The solar dryer consists of the following major components:

- An unglazed transpired solar collector for day time use.
- A biomass gasifier to supply hot air to the rock bed.
- A heat exchanger to transfer heat from the stove flue gas to the air.
- A rock bed thermal storage system that was connected to a stove/heat exchanger unit.
- A mixing chamber to obtain delivery air at both day and night time.

Schematic of the solar biomass heating system is as shown in Figure 4-6.

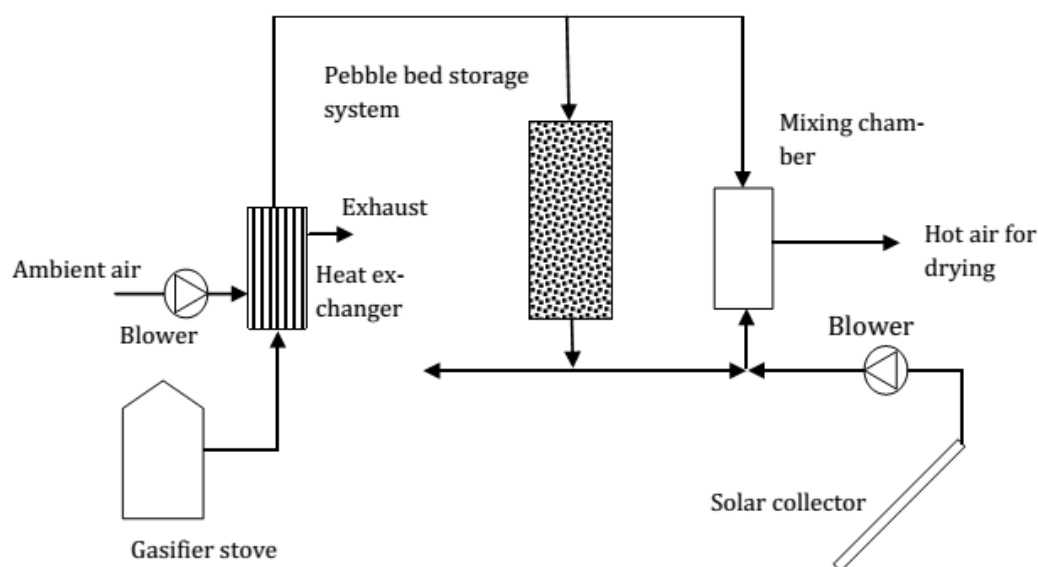


Figure 4-6: Schematic layout of the Solar Biomass Heating System.

The solar drying system operated differently in day time and night time conditions. In day time, the solar collector supplied the complete hot air when there was sufficient solar radiation. In the event of insufficient solar radiation, part of the rock bed will supply the deficient energy. During day time, the stove was also operated to charge the rock bed with heat but was shut down in the evening. During night time, ambient air and hot air extracted from the rock bed entered the mixing chamber to obtain the desirable drying temperature of 55 – 60°C. The temperature was regulated by adjusting the ratio of ambient air mixing with air from the rock bed.

For chili drying a solar drying chamber (1.2 m x 1 m x 1.2 m) fitted with a rotary wind ventilator, 22 kg of chilies was spread onto four wire mesh trays of 0.96 m x 1.13 m each. Drying

air of 60 °C was chosen as the optimum temperature for product quality requirement. Eucalyptus wood chips (< 3 cm long) were used as fuel for the biomass stove.

#### 4-1-4: Nuts Drying:

Nuts are dried inside a solar assisted dryer that consists of a drying cupboard, air collector, an auxiliary heater and a circulation fan.

Solar drying of nuts was by dryer consists of a solar collector system (2.75 m long x 1.75 m width), absorbers, single pass cover, black plate and insulation. Absorber was made of blacked painted zinc plate (0.05 cm thick) and covered with glass (0.5 cm thick). A biomass burner was used as a backup heating system that used bricks as heat storage and installed just beneath the drying chamber (Figure 4-7) [22].

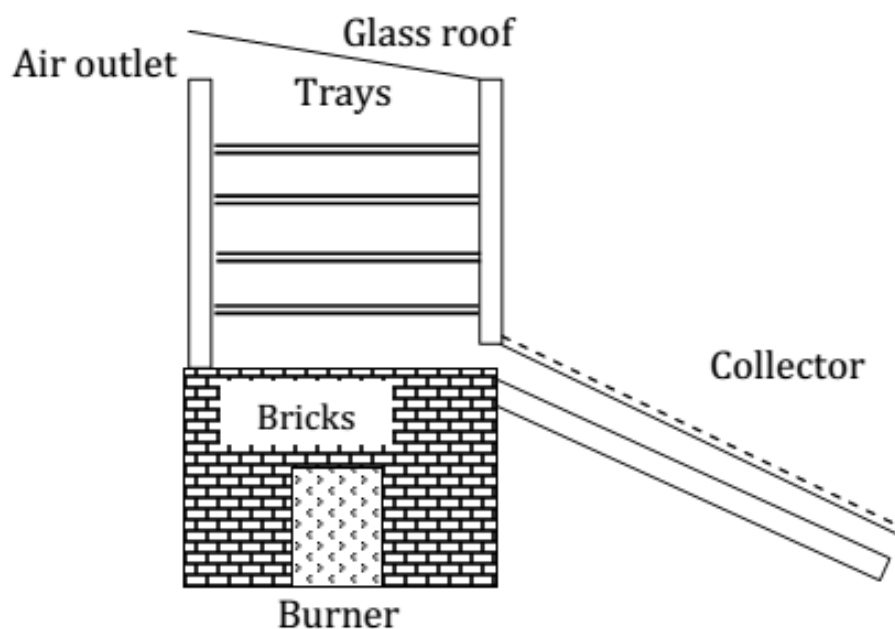


Figure 4-7: Side view of the Solar Dryer with Biomass Burner.

Drying at day time was relatively shorter than the night time at less than 10 hours drying duration. However, it took about 3 days to dry 64 kg of nuts when the burner was not used at all during night time. The system efficiency was found to be 21.3% and 23%. The back-up heater was found to have overall efficiency of 40% with caloric value of wood at 13.1 MJ/kg.



**4-1-5: Tobacco Drying:**

Two types of greenhouse solar dryers, namely the loading supporting wall design and the shell design, as shown in Figure (4-8).

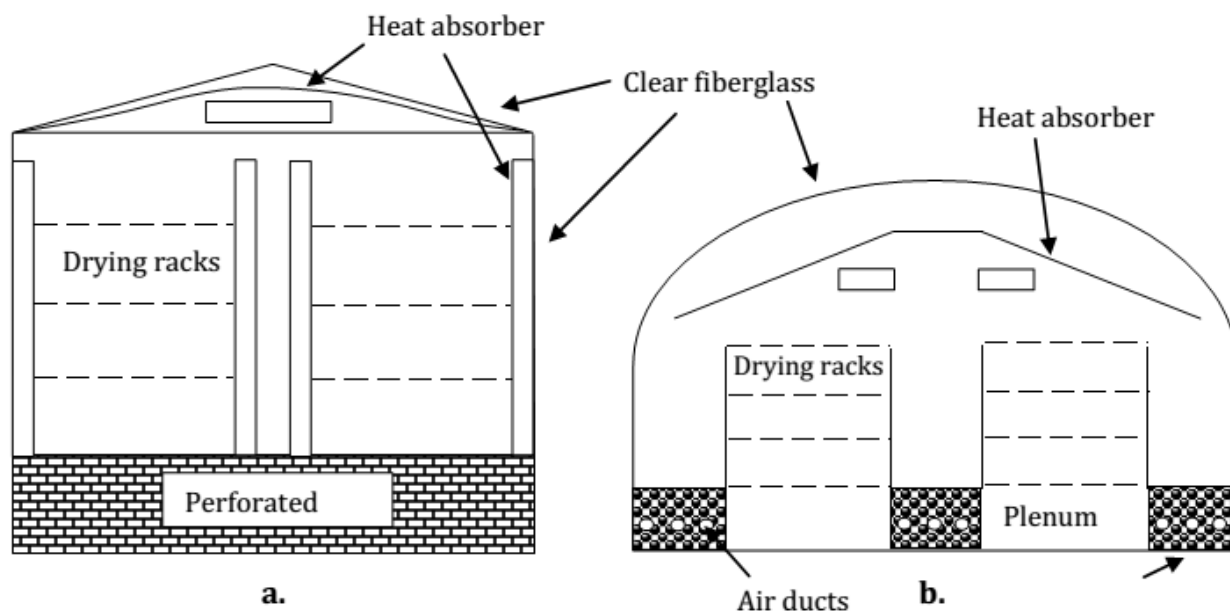


Figure 4-8: Greenhouse solar dryer type a) load supporting wall design and b) shell design (not to scale)

In the load supporting wall design, the tobacco bulk racks were supported by exterior and interior walls. Solar radiation was transmitted through the clear corrugated fiber-glass and absorbed by the black plastic heat absorber inside the structure. Forced air was supplied to transfer the heat inside the curing compartment. The stagnant air space between the transparent exterior and the heat absorber acted as an insulation layer. The concrete slab and block foundation served as an additional heat storage system.

In the shell design, the greenhouse structure was covered with clear corrugated fiber-glass to form a large solar collector with an integrated gravel energy storage system for night time usage. An auxiliary fan to circulate the air over the absorbers and portable frames were used to support the tobacco racks. The gravel energy system was designed to store excess solar energy. Air was heated by the black surfaces of the absorber panels and gravel bed and it was then

forced through the gravel and bottom air ducts by the fan. Soil drainage pipes were installed at the base to distribute the airflow uniformly through the gravel base.

Solar tobacco dryer of 1-ton fresh leaves capacity and measured 3.6 m x 3.6 m x 4.8 m in dimension. An array of 38.5 m<sup>2</sup> flat plate solar heaters and a 6 m<sup>2</sup> rock bed unit were also installed. Forced air was supplied by two units of blower at 1.5 kW and 0.75 kW each. liquid gas was used as an auxiliary fuel source in this system. It was found that average fuel saving of 28% was possible and average thermal efficiency was estimated at 40.5%. liquid gas consumption of 0.48 kg or 22.2 MJ per kg of cured leaves was achieved during drying [23].

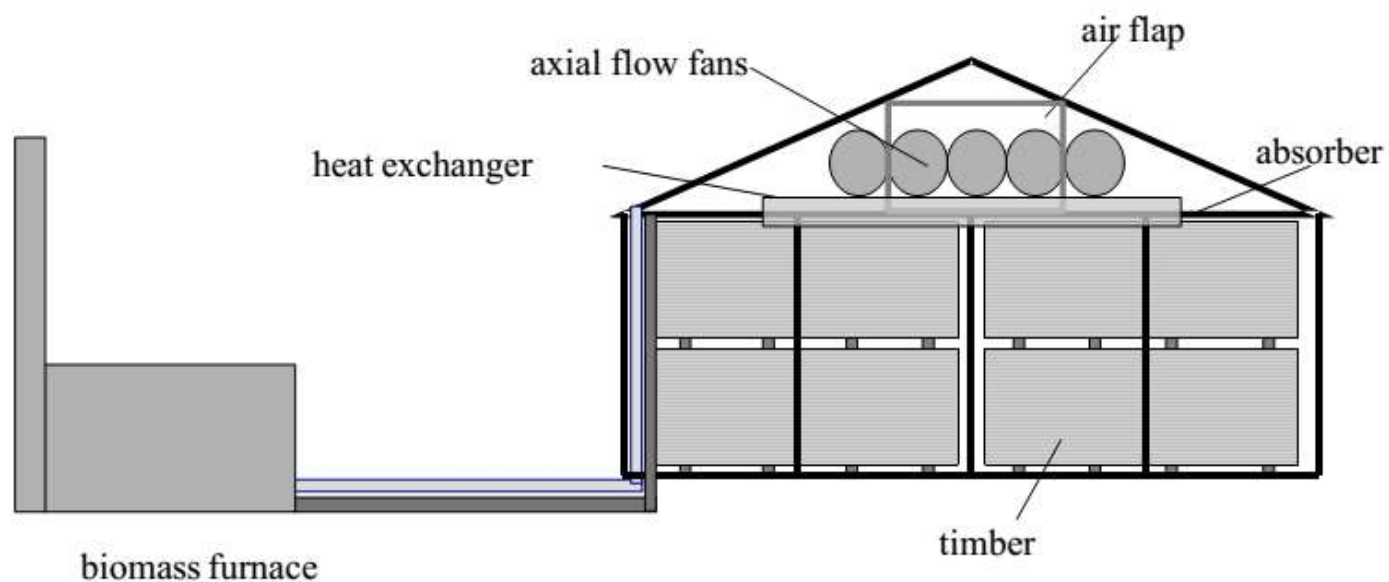
#### ***4-1-5: Timber and Wood Drying:***

Timber drying is a highly energy intensive process and this operation consumes about 70% of the total energy used in the production of most wood products.

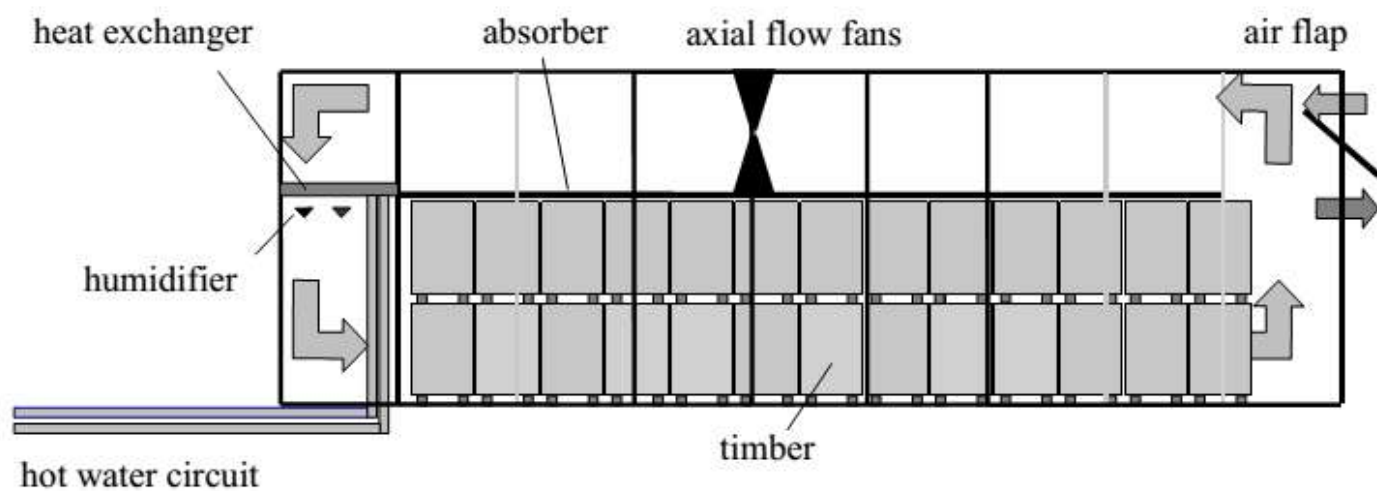
The structure of dryers (Figures 4-9 and 4-10) consists of rectangular aluminum profiles which are corrosion-resistant. The drying chamber is 10 m wide and up to 20 m long. The side walls are 3 to 4 m in height and the roof is inclined at an angle of 22 degrees. Each segment is covered with a transparent foil, providing a transmittance of 83 % for direct and 68 % for diffuse radiation [20].

The gable ends of the drying chamber are covered by polycarbonate double-skin sheets. For loading and unloading the dryer two revolving doors are installed over the full width of the drying chamber at the front side.

A specially developed microprocessor control regulates several axial flow fans, a humidifier and a backup woodchip furnace, providing the heat during night and unfavorable weather conditions. The drying regime is adjusted automatically according to the type of wood, the board thickness and the ambient air temperature.



Figures 4-9: Cross section of the solar-assisted drying kiln.



Figures 4-10: Longitudinal section of the solar-assisted drying kiln.

#### 4-1-6: Rice Drying:

Rice is one the most consumed cereal crops in the world. The harvested paddy usually contains very high moisture content in between (20 – 25) % and it needs to be dried down to (12 – 14) % moisture contents.

Solar dryer shown in Figure (4-11) was designed for the particular requirements of rice but the principles hold for other products and design types, since the basic need to remove water is the same [13].

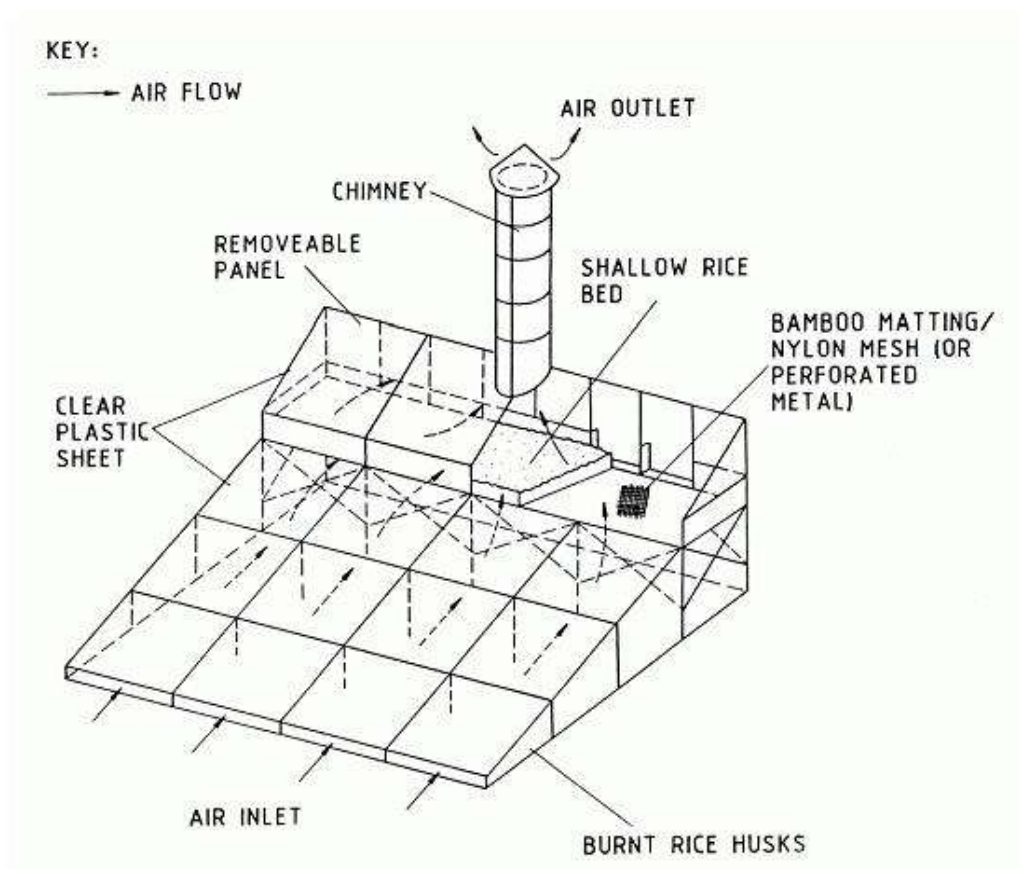


Figure 4-11: Solar Rice Dryer

#### 4-1-7: Corn Drying:

This solar drying system consists of a set of solar collectors, a heat pump and a mechanical grain stirrer (Figure 4-12). Heat was generated from the joint solar collector and heat pump system. The purpose of installing the heat pump was to solve the problem of the intermittent availability of the solar radiation.

The components installed in this drying system are as shown in Table (4-4). An air duct connected the solar assisted heat pump system to the bottom part of the granary. During trials, it was observed that the average temperature difference between ambient air and granary inlet air was about 8.9 °C while average relative humidity varied from 13.6% to 37.7% lower than the ambient air. It took about 240 hr to reduce the moisture content of the corn from 16.6% to 14.5%. Power consumption per grain ton to reduce the moisture content by 1 % was 1.24 kWh and the value was much lower than the official standard (2.0 kWh) [21].

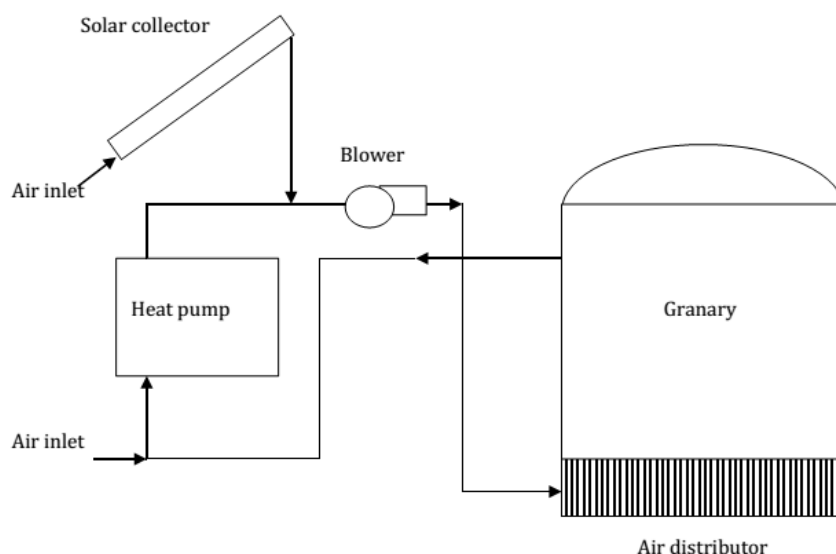


Figure 4-12: The schematic layout of the solar assisted heat pump granary

Table 4-4: Details of the components installed

Component	Specification
Solar air collector	4 m x 6 m enclosing a total area of 96 m <sup>2</sup>
Air source heat pump	Compressor 22 kW
Grain stirrer	2.2 kW and 4 m length auger
Granary	37.2 m x 22.9 m x 7.8 m and capacity 3.7 ton

**4-1-8: Fish Drying:**

Drying is the traditional method of preserving fish. Fresh fish contains up to 80% of water and it is a highly perishable material. When moisture content is reduced to 25%, contaminating agents cannot survive and autolytic activity is greatly reduced. However, to prevent mold growth during storage, moisture content must be reduced to 15%.

The Hohenheim tunnel dryer (Figure 4-14) can be used for drying of fish. 150 kg of silver fish were dried from 66 % down to 16 % in 5 days. Comparable samples dried with the traditional methods had a moisture content of 32.84 % after 5 days.

The temperature of the drying air at the collector outlet varied from 35.1 °C to 52.2 °C during drying. The fish was initially treated with dry salt and stacked for about 16 hours before drying [18].

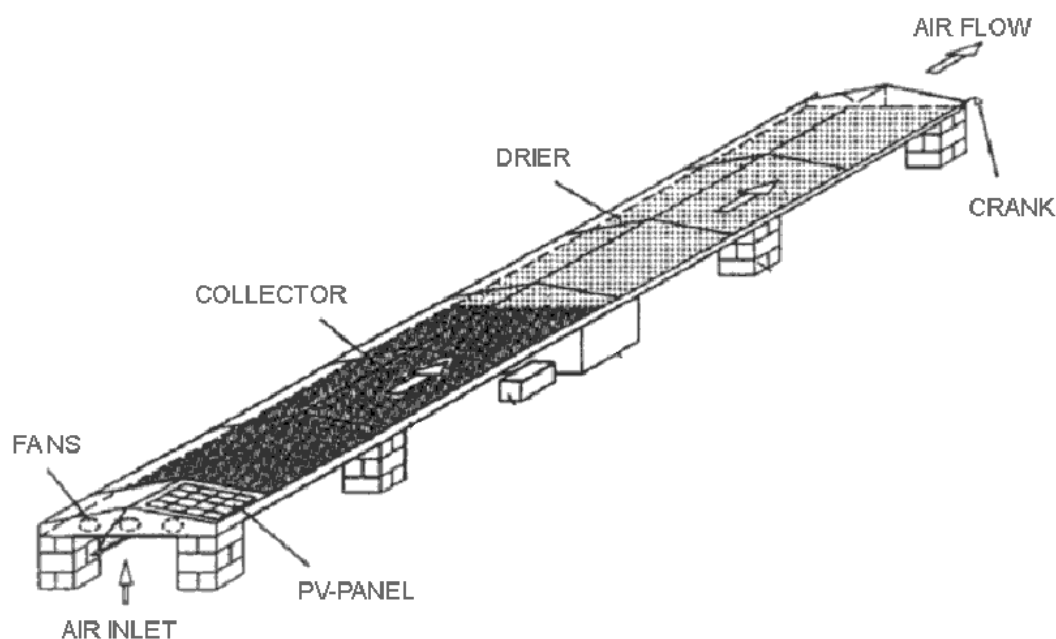


Figure 4-13: Solar Tunnel Dryer.

The three major dryer components, as shown in Figure (4-13), are the solar collector, food dryer compartment, and the airflow system. Air is circulated by fans, which use from 20-40 W of power from a photovoltaic panel, a generator, or a central utility. Air is forced into the

solar collector by the fans where it is heated by the sun, and then flows on to the food dryer section.

An advantage of the PV powered system is that, depending on the solar radiation, the air throughput is automatically adjusted by the speed of the fans. The plastic cover may be constructed from a sheet of greenhouse type UV-stabilized polyethylene.

It has produced a set of design specifications to help ensure quality performance. As long as these design specifications are followed, considerable opportunities exist for successful variation of the dryer. Table 4-5 shows some of the options viable for making each part of the dryer and Table 4-6 shows technical data of the tunnel dryer [18].

Table 4-5: Options for adapting a solar tunnel dryer

<b>PART</b>	<b>OPTIONS</b>
Support	Stone, slate, wood, metal, loam, barrels
Frame	Steel sheeting, wood, plywood, slate, concrete, stone, loam
Heat insulation	Polyurethane, Styrofoam, building insulation, cork, flax, straw, coconut fibers, wood shavings, leaves
Sheeting (cover)	LD-PE, LLD-PE, PTFE, PVC, PE-EVA
Winding shaft	Steel pipe, plastic, wood, bamboo, wicker
Power source	Photovoltaic cells, utility power, diesel or petrol generator

Table 4-6: Technical data of the tunnel dryer

Length	18 m
Width	2 m
Collector area	16 m <sup>2</sup>
Drying area	20 m <sup>2</sup>
Air flow rate	400-1200 m <sup>3</sup> /h
Air temperature	30-80°C
Power requirement	20 - 40 W
Thermal energy gain from solar radiation	up to 60 kWh/d ( $\cong$ 15 kg firewood)
drive of fans	solar panel
Number of fans	3
Price	US\$ 5,250 (+US\$ 250 for PV)
Products	Indirect operation ideal for sensitive products
Climate	Operation in arid and humid regions; adaptable to local climate
Control	Self regulated airflow and temperature (solar panel type)

#### ***4-2: Product Quality Consideration:***

The quality aspect of dried product is important in any drying system especially in solar and sun drying. This is mainly due to the possible extended drying duration as the source of solar radiation depends on the weather condition.

The prolonged drying duration, coupled with unfavorable drying condition could contribute to product spoilage (mold growth). Typically, the product quality of any dried products can be classified into the physical, chemical, biological and nutritional parameters whichever is applicable to both edible and non-edible products.

Not all commodities can be benefited from the use of solar drying in terms of quality improvement or no significant effect on quality, especially when compared against sun drying. However, certain products are better when dried under mild drying condition as compared to hot air drying.

Certain products need to be cured for reasons related to physical and chemical changes, and this cannot be accelerated via high temperature drying. This is especially true for product that undergoes flavor development process [17].



***Chapter -5-***  
***Conclusion and***  
***Suggestions***

## **5: - Conclusion and Suggestions:**

### **5-1: Conclusions: -**

In this project, (Different Types of Solar Dryers - Theoretical Study), The following conclusions of the present project can be drawn:

a- The classification of solar dryers clearly illustrates that the solar dryer designs can be grouped systematically according to their operating temperature ranges, heating sources/modes and operational modes.

b- It is difficult to have one single criteria for the selection of a solar dryer for a specific region or a product as solar insolation and other parameters change frequently with geographical location, however the general rules of thumb are mentioned to assist in making the final selection.

c- The final selection is generally based on the available insolation rate, production throughput, flexibility requirements, cost of fuel to run accessories as well as on the experience and judgment of the fabricator.

d- As the solar dryer has a long life of about 20-40 years, the effect of a poor design can have a long-term impact on the economic health of the dryer.

e- One of the most important potential applications of solar energy is the solar drying of agricultural products. It has been established that solar drying of fruits and vegetables is technically feasible and economically viable. Losses of fruits and vegetables during their drying in developing countries are estimated to be 30–40% of production.

f- Solar drying has proved to be viable in drying various agricultural commodities provided the surrounding conditions (weather, insolation, location) are conducive for the implementation of this type of drying technique and solar drying system preferably using local materials and skills.

g- There are still many issues that must be overcome especially in the transfer of technology and the commercialization of this drying technology to the potential users. Training, guidance and management of the whole processing steps, which includes solar drying, should be emphasized to ensure quality control of the dried product.

h- The postharvest losses of agricultural products can be reduced drastically by using well-designed solar drying systems. Drying time can be further reduced using the same system with heat storage material.

i- Farmers can choose solar dryers according to their individual requirements. and it is necessary to develop a simple, effective and economical natural convection solar dryer (multipurpose solar dryer capable of drying a variety of fruits and vegetables).

j- Among the different types of solar dryers, the indirect mode forced convection solar dryer has been demonstrate to be superior in the speed and quality of drying. Incorporation of sensible and/or latent heat storage media within the solar drying systems accelerate the drying process during the night time and low intensity solar radiation periods and exclude the need for using auxiliary heat sources during low solar radiation seasons.

#### **5-2: - Suggestions for Future Work:**

The following can be considered for further experiments works:-

a- Provide the project for small design of solar dryer experimentally (by experimenting with a one design (active or passive solar dryer)).

b- Consideration economic estimation and the efficiency of solar dryers in climate conditions of Iraq.

c- The relevant authorities have to be present and influential in encouraging people to turn to such alternative energy systems. The relevant authorities should encourage and support renewable energy and should provide technical assistant to potential users.

d- Encouragement innovation and technological advancements to better drying processes, more efficient in energetic terms and allowing a better preservation of the organoleptic and nutritional qualities. The applicability of the process to a wide range of foods, with diverse characteristics render this operation a prominent position in the processing food industries.

# ***References***

***References:***

- 1- Jyoti Singh, (2015), Journal of Mechanical and Mechanics Engineering Volume 1 Issue 1, p.p. 14-24.
- 2- Sharma, S., Ray, R. A., Sharma, K., (1987), Comparative study of solar dryers for crop drying. Invention Intelligence, 22, pp. 105-113.
- 3- Sharma, G. P.; & Prasad, S. Effective moisture diffusivity of garlic cloves undergoing microwave convective drying. Journal of Food Engineering 2004, 65, 609–617.
- 4- Sharma, A., Chen, C.R., Lan, N. V., 2009, Solar-energy drying systems: A review, Renewable and Sustainable Energy Reviews, 13, pp. 1185-1210.
- 5- Hankins, Mark. 1995: Solar Electric Systems for Africa. Commonwealth Science Council and AGROTEC. pp 14-16.
- 6- Hislop, D. (1992): Energy Options – Chapter 3: Heat from Solar Energy. Intermediate Technology Development Group. pp 43-47.
- 7- Vargas, Tania V. Camacho, Sylvia A. (1996): Solar Drying of Fruits and Vegetables: Experiences in Bolivia. FAKT, Energetica. 65 pgs.
- 8- VANDERHULST, P., LANSER, H., BERGMAYER, P., FOETH, F., ALBERS, R. (1990): Solar Energy - Small scale applications in developing countries, Amsterdam.
- 9- Ekechukwu, O.V., (1999), Review of solar-energy drying systems I: an overview of drying principles and theory, Energy Conversion and Management, 40, pp. 593–613.
- 10- Werner Weiss and Josef Buchinger, Arbeit gemeinschaft ERNEUERBARE, ENERGIE Institute for Sustainable Technologies.
- 11- Ching Lik Hii et.al. (2012), Solar Drying: Fundamentals, Applications and Innovations, ISBN: 978-981-07-3336-0
- 12- IEA-SHC: Solar Air Systems, (1998).
- 13- GREEN, M.G., SCHWARZ, D. (2001): Solar Drying Technology for Food Preservation, gtz-gate.

- 14- Sreekumar, A. (2010): Techno-economic analysis of a roof-integrated solar air heating system for drying fruit and vegetables, *Energy Conversion and Management*, 51, pp. 2230-2238.
- 15- Raquel P. F. Guiné, (2018): The Drying of Foods and Its Effect on the Physical-Chemical, Sensorial and Nutritional Properties, *international Journal of Food Engineering* Vol. 4, No. 2, June.
- 16- R. P. F. Guiné, (2015): Food Drying and Dehydration: Technology and Effect on Food Properties, Germany: LAP Lambert Academic Publishing GmbH & Co.
- 17- Bassey, M.W., (1989), Development and Use of Solar Drying Technologies. In Nigerian Solar Energy Forum (NASEF'89). Special Technical Paper.
- 18- Perera, C.O., (2005), Selected Quality Attributes of Dried Foods, *Drying Technology*, 23, pp. 717-730.
- 19- GREEN, M.G., SCHWARZ, D. (2001): Solar Drying Equipment: Notes on three dryers, gtzgate,
- 20- BUX, M., MÜHLBAUER, W., BAUER, K., KÖHLER, B. (2001): Solar Assisted Drying of Timber in Industrial Scale, *Southern African Forestry Journal*.
- 21- Li, Y et al. (2011), Experimental Investigation on a Solar Assisted Heat Pump In-Store Drying System, *Applied Thermal Engineering*, 31, pp. 1718-1724.
- 22- Tarigan, E. and Tekasakul, P. (2005): A Mixed-mode Natural Convection Solar dryer with Biomass Burner and Heat Storage Backup Heater, In ANZSES 2005: Renewable Energy for a Sustainable Future - A challenge for a post carbon world, Otago University, Dunedin, New Zealand, 28 - 30 November 2005. Pp. 1-9.
- 23- Huang, B.K., Bowers Jr, C.G., (1986): Development of Greenhouse Solar Systems for Bulk Tobacco Curing and Plant Production, *Energy in Agriculture*, 5, pp. 267-284

# ***Appendix***

## Appendix -1: Initial Moisture Content of Different Crops

### Crop Data

The crop data are an extract of the study « Potential for Solar Drying in the World », prepared by Enermodal Engineering Ltd., Canada and ECOFYS Energy & Environment, Netherlands [12].

#### Apples

<b>Initial Moisture Content:</b>	80-85 %	
<b>Final Moisture Content:</b>	20-24 %	
<b>Energy Required (MJ/kg):</b>	1.502	
<b>Maximum Temperature:</b>	70 °C	
<b>Storage</b>	Leather is wrapped in polypropylene	
<b>Drying Methods</b>	<b>Low Temperature</b>	<b>High Temperature</b>
	1. Tunnel 2. forced air dehydrator for leather	3. dry sulphuring 4. wet sulphuring
<b>Required drying time</b>	1. 5-6 hours 2. 3.5 hours	3. 30-40 min 4. 10 min
<b>Required drying temperature</b>	1. 75-55 °C 2. 45 °C	

#### Apricots

<b>Initial Moisture Content:</b>	85 %	
<b>Final Moisture Content:</b>	15-25 %	
<b>Energy Required (MJ/kg):</b>	1.666	
<b>Maximum Temperature:</b>	65 °C	
<b>Storage</b>	Leather is wrapped in polypropylene	
<b>Drying Methods</b>	<b>Low Temperature</b>	<b>High Temperature</b>
	1. Tunnel 2. forced air dehydrator for leather 3. sulphuring 4. sun drying	
<b>Required drying time</b>	1. 10-15 hours 2. 3.5 hours 3. limited through-put time 4. 4,5 days	
<b>Required drying temperature</b>	1. 70-60 °C 2. 45 °C	°C

In apricots, the decomposition of chlorophyll causes a positive effect on the colour. Therefore direct exposition to solar radiation is recommended.[1]



## Bananas

<b>Initial Moisture Content:</b>	70-80 %	
<b>Final Moisture Content:</b>	7-15 % 2 % (powder) 8 % (flour)	
<b>Energy Required (MJ/kg):</b>	1.679	
<b>Maximum Temperature:</b>	70 °C	
<b>Storage</b>	Stored in bundles, hung on racks in warehouse. Wrapped in leaves and bound tightly, vacuum sealed, dry conditions; may be treated with sulphating or by fumigation with methyl bromide (dried products) or an antioxidant (chips) Fruit bars are wrapped in cellophane	
<b>Drying Methods</b>	<b>Low Temperature</b>	<b>High Temperature</b>
	<ol style="list-style-type: none"> <li>1. Sun-drying</li> <li>2. oven-drying</li> <li>3. batch or in-bin drying after osmotic dehydration for candied fruit</li> <li>4. warehouse drying</li> <li>5. spray or drum-drying (powder)</li> </ol>	<ol style="list-style-type: none"> <li>6. Tunnel or cabinet</li> <li>7. osmotically (2000 ppm SO<sub>2</sub>) usually followed by sun drying or air drying</li> <li>8. sun and mechanical</li> <li>9. forced air dehydrator for leather</li> </ol>
<b>Required drying time</b>	<ol style="list-style-type: none"> <li>1. several days (4-6)</li> <li>2. several hours or days</li> <li>3. several hours</li> <li>4. several hours</li> <li>5. 7-8 hours (flour)</li> </ol>	<ol style="list-style-type: none"> <li>6.</li> <li>7. 2 hours followed by a day of solar</li> <li>8. 10 hours solar plus 16 hours electric or steam power (fruit bars)</li> <li>9. 3.5 hours</li> </ol>
<b>Required drying temperature</b>	30-70 °C 60 °C (tunnel for powder) 75 °C inlet temperature and 45 °C outlet temp. (flour)	70 °C 45 °C

## Barley

<b>Initial Moisture Content:</b>	15-20 %	
<b>Final Moisture Content:</b>	13-14 %	
<b>Energy Required (MJ/kg):</b>	0.055-0.168	
<b>Maximum Temperature:</b>	43 °C for mc > 24 % 49 °C for mc < 24 % 60 °C for grains to be milled if mc > 25 % 66 °C for grains to be milled if mc < 25 % 120 °C for grain for feed 55 °C for barley destined for brewery	
<b>Storage</b>	In silos without aeration and circulation In silos with sufficient aeration In ventilated storage bags	
<b>Drying Methods</b>	<b>Low Temperature</b>	<b>High Temperature</b>
	De-central in storage driers (silos, floor)	De-central batch dryers at farms or central large-scale continuous process at drying facility
<b>Required drying time</b>	Days-weeks; drying during storage	Minutes; drying and storage separately
<b>Required drying temperature</b>	Δ 3-5 °C	50 – 250 °C

## Cassava, Mainoc, Yuca (*Manihot esculenta*)

<b>Initial Moisture Content:</b>	62 – 75%	
<b>Final Moisture Content:</b>	14-17 %	
<b>Energy Required (MJ/kg):</b>	1.105	
<b>Maximum Temperature:</b>	150 °C	
<b>Storage</b>	In-ground, in water as roots; in silos as chips; sealed polyethylene bags as gari	
<b>Drying Methods</b>	<b>Low Temperature</b>	<b>High Temperature</b>
	1. Chips dried in sun 2. Chips in cabinet solar dryer 3. Tunnel Dryers 4. Flour and tapioca from Drums	5. oven dried 6. pneumatic dryers
<b>Required drying time</b>	1. several days-weeks 2. several days (92 h) 3. several hours 4. several hours	5. several hours 6. several hours
<b>Required drying temperature</b>	30-60 °C	
<b>Drying Constant</b>	Kc = 0.031, ke=0.012 for Chips	

## Cassava leaves

<b>Initial Moisture Content:</b>	80 %	
<b>Final Moisture Content:</b>	14 %	
<b>Energy Required (MJ/kg):</b>	1.586	
<b>Maximum Temperature:</b>		
<b>Storage</b>	Small huts or by cooking pit or oven	
<b>Drying Methods</b>	<b>Low Temperature</b>	<b>High Temperature</b>
	1. Sun drying 2. Leaves in cabinet solar dryer 3. incidental drying above cooking pit or oven	
<b>Required drying time</b>	1. several days 2. two days (46 h) 3. sometimes weeks	
<b>Required drying temperature</b>	30-60 °C	
<b>Drying Constant</b>	kc=0.047, ke=0.012	

## Chillies and Peppers

<b>Initial Moisture Content:</b>	75-80 %	
<b>Final Moisture Content:</b>	5-14 %	
<b>Energy Required (MJ/kg):</b>	1.610	
<b>Maximum Temperature:</b>	90 °C	
<b>Storage</b>	Bags and bulk storage in warehouse	
<b>Drying Methods</b>	<b>Low Temperature</b>	<b>High Temperature</b>
	Sun drying	Kiln drying
<b>Required drying time</b>	Several days (6-8)	Several hours
<b>Required drying temperature</b>	40 °C	90 °C

## Cocoa Beans

<b>Initial Moisture Content:</b>	60-80 %; 50-55 %	
<b>Final Moisture Content:</b>	25-30 %; 6-7 %	
<b>Energy Required (MJ/kg):</b>		
<b>Maximum Temperature:</b>		
<b>Storage</b>		
<b>Drying Methods</b>	<b>Low Temperature</b>	<b>High Temperature</b>
	1. sun drying 2. batch or in-bin drying with wood or crop waste, coal or diesel fuel burned dryers 3. solar dryers drying during storage (45-50 °C)	Central large-scale continue process at drying facility; drying and storage separately
<b>Required drying time</b>	1. Several days (4-9) 2. several hours (32-42 h) 3. several hours (48 h)	Minutes
<b>Required drying temperature</b>	30-60 °C	

## Coffee

<b>Initial Moisture Content:</b>	45-65 %	
<b>Final Moisture Content:</b>	9-12 %	
<b>Energy Required (MJ/kg):</b>	0.855- 0.865	
<b>Maximum Temperature:</b>		
<b>Storage</b>	Bags and bulk storage in warehouses and silos	
<b>Drying Methods</b>	<b>Low Temperature</b>	<b>High Temperature</b>
	1. sun drying 2. batch or in-bin drying with wood or crop waste burned for heat 3. solar drying	Roasting
<b>Required drying time</b>	1. Several days (3-7) 2. several hours 3. several hours (40-58)	
<b>Required drying temperature</b>	30-60 °C	

For Arabica coffee, a period of exposure to sunlight is considered inviolable for the development of full flavour in the roasted bean.[3-5]

## Grapes

<b>Initial Moisture Content:</b>	75- 80 %	
<b>Final Moisture Content:</b>	15-20 %	
<b>Energy Required (MJ/kg):</b>	1.444	
<b>Maximum Temperature:</b>	70 °C	
<b>Storage</b>	Leather is wrapped in polypropylene	
<b>Drying Methods</b>	<b>Low Temperature</b>	<b>High Temperature</b>
	1. sun drying 2. Forced air dehydrator for leather	
<b>Required drying time</b>	1. 8-10 days 2. 3.5 hours	
<b>Required drying temperature</b>	45 °C	

Continuous air flow required during the first phase of solar drying.[1]

In grapes, the decomposition of chlorophyll causes a positive effect on the colour. Therefore direct exposition to solar radiation is recommended.[1]

## Mushrooms

<b>Initial Moisture Content:</b>	%	
<b>Final Moisture Content:</b>	%	
<b>Energy Required (MJ/kg):</b>		
<b>Maximum Temperature:</b>		
<b>Storage</b>	Opaque, air-tight containers (drums or packages), sometimes with a desiccants	
<b>Drying Methods</b>	<b>Low Temperature</b>	<b>High Temperature</b>
<b>Required drying time</b>		
<b>Required drying temperature</b>	°C	°C

## Maize

<b>Initial Moisture Content:</b>	20-35 %	
<b>Final Moisture Content:</b>	8-15 %	
<b>Energy Required (MJ/kg):</b>	0.254 – 0.565	
<b>Maximum Temperature:</b>	60 °C 43 °C (then seeds lose their viability) 43 °C for mc > 24 % 49 °C for mc < 24 % 60 °C for grains to be milled if mc > 25 % 66 °C for grains to be milled if mc < 25 % 120 °C for grain for feed	
<b>Storage</b>	- at households stored in various ways from in the cob to sealed containers - on larger farms in special constructions (in bags or in bulk) - central large-scale farmers and traders store amize (12-13 %) in bags or bulk in warehouses or silos	
<b>Drying Methods</b>	<b>Low Temperature</b>	<b>High Temperature</b>
	- sun and field and banda( wood fire in storage (Africa) followed by incidental (Gulf of Guinea), tap (elevated storage)(Cameroon), bliva (elevated pile of cobs), maize crib (tap-type but better made)(Nigeria), IRRI hot air dryer - shallow batch dryer (2.4-6 m <sup>3</sup> /min/m <sup>2</sup> )	
<b>Required drying time</b>	Several weeks	Several hours
<b>Required drying temperature</b>	On average less then 35 °C	

## Mangoes

<b>Initial Moisture Content:</b>	80-85 %	
<b>Final Moisture Content:</b>	12-18 %	
<b>Energy Required (MJ/kg):</b>	1.564	
<b>Maximum Temperature:</b>	70 °C	
<b>Storage</b>	Oval bundles and hung Larger amounts stored in millet granaries Fruit bars are wrapped in cellophane Leather is wrapped in polypropylene	
<b>Drying Methods</b>	<b>Low Temperature</b>	<b>High Temperature</b>
	1. sun or solar (decentral small-scale batch system at farm) 2. tunnel 3. vacuum-drying 4. forced air dehydrator for leather	5. osmotically (8000 ppm SO <sub>2</sub> ) 6. sun and mechanical (fruit bars)
<b>Required drying time</b>	1. 1-2 weeks 2. – 3. – 4. 2 hours	5. – 6. 10 hours solar plus 16 hours electric or steam power
<b>Required drying temperature</b>	1. 70 °C; 55 °C in last stage of drying	6. 55 °C at beginning to a high of 70°C

## Papayas

<b>Initial Moisture Content:</b>	%	
<b>Final Moisture Content:</b>	%	
<b>Energy Required (MJ/kg):</b>		
<b>Maximum Temperature:</b>		
<b>Storage</b>	Leather is wrapped in polypropylene	
<b>Drying Methods</b>	<b>Low Temperature</b>	<b>High Temperature</b>
	Forced air dehydrator for leather	Osmotically (2000 ppm SO <sub>2</sub> )
<b>Required drying time</b>	3.5 hours	4 hours
<b>Required drying temperature</b>	45 °C	70 °C

Pine apples  
Turn black above 47 °C

## Potatoes

<b>Initial Moisture Content:</b>	70-75 %	
<b>Final Moisture Content:</b>	8-13 % < 4 % for powder	
<b>Energy Required (MJ/kg):</b>	1,453	
<b>Maximum Temperature:</b>	75-85 °C	
<b>Storage</b>	Warehouse/silo	
<b>Drying Methods</b>	<b>Low Temperature</b>	<b>High Temperature</b>
	Sun (for chips) Plates heated with hot water, under vacuum	Drum (for powder) Spraying in hot air (powder)
<b>Required drying time</b>	Sometimes several days	< 1 hour 1/50 s
<b>Required drying temperature</b>	30 – 60 °C 50-70 °C	75-85 °C 130-150 °C

## Rice

<b>Initial Moisture Content:</b>	20-30 %	
<b>Final Moisture Content:</b>	12-18 %	
<b>Energy Required (MJ/kg):</b>	0.218 – 0.351	
<b>Maximum Temperature:</b>	50 °C 43 °C for mc > 24 % 49 °C for mc < 24 % 60 °C for grains to be milled if mc > 25 % 66 °C for grains to be milled if mc < 25 % 120 °C for grain for feed	
<b>Storage</b>	In silos without aeration and circulation In silos with sufficient aeration In ventilated storage bags	
<b>Drying Methods</b>	<b>Low Temperature</b>	<b>High Temperature</b>
	De-central batch drying system at farms (silos, floor)	Central large-scale continuous-flow driers and storage driers
<b>Required drying time</b>	Days-weeks; drying during storage	Minutes; drying and storage separately
<b>Required drying temperature</b>	< 50 °C	

## Sugar cane

<b>Initial Moisture Content:</b>	75 %	
<b>Final Moisture Content:</b>	%	
<b>Energy Required (MJ/kg):</b>		
<b>Maximum Temperature:</b>		
<b>Storage</b>	Raw sugar stored in piles in warehouses before shipping to a refinery	
<b>Drying Methods</b>	Following other treatments, sugar is boiled to obtain crystallized form	
<b>Required drying time</b>		
<b>Required drying temperature</b>	°C	°C

## Tea

<b>Initial Moisture Content:</b>	60-80 %	
<b>Final Moisture Content:</b>	25-30 %; 3 % ??	
<b>Energy Required (MJ/kg):</b>	1.203	
<b>Maximum Temperature:</b>	140 °C	
<b>Storage</b>		
<b>Drying Methods</b>	<b>Low Temperature</b>	<b>High Temperature</b>
	1. sun drying 2. batch or in-bin drying with wood or crop waste burned for heat 3. solar drying	4. withering – uses warm air 5. fermentation – moist air at 95 % RH 6. tray dryer or fluidized bed dryer for drying by hot air
<b>Required drying time</b>	1. Several days 2. several hours 3. several hours	4. 16-20 hours 5. 1-2 hours 6. 24-26 minutes
<b>Required drying temperature</b>	30-60 °C	4. 35 °C 5. 25-30 °C 6. 100-140 °C

## Tobacco Leaves

<b>Initial Moisture Content:</b>	70-85 %	
<b>Final Moisture Content:</b>	11-25 %	
<b>Energy Required (MJ/kg):</b>	1.592 – 1.997	
<b>Maximum Temperature:</b>	70 °C	
<b>Storage</b>		
<b>Drying Methods</b>	<b>Low Temperature</b>	<b>High Temperature</b>
	1. sun-drying 2. batch or in-bin drying with wood or diesel fuel burned	Batch drying with diesel fuel
<b>Required drying time</b>	1. several weeks (30 – 40 days) 2. several days to several weeks (15- 20 days)	Several hours
<b>Required drying temperature</b>	30-60 °C	18-75 °C

## Tomatoes

<b>Initial Moisture Content:</b>	75 %	
<b>Final Moisture Content:</b>	35 %, < 4 % (powder)	
<b>Energy Required (MJ/kg):</b>	0.963	
<b>Maximum Temperature:</b>		
<b>Storage</b>	Opaque, air-tight containers (drums or packages), sometimes with a desiccant	
<b>Drying Methods</b>	<b>Low Temperature</b>	<b>High Temperature</b>
	1. sun-drying 2. drum drying for powder 3. vacuum dehydration for concentrated juices and sauces 4. plates heated with hot water under vacuum (powder)	After boiling: 1. conduction 2. tunnel spraying in hot air (powder)
<b>Required drying time</b>		1/50 s
<b>Required drying temperature</b>	30-60 °C	95 °C

## Wheat

<b>Initial Moisture Content:</b>	15-20 %	
<b>Final Moisture Content:</b>	13-14 %	
<b>Energy Required (MJ/kg):</b>	0.055 – 0.193	
<b>Maximum Temperature:</b>	43 °C for mc > 24 % 49 °C for mc < 24 % 60 °C for grains to be milled if mc > 25 % 66 °C for grains to be milled if mc < 25 % 120 °C for grain for feed	
<b>Storage</b>	In silos without aeration and circulation In silos with sufficient aeration In ventilated storage bags	
<b>Drying Methods</b>	<b>Low Temperature</b>	<b>High Temperature</b>
	Shallow batch dryer (2.4 – 6 m <sup>3</sup> /min/m <sup>2</sup> ) De-central in storage driers (silos, floor)	De-central batch dryers at farms or central large-scale continuous process at drying facility
<b>Required drying time</b>	Days-weeks; drying during storage	Minutes; drying and storage separately
<b>Required drying temperature</b>	45 °C	60 – 250 °C

## Wood

<b>Initial Moisture Content:</b>	40-200 %	
<b>Final Moisture Content:</b>	8-10 %	
<b>Energy Required (MJ/kg):</b>		
<b>Maximum Temperature:</b>	60 °C	
<b>Storage</b>	Stacked; protected from the elements; in environment in which it is to be used	
<b>Drying Methods</b>	<b>Low Temperature</b>	<b>High Temperature</b>
	Air dry	Kiln dry
<b>Required drying time</b>	Several months	Several weeks
<b>Required drying temperature</b>	Ambient	



**A-2-1: Examples of Dried Foods [15]:**

**A- Fruits:**

Many fruits have been for long dried in the sun, including grapes, figs, dates, pears, peaches and apricots (Figure A-2-1). Nevertheless, the hot air for drying is also amply applied to fruits such as apple slices, apricot halves, pineapple slices or pears in halves or quarters.



Figure A-2-1: Examples of fruits dried in the sun.

Other drying methods like vacuum (Figure A-2-2) drying or combined methods can be used to dry fruit, such as kiwi, mango and banana.



Figure A-2-2: Examples of fruits dried in vacuum.

The osmotic dehydration is applied to orange, pineapple, kiwi, apple, cherry, papaya, coconut, strawberry, among many others (Figure A-2-3).



Figure A-2-3: Examples of fruits processed by osmotic dehydration

In general fruits are not blanched but are sulphurated by exposure to vapors resulting from the burning of Sulphur, to control minimize browning reactions. Fruit purees can be drum dried to obtain powders or flakes, like in the case of banana, apricot, mango and peach. Some of these products are hygroscopic and sticky, so it is beneficial to add glucose syrup to facilitate removal of the product from the drum and its subsequent handling. For the drying of fruit juices can be used atomization or spray drying (Figure A-2-4).



Figure A-2-4: Examples of fruit juices processed by spray drying.

### ***B. Horticultural Products:***

Many vegetables can be found in the dried form, such as the tomatoes that are dried in the sun in some countries bordering the Mediterranean. Most vegetables are blanched and/or sulphurated before drying. Many different types of dryers are used for drying

vegetables such as trays, tunnels or fluidized beds, which use hot air in temperatures normally ranging from 50 to 110 °C. Among the dried vegetables stand the green beans, peppers, cabbage, carrots, celery, spinach and broccoli (Figure A-2-5). Some vegetables such as garlic, mushrooms, peas and onions are not sulphatic to preserve their delicate taste and aroma, that otherwise would be much affected.



Figure A-2-5: Examples of dried vegetables.

### ***C. Herbs and Spices:***

Herbs and spices can be dried in vacuum dryers to produce products with better organoleptic qualities than those produced by hot air drying. This is why the aromatic herbs for culinary uses are dried in vacuum, so as to preserve their volatile compounds responsible for the aroma and flavor. Some herbs like parsley or thyme can be dried without bleaching or sulphation. The plants dried for infusions are also dried in vacuum to preserve their bioactive compounds responsible for their beneficial health effects.

### ***D. Dairy Products:***

The use of drying to preserve milk for applications in baby food dates from 1902, being the milk powders divided into whole milk and skimmed milk powders. The whole

raw milk is centrifuged to produce skimmed milk with 0.05% fat, which is then heat-treated, with an intensity that determines whether the powder produced is classified as low-heat, medium heat or high heat. The more intense the thermal treatment, the lower the amount of soluble serum proteins (albumin and globulin) remaining in the powder. The low-heat powder is used in recombined dairy products, such as cheese and baby food; the medium-heat powder is used in the production of concentrated recombined dairy products; and the high heat powder is mainly used in the bakery and chocolate industries. The milk is then concentrated to a total solids content in the range 40-55% using a multiple effect evaporator. The skimmed milk is mainly produced by spray drying.

### ***E. Fish***

Traditional methods of extending the shelf life of fish include salting and smoking. The salting corresponds to an osmotic dehydration in which the salt is introduced into fish to reduce the water activity (Figure A-2-6).



Figure A-2-6: Salted fish

The smoking involves exposure of fish to wood smoke (Figure A-2-7), which can be done at a relatively low temperature, up to 30 °C, in which case the process is known as cold smoking. During smoking there may occur a loss of moisture of 10-11% and the cold smoked fish products can be refrigerated, which gives them a shelf life of about 7 days. The hot smoking is carried out at temperatures up to 120 °C, and these products may have

sufficiently low water activity which allows them to be stable without refrigeration. Lyophilized fish products are also available, but due to the high cost of this type of processing, lyophilization is used only for relatively expensive products such as shrimps.



Figure A-2-7: Smoked fish

#### ***F. Meat:***

Cooked minced meat (chicken, beef, lamb and pork) may be dried by hot air in tray dryers, conveyors, fluidized beds or rotary driers until a moisture content of 4-6% (wet basis). When dried, chicken meat is the most stable while pork is the least. The main cause of deterioration of such products is the oxidation of fat that leads to rancidity. The cooked minced meat can also be dried under vacuum, allowing obtaining better products, but also at a higher cost. Both raw and cooked meat in the form of steaks, slices, cubes or minced can be lyophilized to a moisture content of 1.5-3.0% (wet basis), at an even higher cost.

### ***A-2-1: Effects of Drying on Food Properties:***

#### ***A. Microstructure and Texture***

Factors that affect the structure of dehydrated fruits and vegetables are the type of pre-treatment applied to the materials (blanching, peeling, cutting, ...) together with the intensity with which it is applied.

Blanching is a previous operation of great importance in drying materials of plant origin, because it neutralizes the polyphenol oxidase. Even when it is well done, it causes textural changes owing to starch gelatinization, cellulose crystallization and internal



tensions originated by localized variations in moisture. These originate ruptures and compressions which cause permanent distortions in the cells, providing them with a roughed aspect. When rehydrated these foods absorb water more slowly and fail to gain back the firm texture of the original raw material.

The dehydration temperature and rate have great influence on the texture of the food and, in general, faster processes and higher temperatures cause greater changes.

The water that migrates to the surface carries solutes from the food, originating tensions in the structure, variable according to the type of food, its composition and the processing parameters. The drying may cause some changes in mechanical properties, structure, volume, porosity and density of the foods.

The high temperature causes profound physical and chemical alterations on the surface of the foods, thus leading to the formation of a hard impenetrable surface layer, which keeps the foods dried at the surface but moist inside. The structural changes during drying influence the texture of the final product, according to the rate of water elimination. If shrinkage occurs, like in the air-dried foods, a very dense structure is formed and the dried product is harder (Figure A-2-8).



Figure A-2-8: Highly porous freeze-dried fruits (strawberries and bananas)

On the contrary, if no shrinkage occurs, like in the case of lyophilized foods, a highly porous structure is formed and the product has a smoother texture (Figure A-2-9).



Figure A-2-9: Dense air-dried fruits (raisins and peaches).

**B. Color:**

Enzymatic browning is one of the important browning reactions in fruits and vegetables during thermal processing and that includes drying (Figure A-2-10).

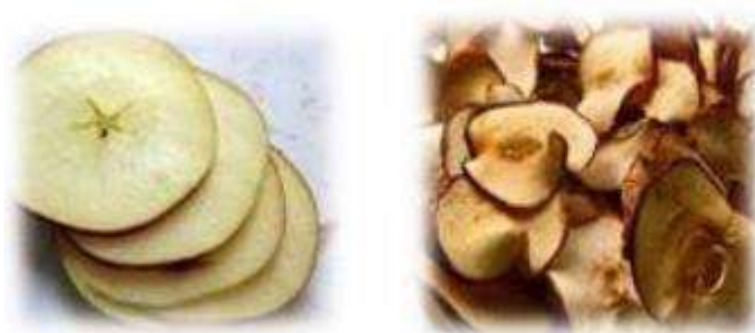


Figure A-2-10: Darkening of apple slices during drying due to polyphenol oxidase activity.

The enzyme PPO is widely distributed among plant materials and may cause undesirable color and flavor changes during post-harvest processing, due to enzymatic browning, when in the presence of oxygen. Therefore, enzyme deactivation is usually an essential treatment prior to any preservation process such as drying, and which largely determines the product quality.

Dehydration alters the surface characteristics of the food, and thus the color and reflectance. Chemical changes in pigments such as carotene and chlorophyll are produced by heat and oxidation that occur during drying (Figure A-2-11). In general, the longer the process and the higher the temperature, the greater are the losses in these pigments.



Figure A-2-11: Discoloration of pigments with drying (carotenoids and chlorophyll).

The optimum pH for the activity of the PPO is between 6 and 7, so that for  $\text{pH} \leq 4$  it becomes inactive. Hence it is recommended the addition of citric or ascorbic acid to lower the pH. On the other hand, Sulphur compounds (exposure to the vapors resulting from the burning of Sulphur or dipping in aqueous solutions of bisulphite or metabisulphite) have also been used to avoid the browning reactions. However, in some cases we must pay attention to the concentrations used to avoid unpleasant flavors.

Finally, the activity of PPO is also inhibited in the absence of the oxygen, for which the reduction of the oxygen concentration of the drying atmosphere is also beneficial, such as when the drying is done under vacuum.

Among the non-enzymatic browning reactions stand the Maillard and the caramelization reactions. The Maillard reaction involves the amino acids and the reducing sugars resulting in the formation of melanoidins, with consequent loss of nutritive value. These reactions start at 70 °C and their rate is dependent on the type of sugars present in the food. Also, the foods with water activity in the range 0.5-0.8 are more susceptible to nonenzymatic browning. Caramelization reactions happen with sugars for temperatures higher than 120 °C originating dark products named caramels.



### ***C. Chemical Composition and Nutritional Value:***

Drying can significantly alter the food chemical composition and nutrients, with an extension variable according to the type of food, drying method, intensity of treatment and operating conditions (Figure A-2-12).

Changes in nutritional value of dried foods may be due to preparation systems (pre-treatments), drying conditions (particularly temperature) or storage conditions (after drying). Some measures that can be taken to reduce nutrient losses include: minimize drying time, use lower temperatures, and during storage maintain low levels of moisture and oxygen concentration.



Figure A-2-12: Effect of drying on food nutrients.

The water solubility of vitamins is variable. As drying proceeds, some vitamins (ex. riboflavin) reach oversaturation and precipitate and therefore lower losses occur. Others (ex.

vitamin C) are maintained dissolved until the moisture content in the food is very low, and react with the solutes at a greater rate as the process advances. The vitamin C is particularly affected by heat and oxidation and also the thiamine is relatively sensitive to heat. The liposoluble vitamins are more stable to heat and oxidation (with losses < 10 %), but may react with peroxides resulting from lipid oxidation.

The liposoluble nutrients (ex. Essential fatty acids and vitamins A, D, E and K) are present mostly in the dry matter of the food and that why the losses during drying are not so important. The dietary minerals (copper and iron) act as catalyzers in oxidation reactions of unsaturated lipids and are dissolved in the aqueous phase of the food. Hence, during drying water is eliminated and their reactivity diminishes, thus giving a better preservation of the nutritional value. The biological value and digestibility of proteins in most foods does not change with drying. However, it may occur denaturation in some foods and under some operating conditions.

#### ***D. Aroma:***

Heat originates losses in volatile components from the food, according to the processing temperature, the vapor pressure of the volatile substances, their solubility in water vapor and the concentration of solids in the food. Some methods for protecting the flavor of dehydrated food include: working at low temperature and/or use vacuum, promote the activation of natural enzymes in the foods or add external enzymes which originate aromatic substances from the natural aroma precursors, use compounds fixators of aroma, and do the recovery of the volatile compounds to add the again to the product.

## ملخص المشروع:

التجفيف الشمسي هو أحد تطبيقات الطاقة الشمسية الفعالة وهو يعني إزالة الرطوبة من المنتج الزراعي والتجفيف مفيد في الحفاظ على المنتجات الزراعية والغذائية لفترة طويلة حيث يمنع المنتج من التلف والتلوث. يتضمن التجفيف استخدام الحرارة لتبخير الرطوبة وإزالة بخار الماء بعد فصله عن المنتجات الغذائية وبالتالي فهي عملية نقل حرارة وكتلة مشتركة ومتزامنة ويجب توفير الطاقة من أجلها. تمنع إزالة الرطوبة نمو وتكاثر الكائنات الحية الدقيقة مثل البكتيريا والخمائر والعفن التي تسبب التسوس وتقلل تدهور المنتج بسبب الرطوبة وإن عملية التجفيف تؤدي إلى انخفاض وزن وحجم المنتج وبالتالي تقليل تكاليف التعبئة والتخزين والنقل، وتتيح إمكانية تخزين المنتج في درجات الحرارة المحيط.

هناك العديد من المنتجات التي يتم تجفيفها بواسطة المجففات الشمسية مثل الفواكه والحبوب والأخشاب والأسماك. إن التجفيف المفتوح بالشمس يعني أن المنتجات تتعرض مباشرة للشمس، مما يسمح لها بامتصاص الأشعة الشمسية وأن هذه الطريقة لها العديد من العيوب مثل الجودة الرديئة وتلوث المنتج ويمكن التخلص من هذه العيوب عن طريق غير مباشر بواسطة المجففات الذي تُستخدم لتجفيف المنتجات كتطبيق للطاقة الشمسية. في هذا المشروع، درسنا التقنيات المختلفة للتجفيف وأنماط مختلفة من التجفيف الشمسي.

إن الطرق المختلفة للتجفيف الشمسي هي التجفيف الشمسي المباشر والتجفيف الشمسي غير المباشر والتجفيف الشمسي المختلط.

الغرض من المجفف هو توفير مزيد من الحرارة للمنتج أكثر من تلك المتوفرة بشكل طبيعي في ظل الظروف المحيطة، وبالتالي زيادة ضغط بخار رطوبة المنتج بشكل كافٍ. لذلك، تتم إزالة الرطوبة من المنتج ويقلل المجفف أيضاً بشكل كبير من الرطوبة النسبية لهواء التجفيف، ومن خلال القيام بذلك، تزداد قدرته على حمل الرطوبة مما يضمن محتوى رطوبة منخفضاً بدرجة كافية.

ثبت أن استخدام أنظمة التجفيف بالطاقة الشمسية للمنتجات الزراعية للحفاظ على الفواكه والخضروات والمحاصيل الأخرى رخيص الثمن وموثوق به وصديق للبيئة، كما أنه يوفر بديلاً عملياً لتقنيات التجفيف التقليدية.

إن الطريقة التقليدية للتجفيف الشمسي تسبب مشاكل الغبار والقوارض والحشرات وكذلك فقدان اللون وتوفر مجففات الطاقة الشمسية مزايا منتجات ذات جودة أفضل، وفترات تجفيف أقصر، وتقليل فقد المواد المراد تجفيفها. يمكن تصنيف المجففات الشمسية على أنها مباشرة أو غير مباشرة، مع فئات فرعية حيث يتم تصنيف أنظمة التجفيف بالطاقة الشمسية بشكل أساسي وفقاً لأنماط التسخين الخاصة بها والطريقة التي يتم بها استخدام الحرارة الشمسية ويتم تصنيفها أساساً إلى طريقتين رئيسيتين (المجففات النشطة والمجففات السلبية).

يستعرض هذا المشروع حالة الأنواع المختلفة من المجففات الشمسية المستخدمة على نطاق واسع اليوم وكذلك عملية التجفيف التي يتم إجراؤها أثناء تجفيف المنتجات الغذائية المختلفة والنسبة المئوية التي تحتوي على الرطوبة في

المنتجات الغذائية المختلفة وتمت مناقشة المجففات غير المباشرة والمباشرة والمختلطة التي أظهرت إمكانيات في تجفيف المنتجات الزراعية.

كما تم تسليط الضوء أيضًا على العوامل المؤثرة والتأثير البيئي الذي يلعب دورًا حيويًا في قطاع التجفيف الشمسي ونقول إن المجفف الشمسي غير المباشر أكثر ملاءمة من المجففات الأخرى وإن إعادة تدوير الهواء في المجفف الشمسي الغير مباشر يمكن أن يقلل من وقت تجفيف المنتج بالمقارنة مع المجففات الشمسية غير المباشرة العادية اي ان المجفف الذي يحتوي على إعادة تدوير للهواء له كفاءة أكثر من المجففات الأخرى.

يمكن استخدام المواد المتوفرة محليًا لبناء مجففات شمسية كما يمكن تصميم أنظمة التجفيف باستخدام الألواح الشمسية الكهروضوئية ونظرًا لأن الطاقة الشمسية متقطعة، فإن عملية تخزين الطاقة الحرارية والكهربائية ضروري للاستفادة من الطاقة المتجددة بشكل قابل للتطبيق في التجفيف ولتقليل استخدام النفط أو الغاز، يمكن استخدام الطاقة الحيوية للتسخين في حالة عدم توفر الشعاع الشمسي.

لقد تم شرح ومناقشة أنواع عديدة من أنظمة التجفيف الشمسي المصممة والمطورة لتحسين عملية التجفيف لتوفير الطاقة وتحسين جودة المنتج والاستفادة من مصادر الطاقة المجانية والمتجددة وغير الملوثة التي توفرها الشمس. في هذا المشروع ، تم استعراض وشرح تقنية وأداء منظومات التجفيف الشمسي حسب نوع المنتج المراد تجفيفه وأظهر استخدام أنظمة التجفيف الشمسي في الحفاظ على الخضار والفاكهة والمحاصيل أنه عملي واقتصادي ومتوافق من الناحية البيئية.



وزارة التعليم العالي والبحث العلمي  
كلية دجلة الجامعة  
قسم هندسة تقنيات التبريد والتكييف

# الأنواع المختلفة من المجففات التلمسية دراسة نظرية

مشروع تخرج

مقدم إلى مجلس كلية دجلة الجامعة/ قسم هندسة تقنيات التبريد والتكييف وهو جزء من متطلبات  
نيل درجة بكالوريوس هندسة في تقنيات التبريد والتكييف

من قبل

ايمن تركي ساكن صالح

ظافر عمار حميد سلمان

محمد عبد الرحيم نعمه جوده

منذر عوده ضهد عاصي

نصيف جاسم محمد غزال

بإشراف

المدرس المساعد

عامر فاضل حسين

*Ministry of Higher Education and Scientific Research*

*Dijlah University College*

*Refrigeration and Air Conditioning*

*Technologies Engineering Department*



## **Design a Heat Exchanger for a Chiller System Used for Cooling in Plastic Factories**

**A project**

**Submitted to the Refrigeration and Air Condition Technology Engineering  
Department at Dijlah University College in partial fulfillment of the requirements  
for Degree of Bachelor in Refrigeration and Air Conditioning Technologies  
Engineering Department**

**By:**

- **Ahmed Adi Mhameed**
- **Abbas Ihsan Faleh**
- **Ahmed fayez hussain**
- **safaa kadhim Habeeb**
- **Ali Fahm Habeeb**

**Supervisor**

**by**

**Lec. Maha Ali Hussein**

**1442 A.H.**

**2021 A.D.**

بسم الله الرحمن الرحيم

(( وَقُلْ اَعْمَلُوا فَسَيَرَى اللّهُ عَمَلَكُمْ وَرَسُولُهُ وَالْمُؤْمِنُونَ وَسَتُرَدُّونَ  
إِلَىٰ عَالِمِ الْغَيْبِ وَالشَّهَادَةِ فَيُنَبِّئُكُم بِمَا كُنتُمْ تَعْمَلُونَ » التوبة -

(( 105

صدق الله العظيم



## ***Supervisor Certificate***

*We certify that this project entitled ((Design a Heat Exchanger for a Chiller System Used for Cooling in Plastic Factories))*

*Prepared by:*

- ***Ahmed Adi Mhameed***
- ***Abbas Ihsan Faleh***
- ***Ahmed fayez hussain***
- ***safaa kadhim Habeeb***
- ***Ali Fahm Habeeb***

*Has been carried out completely under our supervision at the Dijlah university college in partial fulfillment of the requirements for Degree of Bachelor in Refrigeration and Air Conditioning Technologies Engineering.*

*Signature:*

***Maha A. Hussein***

*Date: 20/06 /2021*

*Approved by the head of Air condition and refrigeration engineering department:*

*Signature*

*Dr.*

*Head of Refrigerating and Air  
Conditioning Engineering Department*

*Date:    /    /2021*



# ***Examining committee certificate***

**We certify that this project entitled ( Design a Heat Exchanger for a Chiller System  
Used for Cooling in Plastic Factories )**

**Submitted by:**

- ***Ahmed Adi Mhameed***
- ***Abbas Ihsan Faleh***
- ***Ahmed fayez hussain***
- ***safaa kadhim Habeeb***
- ***Ali Fahm Habeeb***

and as an examining committee examined the students in its content and that  
our opinion it meets the standards of a project for the for Degree of Bachelor  
Refrigeration and Air Conditioning Technologies Engineering.

Signature

***Maha A. Hussein***

***Date: / /2021***

***(supervisor)***

***Signature***

***Name:***

***Date: 01 /07 /2021***

***(Member)***

***Signature***

***Name:***

***Date: 01/07 /2021***

***(Member)***

## الإهداء

بمن ارسله الله رحمة للعالمين واماماً للمتقين وحجة على الخلائق اجمعين محمد  
لمى الله عليه واله وسلم) الى من وكلهم الله بالهبة والوقاء الى من علمونا العطاء بدون  
ار الى من تجلى اسمه بكل افتخار (والدي العزيز) الى كل ما في الوجود بعد الله ورسوله  
بي وقوتي وملاذي بعد الله (امي الغالية) الى من اثروني على انفسهم الى  
من علموني وساعدوني الى من اظهروا لي ما هو اجل من الحياة (اخوتي  
نواتي) الى من كانوا ملاذي وملجئي الى من تذوقت معهم اجمل اللحظات الى  
من سنقتقدم واتمنا ان يفقدونا الى من جعلهم الله اخوتي بالله ومن احببتهم بالله

(طالبة قسم هندسة تقنيات التكيف والتبريد)

## ***Abstract***

In this project a water cooling heat exchanger (condenser) has been designed to use in a chiller system according to a plastic factory requirements. The design based on the trial and error method by assuming the number of inner tubes with one pass and two pass pipes. Also, the difference temperature between the outer surface of the pipes with the refrigerant was assuming. The results showed that as the number of one pass tube increases the Reynolds number, the overall heat transfer coefficient, pressure drop and the tube length decreases. The design specifications is chosen for the heat exchanger (condenser) are:

- Shell and tube heat exchanger with one pass tubes.
- Number of tubes is 25 with 2.7m length and 14 mm inner diameter



# *Content*

## **CHAPTER ONE**

1.1 Introduction .....	1
1.2 Heat Transfer Modes.....	2
1.2.1 Conduction .....	2
1.2.2 Convection.....	3
1.3 Heat Exchangers.....	5
1.3.1 Heat Exchanger classification.....	5

## **CHAPTER TWO.....8**

Chilled- Water System.....	8
2.1 Introduction.....	8
2.2 Chiller System Working Principles.....	8
2.3 Condensers for High Pressure Chillers.....	10
2.3.1 Water-Cooled Condensers.....	10
2.4 Refrigerant in Chiller System.....	11
2.4.1 Thermodynamic And Thermo-Physical Properties:.....	12
2.4.2 R22 Refrigerant fluid.....	13
2.4.2 R22 Refrigerant fluid.....	14

## **CHAPTER THREE.....16**

### **Shell and Tube Exchangers: Construction Details.....16**

3.1 Overall heat-transfer coefficient.....	16
3.2 Liquid in tubes; heat transfer and pressure drop.....	18
3.3 Pressure Drop across Tubes.....	19
3.4 Required condensing capacity.....	20
3.5 Condensing heat transfer coefficient across shell.....	20

## **CHAPTER FOUR.....23**

### **Design Calculation.....23**

4.1 Design Procedure.....	23
4.2 Calculations.....	24
Properties (R_22) AT 50 From Table (B - 1).....	26

## **CHAPTER FIVE.....42**

Discussion and Conclusion.....	42
5.1 Discussion.....	42
References:.....	46

# CHAPTER ONE

## Introduction

### 1.1 Introduction

A heat exchanger is a device that is used for transfer of thermal energy (enthalpy) between two or more fluids, between a solid surface and a fluid, or between solid particulates and a fluid, at differing temperatures and in thermal contact, usually without external heat and work interactions. Heat exchangers have many applications in industrial and engineering fields. In most of these applications, heat is transferred through heat exchangers as in the chemical, electrical, power, petroleum, air-conditioning, refrigeration, cryogenic, heat recovery, and manufacturing industries. Heat exchange involve convection in each fluid and conduction through the separating wall. Heat can flow only from hotter to cooler fluids, as per the second law of thermodynamics [1]. The actual design of heat exchangers is a complicated problem. It involves more than heat-transfer analysis alone. Saving material and energy are common objectives for heat sink design optimization. One of the important issues that should be defined during the design work, taking in consideration the cost of material, is the optimization of the heat efficiency. The optimization function can consider minimum weight for a specified heat flow, placement of individual fins to form channels or fin profile based on a set of specified conditions (for instance the dissipation from the fin faces, minimum mass, minimum pressure drop etc). In order to intensify the heat transfer from the heat exchanger surface to fluid, it is possible to increase convection coefficient (by growing the fluid velocity), widen temperature difference between surface and fluid or increase the surface area across which convection occurs. Extended surfaces, in the form of longitudinal or

radial fins are common in applications where the need to enhance the heat transfer between a surface and an adjacent fluid exists [2].

## 1.2 Heat Transfer Modes

Heat can be transferred in three different modes: *conduction*, *convection*, and *radiation*. All modes of heat transfer require the existence of a temperature difference, and all modes are from the high-temperature medium to a lower-temperature one.

### 1.2.1 Conduction

Conduction is the transfer of energy from the more energetic particles of a substance to the adjacent less energetic ones as a result of interactions between the particles. Conduction can take place in solids, liquids, or gases. In gases and liquids, conduction is due to the collisions and diffusion of the molecules during their random motion. In solids, it is due to the combination of vibrations of the molecules in a lattice and the energy transport by free electrons. The rate of heat conduction through a medium depends on the geometry of the medium, its thickness, and the material of the medium, as well as the temperature difference across the medium [3].

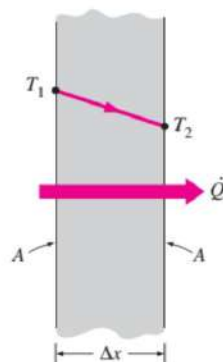
Consider steady heat conduction through a large plane wall of thickness  $\Delta x = L$  and area  $A$ , as shown in Fig. (1.1). The temperature difference across the wall is  $\Delta T = T_2 - T_1$ . Experiments have shown that the rate of heat transfer  $Q$  through the wall is doubled when the temperature difference  $\Delta T$  across the wall or the area  $A$  normal to the direction of heat transfer is doubled, but is halved when the wall thickness  $L$  is doubled. Thus we conclude that the rate of heat conduction through a plane layer is proportional to the temperature difference across the layer



and the heat transfer area, but is inversely proportional to the thickness of the layer. That is,

$$\dot{Q}_{\text{cond}} = kA \frac{T_1 - T_2}{\Delta x} = -kA \frac{\Delta T}{\Delta x} \quad (\text{W}) \quad \dots\dots\dots 1.1$$

Where the constant of proportionality  $k$  is the **thermal conductivity** of the material, which is a measure of the ability of a material to conduct heat.



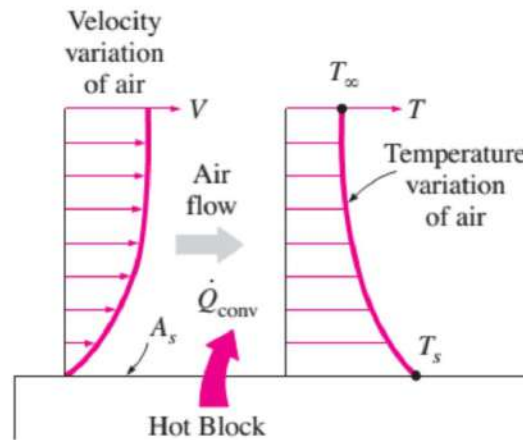
**Fig. (1-1):** Heat conduction through a large plane wall of thickness  $\Delta x$  and area  $A$

### 1.2.2 Convection

Convection is the mode of energy transfer between a solid surface and the adjacent liquid or gas that is in motion, and it involves the combined effects of conduction and fluid motion. The faster the fluid motion, the greater the convection heat transfer. In the absence of any bulk fluid motion, heat transfer between a solid surface and the adjacent fluid is by pure conduction. The presence of bulk motion of the fluid enhances the heat transfer between the solid surface and the fluid, but it also complicates the determination of heat transfer rates [3].

Consider the cooling of a hot block by blowing cool air over its top surface (Fig. 1.2). Heat is first transferred to the air layer adjacent to the block by conduction. This heat is then carried away from the surface by

convection, that is, by the combined effects of conduction within the air that is due to random motion of air molecules and the bulk or macroscopic motion of the air that removes the heated air near the surface and replaces it by the cooler air.



**Fig. (1.2):** Heat transfer from a hot surface to air by convection

Convection is called **forced convection** if the fluid is forced to flow over the surface by external means such as a fan, pump, or the wind. In contrast, convection is called **natural** (or **free**) **convection** if the fluid motion is caused by buoyancy forces that are induced by density differences due to the variation of temperature in the fluid.

The rate of convection heat transfer is observed to be proportional to the temperature difference, and is conveniently expressed by **Newton's law of cooling** as:

$$\dot{Q}_{conv} = hA_s (T_s - T_\infty) \quad (W) \quad \dots\dots\dots 1.2$$

where  $h$  is the convection heat transfer coefficient in  $W/m^2 \cdot ^\circ C$ ,  $A_s$  is the surface area through which convection heat transfer takes place,  $T_s$  is the surface temperature, and  $T_\infty$  is the temperature of the fluid



sufficiently far from the surface. Note that at the surface, the fluid temperature equals the surface temperature of the solid.

The convection heat transfer coefficient  $h$  is not a property of the fluid. It is an experimentally determined parameter whose value depends on all the variables influencing convection such as the surface geometry, the nature of fluid motion, the properties of the fluid, and the bulk fluid velocity.

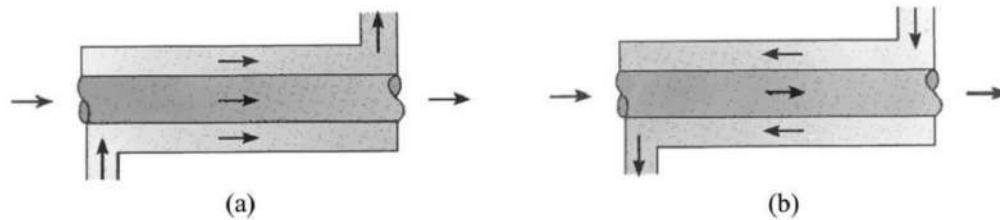
### **1.3 Heat Exchangers**

The general function of a heat exchanger is to transfer heat from one fluid to another. The basic component of a heat exchanger can be viewed as a tube with one fluid running through it and another fluid flowing by on the outside. There are thus three heat transfer operations that need to be described [4]:

- 1) Convective heat transfer from fluid to the inner wall of the tube
  - 2) Conductive heat transfer through the tube wall
  - 3) Convective heat transfer from the outer tube wall to the outside fluid.
- Heat

#### **1.3.1 Heat Exchanger classification**

exchangers are typically classified according to flow arrangement and type of construction. The simplest heat exchanger is one for which the hot and cold fluids move in the same or opposite directions in a concentric tube (or double-pipe) construction. In the parallel-flow arrangement of Figure 1.3 a, the hot and cold fluids enter at the same end, flow in the same direction, and leave at the same end. In the counter flow arrangement of Figure 1.3 b, the fluids enter at opposite ends, flow in opposite directions, and leave at opposite ends [2].



**Fig. (1.3):** Concentric tubes heat exchangers. (a) Parallel flow. (b) Counter flow

The heat transfer surface in heat exchangers can be arranged in several forms. Heat exchangers are therefore also classified as [2]:

- **Double pipe heat exchangers.** Double pipe heat exchangers are cheap for both design and maintenance, making them a good choice for small industries. In these exchangers one fluid flows inside the tube and the other fluid flows on the outside. Although they are simple and cheap, their low efficiency coupled with the high space occupied in large scales, has led modern industries to use more efficient heat exchangers like shell and tube.
- **Shell and tube heat exchangers.** Shell and tube heat exchangers in their various construction modifications are probably the most widespread and commonly used basic heat exchanger configuration in industry. Shell-and-tube heat exchangers are further classified according to the number of shell and tube passes involved. Shell and tube heat exchangers are typically used for high-pressure applications (with pressures greater than 30 bar and temperatures greater than 260 °C). This is because the shell and tube heat exchangers can withstand high pressures due to their shape. In this type of heat exchanger, a number of small bore pipes are fitted between two tube plates and primary fluid flows through these tubes. The tube bundle is placed inside a shell and the secondary fluid flows through the shell and over the surface of the tubes. In nuclear engineering, this design of heat exchangers is widely used

as in case of steam generator, which are used to convert feedwater into steam from heat produced in a nuclear reactor core. To increase the amount of heat transferred and the power generated, the heat exchange surface must be maximized. This is obtained by using tubes. Each steam generator can contain anywhere from 3,000 to 16,000 tubes, each about 19mm diameter.

- **Plate heat exchangers.** A plate heat exchanger is a type of heat exchanger that uses metal plates to transfer heat between two fluids. This arrangement is popular with heat exchangers using air or gas as well as lower velocity fluid flow. The classic example of a heat exchanger is found in an internal combustion engine in which an engine coolant flows through radiator coils and air flows past the coils, which cools the coolant and heats the incoming air. When compared to shell and tube exchangers, the stacked-plate arrangement typically has lower volume and cost. Another difference between the two is that plate exchangers typically serve low to medium pressure fluids, compared to medium and high pressures of shell and tube.



## **CHAPTER TWO**

### **Chilled- Water System**

#### **2.1 Introduction**

Refrigeration is the process of removing heat from a place where it is not wanted and transferring that heat to a place where it makes little or no difference. A chiller is one of refrigeration machine that removes heat from a liquid via a vapor-compression, adsorption refrigeration, or absorption refrigeration cycles. This liquid can then be circulated through a heat exchanger to cool equipment, or another process stream (such as air or process water). As a necessary by-product, refrigeration creates waste heat that must be exhausted to ambience, or for greater efficiency, recovered for heating purposes. The condensing side of the chiller can be either air or water cooled. Even when liquid cooled, the chiller is often cooled by an induced or forced draft cooling tower.

Chilled water is used to cool and dehumidify air in mid- to large-size commercial, industrial, and institutional facilities. Water or liquid chillers can be liquid-cooled or air-cooled. Water or liquid-cooled systems can provide efficiency and environmental impact advantages over air-cooled systems [5].

#### **2.2 Chiller System Working Principles**

In most process cooling applications, a pumping system circulates cool water from the chiller to the process. This cool fluid removes heat from the process and the warm fluid returns to the chiller. The process water is the means by which heat transfers from the process to the chiller [6].

Process chillers contain a chemical compound, called a refrigerant. There are many types of refrigerant and applications depending on the temperatures required but they all work on the basic principle of compression and phase-change of the refrigerant from a liquid to a gas and back to a liquid. This process of heating and cooling the refrigerant and changing it from a gas to a liquid and back again is the refrigeration cycle.

The refrigeration cycle starts with a low-pressure liquid/gas mix entering the evaporator. In the evaporator, heat from the process water boils the refrigerant, which changes it from a low-pressure liquid to a low-pressure gas as can be seen in Fig.(2-1). The low-pressure gas enters the compressor where it is compressed to high-pressure gas. The high-pressure gas enters the condenser where ambient air or condenser water removes heat to cool it to a high-pressure liquid. The high-pressure liquid travels to the expansion valve, which controls how much liquid refrigerant enters the evaporator, thereby beginning the refrigeration cycle again.

There are two types of condensers used in chillers; air-cooled and water-cooled. An air-cooled condenser uses ambient air to cool and condense the hot refrigerant gas back down to a liquid. It can be located inside the chiller or can be remotely located outside, but ultimately it rejects the heat from the chiller to the air. In a water-cooled condenser, water from a cooling tower cools and condenses the refrigerant.

## WATER-COOLED CHILLER DIAGRAM

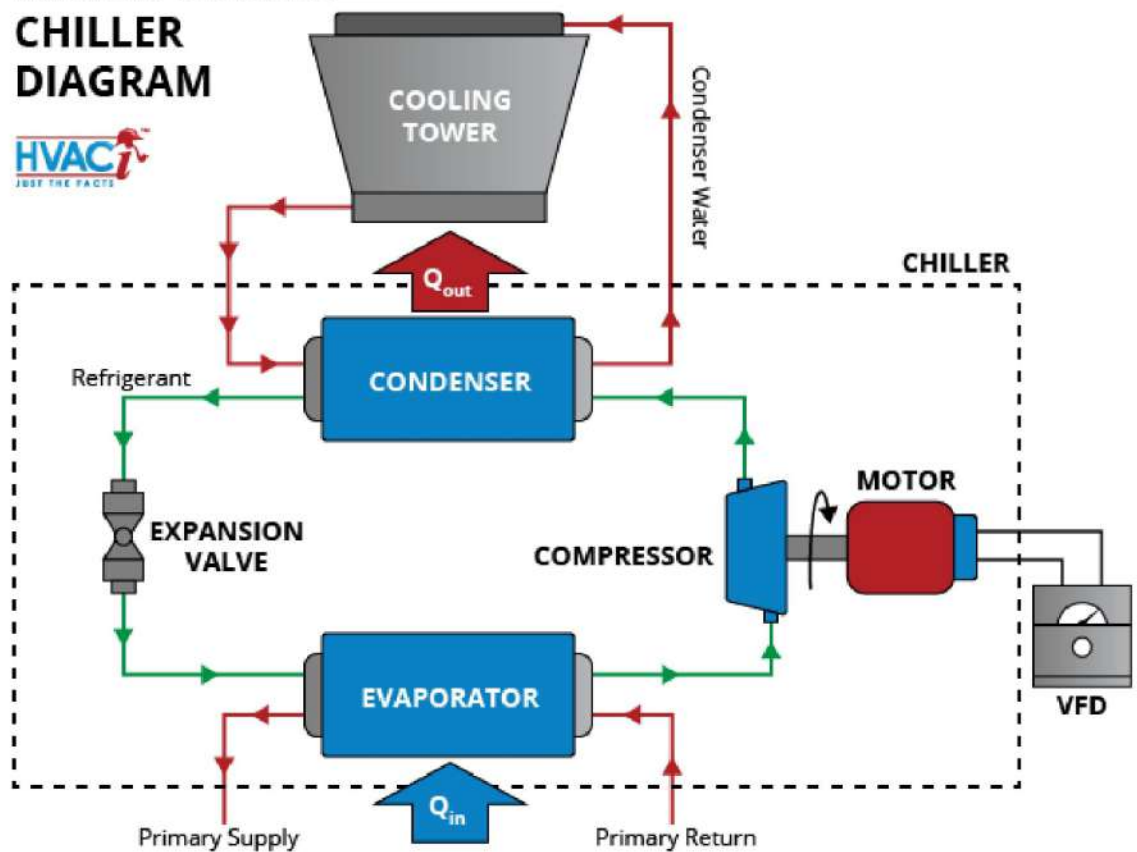


Figure (2-1): Chiller System

### 2.3 Condensers for High Pressure Chillers

The condenser is the component that transfers heat out of the system. The condenser for high-pressure chillers may be either water-cooled or air-cooled. Both will absorb the heat and transfer it out of the system, usually to the atmosphere.

In some manufacturing processes, the heat may be recovered and used for other purposes [6].

#### 2.3.1 Water-Cooled Condensers

Water-cooled condensers used for high-pressure chillers are the shell-and-tube type with the water circulating in the tubes and the



refrigerant around the tubes. The shell must have a working pressure to accommodate the refrigerant used and a water-side working pressure of 150 to 300 psig. The hot discharge gas is normally discharged into the top of the condenser, **Fig.(2-2)**. The refrigerant is condensed to a liquid and drips down to the bottom of the condenser, where it gathers and drains into the liquid line. The heat exchange can be improved by use of extended surfaces on the refrigerant side of the condenser tube.

The inside of the condenser tubes may also be grooved for improved water-side heat exchange. Condensers must also have a method for piping the water into the shell. There are two basic types of connections to the water box that is attached to the condenser shell. In a standard water box, the piping is attached to the removable water box and some of the piping must be removed before the inspection cover can be removed on the piping end. A marine water box has a removable cover for easy access to the piping end of the machine. Tube access is more important for the condenser than the evaporator in most installations because the water in the cooling tower is open to the atmosphere and more likely to carry dirt and other foreign matter into the condenser. Some comfort-cooling installations serve both cooling and heating needs at the same time. While the outside of the building may need heat in the winter, the inside or core of the building may be generating heat from lighting and equipment that needs to be removed. These installations may have what is known as double-bundled condensers, which are two condensers in one shell. When the heat can be used for the building perimeter, the warm condenser water can be circulated in the heating circuit [6].

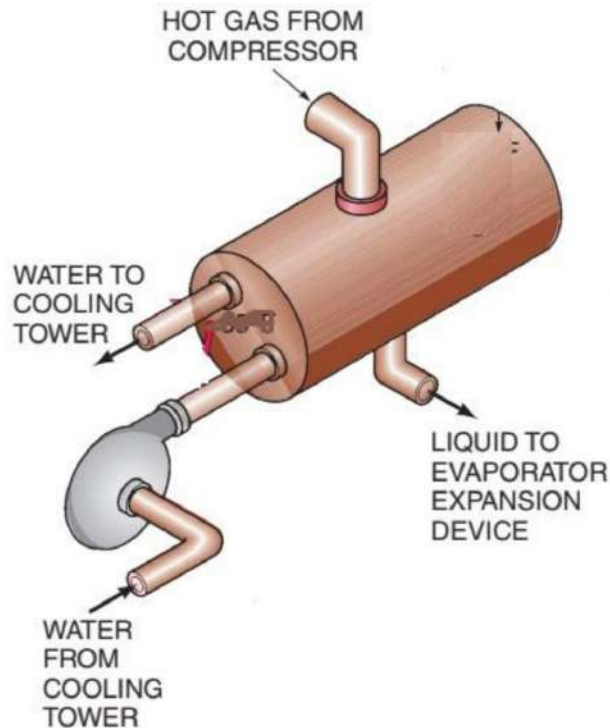


Figure (2-2): Shell and Tube Condenser

## 2.4 Refrigerant in Chiller System

The thermodynamic efficiency of a refrigeration system depend very much on the type of refrigerant selected for a given application. In principle, any fluid can be used as a refrigerant. Many fluids can be used as refrigerants in vapor compression refrigeration systems. Air also be considered as a refrigerant used in an air cycle refrigeration system. Selection of refrigerant for a particular application is based on the following requirements:

- 1- Thermodynamic and thermo-physical properties
- 2- Environmental and safety properties, and
- 3- Economics



### **2.4.1 Thermodynamic And Thermo-Physical Properties:**

- a) Suction pressure: At a given evaporator temperature, the saturation pressure should be above atmospheric for prevention of air or moisture ingress into the system and ease of leak detection. Higher suction pressure allows for smaller compressor displacement is better as it leads to
- b) Discharge pressure: At a given condenser temperature, the discharge pressure should be as small as possible to allow light-weight construction of compressor, condenser etc.
- c) Pressure ratio: Should be as small as possible for high volumetric efficiency
- d) Latent heat of vaporization: Should be as large as possible so that the required mass flow rate per unit cooling capacity will be small.
- e) Isentropic index of compression: Should be as small as possible so that the temperature rise during compression will be small.
- f) Liquid specific heat: Should be small so that degree of sub-cooling will be large leading to smaller amount of flash gas at evaporator inlet.
- g) Vapor specific heat: Should be large so that the degree of superheating will be small.
- h) Thermal conductivity: Thermal conductivity in both liquid as well as vapor phase should be high for higher heat transfer coefficients.
- i) Viscosity: Viscosity should be small in both liquid and vapor phases for smaller frictional pressure drops.

### 2.4.2 R22 Refrigerant fluid

R22 refrigerant is one of the most commonly used refrigerants in the air conditioning systems. R22 is the short name for the halocarbon compound  $\text{CHClF}_2$  (monochlorodifluoromethane), which is used as the refrigerant. R stands for the refrigerant. In the number “22” second “2” denotes the number of the fluorine atoms in the compound [7].

The boiling point of R22 is -40.8 degree Celsius (-41.4 degree F). Due to its low boiling point this refrigerant was initial developed for the low temperature applications like domestic and farm freezers and in industrial refrigeration applications. Even at present R22 is extensively used in the industries for liquefaction of the gases like chlorine, for supplying chilled water to various processes, machines, chillers of central air conditioning systems, etc. . R22 is non-toxic and it is non-flammable that makes this refrigerant highly safe for the domestic and industrial purposes.

The discharge temperature of R22 is quite high, hence the degree of superheat in the systems using this refrigerant should be minimum. The compression ratio for the systems using this refrigerant should also be low, and if it is high intercooling between the two stages of the compression should be kept. **R22 Refrigerant has many Advantages:**

**1) Has less effect on ozone layer:** It has lesser ozone destruction capability. The ozone destruction potential of R22 is only 5% of refrigerant R11, which has the highest ozone destruction potential.

**2) Low compressor displacement:** For producing the same compression the displacement required by the compressor with refrigerant R22 is small compared to refrigerant R12. In fact the displacement required for R22 is 60% of that required for R12. This means that for the given displacement

of the compressor the system using refrigerant R22 produces 65% more refrigeration capacity than the system using the refrigerant R12. This translates into higher refrigeration efficiency and lower power consumption, which is very crucial in the large industrial applications though it is important for the domestic applications as well.

**3) Greater water absorbing capacity:** Refrigerant R22 has greater water absorbing capacity than R12. This is very important in low temperature applications since the water in refrigerant R22 would have less troubling effects on the refrigeration system. Anyways, even minor amount of water in the refrigeration system is undesirable.

## **CHAPTER THREE**

### **Shell and Tube Exchangers: Construction Details**

The shell and tube exchanger is by far the most commonly used type of heat-transfer equipment used in the industries. The advantages of this type are:

1. The configuration gives a large surface area in a small volume.
2. Good mechanical layout: a good shape for pressure operation.
3. Uses well-established fabrication techniques.
4. Can be constructed from a wide range of materials.
5. Easily cleaned.
6. Well-established design procedures.

Essentially, a shell and tube exchanger consists of a bundle of tubes enclosed in a cylindrical shell. The ends of the tubes are fitted into tube sheets, which separate the shell-side and tube-side fluids. Baffles are provided in the shell to direct the fluid flow and support the tubes. The most widely used types of condensers

are shell-and-tube heat exchangers. The common used configuration where the gas is passed through the shell and the liquid in tubes. The reason is that volume flow rates of gases are high relative to those of liquids and would result in high pressure drops if forced through the tubes.



### 3.1 Overall heat-transfer coefficient

The overall heat-transfer coefficient for a condenser is the proportionality constant, which, when multiplied by the heat-transfer area and the mean temperature difference between the fluids, yields the rate of heat transfer. If heat flows across a tube between refrigerant on the outside and water on the inside, for example, under steady-state conditions the rate of heat transfer  $q$  in watts is the same from the refrigerant to the outside surface of the tube, from the outside to the inside surface of the tube, and from the inside condenser is the proportionality constant, surface of the tube to the water. The expressions for  $q$  in each of these transfers are, respectively [7],

$$q = h_o A_o (t_o - t_{os}) \quad \dots\dots\dots(3-1)$$

$$q = \frac{k}{x} A_m (t_{os} - t_{is}) \quad \dots\dots\dots(3-2)$$

$$q = h_i A_i (t_{is} - t_i) \quad \dots\dots\dots(3-3)$$

where  $q$  = rate of heat transfer, W  
 $h_o$  = heat-transfer coefficient on outside of tube, W/m<sup>2</sup> · K  
 $A_o$  = outside area of tube, m<sup>2</sup>  
 $t_o$  = refrigerant temperature, °C  
 $t_{os}$  = temperature of outside surface of tube, °C  
 $k$  = conductivity of tube metal, W/m · K  
 $x$  = thickness of tube, m  
 $t_{is}$  = temperature of inside surface of tube, °C  
 $A_m$  = mean circumferential area of tube, m<sup>2</sup>  
 $h_i$  = heat-transfer coefficient on inside of tube, W/m<sup>2</sup> · K  
 $A_i$  = inside area of tube, m<sup>2</sup>  
 $t_i$  = water temperature, °C

To express the overall heat-transfer coefficient the area on which the coefficient is based must be specified. Two acceptable expressions for the overall heat-transfer coefficient are,

$$q = U_o A_o (t_o - t_i) \quad \dots\dots\dots(3-4)$$

$$q = U_i A_i (t_o - t_i) \quad \dots\dots\dots(3-5)$$

where  $U_o$  = overall heat-transfer coefficient based on outside area,  $W/m^2 \cdot K$   
 $U_i$  = overall heat-transfer coefficient based on inside area,  $W/m^2 \cdot K$

From Eqs. (3-4) and (3-5) it is clear that  $U_o A_o = U_i A_i$ . The U value is always associated with an area. Knowledge of  $U_o$  or  $U_i$  facilitates computation of the rate of heat transfer (q).

To compute the U value from knowledge of the individual heat-transfer coefficients, first divide Eq. (3-1) by ( $h_o A_o$ ), Eq. (3-2) by ( $k A_m/x$ ), and Eq. (3-3) by ( $h_i A_i$ ), leaving only the temperature differences on the right sides of the equations. Next add the three equations, giving:

$$\frac{q}{h_o A_o} + \frac{qx}{k A_m} + \frac{q}{h_i A_i} = (t_o - t_{os}) + (t_{os} - t_{is}) + (t_{is} - t_i) \quad \dots\dots\dots(3-6)$$

$$= t_o - t_i$$

Alternate expressions for ( $t_o - t_i$ ) are available from Eqs. (3-4) and (3-5):

$$t_o - t_i = \frac{q}{U_o A_o} = \frac{q}{U_i A_i} \quad \dots\dots\dots(3-7)$$

Equating Eqs. (3-6) and (3-7) and canceling q provides an expression for computing the U values:

$$\frac{1}{U_o A_o} = \frac{1}{U_i A_i} = \frac{1}{h_o A_o} + \frac{x}{k A_m} + \frac{1}{h_i A_i} \quad \dots\dots\dots(3-8)$$

The physical interpretation of the terms in Eq. (3-8) is that  $1/U_o A_o$  and  $1/U_i A_i$  are

the total resistances to heat transfer between the refrigerant and water.

This total

resistance is the sum of the individual resistances

1. From the refrigerant to the outside surface of the tube  $1/h_o A_o$

2. Through the tube  $x/(k A_m)$

3. From the inside surface of the tube to the water  $1/h_i A_i$

### 3.2 Liquid in tubes; heat transfer and pressure drop

The expression for the heat transfer coefficient for fluids flowing inside tubes,

$$Nu = C Re^n Pr^m \dots\dots\dots(3-9)$$

where  $n$  and  $m$  are exponents. The constant  $C$  and exponents in the equation are

$$\frac{hD}{k} = 0.023 \left( \frac{VD\rho}{\mu} \right)^{0.8} \left( \frac{c_p \mu}{k} \right)^{0.4} \dots\dots\dots(3-10)$$

where  $h$  = convection coefficient,  $W/m^2 \cdot K$

$D$  = ID of tube, m

$k$  = thermal conductivity of fluid,  $W/m \cdot K$

$V$  = mean velocity of fluid, m/s

$\rho$  = density of fluid,  $kg/m^3$

$\mu$  = viscosity of fluid,  $Pa \cdot s$

$c_p$  = specific heat of fluid,  $J/kg \cdot K$

Equation (3-9) is applicable to turbulent flow, which typically prevails with the velocities and fluid properties experienced in most commercial evaporators and condenser [7].

### 3.3 Pressure Drop across Tubes

As the fluid flows inside the tubes through a condenser, a pressure drop occurs both in the straight tubes and in the U-bends or heads of the heat exchanger. Some drop in pressure is also attributable to entrance and exit losses. The expression for pressure drop of fluid flowing in straight tubes [7],

$$\Delta p = f \frac{L}{D} \frac{V^2}{2} \rho \quad \dots\dots\dots(3-11)$$

where  $\Delta p$  = pressure drop, Pa  
 $f$  = friction factor, dimensionless  
 $L$  = length of tube, m

The values suggested below can be used as a general guide, and will normally give designs that are near the optimum[8]:

#### *Liquids*

Viscosity	<1 mN s/m <sup>2</sup>	35 kN/m <sup>2</sup>
	1 to 10 mN s/m <sup>2</sup>	50–70 kN/m <sup>2</sup>

### 3.4 Required condensing capacity

The required rate of heat transfer in the condenser is predominately a function of the refrigerating capacity and the temperatures of evaporation and condensation. The condenser must reject both the energy absorbed by the evaporator and the heat of compression added by the compressor. A term often used to relate the rate of heat flow at the condenser to that of the evaporator is the heat-rejection ratio [7],

$$\text{Heat-rejection ratio} = \frac{\text{rate of heat rejected at condenser, kW}}{\text{rate of heat absorbed at evaporator, kW}} \quad \dots\dots(3-12)$$



A graph of typical values of heat-rejection ratios is shown in Fig. (A-1) in Appendix (A).

### 3.5 Condensing heat transfer coefficient across shell

The basic equation for calculating the local coefficient of heat transfer of vapor condensing on a vertical plate was developed by Nusselt [9] by pure physical analysis. The equation for the local condensing coefficient is,

$$\frac{h_{cv}x}{k} = \left( \frac{g\rho^2 h_{fg} x^3}{4\mu k \Delta t} \right)^{1/4} \dots\dots\dots(3-13)$$

where  $h_{cv}$  = local condensing coefficient on vertical plate,  $W/m^2 \cdot K$   
 $x$  = vertical distance measured from top of plate, m  
 $g$  = acceleration due to gravity =  $9.81 \text{ m/s}^2$   
 $\rho$  = density of condensate,  $kg/m^3$   
 $h_{fg}$  = latent heat of vaporization,  $J/kg$   
 $\mu$  = viscosity of condensate,  $Pa \cdot s$   
 $\Delta t$  = temperature difference between vapor and the plate,  $K$

The equation for the mean condensing coefficient for vapor condensing on the outside of horizontal tubes is,

$$h_{ct} = 0.725 \left( \frac{g\rho^2 h_{fg} k^3}{\mu \Delta t ND} \right)^{1/4} \text{ W/m}^2 \cdot K \dots\dots\dots(3-14)$$

where  $N$  = number of tubes in vertical row  
 $D$  = OD of tube, m

### 3.6 Pressure Drop across Shell

calculate the shell-side pressure drop from [10]:

$$\Delta P_s = 8. \tau \left( \frac{D_s}{d_e} \right) \left( \frac{L}{l_B} \right) \frac{\rho u_s^2}{2} \dots\dots\dots(3-15)$$

where  $L$  = tube length,  
 $l_B$  = baffle spacing.

$F$  = friction factor from figure (A-2)

The parameters in the equation can be calculated as follows:  
the area for cross-flow  $A_s$  for the hypothetical row of tubes at the shell equator, given by:

$$A_s = \frac{(p_t - d_o)D_s l_B}{p_t} \dots\dots\dots(3-16)$$

where  $p_t$  = tube pitch,  
 $d_o$  = tube outside diameter,  
 $D_s$  = shell inside diameter, m,  
 $l_B$  = baffle spacing, m.

An estimate of the shell diameter  $D_s$  can be obtained from equation (3-17), which is an empirical equation based on standard tube layouts:

$$D_b = d_o \left( \frac{N_t}{K_1} \right)^{1/n_1} \dots\dots\dots(3-17)$$

where  $N_t$  = number of tubes,

$d_o$  = tube outside diameter, mm.

Table 3-1. Constants for use in equation 3-17

Triangular pitch, $p_t = 1.25d_o$					
No. passes	1	2	4	6	8
$K_1$	0.319	0.249	0.175	0.0743	0.0365
$n_1$	2.142	2.207	2.285	2.499	2.675

Calculate the shell-side mass velocity  $G_s$  and the linear velocity  $u_s$ :

$$G_s = \frac{W_s}{A_s}$$

$$u_s = \frac{G_s}{\rho} \dots\dots\dots(3-17)$$

where  $W_s$  = fluid flow-rate on the shell-side, kg/s,  
 $\rho$  = shell-side fluid density, kg/m<sup>3</sup>.

Calculate the shell-side equivalent diameter (hydraulic diameter), for triangular pitch arrangement:

$$d_e = \frac{4 \left( \frac{p_t}{2} \times 0.87 p_t - \frac{1}{2} \pi \frac{d_o^2}{4} \right)}{\frac{\pi d_o}{2}} = \frac{1.10}{d_o} (p_t^2 - 0.917 d_o^2) \dots\dots\dots(3-18)$$

Calculate the shell-side Reynolds number, given by:

$$Re = \frac{G_s d_e}{\mu} = \frac{u_s d_e \rho}{\mu} \dots\dots\dots(3-19)$$

## CHAPTER FOUR

### Design Calculation

#### 4.1 Design Procedure

Designing the optimal heat exchanger for a given application involves determining the temperature change of the fluids, the heat transfer coefficient, and the construction of the heat exchanger and relating them to the rate of heat transfer. The following steps were done to design the heat exchanger (condenser):

1. Shell and tube heat exchanger was chosen due to its wide range of application, especially in chiller system.
2. Assume the number of pipes with one pass.
3. Tube diameters in the range 5/8 in. (16 mm) to 2 in. (50 mm) are used. The smaller diameters 5/8 to 1 in. (16 to 25 mm) are preferred for most duties, as they will give more compact, and therefore cheaper, exchangers.
4. The tubes in an exchanger are usually arranged in an equilateral triangular, square, or rotated square pattern. The triangular and rotated square patterns give higher heat-transfer rates. The space between the tubes in triangular arranged can be calculated from  $p_t = 1.25 \times d_o$ .
5. Select the coolant temperatures and calculate an overall logarithmic mean temperature difference.
6. Assume the temperature difference between the tube surface and the R22 is 5 °C. Estimate an overall coefficient from the inside and outside heat transfer coefficients.
7. Calculate the area.

8. Calculate the tube length, shell size, and baffling.
9. The most commonly used type of baffle is the single segmental baffle. The baffle cut is the height of the segment removed to form the baffle, expressed as a percentage of the baffle disc diameter. Baffle cuts from 15 to 45 percent are used. Generally, a baffle cut of 20 to 25 percent will be the optimum, giving good heat-transfer rates, without excessive drop. In this design 20% cutting percent is used, the space between baffles calculated as  $LB = 0.5 D_s$
10. The shell size calculated from  $D_s = D_b + 6 \text{ mm}$
11. Steps 1 to 10 result in a guessed design. Therefore a primary calculation was done by hand then a computer program (Microsoft Excel ) is used to make several trials to obtain a final design.
12. The previous steps were repeated with two pass tubes.

Tables (4-1) to (4-5) show the trials results for one pass tubes heat exchanger

Tables (4-7) to (4-11) show the trials results for two pass tubes heat exchanger



## 4.2 Calculations

### Data

$$TR = 12 \text{ TON}$$

$$QE = 12 * 3.516 = 42.192 \text{ KW}$$

$$T_E = 5^\circ\text{C}$$

$$D_i = 14 \text{ mm}$$

$$D_o = 16 \text{ mm}$$

$$K=25 \text{ tube , one pass}$$

$$H. r. r = 1.29 \text{ from fig. (A-1)}$$

$$H. r. r = \frac{Q_C}{Q_E} \rightarrow 1.29 = \frac{Q_C}{42.192} \rightarrow Q_C = 54.42 \text{ KW}$$

$$LMTD = \frac{(T_C - T_i) - (T_c - T_o)}{LN \frac{T_C - T_i}{T_C - T_o}}$$

$$LMTD = \frac{(50 - 25) - (50 - 33)}{LN \frac{50 - 25}{50 - 33}} = 20.743^\circ\text{C}$$

$$\left[ \frac{1}{U_o * A_o} = \frac{1}{h_o * A_o} + \frac{X}{K * A_m} + \frac{1}{h_i * A_i} \right] * A_o$$

$$\frac{1}{U_o} = \frac{1}{h_o} + \left( \frac{X}{K} * \frac{A_o}{A_m} \right) + \left( \frac{1}{h_i} * \frac{A_o}{A_i} \right)$$

$$\frac{A_o}{A_i} = \frac{\pi \cancel{D_o} L}{\pi \cancel{D_i} L} = \frac{\cancel{D_o}}{\cancel{D_i}} = \frac{16}{14} = 1.142$$

$$D_m = \frac{D_o + D_i}{2} = \frac{16 + 14}{2} = 15 \text{ mm}$$

$$\frac{A_o}{A_m} = \frac{\pi \cancel{D_o} L}{\pi \cancel{D_m} L} = \frac{\cancel{D_o}}{\cancel{D_m}} = \frac{16}{15} = 1.066$$

$$X = \frac{D_o - D_i}{2} = \frac{16 - 14}{2} = 1 \text{ mm}$$

### Properties ( $R_{22}$ ) AT 50 From Table (B - 1)

$$\rho = 1082.3 \text{ Kg/m}^3$$

$$h_f = 263.25 \text{ kg/kg}$$

$$h_g = 417.44 \text{ kg/kg}$$

$$h_{fg} = h_g - h_f$$

$$h_{fg} = 417.44 - 263.25 = 154.19 * 10^3 \text{ j/kg}$$

$$K = 72.3 * 10^{-3} \text{ W/M}^2 * \text{K}$$

$$\mu = 123.1 * 10^{-6} \text{ Pa.S}$$

$$N = \frac{\text{Number of tubes}}{\text{Number of columns}} = \frac{25}{9} = 2.77$$

$$h_o = 0.725 \left( \frac{g * \rho^2 * h_{fg} * k^3}{\mu * \Delta t * N * D_o} \right)^{\frac{1}{4}}$$

$$h_o = 0.725 \left( \frac{9.81 * 1082.3^2 * 154.19 * 10^3 * (72.3 * 10^{-3})^3}{123.1 * 10^{-6} * 5 * 2.77 * 0.016} \right)^{\frac{1}{4}}$$

$$h_o = 1614.933 \text{ W/M}^2 * \text{K}$$

$$Q_c = Q_w$$

$$54.42 = \dot{m}_w * C_p * \Delta t$$

$$54.42 = \dot{m}_w * 4.181 * (33 - 25)$$

$$\dot{m}_w = 1.62 \text{ Kg/s}$$

$$\dot{m}_{tube} = \frac{1.62}{25} = 0.065 \text{ Kg/s}$$

$$\dot{m} = \rho * V * A$$

$$1.62 = 996 * V * \frac{\pi}{4} D^2$$

$$1.62 = 996 * V * \frac{\pi}{4} (0.014)^2 \rightarrow V = 0.424 \text{ m/s}$$

$$R_e = \frac{\rho * V * D}{\mu} = \frac{996 * 0.42 * 0.014}{843.75 * 10^{-6}} = 7007 \text{ Turbulent}$$

$$R_e = \frac{C_p * \mu}{K} = \frac{4181 * 843.75 * 10^{-6}}{611.35 * 10^{-3}} = 5.77$$

$$\frac{h_i * A_i}{K} = N_U = 0.023 * (Re)^{0.8} * (Pr)^{0.4}$$

$$\frac{h_i * 0.014}{611.35 * 10^{-3}} = 0.023 * (7007)^{0.8} * (5.77)^{0.4}$$

$$h_i = 2414.26 \text{ W/M}^2 * \text{K}$$

$$\frac{1}{U_o} = \frac{1}{1614.933} + \left( \frac{0.001}{390} * 1.066 \right) + \left( \frac{1}{2414.26} * 1.142 \right) + (0.000179 * 1.142)$$

$$= 6.192 * 10^{-4} + 2.73 * 10^{-6} + 4.73 * 10^{-4} + 2 * 10^{-4}$$

$$\frac{1}{U_o} = 1.295 * 10^{-3} \rightarrow U_o = 771.65 \text{ W/M}^2 * \text{K}$$

$$Q_c = U_o * A_o * LMTD$$

$$54.42 = 771.65 * A_o * 20.743$$

$$A_o = 3.4 \text{ M}^2$$

$$A_o = K * \pi * D_o * L$$

$$3.4 = 26 * 3.14 * 0.016 * L$$

$$L = 2.7 \text{ m}$$

$$\frac{E}{D} = \frac{0.001}{14} = 0.00007$$

FROM MOODY CHART (A - 3)

$$F = 0.035$$

$$\Delta P = F \frac{V^2}{2} * \frac{L}{D} * \rho$$

$$\Delta P = 0.035 \frac{0.424^2}{2} * \frac{2.7}{0.014} * 996$$



$$\Delta P = 604.3 P_a$$

$$\Delta P = 0.604 \text{ kPa} < 70 \text{ kPa}$$

Table (4-1): Design calculation for one pass pipes, First trial

NO. OF TUPES	NO. OF COLUMNS	N	$\Delta T$ (°C)	$h_o$ (W/m <sup>2</sup> .k)	$m$ (water) (kg/s)	$m$ (tube) (kg/s)	$V$ (water) (m/s)	Re	pr	$h_i$ (W/m <sup>2</sup> .k)	$1/U_o$	$U_o$ (W/m <sup>2</sup> .k)	$A_o$ (m <sup>2</sup> )	L (m)	$\Delta P$ (kpa)	$T_s$ TUBE SURFACE (trail)
10	5	2	5	1751.02	1.63	0.16	1.06	17540.75	5.34	5274.07	0.000963	1037.95	2.53	5.03	7.06	37.70
11	5	2	5	1709.79	1.63	0.15	0.97	15946.14	5.34	4886.88	0.000992	1007.83	2.60	4.71	5.46	37.77
12	5	2	5	1673.00	1.63	0.14	0.88	14617.29	5.34	4558.28	0.001020	980.55	2.68	4.44	4.33	37.84
13	7	2	5	1783.76	1.63	0.13	0.82	13492.89	5.34	4275.55	0.000997	1002.78	2.62	4.01	3.33	38.34
14	7	2	5	1751.02	1.63	0.12	0.76	12529.11	5.34	4029.43	0.001022	978.47	2.68	3.81	2.73	38.41
15	7	2	5	1721.07	1.63	0.11	0.71	11693.84	5.34	3813.06	0.001046	956.01	2.74	3.64	2.27	38.48
16	7	2	5	1693.53	1.63	0.10	0.66	10962.97	5.34	3621.18	0.001069	935.13	2.81	3.49	1.91	38.55
17	7	2	5	1668.06	1.63	0.10	0.62	10318.09	5.34	3449.75	0.001092	915.66	2.87	3.35	1.63	38.61
18	9	2	5	1751.02	1.63	0.09	0.59	9744.86	5.34	3295.55	0.001077	928.28	2.83	3.13	1.35	39.00
19	9	2	5	1727.51	1.63	0.09	0.56	9231.98	5.34	3156.05	0.001098	910.37	2.88	3.02	1.17	39.07
20	9	2	5	1705.50	1.63	0.08	0.53	8770.38	5.34	3029.16	0.001119	893.50	2.94	2.92	1.03	39.13
21	9	2	5	1684.82	1.63	0.08	0.51	8352.74	5.34	2913.20	0.001140	877.56	2.99	2.83	0.90	39.20
22	9	2	5	1665.34	1.63	0.07	0.48	7973.07	5.34	2806.78	0.001159	862.45	3.04	2.75	0.80	39.26
23	9	3	5	1646.94	1.63	0.07	0.46	7626.41	5.34	2708.72	0.001179	848.11	3.09	2.68	0.71	39.32
24	11	2	5	1713.34	1.63	0.07	0.44	7308.65	5.34	2618.05	0.001168	855.91	3.07	2.54	0.62	39.64
25	11	2	5	1695.94	1.63	0.07	0.42	7016.30	5.34	2533.93	0.001187	842.45	3.11	2.48	0.56	39.70
26	11	2	5	1679.40	1.63	0.06	0.41	6746.44	5.34	2455.66	0.001205	829.60	3.16	2.42	0.50	39.75
27	11	2	5	1663.62	1.63	0.06	0.39	6496.58	5.34	2382.62	0.001224	817.31	3.21	2.37	0.46	39.81
28	11	3	5	1648.57	1.63	0.06	0.38	6264.55	5.34	2314.30	0.001241	805.53	3.26	2.32	0.41	39.86

**Table (4-2): Design calculation for one pass pipes, Second trial**

NO. OF TUPES	NO. OF COLUMNS	N	ΔT (°C)	h <sub>o</sub> (W/m <sup>2</sup> .k)	m (water) (kg/s)	m (tube) (kg/s)	V (water) (m/s)	Re	pr	h <sub>i</sub> (W/m <sup>2</sup> .k)	1/U <sub>o</sub>	U <sub>o</sub> (W/m <sup>2</sup> .k)	A <sub>o</sub> (m <sup>2</sup> )	L (m)	ΔP (kpa)	T <sub>s</sub> TUBE SURFACE (trail)
10	5	2	12.3	1398.28	1.63	0.16	1.06	17540.75	5.34	5274.07	0.0011075	902.93	2.91	5.78	8.12	36.61
11	5	2.2	12.2	1367.27	1.63	0.15	0.97	15946.14	5.34	4886.88	0.0011387	878.16	2.99	5.41	6.27	36.68
12	5	2.4	12.2	1339.76	1.63	0.14	0.88	14617.29	5.34	4558.28	0.0011685	855.79	3.07	5.08	4.96	36.75
13	7	1.86	11.7	1443.43	1.63	0.13	0.82	13492.89	5.34	4275.55	0.0011294	885.41	2.96	4.54	3.77	37.28
14	7	2	11.6	1419.06	1.63	0.12	0.76	12529.11	5.34	4029.43	0.0011556	865.35	3.03	4.31	3.09	37.35
15	7	2.14	11.5	1396.88	1.63	0.11	0.71	11693.84	5.34	3813.06	0.0011809	846.83	3.10	4.11	2.56	37.42
16	7	2.29	11.5	1376.57	1.63	0.10	0.66	10962.97	5.34	3621.18	0.0012053	829.65	3.16	3.93	2.16	37.50
17	7	2.43	11.4	1357.86	1.63	0.10	0.62	10318.09	5.34	3449.75	0.0012291	813.63	3.22	3.78	1.83	37.57
18	9	2	11	1437.87	1.63	0.09	0.59	9744.86	5.34	3295.55	0.0012016	832.19	3.15	3.49	1.51	37.99
19	9	2.11	10.9	1420.68	1.63	0.09	0.56	9231.98	5.34	3156.05	0.0012235	817.35	3.21	3.36	1.31	38.07
20	9	2.22	10.9	1404.64	1.63	0.08	0.53	8770.38	5.34	3029.16	0.0012448	803.35	3.27	3.25	1.14	38.14
21	9	2.33	10.8	1389.63	1.63	0.08	0.51	8352.74	5.34	2913.20	0.0012656	790.13	3.32	3.15	1.00	38.21
22	9	2.44	10.7	1375.53	1.63	0.07	0.48	7973.07	5.34	2806.78	0.001286	777.60	3.37	3.05	0.89	38.27
23	9	2.56	10.7	1362.25	1.63	0.07	0.46	7626.41	5.34	2708.72	0.001306	765.70	3.43	2.97	0.79	38.34
24	11	2.18	10.4	1427.98	1.63	0.07	0.44	7308.65	5.34	2618.05	0.001285	778.22	3.37	2.80	0.68	38.70
25	11	2.27	10.3	1415.48	1.63	0.07	0.42	7016.30	5.34	2533.93	0.0013038	766.96	3.42	2.72	0.61	38.76
26	11	2.36	10.2	1403.62	1.63	0.06	0.41	6746.44	5.34	2455.66	0.0013224	756.20	3.47	2.66	0.55	38.82
27	11	2.45	10.2	1392.35	1.63	0.06	0.39	6496.58	5.34	2382.62	0.0013406	745.91	3.52	2.59	0.50	38.89
28	11	2.55	10.1	1381.62	1.63	0.06	0.38	6264.55	5.34	2314.30	0.0013586	736.04	3.56	2.53	0.45	38.95

**Table (4-3): Design calculation for one pass pipes, Third trial**

NO. OF TUPES	NO. OF COLUMNS	N	$\Delta T$ (°C)	ho (w/m <sup>2</sup> . k)	m (water) (kg /s)	m (tube) kg/s	V (water) m/s	Re	pr	hi (W/m <sup>2</sup> .k)	1/Uo	Uo (W/m <sup>2</sup> .k)	Ao (m2)	L (m)	$\Delta P$ (kpa)	T s TUBE SURFACE (trail)
10	5	2	13.4	1368.67	1.63	0.16	1.06	17540.75	5.34	5274.07	0.001123	890.49	2.95	5.86	8.23	36.50
11	5	2.2	13.3	1338.25	1.63	0.15	0.97	15946.14	5.34	4886.88	0.0011546	866.10	3.03	5.48	6.36	36.58
12	5	2.4	13.2	1311.25	1.63	0.14	0.88	14617.29	5.34	4558.28	0.0011847	844.07	3.11	5.16	5.02	36.65
13	7	1.86	12.7	1412.29	1.63	0.13	0.82	13492.89	5.34	4275.55	0.0011447	873.60	3.00	4.60	3.82	37.17
14	7	2	12.6	1388.41	1.63	0.12	0.76	12529.11	5.34	4029.43	0.0011712	853.86	3.07	4.37	3.13	37.24
15	7	2.14	12.6	1366.67	1.63	0.11	0.71	11693.84	5.34	3813.06	0.0011967	835.64	3.14	4.17	2.60	37.32
16	7	2.29	12.5	1346.77	1.63	0.10	0.66	10962.97	5.34	3621.18	0.0012214	818.73	3.20	3.99	2.19	37.39
17	7	2.43	12.4	1328.44	1.63	0.10	0.62	10318.09	5.34	3449.75	0.0012454	802.97	3.27	3.83	1.86	37.46
18	9	2	12	1406.66	1.63	0.09	0.59	9744.86	5.34	3295.55	0.0012171	821.64	3.19	3.53	1.53	37.88
19	9	2.11	11.9	1389.85	1.63	0.09	0.56	9231.98	5.34	3156.05	0.0012391	807.05	3.25	3.41	1.32	37.96
20	9	2.22	11.9	1374.17	1.63	0.08	0.53	8770.38	5.34	3029.16	0.0012606	793.29	3.31	3.29	1.15	38.03
21	9	2.33	11.8	1359.50	1.63	0.08	0.51	8352.74	5.34	2913.20	0.0012816	780.30	3.36	3.19	1.01	38.09
22	9	2.44	11.7	1345.72	1.63	0.07	0.48	7973.07	5.34	2806.78	0.0013021	767.99	3.42	3.09	0.90	38.16
23	9	2.56	11.7	1332.76	1.63	0.07	0.46	7626.41	5.34	2708.72	0.0013222	756.30	3.47	3.00	0.80	38.23
24	11	2.18	11.3	1397.25	1.63	0.07	0.44	7308.65	5.34	2618.05	0.0013004	769.00	3.41	2.83	0.69	38.58
25	11	2.27	11.2	1385.06	1.63	0.07	0.42	7016.30	5.34	2533.93	0.0013194	757.94	3.46	2.76	0.62	38.65
26	11	2.36	11.2	1373.51	1.63	0.06	0.41	6746.44	5.34	2455.66	0.001338	747.37	3.51	2.69	0.56	38.71
27	11	2.45	11.1	1362.53	1.63	0.06	0.39	6496.58	5.34	2382.62	0.0013564	737.26	3.56	2.62	0.51	38.78
28	11	2.55	11.1	1352.08	1.63	0.06	0.38	6264.55	5.34	2314.30	0.0013744	727.58	3.61	2.56	0.46	38.84



**Table (4-4): Design calculation for one pass pipes, Forth trial**

NO. OF TUPES	NO. OF COLU MNS	N	$\Delta T$ (°C)	$h_o$ (w/m <sup>2</sup> . k)	m (water) (kg /s)	m (tube) kg/s	V (water) m/s	Re	pr	$h_i$ (W/m <sup>2</sup> .k)	1/U <sub>o</sub>	U <sub>o</sub> (W/m <sup>2</sup> . k)	A <sub>o</sub> (m2)	L (m)	$\Delta P$ (kpa)	T <sub>s</sub> TUBE SURFACE (trail)
10	5	2	13.5	1366.10	1.63	0.16	1.06	17540.75	5.34	5274.07	0.0011243	889.40	2.95	5.87	8.24	36.50
11	5	2.2	13.4	1335.70	1.63	0.15	0.97	15946.14	5.34	4886.88	0.001156	865.03	3.03	5.49	6.37	36.57
12	5	2.4	13.4	1308.72	1.63	0.14	0.88	14617.29	5.34	4558.28	0.0011862	843.02	3.11	5.16	5.03	36.64
13	7	1.86	12.8	1409.33	1.63	0.13	0.82	13492.89	5.34	4275.55	0.0011462	872.47	3.01	4.60	3.82	37.16
14	7	2	12.8	1385.47	1.63	0.12	0.76	12529.11	5.34	4029.43	0.0011727	852.75	3.08	4.37	3.13	37.23
15	7	2.14	12.7	1363.75	1.63	0.11	0.71	11693.84	5.34	3813.06	0.0011983	834.55	3.14	4.17	2.60	37.31
16	7	2.29	12.6	1343.86	1.63	0.10	0.66	10962.97	5.34	3621.18	0.001223	817.66	3.21	3.99	2.19	37.38
17	7	2.43	12.5	1325.55	1.63	0.10	0.62	10318.09	5.34	3449.75	0.001247	801.92	3.27	3.83	1.86	37.45
18	9	2	12.1	1403.43	1.63	0.09	0.59	9744.86	5.34	3295.55	0.0012187	820.54	3.20	3.54	1.53	37.87
19	9	2.11	12	1386.63	1.63	0.09	0.56	9231.98	5.34	3156.05	0.0012408	805.96	3.26	3.41	1.33	37.94
20	9	2.22	12	1370.97	1.63	0.08	0.53	8770.38	5.34	3029.16	0.0012623	792.23	3.31	3.30	1.16	38.01
21	9	2.33	11.9	1356.31	1.63	0.08	0.51	8352.74	5.34	2913.20	0.0012833	779.25	3.37	3.19	1.02	38.08
22	9	2.44	11.8	1342.54	1.63	0.07	0.48	7973.07	5.34	2806.78	0.0013039	766.95	3.42	3.09	0.90	38.15
23	9	2.56	11.8	1329.58	1.63	0.07	0.46	7626.41	5.34	2708.72	0.001324	755.27	3.47	3.01	0.80	38.22
24	11	2.18	11.4	1393.81	1.63	0.07	0.44	7308.65	5.34	2618.05	0.0013022	767.96	3.42	2.83	0.69	38.57
25	11	2.27	11.4	1381.64	1.63	0.07	0.42	7016.30	5.34	2533.93	0.0013212	756.91	3.47	2.76	0.62	38.64
26	11	2.36	11.3	1370.09	1.63	0.06	0.41	6746.44	5.34	2455.66	0.0013398	746.36	3.52	2.69	0.56	38.70
27	11	2.45	11.2	1359.13	1.63	0.06	0.39	6496.58	5.34	2382.62	0.0013582	736.27	3.56	2.63	0.51	38.76
28	11	2.55	11.2	1348.69	1.63	0.06	0.38	6264.55	5.34	2314.30	0.0013763	726.59	3.61	2.57	0.46	38.82

**Table (4-5): Design calculation for one pass pipes, Fifth trial**

NO. OF TUPES	NO. OF COLUMNS	N	$\Delta T$ (°C)	$h_o$ (W/m <sup>2</sup> . k)	m (water) (kg /s)	m (tube) kg/s	V (water) m/s	Re	pr	$h_i$ (W/m <sup>2</sup> .k)	1/U <sub>o</sub>	U <sub>o</sub> (W/m <sup>2</sup> .k)	A <sub>o</sub> (m <sup>2</sup> )	L (m)	$\Delta P$ (kpa)	T <sub>s</sub> TUBE SURFACE (trail)
10	5	2	13.5	1365.87	1.63	0.16	1.06	17540.75	5.34	5274.07	0.0011245	889.31	2.95	5.87	8.24	36.49
11	5	2.2	13.4	1335.48	1.63	0.15	0.97	15946.14	5.34	4886.88	0.0011562	864.94	3.03	5.49	6.37	36.57
12	5	2.4	13.4	1308.50	1.63	0.14	0.88	14617.29	5.34	4558.28	0.0011863	842.92	3.11	5.16	5.03	36.64
13	7	1.86	12.8	1409.05	1.63	0.13	0.82	13492.89	5.34	4275.55	0.0011463	872.36	3.01	4.60	3.82	37.16
14	7	2	12.8	1385.19	1.63	0.12	0.76	12529.11	5.34	4029.43	0.0011728	852.64	3.08	4.37	3.13	37.23
15	7	2.14	12.7	1363.47	1.63	0.11	0.71	11693.84	5.34	3813.06	0.0011984	834.44	3.14	4.17	2.60	37.31
16	7	2.29	12.6	1343.58	1.63	0.10	0.66	10962.97	5.34	3621.18	0.0012232	817.55	3.21	3.99	2.19	37.38
17	7	2.43	12.5	1325.26	1.63	0.10	0.62	10318.09	5.34	3449.75	0.0012472	801.81	3.27	3.83	1.86	37.45
18	9	2	12.1	1403.10	1.63	0.09	0.59	9744.86	5.34	3295.55	0.0012189	820.43	3.20	3.54	1.53	37.87
19	9	2.11	12.1	1386.30	1.63	0.09	0.56	9231.98	5.34	3156.05	0.0012409	805.85	3.26	3.41	1.33	37.94
20	9	2.22	12	1370.63	1.63	0.08	0.53	8770.38	5.34	3029.16	0.0012624	792.11	3.31	3.30	1.16	38.01
21	9	2.33	11.9	1355.97	1.63	0.08	0.51	8352.74	5.34	2913.20	0.0012835	779.13	3.37	3.19	1.02	38.08
22	9	2.44	11.8	1342.20	1.63	0.07	0.48	7973.07	5.34	2806.78	0.0013041	766.84	3.42	3.10	0.90	38.15
23	9	2.56	11.8	1329.24	1.63	0.07	0.46	7626.41	5.34	2708.72	0.0013242	755.16	3.47	3.01	0.80	38.22
24	11	2.18	11.4	1393.43	1.63	0.07	0.44	7308.65	5.34	2618.05	0.0013023	767.84	3.42	2.83	0.69	38.57
25	11	2.27	11.4	1381.25	1.63	0.07	0.42	7016.30	5.34	2533.93	0.0013214	756.80	3.47	2.76	0.62	38.63
26	11	2.36	11.3	1369.71	1.63	0.06	0.41	6746.44	5.34	2455.66	0.00134	746.25	3.52	2.69	0.56	38.70
27	11	2.45	11.2	1358.74	1.63	0.06	0.39	6496.58	5.34	2382.62	0.0013584	736.15	3.56	2.63	0.51	38.76
28	11	2.55	11.2	1348.30	1.63	0.06	0.38	6264.55	5.34	2314.30	0.0013765	726.48	3.61	2.57	0.46	38.82

Table (4-6): Design calculation for shell side in one pass tubes heat exchanger

No. of tubes	D (bundle) m	D (shell) m	L <sub>b</sub> (m)	As (m <sup>2</sup> )	Gs (kg/m <sup>2</sup> .s)	u <sub>s</sub> (m/s)	de (m)	Re	f	(P <sub>1</sub> -P <sub>2</sub> ) pa
10	0.08	0.09	0.04	0.000738	186.96	0.17	0.01	17267.96	0.06	6.83
11	0.084	0.09	0.04	0.000802	172.08	0.16	0.01	15894.11	0.06	5.47
12	0.087	0.09	0.05	0.000865	159.50	0.15	0.01	14732.37	0.06	4.46
13	0.09	0.1	0.05	0.000928	148.72	0.14	0.01	13736.39	0.06	3.49
14	0.094	0.1	0.05	0.00099	139.37	0.13	0.01	12872.51	0.06	2.94
15	0.097	0.1	0.05	0.001052	131.17	0.12	0.01	12115.68	0.06	2.55
16	0.1	0.11	0.05	0.001114	123.93	0.11	0.01	11446.87	0.06	2.20
17	0.102	0.11	0.05	0.001175	117.48	0.11	0.01	10851.32	0.06	1.91
18	0.105	0.11	0.06	0.001235	111.70	0.10	0.01	10317.43	0.06	1.62
19	0.108	0.11	0.06	0.001296	106.49	0.10	0.01	9835.96	0.06	1.43
20	0.11	0.12	0.06	0.001356	101.76	0.09	0.01	9399.42	0.06	1.27
21	0.113	0.12	0.06	0.001416	97.46	0.09	0.01	9001.71	0.06	1.14
22	0.115	0.12	0.06	0.001476	93.52	0.09	0.01	8637.78	0.06	1.03
23	0.118	0.12	0.06	0.001535	89.90	0.08	0.01	8303.45	0.06	0.93
24	0.12	0.13	0.06	0.001594	86.56	0.08	0.01	7995.18	0.06	0.82
25	0.123	0.13	0.06	0.001653	83.47	0.08	0.01	7710.00	0.06	0.75
26	0.125	0.13	0.07	0.001712	80.61	0.07	0.01	7445.36	0.06	0.69
27	0.127	0.13	0.07	0.001771	77.94	0.07	0.01	7199.10	0.06	0.64
28	0.129	0.14	0.07	0.001829	75.45	0.07	0.01	6969.32	0.07	0.59



**Table (4-7): Design calculation for two pass pipes, First trial**

NO. OF TUPES	NO. OF COLUMNS	N	$\Delta T$ (°C)	$h_o$ (W/m <sup>2</sup> . k)	m (water) (kg /s)	m (tube) kg/s	V (water) m/s	Re	pr	$h_i$ (W/m <sup>2</sup> .k)	1/U <sub>o</sub>	U <sub>o</sub> (W/m <sup>2</sup> .k)	A <sub>o</sub> (m <sup>2</sup> )	L (m)	$\Delta P$ (kpa)	T s TUBE SURFACE (trail)
20	9	2.22	5	1705.50	1.63	0.08	0.53	8770.38	5.34	3029.16	0.00112	893.50	2.94	2.92	1.03	39.13
22	9	2.44	5	1665.34	1.63	0.07	0.48	7973.07	5.34	2806.78	0.00116	862.45	3.04	2.75	0.80	39.26
24	9	2.67	5	1629.51	1.63	0.07	0.44	7308.65	5.34	2618.05	0.0012	834.46	3.14	2.61	0.64	39.38
26	11	2.36	5	1679.40	1.63	0.06	0.41	6746.44	5.34	2455.66	0.00121	829.60	3.16	2.42	0.50	39.75
28	11	2.55	5	1648.57	1.63	0.06	0.38	6264.55	5.34	2314.30	0.00124	805.53	3.26	2.32	0.41	39.86
30	13	2.31	5	1689.48	1.63	0.05	0.35	5846.92	5.34	2190.03	0.00125	799.21	3.28	2.18	0.34	40.19
32	13	2.46	5	1662.44	1.63	0.05	0.33	5481.49	5.34	2079.82	0.00129	778.17	3.37	2.10	0.29	40.29
34	13	2.62	5	1637.44	1.63	0.05	0.31	5159.05	5.34	1981.36	0.00132	758.64	3.46	2.02	0.25	40.39
36	13	2.77	5	1614.20	1.63	0.05	0.29	4872.43	5.34	1892.80	0.00135	740.44	3.54	1.96	0.21	40.49
38	13	2.92	5	1592.53	1.63	0.04	0.28	4615.99	5.34	1812.67	0.00138	723.41	3.63	1.90	0.18	40.58
40	13	3.08	5	1572.24	1.63	0.04	0.27	4385.19	5.34	1739.80	0.00141	707.44	3.71	1.85	0.16	40.67
42	13	3.23	5	1553.18	1.63	0.04	0.25	4176.37	5.34	1673.20	0.00144	692.41	3.79	1.80	0.14	40.75
44	13	3.38	5	1535.22	1.63	0.04	0.24	3986.53	5.34	1612.07	0.00147	678.23	3.87	1.75	0.13	40.84
46	13	3.54	5	1518.25	1.63	0.04	0.23	3813.21	5.34	1555.75	0.0015	664.82	3.95	1.71	0.11	40.92
48	13	3.69	5	1502.19	1.63	0.03	0.22	3654.32	5.34	1503.67	0.00153	652.12	4.02	1.67	0.10	41.00
50	13	3.85	5	1486.93	1.63	0.03	0.21	3508.15	5.34	1455.36	0.00156	640.05	4.10	1.63	0.09	41.07
52	13	4.00	5	1472.42	1.63	0.03	0.20	3373.22	5.34	1410.40	0.00159	628.58	4.17	1.60	0.08	41.14
54	13	4.15	5	1458.60	1.63	0.03	0.20	3248.29	5.34	1368.46	0.00162	617.64	4.25	1.57	0.08	41.22
56	13	4.31	5	1445.40	1.63	0.03	0.19	3132.28	5.34	1329.22	0.00165	607.20	4.32	1.54	0.07	41.29



**Table (4-8): Design calculation for two pass pipes, Second trial**

NO. OF TUPES	NO. OF COLUMNS	N	$\Delta T$ (°C)	$h_o$ (W/m <sup>2</sup> . k)	$m$ (water) (kg /s)	$m$ (tube) kg/s	$V$ (water) m/s	Re	pr	$h_i$ (W/m <sup>2</sup> .k)	$1/U_o$	$U_o$ (W/m <sup>2</sup> .k)	$A_o$ (m <sup>2</sup> )	L (m)	$\Delta P$ (kpa)	$T_s$ TUBE SURFACE (trail)
20	9	2.22	10.87	1404.64	1.63	0.08	0.53	8770.38	5.34	3029.16	0.00124	803.35	3.27	3.25	1.14	38.14
22	9	2.44	10.74	1375.53	1.63	0.07	0.48	7973.07	5.34	2806.78	0.00129	777.60	3.37	3.05	0.89	38.27
24	9	2.67	10.62	1349.72	1.63	0.07	0.44	7308.65	5.34	2618.05	0.00133	754.38	3.48	2.88	0.70	38.41
26	11	2.36	10.25	1403.62	1.63	0.06	0.41	6746.44	5.34	2455.66	0.00132	756.20	3.47	2.66	0.55	38.82
28	11	2.55	10.14	1381.62	1.63	0.06	0.38	6264.55	5.34	2314.30	0.00136	736.04	3.56	2.53	0.45	38.95
30	13	2.31	9.81	1427.42	1.63	0.05	0.35	5846.92	5.34	2190.03	0.00136	735.34	3.57	2.37	0.37	39.31
32	13	2.46	9.71	1408.28	1.63	0.05	0.33	5481.49	5.34	2079.82	0.00139	717.55	3.66	2.27	0.31	39.43
34	13	2.62	9.61	1390.66	1.63	0.05	0.31	5159.05	5.34	1981.36	0.00143	701.01	3.74	2.19	0.27	39.54
36	13	2.77	9.51	1374.36	1.63	0.05	0.29	4872.43	5.34	1892.80	0.00146	685.56	3.83	2.12	0.23	39.65
38	13	2.92	9.42	1359.21	1.63	0.04	0.28	4615.99	5.34	1812.67	0.00149	671.09	3.91	2.05	0.20	39.76
40	13	3.08	9.33	1345.09	1.63	0.04	0.27	4385.19	5.34	1739.80	0.00152	657.48	3.99	1.99	0.17	39.86
42	13	3.23	9.25	1331.87	1.63	0.04	0.25	4176.37	5.34	1673.20	0.00155	644.66	4.07	1.93	0.15	39.96
44	13	3.38	9.16	1319.45	1.63	0.04	0.24	3986.53	5.34	1612.07	0.00158	632.53	4.15	1.88	0.14	40.06
46	13	3.54	9.08	1307.76	1.63	0.04	0.23	3813.21	5.34	1555.75	0.00161	621.05	4.22	1.83	0.12	40.15
48	13	3.69	9.00	1296.72	1.63	0.03	0.22	3654.32	5.34	1503.67	0.00164	610.15	4.30	1.78	0.11	40.24
50	13	3.85	8.93	1286.28	1.63	0.03	0.21	3508.15	5.34	1455.36	0.00167	599.78	4.37	1.74	0.10	40.33
52	13	4.00	8.86	1276.37	1.63	0.03	0.20	3373.22	5.34	1410.40	0.0017	589.89	4.45	1.70	0.09	40.41
54	13	4.15	8.78	1266.95	1.63	0.03	0.20	3248.29	5.34	1368.46	0.00172	580.46	4.52	1.67	0.08	40.50
56	13	4.31	8.71	1257.98	1.63	0.03	0.19	3132.28	5.34	1329.22	0.00175	571.44	4.59	1.63	0.07	40.58

**Table (4-9): Design calculation for two pass pipes, Third trial**

NO. OF TUPES	NO. OF COLUMNS	N	$\Delta T$ (°C)	$h_o$ (W/m <sup>2</sup> .k)	$m$ (water) (kg/s)	$m$ (tube) (kg/s)	$V$ (water) (m/s)	Re	pr	$h_i$ (W/m <sup>2</sup> .k)	$1/U_o$	$U_o$ (W/m <sup>2</sup> .k)	$A_o$ (m <sup>2</sup> )	L (m)	$\Delta P$ (kpa)	$T_s$ TUBE SURFACE (trail)
20	9	2.22	11.86	1374.17	1.63	0.08	0.53	8770.38	5.34	3029.16	0.00126	793.29	3.31	3.29	1.15	38.03
22	9	2.44	11.73	1345.72	1.63	0.07	0.48	7973.07	5.34	2806.78	0.0013	767.99	3.42	3.09	0.90	38.16
24	9	2.67	11.59	1320.52	1.63	0.07	0.44	7308.65	5.34	2618.05	0.00134	745.17	3.52	2.92	0.71	38.29
26	11	2.36	11.18	1373.51	1.63	0.06	0.41	6746.44	5.34	2455.66	0.00134	747.37	3.51	2.69	0.56	38.71
28	11	2.55	11.05	1352.08	1.63	0.06	0.38	6264.55	5.34	2314.30	0.00137	727.58	3.61	2.56	0.46	38.84
30	13	2.31	10.69	1340.16	1.63	0.05	0.35	5846.92	5.34	2190.03	0.00141	711.48	3.69	2.45	0.38	38.99
32	13	2.46	10.57	1378.73	1.63	0.05	0.33	5481.49	5.34	2079.82	0.00141	709.80	3.70	2.30	0.32	39.32
34	13	2.62	10.46	1361.64	1.63	0.05	0.31	5159.05	5.34	1981.36	0.00144	693.56	3.78	2.21	0.27	39.43
36	13	2.77	10.35	1345.85	1.63	0.05	0.29	4872.43	5.34	1892.80	0.00147	678.39	3.87	2.14	0.23	39.54
38	13	2.92	10.24	1331.19	1.63	0.04	0.28	4615.99	5.34	1812.67	0.00151	664.18	3.95	2.07	0.20	39.65
40	13	3.08	10.14	1317.53	1.63	0.04	0.27	4385.19	5.34	1739.80	0.00154	650.83	4.03	2.01	0.18	39.75
42	13	3.23	10.04	1304.76	1.63	0.04	0.25	4176.37	5.34	1673.20	0.00157	638.24	4.11	1.95	0.15	39.85
44	13	3.38	9.94	1292.77	1.63	0.04	0.24	3986.53	5.34	1612.07	0.0016	626.34	4.19	1.89	0.14	39.95
46	13	3.54	9.85	1281.50	1.63	0.04	0.23	3813.21	5.34	1555.75	0.00163	615.07	4.27	1.85	0.12	40.04
48	13	3.69	9.76	1270.87	1.63	0.03	0.22	3654.32	5.34	1503.67	0.00165	604.36	4.34	1.80	0.11	40.14
50	13	3.85	9.67	1260.82	1.63	0.03	0.21	3508.15	5.34	1455.36	0.00168	594.18	4.42	1.76	0.10	40.22
52	13	4.00	9.59	1251.29	1.63	0.03	0.20	3373.22	5.34	1410.40	0.00171	584.48	4.49	1.72	0.09	40.31
54	13	4.15	9.50	1242.25	1.63	0.03	0.20	3248.29	5.34	1368.46	0.00174	575.22	4.56	1.68	0.08	40.40
56	13	4.31	9.42	1233.64	1.63	0.03	0.19	3132.28	5.34	1329.22	0.00177	566.36	4.63	1.65	0.07	40.48

**Table (4-10): Design calculation for two pass pipes, Forth trial**

NO. OF TUPES	NO. OF COLUMNS	N	$\Delta T$ (°C)	$h_o$ (W/m <sup>2</sup> .k)	$m$ (water) (kg/s)	$m$ (tube) kg/s	$V$ (water) m/s	Re	pr	$h_i$ (W/m <sup>2</sup> .k)	$1/U_o$	$U_o$ (W/m <sup>2</sup> .k)	$A_o$ (m <sup>2</sup> )	L (m)	$\Delta P$ (kpa)	$T_s$ TUBE SURFACE (trail)
20	9	2.22	11.97	1370.97	1.63	0.08	0.53	8770.38	5.34	3029.16	0.00126	792.23	3.31	3.30	1.16	38.01
22	9	2.44	11.84	1342.54	1.63	0.07	0.48	7973.07	5.34	2806.78	0.0013	766.95	3.42	3.09	0.90	38.15
24	9	2.67	11.71	1317.35	1.63	0.07	0.44	7308.65	5.34	2618.05	0.00134	744.16	3.53	2.92	0.71	38.28
26	11	2.36	11.29	1370.09	1.63	0.06	0.41	6746.44	5.34	2455.66	0.00134	746.36	3.52	2.69	0.56	38.70
28	11	2.55	11.16	1348.69	1.63	0.06	0.38	6264.55	5.34	2314.30	0.00138	726.59	3.61	2.57	0.46	38.82
30	13	2.31	11.01	1330.12	1.63	0.05	0.35	5846.92	5.34	2190.03	0.00141	708.64	3.70	2.46	0.38	38.95
32	13	2.46	10.68	1375.17	1.63	0.05	0.33	5481.49	5.34	2079.82	0.00141	708.86	3.70	2.30	0.32	39.31
34	13	2.62	10.57	1358.11	1.63	0.05	0.31	5159.05	5.34	1981.36	0.00144	692.64	3.79	2.22	0.27	39.42
36	13	2.77	10.46	1342.34	1.63	0.05	0.29	4872.43	5.34	1892.80	0.00148	677.50	3.87	2.14	0.23	39.53
38	13	2.92	10.35	1327.70	1.63	0.04	0.28	4615.99	5.34	1812.67	0.00151	663.31	3.96	2.07	0.20	39.64
40	13	3.08	10.25	1314.07	1.63	0.04	0.27	4385.19	5.34	1739.80	0.00154	649.98	4.04	2.01	0.18	39.74
42	13	3.23	10.15	1301.32	1.63	0.04	0.25	4176.37	5.34	1673.20	0.00157	637.41	4.12	1.95	0.16	39.84
44	13	3.38	10.05	1289.36	1.63	0.04	0.24	3986.53	5.34	1612.07	0.0016	625.54	4.19	1.90	0.14	39.94
46	13	3.54	9.96	1278.11	1.63	0.04	0.23	3813.21	5.34	1555.75	0.00163	614.28	4.27	1.85	0.12	40.03
48	13	3.69	9.86	1267.50	1.63	0.03	0.22	3654.32	5.34	1503.67	0.00166	603.60	4.35	1.80	0.11	40.12
50	13	3.85	9.78	1257.47	1.63	0.03	0.21	3508.15	5.34	1455.36	0.00169	593.44	4.42	1.76	0.10	40.21
52	13	4.00	9.69	1247.97	1.63	0.03	0.20	3373.22	5.34	1410.40	0.00171	583.76	4.49	1.72	0.09	40.30
54	13	4.15	9.60	1238.95	1.63	0.03	0.20	3248.29	5.34	1368.46	0.00174	574.51	4.57	1.68	0.08	40.38
56	13	4.31	9.52	1230.37	1.63	0.03	0.19	3132.28	5.34	1329.22	0.00177	565.67	4.64	1.65	0.07	40.46



**Table (4-11): Design calculation for two pass pipes, Fifth trial**

NO. OF TUPES	NO. OF COLUMNS	N	$\Delta T$ (°C)	$h_o$ (W/m <sup>2</sup> .k)	$m$ (water) (kg/s)	$m$ (tube) (kg/s)	V (water) (m/s)	Re	pr	$h_i$ (W/m <sup>2</sup> .k)	$1/U_o$	$U_o$ (W/m <sup>2</sup> .k)	$A_o$ (m <sup>2</sup> )	L (m)	$\Delta P$ (kpa)	T s TUBE SURFACE (trail)
20	9	2.22	11.99	1370.63	1.63	0.08	0.53	8770.38	5.34	3029.16	0.00126	792.11	3.31	3.30	1.16	38.01
22	9	2.44	11.85	1342.20	1.63	0.07	0.48	7973.07	5.34	2806.78	0.0013	766.84	3.42	3.10	0.90	38.15
24	9	2.67	11.72	1317.01	1.63	0.07	0.44	7308.65	5.34	2618.05	0.00134	744.05	3.53	2.92	0.71	38.28
26	11	2.36	11.30	1369.71	1.63	0.06	0.41	6746.44	5.34	2455.66	0.00134	746.25	3.52	2.69	0.56	38.70
28	11	2.55	11.18	1348.30	1.63	0.06	0.38	6264.55	5.34	2314.30	0.00138	726.48	3.61	2.57	0.46	38.82
30	13	2.31	11.05	1328.94	1.63	0.05	0.35	5846.92	5.34	2190.03	0.00141	708.30	3.70	2.46	0.38	38.94
32	13	2.46	10.69	1374.74	1.63	0.05	0.33	5481.49	5.34	2079.82	0.00141	708.74	3.70	2.30	0.32	39.31
34	13	2.62	10.58	1357.67	1.63	0.05	0.31	5159.05	5.34	1981.36	0.00144	692.53	3.79	2.22	0.27	39.42
36	13	2.77	10.47	1341.90	1.63	0.05	0.29	4872.43	5.34	1892.80	0.00148	677.39	3.87	2.14	0.23	39.53
38	13	2.92	10.36	1327.27	1.63	0.04	0.28	4615.99	5.34	1812.67	0.00151	663.20	3.96	2.07	0.20	39.64
40	13	3.08	10.26	1313.63	1.63	0.04	0.27	4385.19	5.34	1739.80	0.00154	649.87	4.04	2.01	0.18	39.74
42	13	3.23	10.16	1300.88	1.63	0.04	0.25	4176.37	5.34	1673.20	0.00157	637.31	4.12	1.95	0.16	39.84
44	13	3.38	10.06	1288.92	1.63	0.04	0.24	3986.53	5.34	1612.07	0.0016	625.43	4.19	1.90	0.14	39.93
46	13	3.54	9.97	1277.67	1.63	0.04	0.23	3813.21	5.34	1555.75	0.00163	614.18	4.27	1.85	0.12	40.03
48	13	3.69	9.88	1267.06	1.63	0.03	0.22	3654.32	5.34	1503.67	0.00166	603.50	4.35	1.80	0.11	40.12
50	13	3.85	9.79	1257.03	1.63	0.03	0.21	3508.15	5.34	1455.36	0.00169	593.34	4.42	1.76	0.10	40.21
52	13	4.00	9.70	1247.53	1.63	0.03	0.20	3373.22	5.34	1410.40	0.00171	583.66	4.49	1.72	0.09	40.30
54	13	4.15	9.62	1238.51	1.63	0.03	0.20	3248.29	5.34	1368.46	0.00174	574.41	4.57	1.68	0.08	40.38
56	13	4.31	9.54	1229.93	1.63	0.03	0.19	3132.28	5.34	1329.22	0.00177	565.58	4.64	1.65	0.07	40.46

Table (4-12): Design calculation for shell side in two pass tubes heat exchanger

No. of tubes	D (bundle) m	D (shell) m	L <sub>b</sub> (m)	A <sub>s</sub> (m <sup>2</sup> )	G <sub>s</sub> (kg/m <sup>2</sup> .s)	u <sub>s</sub> (m/s)	de (m)	Re	F	(P <sub>1</sub> -P <sub>2</sub> ) pa
10	0.11045	0.1165	0.05823	0.001356	101.764696	0.09402633	0.0113608	9399.42	0.06	1.26393667
11	0.11548	0.1215	0.06074	0.001476	93.5186819	0.08640736	0.0113608	8637.78	0.0607	1.01632022
12	0.12026	0.1263	0.06313	0.001594	86.5614328	0.07997915	0.0113608	7995.18	0.0612	0.8310206
13	0.12484	0.1308	0.06542	0.001712	80.6087258	0.0744791	0.0113608	7445.36	0.0618	0.67093463
14	0.12924	0.1352	0.06762	0.001829	75.4547408	0.06971703	0.0113608	6969.32	0.0625	0.56798066
15	0.13347	0.1395	0.06973	0.001945	70.9466647	0.06555176	0.0113608	6552.93	0.063	0.48521764
16	0.13755	0.1436	0.07178	0.002061	66.968592	0.06187618	0.0113608	6185.5	0.0638	0.41072674
17	0.1415	0.1475	0.07375	0.002176	63.4309721	0.05860757	0.0113608	5858.75	0.0647	0.3603518
18	0.14533	0.1513	0.07566	0.00229	60.2634911	0.05568095	0.0113608	5566.19	0.0653	0.31730883
19	0.14904	0.155	0.07752	0.002404	57.4101483	0.05304458	0.0113608	5302.64	0.0675	0.28832331
20	0.15265	0.1587	0.07933	0.002517	54.8257759	0.05065673	0.0113608	5063.94	0.0683	0.25818379
21	0.15617	0.1622	0.08108	0.00263	52.4735293	0.04848335	0.0113608	4846.68	0.0689	0.23189901
22	0.1596	0.1656	0.0828	0.002742	50.3230463	0.04649639	0.0113608	4648.05	0.0696	0.20972644
23	0.16295	0.1689	0.08447	0.002854	48.3490759	0.04467253	0.0113608	4465.73	0.0704	0.19087994
24	0.16621	0.1722	0.08611	0.002966	46.5304413	0.04299218	0.0113608	4297.75	0.0709	0.17376838
25	0.16941	0.1754	0.08771	0.003077	44.8492468	0.04143883	0.0113608	4142.47	0.0715	0.15907329
26	0.17254	0.1785	0.08927	0.003188	43.2902633	0.0399984	0.0113608	3998.47	0.0724	0.14678513
27	0.17561	0.1816	0.09081	0.003298	41.8404472	0.03865883	0.0113608	3864.56	0.0738	0.13683901
28	0.17862	0.1846	0.09231	0.003408	40.4885607	0.03740974	0.0113608	3739.69	0.075	0.1276053

## CHAPTER FIVE

### Discussion and Conclusion

#### 5.1 Discussion

Figure (5-1) shows the variation of overall heat transfer coefficient with Reynolds number for one pass and two pass tubes. From the graph, it is seen that, overall heat transfer coefficient gets increased from 726 to 889  $\text{W/m}^2\cdot\text{K}$  for one pass tubes and from 565 to 792  $\text{W/m}^2\cdot\text{K}$  for two pass tubes with increase of Reynolds number. This is due to high mixing and increase turbulence in the cold air layers region which prevents the forming of thick boundary sub-layers. Overall heat transfer coefficient is also dependent on convective heat transfer coefficient so increase in Reynolds number results into higher heat transfer rates.

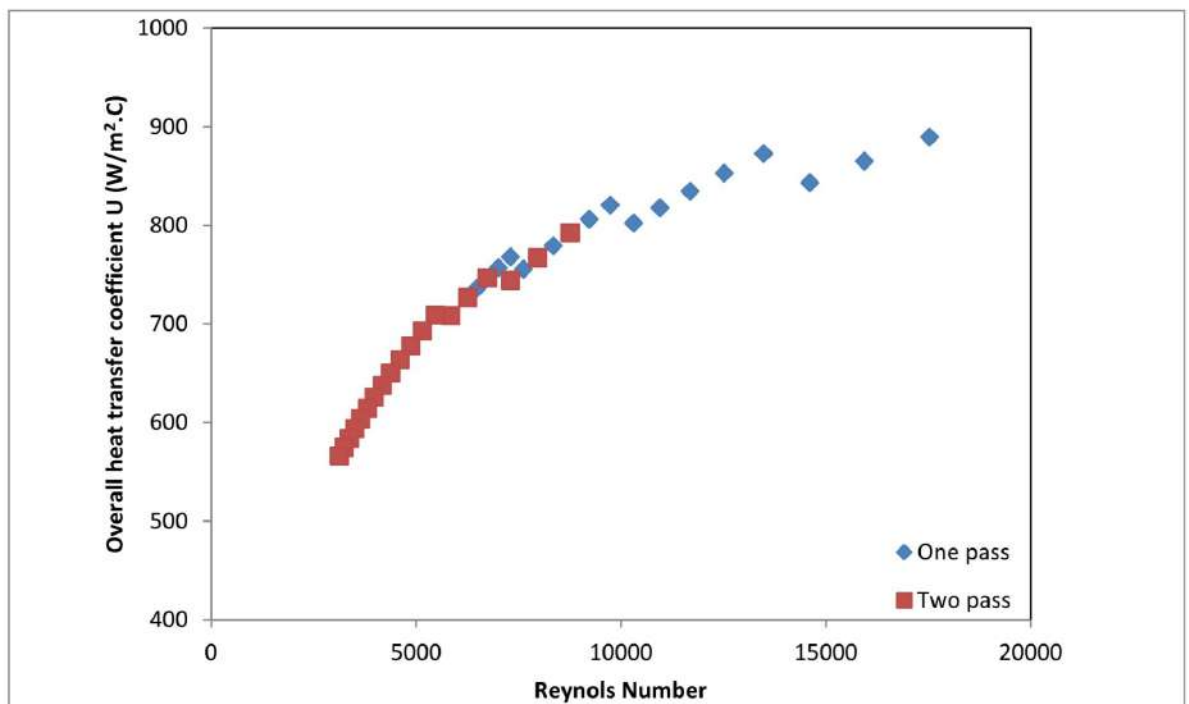


Figure (5-1): Overall heat transfer coefficient vs. Re numbers



Figure (5-2) represents the pressure drop across the pipes with Reynolds number for one pass and two pass tubes. It can be clearly seen that the pressure drop increases as the Reynolds number increases. The increasing in pressure drop will increase the power pumping requirements. For this reason, the Reynolds number should be specified to accomplish a high transfer rate with suitable pressure drop.

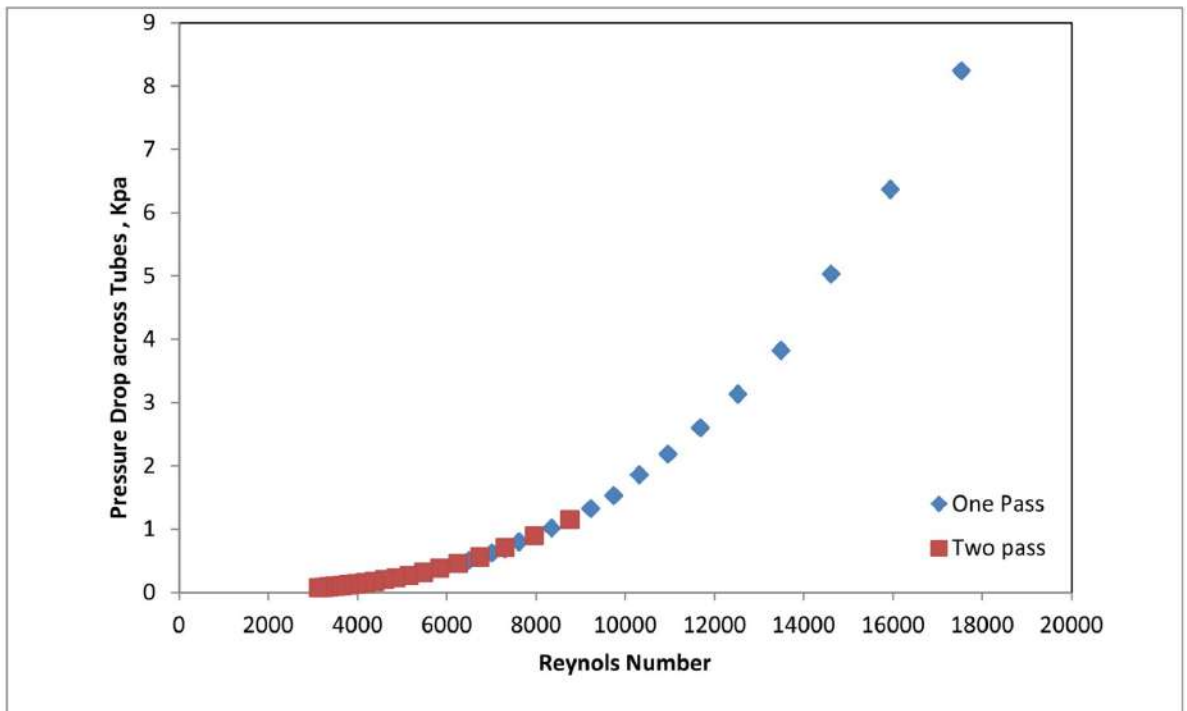


Figure (5-2): Pressure drop vs. Re numbers for the inner pipes

Baffles are used in the shell to direct the path and control the speed of flow. Placing them closer together can cause the fluid to travel more quickly, increasing the pressure drop as well as the heat transfer rate. Generally, a baffle cut of 20 to 25 per cent will be the optimum, giving good heat-transfer rates, without excessive drop. Figure (5-3) illustrate the pressure drop vs. Reynolds number in the shell side for one pass and two pass heat exchanger.

It is clearly seen that as the Reynolds number increases, the pressure drop increases as shown in figure (5-3). Excessive pressure drop will result in poor system performance and excessive energy consumption. Pressure drop across the shell will lead to increase compression pressures in the compressor.

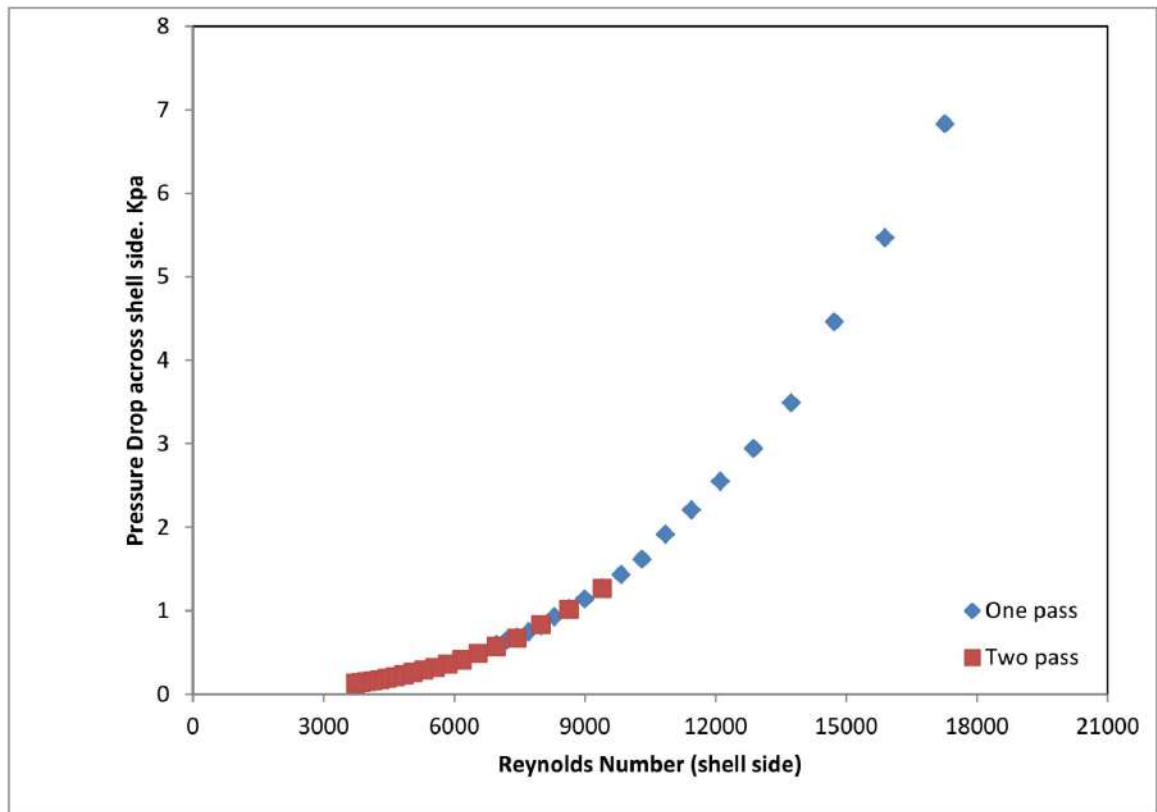


Figure (5-3): Pressure drop vs. Re numbers for the shell side

For the reasons mentioned above, the design specifications is chosen for the heat exchanger (condenser) are:

- Shell and tube heat exchanger with one pass tubes.
- Number of tubes is 26 with 2.7m length and 14 mm inner diameter

This specifications provide very good thermal performance with suitable pressure drop across the inner pipe and in the shell side with acceptalbe total length, as Shown in Figure (5-4).



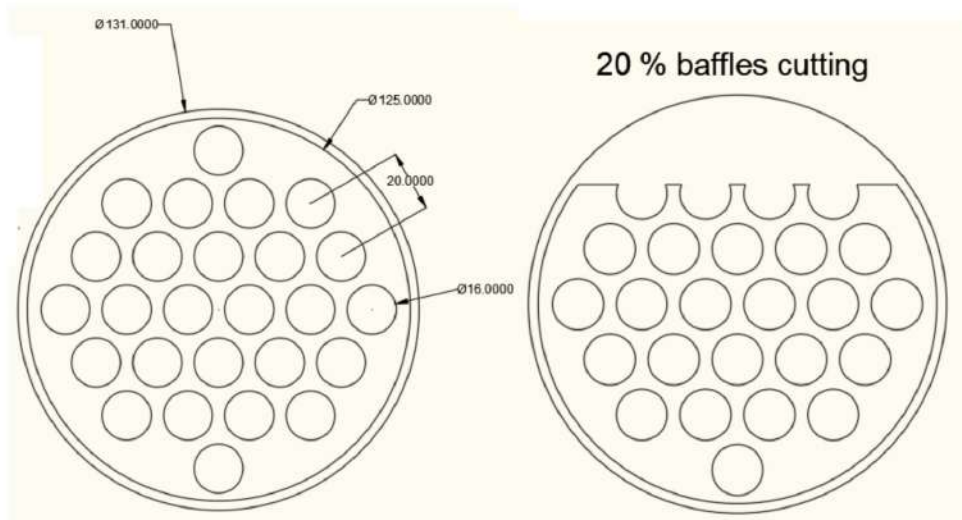


Figure (5-4): The condenser design

Inorder to increase the thermal performance with out increasing the heat exchanger length, twisted tape or swirl tape (Figure 5-5) could be inserted inside the inner pipes. These types of augmentations make the flow inside pipes more turbelent to enhance the heat transfer between the fluids. This method enhance the thermal efficiency with less expensive.

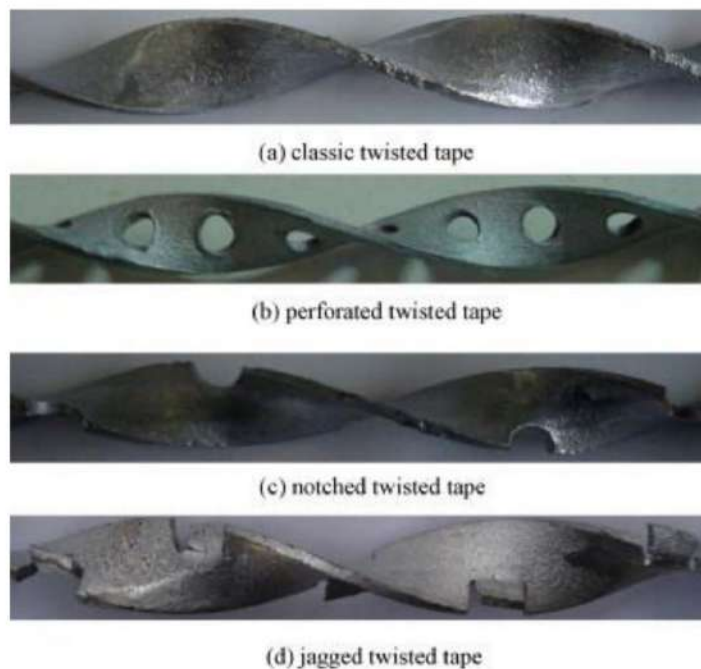


Figure (5-5) Types of twisted tapes inserts

## **References:**

- [1] Bejan Adrian, Kraus Allan D., Heat transfer handbook, vol. 1. John Wiley & Sons; 2003, p. 1030.**
- [2] Ramesh K. Shah, Dušan P. Sekulić, Fundamentals of Heat Exchanger Design, 1<sup>st</sup> edition, John Wiley & Sons, 2003.**
- [3] Holman J. P., "heat transfer", 10<sup>th</sup> edition, 2010.**
- [4] FRANK P. INCROPERA, DAVID P. DEWITT, " Fundamentals of Heat and MassTransfer ", sixth edition, 2007.**
- [5]William C. Whitman, William M. Johnson, John A. Tomczyk, Eugene Silberstein, Refrigeration & Air Conditioning Technology, 7<sup>th</sup> edition, 2013.**
- [6] Herbert W. Stanford, HVAC Water Chillers and Cooling Towers Fundamentals, Application, and Operation, 1<sup>st</sup> edition, 2003.**
- [7] Stoecker W.F., Jones J. W., Refrigeration and Air Conditioning, 2<sup>nd</sup> edition McGraw, New York, 1983.**
- [8] R. K. Sinnott, Coulson & Richardson"s Chemical Engineering: Chemical Engineering Design (volume 6), Butterworth-Heinemann, 4<sup>th</sup> edition, 2005.**
- [9] W. z. Nusselt: Die Oberflaechenkondensation des Wasserdampfes, Ver. Dtsch. Ing., vol. 60, pp. 541-569, 1916.**
- [10] R. K. SINNOTT, Chemical Engineering Design, 4<sup>th</sup> edition, Elsevier Butterworth-Heinemann, 2005.**

## Appendix (A)

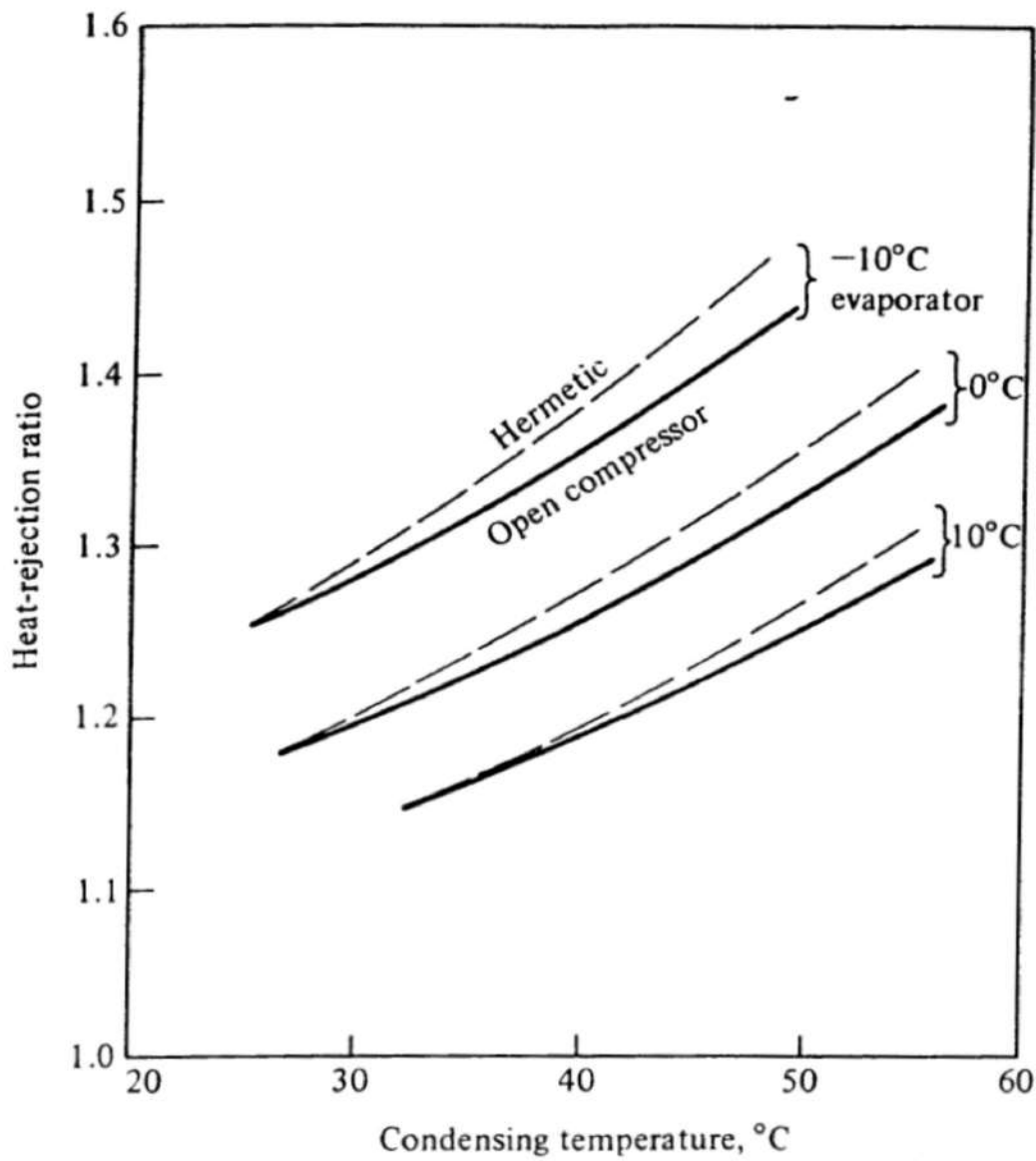


Figure (A-1): Typical values of the ratio of the heat rejected at the condenser to the refrigerating capacity for refrigerants 12 and 22

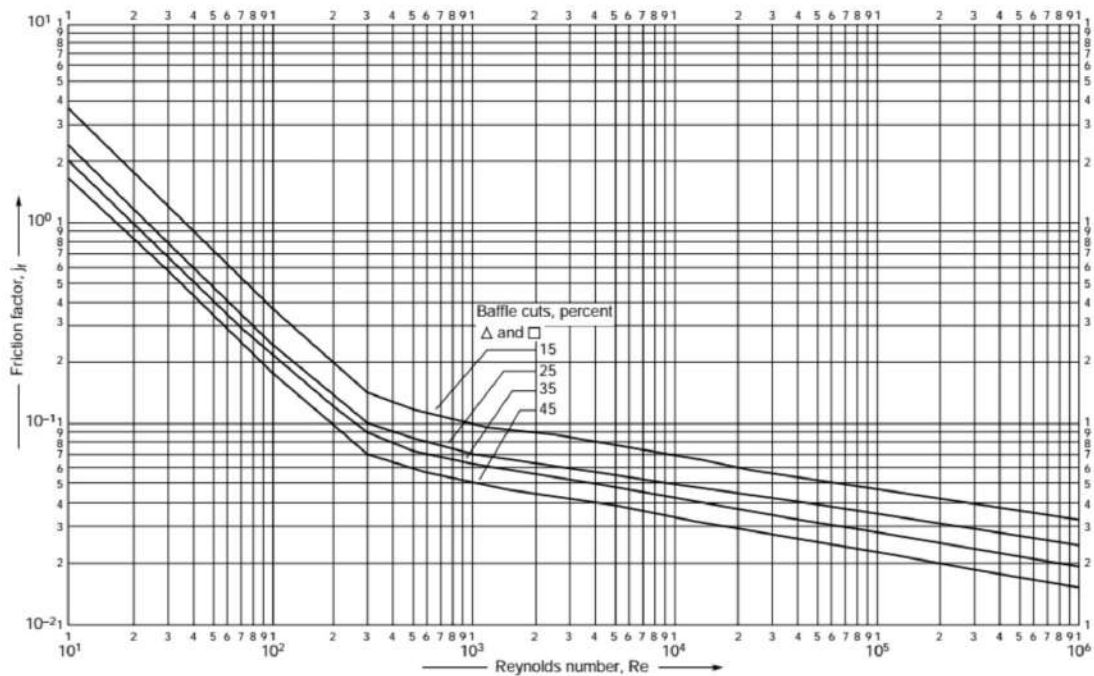


Figure (A-2): Shell-side friction factors, segmental baffles

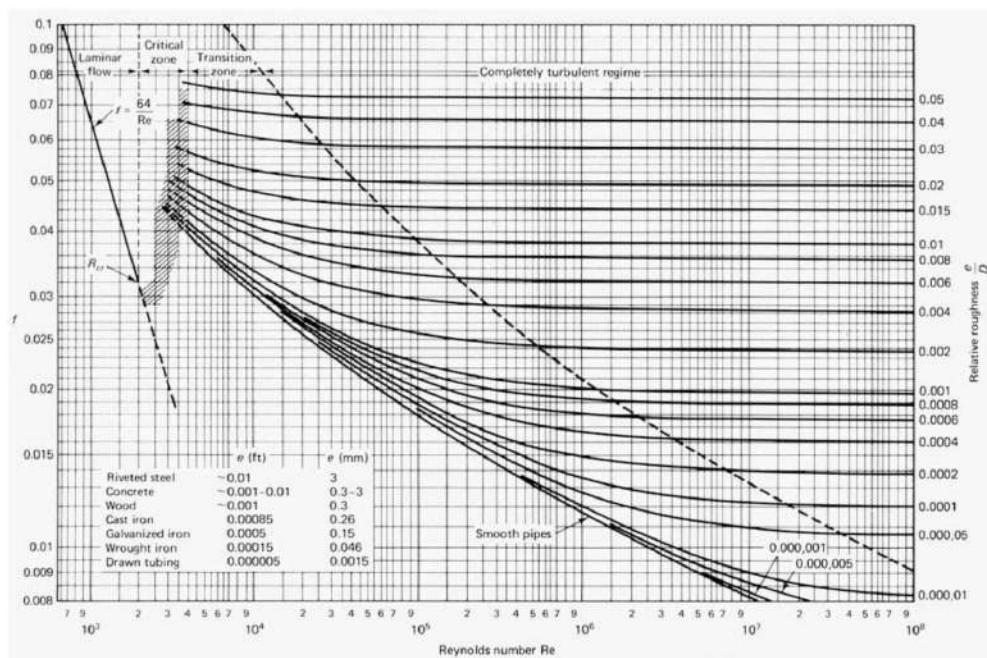


Figure (A-3): Moody Chart



## Appendix B

**Table (B-1): R22 properties**

Refrigerant 22 (Chlorodifluoromethane) Properties of Saturated Liquid and Saturated Vapor																			
Temp., °C	Pres- sure, MPa	Density, kg/m <sup>3</sup> Liquid	Volume, m <sup>3</sup> /kg Vapor	Enthalpy, kJ/kg		Entropy, kJ/(kg·K)		Specific Heat c <sub>p</sub> , kJ/(kg·K)		c <sub>p</sub> /c <sub>v</sub>	Velocity of Sound, m/s		Viscosity, μPa·s		Thermal Cond., mW/(m·K)		Surface Tension, mN/m	Temp., °C	
				Liquid	Vapor	Liquid	Vapor	Liquid	Vapor		Liquid	Vapor	Liquid	Vapor	Liquid	Vapor			
-100.00	0.00201	1571.3	8.2660	90.71	358.97	0.5050	2.0543	1.061	0.497	1.243	1127.	143.6	845.8	7.25	143.1	4.46	28.12	-100.00	
-90.00	0.00481	1544.9	3.6448	101.32	363.85	0.5646	1.9980	1.061	0.512	1.237	1080.	147.0	699.4	7.67	137.8	4.84	26.36	-90.00	
-80.00	0.01037	1518.2	1.7782	111.94	368.77	0.6210	1.9508	1.062	0.528	1.233	1033.	150.3	591.0	8.09	132.6	5.25	24.63	-80.00	
-70.00	0.02047	1491.2	0.94342	122.58	373.70	0.6747	1.9108	1.065	0.545	1.231	986.	153.3	507.6	8.52	127.6	5.68	22.92	-70.00	
-60.00	0.03750	1463.7	0.53680	133.27	378.59	0.7260	1.8770	1.071	0.564	1.230	940.	156.0	441.4	8.94	122.6	6.12	21.24	-60.00	
-50.00	0.06453	1435.6	0.32385	144.03	383.42	0.7752	1.8480	1.079	0.585	1.232	893.	158.3	387.5	9.36	117.8	6.59	19.58	-50.00	
-48.00	0.07145	1429.9	0.29453	146.19	384.37	0.7849	1.8428	1.081	0.589	1.233	884.	158.7	377.8	9.45	116.9	6.69	19.25	-48.00	
-46.00	0.07894	1424.2	0.26837	148.36	385.32	0.7944	1.8376	1.083	0.594	1.234	875.	159.1	368.6	9.53	115.9	6.79	18.92	-46.00	
-44.00	0.08705	1418.4	0.24498	150.53	386.26	0.8039	1.8327	1.086	0.599	1.235	865.	159.5	359.6	9.62	115.0	6.89	18.59	-44.00	
-42.00	0.09580	1412.6	0.22402	152.70	387.20	0.8134	1.8278	1.088	0.603	1.236	856.	159.9	351.0	9.70	114.0	6.99	18.27	-42.00	
-40.8 lb	0.10132	1409.2	0.21260	154.00	387.75	0.8189	1.8250	1.090	0.606	1.236	851.	160.1	346.0	9.75	113.5	7.05	18.08	-40.81	
-40.00	0.10523	1406.8	0.20521	154.89	388.13	0.8227	1.8231	1.091	0.608	1.237	847.	160.3	342.6	9.79	113.1	7.09	17.94	-40.00	
-38.00	0.11538	1401.0	0.18829	157.07	389.06	0.8320	1.8186	1.093	0.613	1.238	838.	160.6	334.5	9.87	112.2	7.19	17.62	-38.00	
-36.00	0.12628	1395.1	0.17304	159.27	389.97	0.8413	1.8141	1.096	0.619	1.239	828.	160.9	326.7	9.96	111.2	7.29	17.30	-36.00	
-34.00	0.13797	1389.1	0.15927	161.47	390.89	0.8505	1.8098	1.099	0.624	1.241	819.	161.2	319.1	10.04	110.3	7.40	16.98	-34.00	
-32.00	0.15050	1383.2	0.14682	163.67	391.79	0.8596	1.8056	1.102	0.629	1.242	810.	161.5	311.7	10.12	109.4	7.51	16.66	-32.00	
-30.00	0.16389	1377.2	0.13553	165.88	392.69	0.8687	1.8015	1.105	0.635	1.244	800.	161.8	304.6	10.21	108.5	7.61	16.34	-30.00	
-28.00	0.17819	1371.1	0.12528	168.10	393.58	0.8778	1.7975	1.108	0.641	1.246	791.	162.0	297.7	10.29	107.5	7.72	16.02	-28.00	
-26.00	0.19344	1365.0	0.11597	170.33	394.47	0.8868	1.7937	1.112	0.646	1.248	782.	162.3	291.0	10.38	106.6	7.83	15.70	-26.00	
-24.00	0.20968	1358.9	0.10749	172.56	395.34	0.8957	1.7899	1.115	0.653	1.250	772.	162.5	284.4	10.46	105.7	7.94	15.39	-24.00	
-22.00	0.22696	1352.7	0.09975	174.80	396.21	0.9046	1.7862	1.119	0.659	1.253	763.	162.7	278.1	10.55	104.8	8.06	15.07	-22.00	
-20.00	0.24531	1346.5	0.09268	177.04	397.06	0.9135	1.7826	1.123	0.665	1.255	754.	162.8	271.9	10.63	103.9	8.17	14.76	-20.00	
-18.00	0.26479	1340.3	0.08621	179.30	397.91	0.9223	1.7791	1.127	0.672	1.258	744.	163.0	265.9	10.72	103.0	8.29	14.45	-18.00	
-16.00	0.28543	1334.0	0.08029	181.56	398.75	0.9311	1.7757	1.131	0.678	1.261	735.	163.1	260.1	10.80	102.1	8.40	14.14	-16.00	
-14.00	0.30728	1327.6	0.07485	183.83	399.57	0.9398	1.7723	1.135	0.685	1.264	726.	163.2	254.4	10.89	101.1	8.52	13.83	-14.00	
-12.00	0.33038	1321.2	0.06986	186.11	400.39	0.9485	1.7690	1.139	0.692	1.267	716.	163.3	248.8	10.98	100.2	8.65	13.52	-12.00	
-10.00	0.35479	1314.7	0.06527	188.40	401.20	0.9572	1.7658	1.144	0.699	1.270	707.	163.3	243.4	11.06	99.3	8.77	13.21	-10.00	
-8.00	0.38054	1308.2	0.06103	190.70	401.99	0.9658	1.7627	1.149	0.707	1.274	697.	163.4	238.1	11.15	98.4	8.89	12.91	-8.00	
-6.00	0.40769	1301.6	0.05713	193.01	402.77	0.9744	1.7596	1.154	0.715	1.278	688.	163.4	233.0	11.24	97.5	9.02	12.60	-6.00	
-4.00	0.43628	1295.0	0.05352	195.33	403.55	0.9830	1.7566	1.159	0.722	1.282	679.	163.4	227.9	11.32	96.6	9.15	12.30	-4.00	
-2.00	0.46636	1288.3	0.05019	197.66	404.30	0.9915	1.7536	1.164	0.731	1.287	669.	163.4	223.0	11.41	95.7	9.28	12.00	-2.00	
0.00	0.49799	1281.5	0.04710	200.00	405.05	1.0000	1.7507	1.169	0.739	1.291	660.	163.3	218.2	11.50	94.8	9.42	11.70	0.00	
2.00	0.53120	1274.7	0.04424	202.35	405.78	1.0085	1.7478	1.175	0.748	1.296	650.	163.2	213.5	11.59	93.9	9.56	11.40	2.00	
4.00	0.56605	1267.8	0.04159	204.71	406.50	1.0169	1.7450	1.181	0.757	1.301	641.	163.1	208.9	11.68	93.1	9.70	11.10	4.00	
6.00	0.60259	1260.8	0.03913	207.09	407.20	1.0254	1.7422	1.187	0.766	1.307	632.	163.0	204.4	11.77	92.2	9.84	10.81	6.00	
8.00	0.64088	1253.8	0.03683	209.47	407.89	1.0338	1.7395	1.193	0.775	1.313	622.	162.8	200.0	11.86	91.3	9.99	10.51	8.00	
10.00	0.68095	1246.7	0.03470	211.87	408.56	1.0422	1.7368	1.199	0.785	1.319	613.	162.6	195.7	11.96	90.4	10.14	10.22	10.00	
12.00	0.72286	1239.5	0.03271	214.28	409.21	1.0505	1.7341	1.206	0.795	1.326	603.	162.4	191.5	12.05	89.5	10.29	9.93	12.00	
14.00	0.76668	1232.2	0.03086	216.70	409.85	1.0589	1.7315	1.213	0.806	1.333	594.	162.2	187.3	12.14	88.6	10.45	9.64	14.00	
16.00	0.81244	1224.9	0.02912	219.14	410.47	1.0672	1.7289	1.220	0.817	1.340	584.	161.9	183.2	12.24	87.7	10.61	9.35	16.00	
18.00	0.86020	1217.4	0.02750	221.59	411.07	1.0755	1.7263	1.228	0.828	1.348	575.	161.6	179.2	12.33	86.8	10.77	9.06	18.00	
20.00	0.91002	1209.9	0.02599	224.06	411.66	1.0838	1.7238	1.236	0.840	1.357	565.	161.3	175.3	12.43	85.9	10.95	8.78	20.00	
22.00	0.96195	1202.3	0.02457	226.54	412.22	1.0921	1.7212	1.244	0.853	1.366	555.	161.0	171.5	12.53	85.0	11.12	8.50	22.00	
24.00	1.0160	1194.6	0.02324	229.04	412.77	1.1004	1.7187	1.252	0.866	1.375	546.	160.6	167.7	12.63	84.1	11.30	8.22	24.00	
26.00	1.0724	1186.7	0.02199	231.55	413.29	1.1086	1.7162	1.261	0.879	1.385	536.	160.2	163.9	12.74	83.2	11.49	7.94	26.00	
28.00	1.1309	1178.8	0.02082	234.08	413.79	1.1169	1.7136	1.271	0.893	1.396	527.	159.7	160.3	12.84	82.3	11.69	7.66	28.00	
30.00	1.1919	1170.7	0.01972	236.62	414.26	1.1252	1.7111	1.281	0.908	1.408	517.	159.2	156.7	12.95	81.4	11.89	7.38	30.00	
32.00	1.2552	1162.6	0.01869	239.19	414.71	1.1334	1.7086	1.291	0.924	1.420	507.	158.7	153.1	13.06	80.5	12.10	7.11	32.00	
34.00	1.3210	1154.3	0.01771	241.77	415.14	1.1417	1.7061	1.302	0.940	1.434	497.	158.2	149.6	13.17	79.6	12.31	6.84	34.00	
36.00	1.3892	1145.8	0.01679	244.38	415.54	1.1499	1.7036	1.314	0.957	1.448	487.	157.6	146.1	13.28	78.7	12.54	6.57	36.00	
38.00	1.4601	1137.3	0.01593	247.00	415.91	1.1582	1.7010	1.326	0.976	1.463	478.	157.0	142.7	13.40	77.8	12.77	6.30	38.00	
40.00	1.5336	1128.5	0.01511	249.65	416.25	1.1665	1.6985	1.339	0.995	1.480	468.	156.4	139.4	13.52	76.9	13.02	6.04	40.00	
42.00	1.6098	1119.6	0.01433	252.32	416.55	1.1747	1.6959	1.353	1.015	1.498	458.	155.7	136.1	13.64	76.0	13.28	5.77	42.00	
44.00																			



Table (B-2) Water properties

Temp., °C	Pres- sure, MPa	Density, kg/m <sup>3</sup> Liquid	Volume, m <sup>3</sup> /kg Vapor	Enthalpy, kJ/kg		Entropy, kJ/(kg·K)		Specific Heat $c_p$ , kJ/(kg·K)			Velocity of Sound, m/s		Viscosity, μPa·s		Thermal Cond., mW/(m·K)		Surface Tension, mN/m	Temp., °C
				Liquid	Vapor	Liquid	Vapor	Liquid	Vapor	Vapor	Liquid	Vapor	Liquid	Vapor	Liquid	Vapor		
0.01a	0.00061	999.8	205.99	0.00	2500.92	0.0000	9.1555	4.220	1.884	1.329	1402.	409.0	1791.2	9.22	561.0	17.07	75.65	0.01
5.00	0.00087	999.9	147.01	21.02	2510.06	0.0763	9.0248	4.205	1.889	1.328	1426.	412.6	1518.3	9.34	570.5	17.34	74.94	5.00
10.00	0.00123	999.7	106.30	42.02	2519.21	0.1511	8.8998	4.196	1.895	1.328	1447.	416.2	1306.0	9.46	580.0	17.62	74.22	10.00
15.00	0.00171	999.1	77.875	62.98	2528.33	0.2245	8.7803	4.189	1.900	1.328	1466.	419.7	1137.6	9.59	589.3	17.92	73.49	15.00
20.00	0.00234	998.2	57.757	83.91	2537.43	0.2965	8.6660	4.184	1.906	1.327	1482.	423.2	1001.6	9.73	598.4	18.23	72.74	20.00
25.00	0.00317	997.0	43.337	104.83	2546.51	0.3672	8.5566	4.182	1.912	1.327	1497.	426.6	890.1	9.87	607.2	18.55	71.97	25.00
30.00	0.00425	995.6	32.878	125.73	2555.55	0.4368	8.4520	4.180	1.918	1.327	1509.	430.0	797.4	10.01	615.5	18.89	71.19	30.00
35.00	0.00563	994.0	25.205	146.63	2564.55	0.5051	8.3517	4.180	1.925	1.327	1520.	433.4	719.3	10.16	623.3	19.24	70.40	35.00
40.00	0.00738	992.2	19.515	167.53	2573.51	0.5724	8.2555	4.180	1.931	1.327	1529.	436.7	653.0	10.31	630.6	19.60	69.60	40.00
45.00	0.00959	990.2	15.252	188.43	2582.43	0.6386	8.1633	4.180	1.939	1.327	1536.	440.0	596.1	10.46	637.3	19.97	68.78	45.00
50.00	0.01235	988.0	12.027	209.34	2591.29	0.7038	8.0748	4.182	1.947	1.328	1542.	443.2	546.8	10.62	643.6	20.36	67.94	50.00
55.00	0.01576	985.7	9.5643	230.26	2600.09	0.7680	7.9898	4.183	1.955	1.328	1547.	446.4	504.0	10.77	649.2	20.77	67.10	55.00
60.00	0.01995	983.2	7.6672	251.18	2608.83	0.8313	7.9081	4.185	1.965	1.328	1551.	449.5	466.4	10.93	654.3	21.19	66.24	60.00
65.00	0.02504	980.5	6.1935	272.12	2617.50	0.8937	7.8296	4.187	1.975	1.329	1553.	452.6	433.2	11.10	659.0	21.62	65.37	65.00
70.00	0.03120	977.7	5.0395	293.07	2626.10	0.9551	7.7540	4.190	1.986	1.330	1555.	455.6	403.9	11.26	663.1	22.07	64.48	70.00
75.00	0.03860	974.8	4.1289	314.03	2634.60	1.0158	7.6812	4.193	1.999	1.331	1555.	458.5	377.7	11.43	666.8	22.53	63.58	75.00
80.00	0.04741	971.8	3.4052	335.01	2643.02	1.0756	7.6111	4.197	2.012	1.332	1554.	461.4	354.3	11.59	670.0	23.01	62.67	80.00
85.00	0.05787	968.6	2.8258	356.01	2651.33	1.1346	7.5434	4.201	2.027	1.333	1553.	464.2	333.3	11.76	672.8	23.51	61.75	85.00
90.00	0.07018	965.3	2.3591	377.04	2659.53	1.1929	7.4781	4.205	2.043	1.334	1550.	466.9	314.4	11.93	675.3	24.02	60.82	90.00
95.00	0.08461	961.9	1.9806	398.09	2667.61	1.2504	7.4151	4.210	2.061	1.335	1547.	469.6	297.3	12.10	677.3	24.55	59.87	95.00
99.97b	0.10133	958.4	1.6732	419.68	2675.53	1.3069	7.3544	4.216	2.080	1.337	1543.	472.2	281.8	12.27	679.1	25.09	58.92	99.97
100.00	0.10142	958.3	1.6718	419.17	2675.57	1.3072	7.3541	4.216	2.080	1.337	1543.	472.2	281.7	12.27	679.1	25.10	58.91	100.00
105.00	0.12090	954.7	1.4184	440.27	2683.39	1.3633	7.2952	4.222	2.101	1.339	1538.	474.7	267.6	12.44	680.5	25.66	57.94	105.00
110.00	0.14338	950.9	1.2093	461.42	2691.06	1.4188	7.2381	4.228	2.124	1.341	1533.	477.1	254.7	12.61	681.7	26.24	56.96	110.00
115.00	0.16918	947.1	1.0358	482.59	2698.58	1.4737	7.1828	4.236	2.150	1.343	1527.	479.5	242.9	12.78	682.6	26.85	55.97	115.00
120.00	0.19867	943.1	0.89121	503.81	2705.93	1.5279	7.1291	4.244	2.177	1.346	1520.	481.7	232.1	12.96	683.2	27.47	54.97	120.00
125.00	0.23224	939.0	0.77903	525.07	2713.10	1.5816	7.0770	4.252	2.207	1.349	1512.	483.9	222.1	13.13	683.6	28.11	53.96	125.00
130.00	0.27028	934.8	0.68600	546.38	2720.08	1.6346	7.0264	4.261	2.239	1.352	1504.	486.0	212.9	13.30	683.7	28.76	52.93	130.00
135.00	0.31323	930.5	0.58173	567.74	2726.87	1.6872	6.9772	4.272	2.274	1.355	1496.	487.9	204.4	13.47	683.6	29.44	51.90	135.00
140.00	0.36154	926.1	0.50845	589.16	2733.44	1.7392	6.9293	4.283	2.311	1.359	1486.	489.8	196.5	13.65	683.3	30.14	50.86	140.00
145.00	0.41568	921.6	0.44596	610.64	2739.80	1.7907	6.8826	4.294	2.351	1.363	1476.	491.6	189.2	13.82	682.8	30.86	49.80	145.00
150.00	0.47616	917.0	0.39245	632.18	2745.93	1.8418	6.8371	4.307	2.394	1.368	1466.	493.3	182.5	13.99	682.0	31.60	48.74	150.00
155.00	0.54350	912.3	0.34646	653.79	2751.81	1.8924	6.7926	4.321	2.440	1.373	1455.	494.8	176.1	14.16	681.1	32.35	47.67	155.00
160.00	0.61823	907.4	0.30678	675.47	2757.44	1.9426	6.7491	4.335	2.488	1.379	1443.	496.3	170.2	14.34	680.0	33.13	46.59	160.00
165.00	0.70093	902.5	0.27243	697.24	2762.81	1.9923	6.7066	4.351	2.540	1.385	1431.	497.6	164.7	14.51	678.6	33.93	45.50	165.00
170.00	0.79219	897.5	0.24259	719.08	2767.90	2.0417	6.6650	4.368	2.594	1.392	1419.	498.9	159.6	14.68	677.0	34.75	44.41	170.00
175.00	0.89260	892.3	0.21658	741.02	2772.71	2.0906	6.6241	4.386	2.652	1.399	1405.	500.0	154.7	14.85	675.3	35.59	43.30	175.00
180.00	1.0028	887.0	0.19384	763.05	2777.21	2.1392	6.5840	4.405	2.713	1.407	1392.	501.0	150.1	15.03	673.3	36.45	42.19	180.00
185.00	1.1235	881.6	0.17390	785.19	2781.41	2.1875	6.5447	4.425	2.777	1.416	1378.	501.9	145.8	15.20	671.1	37.33	41.07	185.00
190.00	1.2552	876.1	0.15636	807.43	2785.28	2.2355	6.5059	4.447	2.844	1.425	1363.	502.7	141.8	15.37	668.8	38.24	39.95	190.00
195.00	1.3988	870.4	0.14089	829.79	2788.82	2.2832	6.4678	4.471	2.915	1.436	1348.	503.4	137.9	15.54	666.1	39.16	38.81	195.00
200.00	1.5549	864.7	0.12721	852.27	2792.01	2.3305	6.4302	4.496	2.990	1.447	1332.	503.9	134.3	15.71	663.3	40.11	37.67	200.00
205.00	1.7243	858.8	0.11508	874.88	2794.83	2.3777	6.3930	4.523	3.068	1.459	1316.	504.3	130.9	15.89	660.3	41.09	36.53	205.00
210.00	1.9077	852.7	0.10429	897.63	2797.27	2.4245	6.3563	4.551	3.150	1.472	1299.	504.6	127.6	16.06	657.0	42.09	35.38	210.00
215.00	2.1058	846.5	0.09468	920.53	2799.32	2.4712	6.3200	4.582	3.237	1.486	1282.	504.8	124.5	16.24	653.4	43.11	34.23	215.00
220.00	2.3196	840.2	0.08609	943.58	2800.95	2.5177	6.2840	4.615	3.329	1.501	1264.	504.8	121.5	16.41	649.7	44.17	33.07	220.00
225.00	2.5497	833.7	0.07840	966.80	2802.15	2.5640	6.2483	4.650	3.426	1.518	1246.	504.6	118.7	16.59	645.6	45.26	31.90	225.00
230.00	2.7971	827.1	0.07150	990.19	2802.90	2.6101	6.2128	4.688	3.528	1.536	1228.	504.4	116.0	16.76	641.3	46.38	30.74	230.00
235.00	3.0625	820.3	0.06530	1013.77	2803.17	2.6561	6.1775	4.728	3.638	1.556	1209.	503.9	113.4	16.94	636.7	47.53	29.57	235.00
240.00	3.3469	813.4	0.05970	1037.55	2802.96	2.7020	6.1423	4.772	3.754	1.578	1189.	503.3	110.9	17.12	631.8	48.73	28.39	240.00
245.00	3.6512	806.2	0.05465	1061.55	2802.22	2.7478	6.1072	4.819	3.878	1.601	1169.	502.6	108.4	17.31	626.7	49.97	27.22	245.00
250.00	3.9762	798.9	0.05008	1085.77	2800.93	2.7935	6.0721	4.870	4.011	1.627	1148.	501.6	106.1	17.49	621.2	51.26	26.04	250.00
255.00	4.3229	791.4	0.04594	1110.23	2799.07	2.8392	6.0369	4.925	4.153	1.655	1127.	500.5	103.9	17.68	615.4	52.61	24.87	255.00
260.00	4.6923	783.6	0.04217	1134.96	2796.60	2.8849	6.0016	4.986	4.308	1.686	1105.	499.2	101.7	17.88	609.2	54.03	23.69	260.00
265.00	5.0853	775.7	0.03875	1159.96	2793.49	2.9307	5.9661	5.051	4.475	1.720	1083.	497.7	99.6	18.07	602.8	55.53	22.51	265.00
270.00	5.5030	767.5	0.03562	1185.27	2789.69	2.9765	5.9304	5.123	4.656	1.757	1060.	496.0	97.5	18.28	595.9	57.11	21.34	270.00
275.00	5.9464	759.0	0.03277	1210.90	2785.17	3.0224	5.8944	5.202	4.855	1.798	1037.	494.1	95.5	18.48	588.7	58.80	20.16	275.00
280.00	6.4166	750.3	0.03015	1236.88	2779.87	3.0685	5.8579	5.289	5.073	1.845	1013.	491.9	93.5	18.70	581.1	60.61	18.99	280.00
285.00</																		



وزارة التعليم العالي والبحث العلمي

كلية دجلة الجامعة الأهلية

قسم هندسة تقنيات التبريد والتكييف

## تصميم مبادل حراري لمنظومة تبريد في معمل بلاستيك

تقديم إلى كلية دجلة الجامعة الأهلية/ قسم هندسة تقنيات التبريد والتكييف وهو جزء من متطلبات نيل  
شهادة البكالوريوس في هندسة تقنيات التبريد والتكييف

من قبل

- احمد عادي محييد
- عباس احسان فالح
- احمد فائز حسين
- صفاء كاظم حبيب
- علي فاهم حبيب

بإشراف

م. مها علي حسين

1442 هـ

2021 م

## الخلاصة

في هذا المشروع ، تم تصميم مبادل حراري للتبريد بالماء (مكثف) لاستخدامه في نظام التبريد وفقاً لمتطلبات مصنع بلاستيك. يعتمد التصميم على طريقة التجربة والخطأ بافتراض عدد الأنابيب الداخلية باتجاه واحد واتجاهين تمرير. أيضاً ، تم افتراض اختلاف درجة الحرارة بين السطح الخارجي للأنابيب مع مادة التبريد. أظهرت النتائج أنه كلما زاد عدد الأنابيب للاتجاه الواحد كلما قل عدد رينولدز وانخفض معامل نقل الحرارة الكلي وانخفض خسارة الضغط مع طول الأنبوب. مواصفات التصميم المختارة للمبادل الحراري (المكثف) هي:

- مبادل حراري ذو أنابيب بممر واحد.
- عدد الأنابيب 26 بطول 2.7 م وقطر داخلي 14 ملم



**Ministry of Higher Education  
and Scientific Research  
Dijlah University College  
Refrigeration and Air Conditioning  
Technologies Engineering Department**



## **Solar Parabola Mirror With Power Generation**

### **A Project**

*Submitted to the Refrigeration and Air Condition Technology  
Engineering Department at Dijlah University College in partial  
fulfillment of the requirements for Degree of Bachelor in Refrigeration  
and Air Conditioning Technologies Engineering Department*

**By:**

***Ammar Abd .Al-Raheem Ammar***

***Omar Maged Aabed***

***Ali Abd Ajaj Ibrahim***

***Muhannad Malik Abd***

***Abdullah Essam Hussein***

***Supervisor by:***

**Lec. Mohammed Hamza**

***1442 A.H.***

***2021 A.D.***

بِسْمِ اللَّهِ الرَّحْمَنِ الرَّحِيمِ

﴿ وَلَقَدْ آتَيْنَا دَاوُودَ وَسُلَيْمَانَ عِلْمًا وَقَالَا الْحَمْدُ  
لِلَّهِ الَّذِي فَضَّلَنَا عَلَى كَثِيرٍ مِنْ عِبَادِهِ الْمُؤْمِنِينَ ﴾

﴿ سورة النمل الآية 15 ﴾

## ***Supervisor Certificate***

***We certify that this project entitled ( Solar Parabola  
Mirror With Power Generation )***

***Prepared by:***

***Ammar Abd Al-Raheem Ammar***

***Omar Maged Aabed***

***Ali Abd Ajaj Ibrahim***

***Muhannad Malik Abd***

***Abdullah Essam Hussein***

***Has been carried out completely under our supervision at the  
Dijlah university college in partial fulfillment of therequirements  
for Degree of Bachelor in Refrigeration and Air  
Conditioning Technologies Engineering.***

***Signature:***

**Lec. Mohammed Hamza**

***Date: / /2021***

***Approved by the head of Air condition and refrigeration  
engineering department:***

**Signature**

**Dr. firas maan**

**Head of Refrigerating and Air  
Conditioning Engineering  
Department**

**Date: / /2021**

# ***Examining committee certificate***

**We certify that this project entitled (*Solar Parabola Mirror With Power Generation* )**

**Submitted by:**

***Ammar Abd Al-Raheem Ammar***

***Omar Maged Aaded***

***Ali Abd Ajaj Ibrahim***

***Muhannad Malik Abd***

***Abdullah Essam Hussein***

**and as an examining committee examined the students in its content  
and that in our opinion it meets the standards of a project for the for  
Degree of Bachelor in Refrigeration and Air Conditioning  
Technologies Engineering.**

**Signature**

**Lec. Mohammed Hamza**

***Date: / /2021***  
***(supervisor)***

**Signature**

**Asst.Lec.Amer Fadel**

**Date: / /2021**

**(Member)**

**Signature**

**Asst.Lec.Maryam Ali**

**Date: / /2021**

**(Member)**

# الاهداء

الى الوطن الغالي وشهداءه

وكل من ضحى من اجل امن وامان هذا الوطن الحبيب

إلى أمهاتنا..... لا أجد كلمات يمكن أن تمنحها حقها فهي ملحة الحب وفرحة العسر

ومثال التفاني والعطاء.

إلى أبائنا .... قدوتنا الأعلى في الحياة فهو من علّمني كيف أعيش بكرامة وشموخ.

أساتذة كلية وحلة الجامعة قسم هندسة التبريد والتكييف كافة وبخصوص الأستاذ المشرف

محمد حمزة داود لما بذله من جهد في توجيهنا وله الشكر

والتقدير

والى

اخواني الطلبة كافة

اوجه لهم تحياتي وجهدنا المتواضع لكم منا التحية

# الشكر والتقدير

الامتنان والشكر والتقدير لكل من ساهم أقدم  
في انجاز هذا البحث وبالأخص استاذي العزيز  
الاستاذ (محمد حمزة داود)  
وكافة اساتذة كلية دجلة الجامعة  
والى زملائي واخواني الطلبة والى الشعب العراقي  
الكريم

## *Abstract*

The research studies the possibility of generating energy using this solar shower system to focus the rays at the focal point of heat generation from the sun which is concentrated in the central point a sterling engine that drives a Stirling piston and generates electrical energy Using such a method is very beneficial because it is environmentally friendly (does not generate pollutants) is technically inexpensive and does not require organic fuel Our project consists of a shower system made of aluminum foil adhesive parts and a Stirling engine The benefit of this project is to produce heat energy and convert it into any form of energy.

## List of symbols

Name	icons	Unit
<i>Energy</i>	$Q_u$	$W$
<i>Area</i>	$A$	$m^2$
<i>Focal Length</i>	$f$	$M$
<i>Diameter</i>	$D$	$M$
<i>Depth</i>	$h$	$M$
<i>Solar Intensity</i>	$I$	$W/m^2$
<i>Collector efficiency factor</i>	$F'$	
<i>Collector flow factor</i>	$F''$	
<i>Temprature</i>	$T$	$C^\circ$

## List of figures

Number	Name	Number Of Page
Figure 1-1	Parabolic Dish	3
Figure 3-1	A 3D illustration and a Graph of a Paraboloid	9
Figure 3-2	Measurement of the intensity of solar radiation	10
Figure 3-3	Working Cycle of an Stirling Engine	11
Figure 3-4	Stirling Engine	11-12

## List of Tables

Number	Name	Number Of Page
Table 3-1	Potential Reflector Mater	13
Table 4-1	Read solar radiation	16-17
Table 4-2	Total Hours Reading	17



<b>Abstract</b>	<b>VI</b>
<b>Chapter one</b>	<b>Number Of Page</b>
INTRODUCTION	2
Parabolic Dish	2-3
<b>Chapter tow</b>	
Previous studies	5-6
<b>Chapter three</b>	
Concentration Ratio	8
Geometry	8-9
Intensity of solar radiation	9-10
Stirling Engine	10-11
Reflector Material Selection	12
Energy Laws	14
<b>Chapter four</b>	
Readings	16-17
Discussion	18
References	19
الخلاصة	20

**Chapter one**

# **Introduction**

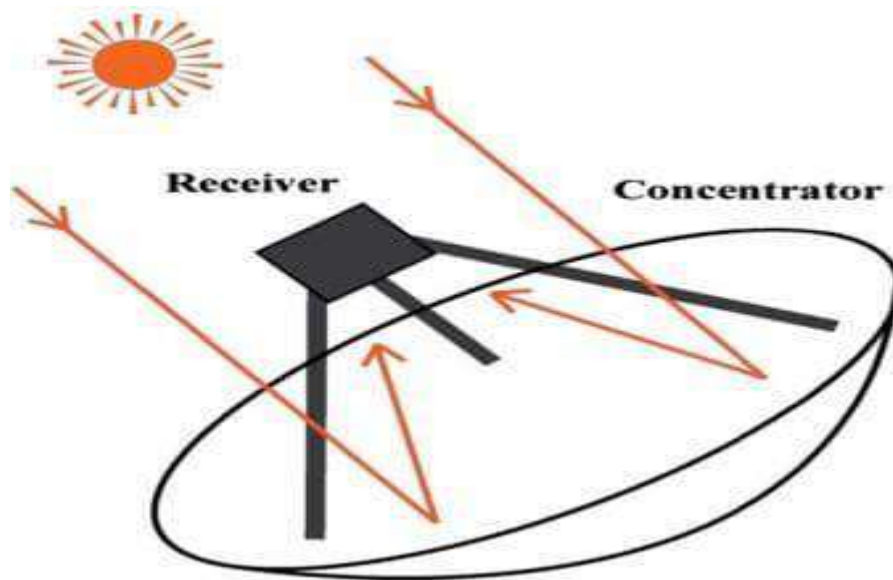
## **1.1 INTRODUCTION**

Solar energy is the most popular renewable energy and it has been heavily utilized over the past decades mainly for electricity generation and water heating. The current technologies such as photovoltaic panels do not permit a high efficiency level as they are limited to an average efficiency of 15 to 18%. Concentrating solar power systems (CSP) are still undergoing research and testing it is believed that they can achieve higher efficiencies between 20 and 25%. A CSP dish is a device that collects solar radiations and concentrates them at a focal point thanks to its reflecting parabolic shape. Besides optical properties a Stirling dish comprehends of a thermodynamic aspect that consists of a Stirling engine converting thermal energy to mechanical energy which in turn is converted to electricity by an electric generator. In order to achieve high efficiencies the design of such a system may be very complex as many aspects have to be optimized and many factors have to be taken into consideration.

### **Parabolic Dish**

Parabolic dish concentrators concentrate light in a point which is called the receiver. They benefit from their geometry to achieve one of the highest efficiencies among all solar energy technologies. These systems collect the beams coming from the sun, and parallel to the axis of the parabola, and reflect them to the focal point where the thermal receiver is located. The collector must be optimally oriented towards sun and that is why most of parabolic dish collectors use a two-axis tracking system to constantly track the position of the sun in the sky. The surface of the collector is covered with reflecting mirrors or other coating materials with high reflection coefficients. This type of concentrators achieves the highest efficiencies since they do not experience much optical loss compared to other CSP technologies. The

present work will shed light on a special parabolic technology which is the Dish Stirling. They can be used either in power plants or for small-scale applications such as for off-grid electricity production for houses. The picture below is a photograph of this type of parabolic dish collectors [1]



*Figure 1-1. Parabolic Dish*

## **1.2 Objective of the project:**

- 1-The objective of this project was to produce thermal energy by solar dish .
- 2- measure solar radiation .

## **Chapter two**

### **Previous Studies**

## 2.1 Previous studies

In the last 50 years a need of renewable energy have been appeared because of the contamination and the high cost of fuel. The solar thermal radiation is the main energy source in the world.many researchers worked on using the solar thermal energy to design Energy is a basic necessity of Life.Sun is the main source of Energy for Earth.

Solar Energy converted and inter- converted to and from various forms, supports Life on Earth.

The development of human ability to harness and utilize energy from various sources has had a major influence on evolution of Human Life and Civilization. Industrial Revolution resulted into great changes in energy conversion and utilization patterns Solar energy is the radiant light and heat from the sun that has been harnessed by humans since ancient times using a range of ever-evolving technologies Solar radiation along with secondary solar resources account for most of the available renewable energy on earth.

Wind power is one of the fastest-growing renewable energy technologies Usage is on the rise worldwide in part because costs are falling Tidal energy.

Energy and Islands Energy and Lunar Energy is a kind of energy and renewable energy in the subject of energy and renewable energy Tidal power harnessed by converting energy from tides into useful forms of power mainly electricity using various methods.

Geothermal energy is an alternative and renewable energy source which is a high thermal energy of natural origin in magma where it is estimated that more than 99% of the mass of the globe is rocks whose temperature exceeds 1000 degrees Celsius. Solar dish collectors (SDC) offer the highest thermal and optical efficiencies of all the current concentrator options (Lovegrove et al 2011). Solar dish collector (SDC) have been widely used to concentrate solar radiation and convert it into medium or high temperature heat including solar cooker (Abu-Malouh et al 2011 Kumaret al 2012 solar hydrogen production (Furler et al 2012) and Dish–Stirling system to generate electricity (Manciniet al 2003 Mills 2004).Coventry and Andraka (2017) reviewed parabolic dish technology and focused on the evolution of dish design by examining features such as mode of tracking structure and mirror design.

The review includes a brief summary of power generation options as well as a discussion about options for storage and hybridisation. Sun is not a point source of light and  $0.32^\circ$  non-parallelism of natural sunlight and imperfections of the collector can provide a reduction in the solar radiation intercepted by the receiver (Stine and Harrigan 1985). Hence improving the optical performance is the main step to optimize the SDC (Li et al 2013).

Considerable theoretical and experimental works on SDC for a large range of industrial applications have been carried out in recent years (Cui et al 2003 Li et al 2011 Lovegrove et al 2011 Reddy and Kumar 2009 Shuai et al 2008 Wang and Siddiqui 2010 Wu et al 2010a 2010b Wua et al 2010).

Solar dishes are very attractive due to their high concentration ratios and versatility (Poullikkas et al 2010).

High concentration ratios allow to control the thermal losses and therefore to obtain high conversion efficiencies (Andraka and Powell 2008).

Also conversion efficiencies severely depend on the optical properties of the reflective surfaces Errors affect the intercept factor which is defined as the ratio of the energy intercepted by the receiver to the energy reflected by the reflector (Sodha et al 1984). The ideal optical configuration for the dish concentrator is a paraboloidal mirror which is very expensive to fabricate its costs increase rapidly with aperture area However in practice it is easier to fabricate a dish concentrator from small elementary mirrors.

The elementary components are known as reflecting petals or facets (Kaushika and Reddy 2000).

## **Chapter three**

# **Experimental Setup**



### 3.1 Concentration Ratio

The most common utilized types of receivers are cavity receivers and they are placed at the focal point thus the concentration of sunrays will occur at its basis. The optical performance of the system is tightly related to the size of the receiver. The concentration ratio is another critical design parameter which refers to the ratio of the aperture's area of the dish to the absorber/receiver's area. For Dish Stirling systems the concentration ratio can reach great values since the application of such systems require a great collector's area. The geometric concentration ratio  $C_g$  is given by the equation below where  $A_{dish}$  and  $A_{rec}$  are respectively the area of the concentrator's aperture and the area of the receiver's basis.[5]

$$C_g = A_{dish} / A_{rec} \quad (1)$$

### 3.2 Geometry

The project consists of an oval dish with a diameter of 0.45 meters and a depth of 0.09 meters and the surface area of the dish 0.159 meters, the receiver area is 0.0002 meters, the focus ratio is 795, and the focal length is 0.141 meters.

An oval dish made of wrought iron was obtained and then a good quality reflective material was placed on it with a thickness of 1.5 mm with good reflectivity, and this is what is available in the local markets, as this project was done with a self-effort by the applicants for research to produce energy at the lowest costs and materials available in The local markets are within the reach of everyone, as the project faced some waste of energy due to the scattering of the reflected beam, and the intensity of the sun's rays is not at the required level for this month (the sixth month), the inability to operate the Stirling Engine due to the small diameter of the reflecting plate, with the researchers having all the information and ideas about energy conversion The solar energy using oval mirrors reflecting into kinetic energy, where an alternative was made to Solar Parabola Mirror With Power Generationa, placing a container of water size 180 ml and fixing it in the focus, and the water temperature was measured before placing it in the focus, where it was 32C and after conducting the experiment it was measured for four consecutive times Where the temperature after 10 minutes became 48C, after 15 minutes it became 53.5 C after 20 minutes it became 54C, after 25 minutes it became 55.2 C, and after 30 minutes it became 56 C and this proves The success of the experiment by a percentage and the conversion of solar radiation into energy.

Dish Stirling is a specific type of parabolic dish collectors. In order to reflect the solar radiation it uses reflecting coating materials or mirrors distributed over its aperture's surface but most importantly it takes advantage of its parabolic shape to concentrate sunlight onto the receiver.

The parabolic solar collector of this device is a paraboloid of revolution which is the shape obtained from revolving a parabola around its axis of symmetry. The paraboloid of revolution, and thus the solar collector we are interested in, has a first important parameter which is the focal length. The focal length defines the distance at which the focal point will be located with respect to the vertex of the parabola. This vertex shows the deepest point of the paraboloid. In spatial geometry, the paraboloid of revolution is parameterized as follows [3]

$$X^2 + Y^2 = 4fz$$

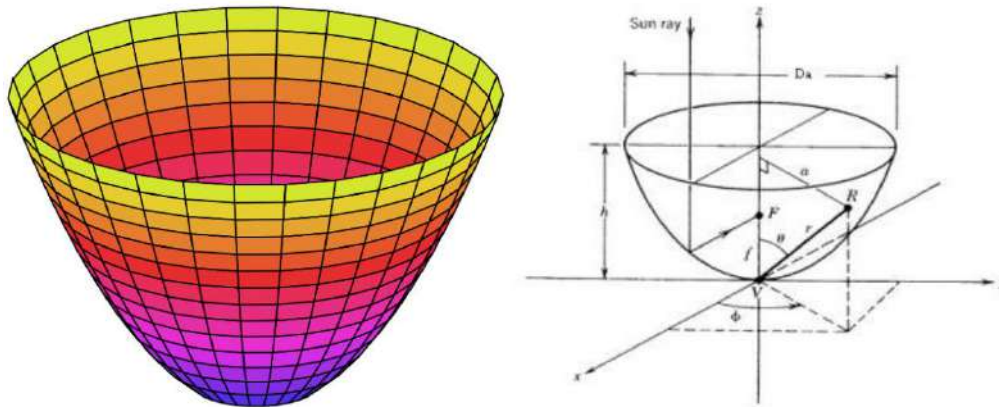


Figure 3-1. A 3D illustration and a Graph of a Paraboloid [4]

The depth and the outer diameter of the paraboloid are other geometric parameters that should be taken into consideration. The depth  $h$  refers to the distance from the center of its aperture to the vertex. On the other hand, the diameter is the diameter of the paraboloid's aperture which is the circular surface of its upper base. These parameters are critical to defining the shape of the solar collector and thus to determining the position of its focal point. If we take the two-dimensional plane, the equation of the parabola will simply be  $y^2 = 4fz$ . As is

directed along the axis and the plane of interest is the  $yz$  plane, the  $y$  parameter is simply the radius of the aperture  $R$ . Therefore, as  $h$  is directed along the  $z$  axis, the equation becomes as follows,  $R^2 = 4fh$  which is equivalent to  $D^2/4 = 4fh$ . Then can be expressed as a function of parameters  $h$  and as shown in equation (2)

$$f = D^2/16h \quad (2)$$

### 3.3 Intensity of solar radiation

Solar radiation at Earth's surface is typically defined as total radiation across a wavelength range of 280 to 4000 nm (shortwave radiation). Total solar radiation, direct beam and

diffuse, incident on a horizontal surface is defined as global shortwave radiation, or shortwave irradiance (incident radiant flux), and is expressed in Watts per square meter ( $\text{W m}^{-2}$ , equal to Joules per second per square meter).

Pyranometers are sensors that measure global shortwave radiation. TES 1333R Datalogging Solar Power Meter incorporate silicon-cell pyranometers, and are only sensitive to a portion of the approximately 350-1100 nm (approximately 80 % of total shortwave radiation is within this range)



Figure 3-2 .Measurement of the intensity of solar radiation

### 3.4 Stirling Engine

The Stirling engine is a type of heat engines which takes advantage from the ability of gases to expand when heated and contract when they are cooled. In the engine, the gas is enclosed in fixed volume cylinders; therefore, its pressure will increase when it is heated and cooled down to decrease its temperature. The pistons of the cylinders are moved out when the pressure of the gas is high and they are moved in when the pressure is low. The movement of the cylinders causes a crank-shaft to rotate and produce mechanical work. The most used engine for solar energy applications is the Alpha Stirling Engine. It consists of a two-cylinder engine with a hot and a cold cylinder. The working principle is obviously similar to any other Stirling engine. The working fluid, which is in this case hydrogen for its high performance according to literature [10], is heated and expand in the cylinder which forces the hot piston to move downward and cause the fluid to move to the cold cylinder where it continues to expand extracting then more energy from it. The momentum of the crankshaft forces the hot piston to the top and extracting the fluid from the cold cylinder where its pressure drops because of the cooling [11]. The regenerator is not used

in all Stirling engines but serves to improve the efficiency of the engine. It is located at the level of the air passage between the two cylinders. Its main purpose is to extract the heat from the hot cylinder when the working gas is flowing towards the cold one; therefore, the heat is being used again in the heating process. The cycle is shown in the figure below

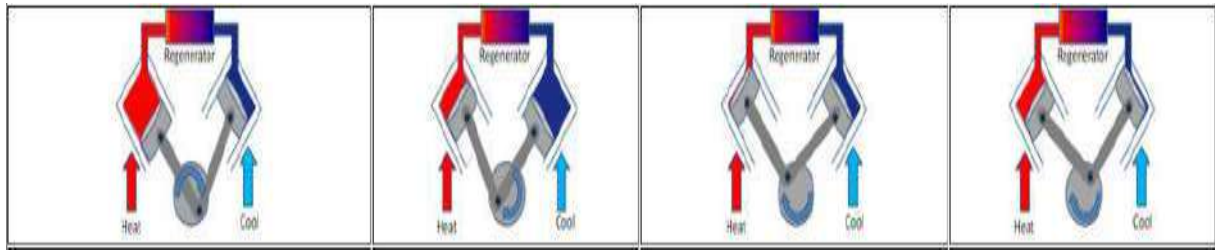


Figure 3-3. Working Cycle of Stirling Engine [11].





Figure 3-4. Stirling Engine

### 3.5 Reflector Material Selection

The selection of the material to be used to reflect the incoming solar radiation is a critical design criterion. It affects heavily the amount of solar radiation transmitted to the receiver. The surface of the collector must be highly reflective in order to minimize the energy absorbed by the reflector material and reflect most of the incident solar radiation to the focal plane. be in the form of a polished metal such as aluminum or stainless steel. The most used material is silver coated glass. The material must also resist climatic conditions to ensure its long-lasting operating lif Some of the reflector materials are proposed in the table below along with their reflectivity and emissivity [8].



### 3-1 Table of Potential Reflector Mater [9]

Materials	Reflective (%)	Emissive (%)
Polymeric film, non metal	98	2
Aluminum, acrylic	98	2
Silver, aluminum acrylic	97	3
Silver, acrylic	95	5
Aluminum	86	14
Aluminum, polyethylene	97	3
Plexiglas with mirror	90	10
Thermoplastic, silver, gold, brass, etc.	80	20
Aluminum mylar	97	3
Polymer, copper, silvered, alumina	97	3
Polished stainless	50	50
Ceramic metallic coating layer	95	5
Glass/silver 4 mm	93.8	6.2
Glass/silver 2 mm	94	6
Glass/silver 1 mm	94.6	5.4
Miro 2-95	88.6	11.4
Miro 3-95	91.1	8.9
Anod aluminum	86.8	13.2
1000.90	89.8	10.2
ECP305+/aluminum	95.6	4.4
ECP305+/glass	96.1	3.9
Sunflex (polymer/aluminum)	86.9	10.1
SA 85/glass	88.1	11.9
SA 85/steel	88.2	11.8
Sol-gel coated silver	95.5	4.5
Sol-gel coated aluminum	91	9

## Energy Laws [2]

$$Q_u = A_a F_R \left\{ S - \frac{A_r U_L}{A_a} (T_i - T_a) \right\} \quad (3)$$

$$F'' = \frac{F_R}{F'} = \frac{\dot{m} C_p}{A_r U_L F'} \left\{ 1 - e^{-A_r U_L F' / \dot{m} C_p} \right\} \quad (4)$$

$$F' = \frac{U_0}{U_L} \quad (5)$$

## **Chapter four**

### **Results**



## 4.1 Readings

The readings were taken from nine solar time in the morning until three solar time in the evening and the interval between one reading and another is only one hour, on the days 10, 11, 12, 13, and 14 of June, where varying rates of energy were recorded and peaked at twelve solar time in the evening, as shown in Tables and charts below

### 4-1 Table Read solar radiation

2021/6/10

Sequence	Solar Time	Reading
1	9:00	820.5
2	10:00	975.4
3	11:00	1076
4	12:00	1126
5	13:00	1104
6	14:00	1015
7	15:00	951.7

2021/6/11

Sequence	Solar Time	Reading
1	9:00	840.1
2	10:00	1024
3	11:00	1140
4	12:00	1145
5	13:00	1112
6	14:00	1003
7	15:00	933.5

2021/6/12

Sequence	Solar Time	Reading
1	9:00	898.2
2	10:00	1063
3	11:00	1143
4	12:00	1162
5	13:00	1148
6	14:00	1110
7	15:00	985.7

2021/6/13

Sequence	Solar Time	Reading
1	9:00	950.9
2	10:00	1019
3	11:00	1124
4	12:00	1132
5	13:00	1101
6	14:00	1032
7	15:00	911.9

2021/6/14

Sequence	Solar Time	Reading
1	9:00	912.1
2	10:00	1028
3	11:00	1103
4	12:00	1144
5	13:00	1113
6	14:00	974.2
7	15:00	857.9

## 4-2 Table of Total highest radiation

sequence	Solar Time	Total Reading	Date
1	9:00	950.9	2021/6/13
2	10:00	1063	2021/6/12
3	11:00	1143	2021/6/12
4	12:00	1162	2021/6/12
5	13:00	1148	2021/6/12
6	14:00	1110	2021/6/12
7	15:00	985.7	2021/6/12

## Discussion

Solar Conting System is considered one of the most important systems affecting energy generation, especially with a continuous and effective energy source like the sun. Solar energy applications using mirrors are better than other solar energy applications in terms of efficiency and because they have the lowest installation and maintenance costs with reasonable thermal efficiency . In this research the intensity and quantity of solar radiation is the variable affecting the highest thermal efficiency of a system. Five experiments were conducted for five days The experiments proved that the produced thermal energy increases with the increase in the intensity of solar radiation and that is the efficiency of the system and it has proven that (Thermal Solar Traffic System) is effective in Iraq within the rate of solar radiation in it.

## References

- [1] I. L. Mohammed, "Design and Development of a Parabolic Dish Solar Thermal Cooker," *International Journal of Engineering Research and Applications*, vol. 3, no. 4, p. 1179-1186, 2013.
- [2] J.A. Duffie, W.A. Beckman (2006), *Solar Engineering of Thermal Processes*, Hoboken, NJ: Wiley..
- [3] M. Günther and R. Shahbazfar, "Solar Dish Technology," in *Advanced CSP Teaching Materials*.
- [4] V. Thakkar, A. Doshi and A. Rana, "Performance Analysis Methodology for Parabolic Dish Solar," *Journal of Mechanical and Civil Engineering*, vol. 12, no. 1, pp. 101-114, 2015.
- [5] T. Dwyer, "The terminology and concepts used to determine the magnitude and direction of incident solar radiation," *CIBSE Journal*, July 2013. [Online]. Available: <https://www.cibsejournal.com/cpd/modules/2013-07/>. [Accessed 18 February 2019].
- [6] SolarPACES, "How CSP Works: Tower, Trough, Fresnel or Dish," 2018. [Online]. Available: <https://www.solarpaces.org/how-csp-works/>. [Accessed 12 02 2019].
- [7] ScienceDirect, "Parabolic Trough-An Overview," [Online]. Available: <https://www.sciencedirect.com/topics/engineering/parabolic-trough>. [Accessed 02 February 2019].
- [8] I. Aoukli, "Anti-Soiling Protective Coating for CSP Reflectors," *Al Akhawayn University, Ifrane*, 2018.
- [9] A. Z. Hafez, K. El-Metwally, A. Soliman and I. Ismail, "Solar Parabolic Dish Stirling Engine System Design, Simulation and Thermal Analysis," *Energy Conversion and Management*, no. 126, p. 60-75, 2016.
- [10] A. Yerbury, A. Coote, V. Garaniya and H. Yu, "Design of a Solar Stirling Engine for Marine and Offshore Applications," *International Journal of Renewable Energy Technology*, vol. 7, no. 1, 2016.
- [11] Electropaedia, "Battery and Energy Technologies," [Online]. Available: [https://www.mpoweruk.com/stirling\\_engine.htm](https://www.mpoweruk.com/stirling_engine.htm). [Accessed 27 March 2019].v42
- [12] A. Asnaghi, S. M. Ladjevardi, P. S. Izadkhast and A. H. Kashani, "Thermodynamics Performance Analysis of Solar Stirling Engines," *ISRN Renewable Energy*, 2012.

## الخلاصة

يدرس البحث إمكانية توليد الطاقة باستخدام نظام الدش الشمسي هذا لتركيز الأشعة عند النقطة المحورية لتوليد الحرارة من الشمس والتي تتركز في النقطة المركزية بمحرك استرليني يقود مكبس ستيرلينغ ويولد طاقة كهربائية باستخدام مثل هذه الطريقة مفيد جدًا لأنه صديق للبيئة

(لا يولد ملوثات) غير مكلف من الناحية الفنية ولا يتطلب وقودًا عضويًا. يتكون مشروعنا من نظام طبق يتكون من أجزاء لاصقة من رقائق الألمنيوم ومحرك ستيرلينغ.

وتتمثل فائدة هذا المشروع في إنتاج الطاقة الحرارية وتحويلها إلى أي شكل من أشكال الطاقة.



وزارة التعليم العالي والبحث العلمي  
كلية دجلة الجامعة الاهلية  
قسم هندسة تقنيات التبريد والتكييف

## انتاج الطاقة باستخدام مرايا ببيضوية عاكسة

### بحث مقدم

الى كلية دجلة الجامعة الاهلية / قسم هندسة تقنيات التبريد والتكييف وهو جزء من متطلبات نيل  
شهادة البكالوريوس في هندسة تقنيات التبريد والتكييف

### من قبل

عمار عبد الرحيم عمار

عمر ماجد عابد

مهند مالك عبد

علي عبد عجاج ابراهيم

عبد الله عصام حسين

بإشراف

م. محمد حمزة داود

1442 هـ

2021 م

*Ministry of Higher Education and Scientific Research*

*Dijlah University College*

*Refrigeration and Air Conditioning*

*Engineering Techniques Department*



# **Study on Fluid Behavior in the Wake Region of Bluff Bodies**

*A project Submitted to the Refrigeration and Air Conditioning Engineering Techniques Department at Dijlah University College in partial fulfillment of the requirements for Degree of Bachelor in Refrigeration and Air Conditioning Engineering Techniques*

***By:***

Noor Esam Abdul-Wahid  
Dhyaa Hayder Kareem  
Wathiq Abbas Jassim  
Salam Ismael Khalil

***Supervisor by:***  
***Dr. Oula M. Hadawi***

***1442 A.H.***

***2021 A.D***

بِسْمِ اللَّهِ الرَّحْمَنِ الرَّحِيمِ

(وَمَا كَانَ الْمُؤْمِنُونَ لِيَنفِرُوا كَافَّةً فَلَوْلَا نَفَرَ

مِنْ كُلِّ فِرْقَةٍ مِنْهُمْ طَائِفَةٌ لِّيَتَفَقَّهُوا فِي الدِّينِ

وَلِيُنذِرُوا قَوْمَهُمْ إِذَا رَجَعُوا إِلَيْهِمْ لَعَلَّهُمْ

يَحْذَرُونَ )

التوبة: 122

صدق الله العظيم



# ***Supervisor Certificate***

***We certify that this project entitled (Study on fluid behavior in the wake region of bluff bodies)***

***Prepared by:***

Noor Esam Abdul-Wahid  
Dhyaa Hayder Kareem  
Wathiq Abbas Jassim  
Salam Ismael Khalil

***Has been carried out completely under our supervision at the  
Dijlah University College in partial fulfillment of the  
requirements for Degree of Bachelor in Refrigeration and Air  
Conditioning Engineering Techniques***

***Signature:***

***Oula M. Hadawi***

***Date: / /2021***

***Approved by the head of Refrigeration and Air Conditioning  
Engineering Techniques Department:***

***Signature***

***Dr. Firas Maan Abdulsattar***

***Head of Refrigerating and Air***

***Conditioning Engineering Department***

***Date: / /2021***

# ***Examining committee certificate***

**We certify that this project entitled (*Study on fluid behavior in the wake region of bluff bodies*)**

Submitted by:

Noor Esam Abdul-Wahid  
Dhyaa Hayder Kareem  
Wathiq Abbas Jassim  
Salam Ismael Khalil

and as an examining committee examined the students in its content and that in our opinion it meets the standards of a project for the Degree of Bachelor in Refrigeration and Air Conditioning Engineering Techniques.

*Signature*

***Dr. Oula M. Hadawi***

***Date: / / 2021***

***(Supervisor)***

*Signature*

***Dr. Firas Maan Abdulsattar***

***Date: / / 2021***

***(Member)***

*Signature*

***Lec. Maha Ali Hussain***

***Date: / / 2021***

***(Member)***

## **Dedication**

Praise be to Allah who gave me health, strength and patience to conduct  
this work

To the fountain of patience and optimism and hope  
**My dear mother**

To the big heart  
**My dear father**

To those who have demonstrated to me what is the most beautiful of life  
**My brothers and sisters**

To the people who paved our way of science and knowledge  
All our  
**Educational Stuff**

To those who support me during my journey my  
**Friends and colleagues**

To the soul of our classmate **Mohammed Abd Raja**, may Allah  
Almighty rest his soul in peace, Amen.

I dedicate this research

**Researchers**

## Contents

List of Figures .....	VI
Abstract .....	1
Chapter 1 – Introduction .....	2
1.1 Flow over a Bluff Body .....	2
1.2 Vortex Shedding .....	2
1.3 The Cylinder in Cross Flow – Flow Considerations .....	4
1.4 Flow Visualization .....	6
1.5 Aim of the Project .....	9
1.6 Objectives .....	9
Chapter 2- Theory .....	10
2.1 Reynolds Number .....	10
2.1.1 Laminar flow .....	11
2.1.2 Turbulent flow .....	12
2.2 Governing equations .....	13
2.2.1 Mass conservation law .....	13
2.2.2 Continuity equation .....	13
Chapter 3 – Experimental Setup and Calculations .....	15
3.1 Materials of Wind Tunnel – Test Rig .....	15
3.2 Calculations .....	18
Chapter 4 - Results and Discussion .....	22
4.1 Results .....	22
Chapter 5 – Future Work .....	25
5.1 Challenges while working on the project .....	25
5.2 Recommendations for Future Work .....	25
References .....	26

## **List of Figures**

Figure 1-1: Vortex Generation	3
Figure 1-2: Different characteristic flow regimes manifested by a cylinder in cross flow [1]	4
Figure 1-3: Boundary layer separation	5
Figure 1-4: Surface flow visualization; oil paint (left) and dye (right)	6
Figure 1-5: Surface flow visualization for formula 1 tests aerodynamics	7
Figure 1-6: Shadowgraph and Schlieren flow visualization	7
Figure 1-7: Flow visualization using smoke, ink and hydrogen bubbles	8
Figure 2-1: One-dimensional system showing control volume	14
Figure 3-1: Wind tunnel	16
Figure 3-2: Implantation the wind tunnel, anemometer, bluff bodies and smoke generator	17
Figure 4-1: Flow over a cylinder	22
Figure 4-2: Flow over a wing	23
Figure 4-4: flow over a sphere	24

## **Abstract**

Flow over a bluff body is a common occurrence associated with fluid flowing over an obstacle or with the movement of a natural or artificial body. Evident examples are the flows past an airplane, a submarine and an automobile, and wind blowing past a bridge and a high-rise building.

The most important phenomenon associated with flow passing a bluff body is the generation of vortices. This vortex shedding occurs over a wide range of Reynolds numbers, causing serious structural vibrations, acoustic noise and resonance, enhanced mixing, and significant increases in the mean drag and lift fluctuations. Therefore, the effective control of vortex shedding is important in engineering applications. The current project aimed at studying the phenomenon of vortex shedding in the wake region of bluff bodies by investigating the possible techniques of flow visualization upstream and downstream the bluff body.

Although many different shapes of bluff bodies exist, three representative shapes were considered in the present project: the circular cylinder, a 2D bluff body with a blunt trailing edge, and the sphere. The circular cylinder and sphere are the representative 2D and 3D bluff bodies, respectively, and their separation points change depending on the Reynolds number. Conversely, in the case of the 2D blunt-based bluff body, the separation is fixed at the trailing edge, and hence the flow suddenly changes at the trailing edge from a boundary-layer flow to a wake, which is quite different from the case of both the circular cylinder and sphere.

## **Chapter 1 – Introduction**

### **1.1 Flow over a Bluff Body**

Flow around bluff bodies is of great importance today not only in automotive industry, but in every industrial department or product that is associated with any kind of flow around an object, posing one of the greatest factors to take into consideration in terms of designing a new car, aero plane, ship, etc. A strong background and knowledge in aerodynamics and the physical mechanisms governing their basic principles and phenomena is essential in order to achieve improvement of the flow through various means. More specifically, in the case of automotive engineering an analysis and results were presented mostly by gaining experimental data on various automotive shapes. However, setting up an experimental process is rigorous and time consuming, especially when the setup has to be altered to achieve the desirable results.

The interaction between a fluid flow and a bluff body is extremely complex. Different response modes and flow phenomena exist depending on the flow characteristics, the body geometry and the structural properties like stiffness and damping. This project, particularly, aims at studying the phenomenon of vortex shedding in the wake region of bluff bodies.

### **1.2 Vortex Shedding**

A vortex is a physics phenomenon that occurs when a gas or a liquid moves in circles. At the center is a vortex line that the matter swirls around. They are formed when there is a difference in the velocity of what surrounds the line. Hurricanes, tornadoes and air moving over a plane wing are examples of vortices. Vortices are a major component of turbulent flow.

Vortex shedding is an oscillating flow and occurs when air flows past a bluff body, figure (1-1). This type of vortex typically causes structural problems as the intensity of the accumulation of the wind around structures results into failure. When a speeding wind becomes in contact with a building's exterior surface, a build up of wind pressure accumulates. Since wind force is a dynamic action, the pressure created at a building's surface also produces vibrations. If the peak wind pressure is high enough, these vibrations can turn into mini earthquakes at certain levels of a structure where the wind direction is passing. This causes a tall building to sway, and if dynamic damping is not provided, the structure could potentially collapse.



Figure 1-1: Vortex Generation



### 1.3 The Cylinder in Cross Flow – Flow Considerations

Examples of cylindrical objects in cross flow (i.e. with the freestream flow direction normal to the cylinder axis) include wind and water flow over offshore platform supports, flow across pipes or heat exchanger tubes, and wind flow over power and phone lines. The drag coefficient for such an object depends strongly on the behavior of the fluid around the cylinder, Figure (1-2). For example, depending on the Reynolds number,  $Re = \rho U D / \mu$ , the flow pattern near the cylinder can vary significantly, where  $\rho$  and  $\mu$  are the fluid density and viscosity,  $U$  is the upstream velocity, and  $D$  is the cylinder diameter. For low velocities (i.e.  $Re_D < 5$ ), the flow around the cylinder is unseparated; whereas for  $5 < Re_D < 40$ , two stationary eddies form immediately downstream of the cylinder. For higher velocities (i.e.  $Re_D > 40$ ), an unsteady wake flow occurs, the width and nature of which depends on the Reynolds number. This behavior is due to the fact that the flow over a cylinder usually experiences boundary layer separation and very strong flow oscillations in the wake region of the body.

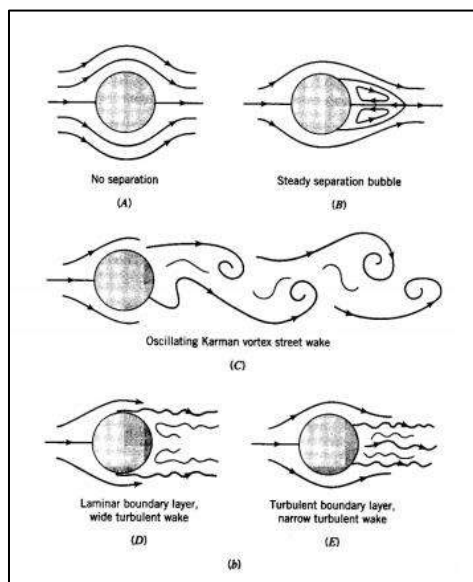


Figure 1-2: Different characteristic flow regimes manifested by a cylinder in cross flow [1]

The flow separation occurs due to boundary layer separation, which means that the flow can no longer follow the profile of the body around which it flows and separates turbulently from it.

Separation occurs when the fluid, no longer able to follow the contour of the (curved) surface and breaks away from it. The breakaway of the boundary layer first occurs at the separation point where the velocity gradient within the boundary layer is equal to zero. Several aspects of this flow are interesting, most notably being the regular vortex-shedding pattern. The flow pattern in the wake of a circular cylinder depends mainly on Reynolds number of the upstream flow and the cylinder diameter. As stated earlier Reynolds number plays the key role in determining the state of such flows. Figure (1-3) shows the stages of boundary layer separation, the point on the cylinder surface at where the free-stream flow hits the cylinder called the stagnation point.

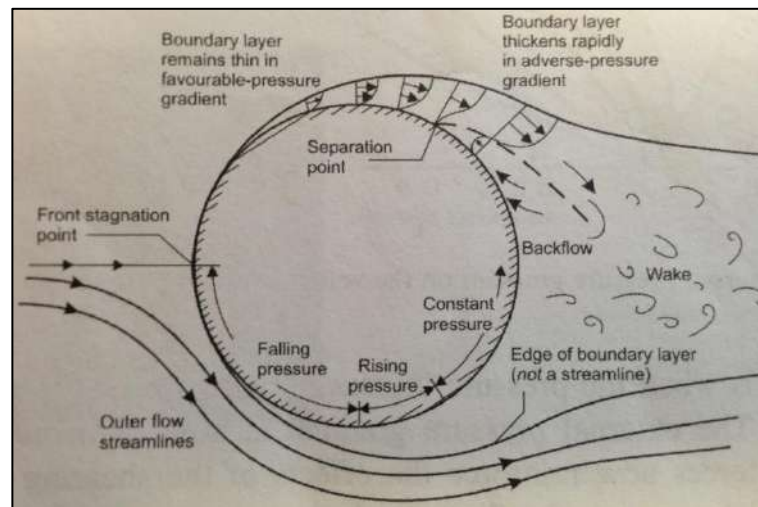


Figure 1-3: Boundary layer separation

Many researches, experimental and numerical, were conducted to study and visualize the vortex shedding in the wake region of a cylinder due to its simple physical shape.

## 1.4 Flow Visualization

Flow visualization is the art of making flow patterns visible. Most fluids (air, water, some oils, etc.) are transparent, thus their flow patterns are invisible to the naked eye without methods to make them this visible.

Historically, such methods included experimental methods. With the development of computer models and CFD simulating flow processes (e.g. the distribution of air-conditioned air in a new car), purely computational methods have been developed.

In experimental fluid dynamics, flows are visualized by three methods:

- **Surface flow visualization:** This reveals the flow streamlines in the limit as a solid surface is approached. Colored oil applied to the surface of a wind tunnel model provides one example (the oil responds to the surface shear stress and forms a pattern), see figure (1-4) and figure (1-5).

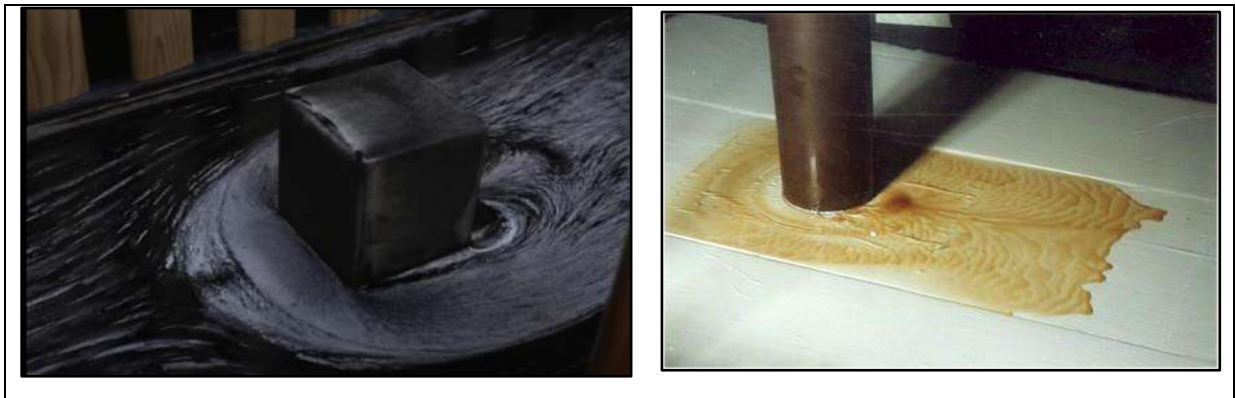


Figure 1-4: Surface flow visualization; oil paint (left) and dye (right)

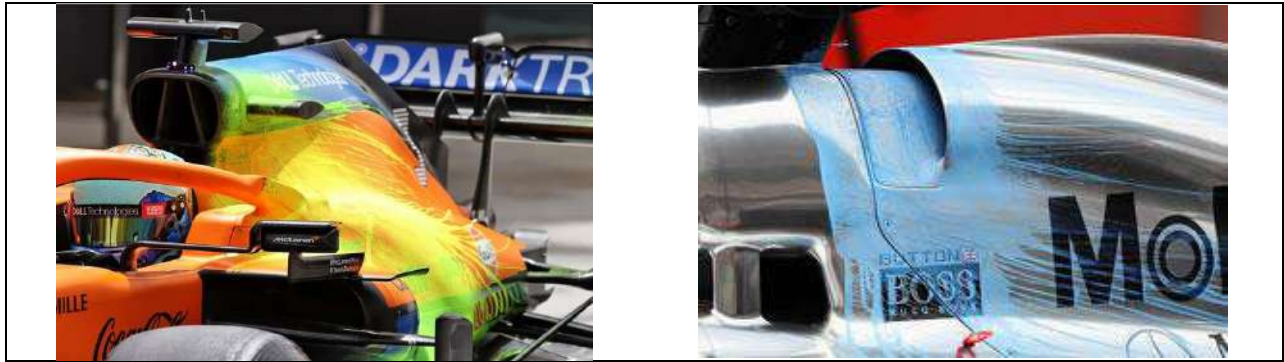


Figure 1-5: Surface flow visualization for formula 1 tests aerodynamics

- **Optical methods:** Some flows reveal their patterns by way of changes in their optical refractive index. These are visualized by optical methods known as the shadowgraph and interferometry. More directly, dyes can be added to (usually liquid) flows to measure concentrations; typically employing the light attenuation or laser-induced fluorescence techniques, see figure (1-6).

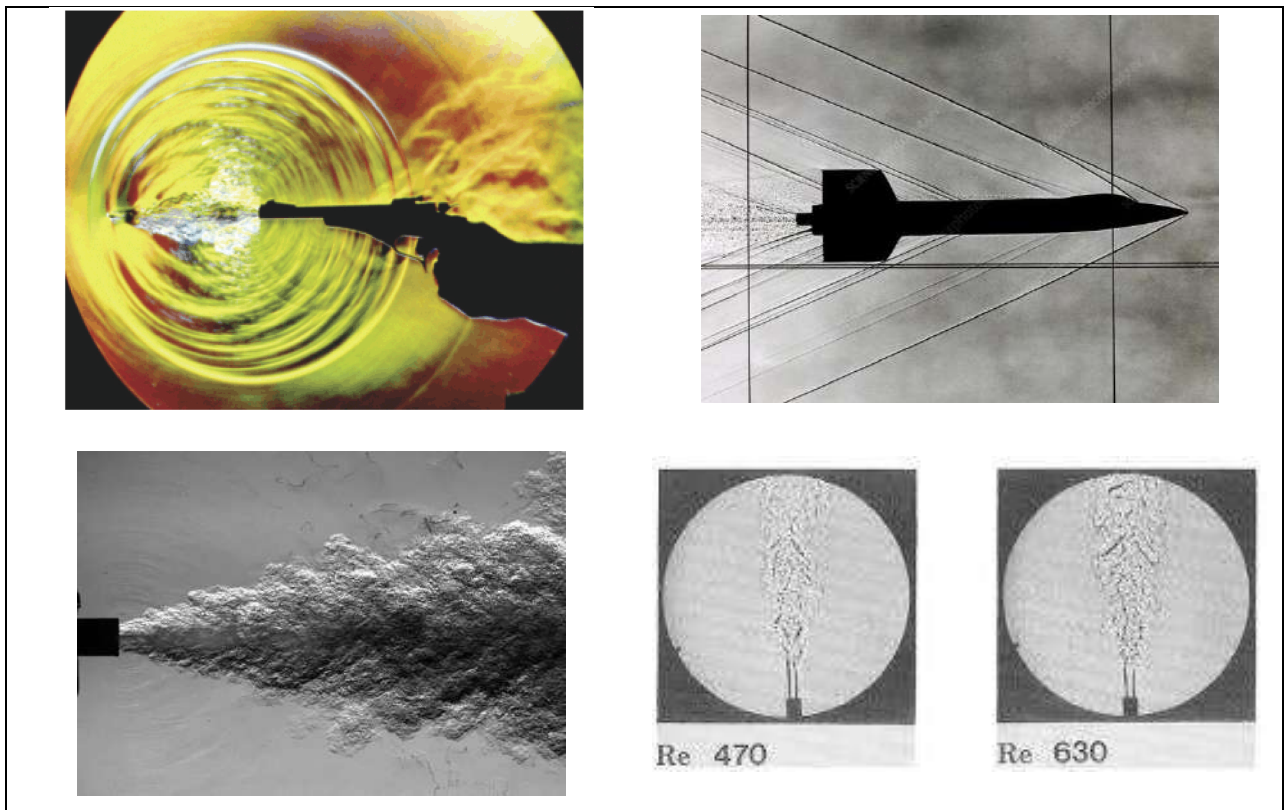


Figure 1-6: Shadowgraph and Schlieren flow visualization

- **Particle tracer methods:** Particles, such as smoke or microspheres, can be added to a flow to trace the fluid motion. The particles can be illuminated with a sheet of laser light in order to visualize a slice of a complicated fluid flow pattern. Assuming that the particles faithfully follow the streamlines of the flow. Particles with densities that match that of the fluid flow will exhibit the most accurate visualization [2], see figure (1-7).

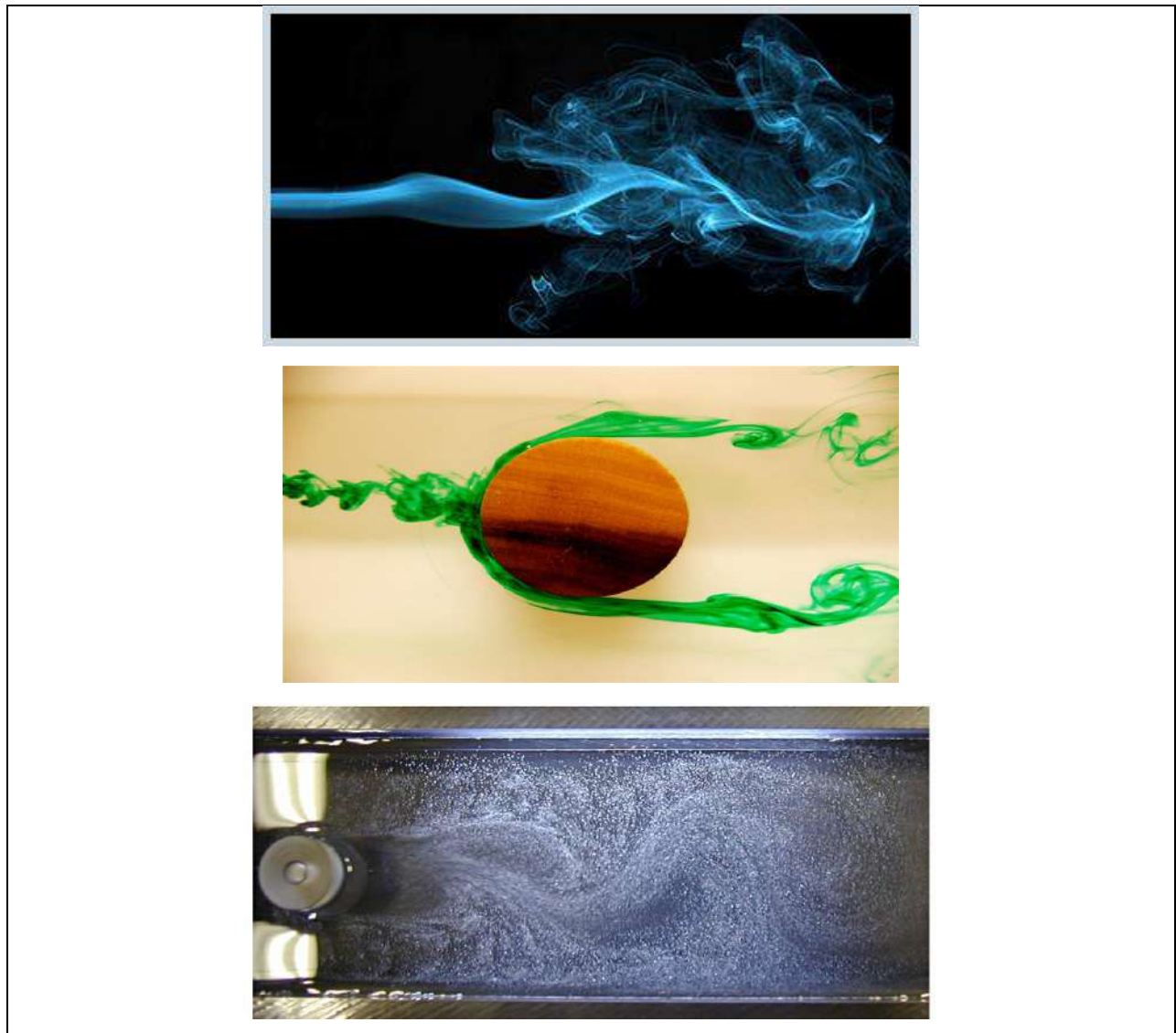


Figure 1-7: Flow visualization using smoke, ink and hydrogen bubbles

Some techniques of Particle tracer methods involve smoke generator, dry ice, hydrogen bubbles (with water flows). In the current project the particle tracer method were investigated intensively.

## **1.5 Aim of the Project**

The aim of the current project is to provide more insight into the complicated flow patterns and explain the physical properties associated with the flow around the body configuration. The behavior the flow structures exhibit around this benchmark test, alongside various parameters that affect the physical phenomena governing the flow around the bluff body in different flow conditions, were be examined.

## **1.6 Objectives**

The objectives of this Research Thesis are the following

- 1) Investigating, experimentally, the flow over bluff body. Cylinder with a circular profile, sphere and wing were considered as bluff bodies.
- 2) Exploring different techniques of flow visualization
- 3) Capturing the phenomena of vortex shedding



## Chapter 2- Theory

### 2.1 Reynolds Number

The Reynolds number (Re) helps predict flow patterns in different fluid flow situations. At low Reynolds numbers, flows tend to be dominated by laminar (sheet-like) flow, while at high Reynolds numbers flows tend to be turbulent. The turbulence results from differences in the fluid's speed and direction, which may sometimes intersect or even move counter to the overall direction of the flow (eddy currents). These eddy currents begin to churn the flow, using up energy in the process, which for liquids increases the chances of cavitation. Reynolds numbers are an important dimensionless quantity in fluid mechanics.

The Reynolds number has wide applications, ranging from liquid flow in a pipe to the passage of air over an aircraft wing. It is used to predict the transition from laminar to turbulent flow, and is used in the scaling of similar but different-sized flow situations, such as between an aircraft model in a wind tunnel and the full-size version.

The Reynolds number is the ratio of inertial forces to viscous forces. The Reynolds number is a dimensionless number used to categorize the fluids systems in which the effect of viscosity is important in controlling the velocities or the flow pattern of a fluid. Mathematically, the Reynolds number, Re, is defined as

$$\text{Re} = \frac{\rho v d}{\mu} \quad (1)$$

Where:

$\rho$  = density ( $kg/m^3$ )

$v$  = velocity (m/sec)

$d$  = diameter (m)

$\mu$  = viscosity (pa/sec)

The Reynolds number is used to determine whether a fluid is in laminar or turbulent flow. Based on the API 13D recommendations, it is assumed that a Reynolds number less than or equal to 2100 indicates laminar flow, and a Reynolds number greater than 2100 indicates turbulent flow.

### **2.1.1 Laminar flow**

In fluid dynamics, laminar flow is characterized by fluid particles following smooth paths in layers, with each layer moving smoothly past the adjacent layers with little or no mixing. At low velocities, the fluid tends to flow without lateral mixing, and adjacent layers slide past one another like playing cards. There are no cross-currents perpendicular to the direction of flow, nor eddies or swirls of fluids. In laminar flow, the motion of the particles of the fluid is very orderly with particles close to a solid surface moving in straight lines parallel to that surface. Laminar flow is a flow regime characterized by high momentum diffusion and low momentum convection.

When a fluid is flowing through a closed channel such as a pipe or between two flat plates, either of two types of flow may occur depending on the velocity and viscosity of the fluid: laminar flow or turbulent flow. Laminar flow occurs at lower velocities, below a threshold at which the flow becomes turbulent. The velocity is determined by a dimensionless parameter characterizing the flow called



the Reynolds number, which also depends on the viscosity and density of the fluid and dimensions of the channel. Turbulent flow is a less orderly flow regime that is characterized by eddies or small packets of fluid particles, which result in lateral mixing. In non-scientific terms, laminar flow is *smooth*, while turbulent flow is *rough*.

### **2.1.2 Turbulent flow**

In fluid dynamics, turbulence or turbulent flow is fluid motion characterized by chaotic changes in pressure and flow velocity. It is in contrast to a laminar flow, which occurs when a fluid flows in parallel layers, with no disruption between those layers.

Turbulence is commonly observed in everyday phenomena such as surf, fast flowing rivers, billowing storm clouds, or smoke from a chimney, and most fluid flows occurring in nature or created in engineering applications are turbulent. Turbulence is caused by excessive kinetic energy in parts of a fluid flow, which overcomes the damping effect of the fluid's viscosity. For this reason turbulence is commonly realized in low viscosity fluids. In general terms, in turbulent flow, unsteady vortices appear of many sizes which interact with each other, consequently drag due to friction effects increases. This increases the energy needed to pump fluid through a pipe.

The onset of turbulence can be predicted by the dimensionless Reynolds number, the ratio of kinetic energy to viscous damping in a fluid flow. However, turbulence has long resisted detailed physical analysis, and the interactions within turbulence create a very complex phenomenon. Richard Feynman has described turbulence as the most important unsolved problem in classical physics.

## **2.2 Governing equations**

In mid-18th century, the French engineer Claude Navier and the Irish mathematician George Stokes derived the well-known equations of fluid motion, known as the Navier- Stokes equations. These equations have been derived based on the fundamental governing equations of fluid dynamics, called the continuity, the momentum and the energy equations, which represent the conservation laws of physics.

### **2.2.1 Mass conservation law**

In physics and chemistry, the law of conservation of mass or principle of mass conservation states that for any system closed to all transfers of matter and energy, the mass of the system must remain constant over time, as the system's mass cannot change, so quantity can neither be added nor be removed. Therefore, the quantity of mass is conserved over time.

### **2.2.2 Continuity equation**

Equation based on the law of conservation of mass. Applying this concept to fluid flow, we ensure that the change of mass in a control volume is equal to the mass that enters through its faces minus the total mass leaving its faces.

The expression of the continuity equation for the system shown in figure (2-1), is as following:

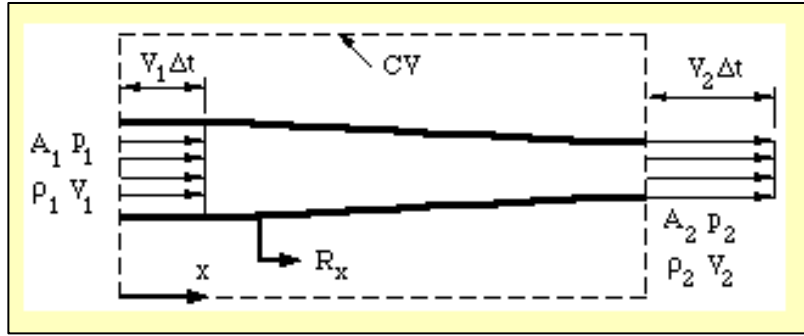


Figure 2-1: One-dimensional system showing control volume

$$\sum Mass_{in} = \sum Mass_{out} \quad (2)$$

$$m_1 = m_2$$

$$\rho * Q_1 = \rho * Q_2$$

$$\rho * V_1 * A_1 = \rho * V_2 * A_2$$

For incompressible fluids, such as air and water, the density  $\rho$  is constant. Therefore the continuity equation can express as:

$$V_1 * A_1 = V_2 * A_2 \quad (3)$$

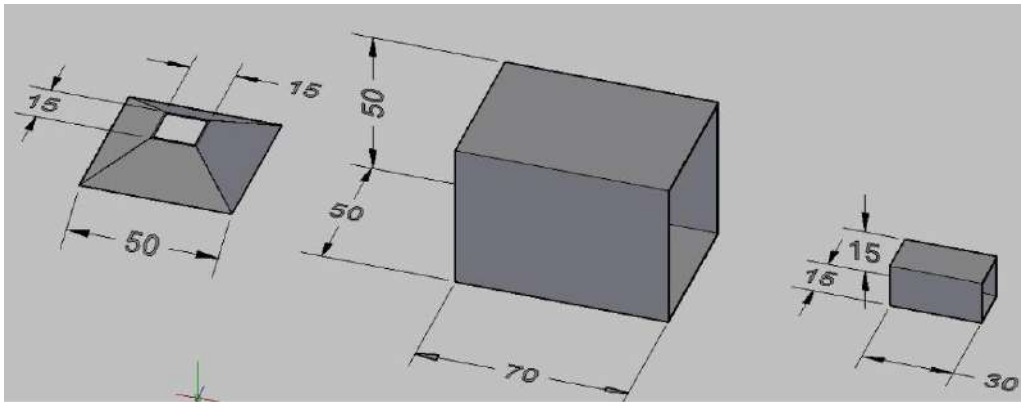
## **Chapter 3 – Experimental Setup and Calculations**

### **3.1 Materials of Wind Tunnel – Test Rig**

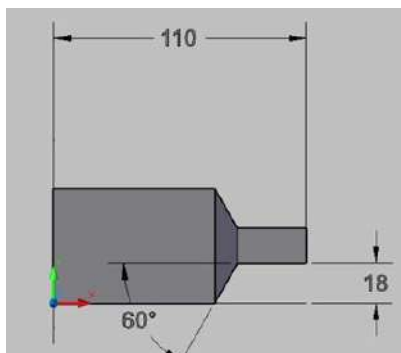
A wind tunnel with a configuration as shown in figure (3-1) and figure (3-2) was designed to study the behavior of a fluid flow in the wake region of bluff bodies. A particular attention was made to visualize the phenomenon of vortex shedding in the wake region. The tunnel consists of a replaceable circular cylinder, which was used as a model of a bluff body, located horizontally inside the wind tunnel of dimensions (100 cm x 50 cm). The flow was forced to pass over the cylinder using a suction fan installed at the exit of the tunnel. A fan speed controller was used to adjust the exit velocity and control the flow rate entering the wind tunnel. The rig walls were made of a perspex material of clear Acrylic sheet of approximately 10 cm thickness to gain optical access to the flow field.

Smoke was utilized as a seeding since the densities of the smoke and air are close enough; this allows a good particle suspension. A smoke generator tool was used to generate the smoke, and it was located at the entrance of the wind tunnel so that the smoke particles can accurately follow the flow.

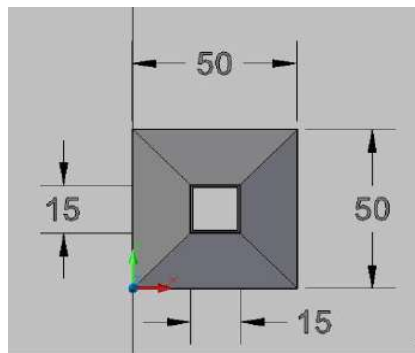
The velocity at the outlet of the rig was measured by using a remote vane digital anemometer. The continuity equation was used to calculate the inlet flow velocity, and then  $Re$  was calculated as well. The following section shows inlet and outlet velocities that are corresponding to the range of Reynolds numbers involved.



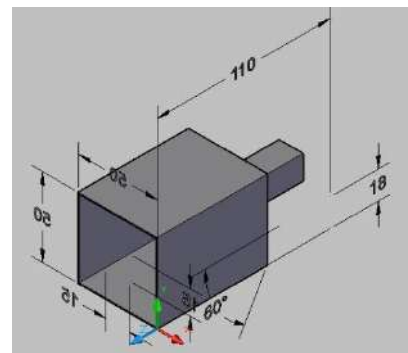
Schematic diagram of the wind tunnel



Side view



Front view



Isometric view

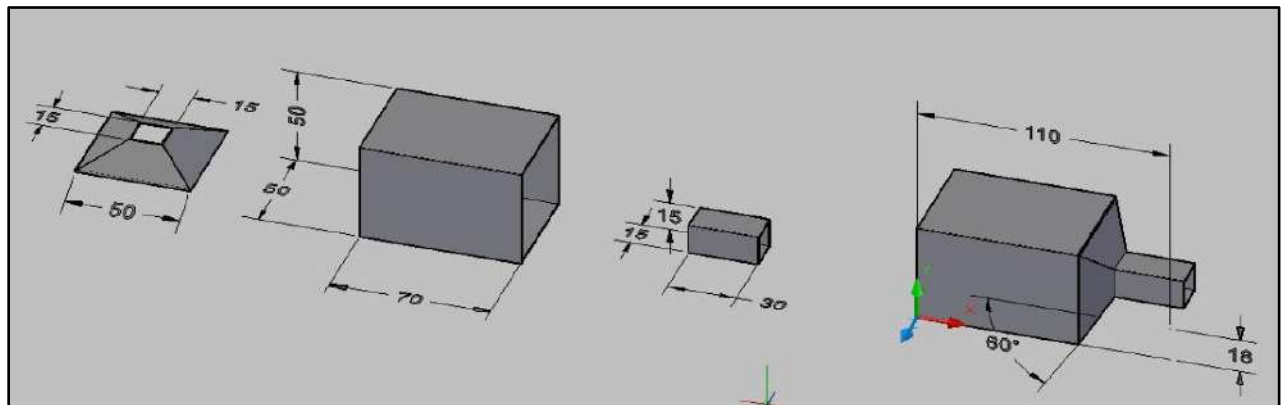


Figure 3-1: Wind tunnel

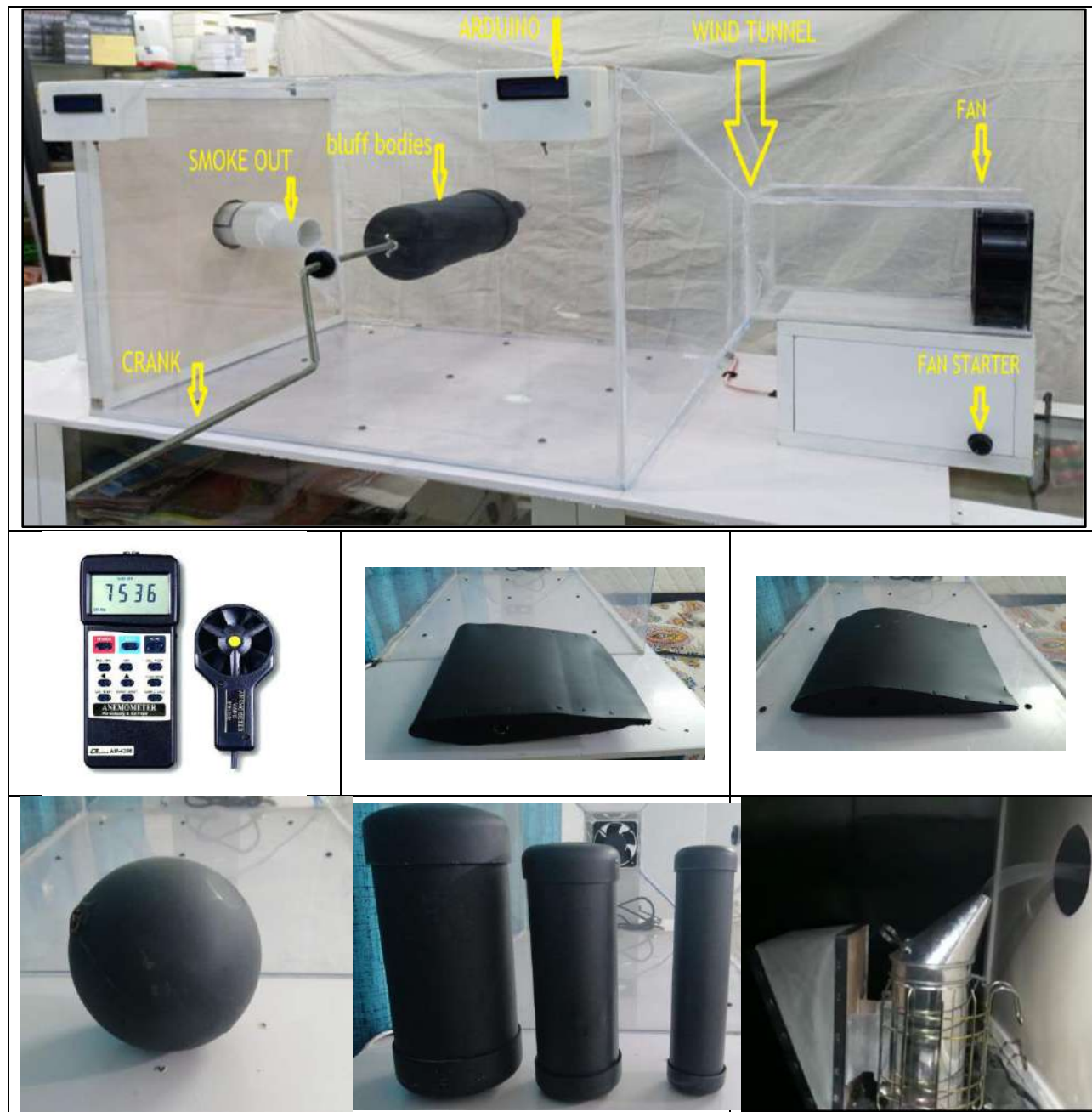


Figure 3-2: Implantation the wind tunnel, anemometer, bluff bodies and smoke generator

### 3.2 Calculations

$$V_1 = \frac{V_2 * A_2}{A_1}$$

$$Re_D = \frac{\rho V_1 D}{\mu}$$

Where:

V = velocity (m/sec)

A = cross- sectional area (m<sup>2</sup>)

Q = volume flow rate m<sup>3</sup>/sec

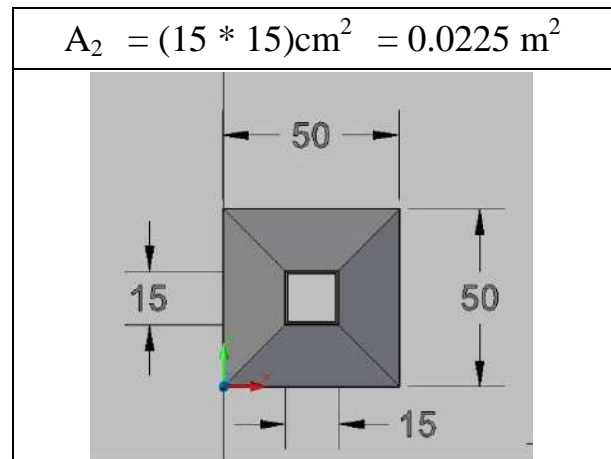
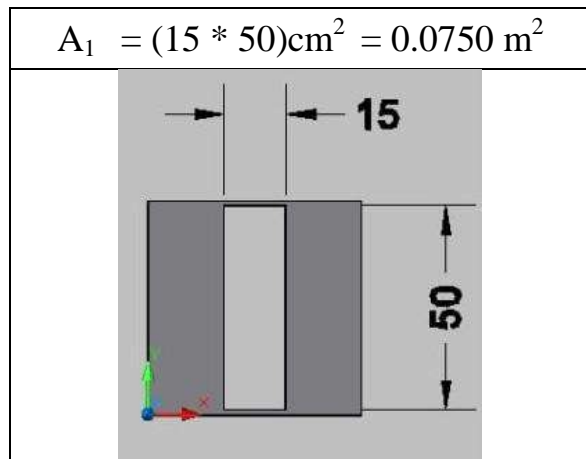
$\rho$  = Fluid density (kg/m<sup>3</sup>)

The calculations of Reynolds number done according to the diameter of the bluff body, circular cylinder D:

2 inch = 0.0508 m

3 inch = 0.0762

4 inch = 0.1016 m



Velocity at the outlet,  $V_2$ , of the tunnel was measured using a digital anemometer and as follow:

	<b>Velocity m/sec</b>
Low	0.057
Medium	0.132
High	0.161

$$A_1 = 15 \times 50 = 750 \text{ cm}^2 \longrightarrow 0.075 \text{ m}^2$$

$$A_2 = 15 \times 15 = 225 \text{ cm}^2 \longrightarrow 0.0225 \text{ m}^2$$

$$V_1 = \frac{V_2 \cdot A_2}{A_1}$$

$$V_{1L} = V_{2L} A_2 / A_1 \longrightarrow V_{1L} = \frac{0.057 \cdot 0.0225}{0.075}$$

$$V_{1L} = 0.0171 \text{ m/s}$$

$$V_{1M} = V_{2M} A_2 / A_1 \longrightarrow V_{1M} = \frac{0.132 \cdot 0.0225}{0.075}$$

$$V_{1M} = 0.0396 \text{ m/s}$$

$$V_{1H} = V_{2H} A_2 / A_1 \longrightarrow V_{1H} = \frac{0.161 \cdot 0.0225}{0.075}$$

$$V_{1H} = 0.0483 \text{ m/s}$$

The density of air at 25 C is ( $\rho=1.2$ ) and ( $\mu=18.27 \cdot 10^{-6}$ )

$$Re_D = \frac{\rho v D}{\mu}$$

$$Re = \frac{1.2 \cdot 0.0171 \cdot 0.1016}{18.27 \cdot 10^{-6}} \longrightarrow Re = 114.11$$

$$Re = \frac{1.2 \cdot 0.0396 \cdot 0.1016}{18.27 \cdot 10^{-6}} \longrightarrow Re = 264.26$$

$$Re = \frac{1.2 \cdot 0.0483 \cdot 0.1016}{18.27 \cdot 10^{-6}} \longrightarrow Re = 322.31$$



**Table 3-1:** Reynold number calculation for **4 inch** diameter cylinder

<b>V1 (m/s)</b>	<b>D (m<sup>2</sup>)</b>	<b>Re<sub>D</sub> = <math>\frac{\rho V1 D}{\mu}</math></b>
L=0.0171	0.1016	114.11
M=0.0396	0.1016	264.26
H=0.0483	0.1016	32.31

$$Re = \frac{\rho V D}{\mu}$$

$$Re = \frac{1.2 * 0.0171 * 0.0762}{18.27 * 10^{-6}} \Rightarrow Re = 85.58$$

$$Re = \frac{1.2 * 0.0396 * 0.0762}{18.27 * 10^{-6}} \Rightarrow Re = 198.19$$

$$Re = \frac{1.2 * 0.0483 * 0.0762}{18.27 * 10^{-6}} \Rightarrow Re = 241.73$$

**Table 3-2:** Reynold number calculation **3 inch** diameter cylinder

<b>V1 (m/s)</b>	<b>D (m<sup>2</sup>)</b>	<b>Re<sub>D</sub> = <math>\frac{\rho V1 D}{\mu}</math></b>
L=0.0171	0.0762	85.58
M=0.0396	0.0762	198.19
H=0.0483	0.0762	241.73

$$Re = \frac{\rho V D}{\mu}$$

$$Re = \frac{1.2 * 0.0171 * 0.0508}{18.27 * 10^{-6}} \Rightarrow Re = 57.05$$




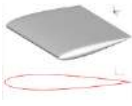
$$Re = \frac{1.2 * 0.0396 * 0.0508}{18.27 * 10^{-6}} \Rightarrow Re = 132.13$$

$$Re = \frac{1.2 * 0.0483 * 0.0508}{18.27 * 10^{-6}} \Rightarrow Re = 161.15$$

**Table 3-3:** Reynold number calculation **2 inch** diameter cylinder

<b>V1 (m/s)</b>	<b>D (m2)</b>	<b>ReD=<math>\frac{\rho v1D}{\mu}</math></b>
L=0.0171	0.0508	57.05
M=0.0396	0.0508	132.13
H=0.0483	0.0508	161.15

**Table 3-4:** Shapes of bluff bodies used in the current research

<b>serial</b>	<b>Object name</b>	<b>shape</b>	<b>Dimensions</b>
1	Sphere		0.1 m
2	Cylinder		2, 3, 4 inch
3	NACA model 0012		Length = 30 cm Width = 25 cm High = 5 cm
4	NACA model 0024		Length = 28 cm Width = 25 cm High = 4 cm

## Chapter 4 - Results and Discussion

### 4.1 Results

The following results, figure (4-1), show flow visualization of a flow over a cylinder. A laminar flow was observed as well as the transient flow. The separation of fluid layer and turbulence downstream were also captured.

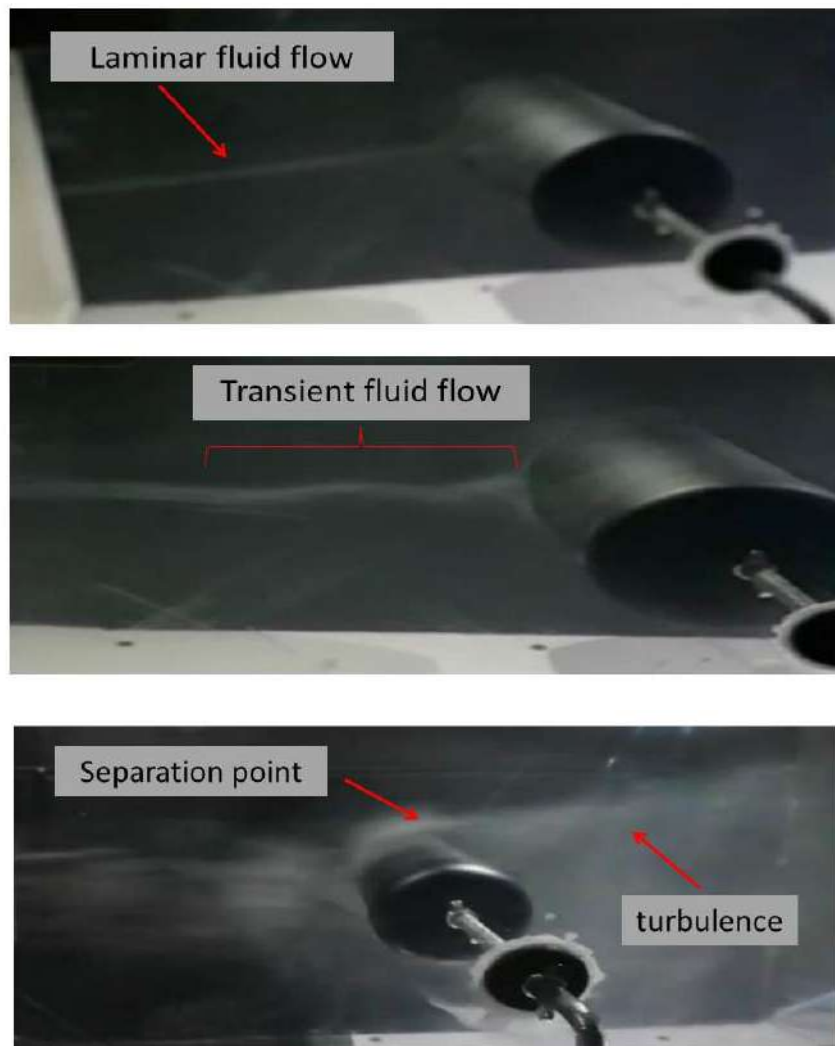


Figure 4-1: Flow over a cylinder

The following results, figure (4-2), represent the flow visualization of a flow over wing bluff body. The experiment successfully visualized the laminar flow in the upstream; also the visualization of the attached boundary layer can be easily noticed on the wing surface.



Figure 4-2: Flow over a wing

The following results, figure (4-3), represent the flow visualization of a flow over a sphere bluff body. The laminar flow and the stagnation point were captured with the help of the smoke.

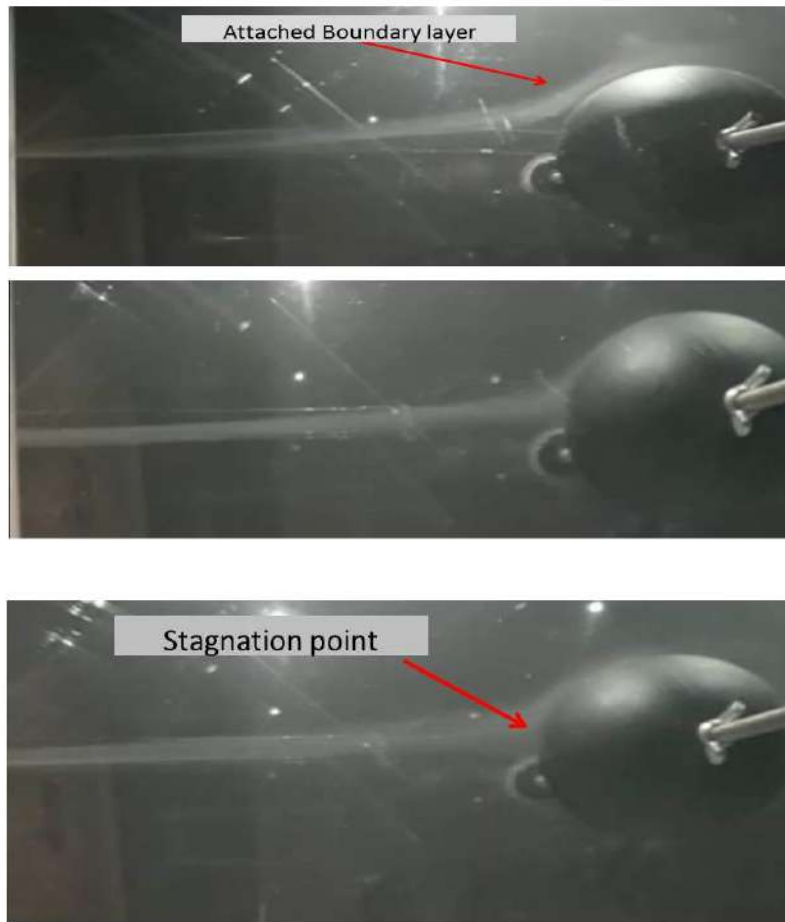


Figure 4-3: flow over a sphere

The design of the wind tunnel used in the current research was able to create a pressure drop to induce the flow passing over the bluff body. The flow pattern was successfully visualized using a smoke generator.

## **Chapter 5 – Future Work**

### **5.1 Challenges while working on the project**

- Finding a source that enables us to see the movement of air, such as a steam generator or a smoke generator.
- Material selection for structure design in terms of safety and visibility
- Finding an air velocity or volumetric flow meter
- Appropriate dimensions for the purpose of consistency between the smoke mass and the speed of the fan's expulsion of air.

### **5.2 Recommendations for Future Work**

For further investigation, it is recommended the following:

1. In order to gain more insight about effect of bluff body on the fluid dynamics, it is recommended measuring flow velocity in the upstream and downstream of the bluff body.
2. Investigating more techniques of flow visualization. This would involve considering using dry ice.
3. Investigating different bluff bodies with different profiles to gain insight about how different profiles may affect the separation of the boundary layer
4. Using high speed camera that can take several frames per minutes for better capturing to the boundary layer separation phenomena

## References

- [1] Munson, B.R., Young, D.F., and Okiishi, T.H., 2006, “Fundamentals of Fluid Mechanics,” 5<sup>th</sup> edition, John Wiley & Sons, p. 526.
- [2]<http://microspheres.us/fluorescent-microspheres/piv-seeding-microparticle-flow-visualization/599.html>.
- [3] Dey, S., Lodh, R. & Sarkar, S., Turbulence characteristics in wall-wake flows downstream of wall-mounted and near-wall horizontal cylinders. *Environmental Fluid Mechanics*, 18(4), pp. 1–31, 2018.
- [4] Panigrahi, P.K., PIV investigation of flow behind surface mounted detached square cylinder. *Journal of Fluids Engineering*, 131(1), 011202, 2009.
- [5] Wang, X.K. & Tan, S.K., Experimental investigation of the interaction between a plane wall jet and a parallel offset jet. *Experiments in Fluids*, 42(4), pp. 551–562, 2007.
- [6] Martinuzzi, R.J., Bailey, S.C.C. & Kopp, G.A., Influence of wall proximity on vortex shedding from a square cylinder. *Experiments in Fluids*, 34(5), pp. 585–596, 2003.
- [7] Taniguchi, S. & Miyakoshi, K., Fluctuating fluid forces acting on a circular cylinder and interference with a plane wall. *Experiments in Fluids*, 9(4), pp. 197–204, 1990.
- [8] Shinneeb, A.M. & Balachandar, R., Effect of gap flow on the shallow wake of a sharp edged bluff body—mean velocity fields. *Journal of Turbulence*, 17(1), pp. 94–121, 2016.
- [9] Shinneeb, A.M. & Balachandar, R., Effect of gap flow on the shallow wake of a sharp edged bluff body—turbulence parameters. *Journal of Turbulence*, 17(1), pp. 122–155, 2016.
- [10] Shinneeb, A.M., Balachandar, R. & Zouhri, K., Effect of gap flow on the shallow wake of a sharp-edged bluff body—Coherent structures. *Physics of Fluids*, 30(6), 065107, 2018.
- [11] CD-adapco, STAR-CCM+ V10.06.009, User Manual, 2015.
- [12] Hirt, C.W. & Nichols, B.D., Volume of fluid (VOF) method for the dynamics of free boundaries. *Journal of Computational Physics*, 39(1), pp. 201–225, 1981.



وزارة التعليم العالي والبحث العلمي  
كلية دجلة الجامعة الاهلية  
قسم هندسة تقنيات التبريد والتكييف

## دراسة سلوك المائع في منطقة العقب

بحث مقدم إلى كلية دجلة الجامعة / قسم هندسة تقنيات التبريد والتكييف  
وهو جزء من متطلبات نيل شهادة البكالوريوس في هندسة تقنيات التبريد والتكييف

من قبل

نور عصام عبدالواحد  
ضياء حيدر كريم  
واثق عباس جاسم  
سلام اسماعيل خليل

بإشراف  
د. علا محمد حداوي

1442 هـ

2021 م



## الخلاصة

في هذا المشروع تم دراسة سلوك المائع في منطقة العقب خلف الاجسام او العوائق. تمت الدراسة من خلال تشييد منظومة فحص متمثلة بنفق رياح. كما تم اختيار ثلاث انواع من العوائق وهي الاسطوانة والكرة و نموذج مصغر لجناح الطائرة. تم استخدام اداة خاصة لتوليد الدخان لغرض تصوير انماط المائع، حيث تم توليد دخان بكثافة منتظمة.

في هذه الدراسة تم تغطية اعداد رينولدز بالنسبة لقطر الاسطوانة كما يلي: 57، 85، 132، 114، 161، 198، 241، 264 و 322.



# **Study the Effect of Cyclic Loads in Mechanical Components Using Programed FEM**

**A project Submitted to the Department of Refrigeration and Air  
Conditioning Techniques Engineering / Dijlah University College  
In partial Fulfillment of the Requirement for the Degree of the  
Bechlorious in Refrigeration and Air Conditioning Techniques  
Engineering**

**Prepared By**

**Ahmed Khaled**

**Bahaa Adnan**

**Farooq Adnan**

**Fouad Taha**

**Qusay Mahmoud**

**Supervised by**

**Dr. Mansoor Ali**

**July 2021**

بِسْمِ اللَّهِ الرَّحْمَنِ الرَّحِيمِ

" وَلَقَدْ آتَيْنَا دَاوُدَ وَسُلَيْمَانَ  
عِلْمًا وَقَالَا الْحَمْدُ لِلَّهِ الَّذِي فَضَّلَنَا  
عَلَى كَثِيرٍ مِنْ عِبَادِهِ الْمُؤْمِنِينَ "

صَدَقَ اللَّهُ الْعَظِيمُ

التمهيد " 15 "

## **ACKNOWLEDGMENT**

The authors wish to express their sincere thanks and profound gratitude to their supervisor *Dr. Mansoor Ali* for his continuous invaluable guidance, sincere effort, helpful discussions and encouragement throughout the preparation of this work.

Thanks to all the Staff Members of the Refrigeration and Air conditioning Department for the facilities offered during the progress of this work.

Thanks are presented to the Staff Members of the College library for their cooperation and help.

Thanks are developed to our family for their patience, care and encouragement.

***Authors***

## **Supervisor Certification**

I certify that this project entitled (**Study the Effect of Cyclic Loads in Mechanical Components Using Programed FEM**) prepared by:

**Ahmed Khaled**

**Bahaa Adnan**

**Farooq Adnan**

**Fouad Taha**

**Qusay Mahmoud**

Has been carried out completely under our supervision at the Dijlah University College as a partial fulfillment of the requirements for the Degree of B.Sc in Refrigeration and Air conditioning Engineering Department.

Signature:

Name : **Mansoor Ali** (Supervisor)

Refrigeration and Air conditioning Engineering Department

Dijlah University College

Date : / /

Approved by the chairman of the Refrigeration and Air conditioning Engineering Department

Signature:

Name :

Chairman of Refrigeration and Air conditioning Engineering Department

Dijlah University College

Date : / /

## **EXAMINATION COMMITTEE**

### **CERTIFICATION**

We certify that we have read this project entitled **(Study the Effect of Cyclic Loads in Mechanical Components Using Programed FEM)**.

Prepared by:

**Ahmed Khaled**

**Bahaa Adnan**

**Farooq Adnan**

**Fouad Taha**

**Qusay Mahmoud**

And as an examining committee, examined the students in its context and that in our opinion it meets the standard project for the Degree of B.Sc in the Refrigeration and Air conditioning Engineering.

Signature:

Name: **Mansoor Ali**

Date:    /    /

(Supervisor)

Signature:

Name:

Date:    /    /

(Member)

Signature:

Name: Dr.

Date:    /    /

(Chairman)

Approved by the Dijlah University College

Signature:

Name:

Date:    /    /

(Dean of the Dijlah University College)

# **DEDICATION**

***To our family and friends  
with love***

***Authors***

## **Abstract**

This project study the fatigue behavior in a mechanical components numerically using Ansys Workbench. There are three models used in this project to study fatigue analysis. First is a rectangular plate with central hole, second is a grooved shaft, and the third model is a stepped bar. The cyclic loads used are fully reversed axial, bending, and torsion loads with different amplitude values.

The theoretical analysis in the project covers the equations of fatigue analysis which are Goodman, Gerber and Soderberg equations that have been used in the programmed finite element analysis.

The results of numerical analysis have been achieved using Ansys workbench (version 16) with suitable element size for meshing process and applying the required cyclic loads and boundary conditions.

The obtained results show that fatigue life (number of load cycles until failure occurs) of any mechanical component must be computed at critical locations of maximum stresses such as holes, notches, and fillets. Also, the fatigue life depends on load type (axial, bending, or torsion) even when the induced stresses in the mechanical component are the same. In the other hand, the generated equivalent alternating stresses are have a maximum values whenever a change in component cross section area due to stress concentration at these regions.



# CHAPTER ONE

## INTRODUCTION

## **Chapter One**

### **Introduction**

#### **1.1 Introduction:**

The failure caused by cyclic stress is called fatigue failure. The fatigue failure originates from a micro-crack (brittle failure) due to stress concentration effect at surface irregularities. Minute irregularities such as grinding scratches, tool marks, inspection stamping, stamped part numbers or surface scales may produce a high value for the stress due to stress concentration and serve as the starting point for the micro crack, which progressively increases until the part breaks into two pieces similar to a brittle fracture. No plastic deformation is observed in the failure surface. Most commonly, the fatigue failure occurs due to reversing bending stress in rotating machineries, less commonly due to reversing torsional shear stress and rarely from reversing axial stress. As the most highly stressed points are on the outer surface for both bending and torsion, crack originates on the outer surface and progresses inwardly. As a consequence of this, a weak decarburized layer on the outer surface of heat-treated parts often produce low endurance limit. Since fatigue cracks are due to tensile stress, a residual tensile stress on the surface of the part constitutes a fatigue hazard. Such a residual tensile stress, for example may arise from a cold working operation on the part without stress relieving. Parts that are finished by grinding frequently have a thin surface layer with high residual stress in tension. Such residual stress combined with the tensile stress from loading, may give a resultant stress sufficiently great to cause a fatigue crack to start. Any residual tensile stress on the surface should be removed, or better still, converted into a layer of compression. Shot blasting, or shot peening operations can induce residual compressive residual stress on surface. Also nitrided and carburized parts have residual compressive stress on the surface. Residual compressive stress on the surface will reduce the tensile

stress from the load, and thus helps to improve fatigue characteristics of the part. Sand blasting of the part should be avoided since the scratches serve as stress risers.

It is well known that the fatigue of structural adhesives depends on the fatigue load as well as the load ratio. These two fatigue loading parameters are related through the fatigue load ratio,  $R$ , which is the ratio of minimum to maximum fatigue load. It is necessary to ensure that the adhesively bonded structural members will not fail as a result of accumulated fatigue damage during their expected service life. Generally, at an early design stage, constant amplitude fatigue experimental tests are performed on coupon-level adhesive joints and S-N curves may be obtained for different load ratio,  $R$ , values. However, it would be expensive to have fatigue data for all possible  $R$  values. Numerical models that are capable of predicting the influence of the  $R$  value on the fatigue behavior can help the engineer to design effectively [1].

## **1.2 Fatigue Nature:**

The concept of "fatigue" arose several times in the Module on Fracture, as in the growth of cracks in the Comet aircraft that led to disaster when they became large enough to propagate catastrophically as predicted by the Griffith criterion. Fatigue, as understood by materials technologists, is a process in which damage accumulates due to the repetitive application of loads that may be well below the yield point. The process is dangerous because a single application of the load would not produce any ill effects, and a conventional stress analysis might lead to an assumption of safety that does not exist.

In one popular view of fatigue in metals, the fatigue process is thought to begin at an internal or surface flaw where the stresses are concentrated, and consists initially of shear flow along slip planes. Over a number of cycles, this slip generates intrusions and extrusions that begin to resemble a crack. A true crack running inward from an intrusion region may propagate initially along one of the original slip planes,

but eventually turns to propagate transversely to the principal normal stress as shown in Fig. (1.1).

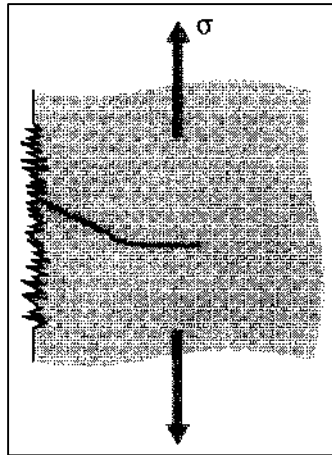


Figure (1.1): Fatigue crack Initiation and propagation in metals.

Fatigue can be defined as “The process of progressive localized permanent structural change occurring in a material subjected to conditions that produce fluctuating stresses and strains at some point or points and that may culminate in cracks or complete fracture after a sufficient number of fluctuations [2].

When the failure surface of a fatigued specimen is examined, a region of slow crack growth is usually evident in the form of a clamshell concentric around the location of the initial flaw (See Fig. (1.2)).



Figure (1.2): Typical Fatigue failure surface.

The clamshell region often contains concentric beach marks at which the crack was arrested for some number of cycles before resuming its growth. Eventually, the crack may become large enough to satisfy the energy or stress intensity criteria for rapid propagation, following the previous expressions for fracture mechanics. This final phase produces the rough surface typical of fast fracture. In postmortem examination of failed parts, it is often possible to correlate the beach marks with specific instances of overstress, and to estimate the applied stress at failure from the size of the crack just before rapid propagation and the fracture toughness of the material.

In general, fatigue or cyclic load has the following properties:

- Cyclic loading produces stresses that are variable, repeated, alternating, or fluctuating
- Fracture at maximum stresses well below yield strength.
- Failure occurs after many stress cycles (such as 100, 000 cycles).
- Failure is by sudden ultimate fracture.
- No visible warning in advance of failure.

### **1.3 S-N Curves:**

Well before a microstructural understanding of fatigue processes was developed, engineers had developed empirical means of quantifying the fatigue process and designing against it. Perhaps the most important concept is the S-N diagram, such as those shown in Fig. (1.3), in which a constant cyclic stress amplitude  $S$  is applied to a specimen and the number of loading cycles  $N$  until the specimen fails is determined. Millions of cycles might be required to cause failure at lower loading levels, so the abscissa is usually plotted logarithmically [2].

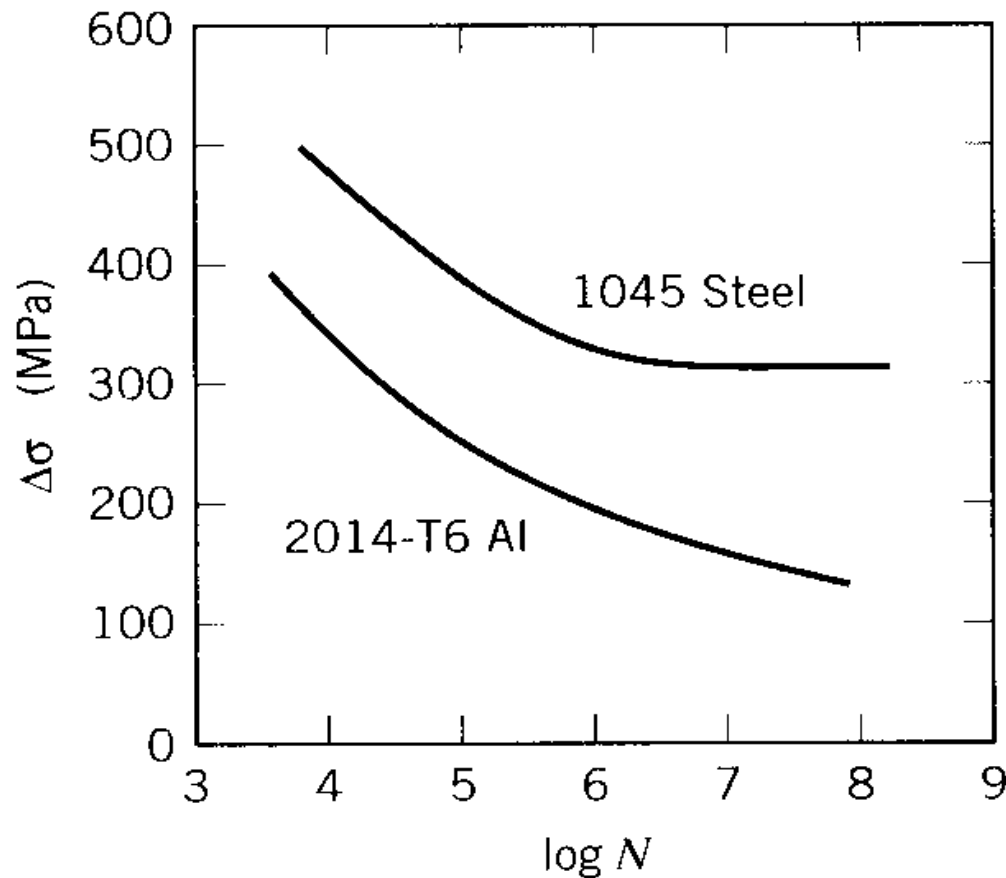


Figure (1.3): S - N curves for aluminum and low-carbon steel.

For high cycle fatigue, the fatigue strength is commonly expressed through an SN curve. Many similar variants of SN curves are used in the literature, e.g. linear, bilinear or nonlinear. Usually they are plotted on double-logarithmic axes, but sometimes the stress axis is linear. Furthermore, the stress axis may be given in either ranges or amplitudes. They are conceptually identical in that they describe “what is the expected life at a given stress amplitude”.

#### **1.4 Failure Stages:**

- Stage I: Initiation of micro- crack due to cyclic plastic deformation.
- Stage II: Progresses to macro-crack which forms plateau-like surface that repeatedly opens and closes, creating bands called beach marks.

- Stage III: Crack has propagated far enough that remaining material is insufficient to carry the load, and fails by simple ultimate failure (see Fig. (1.4)) [3].

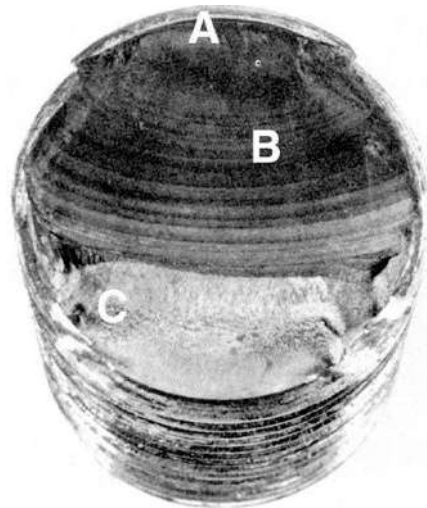


Figure (1.4): Fatigue failure stages: Started at A propagated towards B and finally sudden failure at C.

### **1.5 Fatigue Life Methods:**

There are three major fatigue life models. These Models predict life in terms of number of cycles to failure,  $N$ , for a specific level of loading as following [3]:

1. Stress-life method (used in most designs):
  - Least accurate, particularly for low cycle applications
  - Most traditional, easiest to implement
2. Strain-life method:
  - Detailed analysis of plastic deformation at localized regions
  - Several idealizations are compounded, leading to uncertainties in results
3. Linear-elastic fracture mechanics method:
  - Assumes crack exists
  - Predicts crack growth with respect to stress intensity.

# CHAPTER TWO

## THEORY



## **Chapter Two**

### **Theory**

#### **2.1 Introduction:**

This chapter covers theoretical work of cyclic load analysis. The equations of cyclic load and fatigue in ductile and brittle materials will be covered and derived briefly. Goodman, Gerber and Soderberg equations will be covered and derived in the analysis.

#### **2.2 Design for fatigue stress:**

Unlike a pure reversing stress ( $S_r$ ), a machine part may be subjected to a combined steady and reversing stress. Following design procedure handles such combined stress situation. A generalized stress condition, can be defined as combine purely reversing stress ( $S_r$ ) superimposed on a steady stress ( $S_{avg}$ ). The following stress-time graph shows this combined reversing and steady stress condition. If the stress is varying between  $S_{max}$  and  $S_{min}$ , then the steady (average) stress  $S_{av}$  and reversing stress  $S_r$  can be written as following (figure (2.1)) [4]:

$$S_{av} = \frac{S_{max} + S_{min}}{2}, \quad S_r = \frac{S_{max} - S_{min}}{2} \quad (2.1)$$

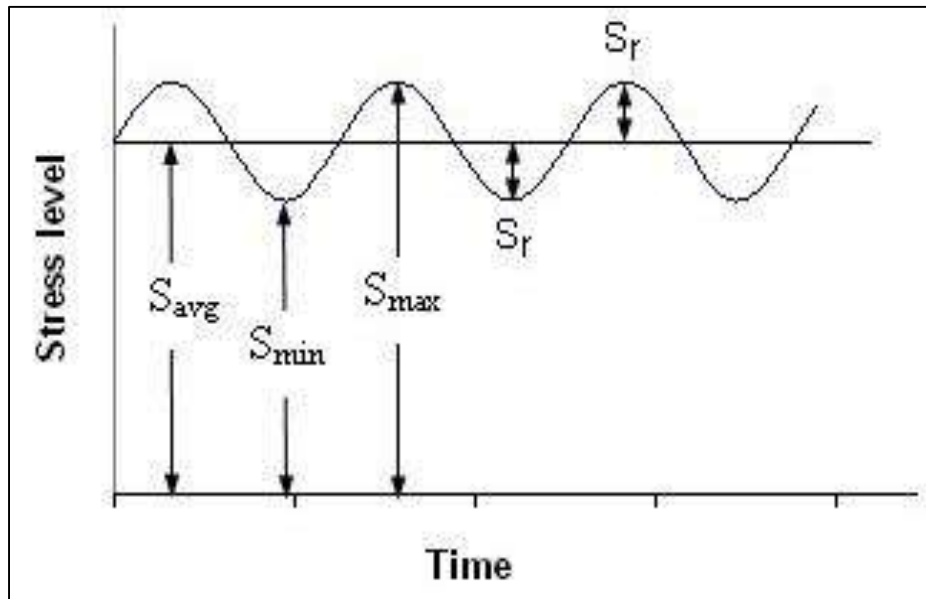


Figure (2.1): Average and reversing stress of cyclic stress.

### **2.3 Soderberg Equation:**

To understand Soderberg's equation, the following cases will be studied (figure (2.2)):

- (i) If a part only contains the steady part of the stress  $S_{avg}$ , (that is  $S_r = 0$ ) then to prevent failure:

$$S_{avg} < S_{yp} / (K * N_{fs}) \quad (2.2)$$

Where  $K$  is the geometric stress concentration factor, and  $N_{fs}$  is the safety factor. Usually parts subjected to fatigue loading are made of ductile material, and for steady stress, we learned that the geometric stress concentration factor can be neglected. Thus the limiting condition is:

$$S_{av} < S_{yp} / N_{fs} \quad (2.3)$$

Which means that  $S_{av}$  can go up to  $S_{yp} / N_{fs}$  when  $S_r = 0$ .

(ii) Similarly, when there is only reversing stress  $S_r$  present, then for safe design:

$$S_r < S_e / (N_{fs} * K_f) \quad (2.4)$$

Where  $K_f$  is the fatigue stress concentration factor. Which means  $S_r$  can go up to  $S_e / (N_{fs} * K_f)$ , when  $S_{av} = 0$ .

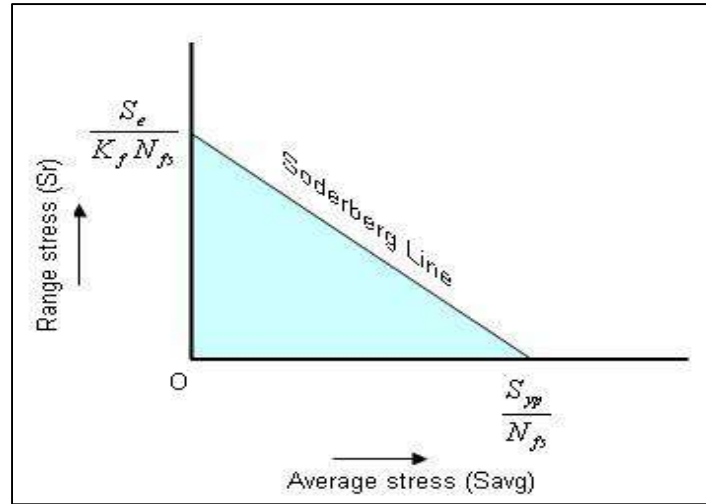


Figure (2.2): Soderberg Equation Line.

If we plot steady stress ( $S_{avg}$ ) along x axis and the range stress ( $S_r$ ) along y axis, then the two extreme stress conditions (i) and (ii) described above, constitute two point on x and y axis. Soderberg Line is obtained by joining these two points. When in a machine part, both types of stress are present simultaneously, if the stress combination ( $S_{avg}$  and  $S_r$ ) is contained in the blue area defined by the Soderberg line, then the part should be safe. Any stress combination falling above the Soderberg's line would be unsafe.

Using intercept form of the equation of straight line (i.e.  $\frac{x}{a} + \frac{y}{b} = 1$ ), the safe design area (blue area) can be defined by:

$$\frac{S_{av}}{\frac{S_{yp}}{N_{fs}}} + \frac{S_r}{\frac{S_e}{K_f N_{fs}}} < 1 \quad (2.5)$$

Multiplying both side by  $\frac{S_{yp}}{N_{fs}}$ :

$$S_{av} + S_r K_f \left( \frac{S_{yp}}{S_e} \right) \leq \frac{S_{YP}}{N_{fs}} \quad (2.6)$$

Equation (2.6) above is called Soderberg Equation for design of a part with combined steady and range stress. Note that, the right hand side of the equation  $\frac{S_{YP}}{N_{fs}}$  is the design limit for normal steady stress  $S_{avg}$ . Because of the presence of the range stress  $S_r$ , the factor  $S_r K_f \left( \frac{S_{yp}}{S_e} \right)$  is added, which is the static equivalent of the range stress  $S_r$  [4].

## 2.4 Goodman Equation:

Because of brittle nature of failure, Goodman proposed the safe design stress for steady stress should be extended to  $S_u/N_{fs}$  instead of  $S_{yp}/N_{fs}$  in Soderberg's equation. This resulted in the safe design space as shown in figure (2.3). The resulted in Goodman Design equation [4]:

$$S_{av} + S_r K_f \left( \frac{S_u}{S_e} \right) \leq \frac{S_u}{N_{fs}} \quad (2.7)$$

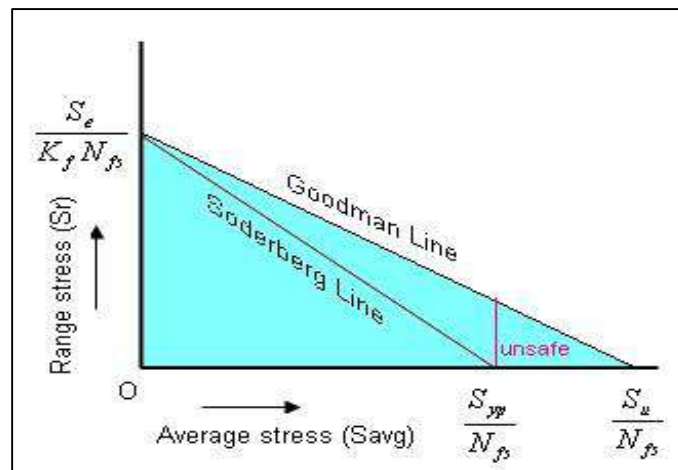


Figure (2.3): Goodman and Soderberg Equations Lines.

Goodman Equation can be obtained from Soderberg equation by replacing  $S_{yp}$  by  $S_u$ .

However, in the safe area defined by Goodman line, when the magnitude of steady stress  $S_{avg}$  becomes more than  $S_{yp}/N_{fs}$ , the part may fail from yielding from plastic deformation. The area is shown as unsafe region.

### **2.5 Modified Goodmans Line:**

To eliminate this shortcoming, a line with  $45^\circ$  angle from the  $S_{yp}/N_{fs}$  point on the x axis as shown in figure (2.4). Mathematically this Modified Goodman space is equivalent to satisfying the following two equations (2.8) and (2.9), simultaneously:

$$S_{av} + S_r K_f \left( \frac{S_u}{S_e} \right) \leq \frac{S_u}{N_{fs}} \quad (2.8)$$

$$S_{av} + S_r K_f \leq \frac{S_{YP}}{N_{fs}} \quad (2.9)$$

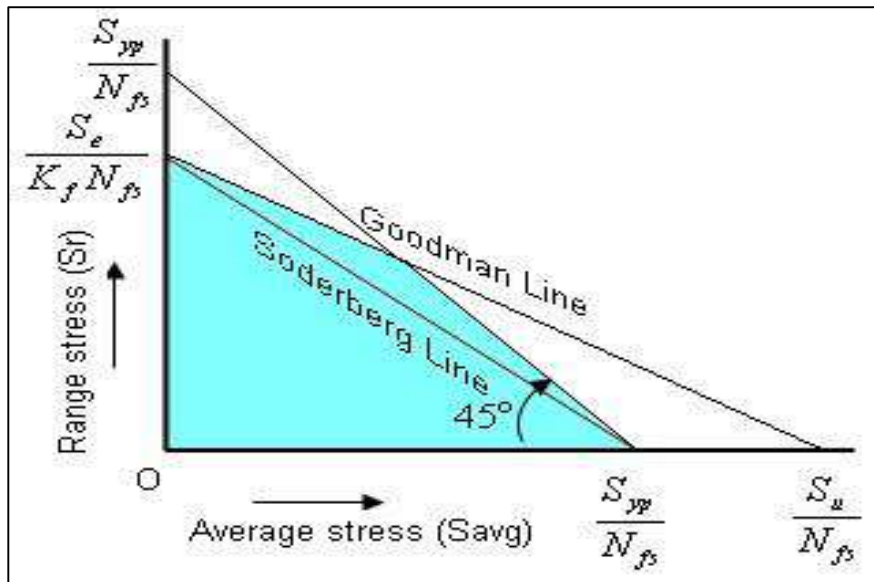


Figure (2.4): Modified Goodman Line.

### **2.6 Gerber Equation:**

This equation is the same as Goodman's equation but it uses a parabola instead of the straight line (see figure (2.5)). Thus, Gerber equation can be written as:

$$\left(\frac{N_{fs} S_{av}}{S_u}\right)^2 + \left(\frac{N_{fs} S_r}{S_e}\right) \leq 1 \quad (2.10)$$

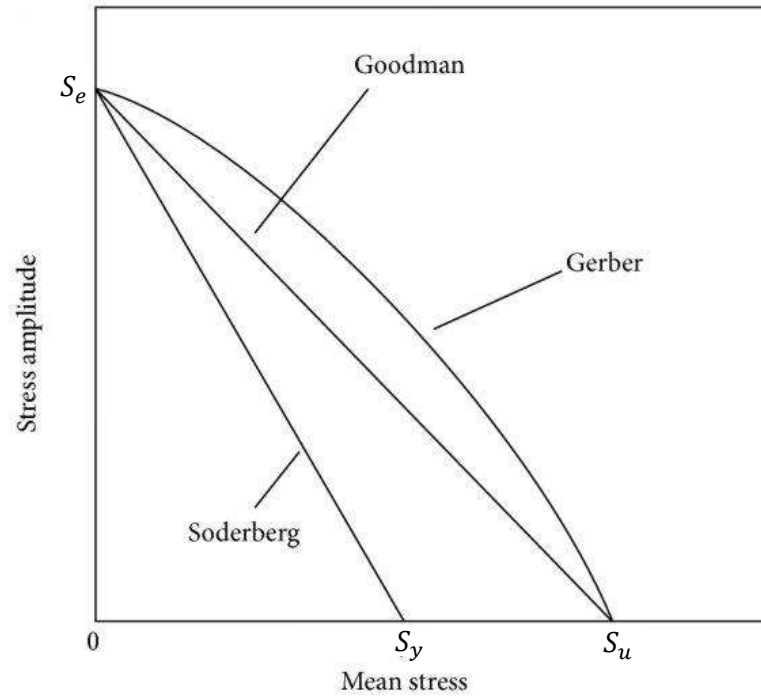


Figure (2.5): Gerber, Goodman and Soderberg Lines.

# **CHAPTER THREE**

## **FINITE ELEMENT ANALYSIS**

## **Chapter Three**

### **Finite Element Analysis**

#### **3.1 Introduction:**

Finite element analysis is used widely in many engineering problems as a numerical solution. There are many software packages used as a programmed finite element, but Ansys package is the widely used method because of its accuracy and wide problem covered by this method. Therefore, Ansys Workbench will be used in this project.

#### **3.2 Finite Element Method:**

The finite element method (FEM) is a numerical technique for solving problems which are described by partial differential equations or can be formulated as functional minimization. A domain of interest is represented as an assembly of finite elements. A continuous physical problem is transformed into a discretized finite element problem with unknown nodal values. For a linear problem a system of linear algebraic equations should be solved.

FEA is essentially a piece-wise process. It can be applied to one-dimensional problems, but more usually there is an area or volume within which the solution is required. This is split up into a number of smaller areas or volumes, which are called finite elements [5].

To summarize in general terms how the finite element method works we list main steps of the finite element solution procedure below:

1. Discretize the continuum. The first step is to divide a solution region into finite elements. The finite element mesh is typically generated by a preprocessor program.



The description of mesh consists of several arrays main of which are nodal coordinates and element connectivities.

2. Select interpolation functions. Interpolation functions are used to interpolate the field variables over the element. Often, polynomials are selected as interpolation functions. The degree of the polynomial depends on the number of nodes assigned to the element.

3. Find the element properties. The matrix equation for the finite element should be established which relates the nodal values of the unknown function to other parameters. For this task different approaches can be used; the most convenient are: the variational approach and the Galerkin method.

4. Assemble the element equations. To find the global equation system for the whole solution region we must assemble all the element equations. In other words we must combine local element equations for all elements used for discretization. Element connectivities are used for the assembly process. Before solution, boundary conditions (which are not accounted in element equations) should be imposed.

### **3.3 Building a Model in Ansys:**

ANSYS is the original (and commonly used) name for ANSYS Mechanical or ANSYS Multiphysics, general-purpose finite element analysis software. All of these products are general purpose finite element self-contained analysis tools incorporating preprocessing (geometry creation, meshing), solver and post processing modules in a unified graphical user interface (GUI).

One of the advantages of “ANSYS” is the user-programmable capability. The ANSYS Command Language contains several thousand commands relating to creating geometry, mesh, boundary conditions, solver settings and many other

features. A subset of these commands are termed ANSYS Parametric Design Language (APDL), and focus on managing parameters, macros, if-then-else branching, do-loops, and scalar, vector and matrix operations [6].

There are two different modes of performing finite element analysis in ANSYS: batch and interactive modes. The batch mode requires an input file of commands and executes it from the command line, while the interactive mode turns on the graphical user interface and shows the result of each user action (picked from a menu or typed as a command) in a graphics window. The batch mode is best suited for those experienced with the ANSYS Command Language.

In this project, only the interactive mode will be used. There are two different modes of inputting commands in ANSYS: graphic mode and text mode. In the graphic mode, the user can pick commands and type in required data values. Thus, there is no need to memorize all commands. This mode is beneficial in a sense that the user can see the result of each command in the graphic window. In the text mode, the user type in commands and data in the command area. In this case, the user should remember what command should be used to perform a particular action [7].

The more general name for a connection between adjacent members is termed a node. For trusses and frames the terms joint and node are interchangeable. Element For trusses and frames element means the same as member. The number of possible directions that displacements or forces at a node can exist in is termed a degree of freedom (dof).

Materials in the Workbench Simulation material library may include a fatigue stress-life curve populated with data from engineering handbooks. Fatigue data has been pre-populated for the Structural Steel and Aluminum Alloy material data files from the MIL-SPEC handbook (MIL-HDBK5H). Since material data is crucial to accurate

fatigue results, Workbench Simulation readily allows the input of this information to new or existing materials by hand or through load history files. The Fatigue Tool will then use the information in the stress-life curves for each material in the model when calculating life, damage, safety factors, etc.

The solution steps in Ansys workbench are listed below [6]:

1. Build the geometrical model of the problem, select element type and define material properties.
2. Mesh the studied geometry to form finite element model using suitable element size such that the accuracy of results is acceptable with reasonable solution time.
3. Apply boundary conditions and loads. These must be acted correctly and carefully.
4. Post-processing the results from result file to show the required results such as stress value, deformation, and model life.

### **3.4 Fatigue Analysis in Ansys Finite Element:**

Fatigue behavior of tested models has been analyzed using structural analysis system in Ansys Workbench with insert fatigue tool. Fatigue tool enables to insert fatigue life analysis, safety factor, and equivalent alternating stress under cyclic loads of axial or bending or torsion type, as well as combined loads. The loads applied in the analysis are chosen as fully reversed because these types of loads are the most serious cyclic load that cause failure of mechanical components.

### **3.5 Models of Fatigue Study and finite element formulation:**

The studied cases that will be used in the analysis are as following (see figure (3.1)):

1. Rectangular plate of 1000mm long and 400mm width with central hole of 250mm diameter. The plate thickness is 15mm.

2. Grooved shaft of 300mm diameter with 50mm groove and 800mm long.
3. Stepped bar consists of two rectangles ( $700 \times 300$ mm and  $300 \times 150$ mm) connected by 40mm fillet. The bar thickness is 35mm.

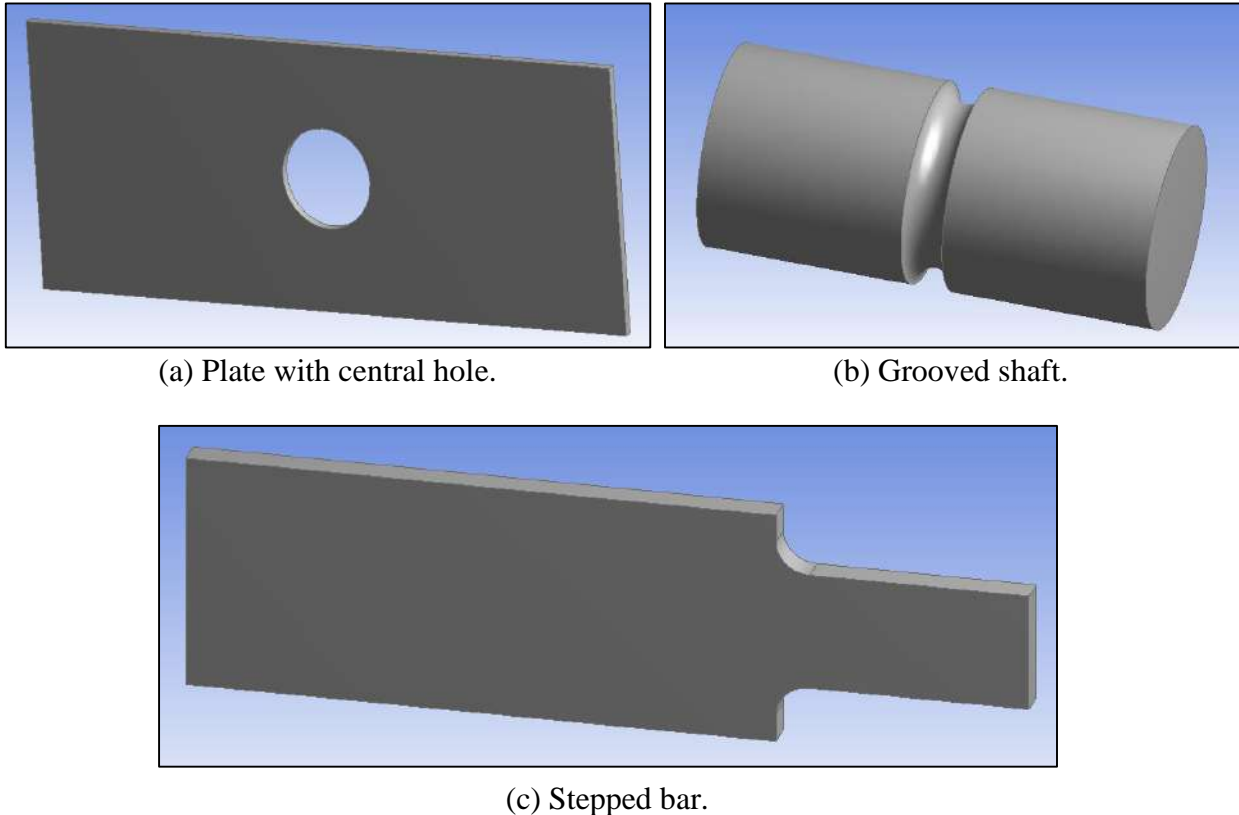
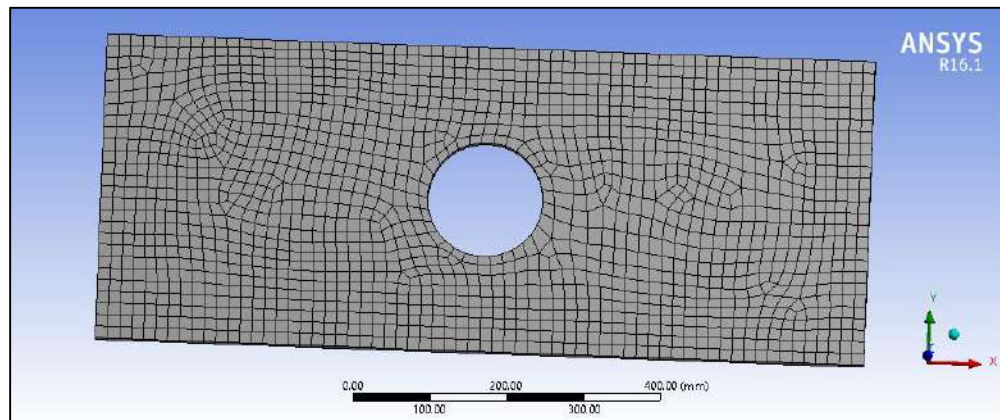


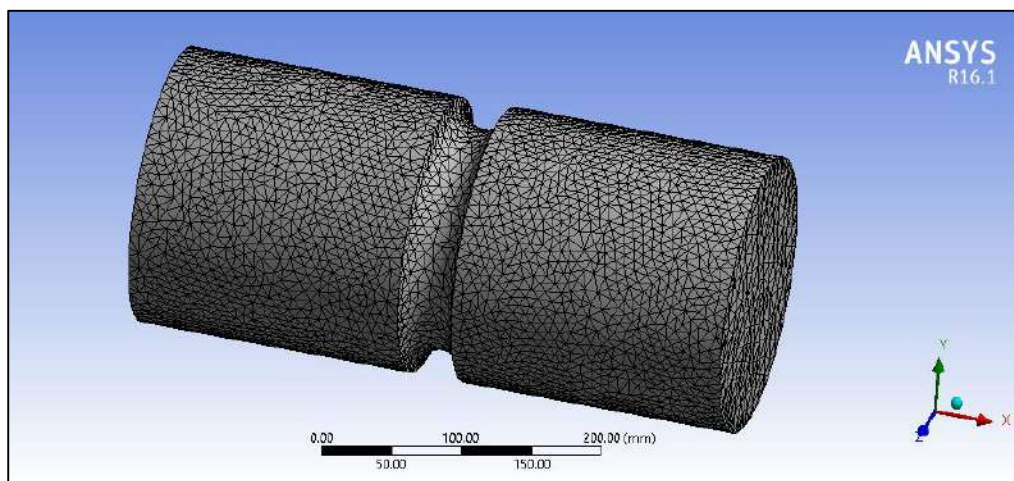
Figure (3.1): Geometry of models used in the fatigue analysis.

Figure (3.2) shows the studied models meshed in Ansys workbench. The total numbers of nodes and elements are as the following: for rectangular plate 11802 nodes and 1611 elements, for grooved shaft 53806 nodes and 32146 elements, and for stepped bar 16564 nodes and 3120 elements.

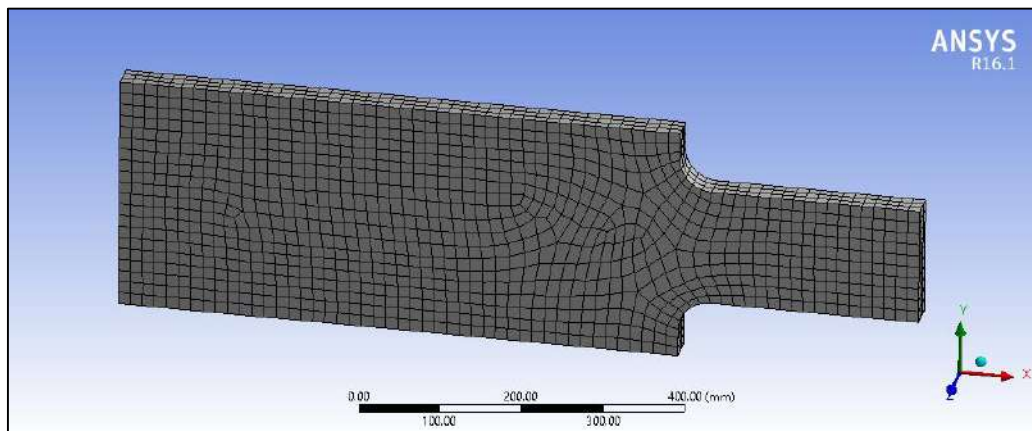
The material used is structural steel of 250 Mpa yield strength, 460 Mpa tensile ultimate tensile strength, 200 000 Mpa Young's modulus, and 0.3 poisson's ratio.



(a) Meshed Plate.



(b) Meshed grooved shaft.



(c) Meshed Stepped Bar.

Figure (3.2): Studied models meshed in Ansys workbench.

# **CHAPTER FOUR**

## **RESULTS, DISCUSSION AND RECOMMENDATIONS**

## **Chapter Four**

### **Results, Discussion and Recommendations**

#### **4.1 Introduction:**

Finite element results of fatigue analysis in rectangular plate with central hole, grooved shaft, and stepped bar under various cyclic load conditions will be achieved in this chapter. Component life under cyclic loads has been computed in Ansys Workbench using fatigue equations introduced in chapter three. These equations are programmed in Ansys and ready to use. The dimensions of all tested models are introduced in chapter three.

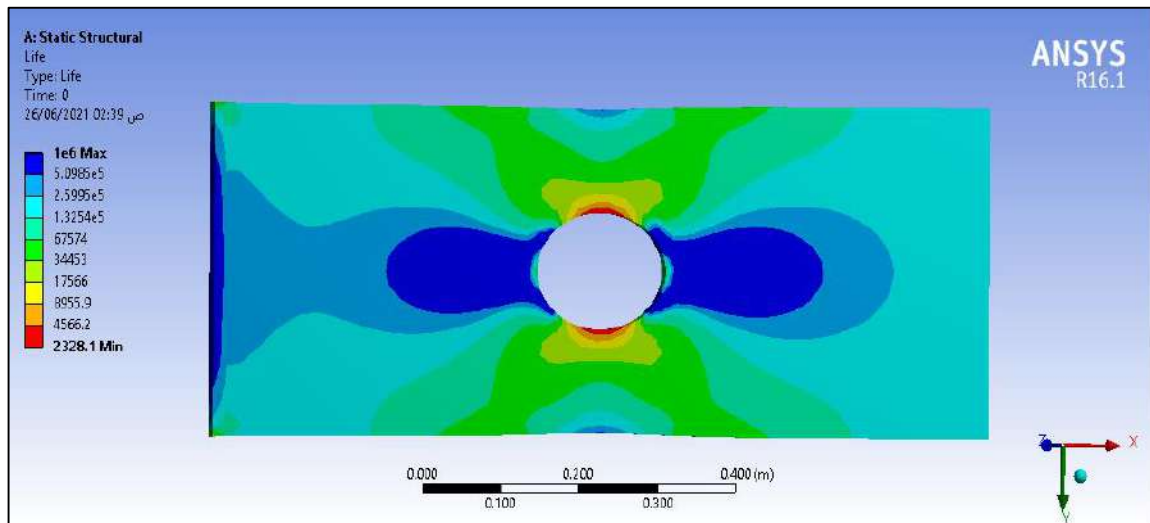
#### **4.2 Results of Fatigue Analysis:**

Figure (4.1a) shows the results of fatigue analysis in rectangular plate with central hole under fully reversed axial load of **700 KN** amplitude. The results show that plate life under this load is **2328.1 cycles** such that when the cycles becomes larger than this number, the failure of component is initiated by small crack at top and lower surfaces of hole because the high value of induced stresses in these region as a result of stress concentration. When the cyclic load is bending of **700 KN** amplitude (vertical load at plate edge), the plate life is **24.589 cycles** as shown in figure (4.1b) and the failure will occurs at top and lower surfaces of hole when the cycles increased.

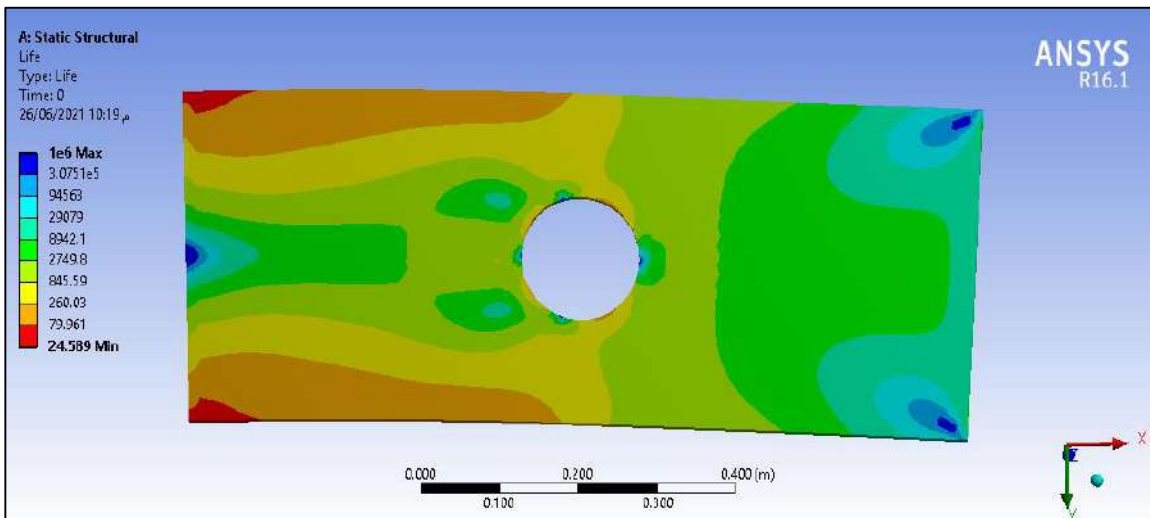
Figures (4.2a), (4.2b), and (4.2c) show the fatigue results in grooved shaft under fully reversed axial load of **1200 KN** amplitude, fully reversed bending load of **1200 KN** amplitude, and fully reversed torsion load of **560 KN.m** amplitude respectively. From these figures, maximum number of load cycles are **166940** for axial load, **182.18** for bending load, and **60.885** for torsion load. These values are computed at



notch (which is the critical failure region because of high stress concentration). The shaft cannot endure any additional cycle.



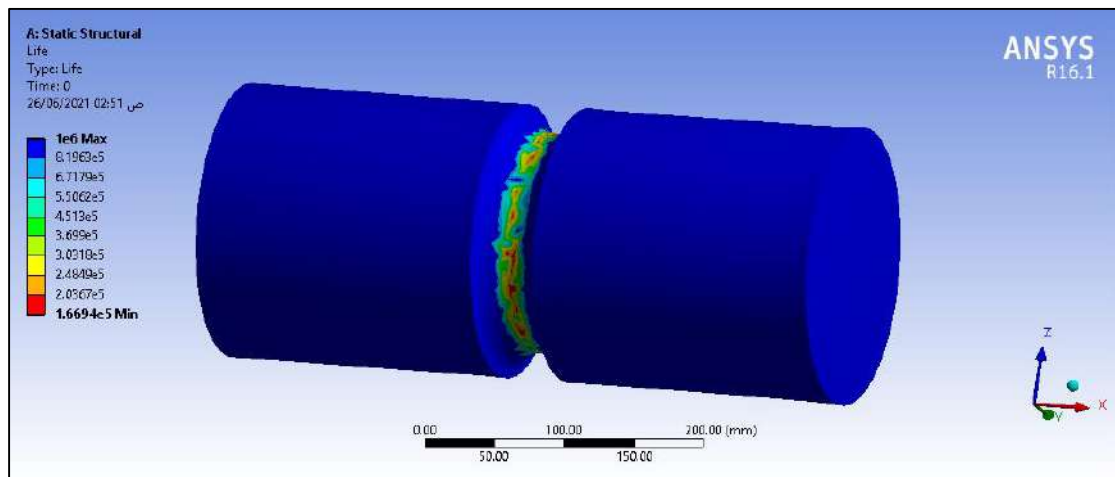
(a)



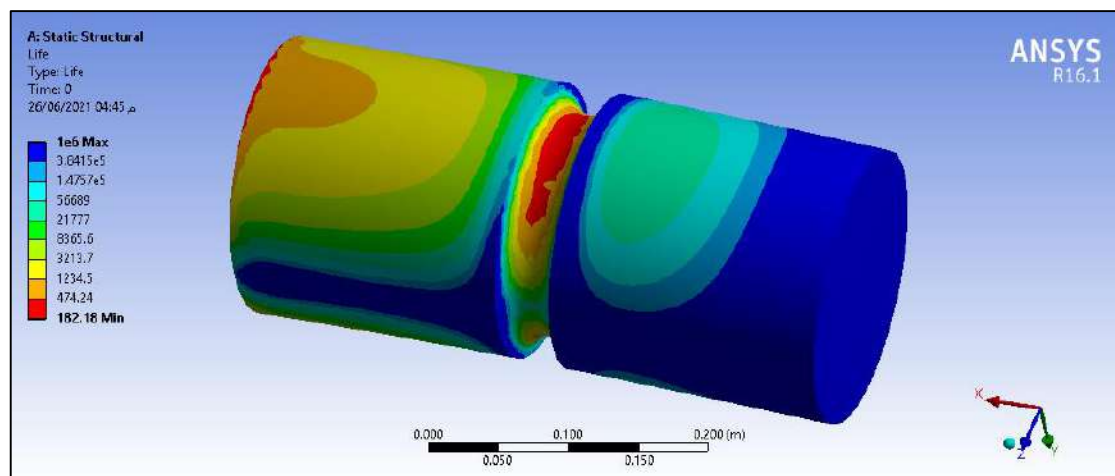
(b)

Figure (4.1): Fatigue life in plate with central hole subjected to fully reversed load: (a) Axial load. (b) Bending load.

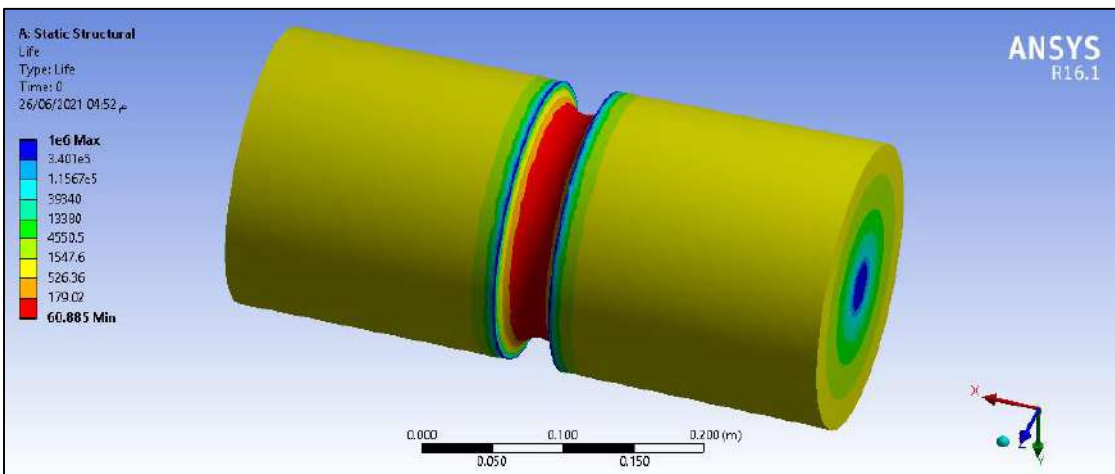




(a)



(b)

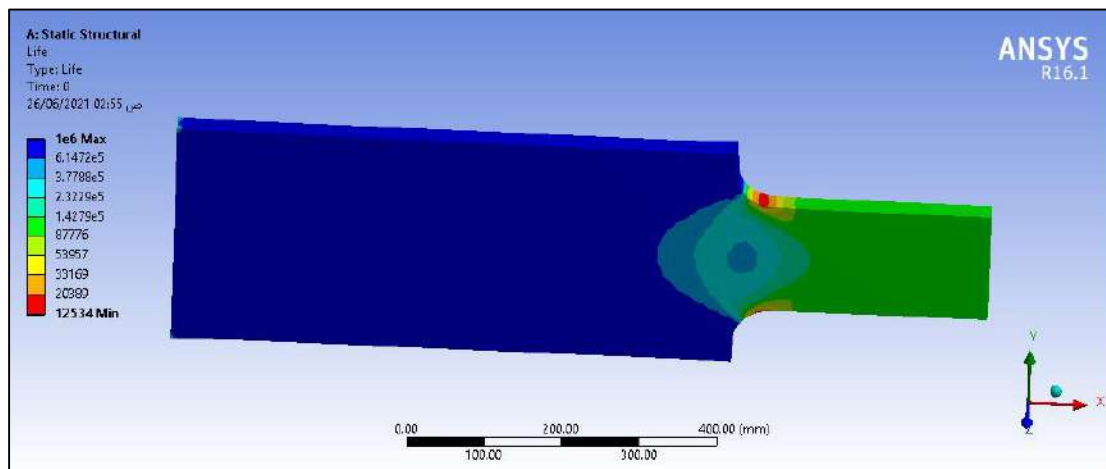


(c)

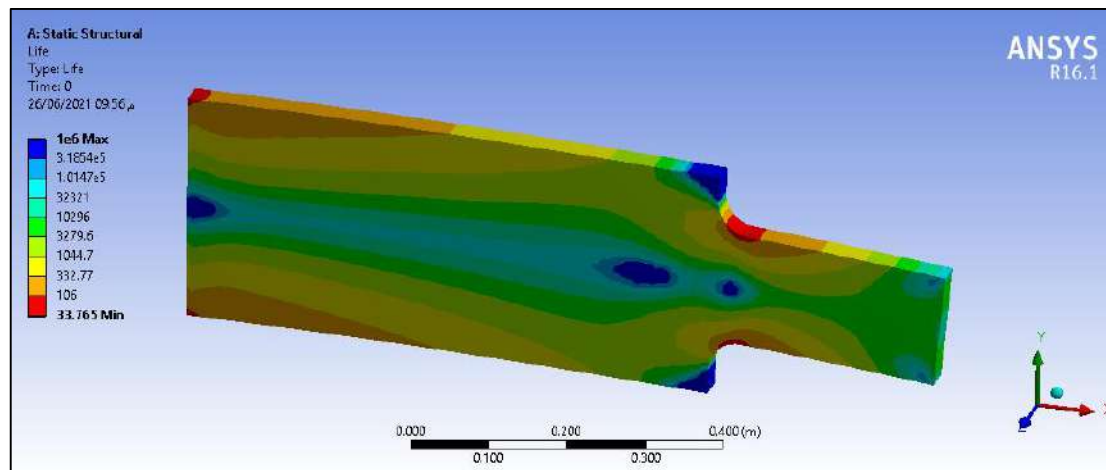
Figure (4.2): Fatigue life in Grooved shaft subjected to fully reversed load:

(a) Axial load. (b) Bending load. (c) Torsion load

Figures (4.3a) and (4.3b) show the fatigue results in stepped bar under fully reversed axial and bending loads of **700 KN** amplitude, respectively. From these figures, stepped bar life is **12534 cycles** under axial load and **33.765 cycles** under bending load. These values are computed at fillet which is consider the critical failure region because of high stress concentration factor and small cross section area. The bar cannot endure any additional cycle above this value.



(a)



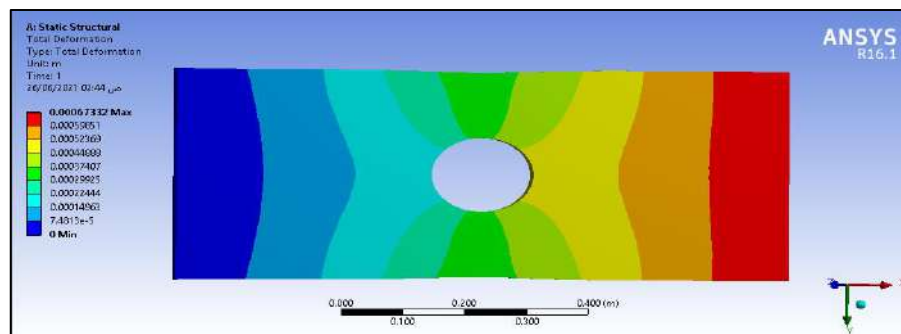
(b)

Figure (4.3): Fatigue life in stepped bar subjected to fully reversed load:

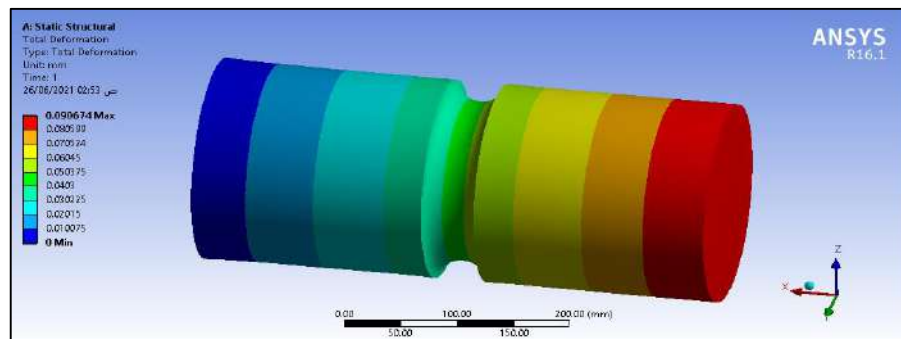
(a) Axial load. (b) Bending load.

### 4.3 Results of deformation and stresses:

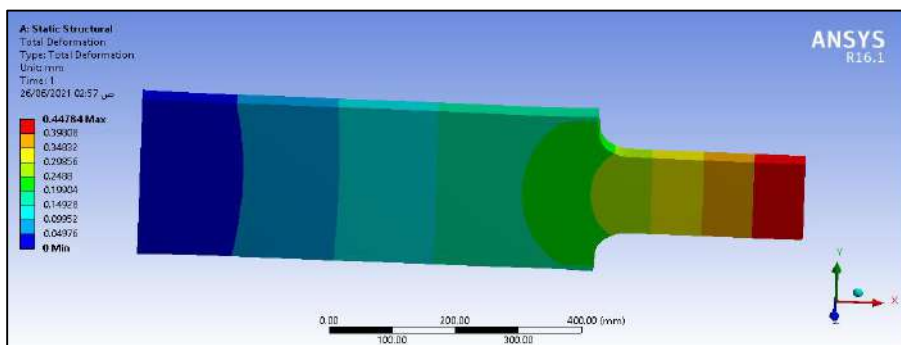
Figures (4.4a), (4.4b) and (4.4c) show the results of total deformation in plate, grooved shaft, and stepped bar respectively under fully reversed axial load of **700 KN** amplitude for both plate and stepped bar, and **1200 KN** amplitude for grooved shaft. From these figures, it is obvious that the deformation is maximum at the applied load edge and decreases gradually toward the fixed edge. This is results from the effect of applied load which tends to deform the nearest edge to the load.



(a)



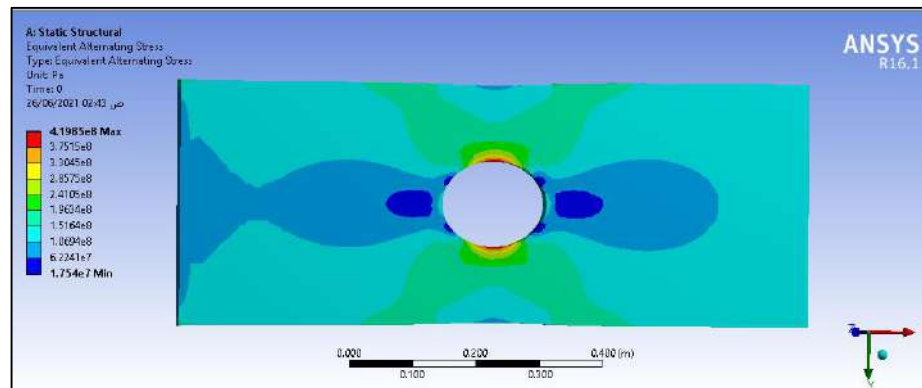
(b)



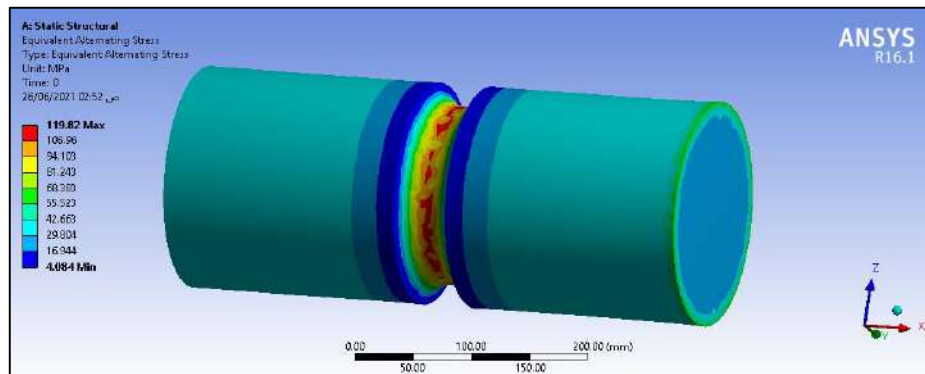
(c)

Figure (4.4): Total deformation under fully reversed axial load: (a) flat plate. (b) Grooved shaft. (c) Stepped bar.

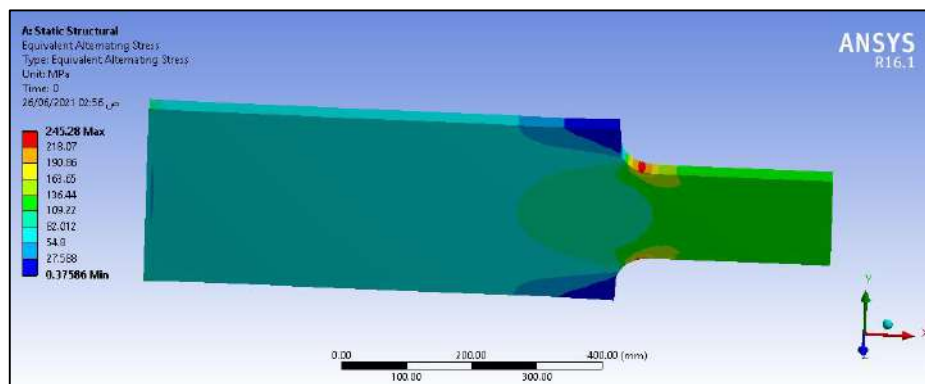
Figures (4.5a), (4.5b) and (4.5c) show the results of equivalent alternating stress in plate, grooved shaft, and stepped bar respectively under the same cyclic loads mentioned above. The alternating stresses have a maximum values at critical regions (hole, notch, and fillet) as a results of high stress concentration at these regions.



(a)



(b)



(c)

Figure (4.5): Equivalent alternating stress under fully reversed axial load: (a) flat plate. (b) Grooved shaft. (c) Stepped bar.

**4.4 Conclusions:**

1. Ansys finite element is an effective method to predict fatigue failure theoretically and can be verified experimentally.
2. Fatigue life of any mechanical component is computed at critical locations (location of maximum stresses) such as holes, notches, and fillets.
3. The results of fatigue under axial load differs from the results under bending load and torsion load even when the induced stresses in the component are the same.
4. Fatigue life of any mechanical component increases with decreasing the amplitude of cyclic load applied.

**4.5 Recommendations for Future Work:**

1. Study the fatigue analysis experimentally to determine the mechanical components life (number of load cycles until fracture occurs).
2. Compare the experimental results with Ansys finite element results to verify the accuracy of Ansys results.
3. Study the effect of changing fillet and notch radii on the resulting fatigue life.
4. Perform the numerical analysis using another program and compare the results with Ansys Workbench results.
5. Study the fatigue behavior under combined stresses of axial, bending, and torsion loads.

# REFERENCES

# REFERENCES

- 1) Mikkel Melters Pedersen, (Introduction to Metal Fatigue- Concepts and Engineering Approaches), 2018.
- 2) David Roylance, (Fatigue), Department of Materials Science and Engineering, Massachusetts Institute of Technology, Cambridge, 2001.
- 3) Ramesh Singh, (Fatigue Failure in Variable Loading).
- 4) Richard Budynas and Keith Nisbett, (Shigley's Mechanical Engineering Design), McGraw-Hill Series in Mechanical Engineering, 10th Edition.
- 5) Geoffrey Modlen, (Introduction to Finite Element Analysis), Department of Manufacturing, University of Manchester, 2010.
- 6) (Fundamental FEA Concepts and Applications), A Guidebook for the Use and Applicability of Workbench Simulation Tools from ANSYS, Inc.
- 7) Colin Caprani, (Structural Analysis II), 2008.

## الخلاصة

هذا المشروع يدرس سلوك الكلال في الاجزاء الميكانيكية عددياً باستخدام برنامج الأنسز. تم استخدام ثلاث نماذج في هذا المشروع لدراسة تحليل الكلال. النموذج الأول هو صفيحة مستطيلة فيها فجوة مركزية، النموذج الثاني هو شفت محرز، و النموذج الثالث هو عتبة مستطيلة متدرجة. الأحمال الدورية المستخدمة هي احمال معكوسة بشكل كامل من النوع المحوري، الحناية، و الالتواء بسعات حمل مختلفة.

التحليل النظري في المشروع غطى معادلات تحليل الكلال التي هي معادلات جودمان، جيربر، و سودربيرج التي تم استخدامها في العناصر المحددة المبرمجة.

نتائج التحليل العددي تم انجازها باستخدام انسز وورك بينج (النسخة 16) مع اختيار حجم عناصر مناسب لعملية التقطيع (ميش) و تطبيق الأحمال الدورية المطلوبة و الشروط المحيطية.

النتائج المستحصلة بيّنت ان عمر الكلال (عدد دورات الحمل حتى حدوث الكسر) لأي جزء ميكانيكي يجب ان تُحسب عند المواضع الحرجة ذات الأجهادات العظمى مثل الفجوات و الحزوز و المتكئات الزاوية. كذلك فإن عمر الكلال يعتمد على نوع الحمل الدوري المسلط (محوري، حناية، أو التواء) حتى و ان كانت الأجهادات المتولدة في الجزء الميكانيكي هي نفسها. من جهة اخرى فإن الأجهادات المتناوبة المكافئة لها اعظم القيم حيثما يكون هناك تغير في مساحة المقطع العرضي للجزء الميكانيكي نتيجةً لتمرکزات الأجهاد عند هذه المناطق.





## دراسة تأثير الأحمال الدورية في الأجزاء الميكانيكية باستخدام طريقة العناصر المحددة المبرمجة

مشروع مقدم الى كلية دجلة الجامعة – قسم هندسة تقنيات التبريد والتكييف  
كجزء من متطلبات منح درجة بكالوريوس هندسة في تقنيات التبريد والتكييف

من قبل

أحمد خالد

بهاء عدنان

فاروق عدنان

فؤاد طه

قصي محمود

باشراف

م.د. منصور علي

*Ministry of Higher Education and Scientific Research*

*Dijlah University College*

*Refrigeration and Air Conditioning*

*Technologies Engineering Department*



## **TESTING OF SINGLE PHASE TRANSFORMER**

*A project*

*Submitted to the Refrigeration and Air Condition Technology  
Engineering Department at Dijlah University College in partial fulfillment  
of the requirements for Degree of Bachelor in Refrigeration and Air  
Conditioning Technologies Engineering Department*

*By:*

**ABDUL SAMAD MAHMOUD ABDUL SAMAD**

**FADEL KARIM SANDAL**

**SAEED JUBEIR HAMAD**

**SUHAIB IBRAHIM KHALIL**

**IMAD HARBI MUSLAH**

*Supervisor by:*

***Assistant.lucther DAWOOD SALMAN***

**1442 A.H.**

**2021 A.D.**

بِسْمِ اللَّهِ الرَّحْمَنِ الرَّحِيمِ

وَمَا أُوتِيتُمْ مِنَ الْعِلْمِ إِلَّا قَلِيلًا

صدق الله العظيم

الاسراء الاية (85)

## *Supervisor Certificate*

*We certify that this project entitled ((**TESTING OF SINGLE PHASE TRANSFORMER**))*

*Prepared by:*

**ABDUL SAMAD MAHMOUD ABDUL SAMAD**

**FADEL KARIM SANDAL**

**SAEED JUBEIR HAMAD**

**SUHAIB IBRAHIM KHALIL**

**IMAD HARBI MUSLAH**

*Has been carried out completely under our supervision at the  
Dijlah university college in partial fulfillment of the  
requirements for Degree of Bachelor in Refrigeration and Air  
Conditioning Technologies Engineering.*

*Signature:*

***Name of lecturer***

*Date: / /2021*

*Approved by the head of Air condition and refrigeration  
engineering department:*

*Signature*

*Dr. Firas Maan Abdel Sattar*

*Head of Refrigerating and Air  
Conditioning Engineering Department*

*Date: / /2021*

# *Examining committee certificate*

We certify that this project entitled ( **TESTING OF SINGLE PHASE TRANSFORMER** )

Submitted by:

**ABDUL SAMAD MAHMOUD ABDUL SAMAD  
FADEL KARIM SANDAL  
SAEED JUBEIR HAMAD  
SUHAIB IBRAHIM KHALIL  
IMAD HARBI MUSLAH**

and as an examining committee examined the students in its content and that in our opinion it meets the standards of a project for the for Degree of Bachelor in Refrigeration and Air Conditioning Technologies Engineering.

Signature

*Assistant.lucther* **DAWOOD SALMAN**

*Date: / /2021*

*(supervisor)*

*Signature*

*Name:*

*Date: / /2021*

*(Member)*

*Signature*

*Name:*

*Date: / /2021*

*(Member)*

## الاهداء

• الى والدي العزيز الذي اختار لي طريق الهندسة  
فأنار لي الطريق طولا وعرضا

• الى اساتذتي الذين اناروا لي الطريق

• اليك يا والدتي يا منبع الحنان تقبلي مني هذا  
الجهد في سبيل الوفاء

وشكرا لكم جميعا

## *Abstract*

*This research is a study of the engineering properties of single-phase transformers and how to calculate their parameters such as total impedance, total resistance and total inductance, and we can also calculate the copper losses that occur in the coils and the ferrous losses that occur in the core.*

<b>N.O</b>	<b>Name</b>	<b>SIMBLE</b>	<b>UNIT</b>
<b>1</b>	<b>VOLTAG</b>	<b>V</b>	<b>V</b>
<b>2</b>	<b>CURRENT</b>	<b>I</b>	<b>A</b>
<b>3</b>	<b>INDUCTANCE</b>	<b>XL</b>	<b><math>\Omega</math></b>
<b>4</b>	<b>FREQUENCY</b>	<b>F</b>	<b>HZ</b>
<b>5</b>	<b>TEMPERATURE</b>	<b>T</b>	<b>C</b>
<b>6</b>	<b>POWER</b>	<b>P</b>	<b>WATT</b>
<b>7</b>	<b>TOTAL CURRENT</b>	<b>IT</b>	<b>A</b>
<b>8</b>	<b>AUXILIARY CURRENT</b>	<b>Ia</b>	<b>A</b>
<b>9</b>	<b>MAIN CURREN</b>	<b>I'm</b>	<b>A</b>
<b>10</b>	<b>TORQUE</b>	<b>Ta</b>	<b>N/M</b>
<b>11</b>	<b>FLUX DENSITY</b>	<b>B</b>	<b>Wb/m</b>
<b>12</b>	<b>FLUX</b>	<b>Q</b>	<b>Wb</b>
<b>13</b>	<b>POWER FACTOR</b>	<b>Cos</b>	<b>Unit Less</b>
<b>14</b>	<b>CAPACITIVE REACTANCE</b>	<b>XC</b>	<b>F<math>\mu</math></b>
<b>15</b>	<b>RESISTANCE</b>	<b>R</b>	<b><math>\Omega</math></b>



N.O	Subject	Page
1	<b>Chapter one</b>	1
1.1	<b>Introduction</b>	2
2	<b>Chapter two</b>	3
2.1	<b>Principle of working</b>	4
2.2	<b>Construction</b>	5
2.3	<b>E.M.F. Equation of a Transformer</b>	7
2.4	<b>Ratios of a Transformer</b>	10
3	<b>Chapter Three Testing of transformer</b>	13
3.1	<b>Indirect Loading Tests on Transformer (O.C. and Tests )</b>	14
3.1.1	<b>Open circuit Test (O.C Test)</b>	14
3.1.2	<b>Short Circuit Test ( S.C Test )</b>	18
4	<b>Chapter Four Calculation</b>	21
4.1	<b>Open circuit test of transformer</b>	22
4.2	<b>Test of short circuit transformer</b>	24
5	<b>Chapter Five</b>	27
5.1	<b>conclusions</b>	28



وزارة التعليم العالي والبحث العلمي

كلية دجلة الجامعة الأهلية

قسم هندسة تقنيات التبريد والتكييف

## TESTING OF SINGLE PHASE TRANSFORMERS

### اختبار محولات احادية الطور

بحث مقدم إلى كلية دجلة الجامعة الأهلية/ قسم هندسة تقنيات التبريد والتكييف وهو جزء من

متطلبات نيل شهادة البكالوريوس في هندسة تقنيات التبريد والتكييف

من قبل

عبد الصمد محمود عبد الصمد

فاضل كريم سندال

سعيد جبير حمد

صهيب ابراهيم خليل

عماد حربي مصلح

بإشراف

م.م داوود سلمان

## الخلاصة

هذا البحث دراسة الخواص الهندسية لمحولات الكهربائية ذات الطور الواحد وكيفية حساب العوامل الخاصة بها مثل الممانعة الكلية والمقاومة الكلية والمحاثة الكلية و كذلك يمكننا حساب الخسائر النحاسية التي تحدث في الملفات والخسائر الحديدية التي تحدث في القلب الحديدي

# **Chapter one**

# **Introduction**

## ***INTRODUCTION***

---

The main advantage of alternating currents over direct currents is that The alternating currents can be easily transferable from low voltage to High or high voltage to low alternation voltages can be raised or lowered as per requirements in the different stages of electrical network as generation transmission , distribution and utilization this is possible with a static device called transformer . The transformer works on the principle of mutual induction . It transfers an electric energy from one circuit to other when there is no electrical connection between the two circuits thus we can define transformer as be.

# **Chapter Two (Theoretical part)**

## 2.1 Principle of working

The principle of **mutual induction** states that when two coils are inductively coupled and if current in one coil is changed uniformly then an e.m.f gets induced in the other coil. This e.m.f can drive a current, when a closed path is provided to it. The transformer works on the same principle. In its elementary form, it consists of two inductive coils which are electrically separated but linked through a common magnetic circuit. The two coils have high mutual inductance. The basic transformer is shown in fig. 2.1.

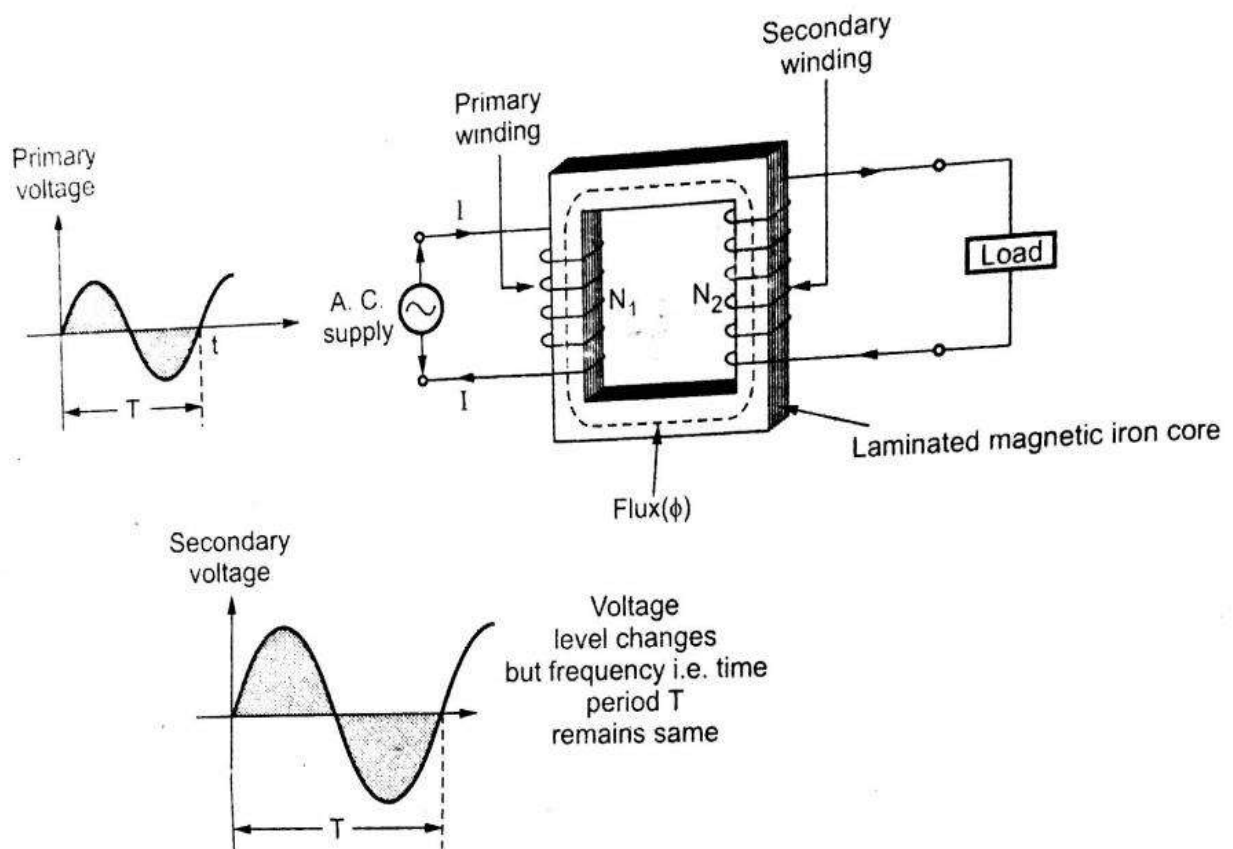


Fig. 2.1 Basic transformer

One of the two coils is connected to a source of alternating voltage . This coil in which electrical energy is fed with the help of source is called **primary winding (P)** . The other winding is connected to load .The electrical energy transformed to this winding is drawn out to the load . This winding is called **secondary winding (S)**. The primary winding has  $N_1$  number of turns while the secondary winding has  $N_2$  number of turns .

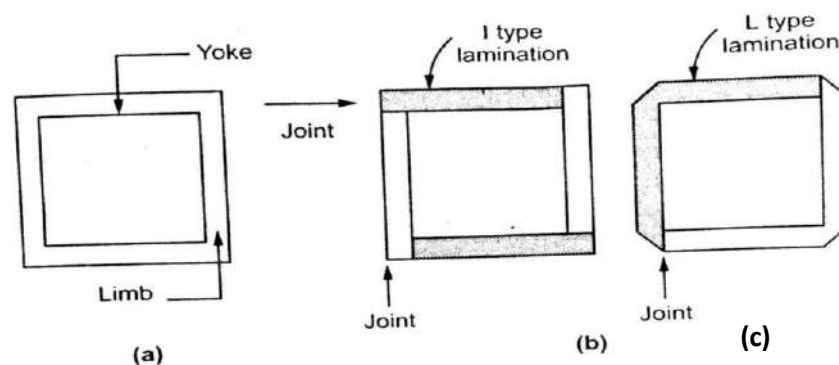
Symbolically the transformer is indicated as shown in the fig. 2.2. When primary winding is excited by an alternating voltage , it circulates an alternating current produced an alternating flux ( $\Phi$ ) which completes its path through common magnetic core as shown dotted in the fig . 1.2. thus an alternating , flux links with the secondary winding. As the flux is alternating , according to faradays law of an electromagnetic inductions, mutually induced e.m.f gets developed in the secondary winding . If load is connected to the secondary winding this e.m.f drives a through it. Thus though there is no electrical contact between the two windings, an energy gets transferred from primary to secondary.

## 2.2 Construction

There are two basic parts of a transformer I (Magnetic Core  
ii) Winding or Coils. The core of transformer is either square or rectangular in size . it is further divided into two parts . the vertical portion on which coils are wound is called **limb** while the top and bottom horizontal portion is called **yoke** of the core. These parts are shown in the fig. 2.2(a).

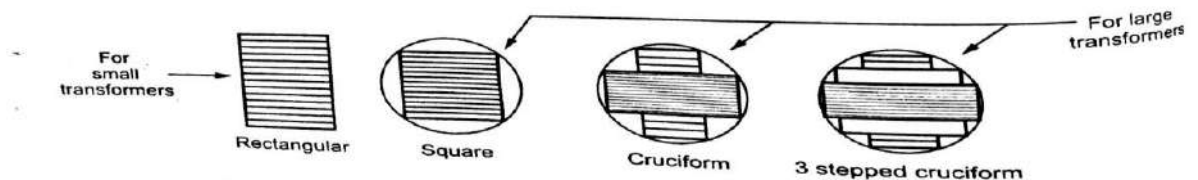


Core is made up of laminations. Because of laminated type of construction, eddy current losses get minimized. Generally high grade silicon steel laminations [0.3 to 0.5 mm thick ] are used. These laminations are insulated from each other by using insulation like varnish. All lamination are varnished. Laminations are overlapped so that to avoid the air gap at the joints. For this generally 'L' shaped or 'I' shaped lamination are used which are shown in the fig. 2.2 (b).



**Fig. 2.2 construction of transformer**

The cross-section of the limb depends on the type of coil to be used either circular or rectangular. The different cross-section of limbs, practically used are shown in the fig. 2.3.



**fig 2.3**

## 2.3 E.M.F. Equation of a Transformer

When the primary winding is excited by an alternating voltage  $V_1$ , it circulates alternating current, producing an alternating flux  $\Phi$ . The primary winding has  $N_1$  number of turns. The alternating flux  $\Phi$  linking with the primary winding itself induces an e.m.f. in it denoted as  $E_1$ . The flux links with secondary winding through the common magnetic core. It produces induces e.m.f.  $E_2$  in the secondary winding. This is mutually induces e.m.f. let us derive the equations for  $E_1$  and  $E_2$ .

The primary winding is excited by purely sinusoidal alternating voltage. Hence the flux produced is also sinusoidal in nature having maximum value of  $\Phi_m$  as shown in the fig. 2.4

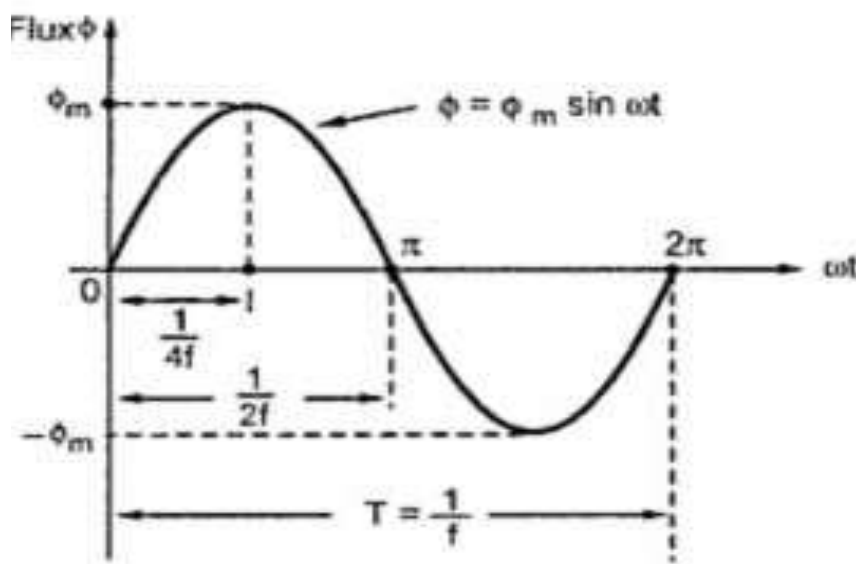


Fig. 2.4 Sinusoidal flux

The various quantities which effect the magnitude of the induced e.m.f. are :

$\Phi$  = Flux

$\Phi_m$  = Maximum value of flux

$N_1$  = Number of primary winding turns

$N_2$  = Number of secondary winding turns

$F$  = Frequency of the supply voltage

$E_1$  = R.M.S. value of the primary induced e.m.f.

$E_2$  = R.M.S. value of secondary induced e.m.f.

From faraday's law of electromagnetic induction the average e.m.f induced in turns is proportional to the average rate of change of flux.

$\therefore$  average e.m.f. turns = average rate of change of flux

$\therefore$  average e.m.f. per turn =  $\frac{d\phi}{dt}$

Now  $\frac{d\phi}{dt} = \frac{\text{change in flux}}{\text{time required for change in flux}} \dots\dots\dots(1-2)$

Consider the  $1/4^{\text{th}}$  cycle of the flux as shown in the fig. 1.11. Complete cycle gets completed in  $1/f$  seconds. In  $1/4^{\text{th}}$  time period, the change in flux is from 0 to  $\Phi_m$ .

$$\begin{aligned}\therefore \frac{d\phi}{dt} &= \frac{\Phi_m - 0}{\left(\frac{1}{4f}\right)} \text{ as } dt \text{ for } 1/4^{\text{th}} \text{ time period is } 1/4f \text{ seconds} \\ &= 4f \Phi_m \quad \text{Wb/sec}\end{aligned}$$

$\therefore$  average e.m.f per turn =  $4f \Phi_m$  volt

As  $\Phi$  is sinusoidal, the induced e.m.f in each turn of both the windings is also sinusoidal in nature. For sinusoidal quantity,

$$\text{Form Factor} = \frac{\text{R.M.S value}}{\text{Average value}} = 1.11 \dots\dots\dots(2-2)$$

**$\therefore$  R.M.S value = 1.11 x Average value**

**$\therefore$  R.M.S value of induced e.m.f per turn**

$$= 1.11 \times 4 f \Phi_m$$

$$= 4.44 f \Phi_m$$

There are  $N_1$  number of primary turns hence the **R.M.S** value of induced e.m.f of

Primary denoted as  $E_1$  is ,

$$E_1 = N_1 \times 4.44 f \Phi_m \quad \text{volts}$$

While as there are  $N_2$  number of secondary turns the R.M.S value of induced e.m.f of secondary denoted  $E_2$  is,

$$E_2 = N_2 \times 4.44 f \Phi_m \quad \text{volt}$$

The expressions of  $E_1$  and  $E_2$  are called e.m.f equations of a transformer

Thus e.m.f equations are,

$$\therefore E_1 = 4.44 f \Phi_m N_1 \quad \text{volts} \quad \text{..... (1)}$$

$$E_2 = 4.44 f \Phi_m N_2 \quad \text{volts} \quad \text{.....(2)}$$

## 2.4 Ratios of a Transformer

Consider a transformer shown in fig. 2.5 indicating various voltages and currents.

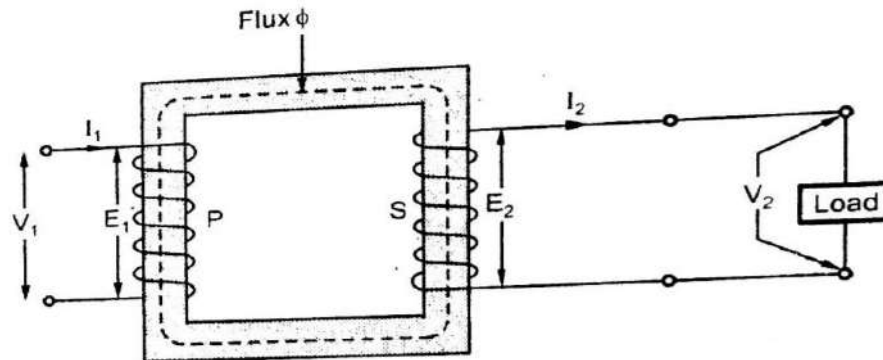


Fig 2.5 Ratios of transformer

### 2.4.1 Voltage Ratio

We know from the e.m.f equations of transformer that

$$E_1 = 4.44 f \Phi_m N_1 \quad \text{and} \quad E_2 = 4.44 f \Phi_m N_2$$

Taking ratio of the two equations we get,

$$\frac{E_2}{E_1} = \frac{N_2}{N_1} = K \quad (3-2)$$

This ratio of secondary induced e.m.f to primary induced e.m.f is known as voltage transformation ratio denoted as **K**.

1. If  $N_2 > N_1$  i.e  $K > 1$ , we get  $E_2 > E_1$  then the transformer is called **step-up transformer**.
2. If  $N_2 < N_1$  i.e  $K < 1$ , we get  $E_2 < E_1$  then the transformer is called **step down transformers**.

3. If  $N_2 = N_1$  i.e  $K = 1$ , we get  $E_2 = E_1$  then the transformer is called **isolated transformer** or **1:1 transformer**.

### 2.4.2 Ideal Transformer

A transformer is said to be ideal if it satisfies following properties:

- i) It has no losses.
- ii) Its winding have zero resistance.
- iii) Leakage flux is zero i.e 100 % flux produced by primary links with the secondary.
- iv) Permeability of core is so high that negligible current is required to establish the flux in it.

Similarly the secondary induced e.m.f  $E_2$  is also same as the terminal voltage  $V_2$  across the load. Hence for an **ideal transformer** we can write,

$$\frac{E_2}{E_1} = \frac{V_1}{V_2} = K$$

No transformer is ideal in practice but the value of  $E_1$  is almost equal to  $V_1$  for properly designed transformer.

### 2.4.3 Current Ratio

For an ideal transformer there are no losses. Hence the product of primary voltage  $V_1$  and primary current  $I_1$ , is the product of secondary voltage  $V_2$  and the secondary current  $I_2$ .

So  $V_1 I_1 = \text{input VA}$  and  $V_2 I_2 = \text{output VA}$

For an ideal transformer,

$$V_1 I_1 = V_2 I_2$$

$$\frac{V_2}{V_1} = \frac{I_1}{I_2} = K$$

# **Chapter Three**

## **Testing of transformer**



### 3.1 Indirect Loading Tests on Transformer (O.C. and Tests )

The efficiency and regulation of a transformer on any load condition and at any power factor condition can be predetermined by indirect loading method. In this method, the actual load is not used on transformer. But equivalent circuit parameters of a transformer are determined by conduction two tests on a transformer which are,

1. Open circuit test (O.C. Test)
2. Short circuit test (S.C Test)

The advantage of this method is that without much power loss the tests can be performed and results can be obtained. Let us discuss in detail how to perform these tests and how to use the results to calculate equivalent circuit parameters.

#### 3.1.1 Open circuit Test (O.C Test)

The experimental circuit to conduct O.C test is shown in the Fig. 3.1

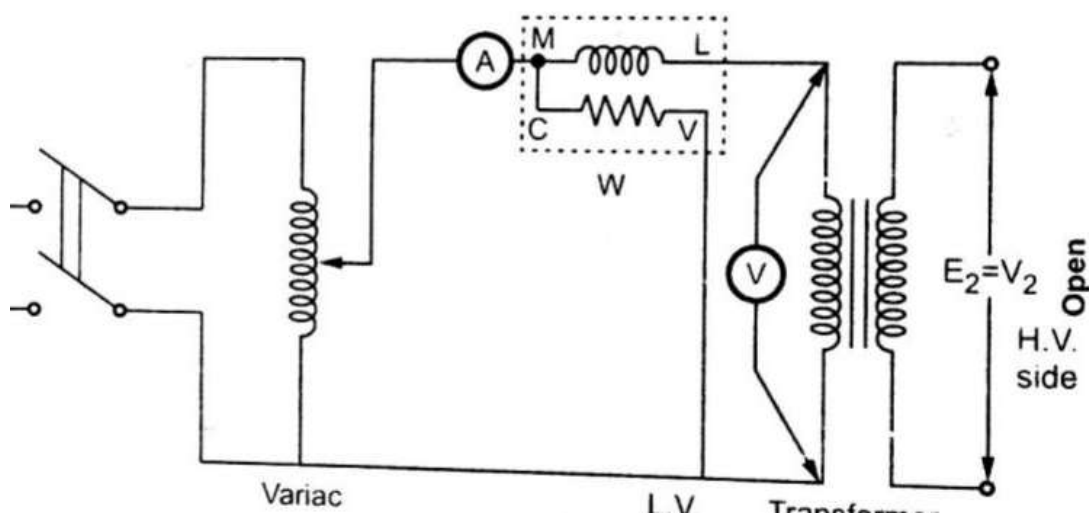


Fig. 3.1 Experimental circuit for O.C test

The transformer primary is connected to a.c supply through ammeter, wattmeter and variac. The secondary of transformer is kept open. Usually low voltage side is used as primary and high voltage side as secondary to conduct O.C. test

The primary is excited by rated voltage, which is adjusted precisely with help of a variac. The wattmeter measures input power. The ammeter measures input current. The voltmeter gives the value of rated primary voltage applied at rated frequency.

Sometimes a voltmeter may be connected across secondary to measure secondary voltage is  $V_2 = E_2$  when primary is supplied with rated voltage. As voltmeter resistance is very high, though voltmeter is connected, secondary is treated to be open circuit as voltmeter current is always negligibly small.

When the primary voltage is adjusted to its rated value with the help of variac, readings of ammeter and wattmeter are be recorded.

The observation table is as follows

$V_o$ volts	$I_o$ amperes	$W_o$ watts
Rated		

$V_o$  = Rated voltage

$W_o$  = Input power

$I_o$  = Input current = no load current

As transformer secondary is open , it is on no load. So current drawn by the primary is no load current  $I_o$ . the two component of this no load current are,

$$I_m = I_o \sin \phi_o$$

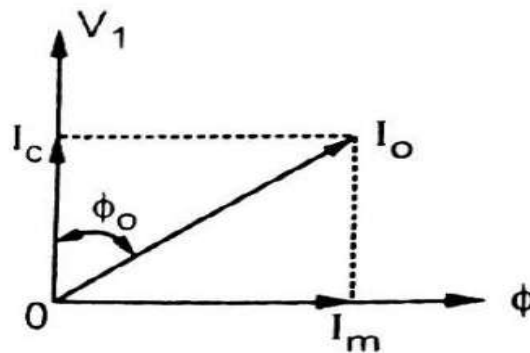
$$I_c = I_o \cos \phi_o$$

Where  $\cos \phi_o$  = No load power factor

And hence power input can be written as,

$$W_o = V_o I_o \cos \phi_o \dots\dots(1-3)$$

The phasor diagram is shown in the fig. 3.2.



**Fig. 3.2**

As secondary is open,  $I_2 = 0$ . Thus its reflected current on primary  $I_2'$  is also zero. So we have primary current  $I_1 = I_o$ . the transformer no load current is always very small, hardly 2 to 4% of its full load value. As  $I_2 = 0$  , secondary copper losses are zero. And  $I_1 = I_o$  is very low. Thus the total copper losses in O.C. test are negligibly small. As against this the input voltage is rated at rated frequency hence flux density in the core is at its maximum value. Hence iron losses are it rated voltage. As output power is zero and copper losses are

$$W_o = P_i = \text{Iron losses}$$

very low, the total input power is used to supply iron losses. This power is measured by the wattmeter i.e.  $W_o$ . hence the wattmeter in O.C. test gives iron losses which remain constant for all the loads.

**Calculations : We know that,**

$$W_o = V_o I_o \cos \phi_o$$

$$\cos \phi_o = \frac{W_o}{V_o I_o} = \text{no load power factor}$$

Once  $\cos \phi_o$  is known we can obtain,

$$I_m = I_o \sin \phi_o$$

and  $I_c = I_o \cos \phi_o$

once  $I_c$  and  $I_m$  are know we can determine exciting circuit parameters as,

$$R_o = \frac{V_o}{I_o} \quad \Omega$$

And  $X_o = \frac{V_o}{I_m} \quad \Omega$

### 3.1.2 Short Circuit Test ( S.C Test )

In this test, primary is connected to a.c. supply through variac, ammeter and voltmeter as shown in the fig. 3.3

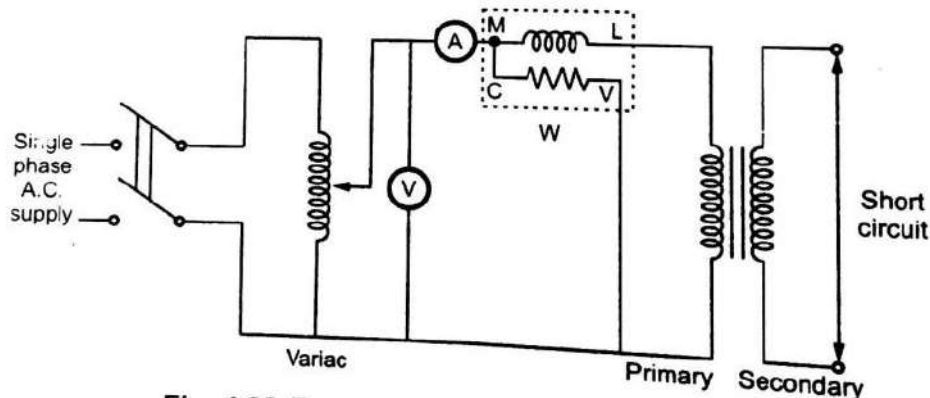


Fig 3.3 Experimental circuit for S.C test

The secondary is short circuited with the help of thick copper wire or solid link. As high voltage side is always low current side, it is convenient to connect high voltage side to supply and shorting the low voltage side.

As secondary is shorted, its resistance is very very small and on rated voltage it may draw very large current. Such large current can cause overheating and burning of the transformer. To limit this short circuit current, primary is supplied with low voltage which is just enough to cause rated current to flow through primary which can be observed on an ammeter. The low voltage can be adjusted with the help of variac. Hence this test is also called **low voltage test** or **reduced voltage test**. The wattmeter reading as well as voltmeter, ammeter reading. Are recorded. The observation table is as follows,

$V_{sc}$ volts	$I_{sc}$ amperes	$W_{sc}$ watts
	Rated	

Now the currents flowing through the winding are rated currents hence the total copper loss is full load copper loss. Now the voltage applied is low which is a small fraction of the rated voltage . the iron losses are function of applied voltage. So the iron losses in reduced voltage test are very small. Hence the wattmeter reading is the power loss which is equal to full load copper losses as iron losses are very low.

$$\therefore W_{sc} = (P_{CU}) F.L = \text{Full load copper loss}$$

**Calculations : From S.C. test readings we can write,**

$$W_{sc} = V_{sc} I_{sc} \cos \phi_{sc}$$

$$\therefore \cos \phi_{sc} = \frac{V_{sc} I_{sc}}{W_{sc}} = \text{short circuit power factor}$$

$$W_{sc} = I_{sc}^2 R_{1e} = \text{copper loss}$$

$$\therefore R_{1e} = \frac{W_{sc}}{I_{sc}^2}$$

**While**  $Z_{1e} = \frac{V_{SC}}{I_{SC}} = \sqrt{R_{1e}^2 + X_{1e}^2}$

$\therefore X_{1e} = \sqrt{Z_{1e}^2 - R_{1e}^2} \dots\dots\dots(2-3)$

Thus we get the equivalent circuit parameters **R<sub>1e</sub>**, **X<sub>1e</sub>** and **Z<sub>1e</sub>**. knowing the transformation ratio **K**, the equivalent circuit parameters referred to secondary also can be obtained.

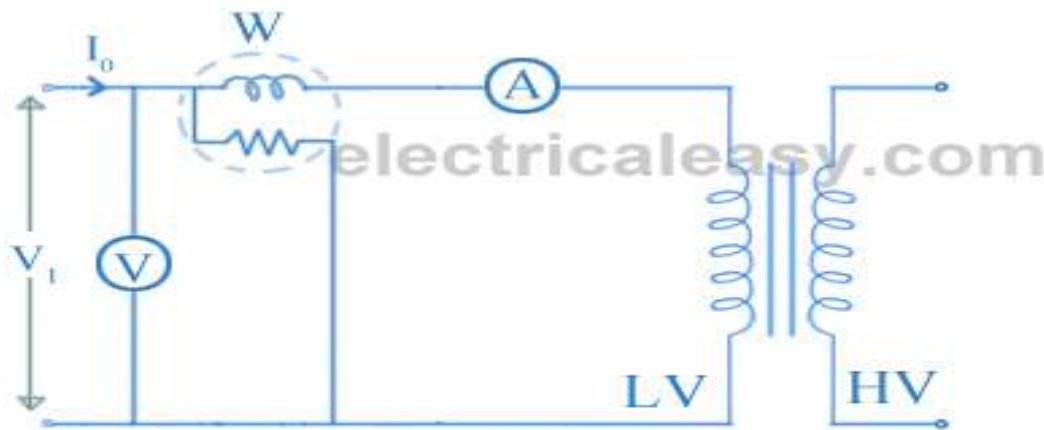
# **Chapter Four**

## **Calculation**



## 4.1 Open circuit test of transformer

Through these reading ,It is possible to know and calculate the values and parameters of the transformer such as resistance of the core ( $R_c$ ) and magnetic reactance ( $X_m$ ) and the core current ( $I_c$ ) and magnetising current ( $I_m$ ) and the copper losses ( $P_{cu}$ ).

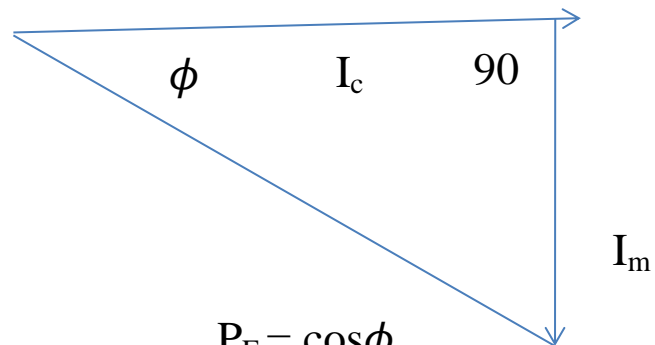


$$I_o = I_c + I_m \dots\dots(4-1)$$

$$I_o = \frac{V_1}{R_c} + \frac{V_1}{X_m}$$

$$R_c = \frac{V_1}{I_c}$$

$$X_m = \frac{V_1}{I_m}$$



$$P_F = \cos \phi$$

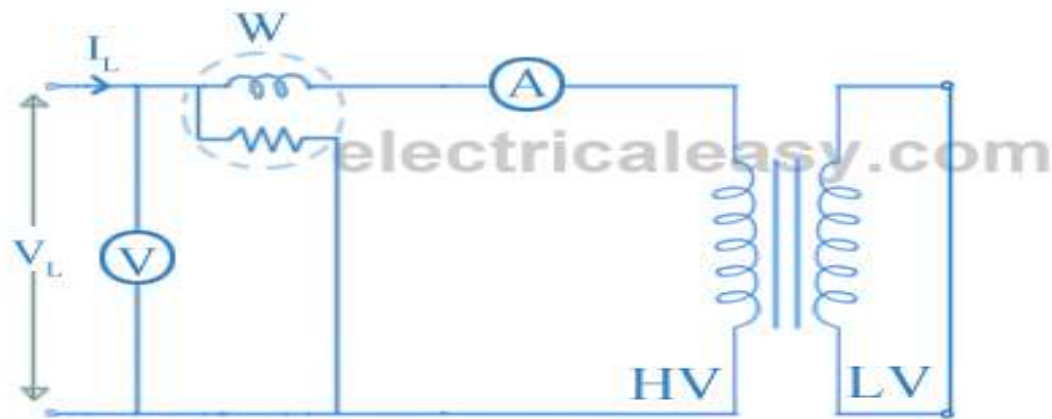
$$I_c = I_o \cos \phi$$

$$I_m = I_o \sin \phi$$

	$V_1=46V$	$V_1=92V$	$V_1=138V$	$V_1=184V$	$V_1=230V$
<b><math>V_1</math> rated</b>	<b>20%</b>	<b>40%</b>	<b>60%</b>	<b>80%</b>	<b>100%</b>
$P_o(w)$	0.8	2.7	5.3	9.2	15
$I_1(A)$	0.041	0.058	0.074	0.088	0.106
$V_2(v)$	24	47.7	72	95	120
$\cos\phi = \frac{P}{V_1 I_1}$	0.42	0.50	0.52	0.56	0.60
$I_c = I_o \cos\phi$	0.017	0.029	0.04	0.05	0.06
$I_m = I_o \sin\phi$	0.037	0.050	0.062	0.076	0.082
$R_c = \frac{v_1}{I_c}$	2700	3172	3450	3680	3833
$X_m = \frac{v_1}{I_m}$	1243	1840	2220	2412	2804
$a = \frac{v_1}{v_2}$	1.92	1.92	1.92	1.92	1.92

## 4.2 Test of short circuit transformer

The short circuit reading enable us to calculate the equivalent Impedance of the circuit ( $Z_{eq}$ ) and equivalent resistance ( $R_{eq}$ ) And equivalent inductance ( $X_{eq}$ ) .



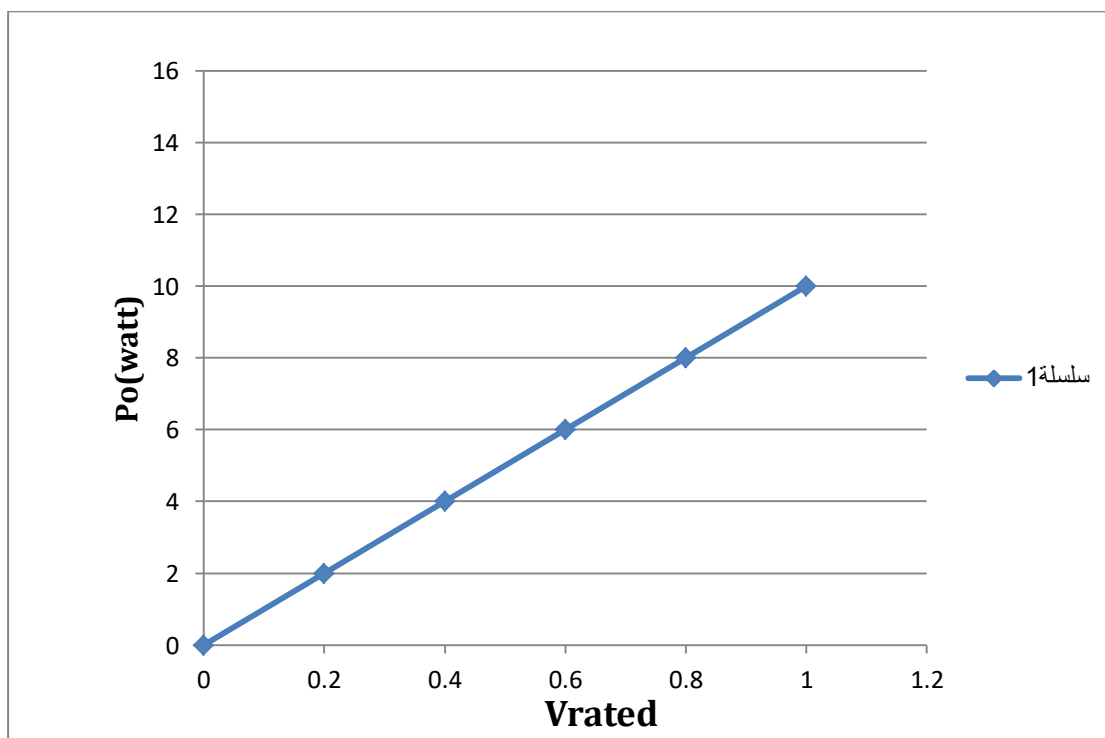
The condition for using the short circuit test transformer is that the ratio of the supplied voltage shall not be more than (10%) of the applied voltage to avoid the passage of high current that leads to damage to the insulators and wires and burning the transformer .

$$X_{eq} = \sqrt{(Z_{eq})^2 - (R_{eq})^2} \dots\dots(2-4)$$

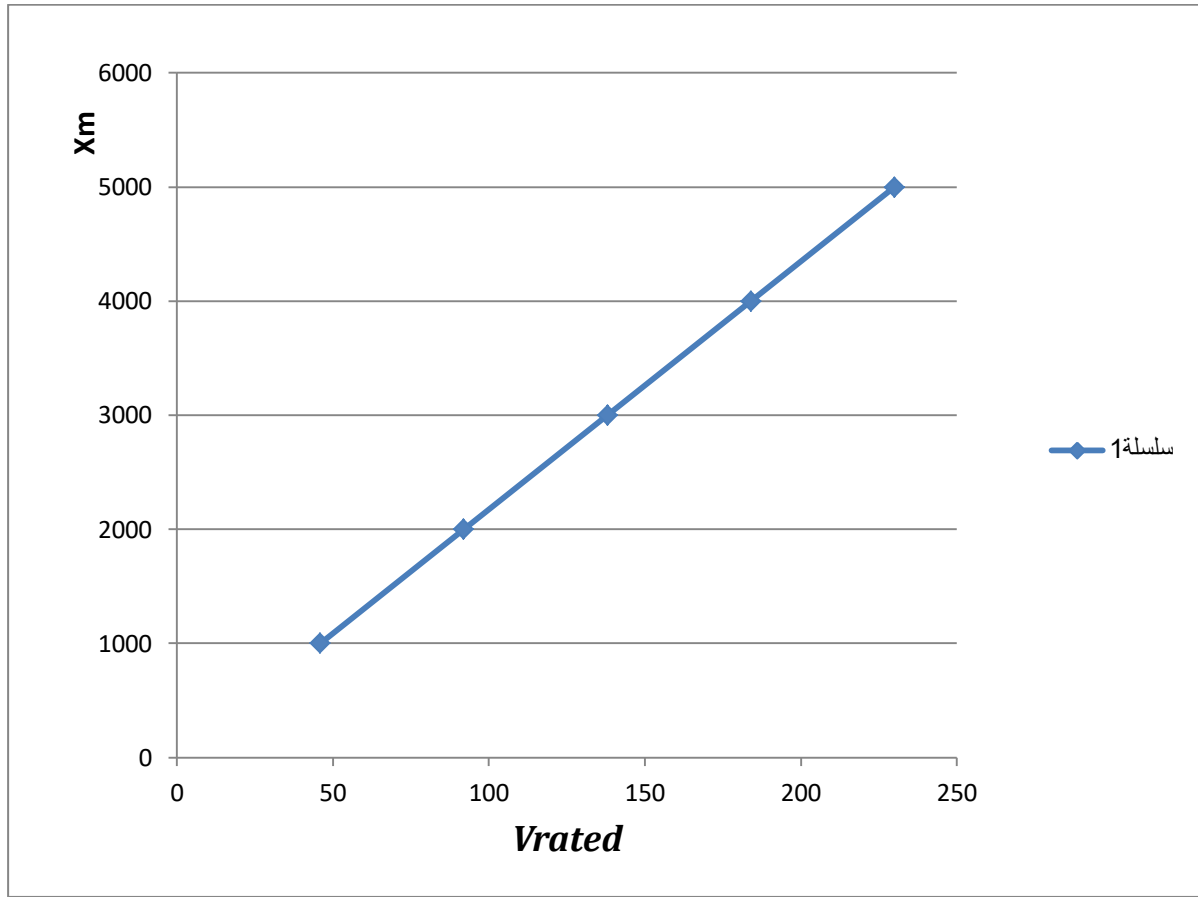
$$P_{sc} = (I_{sc})^2 R_{eq} \dots\dots(3-4)$$

As for ( $I_c$ ) current and the ( $I_m$ ) current neglected because the resistance of each of them is very high and the current dose not pass through ,because of the short circuit secondary

$V_{sc}$ 10% applied	$I_{sc}$ (A)	$Z_{eq}$ ( $\Omega$ )	$R_{eq}$ ( $\Omega$ )	$X_{eq}$ ( $\Omega$ )	$P_{sc}$ (watt)
23V	0.021	1084	793	740	0.35



Relation between Vrated and iron losses



Relation between  $V_{rated}$  and Magnetizing resistance  $X_m$

# **Chapter Five**

## **Conclusions**

## Conclusions

- ✚ Though this research it turns out that there are two types of transformers , which are
  - a. Transformer high voltage (low current)
  - b. Transformer low voltage (high current)
  
- ✚ In both types of these transformers the frequency of the internal voltage remain equal of the frequency of external voltage and this is one of the best benefits of electrical transformer of various types.
  
- ✚ Iron losses of transformer occur in the magnetic core and can be reduce by the following method
  - a. By using grade material silicon stell to reduce hysteresis loss
  - b. Manufacturing core in the form lamination or stacks lamination to reduce eddy current loss.
  
- ✚ Copper losses occur in primary and secondary winding of transformer and they depend on the current with load and current with no load if full load current , we get copper losses full load if half load current then we get copper losses at half , which are less than full load copper losses this called (variable losses). Reduced by using good quality copper conductors with an approqiate cross section area (larger).

## *Reference*

---

- 1- India ,2007 , U-A-Bakshi electrical machine
- 2- India , 2007, B.L Theraja electrical technology



## Abstract:

The electrical energy consumed to cool residential buildings in the city of Baghdad is estimated at about 40% of the electrical energy produced in the city, due to the hot weather conditions in the city, where the temperature in the city reaches 50 degrees Celsius in some summer days that start from May until September. Therefore, care must be taken in choosing the construction materials for buildings, and the quality and thickness of the glass in the windows is an important factor in reducing heat gain during the summer. In this project, a theoretical study was conducted in which the cooling loads of a residential house in the city of Baghdad were calculated, where we obtained results from this study in that the use of Double 8mm thick clear glass with 6mm vacuum achieves a reduction in cooling load by a limit 51.9% compared to using single glass with 4mm thickness and double 8mm thick tinted glass with 6mm vacuum achieves a 41.4% reduction in cooling load compared to using single glass with thickness of 4mm and that the use of double reflective glass with a thickness of 8 mm with a vacuum of 6 mm thickness achieves a 53.7% decrease in the cooling load.

## Content

	<i>Description</i>	<i>Page</i>
<i>Chapter 1</i>	<i>Introduction</i>	<i>5</i>
	<i>Aim of project</i>	<i>6</i>
<i>Chapter 2</i>	<i>Historical review</i>	<i>8</i>
	<i>Factors effecting conditioning calculations</i>	<i>9</i>
	<i>Wind speed:</i>	<i>9</i>
	<i>Air permeation</i>	<i>9</i>
	<i>Building quality and its uses</i>	<i>9</i>
	<i>Design conditions</i>	<i>9</i>
	<i>The Climatic and design conditions of the building,</i>	<i>9</i>
	<i>Method of calculating thermal loads</i>	<i>10</i>
<i>Chapter 3</i>	<i>Theoretical review</i>	
	<i>The equations of calculation</i>	<i>13</i>
<i>Chapter 4</i>	<i>Calculation and result</i>	
	<i>calculation of cooling load for reception room</i>	<i>15</i>
<i>Chapter 5</i>	<i>Discussion and Conclusions</i>	
	<i>Discussion</i>	<i>22</i>
	<i>Conclusions</i>	<i>22</i>
	<i>Recommendations</i>	<i>23</i>
<i>Appendix</i>		<i>26</i>

## List of table:

<i>No.</i>	<i>table</i>	<i>page</i>
<i>1</i>	<i>The climatic and design conditions of the building</i>	<i>10</i>
<i>2</i>	<i>the values of overall heat transfer</i>	<i>16</i>
<i>3</i>	<i>the structural composition of the roof with thermal conductivity</i>	<i>18</i>
<i>4</i>	<i>the cooling load</i>	<i>19</i>
<i>5</i>	<i>cooling load for reception with deferent type of glass</i>	<i>19</i>
<i>6</i>	<i>cooling load calculation for Kitchen</i>	<i>20</i>
<i>7</i>	<i>the cooling load for the building:</i>	<i>20</i>

## List of figures

<b>No.</b>	<b>figures</b>	<b>page</b>
1	4 mm Clear glass	6
2	8 mm Shade glass	6
3	8-6-8 Reflector double glass	6
4	The relationship between Qg and thickness for 3 types of glass	24

## List of Symbol:

<b>Symbol</b>	<b>Description</b>	<b>Units</b>
<i>Q<sub>w</sub></i>	<i>Load through the walls</i>	<i>Ton</i>
<i>U<sub>w</sub></i>	<i>Thermal Transmittance for walls</i>	<i>w/m<sup>2</sup>.c</i>
<i>A<sub>w</sub></i>	<i>Area of Walls</i>	<i>m<sup>2</sup></i>
<i>CLTD<sub>c</sub></i>	<i>Cooling Load Temperature Difference for walls</i>	<i>C</i>
<i>LM</i>	<i>Correction factor of latitude and month</i>	
<i>(25-Tr)</i>	<i>Correction factor of inside temperature</i>	<i>C</i>
<i>Tr</i>	<i>Room temperature</i>	<i>C</i>
<i>(T<sub>m</sub>-29.4)</i>	<i>Correction factor of outside temperature</i>	<i>C</i>
<i>T<sub>m</sub></i>	<i>mean temperature</i>	<i>C</i>
<i>Q<sub>c</sub></i>	<i>Conductive load through the glass</i>	<i>Kw</i>
<i>U</i>	<i>Thermal Transmittance for glass</i>	<i>w/m<sup>2</sup>.c</i>
<i>A</i>	<i>Area of glass</i>	<i>m<sup>2</sup></i>
<i>CLTD</i>	<i>Cooling Load Temperature Difference for glass</i>	<i>C</i>
<i>Q<sub>s</sub></i>	<i>Solar transmission load through the glass</i>	<i>Kw</i>
<i>SC</i>	<i>Shading coefficient</i>	
<i>SCI</i>	<i>solar cooling load factor</i>	
<i>DR</i>	<i>Daily range temperature</i>	<i>C</i>
<i>Q<sub>light</sub></i>	<i>heat gain from lighting</i>	<i>Watt</i>
<i>CLF</i>	<i>Cooling Load Factors</i>	
<i>W</i>	<i>Watts input from electrical lighting plan or lighting load data</i>	<i>Watt</i>
<i>F<sub>u</sub></i>	<i>Lighting use factor, as appropriate</i>	
<i>F<sub>as</sub></i>	<i>special ballast allowance factor, as appropriate</i>	
<i>Q<sub>s</sub></i>	<i>Sensible heat gain from occupancy</i>	<i>Kw</i>
<i>Q<sub>L</sub></i>	<i>Latent heat gain from occupancy</i>	<i>Kw</i>
<i>N</i>	<i>number of people in space</i>	
<i>ACH</i>	<i>Air change per hour</i>	<i>m/hr</i>

# *Chapter 1*

## ***Introduction***

The interest in the window comes from being one of the aesthetics of architectural design and the frequent use of glass for the facades of buildings. The difference in the area of the window often does not exceed the consistency of the design requirements, and through it, the occupants of the room are psychologically linked to the surrounding environment, as well as the main source of access to natural lighting in the room, and because Iraq is within The tropical region has a climate closest to the desert, during which the summer lasts more than seven months, during which the sun shines for a long period of up to 14 hours / day, and the sunny weather averages ( 225 days / year and the radiation rate reaches 430 watts / m.)[1]

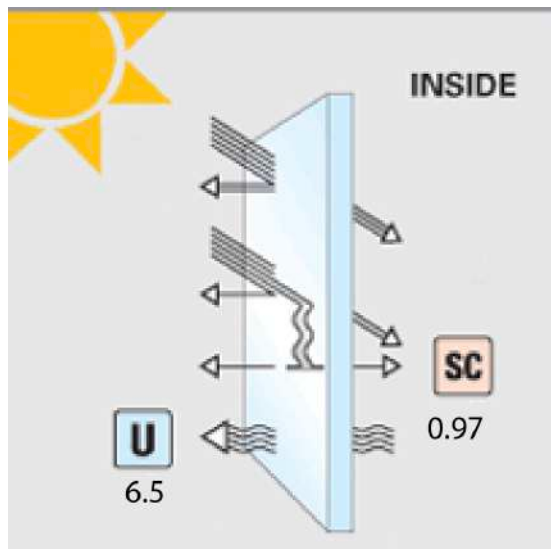
The temperature sometimes reaches 50 degrees Celsius, and thus the outer shell of the building is exposed to huge heat waves that are transmitted inside the building through its walls and ceiling, which dampens the frequency of the transmitted wave, as well as transmitted directly through its windows, which leads to a rise in the temperature of the building space to much higher levels. Which is recommended internationally, so it requires a large energy consumption for the purposes of operating air conditioners (air cooling) to reach the room temperature to a standard level. Where it clearly reduces the psychological connection of the occupants of those buildings with the surrounding environment, in addition to its ineffectiveness in reducing the amount of heat transmitted from the environment with its clear effect in reducing the level of natural lighting inside those rooms and this is reflected in the low distribution of lighting over the entire area of the room, which requires compensation by using Artificial lighting, which consumes direct electrical energy in addition to adding heat loads to the room, which leads to an increase in the cooling load, to the point that it adds thermal loads to the room, which leads to an increase in the cooling load, so this theoretical project was established for the purpose of studying the most appropriate types of glass for these windows, knowing that the proposed types of glass are normal, shaded and reflective, with fixed sizes and variable thicknesses, which are four thicknesses for each type

(4 mm, 6 mm and 8mm and double 8mm each window with 6mm space)

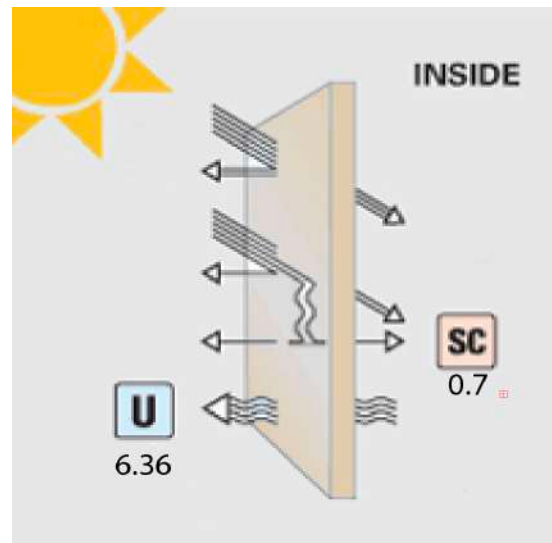
Note that the search area is in the beloved capital Baghdad, latitude 32.2 degrees north and longitude 44.6 east. The research is not related to the direction of the window, but rather is related to calculating the reduction of the amount of heat gained, and the amount of heat released through the window glass

## *Aim of project*

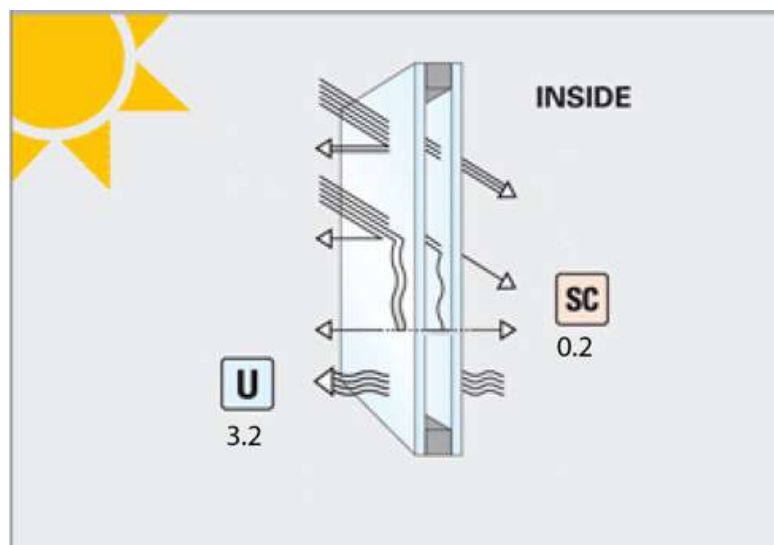
The aim of project is studying the effect of type of glass on the cooling load of house in Baghdad city.



*Figure (1): 4mm Clear glass*



*Figure (2): 8mm Shade glass*



*Figure (3): (8-6-8 )mm Reflector double glass*

## *Chapter 2*

# ***Historical review***

For thousands of years, man has been trying to overcome the difficult environmental conditions surrounding him, such as high heat and humidity, where ancient civilizations in the Nile Valley and Mesopotamia used ceramic pots to cool water, while the affluent in the Chinese and Roman civilizations brought ice from the frozen regions in the north and stored it in private homes for use in cooling. What they need like water and juice. Since then the need for refrigeration, air conditioning and refrigeration has emerged. Willis Carrier is the first to lay the foundations of air conditioning in a scientific way, as he designed the first psychrometric scheme and set its equations. He also presented the first research on the properties of air in 1911 and founded his company known by his name in 1915, which is now one of the largest international companies for the production of air conditioners of all kinds.

Air conditioning is not limited to cooling only, but also includes heating. Heating methods have evolved from old primitive wood stoves to coal or wood heating boilers, and then to heating boilers that operate with mechanical fans that burn light oil fuel or natural gas, and then to the various current heating methods that It was distinguished from its predecessors by its lighter weight, increased capacity and high efficiency, in addition to containing automatic control. With the beginning of the sixties, the spread of central air conditioning systems expanded and was not limited to government buildings only but became an essential part of the construction and reconstruction industry. With the beginning of the seventies, the construction of any new building was not considered valuable. It was not a central air conditioner, and the use of frozen and refrigerated warehouses to preserve foods and meat was widespread. On the industrial level, many Arab and Islamic countries have begun assembling or manufacturing and producing evaporative air coolers, home refrigerators and wall air conditioners, but the advanced refrigeration methods and basic central air conditioning devices of all kinds. It is imported from advanced industrial countries.



**(2-1) Factors Effecting on Cooling Load [1]**

There are several factors that have direct impacts on the conditioning calculations and among these factors are:

**(2-1-1) Wind speed: [1]**

Wind speed is important to air conditioning calculations as it has a direct effect on transaction values Heat transfer and air leakage.

**(2-1-2)- Air permeation: [2]**

The amount of air that penetrates into the building depends on the cracks and mounting holes around the building External doors and windows are mainly based on the provisions of these doors and windows Made and installed. The permeate air imposes an additional load for heating as the temperature must be raised Its temperature is from outside temperature to room air temperature.

**(2-1-3) Building quality and its uses: [2]**

Air conditioning operations differ according to the type of use of the place to be adapted, the air conditioning the factory differs from adapting homes or schools due to the different nature of use It leads to changing the design conditions.

**(2-1-4) Design conditions: [2]**

Set design conditions and temperature selection (indoor and outdoor) depending on The quality of the place and to provide adequate and healthy conditions for the occupants of the space.

**(2-1-5) The Climatic and design conditions of the building,** is showing in, table (1), appendix

The design of external climate conditions is to define the temperature of dry and wet bulb and moisture the relative and daily temperature variation of the outside air. It is the geography of the site for an area the specific determinant of the climate of that region is, and the external design conditions are usually based on measurements Meteorological departments.

As for the internal design conditions of the building, they are defined as the conditions that have an air conditioning system Air permanence and preservation represented by dry bulb temperature and relative humidity are measured These conditions are at a height of (5.1 m), which represents the average height of the human respiratory line.

The choice of internal conditions depends on the external design conditions and the period of residence in the space as well as the type of effort exerted or the nature of the work of the occupants of the space. Based on the foregoing, it can be said Interior and exterior design conditions are based on standard schedules

Table No. (1) Shows the climatic and design conditions of the building [2]

Condition	Summer		Winter	
	DB C	RH %	DB C	RH %
Inside	25	50	22	50
Outside	50	30	0	80

DR= 18.7 For Baghdad

## (2-2) Method of Calculating Thermal Loads

### Thermal Loads Calculate: [3]

The thermal properties of the structural and architectural structure of the building are among the most important foundations on which it is based Designing any heating and cooling system. As the heat is transferred from the inside of the heated case to the outside In winter and from outside to the cooled building in summer, in two main ways:

1- Heat transfer through the walls from the air on one side to the air on the other side.

2- Heat transfer by leaking or penetrating the air itself into the building, so if I want to reduce this heat transfer, the thermal insulation property of the walls must be improved or the use of heat-insulating materials as well as reducing the Infiltration of outside air into the building through the cracks of doors and windows or their frames or as a result of opening them By using sealed doors and windows and treating the cracks.

Heat transfer occurs between two objects whose temperature differs by conduction or convection, or by radiation, or in two ways at the same time.

Conduction is defined as the process of heat transfer from a region of high temperature to a region of low temperature in a certain medium or more than one medium with direct physical contact. Conduction is the only way in which heat is transferred in solid, opaque bodies, and it is also important in fluids, but in non-solid materials it is coupled Usually transmission with pregnancy or sometimes radiation. The load is defined as a process in which energy is transferred by the collective effect of thermal conductivity, thermal storage and mixing movement. The load takes major importance as the method of heat transfer between solid, liquid and gaseous surfaces, and the load is classified according to the method of fluid movement. With natural convection, and when the mixing movement is stimulated

by an external factor such as a pump or a fan, the process is called forced convection. The effectiveness of heat transfer in convection depends on the movement of mixing fluid, and therefore the study of fluid flow characteristics becomes important to know the heat transfer in pregnancy.

As for the other way in which heat is transferred from one body to another, their temperature is different when the two bodies are physically separated in space, even if a complete vacuum separates them, then it is known as radiation, and the heat energy transferred in this way is called radiant heat.

## **2-Sources of Heat Gain: [3]**

The equation of heat loss from inside the heated space to the outside is done by preparing the heat in a manner that sustains a comfortable internal condition for the occupants of the space, and in a similar manner that requires a specific space to remove the heat gain from outside the space inside it so that an internal condition is maintained appropriate to the requirements of comfort and it is appropriate to divide the sources of heat gain into those coming from outside Adapted space, called external sources, and those resulting from within the space, and are called internal sources. There is a second division into perceived thermal gain and latent thermal gain, and this division is necessary to know the percentage of sensible heat within the space and to choose the correct cooling and dehumidification devices.

The external sources of heat gain are summarized as follows:

1- Thermal gain as a result of solar radiation, which is done in two ways:

A - Through glass, which is absorbed into furniture and interior structural surfaces.

B - On the surfaces of external walls and ceilings, which is transmitted by connection to the inside.

2- Heat transfer through the external structural envelope of the space from walls, ceilings and windows due to the difference in the temperature of the outside air and the air inside the room.

## **3- Thermal gain**

as a result of heat transfer from non-air-conditioned neighboring places through structural partitions, floors and ceilings within the air-conditioned space.

## **4- Perceptible and latent thermal gain**

as a result of penetration of the outside air into the space.

## **As for the internal sources, they are:**

1- Electric lighting.

2- A palpable and latent heat from the occupants of the space.

3- Heat from devices and equipment inside the space, such as electric motors, cooking appliances, and the like, and it may be tangible or tangible and latent.

## *Chapter 3*

# ***Theoretical review***

The equation of cooling load calculation are as follows: -

**(3-1) Equation of calculation heat gain throw wall [2]**

$$Q = U_w A_w (T_i - T_o) \text{ ----- (3-1-1)}$$

For glass and window

$$Q = U_g A_g (T_i - T_o) \text{ ----- (3-1-2)}$$

**(3-2) Equation of calculation Infiltration [2]**

Sensible heat

$$Q = 1.22 * V_{inf} * (T_i - T_o) \text{ ----- (3-2-1)}$$

Latent

$$Q = 2940 * V_{inf} * (T_i - T_o) \text{ ----- (3-2-2)}$$

**(3-3) Equation of calculation U [1]**

$$R_t = 1/F_i + X_1/K_1 + X_2/K_2 + X_3/K_3 + X_4/K_4 + 1/F_o \text{ ----- (3-3-1)}$$

$$U_w = 1/R_t \text{ ----- (3-3-2)}$$

**(3-4) Equation of calculation Q and U for glass [1]**

$$Q_{glass} = q_c + q_s \text{ ----- (3-4-1)}$$

$$U = 1 / \sum R = 1 / [ (1/h_o) + (X/K) + (1/h_i) ] \text{ ----- (3-4-2)}$$

$$q_c = U * A * CLTD_c \text{ ----- (3-4-3)}$$

$$q_s = A * S_c * SHG_{max} * CLF \text{ ----- (3-4-4)}$$

$$CLTD \text{ correction} = CLTD + (25.2 - T_R) + (T_O - 29.4) \text{ ----- (3-4-5)}$$

**(3-5) Equation of calculation ventilation [2]**

$$q = U * A * CLTD_c \text{ ----- (3-5-1)}$$

$$\tilde{V} = (v * No.) / 1000 = m^3/s \text{ ----- (3-5-2)}$$

$$Q_{ventilation} = q_l + q_s \text{ ----- (3-5-3)}$$

$$\tilde{V} = (\Psi * ACH) / 3600 \text{ ----- (3-5-4)}$$

$$q_{(inf)} s = 1.22 * \tilde{V}_{inf} * (T_o - T_i) \text{ ----- (3-5-5)}$$

$$q_{(inf)} L = 3000 * \tilde{V}_{inf} * (W_o - W_i) \text{ ----- (3-5-6)}$$

**(3-6) Equation of calculation Lighting**

$$Q = No. * W * FS * FSU * CLF \text{ ----- (3-6-1)}$$

**(3-7) Equation of calculation For people**

$$q_s = No. * q_{sh} \text{ ----- (3-7-1)}$$

$$q_L = No. * q_{Lh} \text{ ----- (3-7-2)}$$

$$Q_{people} = q_s + q_l \text{ ----- (3-7-3)}$$

**(3-8) Equation of calculation For internal load (appliances)**

$$Q_{appliance} = q_{in} * F_u * F_r * CLF \text{ ----- (3-8-1)}$$

$$q_{init} = No. * q_{in} \text{ ----- (3-8-2)}$$

$$Q = No. * W * FS * FSU * CLF \text{ ----- (3-8-3)}$$

## *Chapter 4*

# ***Calculation and results***

**(4-1) sample of calculation of cooling load for reception room**

The heat transfer coefficient of the summer load from the outside at wind speeds of 24 hr / Km

$$h_o = 22.7 \text{ W/m}^2 \cdot \text{c}^\circ [2]$$

The heat transfer coefficient of convection from inside in summer when air is still

$$h_i = 9.37 \text{ W / m}^2 \cdot \text{c}^\circ [2]$$

All values used in this project are taken from special charts and tables with air conditioning and icing.

**(4-1-1) WALL**

The Total Heat Transfer Coefficient for the Walls ( $U_w$ ) is calculated.

$$\begin{aligned} R_t &= 1/F_i + X_1/K_1 + X_2/K_2 + X_3/K_3 + X_4/K_4 + 1/F_o [1] \\ &= 1/9.37 + 0.025/0.81 + 0.24/0.72 + 0.02/0.721 + 0.1/1.3 + 1/22.7 \\ &= 0.61963 \\ U_w &= 1/R_t = 1/0.61963 = 1.61 \text{ W/m}^2 \cdot \text{c}^\circ \end{aligned}$$

**NORTH WALL**

$$\begin{aligned} A &= (5 \times 3) - 3 = 12 \text{ m}^2 \\ \text{CLTD} &\rightarrow \text{from table at time(15)} = 16 \text{ c}^\circ \\ L_m &\rightarrow \text{from table at (Aug)} = -1.1 \\ U &= 1.6 \text{ W/m}^2 \cdot \text{c} \\ T_m &= 39 \text{ c}^\circ \\ \text{CLTDc} &= 27.1 \\ q &= U * A * \text{CLTDc} \\ q(n) &= 520 \text{ watt} = 0.148 \text{ ton} \end{aligned}$$

**EAST WALL**

$$\begin{aligned} A &= (7 \times 3) - 6 = 15 \text{ m}^2 \\ U &= 1.6 \text{ W/m}^2 \cdot \text{c} \\ \text{CLTD} &\rightarrow \text{from table} = 17 \text{ c}^\circ \\ \text{Then CLTDc} &= 28.1 \text{ c}^\circ \\ T_m &= 39 \text{ c}^\circ \\ L_m &= 0 \\ q(E) &= 674.4 \text{ watt} = 0.192 \text{ ton} \end{aligned}$$

## (4-1-2) GLASS

Calculate the overall heat transfer coefficient of glass ( $U_g$ )

Building glass is a normal glass (6 mm) thickness.

( $0.78 \text{ W / m}^2 \cdot \text{c}^\circ$ ) = for thermal conductivity glass

$$R_t = 1/9.37 + 0.006/0.78 + 1/22.7 = 0.1584$$

$$U_g = 1/0.1584 = 6.31 \text{ W/m}^2 \cdot \text{c}^\circ$$

Table No. (2) shows the values of overall heat transfer

Material		$U \text{ w/m}^2 \cdot \text{c}$
Wall		1.61
Roof		4.4
Glass		
clear	4mm	6.5
	6mm	6.47
	8mm	6.36
	22mm	3.2
shade	4mm	6.58
	6mm	6.47
	8mm	6.36
	22mm	3.2
Reflector	4mm	6.58
	6mm	6.47
	8mm	6.36
Reflector double glass	22mm	3.2

The type of glass used is (reflective double glassing)

North Side

$$Q(\text{glass}) = q_c + q_s$$

When

$$q_c = U * A * CLTD_c = 3.2 * 3 * 19 = 0.052 \text{ ton}$$

And

$$q_s = A * S_c * HGS = 3 * 0.2 * 110 = 0.019 \text{ ton}$$

Then

$$Q(\text{glass}) = q_c + q_s = 0.071 \text{ ton}$$



East Side

$$Q(\text{glass}) = q_c + q_s$$

When

$$q_c = U * A * CLTD_c = 3.2 * 3 * 19 = 0.050 \text{ ton}$$

And

$$q_s = A * S_c * SHG = 3 * 0.2 * 123 = 0.020 \text{ ton}$$

Then

$$Q(\text{glass}) = q_c + q_s = 0.7 \text{ ton}$$

$$Q(\text{glass})_{\text{total}} = 0.071 + 0.70 = 0.141 \text{ ton}$$

(4-1-3) DOOR

$$Q(\text{door}) = U * A * CLTD_c$$

$$A = 1.5 * 2.7 = 4 \text{ m}^2$$

$$U = 2.2 \text{ w/m}^2 \cdot \text{c (wood)}$$

$$\Delta t = 11 \text{ c}^\circ$$

$$Q_{\text{door}} = U * A * \Delta t = 2.2 * 4 * (11)$$

$$Q_{\text{door}} = 96.8 \text{ watt} = 0.027 \text{ ton}$$

(4-1-4) VENTILATION

From table we get the average of pure or fresh air for each people

$$v = 3.5 \text{ L/s}$$

$$\text{No. of people} = 6$$

$$\tilde{V} = (v * 6) / 1000 = (3.5 * 4) / 1000 = 0.021 \text{ m}^3/\text{s}$$

$$q_s = 1.22 * \tilde{V} * (45 - 24) = 0.53 \text{ kw} = 0.15 \text{ ton}$$

From chart at  $t(\text{in})$  24 and  $t(\text{out}) = 45$  we get

$$W_o = 0.015 \text{ and } W_i = 0.009$$

$$q_L = 3000 * \tilde{V} * (W_o - W_i) = 0.378 \text{ kw} = 0.108 \text{ ton}$$

$$Q_{\text{ventilation}} = 0.258 \text{ ton}$$

(4-1-5) INFILTRATION

$$\tilde{V} = (\sum V * ACH) / 3600 = (5 * 7 * 3 * 0.5) / 3600 = 0.014 \text{ m}^3/\text{s}$$

$$q(\text{inf})_s = 1.22 * \tilde{V}_{\text{inf}} * (T_o - T_i)$$

$$q(\text{inf})_s = 1.22 * 0.014 * (45 - 24) = 0.35 \text{ kw} = 0.01 \text{ ton}$$

$$q(\text{inf})_L = 3000 * \tilde{V}_{\text{inf}} * (W_o - W_i) = 0.25 \text{ kw} = 0.07 \text{ ton}$$

$$q(\text{infiltration}) = 0.08 \text{ ton}$$

(4-1-6) Light

$$\text{No. of light} = 10$$

$$\text{watt for each one} = 20$$

$$F_s \text{ (from table)} = 1.2$$

$$F_{su} \text{ (from table)} = 1$$

CLF (from table) = 1

$$Q = \text{No.} * W * FS * FSU * CLF = 10 * 20 * 1.2 * 1 * 1$$

$$Q = 240 \text{ watt} = 0.06 \text{ ton}$$

(4-1-7) For People

No. of people = 6

qsh (from table) = 70 w

qLh (from table) = 55 w

$$q_s = \text{No.} * q_{sh} = 6 * 70 = 420 \text{ watt} = 0.12 \text{ ton}$$

$$q_L = \text{No.} * q_{Lh} = 6 * 55 = 330 \text{ watt} = 0.094$$

$$Q_{\text{people}} = 0.21 \text{ ton}$$

(4-1-8) For Internal Load (appliances)

computer, ceiling fan, TV

Assume that each device consumes 200 w

$$Q_{\text{appliance}} = q_{in} * F_u * F_r * CLF$$

$$q_{in} = \text{No.} * q_{in} = 3 * 200 = 600 \text{ watt}$$

From table we get  $F_u$ ,  $F_r$  and CLF value

$$Q_{\text{appliance}} = 43.2 \text{ w}$$

$$Q_{\text{appliance}} = 0.012 \text{ ton}$$

**(4-2) Calculation of the Total Heat Transfer Coefficient for the Roof ( $U_r$ )**

The structural composition of the roof with the type of building material and thermal conductivity.

Table No. (3) shows the structural composition of the roof with thermal conductivity (K.)[2]

Material type	Thickness	Conductivity Thermal (K)(w/m <sup>2</sup> .c°)
Concrete	20	1.7
Plaster and gypsum material	1.6	10.1
Dry sand	10	0.33
asphalt	2.5	0.75
A layer of felt	0.5	2.73

$$R_t = 1/9.37 + 0.1/0.33 + 0.025/0.75 + 0.005/2.73 + 0.2/1.73 + 1/10.1 + 1/22.7 = 0.7035$$

$$U_r = 1/0.7035 = 1.421 \text{ W/m}^2.\text{c}^\circ$$

$$Q_{\text{total}} = Q + 15\% = 1.3 \text{ ton}$$

Table (4) for the cooling load

Room no.	Q total (ton)
<b>First floor</b>	
Kitchen	1.54
Reception	1.3
Living Room	1.69
Room 1	1.26
Room 2	1.4
<b>Second floor</b>	
Room 4	1.54
Room 3	1.3
Living Room	1.69
Room 1	1.26
Room 2	1.4
Roof	4.4
The total load for the building	18.78

Table (5) cooling load calculation for reception with deferent type of glass

type	Thickness	Q galss	Q Total(ton)
clear	4	0.52	1.74
	6	0.51	1.73
	8	0.50	1.72
clear double glass	22	0.34	1.53
shad	4	0.49	1.70
	6	0.48	1.69
	8	0.47	1.67
Shade double glass	22	0.29	1.47
Reflector	4	0.40	1.60
	6	0.39	1.59
	8	0.38	1.57
Reflector double glass	22	0.14	1.30

Table (6) cooling load calculation for Kitchen

type	Thickness	Q galss	Q (ton)
clear	4	0.62	2.09
	6	0.61	2.07
	8	0.60	2.06
clear double glass	22	0.43	1.87
shad	4	0.57	2.03
	6	0.56	2.01
	8	0.54	1.99
Shade double glass	22	0.36	1.78
Reflector	4	0.44	1.87
	6	0.42	1.85
	8	0.40	1.83
Reflector double glass	22	0.15	1.54

Table(7)the cooling load for the building:

Type of Glass	Thickness	Sc	U(w/m <sup>2</sup> .c)	A (m <sup>2</sup> )	Ag/A Total	Qg total	Qg/Q total
<b>clear</b>	4	0.97	6.5	48	14%	3.07	15.35%
	6	0.94	6.47	48	14%	3.02	15.09%
	8	0.92	6.36	48	14%	2.96	14.80%
clear double glass	22	0.8	3.2	48	14%	1.98	9.92%
<b>Shade glass</b>	4	0.83	6.58	48	14%	2.88	14.42%
	6	0.8	6.47	48	14%	2.81	14.06%
	8	0.77	6.36	48	14%	2.74	13.70%
Shade double glas	22	0.6	3.2	48	14%	1.69	8.45%
<b>Reflector</b>	4	0.49	6.58	48	14%	2.39	11.93%
	6	0.46	6.47	48	14%	2.31	11.57%
	8	0.43	6.36	48	14%	2.24	11.21%
Reflector double glass	22	0.2	3.2	48	14%	1.10	5.52%

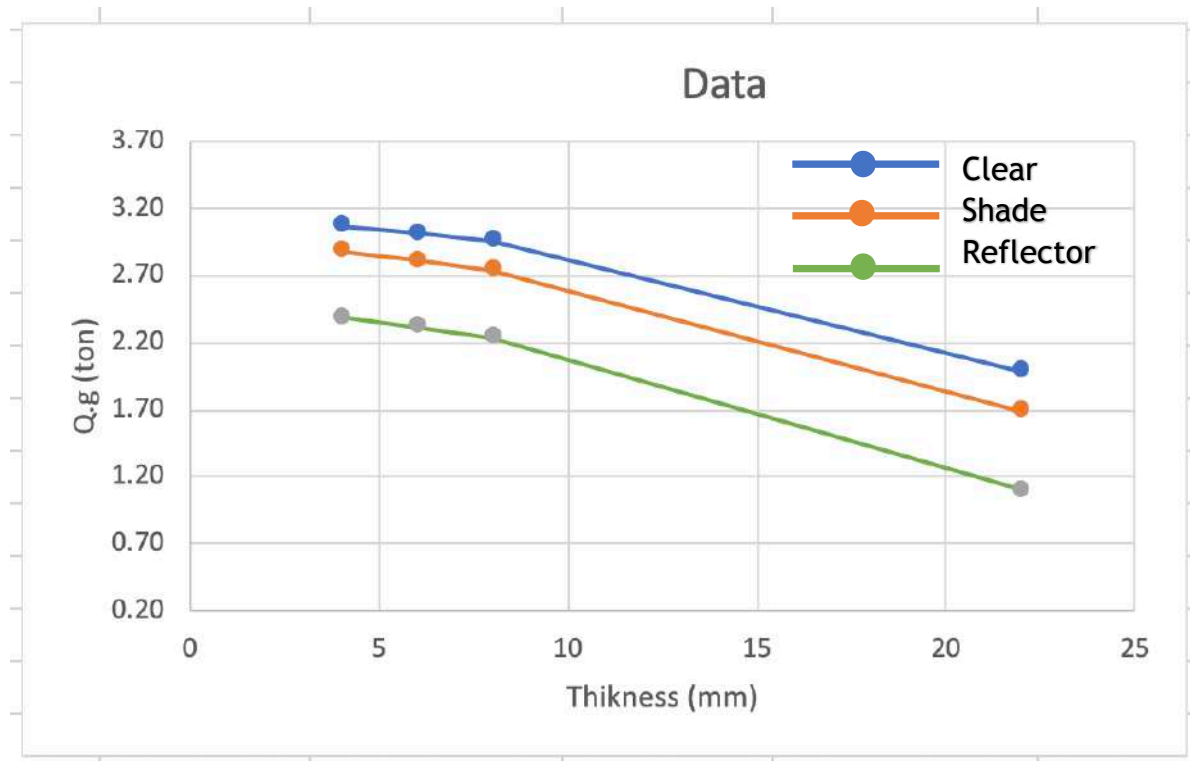


Figure (4): The relationship between  $Q_g$  and thickness for 3 type of glass.

# *Chapter 5*

## ***Discussion and Conclusions***

**(5-1) Discussion**

1. It is evident from the results obtained from the theoretical calculations that the effect of the thickness of the glass does not affect much on reducing the cooling load, and its effect is limited to limits of(2%-3%).
2. The use of double glazing with vacuum and all kinds of clear, tinted and reflective glass has achieved a reduction in the cooling load gained by ( 34.67%-64.%).
3. The results showed that the use of double reflective glass with a thickness of 8 mm with a vacuum of up to 6 mm has achieved a significant reduction in the cooling load gained from the glass by up to 53.7%.

**(5-2) Conclusions**

Through this theoretical study, the following conclusions were reached:

1. The thickness of the glass does not have much effect on reducing the cooling load gained from the glass, and its effect is limited to a limit of(2%-3%).
2. The use of double reflective glass with a thickness of 8 mm with a vacuum of up to 6 mm has achieved a reduction in the cooling load gained by limits ranging from (41.4% - 53.7%) compared to the use of single glass with a thickness of 4 mm and for all types
3. The ratio of the area of the glass to the area of the outer walls is equal to the ratio of the glass load to the total load, so reflective glass should be used with the space in buildings with glass facades

### **(5-3) Recommendations**

We recommend the use of Reflective glass lets optimal light into your space, but also reduces glare from the sun, which eliminates the need for blinds and other window coverings. And when combined with solar controlling low-e coating, this glass can reflect incoming radiant heat energy to keep your HVAC costs low. Also recommend designing buildings with reflective glass Because:

- **Color:** Tinted, reflective architectural glasses offer better harmonization with spandrels, metal panels, extrusions and other building materials. This color enriched glass transmits generous levels of visible light and offers color neutrality, which also enhances the tint of the glass substrate underneath the reflective coating. Today, reflective glasses can also include low-e coatings.
- **Visibility:** Reflective glass also has a special metallic coating that makes it possible to see out, while preventing people from seeing in, in order to preserve privacy during the day. In addition, reflective glass makes it possible to hide computer wires, vents, fans, HVAC components and other building mechanicals.
- **Glare Control:** Reflective glass also impacts visible light transmittance (VLT). Reflective glass allows just the right amount of natural light into a building, while at the same time reduces glare and the need for window blinds and other interior shading devices. In addition, reflective solar control glass reflects a portion of incoming solar radiation, which limits heat penetration into the building and can potentially lower HVAC usage.



- **Exterior Appearance:** Reflective glass provides a bold, crisp exterior appearance, along with a dynamic building surface that changes to reflect the color of the sky, the passing of clouds and the different times of day.

Also recommend the following future studies

Studying the effect of using activated glass on reducing the cooling load acquired in buildings with glass facades about.

## References

---

- 1- د.خالد احمد الجودي, هندسة تكييف الهواء , الطبعة الثانية , ١٩٨٤
- 2- The ASHRAE Handbook 1984
- 3- عاطف علي حسن, تأثير البيئة على درجة حرارة الحيز الداخلي للمبنى, مجلة جامعة ديالى للعلوم الهندسية, المجلد العاشر, الطبعة الأولى , ٢٠١٧
- 4- Yildiz y . Goksal T. and others [ Impact of Window , Wall Surface Area for Different Window Glass Types and Wall Orientation on Building Energy Performance ],vol.6-No:1Jan-2011.
- 5- Shen – H. &Tzonpelilcas A. [ Day lighting and energy analysis of private offices with Automated interior roller shades ] solar energy – vol 86 – issue 2 , 2012

## Appendix:

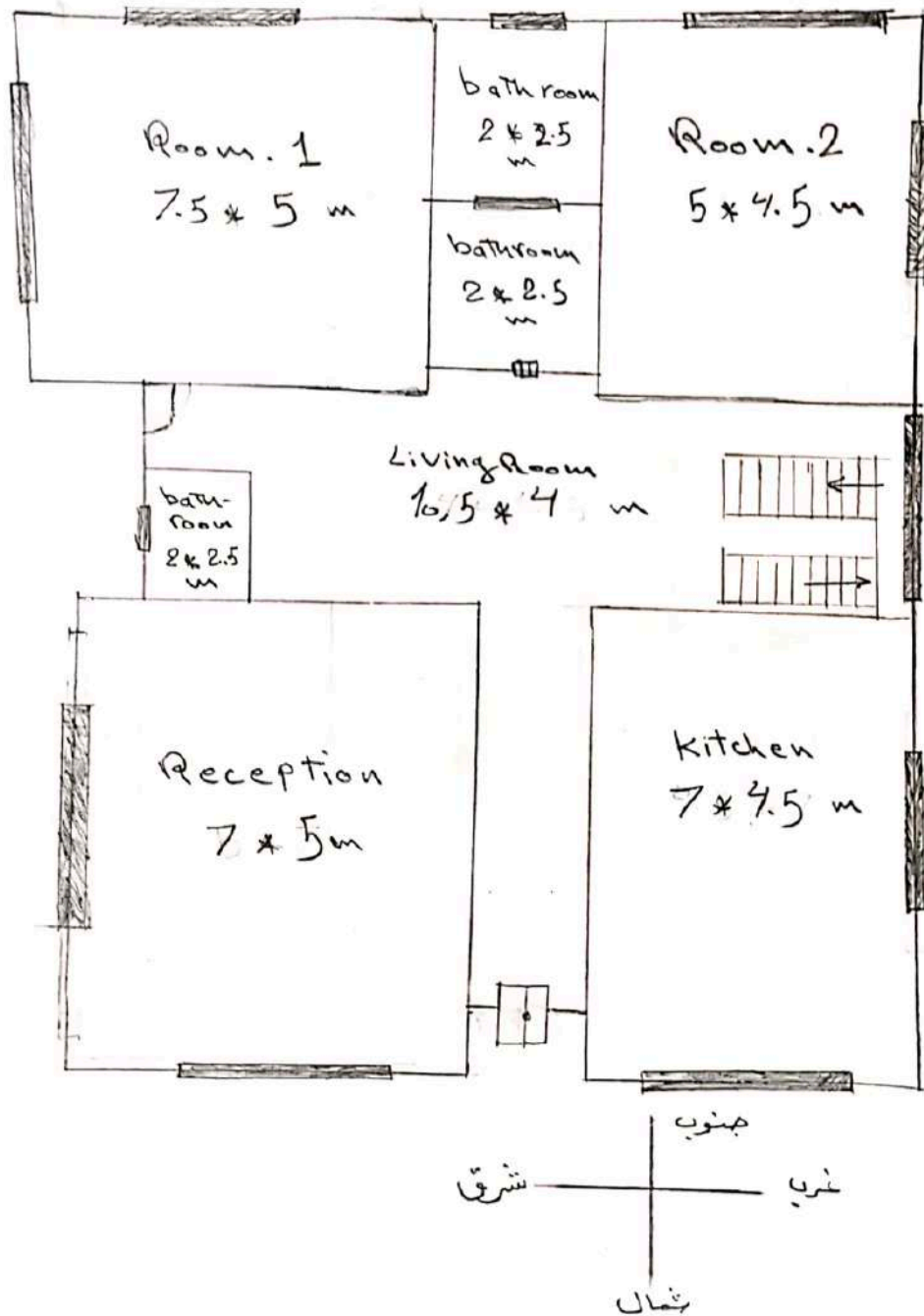
### building specification

1. The walls are built with perforated bricks, 24 cm thick.
2. Window area for rooms 2 \* 1.5 m.
3. The area of the antennas for the bathrooms is 0.5 \* 0.5 m.
4. The map of the first floor is similar to the ground floor.
5. The ceiling is reinforced concrete with a thickness of 20 cm, with thermal insulation of white cork( Alsterbor) material, with a thickness of 5 cm, and dust and sticker with a thickness of 2 cm.
6. The walls are plastered from the outside with cement mortar with a thickness of 2 cm, and from the inside with borac mortar with a thickness of 2 cm.
7. Glass thicknesses of 4 mm, 6 mm and 8 mm are used in different types.

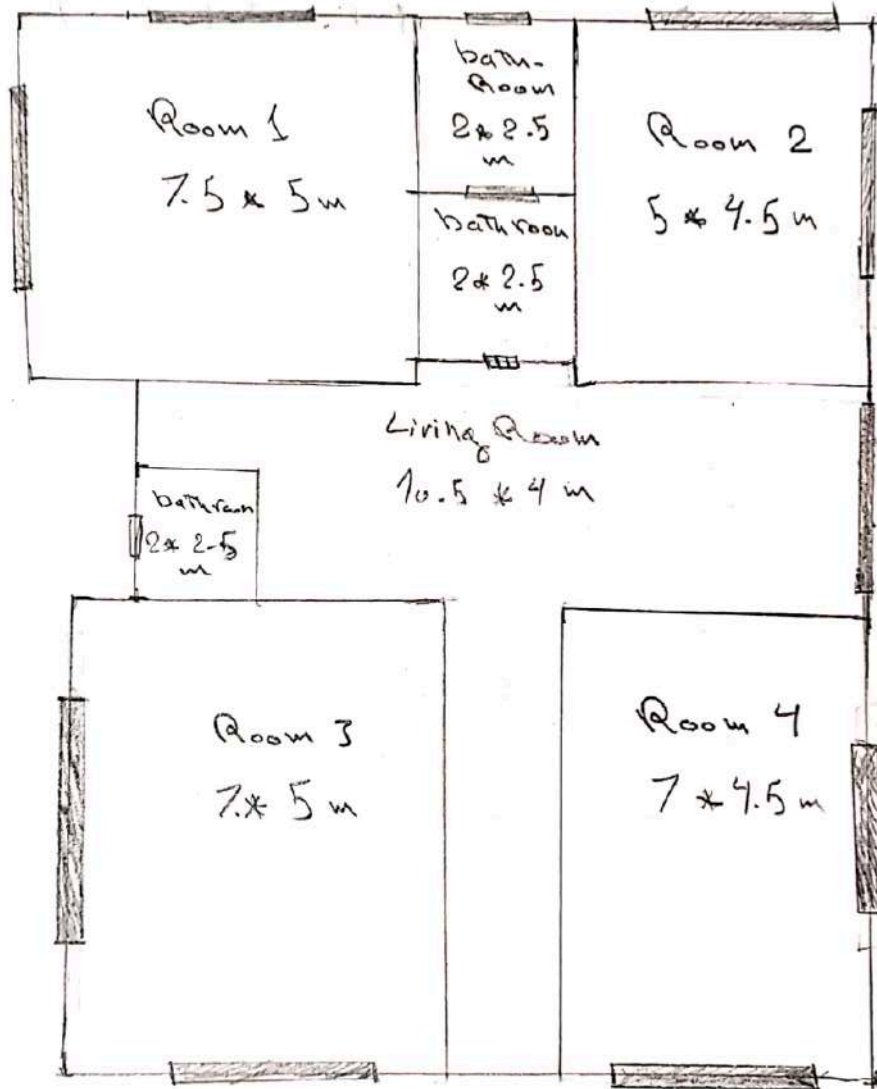
Table No. (2) shows the structural composition of the wall with thermal conductivity (K.)[2]

Material type	Thickness	Conductivity Thermal (K)(w/m <sup>2</sup> .c°)
Ordinary bricks	24	0.72
decorating bricks	10	1.3
Plaster and gypsum material	2.5	0.81
Fichus cement	2	0.721

خارطة دار سكني في مدينة بغداد  
الطابق الاول



خارجه دار سکنی فی مدینة بغداد  
الطابق الثاني



جنوب  
غرب + شرق  
شمال

8 mm  
Glass

8 mm  
Glass

U-value = 3.21 W/m<sup>2</sup>.C

Number of glass layers: Double
Calculation standard: ISO 10292

	Outer pane	Inner pane
Thickness [mm]:	<span style="border: 1px solid black; padding: 2px;">8.0</span>	<span style="border: 1px solid black; padding: 2px;">8.0</span>
Emissivity, front:		<span style="border: 1px solid black; padding: 2px;">0.837</span>
Emissivity, back:	<span style="border: 1px solid black; padding: 2px;">0.837</span>	<span style="border: 1px solid black; padding: 2px;">0.837</span>
Laminated glass?	<input type="checkbox"/>	<input type="checkbox"/>

Gap properties	
Gas type:	<span style="border: 1px solid black; padding: 2px;">Air</span>
Thickness [mm]:	<span style="border: 1px solid black; padding: 2px;">6.0</span>

The reflector double class (8+8+6)

### List of Thermal conductivity(K.):

<i>Material type</i>	<i>K (w/(m<sup>2</sup>.c°))</i>
Ordinary bricks	0.72
decorating bricks	1.3
Plaster and gypsum material	0.81
Fichus cement	0.721
Glass	0.78

### List of the overall heat transfer coefficient (U)

<b>APPLICATION</b>	<b><math>U \text{ w/m}^2.c</math></b>
wall	1.614
Roof	1.421
Glass	6.31
Door	2.25

The reflector glass conduction

t mm	U $\text{w/m}^2.c$	CLTD	CLTDc	A $\text{m}^2$	qc watt	qc ton
4	6.5	8	19	48	370	<b>0.1058</b>
6	6.47	8	19	48	368.7	<b>0.1053</b>
8	6.36	8	19	48	362.52	<b>0.103</b>
8+8+6=22	3.2	8	19	48	182.4	<b>0.052</b>

For solar for one window as a sample

type	A $\text{m}^2$	Sc	SCL (north)	qs watt	qs ton	SCL (west)	qs watt	qs ton
clear	3	0.93	<b>110</b>	307	0.087	<b>436</b>	1190	0.34
shade	3	0.81	<b>110</b>	267	0.076	<b>436</b>	1050	0.30
Reflector	3	0.56	<b>110</b>	184.8	0.052	<b>436</b>	700	0.20
Reflector double glass	3	0.2	<b>110</b>	66.3	0.018	<b>436</b>	261	0.81

the comparison of the overall heat transfer coefficient (U)

Thickness (X) mm	$h_o$ $W/m^2.C$	$h_i$ $W/m^2.C$	$K$ $W/m.C$	$R$ $C/W$	$U$ $W/m^2.C$
4	22.7	9.73	0.78	0.151	6.5
6	22.7	9.73	0.78	0.155	6.47
8	22.7	9.73	0.78	0.157	6.36
$8+8+6$ $=22$	22.7	9.73	$0.78_{and}$ $0.024_{for Air}$	0.174	3.2

تم بحمد الله وفضله

**Ministry of Higher Education and Scientific Research**

**Dijlah University College**

**Refrigeration & Air Conditioning Department**



***The vibration affected by the rotating shaft in cylinder  
on the rate of heat transfer***

**A project**

**Submitted to the Refrigeration and Air Condition Technology Engineering  
Department, Dijlah University College in partial  
Fulfillment requirement for the degree of B.Eng in Refrigeration and Air-  
Conditioning Technology Engineering**

**By:**

**Hussein Ali Talib  
Mohamed Munam Safar  
Mohsen Ali Mohsen  
Saif Aldin Ali Tarish  
Karrar Ali Kuaish  
Fadhel Ahmed Fadhel**

**Supervisor by:**

**Prof.Dr.Kazem Hamza Ghalim**

**Dr. Zaid Ali Hussein**

**2020-2021**



بِسْمِ اللَّهِ الرَّحْمَنِ الرَّحِيمِ

يَرْفَعِ اللَّهُ الَّذِينَ آمَنُوا مِنْكُمْ  
وَالَّذِينَ أُوتُوا الْعِلْمَ دَرَجَاتٍ وَاللَّهُ  
بِمَا تَعْمَلُونَ خَبِيرٌ

سورة المجادلة الآية

رقم ١١

## الاهداء

أهدي عملي هذا الى عائلتي بعد التوفيق من الله تبارك وتعالى  
وشكري الوافر الى استاذي ومشرفي على هذا العمل الدكتور كاظم  
حمزة غليم والدكتور زيد علي حسين لتفانيهم وجهدهم الدؤوب معي  
لانجاز عملي ولا انسى حبي وتقديري لكافة اساتذتي الاجلاء والكادر  
الفني في قسم هندسة التبريد والتكييف وتمنياتي ان نصل الى مستوى  
افضل لخدمة وطننا الحبيب.

طلبة المشروع

# ***Examining committee certificate***

*Project Title*

***The vibration affected by the rotating shaft in cylinder  
on the rate of heat transfer***

*Submitted by*

**Mohamed Munam Safar**

**Hussein Ali Talib**

**Saif Aldin Ali Tarish**

**Karrar Ali Kuaish**

**Fadhel Ahmed Fadhel**

*Has been carried out completely under our supervision at the Dijlah university college in  
partial fulfillment of the requirements for degree if B.Eng.*

*In Refrigeration and Air Conditioning Techniques Engineering Department*

*Signature*

**Prof.Dr.Kazem Hamza Ghalim**

**Dr. Zaid Ali Hussein**

*Date: / /2021*

*(supervisor)*

*Signature*

*Name:*

*Date: / /2021*

*(Member)*

*Signature*

*Name:*

*Date: / /2021*

*(Member)*

## ***Supervisor Certificate***

*We certify that this project entitled ((The vibration affected by the rotating shaft in cylinder on the rate of heat transfer))*

*Prepared by:*

*Hussein Ali Talib  
Mohamed Munam Safar  
Mohsen Ali Mohsen  
Saif Aldin Ali Tarish  
Karrar Ali Kuaish  
Fadhel Ahmed Fadhel*

*Has been carried out completely under our supervision at the Dijlah university college in partial fulfillment of the requirements for degree of B.Eng in Air Conditioning and Refrigeration Engineering.*

*Signature:*

*Prof.Dr.Kazem Hamza Ghalim*

*Dr. Zaid Ali Hussein*

*Date: / /2021*

*Approved by the charm in of Air condition and refrigeration engineering department:*

*Signature*

*Dr.*

*Charmin of Refrigerating and Air Conditioning Engineering Department*

*Date: / /2021*

### **Abstract**

Experimental work has been made for forced convection heat transfer for developing turbulent air stream for rotating isolated inner cylinder and uniformly heated outer cylinder.

The experimental investigation included a set of experiments carried out to study the forced convection heat transfer media. The experimental setup consists of a concentric cylindrical annulus with 80mm inner cylinder and 160 mm outer cylinder diameters with a heated length of 500 mm of the outer cylinder exposed to a permanent heat flux whereas the inner cylinder was isolated. The experimental and numerical study covers Re number various from 2484 to 3904, Ra number various from  $3.5 \times 10^7$  to  $2.45 \times 10^8$ , rotation speed from 0 to 2000 rpm.

The experimental results demonstrate the variation of wall temperature along inner, outer cylinders and the local Nusselt numbers. The experimental results show that the surface temperature. The  $\overline{Nu}$  number increases 60.2% when Re number increases from 500 to 2000 at minimum level and 54.87% at maximum level. The maximum effect of porosity at  $Re = 3904$  and  $Ra = 2.45 \times 10^8$  where average Nusselt number increases by 15% when porosity becomes 0.4 and 30% when porosity decreases to 0.2. Effect of rotation speed on the average Nusselt number  $\overline{Nu}$  increases with Ra number increase and Re number decrease. Average Nusselt numbers increases by 30.53% when rotation speed reaches to 2000

rpm at high Ra number and small Re number. The axial flow is more affective in heat transfer process than rotation for inner cylinder, where its effect is higher than the rotation effect. The results of the temperature profiles have discovered that the secondary stream formed by free convection has an important effect on the heat transfer process and the results disclose a rise in the Nu number values as Re, Ra, porosity and  $\Omega$  increase.

## **Table of Contents**

### **Subject**

Table of Contents  
Nomenclature

### Chapter One : Introduction

1.1 Background

1.2 Literature survey

### Chapter Two: Literature Review

#### 2.1 The test rig

2.1.1 Heating System

2.1.2 Variac

2.2 Measurements

2.2.1 Temperature measurement

2.2.2 Input voltage and current

2.3 Experimental setup

2.4 Experimental procedure

2.4.1 Heat Transfer Calculations

2.4.2 Heat Flux

2.4.2 The Rayleigh Number

2.4.3 The Reynolds Number

#### 2.4.4 The Nusselt Number

### Chapter three: Results and Discussions

### Chapter Four: Experimental Apparatus and Procedure

#### 4.1 Conclusions

#### 4.2 Recommendations

## NOMENCLATURE

### Latin Symbols

Symbol	Description	Units
$A_c$	Cross sectional area of annulus	$m^2$
$D_h$	Hydraulic diameter	m
E	Voltage	V
$g$	Gravitational acceleration	$m/s^2$
$h$	Heat transfer coefficient	$W/m^2.K$
I	Current	A
$k$	Thermal conductivity	$W/(m K)$
$l$	Length of annulus	m
$q''$	Imposed heat flux on the outer cylinder	$W/m^2$



Symbol	Description	Units
T	Temperature	°C
u	Velocity component	m/s
z	Axial direction	m
Z	Dimensionless axial coordinate	-

## Dimensionless Numbers

Number	Description
Gr	Grashof number, $Gr = \frac{Ra}{Pr}$
$\overline{Nu}$	Average Nusselt Number
$Nu_z$	Local Nusselt Number, $Nu_z = \frac{h D_h}{k}$
Pr	Prandtl Number, $Pr = \nu/\alpha_m$
Ra	Rayleigh Number
Re	Reynolds Number

## CHAPTER ONE

### Introduction

## **1.1 Background**

Heat transfer occurs whenever temperature differences exist within the system or between the system and its surroundings. The three modes of heat transfer are conduction, convection and radiation. However, for any given system, each mode of heat transfer can in many cases be studied separately and the results can be combined to give the total heat transfer rate from the system. However, in some cases, heat transfer from a system may involve a combination of two or three of the modes of heat transfer which interact with each other.

In the present work, a study of forced convection from a cylinder is carried out. forced convection from cylinder occur when there is a relative motion between a hot surface and a fluid flowing over the surface and there is a temperature difference between the surface and the fluid. The convective heat transfer rate depends on the characteristics of the fluid flow. Therefore, convective heat transfer can be classified according to the nature of the fluid flow and in particular on whether the flow is laminar or turbulent. So the force convection is a mechanism, or type of heat transport, in which the fluid motion is generated by any external source (like a pump, fan, suction device, etc.) Natural convection occurs only by density differences in the fluid occurring due to temperature gradients. In natural convection, cooler fluid surrounding a heat source receives heat, becomes less dense and rises. This cooler fluid is then heated and the process continues, forming convection current.

Forced convection from horizontal heated cylinder is an important problem relevant to many practical applications, such as flow over tubes of HVAC system, in resistive heating of electronic components, heat loss from process piping, steam heated coils and electric immersion heater in

process vessels, heat removal from spent nuclear fuel bundles and cooling of nuclear reactor core after loss of coolant accident, space shuttle launch pads and wasted nuclear rods stored in repositories.

## **1.2 Literature survey**

Force convective heat transfer from vertical cylinders has been studied for many years, a comprehensive review of these studies are presented in many heat transfer books such as **Al Zahrani (2009) [1]**, **Adegun (2004) [2]**, **Al-Hafidh (2012) [3]**, **Hussain (2010) [4]**, **Kamath (2011)[5]** and **Holman (2010)[6]**.

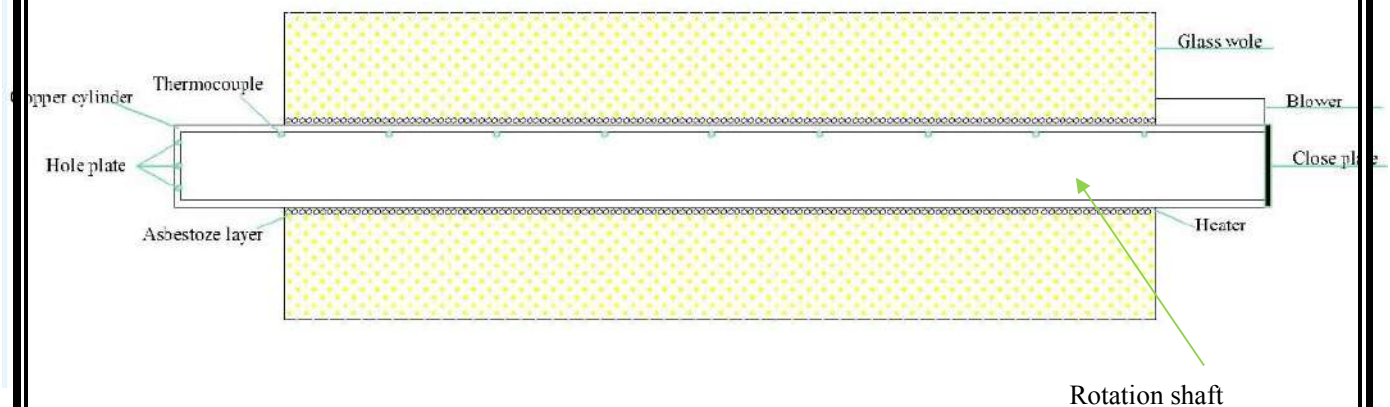
The aim of present work is to obtained the effect of rotation speed on heat transfer processes and find the empirical correlations between overall Nusselt and Reynolds numbers to characterize force convection heat transfer for heated cylinder.

## CHAPTER TWO

### Experimental setup and calculation procedure

#### 2.1 The test rig

Forced convection of air flow through horizontal heated cylinder is investigated experimentally. The objective of the current experimental work is to deduce an empirical equation for the average Nusselt number as a function of Reynolds and Rayleigh numbers.



**Figure (2.1)** Side view of schematic diagram of experimental setup



**Figure (2.2)** The experimental test rig.

The aim of the manufactured test rig is to examine the forced convection heat transfer from heated horizontal cylinder at different heat fluxes with rotation inner cylinder. Another objective is to correlate the experimental data of overall Nusselt number with the Reynolds number.

The following is an explanation of the main parts of the test rig, the purpose of use and the materials used in the construction.

### **2.1.1 Heating System**

The external cylinder surface is electrically heated using an electric heater as presented in figure (2.1). It contains of a nickelchrome wire of 1 mm in diameter and a resistance of (1.5 ohm/m), which was electrically insulated by heat treated fiber glass sleeving and wrapped around the outer cylinder. The heater was provided by AC-current from the voltage

regulator, to regulator supplied current according to the required heat flux. Heater was covered by three layers of 5 mm asbestos rope to ensure a good heater fixing and to provide an initial insulation to the test section. Then the whole test section was well insulated outside with three layers of 50.8 mm thickness of glass wool, which was mounted by means of plastic taps. The tubular heaters and the outer cylinders have the same length of 500 mm. Out of this length; only 400 mm acts as an active heated length. The horizontal cylinder (length 500 mm and diameter 3 in) is made of copper because of its high thermal conductivity.

### **2.1.2 Variac**

Variac is the trademark name of a variable autotransformer. A variable autotransformer is a single-coil transformer in which two portions of the same coil are used as the primary and the secondary. Variable autotransformers are used for the same purposes as regular transformers but handle lower voltages. They also differ from regular autotransformers in that they are equipped with automatic switchgear in order to automatically step a voltage up or down, depending on preset conditions. Variable autotransformers automatically regulate voltages for industrial equipment, simulate power line conditions, and control switches that are dependent on external events. Variable autotransformers are also used as automatic alternatives to regular autotransformers, which can be used in any situation that a regular transformer can be. They are lighter, less expensive, and handle lower voltages, generally ranging between 110 V and 260 V.

The variac shown in Figure (2.3) is used as an autotransformer that automatically regulate the voltage for the thin vertical cylinders during the tests. It was connected to the heaters to control the input voltage and thereby the power with the following specifications: input 380 V, output 0-260 V, 50~60 HZ, max. 6.5 A.



**Figure (2.3)** The variac

## **2.2 Measurements**

The main types of measurements undertaken through the experiments can be classified into the following main categories.

### **2.2.1 Temperature measurement**

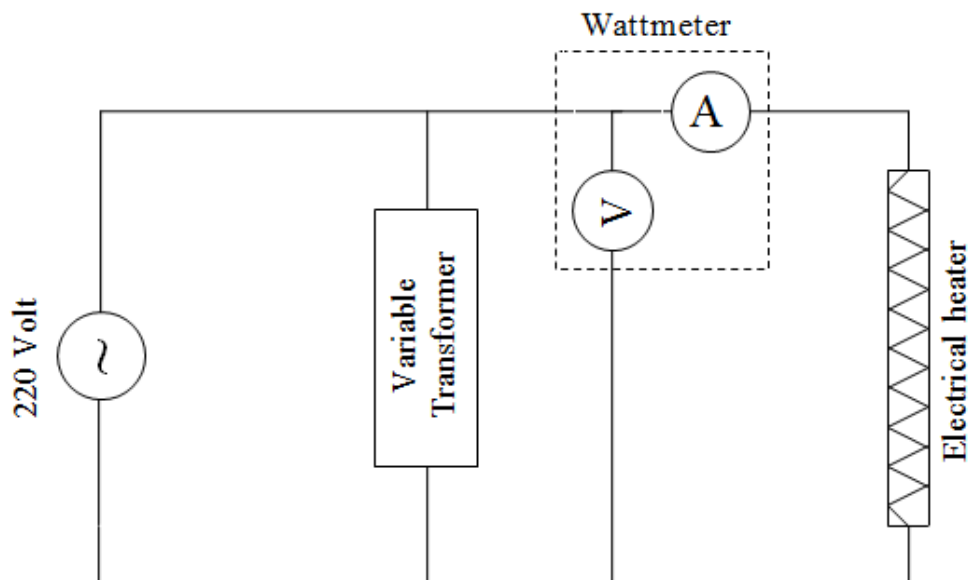
The temperatures at various locations on the surface of the thin vertical cylinders were measured by calibrated K- type thermocouples connected to data acquisition ( TPM -900) as shown in figure Figure (2.5) .The measurements include the temperatures of the surface of the cylinder and the reading of the thermocouples are shown in Figure (2.5). The temperatures of bulk fluid (air) were also measured at inlet and exit slits.



**Figure (2.5)** Digital temperature recorded

### 2.2.2 Input voltage and current

Heater wires were connected to the variac linked to a digital wattmeter to measure the input voltage while one of these wires was associated with digital clamp-on multimeter to measure the input current.



**Figure (2.6)** Electrical Circuit of Heater.



## **2.3 Experimental setup**

The test rig was handmade fabricated. The materials used to construct the test rig were copper cylinder, silicon sealant, shrink plastic pipes, fixer rings, electric wires and blower.

The tested cylinder was made from weathered copper with a standard thickness of almost 3 mm. The cylinder has an outer diameter of 160mm and a total length 500 mm. Each cylinder was drilled at nine equidistance axial positions making small holes. The distance between each hole is 50 mm. Thin thermocouple wires, 1.5 mm outer diameter including fiber glass insulation, of type K (copper constantan) with welded tips were embedded into the cylinder wall from the inner surface and adjusted to keep its tip at the outer surface of the cylinder wall. A tubular heater which has the same length of cylinder, was inserted in the copper cylinder to act as a heat source. Rotational shaft as shown in figure (2.2) was fixed inside the annulus with 80 mm diameter and made from stainless steel hollow shaft instead of solid shaft to decrease the vibration.

## **2.4 Experimental procedure**

The experiments are repeated with varying the following parameters to study their effect on the temperature distribution, and Nusselt number. These parameters are:

1. Heat flux at outer cylinder (400, 1000, 2000 and 2800 W/m<sup>2</sup>).
2. Rotation speed (500, 1500 and 2000 rpm).
3. Air flow rate (35, 40, 45, 50 and 55 m<sup>3</sup>/hr).

To carry out an experiment, the following procedure was followed:

1. The centrifugal fan was switched on and a regulating valve was used for adjusting the required air flow rate.

2. The electrical heater was switched on and the heater input power then adjusted to give the required heat flux.
3. The apparatus was left at least one hours to reach steady state condition. The thermocouples readings were measured every 10 minutes by data acquisition system until the reading became constant (temperature did not vary by more than 0.2°C in 10 min), a final reading was recorded.
4. The electrical motor was switched on to rotate the internal cylinder. An inverter was used for adjusting the required rotation speed.
5. The rotation speed was increased to cover another run in a smaller period of time and get steady state conditions for next rotation speed and same air flow rate and heat flux.
6. The air flow rate could be increased to cover another runs for next Reynolds number.
7. The input power to the heaters could be decreased to cover another runs for next heat flux and steps 5 and 6 was repeated.

During each test run, the following readings were recorded:

- a- The heater power in Watts.
- b- The readings of the thermocouples in °C.

#### **2.4.1 Heat Transfer Calculations**

#### **2.4.2 Heat Flux**

The net heat flux to is determined from recording the electrical power supplied to the heater and applying the following equation;

$$P_E = I \times E , \quad \text{.....(2.1)}$$

$$q'' = \frac{P_E}{2\pi r l} \quad \text{.....(2.2)}$$

Heat losses from the heater across asbestos and fiber glass wool

layers were calculated to be 3%. These losses are subtracted from the electric power to obtain the actual heat transfer rate. The losses in heat flux were calculated from measuring the temperature of the outer surface of the insulation layer by three thermocouples. This loss in heat flux is the resulting of the convection and conduction heat transferred through the insulation layer to the surrounding.

### 2.4.2 The Rayleigh Number

In the constant heat flux case, the dimensionless group, Rayleigh number is calculated as:

$$Ra = \frac{g\beta q'' D_h^4}{k\nu} \dots\dots\dots(2.3)$$

### 2.4.3 The Reynolds Number

$$Re = \frac{u_m D}{\nu} \dots\dots\dots(2.3)$$

### 2.4.4 The Nusselt Number

$$Nu_z = \frac{h_z D_h}{k} = \frac{q_w D}{k(T_{2z} - T_b)} \dots\dots\dots(2.4)$$

The average Nusselt number can be calculated by integrating equation (2.4) over the entire length of the heated wall using a numerical integrating method (Simpson's rule) as:

$$\overline{Nu} = \frac{1}{L} \int_{Z=0}^{Z=L} Nu_z dZ \dots\dots\dots(2.5)$$

## Chapter Three

### Results and Discussions

The main objective of this chapter is to introduce and analyze the experimental of the present work for forced convection air flow through horizontal cylinder and uniformly heated outer cylinder with rotation inner cylinder.

#### 3.1 Experimental Results

##### 3.1.1 Temperature Variation

In general, the change of surface temperature along the annulus may be influenced by several parameters such as Ra number, Re number and rotation speed of inner cylinder.

The temperature variation in longitudinal direction for outer cylinder is drawn for selected runs in figures ((3.1) – (3.2)). Figure (3.1) illustrates the change of the surface temperature along outer cylinder for various Rayleigh number and for three different values of other parameters. This figure reveals that the outer surface temperature increases with the dimensionless axial direction ( $Z$ ). The rate of surface temperature rise is directly proportional to the Rayleigh number. At lower value of Rayleigh number, it can be noticed that the surface temperature along the annulus is approximately constant. The temperature increases with increasing Rayleigh number as a result of increase in heat flux on the outer surface. The temperature increases more with dimensionless axial distance ( $Z$ ) and it reaches to maximum value at the outlet of the annulus. This rise in temperature with axial distance increases more with increase in Rayleigh number. This could be referred to increase the thermal boundary layer growth when heat flux increases.

Figure (3.2) shows the influence of Reynolds number change on the outer cylinder surface temperature at constant heat flux. It is clear that the rising of Reynolds number decreases the surface temperature when heat flux kept permanent. The increase in air flow leads to increase the convected heat by air and therefore the surface temperature decreases and also decreases with axial distance. It is necessary to mention that as flow rate of air inside annulus decreases the outer cylinder surface temperature since the forced convection is the dominate factor in the heat transfer process.

Figure (3.3) illustrates the influence of rotation speed of inner cylinder on the outer cylinder surface temperature for three different values of other parameters. It illustrates that the rising of rotation speed generally decreases the surface temperature as a result of increase in mixing between hot and cold streams. But when Reynolds numbers increase, surface temperature increases slightly at low rotation speed. This increase is because the inner cylinder creates a layer of air that does not have enough momentum to increase mixing inside the annulus.

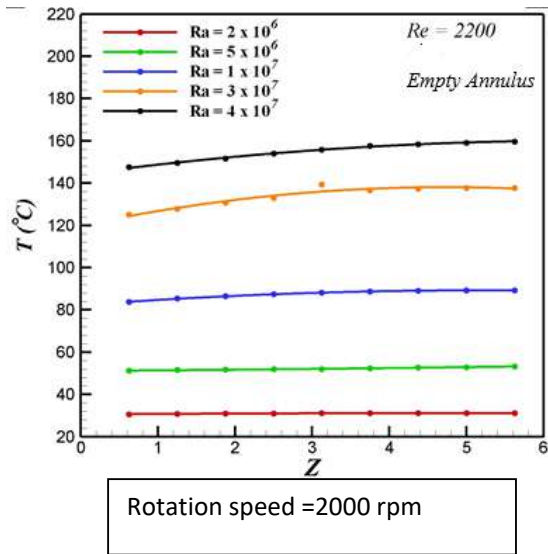
### **3.1.2 Local Nusselt Number**

The change of  $(Nu_z)$  for outer cylinder with axial distance is drawn for a chosen run in figures (3.4) to (3.6). As seen from these figures, the local Nusselt number in all situations decreases with the rising in the dimension less distance  $(Z)$ , meanwhile the heat transfer coefficient depends on the variance in surface temperature and bulk temperature. This behavior is predictable as the highest temperature difference between the hot surface and the entering cold air happens at the entrance of test section especially at higher Rayleigh number. Therefore, the largest heat transfer amount happens in the inlet of the annulus. When the air travels inside the annulus, the local air temperature rises so efficiently rising the local wall

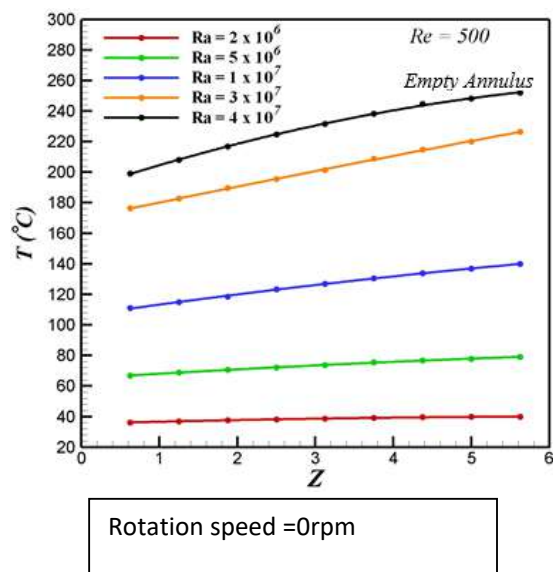
temperature and decreasing the  $Nu_z$  number along the path of flow. It is obvious from this figure that at higher Ra number, the results of the  $Nu_z$  number were larger than the results of lower Ra number. This may be attributed to the secondary flow influence which rises when the heat flux rises; this leads to larger heat transfer coefficient.  $Nu_z$  number decreases with axial distance from inlet section. This decrease is greater at high Ra number due to the faster increase of the thermal boundary layer thickness. This layer leads to reduce in heat transfer coefficient and heat transfer process between hot surface of outer cylinder and air. Local Nusselt number decreases by 70% when Rayleigh number decreases from  $4 \times 10^7$  to  $1 \times 10^6$  at maximum level. While it decrease by 68.7% at minimum level.

The effects of Reynolds number on local Nusselt number variation with dimensionless axial distance are shown in figure (3.5). Momentum of air is increased with increasing Reynolds number, this leads to increase in heat transfer rate. Reynolds number increases local Nusselt number at  $Z = 3.125$  by 34.5% when it increases from 500 to 2200 at maximum level while it increases Nusselt number 44.3% at minimum level.

The  $Nu_z$  number increases with rising in rotation speed as shown in figure (3.6). The rotation of inner cylinder increases the mixing process of the hot and cold air. The rotation speed affects more at high Rayleigh number because the temperature difference is high between the hot surface and cold stream. Nusselt number increases 27.31% when rotation speed reaches to 2000 rpm at maximum level while it increases 39.91 % at minimum level

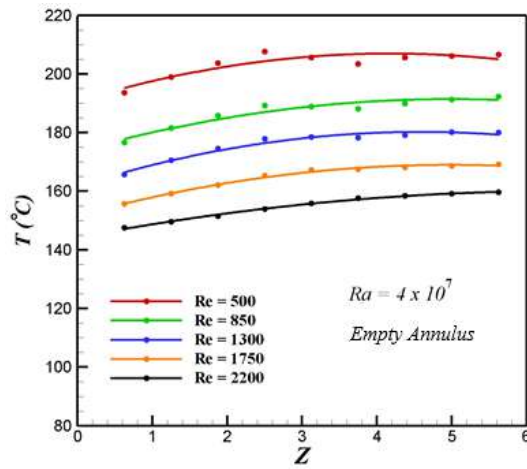


(a)



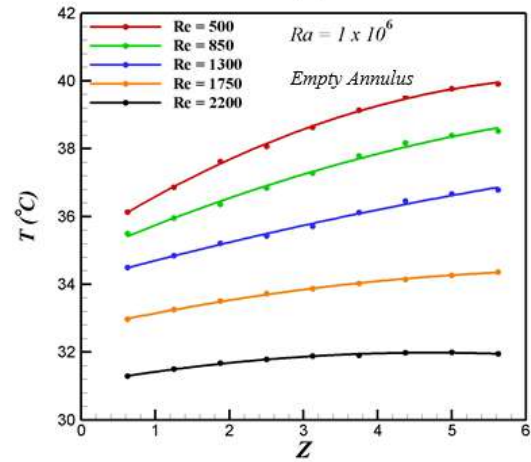
(b)

Figure (3.1): Effect of Rayleigh Number on the Longitudinal Variation of the Experimental Surface Temperature of the Outer Cylinder



(a)

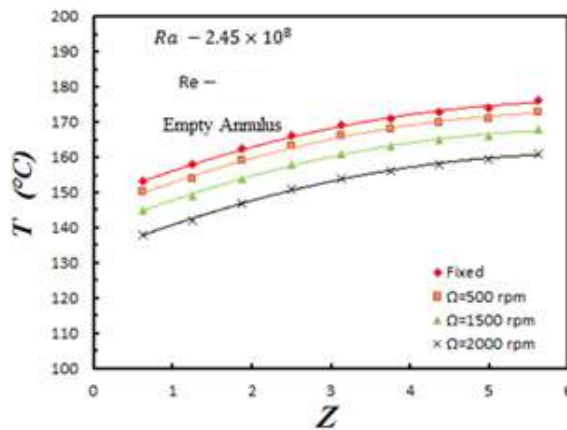
Rotation speed = 2000 rpm



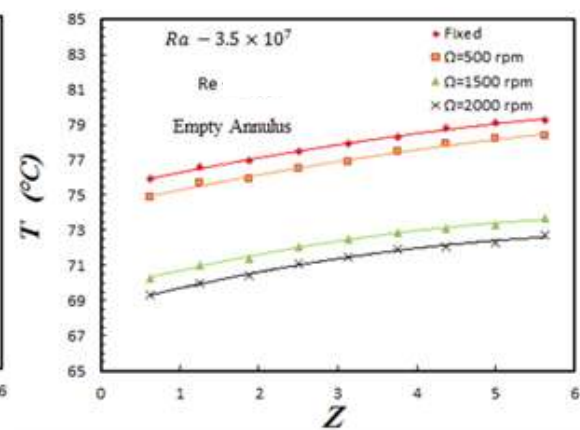
(b)

Rotation speed = 0 rpm

Figure (3.2): Effect of Reynolds Number on the Longitudinal Variation of the Experimental Surface Temperature of the Outer Cylinder



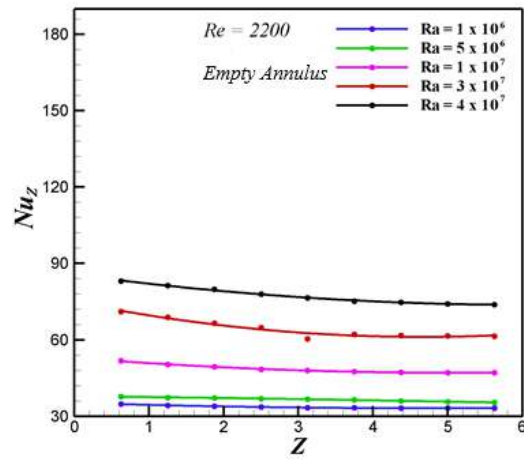
(a)



(b)

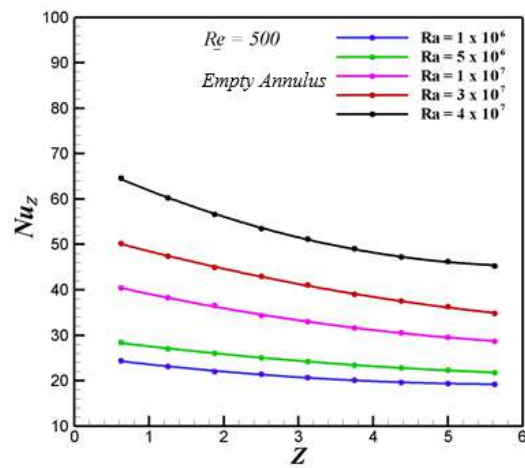
Figure (3.3): Effect of Rotation Speed on the Longitudinal Variation of the Experimental Surface Temperature of the Outer Cylinder





Rotation speed = 2000 rpm

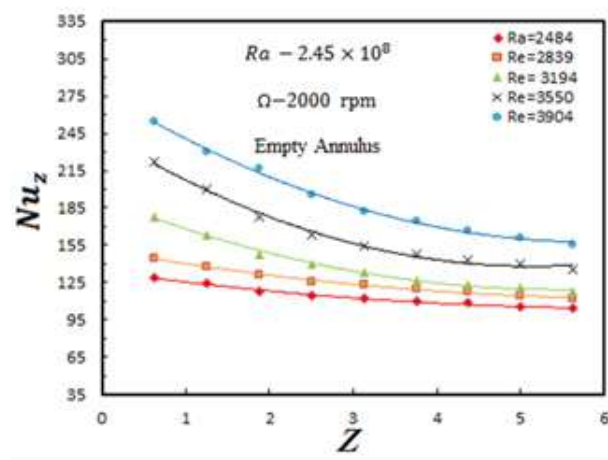
(a)



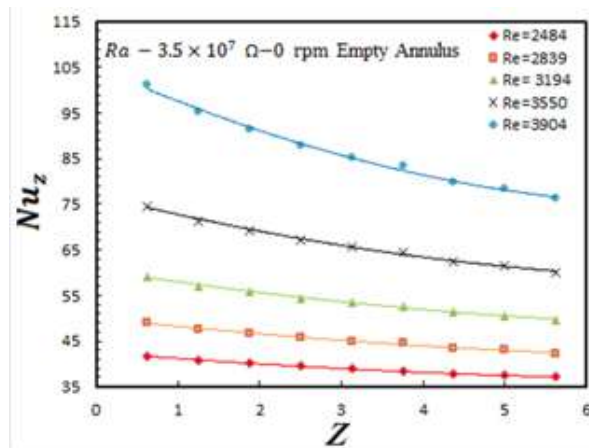
Rotation speed = 0 rpm

(b)

Figure (3.4): Effect of Rayleigh Number on the Longitudinal Variation of the Experimental Local Nusselt Number of the Outer Cylinder

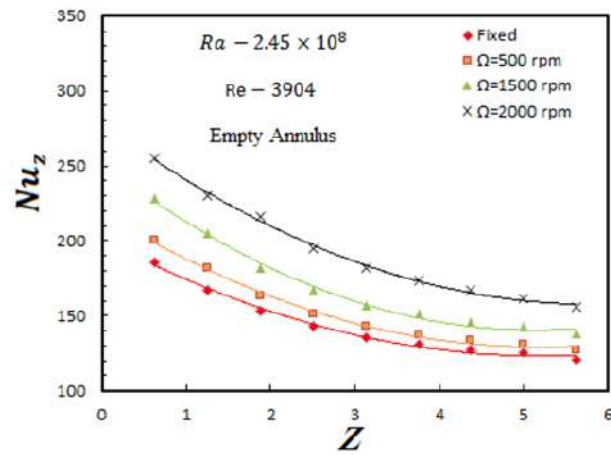


(a)

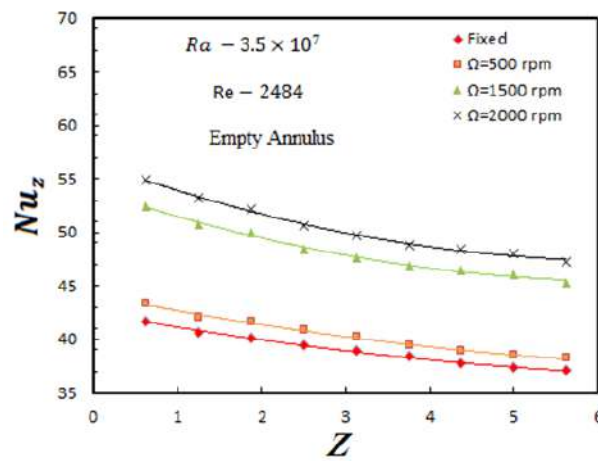


(b)

Figure (3.5): Effect of Reynolds Number on the Longitudinal Variation of the Experimental Local Nusselt Number of the Outer Cylinder



(a)



(b)

Figure (3.6): Effect of Rotation Speed on the Longitudinal Variation of the Experimental Local Nusselt Number of the Outer Cylinder

## Chapter Four

# Conclusions and Recommendations

### 4.1 Conclusions

For the experimental results, the following conclusions can be made:

1. The experimental surface temperature of outer cylinder increases with longitudinal direction while the local Nusselt number of the outer cylinder decreases.
2. The local Nusselt number of the outer cylinder decreases with the decrease of Rayleigh number by 70% at maximum level and 68.7% at minimum level when Rayleigh number decreases from  $4 \times 10^7$  to  $1 \times 10^6$ . While it increases with Reynolds number increase by 34.5% at maximum level and 44.3% at minimum level when Reynolds number increases from 500 to 2200
3. Effect of rotation speed on the average Nusselt number increases with Rayleigh number increase and Reynolds number decrease. Average Nusselt numbers increases by 30.53% when rotation speed reaches to 2000 rpm at high Rayleigh number and low Reynolds number.
4. Reynolds number affected clearly on heat transfer rate because they affected on the flow resistance.

## 4.2 Recommendations

An extension of the present experimental is recommended for future work to study the forced convection of laminar air flow through horizontal cylinder and uniformly heated outer cylinder includes:

Recommendations in this part can be given in the following points:

1. Different annulus lengths are used to investigate the effect of  $L/d$  ratio.
2. Studying the behavior of other fluids such as water and oil, etc.
3. Studying the effect of inclination angle of the annulus.
4. Studying the effect of vibration on heat transfer rate.

## References

- Al Zahrani, M. S., and Kiwan, S., "mixed Convection Heat Transfer in The Annulus between Two Concentric Vertical Cylinders Using Porous Layers", *Transport Porous Media*, Vol. 76, pp. 391-405, (2009).
- Adegun, I., K., and Bello-Ochend, F., L., "Convective and Radiative Heat Transfer in an Inclined Rotating Rectangular Duct with a Centered Circular Tube", *J. of Braz. Soc. of Mech. Sci and Eng*, Vol. xxvi, No.3, pp.323-329, (2004).
- Al-Hafidh, M. H., Safwat, L.S., "Mixed Convective and Radiative Heat Transfer in Horizontal Concentric and Eccentric Cylindrical Annuli", *Journal of Engineering*, Vol. 18, No. 5, pp. 552-570, (2012).
- Hussain, I., Y., Al-Safi, M., A., "Developing Laminar Mixed Convection Heat Transfer through Concentric Annuli", *Journal of Engineering*, Vol. 16, No. 3, pp. 5644-5662, (2010).
- Kamath, P., M., Balaji, C., and Venkateshan, S., P., "Experimental Investigation of Flow Assisted Mixed Convection in High Porosity Foams in Vertical Channels", *International Journal of Heat and Mass Transfer*, Vol. 54, pp. 5231-5241, (2011).
- Holman, J., P., "Heat Transfer", 10<sup>th</sup> Edition, McGraw-Hill Higher Education, (2010).

## الملخص

أجريت دراسة عددية وعملية على انتقال الحرارة بالحمل القسري لجريان متطور للهواء خلال حيز اسطواناني حلقي لاسطوانة داخلية دوارة معزولة واسطوانة مضطرب خارجية ثابتة و مسخنة بشكل منتظم.

شملت الدراسة العملية مجموعة من التجارب التي أجريت لدراسة انتقال الحرارة بالحمل القسري. يتكون الجهاز التجريبي من اسطوانة حلقة متركزه تحتوي على ٨ سم اسطوانة داخلية ١٦ سم اسطوانة خارجية بطول تسخين ٥٠ سم معرضة لفيض حراري منتظم بينما ، 3904-2484 الاسطوانة الداخلية تكون معزولة. تغطي الدراسة العملية والعددية رقم رنولدز ، سرعة دوران ٠ - ٢٠٠٠ دورة في الدقيقة،  $2.45 \times 10^8$  -  $3.5 \times 10^7$  رقم رايلي يتراوح بين

تبين النتائج العملية التغير في درجة حرارة السطح على طول الاسطوانة الداخلية والخارجية ورقم نسلت الموقعي والمتوسط. أظهرت النتائج العملية أن درجة حرارة السطح في حالة وجود المادة المسامية هي أقل منها في حالة الاسطوانة الحلقية الفارغة ورقم نسلت الموقعي عندما يزداد رقم رينولدز من 60.2% يزداد عندما تقل المسامية. متوسط عدد نسلت يزداد بنسبة عند اعظم مستوى. تأثير سرعة الدوران على متوسط رقم نسلت يزيد مع زيادة رقم رايلي عندما تصل سرعة دوران الى 30.53% وانخفاض رقم رينولدز. متوسط رقم نسلت يزداد بنسبة ٢٠٠٠ دورة في الدقيقة عند اعلى رقم رايلي و أقل رقم رينولدز. الجريان المحوري اكثر فعالية في عملية انتقال الحرارة من دوران الاسطوانة الداخلية، حيث يكون تأثيره اعلى من تأثير التدوير. كشفت نتائج مخطط درجة انخفاض الضغط العملي بتأثر بشكل كبير مع المسامية ورقم رينولدز. الحرارة ان التدفق الثانوي الناتج من الحمل الحراري الطبيعي له أثر كبير على عملية انتقال الحرارة وتكشف النتائج عن زيادة في رقم نسلت مع زيادة كل من رقمي رايلي ورينولدز وسرعة  $Ra, Re, Re\Omega Da$ ..الدوران.



وزارة التعليم العالي والبحث العلمي  
كلية دجلة الجامعة الاهلية  
قسم هندسة تقنيات التبريد والتكييف

## الاهتزاز المتأثر بعمود الدوران في أسطوانة على معدل انتقال الحرارة

بحث مقدم إلى كلية دجلة الجامعة الأهلية/ قسم هندسة تقنيات التبريد و التكييف وهو جزء من متطلبات نيل درجة  
بكالوريوس في هندسة تقنيات التبريد والتكييف

من قبل

حسين علي طالب

محمد منعم صفر

محسن علي محسن

سيف الدين علي طارش

كرار علي كويش

فضل احمد فاضل

بإشراف

أ.د كاظم حمزة غليم

د. زيد علي حسين



۲۰۲۱-۲۰۲۰

*Ministry of Higher Education and Scientific Research  
Dijlah University College  
Refrigeration & Air Conditioning Techniques  
Engineering Department*



## **Theoretical and experimental study on the effect of bending on weld joint properties of refrigeration tubes**

*A project*

*Submitted to the Refrigeration and Air Condition Techniques Engineering  
Department*

*Dijlah University College in partial  
Fulfillment requirement for the degree of B. Eng. in Refrigeration and  
Air-Conditioning Technology Engineering*

*By:*

- *Riyadh Mohsen Saleh*
- *Raad Kazem Abdul Hassan*
- *Rafid Rashed abd al-sada*
- *Haider Abid Al-Razaq falh*
- *Khairy Qasim mahmd*

*Supervisor by:*

***Assit. Prof.Dr. Ezzet Hameed***

***2020-2021***

بِسْمِ اللَّهِ الرَّحْمَنِ الرَّحِيمِ

{ يَرْفَعِ اللَّهُ الَّذِينَ آمَنُوا مِنْكُمْ وَالَّذِينَ أُوتُوا الْعِلْمَ دَرَجَاتٍ }

صدق الله العلي العظيم

{ المجادلة: ١١ }

## *Supervisor Certificate*

*We certify that this project entitled ((**Theoretical and experimental study on the effect of bending on weld joint properties of refrigeration tubes**))*

*Prepared by:*

- *Riyadh Mohsen Saleh*
- *Raad Kazem Abdul Hassan*
- *Rafid Rashed abd al-sada*
- *Haider Abid Al-Razaq falh*
- *Khairy Qasim mahmd*

*Has been carried out completely under our supervision at the Dijlah university college in partial fulfillment of the requirements for Degree of Bachelor in Refrigeration and Air Conditioning Technologies Engineering.*

*Signature:*

**Assit. Prof.Dr. Ezzet Hameed**

*Date: / /2021*

*Approved by the head of Air condition and refrigeration engineering department:*

*Signature*

*Dr.*

*Head of Refrigerating and Air  
Conditioning Engineering*

*Department*

*Date: / /2021*

## *Examining committee certificate*

We certify that this project entitled (*Theoretical and experimental study on the effect of bending on weld joint properties of refrigeration tubes*)

Submitted by:

- *Riyadh Mohsen Saleh*
- *Raad Kazem Abdul Hassan*
- *Rafid Rashed abd al-sada*
- *Haider Abid Al-Razaq falh*
- *Khairy Qasim mahmd*

*and as an examining committee examined the students in its content and that in our opinion it meets the standards of a project for the for Degree o Bachelor in Refrigeration and Air Conditioning Technologies Engineerin*

*Signature*

**Assit. Prof.Dr. Ezzet Hameed**

*Date: / /2021*

( )

*Signature*

*Name:*

*Date: / /2021*

( )

*Signature*

*Name:*

*Date: / /2021*

( )

## الأهداء

تعالوا لنقف جميعاً وقفة إجلال وإكبار لأمهات الشهداء اللواتي قدمن فلذات أكبادهن لأجل عزة وكرامة الوطن لن أنسى ماحيينا موقف تلك الام التي قدمت ابنها شهيداً دفاعاً عن الوطن إلى من يضحون بدمائهم من اجلنا إلى من تركوا بيوتهم من اجل الدفاع عن بلدهم إلى من ندين لهم بالفضل قواتنا الأمنية من الجيش والحشد الشعبي لابد لنا نحن نخطو خطواتنا الأخيرة في الحياة الجامعية من وقفة نعود إلى أعوام قضيناها في رحاب الجامعة مع أساتذتنا الكرام الذين قدموا لنا الكثير باذلين بذلك جهودا كبيرة في بناء جيل الغد لتبعث الأمة من جديد وقبل أن نمضي تقدم أسمى آيات الشكر والامتنان والتقدير والمحبة إلى الذين حملوا أقدس رسالة في الحياة إلى الذين مهدوا لنا طريق العلم والمعرفة

إلى جميع أساتذتنا الأفاضل

**"كن عالماً. فإن لم تستطع فكن متعلماً ، فإن لم تستطع فأحب العلماء ،فإن لم تستطع فلا تبغضهم"**

وأخص بالتقدير والشكر

**الدكتور : محرز حميد**

وكذلك نشكر كل من ساعدنا من جميع الاستاذة الكرام في القسم ومن خارجه الذين كانوا عوناً لنا في بحثنا هذا ونورا يضيء الظلمة التي كانت تقف أحيانا في طريقنا

إلى من زرعوا التفاؤل في دربنا وقدموا لنا المساعدات والتسهيلات والأفكار والمعلومات ، ربما دون يشعروا بدورهم بذلك فلهم منا كل الشكر والتقدير

## **ACKNOWLEDGEMENTS**

## **ABSTRACT**

### **CHAPTER / 1**

#### **1 INTRODUCTION**

- 1.1 General Background
- 1.2 Problem Statement
- 1.3 The objective of the project
- 1.4 Scope of Project
- 1.5 Lay out of Project

### **CHAPTER / 2**

#### **2 LITERATURE REVIEW**

- 2.1 Introduction
- 2.2 Definition of Welding
- 2.3 Types of Welding processes
  - 2.3.1 Arc Welding
  - 2.3.2 TIG Welding
  - 2.3.3 Oxy-acetylene welding
  - 2.3.4 Plasma welding
- 2.4 Weld quality
  - 2.4.1 Joint preparation
  - 2.4.2 Striking the arc
  - 2.4.3 Pores
  - 2.4.4 Lack of fusion
  - 2.4.5 End craters
  - 2.4.6 Post weld treatment
- 2.5 Destructive Testing
  - 2.5.1 Tensile Test
  - 2.5.2 Bending Test
  - 2.5.3 Hardness test
- 2.6 Non-destructive Testing
  - 2.6.1 Dye penetrant
  - 2.6.2 X-ray test
- 2.7 Weld Joints Design

## **CHAPTER / 3**

### **3 EXPERIMENTAL WORK**

- 3.1 chemical composition Test
- 3.2 Sample Preparation
- 3.3 visual test for specimen
  - 3.3.1 cutting process of the specimen
  - 3.3.2 Mechanical Testes for Primary Sample
- 3.4 Specimen Welding Process
- 3.5 Destructive Testing
  - 3.5.1 Tensile Test
  - 3.5.2 Bending Test
  - 3.5.3 Hardness test
  - 3.5.4 Compression composition test

## **CHAPTER / 4**

### **4 RESULT AND DISCUSSION**

## **CHAPTER / 5**

### **5 CONCLUSION**

### **6 REFERENCES**



## *Abstract*

Welding is a common process for joining metals using a large variety of applications. Welding occurs in several locations, from outdoors settings on rural farms and construction sites to inside locations, such as factories and job shops. Welding processes are fairly simple to understand, and basic techniques can be learned quickly. Welding is the joining of metals at a molecular level. A weld is a homogeneous bond between two or more pieces of metal, where the strength of the welded joint exceeds the strength of the base pieces of metal.

At the simplest level, welding involves the use of four components: the metals, a heat source, filler metal, and some kind of shield from the air. The metals are heated to their melting point while being shielded from the air, and then a filler metal is added to the heated area to produce a single piece of metal. It can be performed with or without filler metal and with or without pressure.

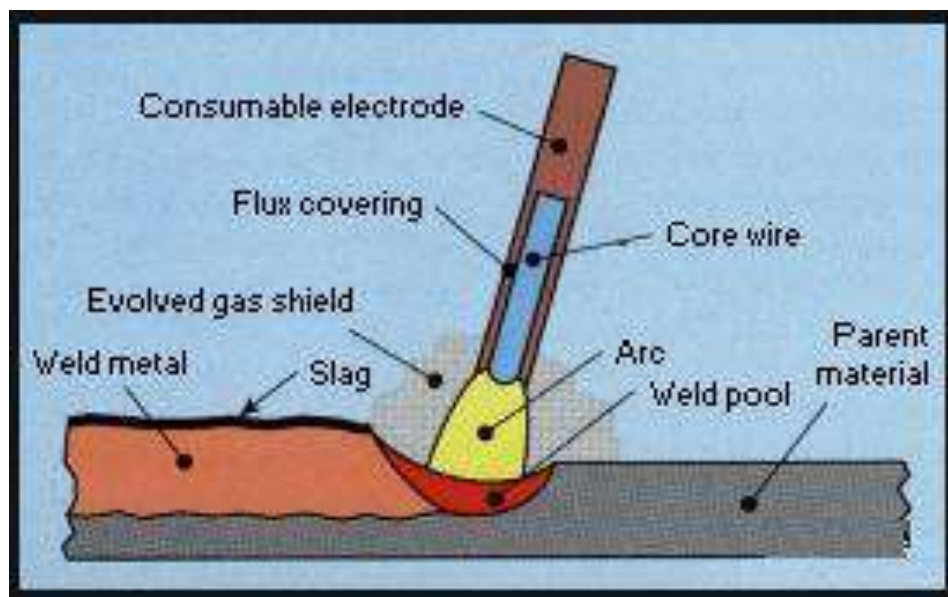
Welders and methods are presented for short-circuit arc welding a workpiece using a modified series arc welding configuration with two electrodes via a sequence of welding cycles, in which each cycle includes an arc condition a short-circuit condition, wherein one or both electrode currents are selectively reversed during a reverse boost portion of the welding cycle to transfer molten metal from the second electrode to the first electrode prior to a short-circuit condition of a sub sequent welding cycle. The process of welding is quite complex and the strength of weldment is highly dependent on metallurgy, welding procedure and the skill of the welder. The influence of following the stander procedure in welding process to identify the perfect welding method for pipe in air conditioning system for preventing leakages according to the welding standers is the main objective of this project.

The mechanical tests (Tensile, Bending and Compression) which are for welded joints especially for pipe welding for current objective offers a great identical with standers. More than forty years ago there the first attempt was reported to model a travelling point heat source for the case of welding process. The stationary and dynamic heat sources are frequently modeled for many manufacturing processes. Finally following of the stander procedure for welding process prevents any damages may appear in it. On the other hand, and for future work take in consideration the effect of welding parameters effect.

# 1-INTRODUCTION

## 1.1 General Background

Methods for joining metals have been known for thousands of years, but for most of this period the only form of welding was forge welding by a blacksmith. A number of totally new welding principles emerged at the end of 19th century; sufficient electrical current could then **be** generated for *resistance welding* and *arc welding*. Arc welding was initially carried out using carbon electrodes, developed by Bemoods, and was shortly followed by the use of steel rods. The Swede Oskar Kjellberg made an important advance when he developed and patented the coated electrode. The welding result was amazing and formed the foundation of the ESAB welding company.



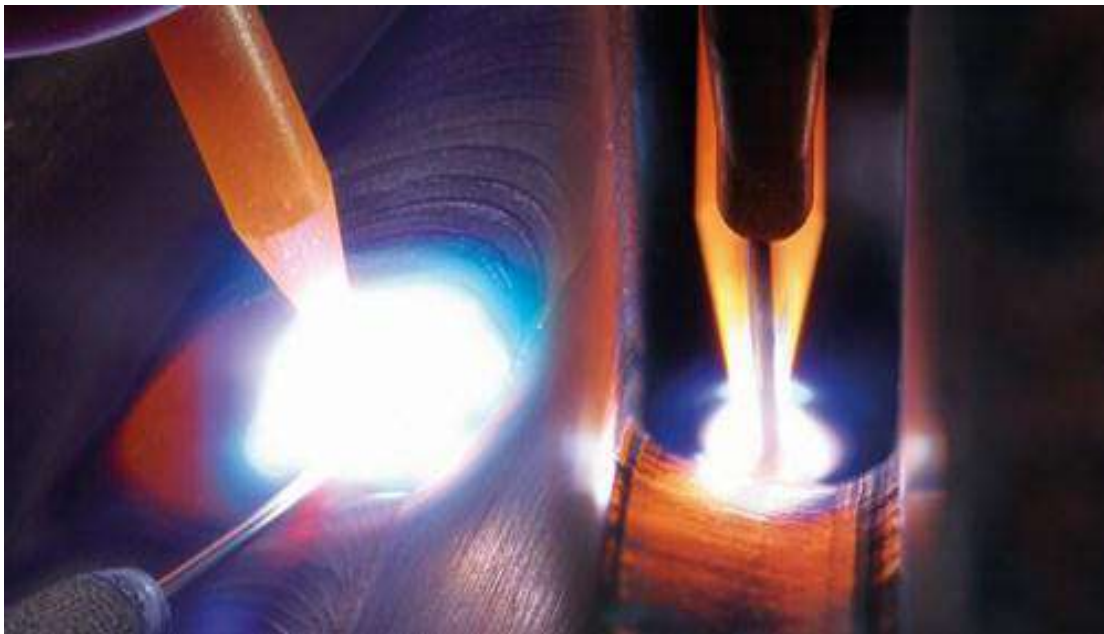
**Figure 1.1: Principle of Manual Metal Arc welding.**

Another early method of welding which was also developed at that time was *gas welding*. The use of acetylene and oxygen made it possible to produce a comparatively high flame temperature,  $3100^{\circ}\text{C}$ , which is higher than that of other hydrocarbon-based gas. The intensity of all these heat sources enables heat to be generated in, or applied to, the workpiece quicker than it is conducted away into the surrounding metal. Consequently, it is possible to generate a molten pool, which solidifies to form the unifying bond between the parts being joined.



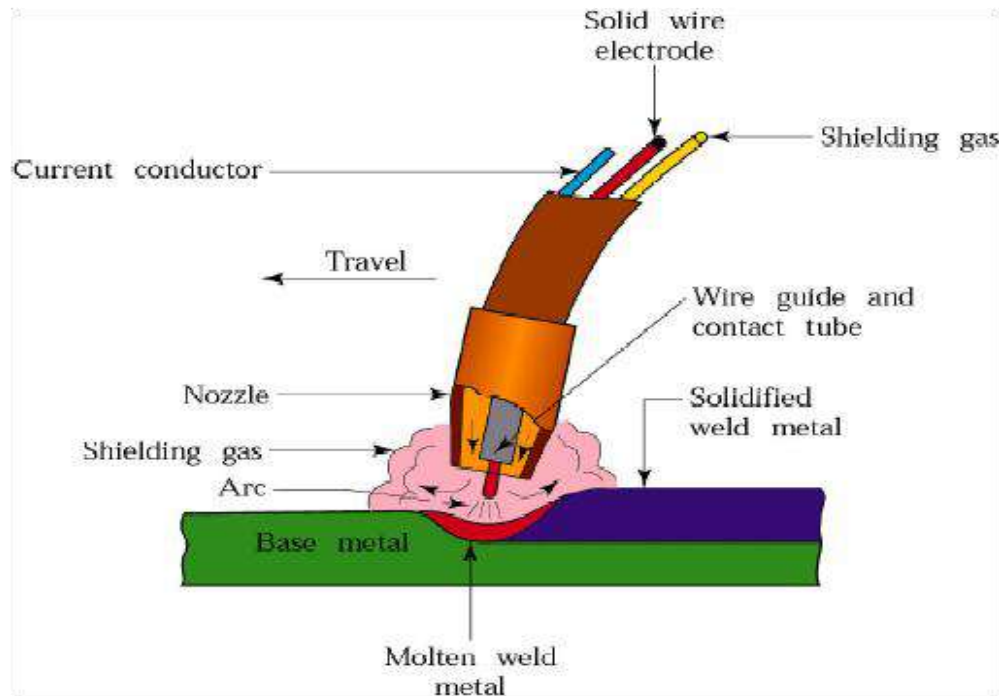
**Figure 1.2: Submerged arc welding.**

Later, in the 1930s, new methods were developed. Up until then, all metal-arc welding had been carried out manually. Attempts were made to automate the process using a continuous wire. The most successful process was *submerged arc welding* (SAW) where the arc is "submerged" in a blanket of granular fusible flux. During the Second World War the aircraft industry required a new method for the welding of magnesium and aluminium. In 1940 experiments began in the USA with the shielding of the arc by inert gases. By using an electrode of tungsten, the arc could be struck without melting the electrode, which made it possible to weld with or without filler material. The method is called *TIG welding* (Tungsten Inert *Gas*).



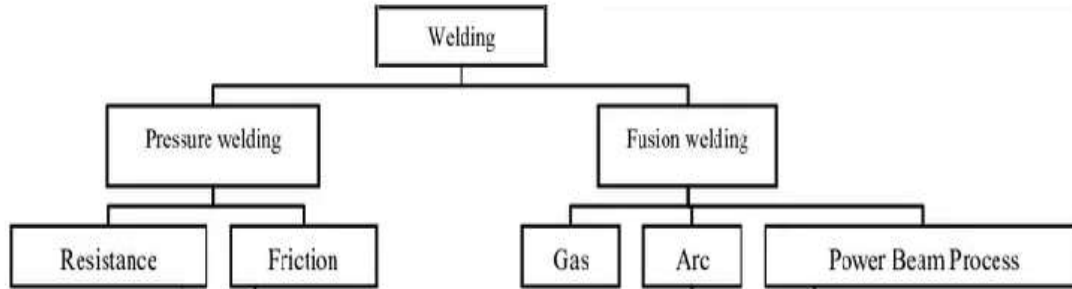
**Figure 1.3: The TIG welding method**

Some years later the **MIG welding process** (Metal Inert Gas) was also developed using a continuously fed metal wire as the electrode. Initially, the shielding gases were inert such as helium or argon. Zaruba and Potapevski tried to use CO<sub>2</sub> as this was much easier to obtain and by using the "dip transfer" method they did manage to reduce some of the problems caused by the intense generation of spatter; however when using a relatively reactive gas such as CO<sub>2</sub> or mixed gases such as argon/CO<sub>2</sub>, the process is generally called MAG welding (Metal Active Gas)



**Figure 1.4: The MIG/MAG welding method.**

The power-beam processes **electron beam (EB) welding** and **laser welding** have the most intensive of heat sources. The breakthrough of EB-welding came in 1958. The aircraft and nuclear power industries were the first to utilize the method. The main characteristics of EB-welding are its deep and narrow penetration. It's one limitation is the need for a vacuum chamber to contain the electron beam gun and the work piece. In some respects, **Laser welding** (and cutting) have ideal characteristics. The laser beam is a concentrated heat source, which permits high speed and very low distortion of the work piece, unfortunately, a high power laser is large and expensive. The beam must also be conducted to the joint in some way. The light from a CO<sub>2</sub> laser must be transmitted by mirrors, while that from a Nd: YAG-laser can be carried by a thin glass fiber, which makes it attractive for use with robotic welding. In the future it should be possible to utilize lightweight diode lasers with sufficient power for welding. The diode laser has a higher efficiency in converting electrical energy into the light beam. Although it has not yet been possible to produce diode lasers with the same power output and beam quality as present welding laser sources; these are already being used for welding metal up to about 1 mm thick. The low weight and size make them an interesting power source for use with robotic welding.



**Figure 1.5: Schematic presentation of the most common welding methods**

## **1.2 Problem Statement**

- Welding is used in different environments in air, underwater and space. It is also applicable in different areas such as construction, petroleum industries, aircraft industries, transportation, machine manufacturing, household manufacturing, repair and maintenance

## **1.3 The objective of the project**

Welding is very important process to complete the qualified operation of air conditioning system[6]. Therefore the main objective of this project is to identify the perfect welding method for pipe in air conditioning system for preventing leakages according to the welding standards by conducting destructive and nondestructive test.

## **1.4 Scope of Project**

An experimental work for pipe welding that following the standards of welding (ASTM), with main objective; to characterize the perfect pipe welding method by using Arc welding.

## **1.5 Lay out of Project**

Lay out of project followed these sections:

Chapter One: introduction / Chapter Two: Literature Review / Chapter Three: Experimental Work / Chapter Four: Result and Discussion / Chapter Five: Conclusion



## 2- LITERATURE REVIEW

### 2.1 Introduction

Welding is widely used technique for obtaining good quality weld joints in structural components. The higher deposition rate and superior surface quality give arc welding an edge over other welding techniques in industrial applications[7]. Presently, industries have concentrated their efforts in the establishment of the relationship between input parameters and weld bead geometry so that the process can be automated to achieve high production rate and controlled bead quality[8].

In the fabrication of large diameter pipes, Steel workpiece sheets are rolled and formed into a cylindrical shape, and lateral edges of the rolled sheet are joined to form a longitudinal pipe seam. The seam joint is typically welded to finish the cylinder shape, where the welded seam must be of adequate strength to maintain fluid seal for transfer of fluids or gas within the finished pipe. In welding the pipe seam, it is initially desirable to tack weld the seam edges to one another to create a joint for holding the seam together. Thereafter, inner and outer welding steps fill the remainder of the seam grooves, wherein the initial tack weld is completely consumed by the Subsequent inner and outer groove welds. One problem associated with the prior short circuit tack weld approach for pipe seams is relatively low amount of metal deposited per unit of time (low deposition rate), wherein the deposition rate is limited by the low heat limitation in order to prevent burn through. In this regard, a large current flows to the workpiece immediately after the short-circuit condition begins, which could potentially blow through the pipe[9]. As a result, the arc Voltage and/or current must be kept relatively low to avoid driving the welding arc through the workpiece seam, whereby the deposition rate of the buried arc approach is limited. Thus, conventional MIG arc welding and other prior welding processes are too slow for the demands of pipe welding operations, particularly for the initial pipe seam tack weld, without risking arc drive-through. Consequently, there is a continuing need for improved pipe seam tack welding processes and welding systems to provide high deposition rates and lineal welding speeds with improved seam integrity without undue spatter, arc drive through, or excessive workpiece heating, for tack welding of longitudinal pipe seams in a pipe mill[10].

According to above and additionally the quality of pipe welding must be taken in consideration with handling the load that effect on it where it will be used in air conditioning system, which is the main objective of this project.

## 2.2 Definition of Welding

Welding is a fabrication process whereby two or more parts are fused together by means of heat, pressure or both forming a join as the parts cool. Welding is usually used on metals and thermoplastics but can also be used on wood. The completed welded joint may be referred to as a weldment. Some materials require the use of specific processes and techniques. A number are considered 'unweldable,' a term not usually found in dictionaries but useful and descriptive in engineering[11].

The parts that are joined are known as a parent material. The material added to help form the join is called filler or consumable. The form of these materials may see them referred to as parent plate or pipe, filler wire, consumable electrode (for arc welding), etc.[12]

Consumables are usually chosen to be similar in composition to the parent material, thus forming a homogenous weld, but there are occasions, such as when welding brittle cast irons, when a filler with a very different composition and, therefore, properties is used. These welds are called heterogeneous. The completed welded joint may be referred to as a weldment.[13]

## 2.3 Types of Welding

### 2.3.1 Arc Welding

#### I. Shielded Metal Arc Welding Process (SMAW)

The shielded metal arc welding, also known as manual metal arc (MMA) welding, which uses a consumable electrode coated in flux to lay the weld. An electric current, in the form of either alternating current or direct current from a welding power supply is used to form an electric arc between the electrode and the metal to be joined. As the weld is laid the flux coating of the electrode disintegrates and providing shielding gas and a layer of slag to protect the weld area from atmospheric contamination [14]. The shielded metal arc welding process is one of the oldest and most widely used methods of joining metals by welding.

In shielded metal arc welding currents typically used in range between 30 to 300 A and voltages from 15 to 45 V depending on the metals being welded, electrode types and length and depth of weld penetration required[15]. Fig.2.1 shows the shielded metal arc welding process

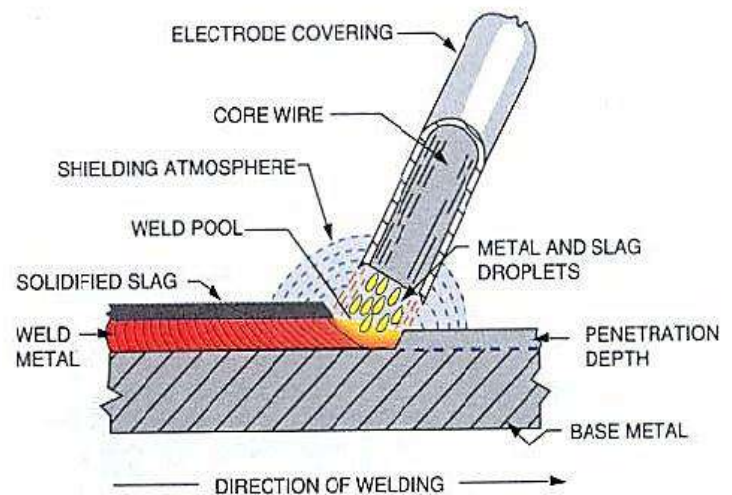
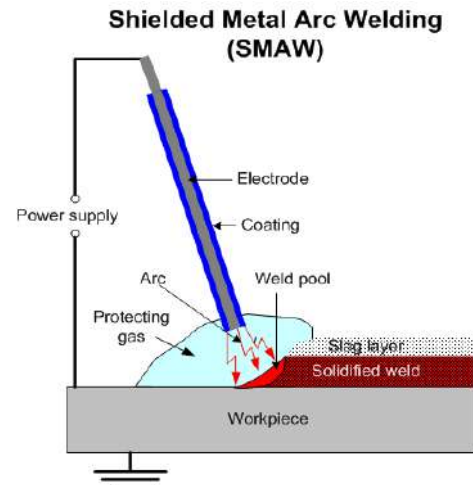


Fig.2.1: Shielded Metal Arc Welding Process[1]

## ***Equipment and Power Supply***

The shielded metal arc welding equipment typically consists of a constant current welding power supply and an electrode with an electrode holder, a ground clamp, welding cables. The shielded metal arc welding process use different types of polarity which depends primarily upon the electrode being used and the desired properties of the weld. Direct current with a negatively charged electrode (DCEN) causes heat to build up on the electrode, increasing the electrode melting rate and decreasing the depth of the weld. Reversing the polarity so that the electrode is positively charged (DCEP) and the work piece is negatively charged increases the weld penetration. The shielded metal arc welding process consists of a step-down transformer to reduce the voltage and increase the current and for direct current models a rectifier used which converts alternating current into direct current[16].



**Fig.2.2: Set up Shielded Metal Arc Welding process.**

## **II. The Main characteristics of Shielded Metal Arc Welding Process[17].**

- The equipment is simple, portable and inexpensive.
- Wide variety of metals, welding positions and electrodes are applicable.
- Suitable for indoor and outdoor applications.
- It can be used in area of limited access.
- The process is suitable for most of the commonly used alloys and metals.
- The process is less sensitive to draft and wind than gas shielded arc welding.
- The shielded metal arc welding electrodes provide a fast freeze weld slag that can assist in the control of the weld.
- In contrast to the alternate welding processes, the shielded metal arc welding process requires minimum weld process expertise.
- The electrode manufacturers can formulate the shielded metal arc welding electrode flux to meet specific chemistry and mechanical requirements.

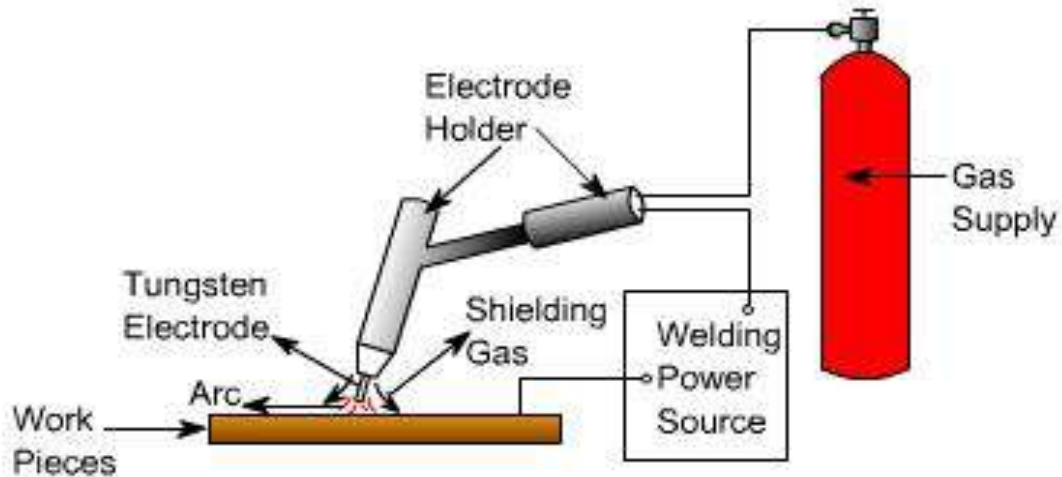
## **III. Shielded Metal Arc Welding Electrodes**

The shielded metal arc welding electrodes are coated metal in mixture of flux, which gives off gases as it decomposes to prevent weld contamination, introduces deoxidizers to purify the weld and provides slag layer to protect weld surface, improves the arc stability, and provides alloying elements to improve the weld quality [16]. The types of welding electrodes used would decide the weld properties such as strength, ductility and corrosion resistance.



### 2.3.2 TIG Welding

TIG welding (also called Gas Tungsten Arc Welding, GTAW) involves striking an arc between a non-consumable tungsten electrode and the workpiece. The weld pool and the electrode are protected by an inert gas, usually argon, supplied through a gas cup at the end of the welding gun, in which the electrode is centrally positioned.



**Figure 2.3: Schematic diagram of TIG welding equipment.**

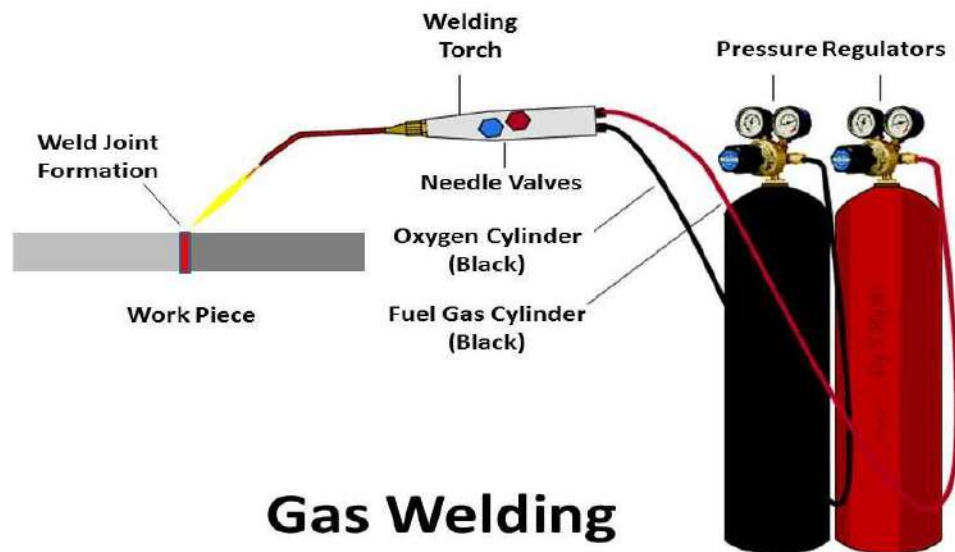
TIG welding can also be used for welding with filler material, which is applied in rod form by hand similar to gas welding. Tools for mechanized TIG welding are used for applications such as joining pipes and welding tubes into the end plates of heat exchangers. Such automatic welding tools can incorporate many advanced features, including mechanized supply of filler wire. The main application for TIG welding is welding of stainless steel, welding of light metals, such as aluminum and magnesium alloys, and the welding of copper. It is also suitable for welding all weldable materials, apart from lead and zinc, with all types of joints and in all welding positions. However, TIG welding is best suited to thin materials, from about 0.5 mm up to about 3 mm thick. In terms of productivity, TIG welding cannot compete with methods such as short arc welding[18].

### 2.3.3 Oxy-acetylene welding

The main application for TIG welding is welding of stainless steel, welding of light metals, such as aluminum and magnesium alloys, and the welding of copper. It is also suitable for welding all weldable materials, apart from lead and zinc, with all types of joints and in all welding positions. However, TIG welding is best suited to thin materials, from about 0.5 mm up to about 3 mm thick. In terms of productivity, TIG welding cannot compete with methods such as short arc welding.

Oxyacetylene welding, also known as Oxy-fuel Welding (OFW), includes any welding operation that uses combustion with oxygen as a heating medium. With this family of processes, the base metal and a filler rod are melted using a flame produced at the tip of a welding torch. Fuel gas and oxygen are combined in the proper proportions inside a mixing chamber in the torch. Molten metal from the plate

edges and filler metal, if used, intermix in a common molten pool and join when cooling. Commonly-used fuel gases include acetylene, propylene, propane and natural gas. The equipment used in oxyacetylene welding is low in cost, usually portable, and versatile enough to be used for a variety of related operations such as bending and straightening, preheating, post heating, surfacing, brazing, and braze welding. Among commercially available fuel gases, acetylene most closely meets the requirements for all these applications. Cutting attachments, multi-flame heating nozzles and a variety of special application accessories add greatly to the overall versatility of the basic oxyacetylene welding equipment. With relatively simple equipment changes, manual and mechanized oxygen cutting operations can be performed. Metals normally welded include carbon and low alloy steels and most nonferrous metals[19].



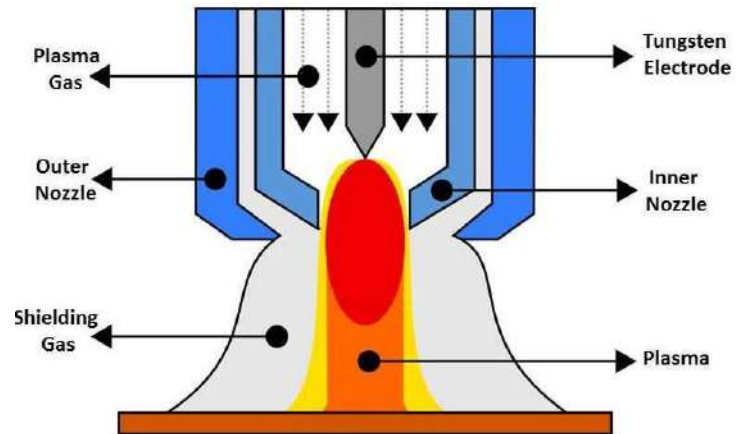
## Gas Welding

Figure 2.4: A gas welding set

### 2.3.4 Plasma welding

The plasma welding method employs an inner plasma gas and outer shielding gas, as shown in Figure 2.5. The plasma gas flows around a retracted centered electrode, which is usually made of tungsten. The shielding gas flows through the outer jet, serving the same purpose as in TIG welding.

A plasma arc is considerably straighter and more concentrated than, for example, a TIG arc, which means that the method is less sensitive to arc length variations: see Figure 2.6. The plasma welding process can accept



### Principle of Plasma Arc Welding

Figure 2.5: Schematic diagram of plasma welding

variations of 2-3 mm in the arc length without significantly altering the heat input to the workpiece. This is approximately ten times better than the corresponding value for TIG welding. However, because the arc is narrower, more accurate transverse control is important, which means that the method is normally used in mechanized welding[20].

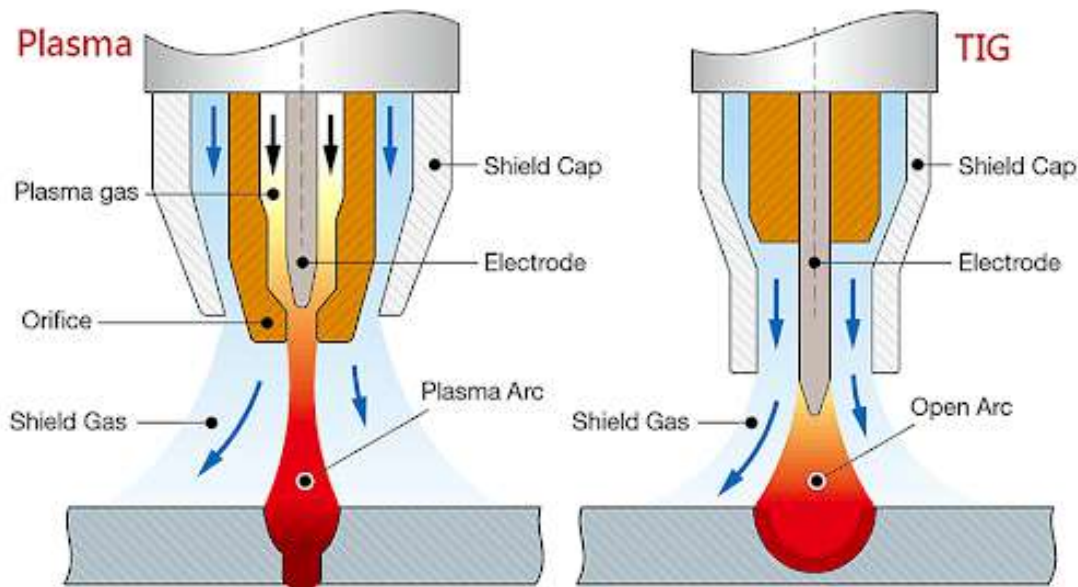


Figure 2.6: The plasma arc is not as conical as the TIG arc.

## **2.4 Weld quality**

Welded constructions may be vehicles, pressure vessels, cranes, bridges and others. It is an important task to ensure the welding quality. Quality systems are specified in standards. They include tasks and responsibilities for the welding coordination (EN 719), approval testing of welders (EN 287) and specification and approval of welding procedures (EN 288). The reader will be introduced shortly to the work that has to be done before and after welding to ensure overall quality. The most common imperfections in welds are also described together with the most common causes on why they occur[20].

### **2.4.1 Joint preparation**

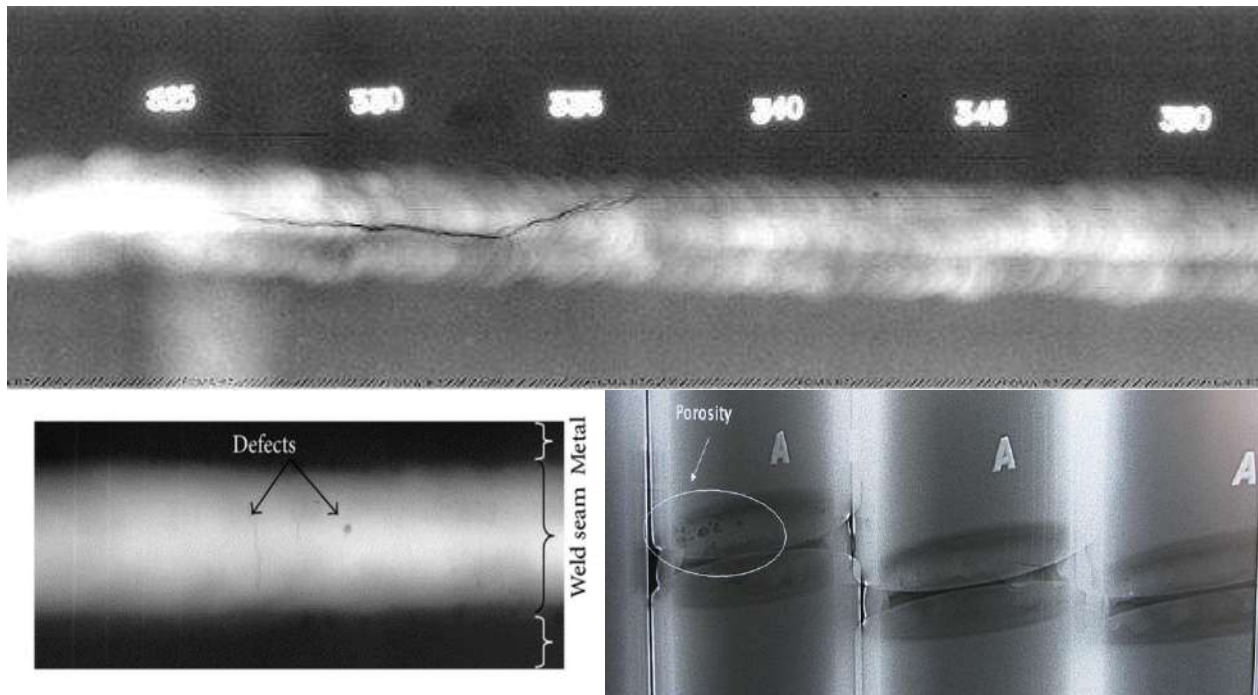
Before commencement of welding, the joint surfaces and area around the weld should be cleaned. Moisture, dirt, oxides, rust and other impurities can cause defective welds. Stainless steels and aluminum need special care. Aluminum joints have to be cleaned by degreasing with alcohol or acetone. The oxide must be removed by a stainless-steel brush or other ways. Welding must be carried out in conjunction with cleaning before new oxide builds up. High-quality stainless-steel joints need to be cleaned in a similar way. Tools and brushes must be made of stainless steel[19].

### **2.4.2 Striking the arc**

The normal procedure for striking the MIG/MAG welding arc is for the gas supply, the wire feed unit and the power unit all to be started before the welder presses the trigger switch on the welding torch. This is also the method that is generally preferred in most cases, as it results in the quickest start. However, problems can arise: for example, the wire may hit the joint, or there may be one or more false starts before a weld pool is created and the welding stabilizes[21].

Creep starting provides a gentler start. The wire is fed forward at reduced wire feed speed until electrical contact is established with the workpiece, after which the wire feed speed increases to the set value. Sputtering during starting is a problem that can occur from a number of causes. The tendency to sputter increases if the inductance is high and the voltage is low. Welding data that may operate satisfactorily once welding has started is perhaps less suitable when starting to weld[21].

Gas pre-flow is used when welding sensitive materials, such as aluminium or stainless steel. The gas flow starts a short (and adjustable) time before the arc is struck. The function ensures that there is proper gas protection of the workpiece before welding starts. Note, however, that if the gas hose between the gas bottle and the wire feeder is long, it can act as a 'store' for compressed gas, which is then released as an uncontrolled puff of gas when the gas valve opens, involving a risk of creating turbulence around the weld, with reduced protection from the gas. However, a gas-saving valve is available as an accessory, reducing the pressure from the gas bottle and thus eliminating the risk of a puff of gas. The gas pre-flow function will also eliminate this problem because the puff is rather short. The hot start facility increases the wire feed speed and arc voltage for a controllable time during the start of welding. It reduces the risk of poor fusion at the start, before full heat inflow has become established[22].



**Figure 2.7 X-ray picture of an aluminum weld containing defect.**

### 2.4.3 Pores

Pores in the weld metal are often caused by some disturbance in the gas shield, but there are also different reasons[23].

- Wrong setting of gas flow. The flow must be enough; it should be adjusted according to the welding current. Too high amount of gas will cause problems with turbulence in the gas nozzle.
- Draught in the place of welding. Airspeed above 0.5 m/s can interfere with the gas stream from the gun (somewhat depending on the setting of the gas flow).
- Defect equipment. Clogged channels or leakage can prevent the gas from flowing. Control if possible by measuring directly on the opening of the gas nozzle.
- Clean the inside of the nozzle regularly from spatter. The joint surfaces are contaminated with oil, rust or painting.



#### 2.4.4 Lack of fusion

Problems with lack of fusion between weld and parent metal have different reasons[24, 25].

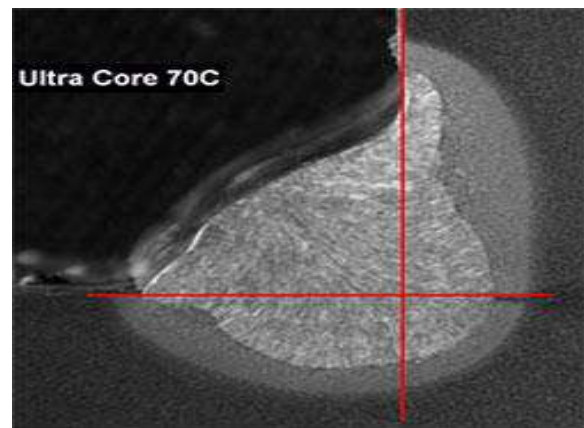
- Incorrect setting. Low voltage or long electrode stick-out will result in welding where the added heat is not in proportion to the amount of filler material.
- If the melted metal in the pool tends to flow before the arc. This can be caused if the weld is sloping, and if the welding torch is not properly aligned with the direction of the weld. The problem will also be worse if there is a large weld pool as a result of high heat input and slow travel speed of the welding torch.
- The large thermal dissipation at thick workpieces.
- Unfavorable geometry or too narrow joint angle.
- The arc is directed in the wrong way (misalignment) and one edge of the joint is heated insufficiently.

#### 2.4.5 End craters

End craters arise as a result of direct interruption in welding. This allows a crack or crater to form in the final part of the metal to solidify, as a result of shrinkage forces during solidification. When grains from opposite sides grow together, low melting-point constituents and impurities can be swept ahead of the solidification front to form a line of weakness in the center of the weld. The craters felling function available in advanced power sources can be used to avoid the creation of craters when welds are finished. The arc continues to provide a reduced heat input while the weld pool solidifies. This has the effect of modifying the solidification process so that the final part of the weld pool solidifies at the top, thus avoiding the formation of a crater[26]



**Figure 2.9** A crack may appear as an effect of direct interruption of the welding.



**Figure 2.8** Example of a fillet weld with lack of fusion against the base plate.

### 2.4.6 Post weld treatment

The corrosion resistance of stainless steels is degraded if oxides from welding remain. Special root gas is used to avoid oxidation and chemical and mechanical post weld treatment has to be done[27].

## 2.5 Destructive Testing

### 2.5.1 Tensile Test

The tensile experience in mechanical engineering and architecture is a standard test to determine the main properties of materials such as yield strength, yield strength, cut limit, and others. This test breaks the sample piece. A sample of the material having a specific section is prepared for a tensile test. Attached to both ends of the tensile device, an increased tensile force is attached to it until the sample pieces are limited.

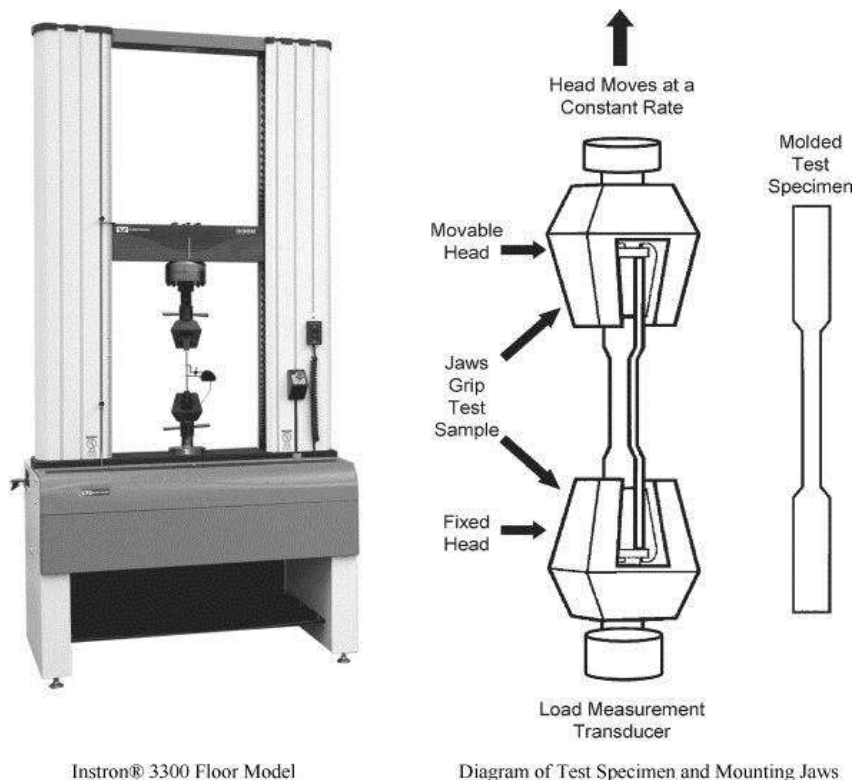
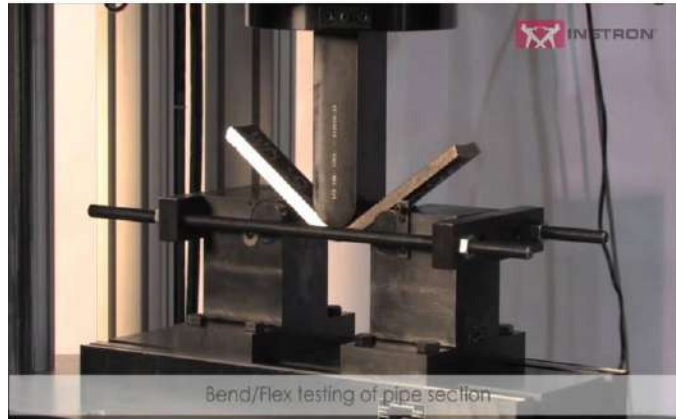
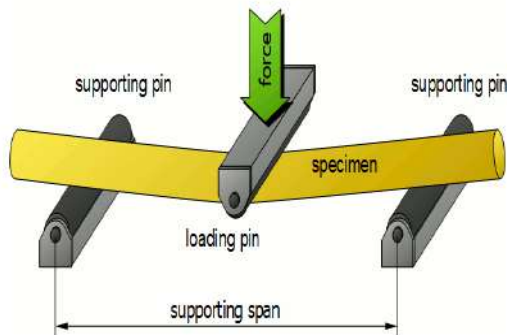


Figure 2.10: sample assessment at tensile test

### 2.5.2 Bending Test

A three-point curvature flexural test together produces values for flexural elasticity, flexural stress, flexural tension and flexural response and flexural tension in the material. The main advantage of a three-point bending test is the ease in preparing and testing samples.



**Figure 2.11 bending test layout**

### 2.5.3 Hardness test

. hardness test is a method employed to measure the hardness of a material. Hardness refers to a material's resistance to permanent indentation. There are numerous techniques to measure hardness and each of these tests can identify varying hardness values for a single material under testing. The hardness test is a mechanical test for material properties which are used in engineering design, analysis of structures, and materials development. The principal purpose of the hardness test is to determine the suitability of a material for a given application, or the particular treatment to which the material has been subjected. The ease with which the hardness test can be made has made it the most common method of inspection for metals and alloys.

## 2.6 Non-destructive Testing

### 2.6.1 Dye penetrant

Dye penetrant inspection (DP), also called liquid penetrate inspection (LPI) or penetrant testing (PT), is a widely applied and low cost inspection method used to check surface-breaking defects in all non-porous materials (metals, plastics, or ceramics). The penetrant may be applied to all non-ferrous materials and ferrous materials; although for ferrous components magnetic-particle inspection is often used instead for its subsurface detection capability. LPI is used to detect casting, forging and welding surface defects such as hairline cracks, surface porosity, leaks in new products, and fatigue cracks on in-service components

Dye penetrant test is a surface testing method, and is used to reveal discontinuities in the surface of non-porous materials.





**Figure 3-10: dye penetrant test for welded joints**

### 2.6.2 X-ray or Radiography test

Radiography is used to reveal primarily internal volumetric discontinuities. The films are evaluated against the required quality level. Use of this method is limited by the thickness of the weld, which should not exceed 50 mm as shown in figure below.



**Figure 3-11: Radiography equipment test**

## 2.7 Weld Joints Design

A welded joint is a permanent joint which is obtained by the fusion of the edges of the two parts to be joined together, with or without the application of pressure and a filler material. The heat required for the fusion of the material may be obtained by burning of gas (in case of gas welding) or by an electric arc (in case of electric arc welding). The latter method is extensively used because of greater speed of welding. Welding is extensively used in fabrication as an alternative method for casting or forging and as a replacement for bolted and riveted joints. It is also used as a repair medium *e.g.* to reunite metal at a crack, to build up a small part that has broken off such as gear tooth or to repair a worn surface such as a bearing surface.

### Types of Welded Joints

Following two types of welded joints are important from the subject point of view:

1. Lap joint or fillet joint, and 2. Butt joint.

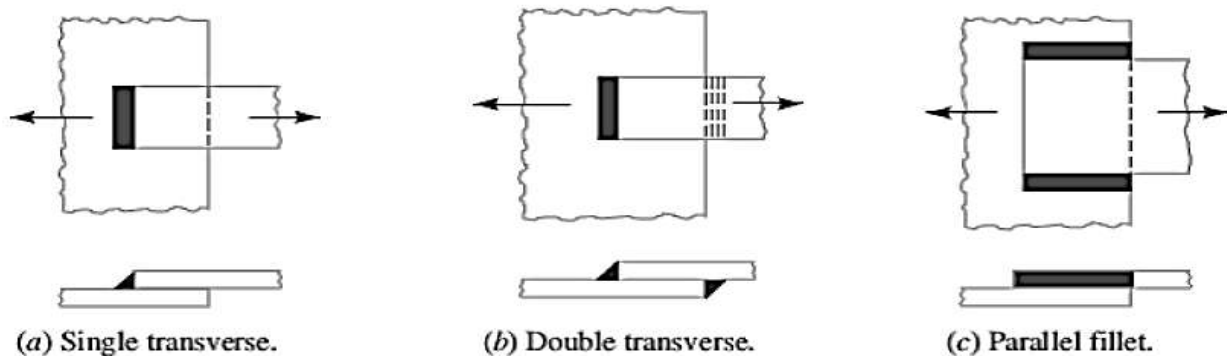


Fig.1. Types of Lab and Butt Joints

### Lap Joint

The lap joint or the fillet joint is obtained by overlapping the plates and then welding the edges of the plates. The cross-section of the fillet is approximately triangular. The fillet joints may be

1. Single transverse fillet, 2. Double transverse fillet and 3. Parallel fillet joints.

The fillet joints are shown in Fig.1. A single transverse fillet joint has the disadvantage that the edge of the plate which is not welded can buckle or warp out of shape.

### Butt Joint

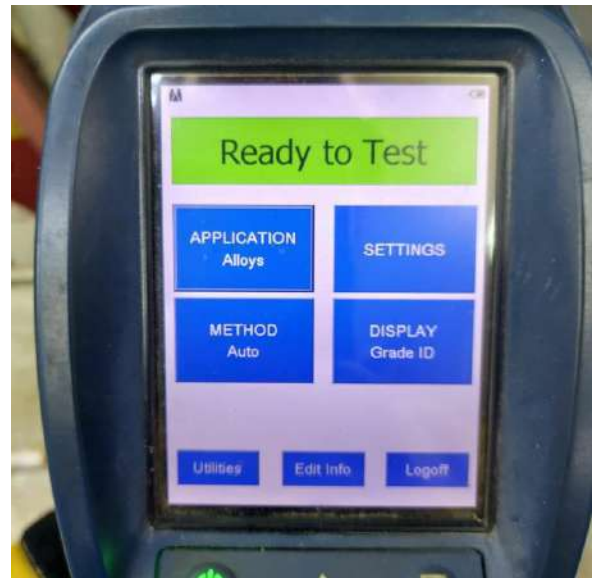
The butt joint is obtained by placing the plates edge to edge as shown in Fig.2. In butt welds, the plate edges do not require beveling if the thickness of plate is less than 5 mm. On the other hand, if the plate thickness is 5 mm to 12.5 mm, the edges should be beveled to V or U-groove on both sides.



## 3-EXPERIMENTAL WORK

### 3.1 chemical composition Test

According to ASTM standard the chemical test done to specify A106-02 chemical components. Chemical composition analysis is conducted for a wide range of purposes from material identification and characterization to quality control monitoring. The analysis provides valuable information about the elements of a test sample. Chemical composition analysis or elemental analysis can be qualitative (determining what elements are present), and it can be quantitative (determining how much of each are present). This test done with two parts: chemical component and radiation



**Figure 4-1: The Chemical composition test of the specimen**

The radiation test was carrying on for the primary sample to avoid the radiation pollution as shown in figure bellow.

### 3.2 Sample Preparation

Welding is widely used technique for obtaining good quality weld joints in structural components. Welding is one of the most important and versatile means of fabrication available to industry. Welding is used to join hundreds of different commercial alloys in many different shapes. Actually, many products could not even be made without the use of welding, for example, guided missiles, nuclear power plants, jet aircraft, pressure vessels, chemical processing equipment, transportation vehicle, air conditioning systems and literally thousands of others. Many of the problems that are inherent to welding can be avoided by proper consideration of the particular characteristics and requirements of the process.

Pipe welding in air conditioning systems is very important process for completing the system cycle and joining system parts each other. Air conditioning systems parts operated with high difference temperature. A106-02 Grade C, Seamless Carbon Steel Pipe is widely used for high temperature differences systems. Therefore, the selection process was done, and A106-02 Seamless Carbon Steel Pipe for current study, as shown below.

### 3.3 visual test for specimen

Primary Sample was selected and preparing it for taking the measurements for sample cutting to overcome the testes.



**Figure 4-2 the specimen measurement**

### 3.3.1 cutting process of the specimen

The samples preparing for mechanical tests have different shape according to the test as shown below.



**Figure 4-3: the specimen Preparation (pipe cutting)**



### 3.3.2 Destructive Testing

Experimental setting of primary sample for axial bending test as shown in figure below.

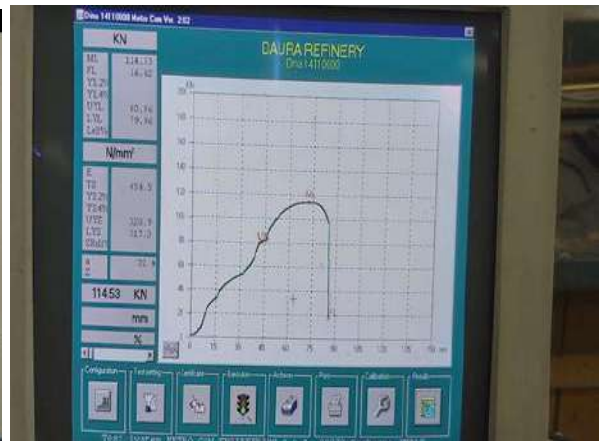
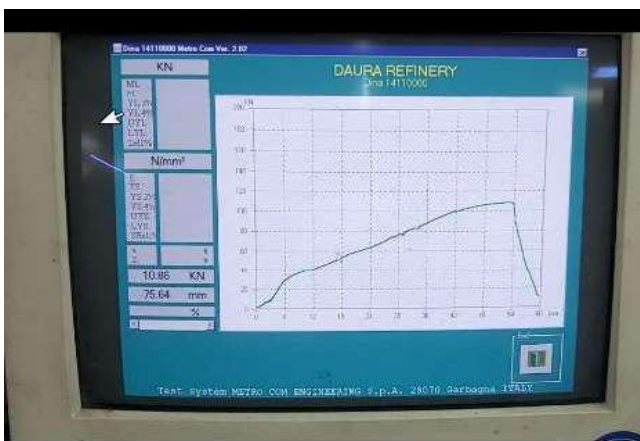


Figure 4-5: primary sample setting for axial bending and Tensile Test (welded and unwelded specimen)

### 3.4 Specimen Welding Process

Three pass welding process has been carried out for the primary sample; However, this sample was divided according to the sample mechanical test as shown in figure below.



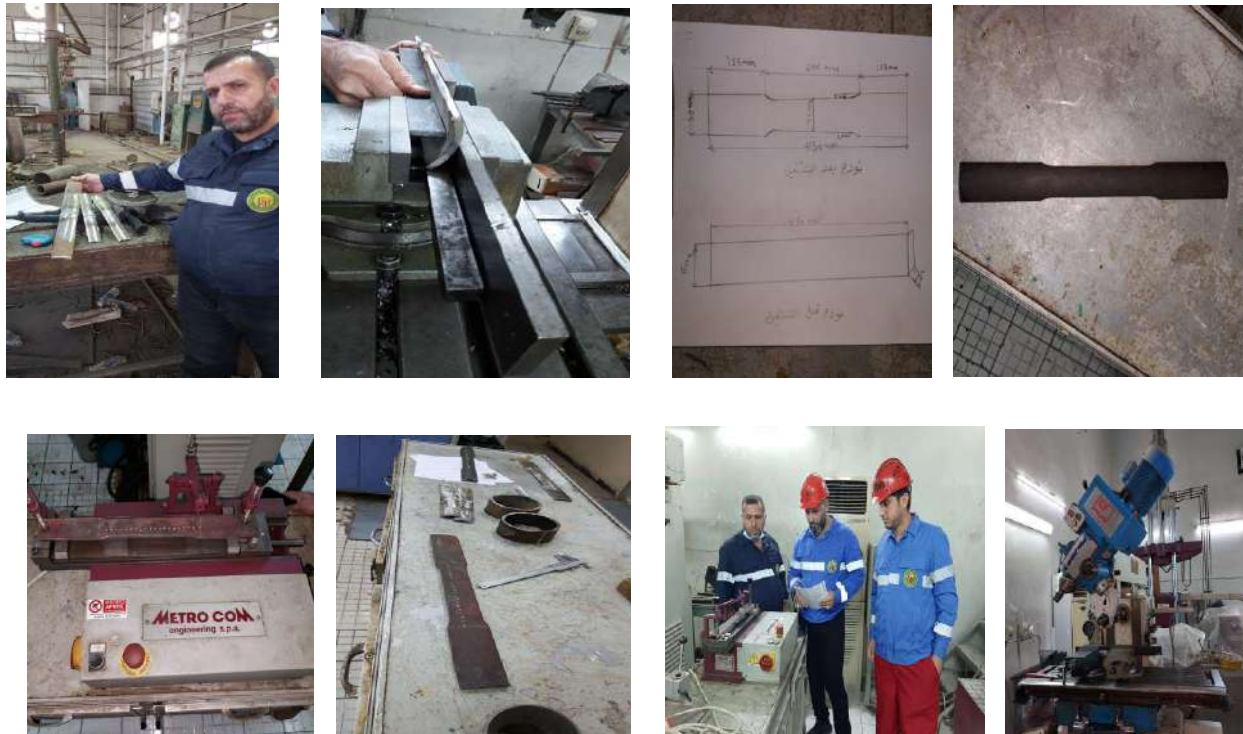


**Figure 4-6: Preparation of Welding Specimen**

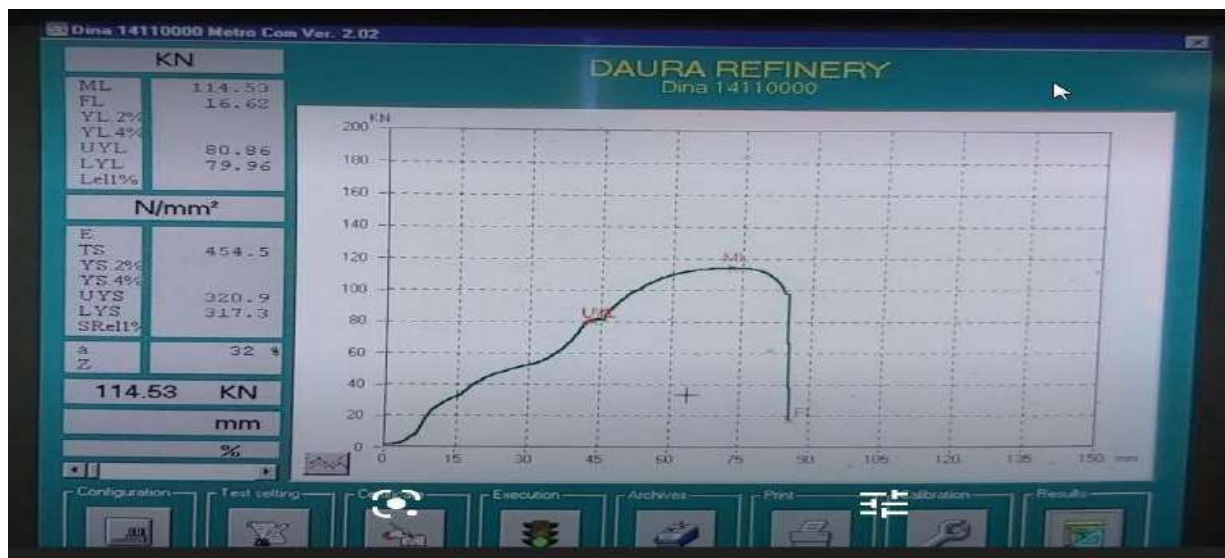
### 3.5 Destructive Testing

#### 3.5.1 Tensile Test

The ultimate tensile strength of the machined specimens is measured in a calibrated Universal tensile testing machine which has a capacity of 60 tons. Tensile test was carried out according to the ASTM standards. Figure shows the test specimen as shown in figure below.



**Figure 4-4: specimen preparing for Tensile Test**



**Figure 4-10: Tensile Test arrangement**

An excellent result will be achieved if it is possible to design the various elements of the structure such that they are subjected mainly to tensile stresses. The entire cross-section of the material then plays its part in carrying the load, thus utilizing the material in the optimum manner to produce light, cheap designs. The material shall conform to the requirement as tensile properties prescribed in table 2. Computed elongation values are contained in table 3 and table 4 as mentioned in ASTM standard. The result as shown in figure 4-4 gave good machining with tables of standard.

TABLE 2 Tensile Requirements

	Grade A (Explanatory Note 2)		Grade B		Grade C	
Tensile strength, min. psi (MPa)	48 000 (330)		60 000 (415)		70 000 (485)	
Yield strength, min. psi (MPa)	30 000 (205)		35 000 (240)		40 000 (275)	
	Longi- tudinal	Transverse	Longi- tudinal	Transverse	Longi- tudinal	Transverse
Elongation in 2 in. or 50 mm, min. %						
Basic minimum elongation transverse strip tests, and for all small sizes tested in full section	35	25	30	16.5	30	16.5
When standard round 2-in. or 50-mm gage length test specimen is used	28	20	22	12	20	12
For longitudinal strip tests	A.B		A.B		A.B	
For transverse strip tests, a deduction for each 1/16-in. (0.8 mm) decrease in wall thickness below 1/4 in. (7.9 mm) from the basic minimum elongation of the following percentage shall be made		1.25 <sup>C</sup>		1.00 <sup>C</sup>		1.00 <sup>C</sup>

<sup>A</sup> The minimum elongation in 2 in. (50.8 mm) shall be determined by the following equation:

$$e = 625 000 A^{0.5} / U^{0.5}$$

where:

e = minimum elongation in 2 in. (50.8 mm), %, rounded to the nearest 0.5 %.

A = cross-sectional area of the tension test specimen, in.<sup>2</sup>, based on specified outside diameter or nominal specimen width and specified wall thickness rounded to the nearest 0.01 in.<sup>2</sup> (if the area thus calculated is greater than the value 0.75 in.<sup>2</sup> shall be used), and

U = specified tensile strength, psi.

<sup>B</sup> See Table 4 for minimum elongation values for various size tension specimens and grades.

<sup>C</sup> Table 3 gives the computed minimum values.

TABLE 3 Computed Transverse Elongation<sup>A</sup>

Wall Thickness		Elongation in 2 in. or 50 mm, min. %	
in.	mm	Grade A, Transverse	Grades B and C, Transverse
1/4 (0.312)	7.9	25.00	16.50
1/4 (0.281)	7.1	23.75	15.50
1/4 (0.250)	6.4	22.50	14.50

<sup>A</sup> This table gives the computed minimum elongation values for each 1/16-in. (0.8-mm) decrease in wall thickness. Where the wall thickness lies between two values shown above, the minimum elongation value is determined by the following equation:

Grade  
A  
B and C

Direction of Test  
Transverse  
Transverse

Equation  
 $E = 40t + 12.50$   
 $E = 32t + 6.50$

where:

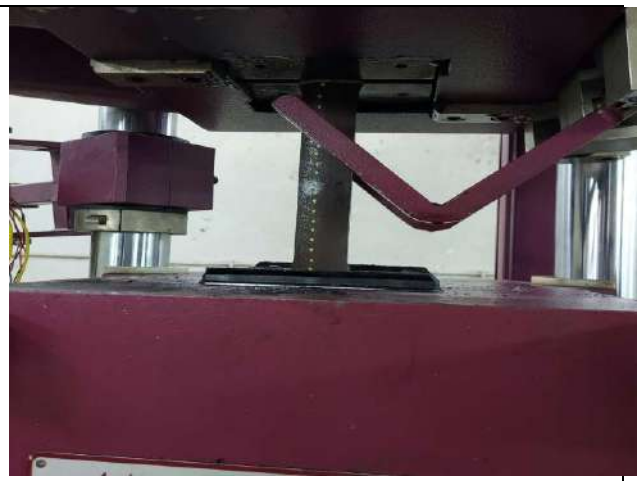
E = elongation in 2 in. or 50 mm, %, and

t = actual thickness of specimen, in.





A



B



**Figure 4- 8: A sample arrange, B sample connection with tensile test machine, C failure of sample, D output results.**

### 3.5.2 Bending Test

For bending test; If it is not possible to avoid having to transfer the loads by bending the structural parts, the first step is to attempt to place the material as far away from the centre of gravity of the cross section as possible and the setting for this test is shown in figure below.



If it is not possible to avoid having to transfer the loads by bending the structural parts, the first step is to attempt to place the material as far away from the center of gravity of the cross section as possible. After the test and X-ray test for welded joints, the weld process showing a high quality and no deformation and cracks appears in the welded joint after the test as shown in figure 4-5. Therefore, bending test for welded joints take place as shown in figure 4-6.

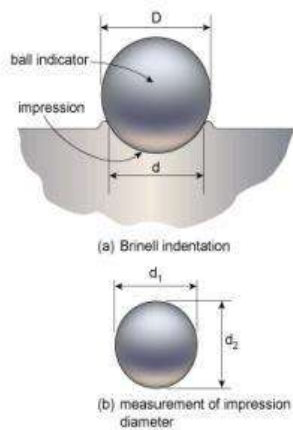


**Figure 4- 9: welded joint after bending test**



### 3.5.3 Hardness test

**The Brinell hardness** test method consists of indenting the test material with a 10 mm diameter hardened steel or carbide ball subjected to a load of 3000 kg. For softer materials the load can be reduced to 1500 kg or 500 kg to avoid excessive indentation. The full load is normally applied for 10 to 15 seconds in the case of iron and steel and for at least 30 seconds in the case of other metals. The diameter of the indentation left in the test material is measured with a low powered microscope. The Brinell hardness number is calculated by dividing the load applied by the surface area of the indentation. When the indenter is extracted to 153 H.B.



$$BHN = \frac{P}{\frac{\pi D}{2} [D - \sqrt{D^2 - d^2}]}$$

Where:

$P$  is the test load [kg]

$D$  is the diameter of the ball [mm]

$d$  is the average impression diameter of indentation [mm]



### 3.5.4 Compression test

Arranging for the loads in the structure to be carried as compressive loads also makes good use of the material. However, the strength of a cylinder structure can be reduced by the risk of buckling or other instability phenomena. The critical buckling load is independent of the strength of the material. This means that, when designing slender structures in which the risk of buckling determines the load carrying capacity, it does not help to choose an alternative material having higher structural strength.

On the other hand, the modulus of elasticity of the material plays a decisive part in determining the load-carrying capacity of slender structures. In the case of cylinder structures that are welded and subjected to compressive loads, the longitudinal residual compressive stresses acting on each side of the weld, also have a negative effect on the load-carrying capacity. In the case of cistern-like structures in particular, the true buckling stress is considerably lower compared to theoretically calculate buckling stress. After the welding process and doing the compression test for sample while the X-ray test showing that there is no deformation and cracks appears in welded joint as shown in figure 4-7.



Figure 4- 11: A sample arrange, B sample connection with compression test machine, C failure of sample, D output results.





## 4-RESULT

### 4.1 Introduction

Welding is one of the most important and versatile means of fabrication available to industry. Welding is used to join hundreds of different commercial alloys in many different shapes. The procedure of qualitative welding process full in many steps first of all; testing the chemical components of steel, secondly doing the nondestructive tests such as Y-ray and Dye penetrant. Finally, the mechanical tests for welded joints such as the tensile, bending and compression tests. Therefore, this chapter related with these results of these tests.

### 4.2 Compression composition test

As shown in figure 4-1, the results of chemical test for A106-02- Grade C pipe have a great identically with ASTM stander as shown in table 1.

---

C	SI	MN	P	S	FE
0.15	0.22	0.65	0.01	0.02	98.8

---

Table 1: pipe sample chemical results

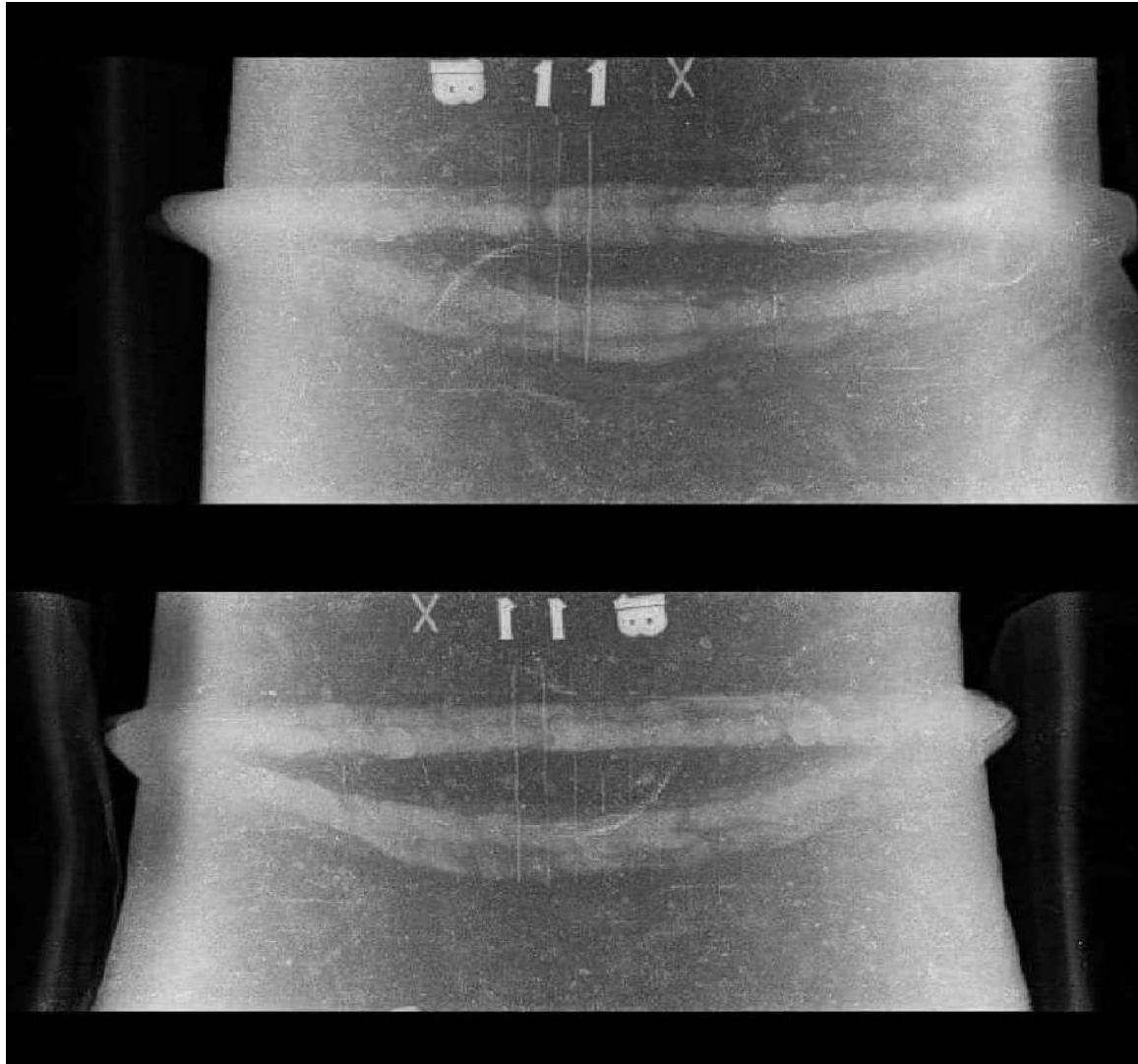
TABLE 1 Chemical Requirements			
	Composition, %		
	Grade A	Grade B	Grade C
Carbon, max <sup>A</sup>	0.25	0.30	0.35
Manganese	0.27–0.93	0.29–1.06	0.29–1.06
Phosphorus, max	0.035	0.035	0.035
Sulfur, max	0.035	0.035	0.035
Silicon, min	0.10	0.10	0.10
Chrome, max <sup>B</sup>	0.40	0.40	0.40
Copper, max <sup>B</sup>	0.40	0.40	0.40
Molybdenum, max <sup>B</sup>	0.15	0.15	0.15
Nickel, max <sup>B</sup>	0.40	0.40	0.40
Vanadium, max <sup>B</sup>	0.08	0.08	0.08

<sup>A</sup> For each reduction of 0.01 % below the specified carbon maximum, an increase of 0.06 % manganese above the specified maximum will be permitted up to a maximum of 1.35 %.

<sup>B</sup> These five elements combined shall not exceed 1 %.

### 4.3 X-ray tests

For the purpose of comparison and illustration, this study uses several characterization techniques to analyze the chemistry of mild steel welding process. X-ray diffraction shows that mild steel gas metal arc welding is predominantly magnetite while the mild steel shielded metal arc welding. Welds deposited using electrodes in the dried condition were subjected to X-ray inspection to verify weld soundness, and no substantial increase in weld porosity was observed in the E8010-G deposits either. Therefore, it may be difficult in the field to determine the condition of the electrodes based on their performance during welding. as shown in figure 4-2.



**Figure 4-12: X-ray test for welded joints**

While the dye penetrant test is a Liquid penetrant testing is also a surface testing method, and is used to reveal discontinuities in the surface of non-porous materials shown in figure4-3.

## DISCUSSION

The main objective for selecting this project is the important need for understanding the welding process of pipes which is mainly used in refrigeration system.

It is known that all fluid of cooling is flowing inside the pipes of system whether large or medium or small size. So is a need to get good knowledge of the theory and practice for common method of pipe welding, such as arc welding, Oxy-Acetylene welding and gas tungsten arc welding, also known as Tungsten Inert

Gas (TIG) welding.

From tensile test the tensile strength was (454 n/m<sup>2</sup>) and the yield strength was (320 n/m<sup>2</sup>). The results were compared with standard (requirement)

which was (380MPa) this mean that the experimental results the bending test of the weld joint show crack free or any weld defect that is mean the test is accepted according to

are acceptable.

standard as shown in figure (4-10).

X-ray test were conducted for the all joints to make shore that the weld way free from any defects.

The weld joint is sound and high integrity because the welding design and preparation was conducted according to stander.

X-ray test were also conducted for all weld joints, the results showed in fig (4-12)

The results were acceptable according to standards because the sizes of all porosity are small and do not affect the weld integrity and also do not affect the mechanical properties of the weld joint.

Liquid penetrant was also used to make sure that there is no surface defect or any cavity on the surface and the results were also acceptable, that because skilled welder was done the weld job.

## 5 - CONCLUSION

- The sample was examined and found to be weldable
- Through this experience, it has been proven that the metal is weldable, and we did not get internal or external defects
- Good results were obtained for the bending test and tensile test, and the results were close to international specifications
- The characteristics between the welded and non-welded sample were close, and this indicates that the welding process was completed according to the specifications after preparing a suitable welding system to obtain these results.
- It was found that the mechanical properties are close to the standard

## REFERENCES

- [1] Gurpreet Singh SidhuSukhpal Singh Chatha. "Role of shielded metal arc welding consumables on pipe weld joint." *International Journal of Emerging Technology and Advanced Engineering* 2, no. 12 (2012).
- [2] William J Rahmeyer. "Pressure loss coefficients of threaded and forged weld pipe fittings for ells, reducing ells, and pipe reducers." *ASHRAE Transactions* 105 (1999): 334.
- [3] Mohammad Shah Alam. "Structural integrity and fatigue crack propagation life assessment of welded and weld-repaired structures." (2005).
- [4] T Bartlett Quimby. "A beginner's guide to the steel construction manual." *University of Alaska Anchorage* || August (2008).
- [5] P KahJ Martikainen. "Current trends in welding processes and materials: improve in effectiveness." *Rev. adv. mater. Sci* 30, no. 2 (2012): 189-200.
- [6] George A Antaki, *Piping and pipeline engineering: design, construction, maintenance, integrity, and repair*. 2003: CRC Press.